UNIVERSITY OF SOUTHAMPTON

FACULTY OF ENGINEERING, SCIENCE &

MATHEMATICS

School of Ocean and Earth Sciences

The Evolutionary History and Phylogeny of the Lithodinae (Decapoda: Anomura: Lithodidae)

by

Sarah Marie Snow (k/a Sally Hall)

Thesis for the degree of Doctor of Philosophy

Submitted April 2010

"*Quis hic locus, quae regio, quae mundi plaga?*

What seas what shores what grey rocks and what islands."

– T.S. Eliot, Marina.

UNIVERSITY OF SOUTHAMPTON

ABSTRACT

FACULTY OF ENGINEERING, SCIENCE AND MATHEMATICS

SCHOOL OF OCEAN AND EARTH SCIENCES

Doctor of Philosophy

THE EVOLUTIONARY HISTORY AND PHYLOGENY OF THE LITHODINAE (DECAPODA: ANOMURA: LITHODIDAE)

By Sarah Marie Snow (k/a Sally Hall)

The anomuran sub-family Lithodinae comprises a great diversity of morphological and ecological forms, whose global radiation has not been specifically addressed since the modern syntheses of plate tectonics, oceanography, species theory and cladistic systematics. The focus of this thesis was to investigate the origin and radiations of the deep-sea Lithodinae as a case study for interchanges between deep and shallow oceans in mobile benthic fauna. Molecular sequences were obtained from six genes (for 47 species belonging to 10 genera of Lithodidae) and different aspects of morphology were examined in order to identify nested monophyletic groups based on shared, derived characteristics. The hypothesis that lineage-specific temperature tolerances influence the distribution of deep- and shallow-water groups was tested by examining habitat alongside phylogeny.

Lithodid ancestors are likely to have had a north Pacific, shallow-water distribution and planktotrophic larvae. Some shallow-water populations of Lithodidae are tied to locations north of 30°N because of the restricted thermal tolerance of pelagic larval stages; however, life-history changes allowed the subfamily Lithodinae to expand through the global deep sea, where they are now living at the frontier of their lower temperature threshold in the Southern Ocean. Phylogenies indicate the importance of large-scale dispersals within deep-sea groups, linked to the cold deep-water currents that connect the major oceans. The subfamily Lithodinae includes examples of at least two genera in which diverse morphologies have arisen within the deep ocean in the absence of discernable barriers to gene flow. Adult migration and larval dispersal partially explain the widespread occurrence of the Lithodidae, but this does not indicate that lithodids roam the ocean depths unconstrained by physical or chemical conditions. Climate change throughout the Cenozoic has substantially altered the marine environment and shaped the distribution and radiation of the extant Lithodidae. In the forthcoming years, measurable changes in ocean temperature, ocean currents and benthic habitat will affect the distribution of the lithodids and the communities they live in, as they have in the past.

CONTENTS

TABLES

FIGURES

APPENDICES

DECLARATION OF AUTHORSHIP

I, Sarah Marie Snow (k/a Sally Hall) declare that this thesis entitled

> The Evolutionary History and Phylogeny of the Lithodinae (Decapoda: Anomura: Lithodidae)

and the work presented in this thesis are both my own, and have been generated by me as the result of my own original research. I confirm that:

- This work was done wholly or mainly whilst in candidature for a research degree at this University;
- Where any part of this thesis has been previously submitted for a degree or any other qualification at this University or any other institution, this has been clearly stated;
- Where I have consulted the published works of others, this is always clearly attributed;
- Where I have quoted from the work of others, the source is always given. With the exception of such quotation, this thesis is entirely my own work;
- I have acknowledged all main sources of help;
- Where this thesis is based on work by myself jointly with others, I have made clear exactly what work was done by others and what was contributed myself;
- Parts of this work have been published before submission:

Hall S, Thatje S (2009a) Global bottlenecks in the distribution of marine Crustacea: temperature constraints in the family Lithodidae. *Journal of Biogeography* 36(11): 2125-2135.

Hall S, Thatje S (2009b) Four new species of the family Lithodidae (Decapoda: Anomura) from collections of the National Museum of Natural History, Smithsonian Institution. *Zootaxa* 2302: 31-47.

Palero F, **Hall S**, Clark PF, Johnston D, Mackenzie-Dodds J, Thatje S (2010) DNA extraction from formalin-fixed tissue: new light from the deep sea. *Scientia Marina* 74(3): 465-470.

Thatje S, **Hall S**, Held C., Hauton C, Tyler P (2008) Encounter of *Paralomis birsteini* on the continental slope of Antarctica, sampled by ROV. *Polar Biology* 31(9): 1143-1148.

Signed:

Date:

ACKNOWLEDGEMENTS

I sincerely thank Dr Stefanie Duff and the University of Alberta for their contribution of molecular and distributional data on the North Pacific Lithodidae to this thesis, where acknowledged in the text.

I am grateful to the crew of RV James Clark Ross and the ROV-*Isis* team (NOCS) for help and assistance at sea, and to Julian Dowdeswell (SPRI, Cambridge) for the organization of leg JCR166. The ROV cruise on board RV James Clark Ross was funded by NERC (project no. NE/D008352/1, PI Tyler). The material collected on cruise Mauritania 2007 and examined at the Instituto Español de Oceanografía, Vigo was kindly made available by Ana Ramos.

Molecular work was made possible by a short-term grant from the German Academic Exchange Service (DAAD) and a Research Grant through The Royal Society (2006-R2). Molecular work was done at the Alfred Wegener Institute for Polar Research (Bremerhaven, Germany), and the Natural History Museum, London (NHM), with invaluable help and advice from Drs Christoph Held, Florian Leese, Ferran Palero, Michael Raupach, Peter Rehm and Jackie Mackenzie-Dodds. Thanks also to Frances O'Hara for her tedious hours in spent in the lab trying to get PCR reactions to work.

Museum work within Europe was supported by the Marine Biodiversity and Ecosystem Functioning Network of Excellence (MarBEF) under the 6th European Framework Programme (Contract no. GOCE-CT-2003-505446) and through a NERC PhD studentship. I would like to thank staff at the National Museum of Natural History, Smithsonian Institute, Washington DC (USNM), especially Rafael Lemaitre and Karen Reed; Régis Cleva at the Muséum national d'Histoire naturelle, Paris (MNHN); Paul Clark at the Natural History Museum (NHM), London; Enrique Macpherson and Pedro Abelló at the Institut de Ciències del Mar, Barcelona; Michael Türkay at the Senckenberg Museum, Frankfurt; and Ana Ramos and her group at Instituto Español de Oceanografía, Vigo. This study would not have been possible without such a wide range of material made available by these institutions.

I thank all of those people that have read various drafts of manuscripts for this thesis and other published works, including editors and reviewers for the Journal of Biogeography, Zootaxa, Polar Biology and Scientia Marina. Particularly, I thank Professor Paul Tyler and Kirsty Morris, Chris Beer and Chris Allen for commenting on drafts. I thank my family and friends, especially my parents and husband for their support. Finally, I thank my main supervisor, Dr Sven Thatje, for his incredible enthusiasm and almost unfailing optimism that have guided me through the peaks and troughs of scientific endeavour.

PAGE 13 IS BLANK

CHAPTER SUMMARIES

Chapter A1: Molecular Phylogeny of the Lithodidae

To examine the hypothesis of a basal position for the soft-bodied North Pacific Hapalogastrinae, the monophyly of shallow and deep-water groups of Lithodinae was tested. Mitochondrial and nuclear genes (COI, COII, 16S, 18S, 28S, ITS) of 47 species (10 genera) of Lithodidae were analysed to search for scenarios of evolution that optimally reflected the patterns of molecular divergence observed between species. Phylogenetic trees based on the shared, derived features present in single gene-fragments largely corroborated those based on 'total molecular evidence (TE_B)'. There was a low level of genetic variation within the subfamily Lithodinae; typically variable regions of ribosomal genes (18S and 28S) have only a few nucleotide substitutions separating genera. This indicates a recent sequence divergence, or raises the possibility of a particularly slow rate of mutation in this lineage. Phylogenetic trees strongly indicate the monophyly of most of the lithodid genera currently accepted on the basis of morphology. Tree topologies suggest that deep-sea radiations have occurred independently in at least two (*Paralomis* and *Lithodes*) of the three globally distributed genera from a shallow-water ancestor.

Chapter B1: King crabs up-close: ontogenetic changes in ornamentation in the family Lithodidae (Decapoda: Anomura), with a focus on the genus *Paralomis*

Evidence of ontogenetic change in the surface ornamentation of lithodids has previously been studied for one species of *Paralomis* (*P. granulosa* Jaquinot); however, its wider occurrence within the genus has never been formally examined. Growth-related change in dorsal spines and tubercles was considered, using growth-series from eight species of *Paralomis*. Tubercular structures from adult specimens of 24 additional species of *Paralomis* are figured in order to provide a reference for future diagnosis. This study highlights one aspect of ontogenetic change between juvenile crab stages and mature adults, which is an important theme in the life history of the Lithodinae. Changes such as these need to be considered when identifying species of *Paralomis*.

Chapter B2: Morphological phylogeny of the *Lithodes* genus

The genus *Lithodes* contains 21 species, which are known to inhabit most of the world's oceans, including one representative (*L. murrayi*) in the Bellingshausen Sea, Southern Ocean. *Lithodes* species typically inhabit depths greater than 200 m, although above 40 degrees of latitude (north and south) some *Lithodes* species are found in shallower

waters. Closely related genus *Paralithodes* contains 6 species, all of which are endemic to the North Pacific, above 30 °N, generally shallower than 300 m. Linear measurements and multi-state discrete morphological characters, were collected for 158 specimens belonging to 17 species of *Lithodes* and *Paralithodes*, and were used to produce two independent estimations of *Lithodes* phylogeny. Results presented here strongly indicate that central and Southern Pacific lineages of *Lithodes* are closely related to one another and to the Indian Ocean and South Atlantic *Lithodes* species. A transition from the North Pacific to the Atlantic was made by the ancestors of *L. maja* and/ or *L. santolla* and *L. confundens*. Subsequent range-expansion followed a deep-water pathway from the Atlantic, through the southern Indian Ocean to the Central Pacific.

Chapter B3: Morphological Phylogeny of the genus *Paralomis*

Paralomis is the largest genus of the Lithodidae, which is represented by 61 species, including at least two in the Southern Ocean. Twenty-five *Paralomis* species were systematically studied using morphometric and descriptive morphological characters. Distance matrices were produced by these two methods, and combined for analysis with Fitch-Margoliash tree-search criteria. Results showed that the pattern of global radiation in *Paralomis* is complex, with at least four distinct sub-groups. The east Pacific coastline was important in the meridional radiation of at least two of these lineages, and inter-oceanic circulation in the Southern Hemisphere could have been important for long-distance dispersal. These radiations at slope-depths (500-2000 m) relate to a time prior to the closing of equatorial links between the Pacific and the Atlantic, and after the opening of the circum-Antarctic waterways.

Chapter C1: Global bottlenecks in the distribution of marine Crustacea: temperature constraints in the family Lithodidae

Members of the family Lithodidae share preferences for cold-water environments; however, the specific role of temperature in governing lithodid biogeography has not been examined to date. It was hypothesized that lineage-specific temperature thresholds underlie differences in the distribution of the two lithodid subfamilies. Descriptions of 90 species of lithodids, sampled at 871 locations worldwide, were obtained from a wide range of published and original sources. For each specimen, the water temperature at the time and locality of collection was recorded. The link between the habitat temperature range and the position of taxa within the lithodid phylogeny was examined. Phylogenetic evidence indicated that the deep-water lithodid lineages had ancestors that inhabited the coastal waters of the North Pacific. Adults of North Pacific

lithodid taxa were found in regions where water temperatures ranged from 0º to 25°C; however, deep-water lineages of the Lithodinae were absent in waters exceeding temperatures of 13°C. Despite the range of temperatures tolerated by adults, North Pacific intertidal/subtidal genera were restricted to regions that had water temperatures of less than 16°C during periods of larval development.

O: INTRODUCTION

O.1 Scope of the thesis

The family Lithodidae Samouelle 1819 comprises a great diversity of morphological and ecological forms: from abyssal crabs with walking legs longer than a metre, to intertidal forms such as the genus *Cryptolithodes* Brandt 1848, which has tiny legs covered by a laterally expanded carapace (Bowman 1972). In the deep sea, the large subfamily Lithodinae includes species occupying hydrothermal vent environments (de Saint Laurent & Macpherson 1997), as well as species amongst the few known 'reptant' decapods from the Southern Ocean (Thatje & Arntz 2004). Study of the origins of the Lithodidae has increased in recent decades (Zaklan 2002a), with particular interest being placed on the putative relationship between primitive lithodids and hermit crabs of the family Paguridae. In this thesis I will investigate the process of global radiation in groups of deep-sea Lithodinae (Bouvier 1896, Makarov 1938): a topic that has not specifically been addressed since the advent of cladistic systematics (Hennig 1966). This will be done in three sections:

A. The production of a molecular phylogeny to investigate the origins of the deep-sea Lithodinae from within the Lithodidae.
B. Elucidation of phylogenetic relationships within deep-sea lithodine genera *Paralomis* and *Lithodes* as case-studies of deep-sea radiations.
C. Comparison of potential geographical and physiological boundaries with the present distribution of the deep-sea Lithodinae and their shallow-water relatives in South America.

O.2 The Anomura

O.2.1 Lithodid biological definition and classification

The family Lithodidae is divided into two sub-families: Lithodinae (10 genera) Samouelle 1819, and Hapalogastrinae (5 genera) Brandt 1850 (117 species in total, Appendix A). The Lithodidae were recently elevated to the taxonomic rank of superfamily (Lithodoidea, McLaughlin et al 2007), containing families Lithodidae and

Hapalogastridae. This rank is based on the results of a morphological phylogeny (McLaughlin et al 2007), which called for a radical rearrangement of anomuran systematics. For stability, prior to a unifying consensus between molecular and morphological analyses, I will refer to the family Lithodidae in its former sense (Samouelle 1819), containing subfamilies Hapalogastrinae and Lithodinae.

-Diagnosis

The Lithodidae are crab-like anomurans which lack uropods in both sexes, as well as having a sexually dimorphic abdominal asymmetry. Males lack all pleopods (abdominal appendages) and females lack pleopods 2-5 on one (usually the right, Zaklan 2000) side. The Hapalogastrinae have a short, broad, triangular rostrum; external obliteration of the cervical groove; weakly defined abdominal segmentation; and complete loss of calcification on abdominal tergites 2–5. The Lithodinae have calcified abdominal tergites in the form of plates or nodules, as well as a developed trispinose rostrum (Macpherson 1988a, McLaughlin et al 2007).

O.2.2 Classification of the Lithodidae within the Decapoda

The infraorder Anomura MacLeay 1838 is classified within the group 'reptantia': the decapods in which the thoracic appendages are aligned to allow for walking (McLaughlin 1983a, Martin & Davis 2001, Dixon et al 2003). Anomurans are unified morphologically by a novel arrangement of the coxosternal joints of the walking legs and the presence of *linea anomurica* on the lateral margins of the carapace (Makarov 1938, Dixon et al 2003). Until recent revisions, four superfamilies existed within the Anomura: Lomisoidea, Galathoidea, Hippoidea and the Paguroidea (which often contains the family Lithodidae, McLaughlin & Holthuis 1985, McLaughlin et al 2007).

-Classification of the Lithodidae within the Anomura

The phylogeny and systematics of the Anomura is a source of much debate (Richter & Scholtz 1994, McLaughlin et al 2007). Developmental and morphological evidence ally lithodids variously with the Paguridae, the Lomisidae and the Galathoidea; however, molecular reconstructions have invariably demonstrated a link between the Lithodidae and the Paguridae (hermit crabs, Cunningham et al 1992, Zaklan 2002a, Morrison et al 2002). Lithodids are in many ways dissimilar to derived hermit crabs, and share several 'ancestral' features with the stem Anomura (Richter & Scholtz 1994); however, detailed analysis of morphology reveals a lot of apparently conflicting evidence, which will be discussed briefly here.

--Carcinisation in the Anomura

Carcinisation is the process of morphing from the ancestral shrimp or lobster-like body plan to one in which the abdomen is held close to the sternum and the carapace is significantly broader than long. Numerous instances of carcinisation are observed within the Anomura in addition to the family Lithodidae: including *Lomis hirta* (Lomisidae), *Birgus latro* (Linnaeus 1767, Paguroidea: Coenobitidae), and *Probeebei mirabilis* (Boone 1926: Paguroidea). Morrison et al (2002) presented genetic evidence that carcinisation has occurred multiple times in parallel within the Anomura, under an unknown selective pressure. McLaughlin & Lemaitre (1997) provide a detailed review. Lithodids of the subfamily Hapalogastrinae are amongst the only anomurans that have a fully uncalcified abdomen and have also undergone full carcinisation (Zaklan 2002a).

--Paguroidea theories

The taxon Paguroidea typically contains families Pylochelidae (symmetrical hermit crabs, McLaughlin & Lemaitre 2009), Parapaguridae (terrestrial hermit crabs, Martin & Davis 2001), Coenobitidae (including the terrestrial robber crab, *Birgus latro*), Diogenidae (left-handed hermit crabs, Ortmann 1892), Paguridae (right-handed hermit crabs), and the Lithodidae (Richter & Scholtz 1994). The evidence to support the placement of the Lithodidae within this taxon includes: the presence of an accessory ampulla in the spermatophore and morphology of the spermatozoa, which ally *Lithodes* with the Paguroidea and particularly the Paguridae (Tudge et al 1998); the similarity of the larval scaphognathites in the Lithodidae and other pagurioid families (Van Dover et al 1982); and uncalcified abdominal tergites 2–5, which exist in the Hapalogastrinae and the shell-dwelling pagurids (Richter & Scholtz 1994). The most compelling morphological evidence for a link between the Paguridae and the Lithodidae comes from the asymmetry of the abdomen in females and the shared reduction in the number of pleopods on abodominal segments (Richter & Scholtz 1994). The morphological transition from a shell-dwelling hermit crab to a carcinised lithodid requires the re-acquisition of primitive character states, including well-developed 4th pereiopods (in both megalopae and adults, MacDonald et al 1957); the calcification of the dorsolateral carapace and the abdominal tergites of the Lithodinae; and the 'reaquisition' of 1st abdominal pleopods in females (Richter & Scholtz 1994). Such reversions are given different weight in different studies (Stiassny 1992), but an improving understanding of genetics has revealed potential mechanisms for explaining these phenomena (e.g. Averof & Patel 1997).

--Lomisoidea theories

Martin & Abele (1986) described a close relationship between *Lomis hirta* (Lomisidae) and the Lithodidae, based on a shared loss of ocular acicles, a loss of uropods, and further features relating to their shared carcinised state. This grouping was resolved close to a clade containing the remaining families of the Paguroidea, and separate from the Galathoidea and the Hippoidea. A close relationship between lithodids and *Lomis* does not explain the evidence of the shared characters between the Lithodidae and the Paguroidea (Richter & Scholtz 1994, Tudge et al 1998).

--Lithodoidea theories

McLaughlin et al (2007) do not support the idea of a close relationship between the Lithodidae and the Paguroidea, instead linking the lithodids loosely with the Hippidae (e.g. genus *Emerita*) and the Aeglidae. The distance between the Lithodidae and all other taxa was considered to be so great that they were elevated in systematic rank. In this scenario, all similarities between the Paguridae and the Lithodidae are assessed as being either convergent or misinterpreted in previous analyses. Particularly, this view is supported by an ontogenetic study of abdominal calcification, female abdominal asymmetry and pleopod development in both sexes. These reveal similar but not necessarily homologous mechanisms for plate differentiation and pleopod reduction in lithodids and the pagurids (McLaughlin et al 2004). In *Pagurus* megalopae, the 2nd abdominal plate is intact (Carvacho 1988), losing its distinction through dechitinisation after the moult to crab-stage 1. In the Hapalogastrinae, the megalopal tergites fail to calcify at metamorphosis, whereas in the Lithodinae (which have well-calcified abdominal plates or nodules in adults **Fig B3.13**), the intact megalopal abdominal tergites divide by narrow inter-plate decalcification in late juvenile crab stages (McLaughlin et al 2004). This is contrary to the long-standing hypothesis that lithodid abdominal morphology is the product of secondary calcification of a pagurid-like abdomen, followed by the sequential fusion of calcified nodules into larger plates (Boas 1880).

O.2.3 Relationships between lithodid genera: Historical perspective

Bouvier (1895) based his theories of lithodid evolutionary history on Boas' earlier study of abdominal calcification (1880), as well as on characters of the rostrum and the antennal acicles (Makarov 1938). He suggested that the abandonment of shell-dwelling in the earliest lithodids led to carcinisation and calcification of the abdomen (Boas 1880). *Hapalogaster* was the most 'primitive' extant lithodid genus, which gradually moved out of the shelter of kelp forests and into shallow gravel-bottom environments

(Zaklan 2002a). In this scheme, the deep-sea species *Neolithodes* was the most primitive taxon of the Lithodinae, based on the division of its abdominal tergites into numerous weakly calcified nodules. The divergence within the Lithodinae was the result of a split in the paraphyletic *Paralithodes* genus, with *P. brevipes, Paralomis, Lopholithodes* and *Rhinolithodes* descendents of one lineage and *P. camtschatica* descended from a common ancestor with the genus *Lithodes*. The heavily calcified, highly specialised *Cryptolithodes* was considered to be the 'pinnacle' of the evolutionary line (Bouvier 1895, Makarov 1938). This view was formulated prior to the development of a cladistic approach to systematics (after Hennig 1966) and developmental studies (McLaughlin et al 2004) lead us to question these assumptions.

Representitives of all lithodid genera can currently be found in the North Pacific, whereas only a subset of these is found in the Atlantic and Indian Oceans. The Hapalogastrinae, regarded as morphologically primitive, are found only in the North Pacific, with 89% of species found in the eastern part of this region and only 45% in the western (Zaklan 2002a). Makarov (1938) hypothesised the spread of the ancestral Hapalogastrinae along the Aleutian ridge into the North West Pacific, and along coastlines towards Japan and Baja California at the southern extremities of their range (Zaklan 2002b). The Hapalogastrinae have still never been found outside the North Pacific in fossil or modern manifestations (Appendix E). From this evidence, the north eastern Pacific coastline of North America is considered to be the evolutionary environment for the incipient Lithodidae and their global, deep-sea distribution is the result of a later ecological adaptation (Bouvier 1896, Makarov 1938, Zaklan 2002a).

O.2.4 Geological and molecular clock

Using a calibrated molecular clock, Cunningham et al (1992) estimated that the Lithodidae are millions of years younger (13–25Ma BP) than the Paguridae, which are known from fossils in the Cretaceous (113 Ma BP). The approach of that study has been challenged as simplistic (Bromham & Penny 2003, Drummond et al 2006, McLaughlin et al 2007); however, no updated estimates have been offered. By more recent methods, the age of the anomuran divergence has been calculated at more than 325 Ma BP (Porter et al 2005). The fossil record of decapods is rich from the Cretaceous onwards (Schram 1986), and the anomuran family Aeglidae are known from this period (Feldmann 1984). Deep-water decapods are underrepresented in the fossil record (Feldmann 2003); decomposition of the arthrodial membrane followed by disarticulation can disperse body segments and make samples unidentifiable (Plotnick 1986). The only lithodid fossil record is *Paralomis debodeorum* Feldmann (1998) from the mid–late Miocene in New Zealand.

O.3 Aspects of change in the marine environment throughout the Cenozoic

O.3.1 The modern marine environment

Physical and chemical properties of an environment have an effect on the distribution and adaptations of lineages over time. Seventy-one percent of the earth's surface is marine and approximately 65 % is deep sea (Sverdrup et al 1942, Briggs 1991), yet the challenges facing animals in the deep sea are not fully understood. The average depth of the ocean is approximately 4 km and the deepest trenches extend to up to 10 km below the surface. The modern continental shelf is typically 100–200 m deep, although that of the Antarctic continent is depressed by the weight of the ice-cap and scoured by ice to depths around 500 m. The deep sea conventionally begins at the shelf-break (c. 200 m), where the sea-floor gradient increases and the continental slope descends to the continental rise (3000–4000 m) and abyssal plain (>4000 m, Gage & Tyler 1991). Tectonic systems govern the geography of the oceans over time, and the relatively homogenous topology of the abyssal ocean floor is punctuated with ridges, trenches, volcanoes, and hydrothermal vents (Anikouchine & Sternberg 1973).

Modern average surface temperatures (3–100 m deep) at high northern latitudes (60 °N) are 2–4 °C, with more than a 20 °C gradient in surface temperature to the equatorial Atlantic (26–27 °C) and Pacific (28–29 °C) (Nikolaev et al 1998). Water temperature below the surface mixed layer declines rapidly to current global deep-water temperatures between 1 and 4 °C (Thistle 2003). Surface temperature fluctuations can be large, especially in temperate regions, which are seasonally variable. Local polar surface temperatures are relatively constant on an annual cycle, with minimum temperatures in some places reaching approximately -1.8 °C (Lamb 1977).

In addition to temperature, the deep sea poses challenges to life, such as darkness, low energy availability and high barometric pressures. Light intensity declines exponentially with depth, such that no measurable light penetrates to 1000 m below the surface (aphotic zone, Gage & Tyler 1991). With the exception of chemoautotrophic primary production at vent and seep localities (Van Dover 2000), the deep sea is dependent on energy flux from the euphotic zone (0–100 m) in the form of particulate organic carbon (POC) (Anikouchine & Sternberg 1973). Depending on the composition of the plankton, POC decreases from the continental shelf to the abyssal plain because of trophic activity in the water column and clines in primary production at the surface (Gage & Tyler 1991). Pressure increases linearly with depth: approximately 1 atmosphere per 10 m. It is not uncommon for slope species to have a bathymetric range of 1000 m (Brey et al 1996), so they need the capacity to tolerate 100-fold increases in pressure and its associated effects on physiology (Hochachka & Somero 1984, Mestre et al 2009).

With a few exceptions, the deep sea has a salinity of around 35 psu and is relatively insulated from major fluctuations caused by the input of fresh water. Oxygen is not, in general, a limitation to life in the deep sea because the majority of deep water sinks from oxygen-saturated surface layers in high-latitude regions (Thistle 2003); however, seasonal oxygen minimum zones within stratified water columns may affect the distribution of the benthos at different depths (Wishner et al 1995). Paradoxically, the deep sea is insulated from physical conditions at the surface and also heavily reliant on photosynthetic and gas exchange processes occurring in the upper 100 m of the water column.

O.3.2 Oceanic circulation (modern)

Oceanic circulation occurs on a global scale and links the world's large oceans, allowing limited mixing of physical and biological components in the water. Latitudinal differences in air temperatures produce stable planetary wind systems which, in conjunction with planetary motion (Coriolis forces), drive oceanic surface circulation as subtropical and sub-polar gyres (Tomczak & Godfrey 1994). The topology of southern sub-polar ocean basins is such that strong eastward winds at 40–60 °S drive a continuous circumpolar current (The ACC, Section O.3.2.1); in the Southern Ocean, gyres only form in bays such as the Weddell and Ross Seas (Deacon 1937).

Vertical and meridional transport of water in the deep seas is additionally the product of latitudinal gradients in water density (temperature and/or salinity). Cold (0– -0.8 °C), saline Antarctic bottom water (AABW) is formed by the submergence of extremely dense surface waters under sea-ice in the Ross Sea and Weddell Sea (Jacobs et al 1970, Deacon 1984). This is the densest body of water in the ocean systems and it flows northwards, spreading along the sea floor into the Northern Hemisphere. North Atlantic deep water (NADW) is formed around Greenland in the Norwegian Sea and spreads southwards through the Atlantic to form part of the circumpolar deep water at high southern latitudes (Tomczak & Godfrey 1994). Thus, currents in the Atlantic are an important part of global thermohaline circulation. No equivalent North Pacific deep water is created because of the combined effect of a shallow Pacific-Arctic connection at the Bering Sea and low sea-surface salinity (Thomas 2004).

O.3.2.1 *The ACC past and present*

The modern position of the continents means that Drake Passage, between the Antarctic Peninsula and Cape Horn, forms the only deep-water link between the Pacific and Atlantic Oceans. The Antarctic circumpolar current (ACC) therefore has a significant

effect on global circulation and inter-ocean transfer. It is bounded to the north by the subtropical front at 35–45 °S, where cold sub-Antarctic waters meet warm, saline subtropical waters (Orsi et al 1995, Rintoul et al 2001). To the south, the ACC ends at the Antarctic Divergence (c. 60 °S), where it is marked by the upwelling of deeper waters. Within this range, there are three zones (Subantarctic, Polar, and Southern Antarctic), divided by two fronts (subAntarctic 42–48 °S and Polar c. 50 °S) – each marked by substantial temperature changes and accompanied by increased primary production (Smetacek et al 1997). Although it is driven by strong westerly winds, the ACC is not only a surface feature and there is evidence of eastward flow down to at least 2500 m (Barker & Thomas 2004). The path of the ACC is determined both by the fronts and by the topology of the basins through which it travels (Patterson & Whitworth 1990, Wei & Wise 1992). Where they are not constrained by bottom topography, the latitudinal position of each front meanders (Moore et al 1999), and there is substantial latitudinal variation in the position of the fronts at different longitudes.

Biologically, it is not uncommon for Antarctic plankton to be transferred into subantarctic waters (Antezana 1999), and recent evidence suggests that sub-Antarctic incursions into Antarctic surface waters may also occur at eddies within the ACC (Nowlin & Klink 1986, Gouretski & Danilov 1994, Thatje & Fuentes 2003). The role of the deep-water isolation of Antarctica (28–32.5 Ma BP) and formation of the ACC (at least 25 Ma BP) in curtailing meridional heat exchange is debated (Toggweiler & Samuels 1995, Toggweiler & Bjornsson 1999, Huber & Sloan 2001).

O.3.3 Marine Conditions and events through the Cenozoic

(**dates for boundaries taken from the international commission for stratigraphy 2009 http://www.stratigraphy.org/upload/ISChart2009.pdf).*

Based on molecular and fossil evidence (Cunningham et al 1992, Feldmann 1998), the history of the Lithodidae is confined mainly within the Cenozoic era: 0 – 65.5 million years (Ma) before present (BP). Prior to the Cenozoic, the Cretaceous (145.5–65.5 Ma BP) environment was generally warmer than present, with high sea levels and a small latitudinal gradient in temperature (Nikolaev et al 1998, Zachos et al 2001). During the Cretaceous, tropical sea-surface temperatures may have averaged around 37 °C (Forster et al 2007) and deep-water temperatures were up to 20 °C higher than their present levels (Schnitker 1980, Nikolaev et al 1998). The Tethys Sea, which connected the oceans at tropical latitudes, was a source of the highly saline (dense) warm water that formed a component of northern deep water (2000–4000 m) in the Atlantic and Indian Oceans (Wright et al 1992, Ramsey et al 1998).

The transition from the Mesozoic to the Cenozoic was followed by a gradual global cooling trend, thought to have occurred in four main stages over the last 50 Ma (Lear et al 2000). Over the Cenozoic, the deep sea cooled by more than 12 °C relative to the surface temperature (Lear et al 2000); the overall global average temperature dropped; and a latitudinal gradient of 20–22 °C in sea surface temperature developed (Nikolaev et al 1998), including the formation of permanent ice at both poles by 2.4 Ma BP (Crame 1999). The initiation and progression of global cooling, bathymetric- and latitudinal differentiation are thought to be the cumulative result of a decrease in atmospheric CO_2 (Barker & Thomas 2004) and fundamental rearrangements of ocean basin topology (Von der Heydt & Dijkstra 2006) such as:

- **Antarctic isolation:** Antarctica has lain over the South Pole for around 120 Ma (DiVenere et al 1994), although in the early Cretaceous (124–97 Ma BP) high latitude marine fauna had a temperate affinity (Olivero & Martinioni 1996). By the end of the Cretaceous, the large southern landmass had fragmented and deep-water pathways between Antarctica and Australia had opened (Crame 1999). Substantial cooling and expansion of the east-Antarctic ice cap began around 37 Ma BP, at which time there was already a shallow connection through Drake Passage – the last remaining continental link between Antarctica and the other Southern landmasses (Lawver et al 1992, Crame 1999).
- **Restriction of deep-water oceanic interchange at tropical latitudes:** In the northern Atlantic 14 Ma BP, cold, dense water formed in the Norwegian Sea was 'trapped' behind a high Greenland–Scotland ridge (Woodruff & Savin 1989, Ramsey et al 1998). At 14–13 Ma BP, it is thought that tectonic changes in the North Atlantic allowed cold, dense water to flow out of the Norwegian Sea and into the Atlantic where it replaced warmer water (from the closing Tethys Sea) in the deep sea (Woodruff & Savin 1989).
- **Restriction of Panama seaway:** A deep-water (3000 m) connection between the Atlantic and Pacific Oceans through the Panamanian seaway existed until the early Miocene (25–15 Ma BP). This seaway is thought to have allowed deep North Atlantic water to flow into the Pacific and warm, tropical Atlantic water to enter the Pacific at shallow depths (Lunt et al 2008). Between c. 13–2.6 Ma BP, the tropical connection between the Atlantic and Pacific gradually closed with the uplift of the Panama land-bridge (Haug & Tiedemann 1998), and this

may have strengthened the Atlantic thermohaline circulation (Lunt et al 2008).

Significance of these events for the global climate cooling are debated; however, the importance of the North Atlantic and the Antarctic to modern deep-water circulation indicates that these events of the Eocene and Miocene had a great influence on the development of modern ocean temperatures and global circulation (Shackleton & Kennett 1974).

O.3.3.1 *Recent glacial/ interglacial cycles*

During the Quaternary period (the part of the Cenezoic in the last 2.58 Ma) the earth has been in an ice age. This is characterised by cyclical bipolar glacial advance and retreat, in cycles lasting between 40 and 100 thousand years (ka). Glacial periods are associated with low sea levels and there has been a 100 m rise in sea levels since the last glacial maximum in the northern hemisphere (Rex 1981, http://www.ngdc.noaa.gov /paleo/ctl/clisci100k.html#sea). The last glacial maximum in the Southern Hemisphere (19–23 ka BP) led to Western Patagonia being covered by a glacier stretching from 38–55 °S, including the narrow continental shelf to the west and south (da Silva et al 1997, Hulton et al 2002). Deglaciation began c. 17.5 ka BP and the first marine incursions into the Magellan Strait are thought to have occurred periodically for the last 5 ka (McCulloch et al 2000). These events were mirrored by similar glacial cycles in the northern hemisphere. During the most recent North American glaciation (26–13.3 ka BP, Wisconsin stage) ice sheets extended to about 45 °N in both the east and the west coast of the continent (Thackray 2001).

O.4 Physiological effects of temperature

The change in the temperature profile of the marine environment throughout the Cenozoic was gradual, but substantial. It is likely to have had an impact on the physiology and ecology of marine organisms and to have affected their distribtuion. Reaction rates, including biological enzymatic processes, increase exponentially with increasing temperatures (Atkins & De Paula 2006). At low temperatures metabolic rate (energy consumption and activity in tissues) is lower than at high temperatures (Cossins & Bowler 1987).

Complex animals, with low surface area/volume ratios and specialised tissues, rely on ventilation and circulatory systems to supply their cells with oxygen. Despite a lower metabolic requirement at low temperatures, the activity of tissues involved in critical ventilatory functions (heart, nervous conductivity) decreases such that, at some stage,

oxygen supply does not match demand and aerobic metabolism can not occur (Pörtner 2002). The effect of low reaction rates on physiology can be exacerbated by temperature related decreases in membrane fluidity and by the effect of [Mg^{2+}] on the nervous system (Frederich et al 2000). The magnesium ion (Mg^{2+}) is highly soluble in water and is also increasingly soluble with decreasing temperature. It competes with the Ca^{2+} ion, which normally regulates the release of neurotransmitter substances at synapses, and at high concentrations Mg^{2+} is an effective narcotising agent (Robertson 1953).

At the other end of the scale, increased environmental temperature induces a higher metabolic requirement, which at some stage exceeds ventilatory and enzymatic capacity (Pörtner 2002). Higher metabolic activity also increases the production of highly reactive oxygen radicals which can interfere with cellular processes (Cooke et al 2003). Temperatures above certain critical levels will denature proteins (threshold dependent on the structure of the protein), which can be an irreversible process leading to cell death (Daniel et al 2010).

O.4.1 Physiological temperature thresholds

Ectothermic animals, by definition, have no internal control over core body temperature. Ectotherms are tolerant of certain environmental temperature ranges, thought to be narrower in cold-adapted than tropical animals (Peck & Conway 2000). Adaptation to high or low temperatures can involve trade-offs in the ability of an organism to survive at the opposite extreme (Fields 2001). Both high and low thresholds are related to the physiological ability of the organism to avoid the transition from aerobic to anaerobic metabolism (Pörtner 2002). Between threshold temperatures, supply of oxygen to the tissues matches metabolic demand; beyond these temperatures in both directions, the capacity for aerobic metabolism decreases. Outside the optimal temperature range, basic metabolic processes can be maintained, but non-essential processes such as growth, reproduction and voluntary movement are reduced (Cossins & Bowler 1987, Young et al 2006). Beyond certain critical temperatures all metabolism is anaerobic. Anaerobic processes are not stable over time, as the product (lactate) requires subsequent oxidation before removal as CO_2 and water (Schmidt-Nielsen 1997), so survival under these conditions is time limited (Pörtner 2002).

Thresholds are not the same for different species and can have adaptive significance. Physiologically, adaptation can include processes such as a change in mitochondrial density (Hazel 1995) and expression of proteins or cell membranes with different thermal properties (activation temperature, denaturation temperature, fluidity: Somero 1992, Lin & Somero 1994). In the Southern Ocean, anomuran and brachyuran

crustaceans are almost absent, whereas shrimps (Natantia) are relatively abundant (Thatje et al 2005). This difference has been attributed to the greater ability of natant decapods to regulate [Mg^{2+}] in their haemolymph below sea water concentrations (Frederich et al 2001). As discussed above, Mg^{2+} has a synergistic narcotising effect with decreasing temperature, and the ability to regulate the concentration of the ion might explain this disparity in distribution (Frederich et al 2000).

O.4.2 Effects of temperature on developmental processes

At low temperatures, feeding requirements decrease because of decreasing metabolic costs (Zhou et al 1998). Growth and development are retarded, such that inter-moult interval doubles with a decrease in water temperature from 6 to 3 °C in *Paralomis granulosa* (Anger et al 2003, 2004). Calcagno et al (2005) demonstrated that lower environmental temperatures slowed development to reproductive maturity in *Paralomis granulosa*.

Developmental speed can be particularly important for early life stages, which are vulnerable to seasonal fluctuations in food abundance and size-related predation pressures (Thatje 2004). Nakanishi (1985) and Kurata (1960) reported temperature-determined increases in larval inter-moult periods, as well as longer embryonic development time (maternal brooding) in *Paralithodes camtschatica*. Spawning duration is further protracted in *P. camtschatica* at temperatures of 3 °C (76 days) when compared to 6–9 °C (29 days), although this could be adaptive trait rather than a physiological effect (Shirley et al 1990).

Significantly reduced survival to first moult is reported when lithodid larvae are exposed to temperatures above 13°C (Nakanishi 1981, 1985, Vinuesa et al, 1985) or 15°C (Kurata 1960, Shirley & Shirley 1989, Calcagno et al 2005). 100% larval mortality occurs at -1.8°C in *Paralithodes camtschatica* (Nakanishi 1981) and the minimal temperature at which larval development is possible is around 0–2 °C (Shirley & Shirley 1989, Thatje 2004). Experimentally determined optimal temperatures for larval development are between 5–10 °C, in all examined lithodids, provided salinity is above 20 psu (Anger et al 2003, Jørgensen et al 2005).

O.5 Lithodid life cycles

O.5.1 Life-history adaptations to temperature

Extreme seasonality of primary production is one of the major challenges of life in the polar environment (Holm-Hansen 1985); this is coupled with a slow-down of developmental rates in cold water in comparison to tropical organisms (Bosch et al 1987, Pearse et al 1991). The adoption of a lecithotrophic larval mode of development

allows independence from seasonal primary production and enables tolerance of the protracted development times associated with cold waters in polar and deep-sea environments (Shirley & Zhou 1997, Thatje 2004). Latitudinal clines in fecundity (Wägele 1987, Gorny 1992) are indications of the increased cost of reproduction at high latitudes and the transition to a reproductive strategy with increased energy investment per offspring (Atkinson et al 2001, Thatje 2004). Lithodids are predominantly cold-water animals (although this is particularly the case for the deep-water Lithodinae, Hall & Thatje 2009a) and aspects of their life history are congruent with an adaptation to cold-water conditions.

O.5.2 Adult life

In all arthropods, including the Lithodidae, size doesn't increase continuously as a function of age. Growth occurs only in relation to the moult cycles and each incremental increase is dependent on temperature, nutritional and reproductive condition, as well as pre-moult size. The increments of growth (in males) generally increase up to reproductive maturity and then begin to decrease as proportionally more energy is partitioned into reproduction (McCaughran & Powell 1977). Intermoult periods are of variable length, ranging from annual synchronous moults in *P. camtschatica* (Stevens 2006) to 1120 day asynchronous cycles in mature *P. spinosissima* (Reid et al 2007). In most cases, moults are closely connected to egg extrusion and fertilisation events (Hoggarth 1993, Stevens 2006). Size at maturity varies between species, sexes and in relation to environmental temperature (Hoggarth 1993) (and, of course, final adult size); males are usually slightly larger than females at maturity (Zaklan 2002b).

O.5.3 Early life history

-Eggs

In lithodids, eggs are carried on the female abdominal pleopods on the left-hand side of abdominal segments 2–5, and also on both sides of the 1st abdominal segment in some groups (Makarov 1938). Eggs are extruded onto the pleopods and are incubated between the abdomen and the sternum for between 1–2 years, depending on the species; the environmental conditions (e.g Nakashini 1985, Paul & Paul 2001, Stevens 2006); and the synchronicity of spawning (Reid et al 2007).

Egg size is broadly related to the volume of yolk sequestered into each egg by the mother. Yolk has both protein and lipid components, which are used selectively through embryonic development and, in some cases, are the exclusive energy source for development until metamorphosis to the first crab stage (Anger 1996, Shirley & Zhou

1997, McLaughlin et al 2001, Paul & Paul 2001, Kattner 2003). Near South Georgia in the sub-Antarctic, there is an increase in egg size with depth from *Paralomis spinosissima* to *Paralomis formosa* (Morley et al 2006). Egg diameter of *Paralithodes camtschatica* and *P. platypus* range from 0.8–1.2 mm, whereas those of *Lithodes aequispina* and *L. couesi* (from the same localities) are more than 2.2 mm in diameter (Zaklan 2002b, see red dots Fig **B2**.9), indicating the different reproductive strategies (zoeal planktotrophy or lecithotrophy) within the Lithodidae.

-Hatching

In all lithodids, hatching is protracted in comparison to decapod groups from similar environments. In each female, larval release at 6–8 °C takes between 17 (*Placetron*, Crain & McLaughlin 2000) and more than 61 days (*Paralomis granulosa,* Thatje et al 2003). Many other decapods have highly synchronous hatching events lasting only minutes or hours, which are often triggered by extrinsic factors (Forward 1987, Ziegler & Forward 2005; Lovrich & Thatje 2006). *Paralithodes camtschatica* takes 28.8 ± 4 days (Shirley et al 1990) to complete larval release – a process that is initiated by temperature cues (4 °C, Stevens 2006). This protracted release occurs despite the fact that its planktotrophic larvae are highly dependent on specific seasonal plankton blooms (Paul et al 1989, Shirley et al 1990, Starr et al 1994). Protracted larval release – investing fewer larvae per day – is thought to be a bet-hedging behaviour, which can increase overall fitness in an unpredictable environment. This may be particularly crucial in species that invest long periods of time into brooding (up to two years in some known cases, Lovrich & Vinuesa 1999, Reid et al 2007) and have a low fecundity because of the cost of increased maternal energy investment into single offspring (Thatje 2004, Morley et al 2006). Deep-water lithodids with lecithotrophic larvae (e.g. *Paralomis spinosissima,* Reid et al 2007) are particularly disconnected from seasonal temperature variations at the surface (Sloan 1985). Females of studied *Lithodes* and *Paralomis* release larvae asynchronously (Reid et al 2007); in *L. aequispinus*, for example, adults of all reproductive stages are found throughout the year below 200 m (Shirley & Zhou 1997, Paul & Paul 2001).

-Larval stages

Variation in number and duration of larval stages occur within the Lithodidae, and there is a pattern of abbreviation of larval development in the Lithodinae (Thatje 2004). All Hapalogastrinae have at least four zoeal stages prior to the megalopa (Crain & McLaughlin 2000); four or five stages have been observed in lithodine species *Lopholithodes mandtii* (Crain & McLaughlin 2000) and *Paralithodes camtschatica*

(Kurata 1960, Nakanishi 1985). Three zoeal stages are found in *Lithodes maja* (Anger 1996), *L. santolla* (Campodicono & Guzman 1971) and *L. aequispina* (Crain & McLaughlin 2000); and a further reduction to two stages is observed in *Paralomis granulosa* (Anger et al 2003), *P. spinosissima* (Watts et al 2006) and *Paralomis* spp. (Konishi & Taishaku 1994). This may be a concession to the greatly protracted development times and associated risks of moulting in colder waters (Thatje 2004).

Zoeal planktotrophy is found in most North Pacific Lithodinae and Hapalogastrinae. Species *Paralithodes camtschatica* (Paul et al 1989, Epelbaum & Borisov 2006), *Placetron wossnessenskii* (Crain 1999), *Lopholithodes foraminatus* (Duguid & Page 2009), *L. mandtii* (Jensen 1995), *Acantholithodes hispidus* (Hong et al 2005), *Cryptolithodes expansus* (Kim & Hong 2000), *Paralithodes brevipes* and *P. platypus* are all known to have food-dependent zoeal stages.
Lecithotrophic development occurs in all studied *Lithodes* and *Paralomis* and is speculated for *Neolithodes* (Anger 1996, Shirley & Zhou 1997, Watts et al 2006, Morley et al 2006, Thatje & Mestre 2010). An obligatory non-feeding larval mode is accompanied by physiological evidence in lithodids, such as the reduced development of mouthparts (Campodicono & Guzman 1981, McLaughlin et al 2001, Watts et al 2006) or a lack of digestive enzymes (Saborowski et al 2006). There is a variation in lecithotrophic adaptation within the non-feeding lithodid larvae (Anger 1996, Kattner et al 2003), with mouthparts slightly better developed in *Paralomis spinosissima* and *P. granulosa* compared to *L. santolla* (Watts et al 2006), as well as a variation in yolk composition and energy content (Kattner et al 2003, Thatje & Mestre 2010).

Larval behaviour, as observed in laboratory experiments, is dependent on feeding mode. Planktotrophic larvae of *Paralithodes camtschatica* (Paul & Paul 1980), *Paralithodes platypus* (Paul et al 1989), and *Lopholithodes foraminatus* (Duguid & Page 2009) are phototactic. They display diurnal migration (or reverse diurnal migration), moving through the water column in what is thought to be a food-searching behaviour (Paul et al 1989). Non-feeding zoeae, including *Lithodes aequispina* (Jewett et al 1988, Shirley & Zhou 1997), *Lithodes maja* and *Lithodes santolla*, *Paralomis granulosa* (Vinuesa et al 1985, 1999) are not active swimmers and are thought to have an epibenthic, demersally drifting habit (Lovrich 1999, Thatje 2004).

-Megalopa and settlement

The megalopa is the final swimming pre-crab stage, preceding metamorphosis and settlement as a juvenile benthic instar. There is evidence that all Lithodidae have

lecithotrophic megalopal stages, regardless of the feeding mode of the preceding zoeal stages (Miller & Coffin 1961, Anger 1989, Abrunhosa & Kittaka 1997, Duguid & Page 2009). This secondary lecithotrophy might enable a prolonged period in the water column to search for suitable settlement habitats and has been suggested to be an evolutionary relic from pagurid ancestors (Anger 1989, Duguid & Page 2009). Megalopal stages are selective of settlement habitat and (at least in *Paralithodes camtschatica*) are able to temporarily delay settlement over mud and silt in favour of finding a complex environment (Stevens 2003).

-Early crab stages

After metamorphosis, early stage (juvenile) lithodid crabs seek protected environments (such as kelp holdfasts in shallow-water species) and display solitary behaviour (Loher & Armstrong 2000). Habit and habitat of juveniles is often substantially different to that of adults, and there is evidence of ontogenetic bathymetric migrations in several species in response to differential requirements of life-stages for temperature, oxygen and food (Abelló & Macpherson 1991, Hoggarth 1993, Loher & Armstrong 2000, Pereladov & Miljutin 2002). As the crabs progress towards reproductive maturity, they begin to exhibit 'podding' behaviour, in which large single sex groups of crabs perform annual migrations; males and females only usually mixing during reproductive seasons (Abelló & Macpherson 1991, Stevens 2003).

In summary, a range of reproductive strategies are present in the Lithodidae, most notably a division between species with planktotrophic and lecithotrophic larval development stages. Features common to the lithodids may affect their population dynamics and distribution:

- all lithodids release larvae over protracted periods of weeks or months as a way to promote survival in unpredictable environments.
- lithodids have a pattern of progressively abbreviated larval development from the Hapalogastrinae (4 zoeal stages) to a minimum of 2 zoeal stages in the Lithodinae.
- larvae of deep-sea species are demersal and this may affect dispersal potential.
- fertilisation events are often seasonally synchronised and involve mass migrations of adults to suitable mating grounds.

- behaviour of both adult and larval stages is influenced by reproductive mode and environmental temperature, particularly the direction and scale of bathymetric ontogenetic migration.

O.6 Species and speciation in the deep ocean

O.6.1 Species

The idea of species has existed since the earliest recorded studies of biology. Pre-Darwinian systems of classification, from Aristotle to Linnaeus, view species as distinct and immutable entities in which all variety is deviant from the example form (Sokal & Crovello 1970, de Queiroz 2007). Darwin's (1859) view that that species are constructs of convenience, drawn on a 'seamless continuum' of extant and extinct varieties, is one which still incites debate (Mayr 1957, Ereshefsky 2009). The question is whether there is a meaningful difference between taxonomic levels such as genus, species and variety (Darwin 1859, Mallet 1995, Goldstein & DeSalle 2005), and whether we can identify (or at least define) what that difference is. Although the philosophy of the existence and significance of species continues to be discussed, species are recognised as 'common sense' discontinuities in nature (Huxley 1942, Mayr 1963, Sokal & Crovello 1970).

At least seven accepted definitions of species exist in modern biology (Mallet 1995); some attempting to produce an all-encompassing concept (Monism, Templeton 1989), whereas some accept that there are many biological processes that can produce functional evolutionary units – species – and which allow the context to dictate the species definition (Ereshefsky 1998). In the majority of cases, these concepts define the same sets of organisms, albeit with different theoretical boundaries (Goldstein & DeSalle 2005). Given that the focus of this study is on sexually reproductive, benthic Metazoa, I will discuss only a selection of relevant concepts.

-Biological Species Concept (BSC)

Dobzhansky's (1936) and Mayr's (1963) species concept is widely employed in the study of sexually reproductive (and dioecious) animals. Species are groups of actually or potentially interbreeding populations which are reproductively isolated from other such groups (Mayr 1963). Reproductive isolation is an incompatibility of mating system, habitat preference, or post-zygotic isolation such as chromosome incompatibility. The genetic basis for the vast majority of reproductive isolation is unknown, the best examples being egg–sperm interaction in sea urchins (e.g. Metz & Palumbi 1996). A modification on the reproductive isolation concept is one of

recognition, where species are groups of organisms which recognise one another as mates, regardless of whether a genetic hybridisation would be theoretically viable (Paterson 1985). Species identification (by taxonomists) in natural populations relies on the fact that populations reproductively isolated from one another will display concordant differences in a suite of additional characters because of genetic drift or selection (Avise & Ball 1990, Knowlton 2000).

-Ecological Species Concept (ESC)

Species are sets of organisms adapted to a particular niche. According to this concept, individuals of **intermediate** adaptation are less fit than either of the parent populations and are selected against. Reproductive isolation is not necessary in this concept, because even where ranges overlap and hybridisation is prevalent, fusion of the two populations will not occur. As ecological niches can be ephemeral, the species are not necessarily stable over time (Simpson 1961, Grether 2005).

-Phylogenetic Species Concept (PSC)

The PSC is defined as separating two groups that have **any** fixed difference between them; as such it is a practical rather than a mechanistic concept (Carcraft 1989, Avise & Ball 1990, Turelli et al 2001). Genetic studies, among other things, have shown that a difference can be found between any pair of individuals if the appropriate part of the genome is examined. It is now considered that the PSC is more appropriate when a suite of characters is used to distinguish species (Knowlton 2000). Species are the minimal units to which the term 'monophyletic' can be applied: they begin at the boundary between a reticulating network and a divergent genealogy (Hennig 1966, Medwar & Medwar 1983, Carcraft 1983, 1989, de Queiroz & Donoghue 1988, Kluge 1990).

O.6.2 Speciation in the Sea

How we define 'species' dictates what we mean by speciation; however, speciation in its broadest sense produces the discrete units of diversity observed in the natural world. Three theoretical scenarios of speciation are prevalent in the literature (allopatry, sympatry and parapatry) and most (although not all, Mayr 1963) sources would agree that more than one mechanism can be found in nature (Slatkin 1987, Turelli et al 2001).

-Allopatric speciation

Allopatric speciation occurs when a population is physically separated for enough time to allow reproductively isolating mechanisms and/or other significant morphological

traits to arise. This phenomenon is thought to occur particularly where a small sample of genes from the parental population is present in each 'daughter' population (Mayr 1954). Allopatric speciation requires that hybrids are less viable than the parent populations (or that they don't form at all) so that new 'species' will not merge on reintroduction (Dobzhansky 1936, Mayr & Ashlock 1991, Turelli et al 2001).

-Parapatric speciation

Parapatric speciation occurs within a contiguous population where there is no physical isolation, and gene flow can be assumed to occur throughout the process. The marine environment is conducive to large-scale movements of gametes, individuals and populations (Gage & Tyler 1991). Species typically have large population sizes, distributed (perhaps sparsely) over large ranges. Over large distances, it is possible that gene flow is too rare to bind species together as a cohesive unit over their whole range, allowing local adaptation and genetic drift in the semi-isolated populations (Erlich & Raven 1969). Gene flow can act to homogenise species, but this will only happen if the selective advantage of local adaptation is low compared to the level of mixing (Slatkin 1987, Barton 1989). If hybrid fitness for two locally adapted populations is lower than parental fitness, then a preference for inbreeding could be selected (Harrison 1990, Ridley 2004, Nosil & Crespi 2006).

Sympatric speciation, in which two species are formed without any geographical separation, is the most controversial theory. Sympatry can describe the natural distribution of sister species; however, in many cases the observed overlapping distribution is secondary to their speciation (Baraclough & Vogler 2000). Sympatric species often exhibit ecological differences, such as zonation by depth in the deep sea (France & Kocher 1996).

-Environmental stability and homogeneity in the deep sea

Most speciation theories rely to some extent on differential adaptation to ecological niches, which occurs in the presence of a heterogeneous or disrupted environment. The benthic deep-sea biome is one of marked heterogeneity and long-term stability, albeit sparsely punctuated by tectonic activity. Currents in the deep ocean are typically a few cm/sec, and are not strong enough to disturb the sea bed substantially (Gage & Tyler 1991). In some locations on the abyssal plain, however, the currents are strong enough to cause habitat disturbance to soft-bottom communities (Hollister et al 1984).

Marine environments differ in several ways from those applicable to paradigms of speciation on land. Terrestrial animals don't reproduce or disperse by broadcasting gametes or larvae into the environment; in this way, marine animals have more in

common with plants – for which hybridisation and dispersal distances are enigmatic (Gardner 1997). Species ranges in the open ocean are typically broad, with dispersal of larvae and mobile adults being aided by large-scale ocean currents (Miya & Nishida 1997). The deep sea is thought to be characterised by a high degree of genetic similarity within species over large distances (Gardner 1997). Perhaps contrary to this is the evidence of numerous 'cryptic' marine species, in which there is substantial genetic divergence, but little morphological differentiation (Miya & Nishida 1997, Etter 1999, Raupach & Wägele 2006). In addition, the observations of morphological diversity and high number of rare species encountered in deep-sea samples (Rex 1981, Grassle & Maciolek 1992) indicates that speciation does occur in the absence of any discernable barriers to gene flow (Wilson & Hessler 1987, Miya & Nishida 1997).

M: METHODOLOGY AND TERMINOLOGY

M.1 Measurements and data collection

All linear measurements were taken using digital callipers, capable of obtaining internal and external measurements in millimetres to an accuracy of 3 decimal places. Carapace length (CL) is used as a linear indicator of size. It is taken from the baseline of the orbit to the posterior edge of the carapace (Fig **BM**.1). It does not include any crests or spines protruding from the carapace (Macpherson 1988a).

In all cases, photographs were taken using the 'macro' setting of a Sony digital 8.1 megapixel camera with 4x optical zoom. Often, microscopic images were taken (using various light microscopes) by using the macro setting and focussing the camera down the lens of the microscope. Computer programs <*Sigmaplot 11*> and <*Microsoft Excel*> were used for statistical analyses. Distributional data was collected from all samples encountered in this study. Each data point was recorded as a location marker in <*Google Earth*>, along with depth, collection and taxonomic data where available. This distributional file is attached as Appendix E (DVD).

M.2 Phylogenetic nomenclature

Phylogenetic systematics (Hennig 1966) is a method of taxonomic classification based on evolutionary relationships; it aims to identify nested monophyletic groups based on shared, derived characteristics to produce a hierarchical tree (in its mathematical sense). Phylogenetic terms used throughout this manuscript are defined below (de Queiroz & Gauthier 1994):

Terminal taxa: In this case, extant groups which form the set of taxa analysed (the **in-group**).

Characters: Genetic features (or morphological features with a genetic basis) that are inherited and undergo selection as independent units. Character states are different forms of a character that have been lost, gained or changed over evolutionary history.

Nodes: Points of divergence between lineages. Nodes represent the last common ancestor of the divergent lineages.

Branches: Ancestral history as represented by lines on a tree. Branches represent a lineage connecting an ancestral node with a more recent node. Branch lengths often represent the 'distance' between nodes based on the likely number of evolutionary steps.

Clades:

- **branch based**: a group containing all descendents of the last common ancestor of the specified terminal taxa that was not also an ancestor of a more distant taxon.
- **character based**: a group containing all descendents of the terminal taxa since the appearance of the derived character that links those taxa.
- **node based**: a group including the last common ancestor of specified terminal taxa and all of its extant and extinct descendents.

This study deals only with extant terminal taxa, so these definitions are equivalent in practical terms, and will be referred to as clades.

Basal: Clade A is basal in relation to clade B if clade B is contained within clade A.

Monophyletic: A monophyletic taxon contains only lineages branching from a single node. Members of a monophyletic taxon are more closely related to one another by descent than to any taxon outside the clade.

Paraphyletic: Paraphyletic taxa are those for which the last common ancestor is also the ancestor of groups not included in that taxon. It has other clades nested within it.

Polyphyletic: Taxon including members of more than one monophyletic group (and is not monophyletic itself).

Homology: A character state which has a single evolutionary origin as opposed to being the product of evolutionary convergence between two lineages (a homoplasy) (Patterson 1988).

Synapomorphy: Shared, derived characters, which form the basis for cladistic methodologies.

Symplesiomorphy: Characters present in the last common ancestor (LCA) of all taxa on the tree and which are shared between taxa because of this ancestry rather than being a derived condition.

Sister taxa: Two taxa connected by a node, from which there are no other descendents.

Polytomy: A node with more than two descendent lineages. This can represent a multi-way divergence from a single ancestor, but more likely represents a node at which the hierarchical relationships between lineages can not be resolved.

Out-group: The extant taxon used to provide evidence of symplesiomorphies. Any similarity between the out-group and the in-group taxa was present in the last common ancestor. Any differences are either derived within in-group lineages (synapomorphies), or are ancestral features which have since been lost in the out-group lineage. To minimise the latter, extant out-groups are chosen to be close to the last common ancestor of the in-group.

M.3 Theory of computational phylogenetics: search and optimality

Modern cladistic studies have incorporated many types of data, including restriction fragments (Vivek & Simon 1999), allozyme frequencies (Grant et al 1994), molecular sequence data and morphological characters (Zaklan 2002a). The optimal criteria for inclusion of characters - homology, independence, and the ability to code characters consistently and accurately - are comparable, regardless of data-source. The process of formulating hypotheses of evolution from observed shared, derived differences between character states has two components: a method of efficiently generating trees (search), and a criterion by which to identify the 'best' of those trees (optimality).

M.3.1 Search

Computational power and time are important considerations in the choice of search mechanism when taxon numbers and character numbers are large. The most accurate search would generate and examine every possible topology, but the number of trees involved increases rapidly with sample size. Heuristic search methods are used as an alternative for large datasets. Random samples are taken from the set of possible tree topologies and then rearrangements of those trees are made until a 'better' tree is found. These are commonly referred to as 'hill climbing' algorithms, because the search will

iteratively generate better 'related' trees. Hill climbing methods are prone to find local rather than global maxima, and they can be improved by searching multiple initial trees in parallel and using a branch swapping algorithm (sub-tree pruning and regrafting or tree bisection and reconnection (TBR)) to make occasional jumps between topological families (Page & Holmes 1998).

M.3.2 Optimality

Optimality criteria enable the user to score how good a tree is, and several types of optimisation are used in computational phylogenetics. Distance criteria (e.g Minimum Evolution) assess trees based on their total 'length' in terms of evolutionary change: the best tree(s) have the shortest total branch length and assume the least possible evolution has occurred. The most simplistic measure of evolutionary change for any 'sequence' of characters is an enumeration of differences between pairs of sequences (p-distance). The parsimony criterion also requires that the observed data have been produced by the smallest possible number of base changes, and this is done by deriving the character states of hypothesised ancestors at intermediate nodes (Eck & Dayhoff 1966, Kluge & Farris 1969, Fitch 1971).

In molecular phylogenetics, 'characters' refer to homologous loci within genes and there can be one of four character states at each locus: Adenine (A), Cytosine (C), Guanine (G) and Thymine (T). Several factors inherent to the nature of molecular evolution mean that p-distance underestimates true evolutionary distances in predictable ways (Kelchner & Thomas 2006) such as:

- the possibility of multiple mutations at the same site (including the possibility of reversions, which are not unlikely in a system with 4 possible character states).
- the difference in likelihood of transversions (A-C or T-G) and transitions (A-G or C-T), since purines (AG) are larger than pyrimidines (TC) and are mechanically less likely to be substituted for one another (Jukes 1987, Collins & Jukes 1994).
- different selective costs of substitutions at different positions in the genome (for example, in a protein coding gene, substitutions at the 3rd position in a codon are less likely to cause change in translated protein and so they mutate more rapidly than 1st or 2nd positions: Goldman & Yang 1994).
- the potential for a difference in evolutionary rate between lineages (Tamura & Kumar 2002).

Most models of evolutionary change employed in computational molecular phylogenetics are simplified examples of the General Time Reversible model (GTR). This assumes a symmetrical substitution matrix (change from A to G is as likely as G to A) with parameters representing each of 6 possible changes between 4 character states; 4 parameters representing the base frequencies at equilibrium; and one parameter representing the rate per unit time (Tavaré 1986). In addition, the models are often modified by incorporating the Gamma function, which allows the rate of substitution to vary over space (the space of the gene or genome), in addition to time (Page & Holmes 1998).

Likelihood or probability-based analyses (Maximum likelihood or Bayesian analysis) use assumptions about molecular evolution directly to model the chance of obtaining the observed sequence data for a given tree topology (Hasegawa & Yano 1984, Hasegawa et al 1991, Beaumont & Rannala 2004). In these cases, the most probable or most likely tree(s) are selected to represent evolutionary events.

In this study, molecular sequences were obtained from six genes and different aspects of morphology were also examined for separate phylogenetic analyses. Comparison of different data sources can provide a minimal estimate for the amount of error present in the methods if and when analyses do not yield congruous results (Draper et al 2007, Pisani et al 2007). Molecular and morphological data were not combined to produce a single (total evidence) tree (Mickevich 1978, Kluge 1989) because the results of the molecular phylogeny were implicit in rooting the smaller morphological trees; however, the congruence of the results is discussed. Within molecular and morphological data types, where datasets are independent of one another, total-evidence trees were produced by combining the data prior to analysis (Kluge 1989) as well as examining the separate phylogenetic signal from each partition to determine overall congruence of the results.

M.4 Choice of outgroups

In computational phylogenetics, it is usually necessary to designate an out-group in order to determine the polarity of change. If we knew the 'true' evolutionary history of the Lithodidae, the best possible out-group would have diverged from the lithodid lineage immediately before the last common ancestor of all lithodids. As discussed elsewhere in this thesis, the position of the Lithodidae within the Anomura is controversial. Cunningham et al (1992) showed that the genus *Pagurus* is paraphyletic with respect to the Lithodidae; themselves monophyletic. Contrary to this result, more recent morphological revisions of the Anomura have entirely removed the Lithodidae from the Paguridoidea and created a separate super-family Lithodoidea (McLaughlin et

al 2007). It is important in phylogenetic analysis that a taxon within the lithodid clade is not chosen to root the analysis, as this would provide misleading evidence about derived differences.

Possible out-groups selected from within the Anomura include:

- the Paguridae, such as *Pagurus criticornis* Dana 1852, *P. brevidactylus* Stimpson 1859, and *P. leptonyx* Forest & de Saint Laurent 1968 from Brazil, the Gulf of Mexico and Uruguay (Hebling & Rieger 1986); *P. comptus* White from the Beagle Channel, Patagonia (Lovrich & Thatje 2006); *P. longicarpus* Say 1817 from the Western Atlantic.
- the Aeglidae, a family of fresh-water anomurans from South America containing the genus *Aegla* (Perez-Losada et al 2004). These were formerly classified within the anomuran taxon Galatheoidea, but were elevated to super-family level at the same time as the Lithodidae (McLaughlin et al 2007).
- the genus *Emerita,* commonly the 'mole crab' or 'sand crab', which is classified within the family Hippidae (Anomura: Hippoidea), and is found intertidally on the Pacific and Atlantic coasts of America. *Emerita* and *Aegla* are not suggested to have an especially close ancestral relationship with the Lithodidae, but unlike *Pagurus*, the relationship is not overshaddowed by questions of paraphyly or polyphyly.

M.5 Lithodid terminology

In this section, I will briefly cover some aspects of lithodid morphological and anatomical terminology to ensure the terms in this work are accessible. The species *Lithodes galapagensis* and *Paralomis alcockiana*, described in Hall & Thatje 2009 (Appendix F) are used to exemplify typical morphology and homologies between the lithodid (Lithodinae) genera *Lithodes* and *Paralomis*.

The segments of the head (5) and thorax (8) are fused dorsally to produce the carapace, with each segment bearing an appendage (McLaughlin 1983b). Lithodids have two pairs of antennae, the second (and longer) of which sometimes bears an elaborate acicle on the second of five segments (the exopod of the antenna, otherwise known as the scaphocerite or scale, Fig **M**.1a). The corneae are at the end of stalked ocular peduncles (or eyestalks, Fig **M**.1a,c). The thoracic appendages (pereiopods) of which there are five, are modified such that the first pair are chelate (Fig **M**.2d), the following three are similar in size and locomotory (Fig **M**.2b) and the fifth is much reduced and typically held under the carapace where they act to clean the gills and egg mass in

ovigerous females (Pohle 1989). The pereiopods are uniramous and consist of segments dactylus, propodus, carpus, merus (Fig **M**.2b), attached to the sternum through joints on smaller segments: the coxa and the basis (Martin 2005). Lithodids typically have several spines on their carapace, including prominent rostral spines between the eyestalks (Fig **M**.1b,c, Macpherson 1988a). Grooves on the carapace are sites of internal attachment for structural and functional musculature, and they aid in visually delimiting the carapace into gastric, cardiac and branchial regions (Pilgrim 1973, Fig **M**.1a).

Six abdominal segments are present in most of the Decapoda (Pilgrim 1973, McLaughlin 1983b). In the Lithodidae, the first abdominal segment is reduced and usually obscured by the carapace or fused to the second segment. The third to the sixth abdominal segments (Fig **M**.2a) of the Lithodinae are flexed underneath the body, close to the sternum. The appendages of the abdominal segments are pleopods, which are present only on the left-hand side in adult female lithodids and these are used for the attachment of egg-masses in reproductive stages (Pohle 1989).

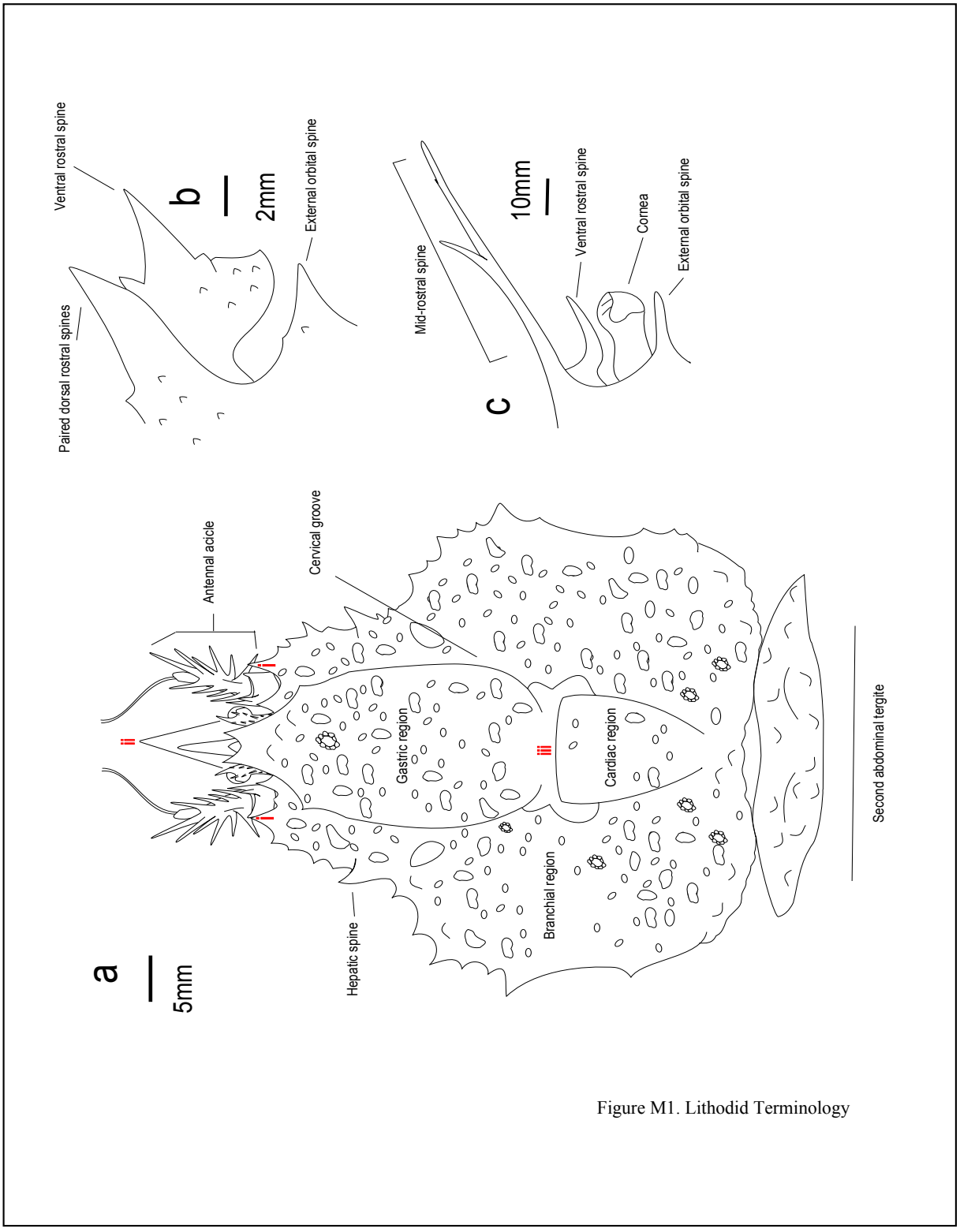

Figure M1. Lithodid Terminology

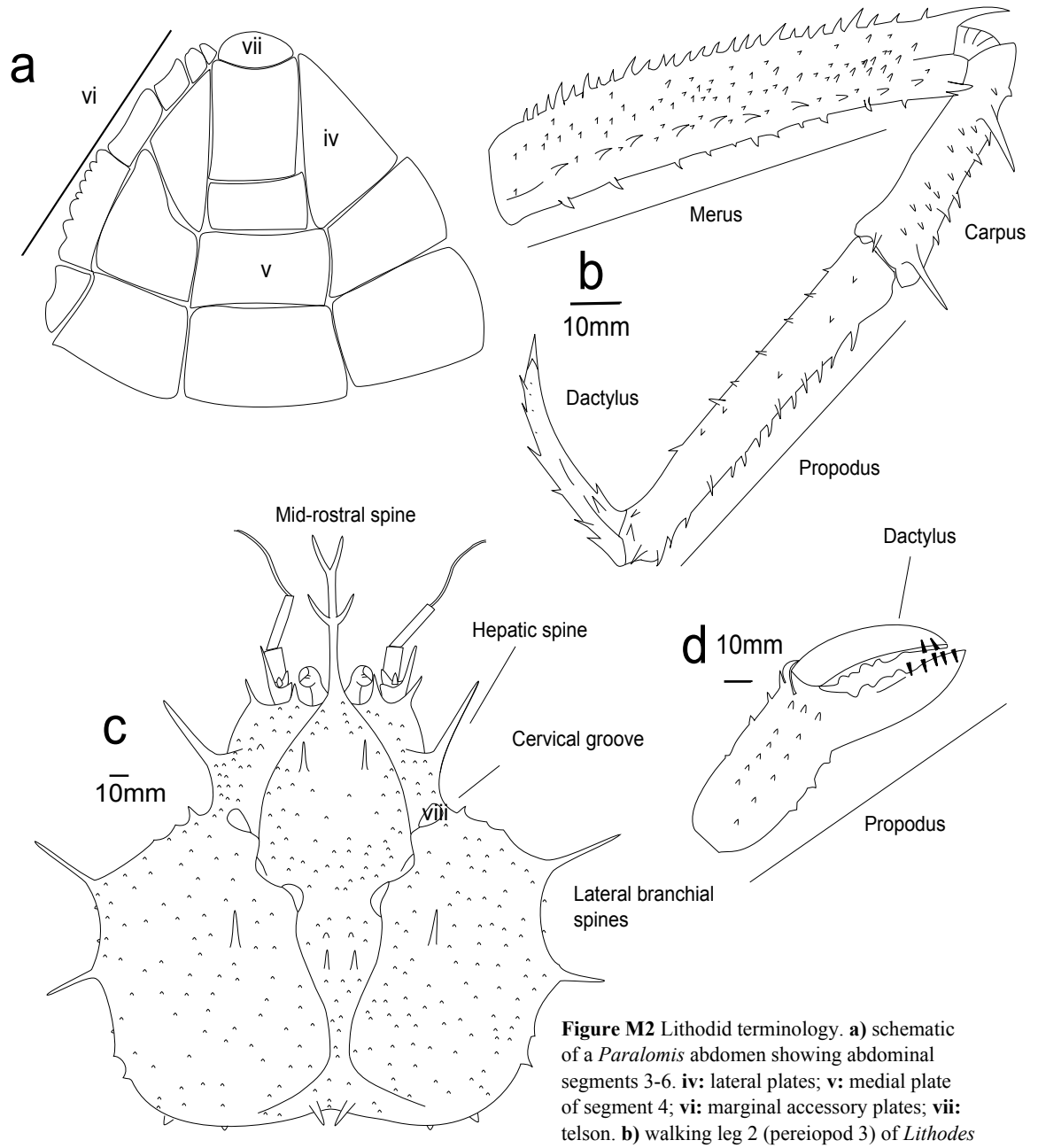

Figure M2 Lithodid terminology. **a)** schematic of a *Paralomis* abdomen showing abdominal segments 3-6. **iv:** lateral plates; **v:** medial plate of segment 4; **vi:** marginal accessory plates; **vii:** telson. **b)** walking leg 2 (pereiopod 3) of *Lithodes galapagensis*. **c)** carapace of *L. galapagensis*. **d)** right chela of *L. galapagensis*. **viii:** cervical 'knob'.

Section A: Genetic evidence for the evolutionary history of the Lithodidae

AO: SECTION INTRODUCTION

AO.1 The genetic basis of species

The nucleic acids (DNA and RNA) are the essential molecules of heredity and cell function, common to all known organisms. In the Metazoa, DNA is found predominantly in the cell nucleus, but also in multiple cellular organelles such as the mitochondria (Brown et al 1979, Henze & Martin 2003). *Drosophila melanogaster*, the 'model' arthropod used for genetic studies, has a nuclear genome of 165 million base pairs of DNA (bp), with an estimated 14,000 genes (Tweedy et al 2009); its mitochondrial genome has approximately 16,000 bp and codes for 2 ribosomal RNA molecules, 22 tRNA molecules and several proteins involved in metabolic pathways (Clary & Wolstenholme 1984). Mutations of the genetic code can be caused by chemical damage, by uncorrected errors during replication and through interactions with viral DNA (Peterson 1985, Greene & Jinks-Robertson 2001, Cooke et al 2003). If changes are not detrimental to cell function, they are propagated by reproduction and can become fixed within an interbreeding population (Barton 1989, Gillespie 1998). Even within a well-mixed population there is some genetic variation between individuals; conversely, there can be selective pressure for sequence conservation in parts of genes across phyla (Slatkin 1987). There is not an established threshold of genetic divergence that is used to imply species formation, not least because mutation rates can vary between different lineages (Britten 1986, Slatkin 1987, Knowlton 2000, Wu 2001). Nevertheless, the consistent genetic differences between homologous genes will become measurably greater over time and there will be some correlation between degree of change and length of separation of two (reproductively, physically or ecologically) isolated populations (Turelli et al 2001, Drummond et al 2003, Bromham & Penny 2003). This cumulative genetic change over time justifies the use of molecular data in the reconstruction of ancestral relationships between species.

AO.2 Molecular techniques overview

The polymerase chain reaction (PCR) and the advent of large-scale, rapid, and relatively inexpensive versions of dideoxy-chain termination sequencing (Sanger et al 1977) made molecular sequence data available as a tool for taxonomists and phylogeneticists towards the end of the 20th century (Mullis et al 1986, Saiki et al 1988, Martin et al 1990). PCR involves the iterative replication of a short piece of DNA (amplicon) from a genomic sequence *in vitro*, which can then be sequenced in a separate reaction (Sanger et al 1977). When double-stranded DNA is heated, the hydrogen bonds between paired bases melt, and when it is cooled the bases rejoin in the

most energetically stable order (Breslauer et al 1986). In PCR, oligonucleotides of synthetic DNA (primers ≈ 20 bp) bind to any somewhat complementary single-stranded DNA (the higher the temperature, the better the match has to be for the duplex structure to be stable). Addition of mononucleotides (dNTPs) and thermostable DNA polymerase, and incubation in the right conditions leads to elongation of primers from their 3' end. This reflects the mechanisms of DNA replication *in vivo*. Repeated melting, annealing and elongation steps enable the exponential increase of amplicon copy number (Sambrook et al 1989).

A number of techniques employ the principle of PCR to amplify sections of genetic code; although some (e.g Random Amplified Polymorphic DNA: RAPD Williams et al 1990) suffer from low degrees of duplicability when the template DNA is fragmented (Skroch & Nienhuis 1995). One of the most common uses of PCR in taxonomic studies is the amplification and comparison of homologous sections of genomic DNA using a single pair of primers. Sequences of more than 1000 bp can be amplified from distantly related organisms even when only small amounts of intact DNA can be isolated (France & Kocher 1996, Palero et al 2010). Even though techniques have improved in speed and cost, the work done to date barely begins to describe the genetic diversity within most organisms – sampling two or three genes from tens of thousands (Etter et al 1999, Wu 2001).

AO.3 Lithodid molecular genetics

Molecular genetics began to influence the study of lithodids in the mid 1990s, when Cunningham et al (1992) used part of the mitochondrial 16S rRNA gene to demonstrate the close affinity of the Lithodidae with the genus *Pagurus* (Paguridae). From this basis, Zaklan (2002a) used parts of nuclear and mitochondrial genes (Cytochrome Oxidase I & II [COI, COII] and rRNA genes 28S, 18S, 16S) to investigate the position of the Lithodidae within the Anomura. Zaklan's target species were chosen to represent the 15 lithodid genera equally and one only species of *Paralomis* and two of *Lithodes* were sampled out of a possible 82 species in those genera (Appendix A). Molecular work since then has accelerated and several other contributors have uploaded lithodid sequences to the international databases (http://www.ncbi.nlm.nih.gov/, Appendix B). Where appropriate, the molecular targets for this thesis are chosen to be compatible with the data obtained in other studies, but with a focus on the globally distributed subfamily Lithodinae rather than divergent lineages at the root of the family Lithodidae.

AO.4 Practical problems with molecular techniques

AO.4.1 Preservation and extraction

Mobile benthic specimens from the deep sea are expensively and rarely encountered, and many of the species currently recognised have been collected only once, often with the holotype and one or two other specimens held as a precious resource by museums (Palero et al 2010). Specimens prized for their morphological novelty are also crucial for studies of genetic diversity and historical radiations (Thatje et al 2008), so it is desirable to overcome barriers to molecular analysis caused by the traditional museum processes of preservation.

Historically, fluid-preserved museum specimens have first been fixed in buffered formalin solution and then later transferred into alcohol or industrial methylated spirit (IMS) for archival storage (France & Kocher 1996). Extraction and amplification of DNA from such traditionally fixed material is difficult (France & Kocher 1996, Boyle et al 2004). It is currently unclear whether difficulties with the PCR amplification are caused by DNA being trapped in a matrix of cross-linked proteins, severe DNA damage caused by low pH or by the presence of PCR inhibitors in solution (Fang et al 2002). Many reports have been published on this topic and numerous protocols have been proposed (Schander & Halanych 2003), but the fact remains that no reproducible, generic method has been reported to date. One of the latest protocols introduced in the literature to solve the problem of DNA extraction from formalin-fixed material is based on critical point drying, a technique used for preparation of samples for electron microscopy (Fang et al. 2002, Palero et al 2010).

AO.4.2 Analysis

Several times in the history of the Metazoa, large amounts of genetic material have been randomly duplicated within a genome, leaving evidence of multiple copies of genes (gene families) (Durand & Hoberman 2006). When comparing genes from different species, it is important that similarities and differences are the result of a common descent (homology) rather than parallel evolution following an intra-genomic duplication (Bensasson et al 2001, Keeling & Palmer 2008). Gene duplications can produce pseudogenes which, when released from selectional constraints, mutate at a rate much higher than the 'original' (functional) copy of the gene. Degradation of function, such as translation-termination codons and frame-shift mutations, can indicate the presence of a pseudogene (Durand & Hoberman 2006). Duplicates can be prone to variation in length because of insertion or deletion mutations, so the occurrence of multiple sizes of PCR product in a single sample can indicate the presence of differences in a multi-copy gene. While there are indicators that genes are unique and

functional, this can not be easily verified, and caution is exercised in the interpretation of these results.

AM: SECTION METHODS

AM.1 Sampling

AM.1.1 Sample procurement

Tissue samples were obtained from several sources in order to get a wide coverage and high number of replicates of lithodid species. Egg and dactylar tissue from preserved museum specimens were obtained with permission from: Natural History Museum, London; Senckenberg Museum, Frankfurt; Musée National d'Histoire Naturelle, Paris; Institut de Ciencies del Mar, Barcelona; United States National Museum of Natural History, Smithsonian Institute, Washington; collections in Chile and Miami; CADIC, Ushuaia, Argentina; and the 'Discovery Collection', National Oceanography Centre, Southampton. Tissue from fresh specimens was obtained from Spanish cruises around Mauritania (2008), French fishing vessels near Kerguelen (2008), ROV Isis from on board RRS James Clark Ross (JCR167), fisheries and dives around the Falklands and South Georgia, and Norwegian commercial fishing vessels.

AM.1.2 Species sampling

To elucidate world-wide relationships between species of Lithodinae, the sampling aim was to obtain molecular sequences from a wide range of the 117 lithodid species described globally. Although obtaining specimens was not a limitation, the difficulty of obtaining non-fragmented DNA from preserved deep-sea samples led to reduced (and slightly unpredictable) success. Approximately 30% of all DNA samples were extracted from ethanol-preserved or frozen tissue, and 70% from formalin-preserved specimens. Including sequences obtained from the NCBI GenBank nucleotide database, 16/61 *Paralomis*, 9/21 *Lithodes* and 3/10 *Neolithodes* species were used in this study, covering approximately one quarter of the species known to exist worldwide (Appendix A, B i-v). In addition, sequences were obtained from NCBI GenBank for some genes of *Cryptolithodes* (2 species), *Hapalogaster* (2 species), *Oedignathus*, *Lopholithodes* (2 species), *Glyptolithodes*, *Phyllolithodes*, *Paralithodes* (3 species) and non-lithodid genera *Aegla*, *Pagurus*, *Emerita* and *Lomis* (Appendix B).

AM.1.3 Gene targets

Appropriate genetic targets for family-level phylogenetic analysis are those that mutate quickly enough for differences to be observed between taxa, but not so quickly that they diverge substantially within an interbreeding population (Brown et al 1979, Wolfe et al 1989, Chuang & Li 2003, Galtier et al 2009). Targeting a gene where there is no detailed prior knowledge of the organism's genome can be done using universal primers that anneal with highly conserved regions of functional copies of the gene (Palumbi & Metz 1991, Folmer et al 1994). Once the target gene has been investigated using universal primers, then for accuracy, duplicability, and resistance to contamination by other organisms, specific internal primers can be designed. Universal primers for mitochondrial genes 16S and Cytochrome Oxidase I (COI) and Cytochrome Oxidase II (COII) exist (see Table A1), which amplify these genes in most eukaryotes. Their structure can be compared with a large amount of data gathered from other organisms, so the viability of the sequence can be ascertained to a degree. Large subunit mitochondrial rDNA (16S), and other rRNA-coding genes are suited to this sort of analysis because their secondary structure is composed of regions that are rigidly constrained, as well as those that are more freely evolving and can show evidence of large deletions or insertions within lineages (Hancock et al 1988). Ribosomal expansion segments are regions of rDNA that are not common to the basic ribosomal structure of prokaryotes and eukaryotes; they tend to be constrained in terms of secondary structure, but at a lower level than the 'core' regions (Larsson & Nygård 2001, McTaggart & Crease 2009). Two sections of the nuclear small subunit ribosomal gene (18S), and three sections of nuclear large subunit rDNA (28S) were examined because of a high rate of sequence divergence observed in the expansion segments of related organisms (Nelles et al 1984, Crease & Taylor 1998, Held 2000). The 'internally transcribed spacer 1' (ITS1) is a region of non-translated DNA which is transcribed along with functional rRNA genes in eukaryotes. Its principally non-structural role means that it is largely free from conservative selection and can be particularly useful for phylogenetic analysis of closely related groups, particularly decapods (Chu et al. 2001, Armbruster & Korte 2006, Chow et al 2009). All of the genes mentioned have a high copy-number within each cell, and for this reason are often readily amplified even without cloning. A caveat is that non-unique genes, especially in the nucleus can have an unpredictable level of heritability, and non-functional versions may exist.

AM.2 Primers

Table A1 Primers used in this study and primer-specific methodological details.

Primer name	**Gene targeted**	**Sequence of synthesised oligonucleotide 5' to 3'**	**Melting (T_m)/ Annealing temperature °C**	**Reference**
16Sar	527-529 bp of in-group mitochondrial rDNA	CGC CTG TTT ATC AAA AAC AT	51.2/48	Palumbi et al (1991)
16Sbr		CCG GTC TGA ACT CAG ATC ACG	61.8/48	Palumbi et al (1991)
LCO1490	658 bp of in-group mtDNA: Cytochrome Oxidase I gene	GGT CAA CAA ATC ATA AAG ATA TTG G	56.4/51	Folmer et al (1994)
HCO2198		TAA ACT TCA GGG TGA CCA AAA AAT CA	58.5/51	Folmer et al (1994)
NURI1	415 bp of 28S nuclear rDNA (Fig **AM**.1a)	GGT AAG CAG AAC TGG CGC TGT GGG	70.41/62	Palero (2009)
NURI2		GGG ATC AGG CTT TCG CCT TGG G	70.44/62	Palero (2009)
28BF/Lsp28BF	683 bp of 28S nuclear rDNA (Fig **AM**.1a)	Primer sequence as designed for *Palinurus*: GGG CCA AGG AGT CCA ACA TGT G Lithodid-specific primer sequence: GGA CCA AGG AGT CTA ACA TGT G	60.3/55	Palero (2009)
28BR		CCC ACA GCG CCA GTT CTG CTT ACC	67.8/55	Palero (2009)
28AF	739 bp of 28S nuclear rDNA (Fig **AM**.1a)	AGT AAG GGC GAC TGA AMM GGG A	59.66/55	Palero (2009)
28AR		CAC ATG TTG GAC TCC TTG GCC CG	70.39/55	Palero (2009)
ITS1F	474 bp of non-coding nuclear DNA	CAC ACC GCC CGT CGC TAC TA	63.5/ 51	Chu et al (2001)
ITS1R		ATT TAG CTG CGG TCT TCA TC	55.3/51	Chu et al (2001)
COIIF	542 bp of mitochondrial Cytochrome	AGC GCC TCT CCT TTA ATA GAA CA	58.9/ 50.5	Zaklan (2002a)
COIIR		CCA CAA ATT TCT	57.6/50.5	Zaklan

	Oxidase II gene.	GAA CAT TGA CCA		(2002a)
18A1	1836 bp of the 18S nuclear rDNA (Fig **AM**.1b)	CTG GTT GAT CCT GCC AGT CAT ATG C	66.55/61	Medlin et al (1988)
1800R		GAT CCT TCC GCA GGT TCA CCT ACG	67.62/61	Medlin et al (1988)
V4for	V4for/ V4rev: 268 bp of 18S rDNA (Fig **AM**.1b)	CGG TTA AAA AGC TCG TAG TTG G	58.83/52	C. Held
V4rev		CCC CCG CCT GTT TCT ATT AG	59.39/52	C. Held

AM.2.1 28S amplicons

Several sets of sequences were available for parts of the anomuran 28S gene on the NCBI GenBank nucleotide database. The longest stretches of lithodid DNA, covering 2478, 2473 and 2474bp respectively are from *Lithodes santolla* (GenBank AY596100.1), *Paralithodes camtschatica* (AB193824.1), and *Paralithodes platypus* (AB193821.1). Lithodid genes from 2 additional genera (*Neolithodes brodiei* x2, *Paralomis formosa, P. elongata*) were sequenced in order to supplement an alignment of *Lithodes santolla* and *Paralithodes* for a preliminary analysis of sequence divergence. The lithodid 28S gene was amplified in three sections in order to probe for levels of inter-specific variation at different locations on the gene. Based on the results of this preliminary analysis (Section **A1**.3.8), the Lsp28SBF and 28SBR primers were used to amplify a partial 28S sequence from a wider lithodid taxon set.

AM.2.2 18S amplicons

1830 bp of the *Lithodes santolla* 18S gene (AF439385.1), and 14 other anomuran sequences of similar length were obtained from the NCBI GenBank database (Appendix B.v). Comparison with the 18S secondary structure of *Drosophila melanogaster* in Hancock et al (1988) shows that this fragment contains the V2 and V4 expansion segments of the molecule. Primers 18A1 and 1800R amplify a theoretical 1800 bp of the gene. V4for and V4rev target 246 bp of ingroup DNA, to ensure that a double-stranded section (where forward and reverse sequences overlap) of this variable region is amplified in all samples (Fig **AM**.1b). To investigate the suitability of the 18S gene for phylogenetic studies in Lithodidae, the genes from 4 species (*Neolithodes brodiei* x2, *Paralomis formosa, P. elongata*) were sequenced for comparison with *L. santolla*.

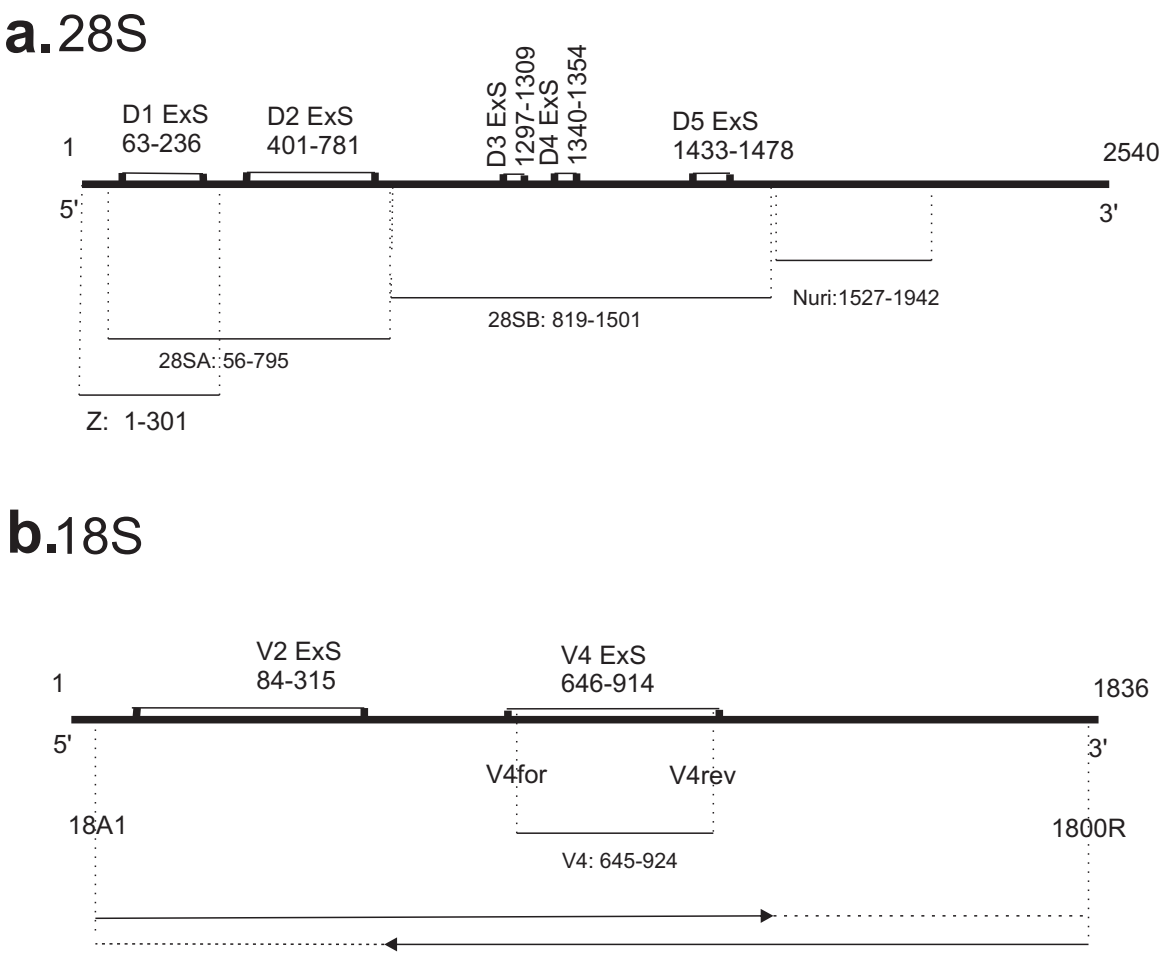

Figure AM.1 Schematic of nuclear rDNA genes, with an indication of regions amplified in this study. Numbers are given for the positions of bases on an aligned sequence of lithodid genes after comparison with the secondary structure of rRNA in *Drosophila melanogaster* (Hancock et al 1998).
a) Large subunit rDNA, 28S gene. D1-D5 are named expansion segments. Narrow lines indicate the relative positions of amplified sequences (Z) from Zaklan (2002a), and three fragments amplified in this study: 28SA, 28SB and NURI.
b) Small subunit rDNA, 18S gene. V1-V4 are expansion segments present in many eukaryotes. V4 is targeted by both long-range primers and short sequence amplification.

AM.3 Tissue sampling protocols

Wherever fresh tissue was obtained for this study, the samples were either frozen whole, or sampled in semi-sterile conditions into cold (0°C) 70% ethanol as soon as possible after death. Frozen tissue, after sampling, was stored in ethanol at 4°C, since repeated freezing and thawing of tissue is detrimental to the structure of DNA (Shikama 1965).

Approximately 1.5mm^3 muscular tissue from one of the elements of the walking legs was sampled through a small incision in the arthrodial membrane. On some occasions, it was only possible to obtain material from gill tissue or from eggs. The success of amplification from embryonic tissue was lower than for muscular tissue, and especially so in formalin preserved samples. Gill tissue was rarely sampled in this study because it was noted that the largely indigestible chitinous structures became stuck in the filters and physically impede DNA collection from Qiagen spin columns. Sampling gill tissue is also a lot more destructive to the specimen than the sampling of muscle through the arthrodial membrane.

Once removed from the specimen with sterile implements (sterilised using a Bunsen burner), the tissue was dried on semi-sterile tissue to remove the preserving fluid. It was then cut into smaller sections to provide digestive enzymes with access to a large surface area. Depending on the method of DNA extraction, the tissue was placed directly into the critical-point drying protocol, or into a Qiagen buffer with proteinase K, which digests the tissue and prevents any autolytic processes (Appendix Ci, ii).

AM.3.1 Methods for well preserved samples

Tissue was placed in 20 µl proteinase K, buffered with 180 µl ATL and incubated at 55 °C for 1-8 hours according to the instructions of the Qiagen *DnEasy Blood and Tissue kit* protocol (Appendix Ci). Selective filtration of the resulting DNA solution was done using Qiagen centrifuge columns, and DNA is eluted after two wash-steps into AE buffer for storage or PCR. All sample extractions were repeated once. All *DnEasy* extractions were performed at AWI, Bremerhaven, Germany.

AM.3.2 Methods for sub-optimally preserved samples

Samples taken from wet-preserved museum specimens, including those for which the Qiagen columnar filtration system isolated DNA, underwent additional extraction using a method based on critical-point drying (Palero et al 2010, Appendix Cii). In order to reduce costs and provide a similar effect to that proposed in (Fang et al. 2002), this study used tetramethylsilane (TMS) as a strong dehydrating agent which maintains tissue structure (Ubero-Pascal et al 2005, Palero et al 2010). Muscle from the dactylus,

was extracted into 50-100 µl TMS solution and incubated for one hour with gentle agitation so that the tissue absorbed the dehydrating agent. The cap of the tube was then opened within a sterile laminar flow cabinet to let the TMS evaporate. Dehydrated tissue was transferred to a 1.5 ml eppendorf tube with 200 µl of 10% Chelex solution in pH 8.0 TE buffer and 20 µl of proteinase K solution (20mg/ml). This was incubated for 2-3 hours at 55 ºC in a thermomixer and then centrifuged for one minute at 10,000 rpm to separate the Chelex from the supernatant. Cells were heat-shocked at 95ºC for 15 minutes. 100 µl of supernatant, containing extracted DNA and minimal Chelex, was transferred into a fresh tube. 1-2 µl of this supernatant was used for each 25 µl PCR reaction (further details in Appendix Cii).

AM.3.3 PCR and cleaning

PCR reactions were conducted using GE Healthcare illustra PuRe-Taq ready-to-go PCR beads: these contain 2.5 units of PuReTaq DNA polymerase, 10 mM Tris-HCl, (pH 9.0 at room temperature), 50 mM KCl, 1.5 mM $MgCl_2$, 200 µM of each dNTP. Beads are temperature-stable until hydration to a total reaction volume of 25 µl, at which time they were stabilised at 4 °C in an ice bucket. Rehydration mixture consisted of nuclease free water, 10 pmol each of forward and reverse primer (Table A1) and approximately 50ng of DNA template in solution (AE or TE buffer). PCR reactions were performed using an *Eppendorf Master Cycler* with temperature profile as follows, according to the guidelines provided for the PuReTaq polymerase, with steps 2-4 repeated 35 times:

1. 2 minutes, 94 °C: initial DNA denaturation.
2. 20 seconds, 94 °C: denaturation
3. 10 seconds, annealing temperature dependent on the melting properties of the primer pair (Table A1).
4. 1 minute, 72 °C: extension
5. 5 minutes, 72 °C: final extension

3 µl of PCR product (+ 1 µl of loading buffer, *peqlab*) was separated by size using electrophoresis on a TBE buffered horizontal 1.5% agarose gel. The results were visualised by staining DNA in an (0.1%) ethidium bromide bath followed by de-staining in a distilled water bath. A 'ladder' of molecular size standards (*Fermentas FastRuler DNA ladder, Middle Range*) was used to quantify the size of amplified DNA when the ethidium bromide stain was visualised under UV light.

PCR products were separated from the residual primers, polymerase and salts using the Qiagen *QIAquick PCR-purification kit*, using the manufacturer's protocol (Appendix Ciii). Dideoxy-chain termination sequencing (Sanger et al 1977) was performed

remotely, either by Eurofins, Germany or Macrogen Inc, Korea. Information given on the Macrogen website states that 20µl of cleaned PCR product and 10µM primer were used for cycle-sequencing under BigDye™ terminator cycling conditions, and the reacted products were purified using ethanol precipitation and separated by size using Automatic sequencer 3730XL.

AM.4 Analysis and verification of results

Sequencing results were returned as chromatograms representing single-strand samples of amplified template DNA. These were interpreted by the <*DNAstar_Seqman*> program (Swindell & Plasterer 1997), and forward and reverse sequences from each sample were matched up to produce a reconstruction of double-stranded DNA. The match between the annealed sequences was compared manually to ensure there was agreement between the forward and reverse sequences, and that there were no artefacts that had been misread by the program. Ambiguous bases at the ends of the sequences were trimmed manually. The chromatogram was additionally checked after polymorphic loci had been identified in alignments of homologous genes to ensure that variable bases were correctly identified by the program and that the sequence was of high quality in that region.

BLAST searches (Altschul et al 1990) were performed by comparing a trimmed sequencing result with other sequences uploaded to the NCBI GenBank database. The search returns a percentage similarity between the input sequence and those stored on the database. This is used both to find additional sequences to support an alignment, and also to check the authenticity of the sequence and the sample amplified.

Alignment was in most cases performed using the <*Clustal W*> program (Larkin et al 2007), which uses pairwise comparison and tree-building methods to align multiple sequences so that biological homology between corresponding bases can be assumed. <*MUSCLE 3.7*> (Edgar 2004a, b)was used to align lithodid sequences with those of other anomuran families for the 16S, 18S and 28S genes in which long sections of base insertions were found; it was an especially powerful algorithm for use with whole taxon-set alignment (AT_A), which included distantly related anomuran genus *Emerita*. Manual inspection of the algorithmically produced alignments was done, whilst incorporating some assumptions about structure and function of the transcribed gene product. For example, those genes coding for rRNA were examined alongside the secondary structure of *Drosophila melanogaster*, and conserved structural 'stems' were identified within the sample set (Hancock et al 1988). Protein coding genes, COI and

COII were examined for codon sense and mutations which altered the reading frame. In any case where alignment was ambiguous (particularly for the out-groups), the bases were replaced with an ambiguity code (N).

Base frequency variations between taxa for the same gene were examined using a Chi-squared statistical test (the 'BASEFREQS' command in <*PAUP*4.0b10*>: Swofford 2000). This established whether there was a significant difference in the frequency of the four nucleotides occurring at equilibrium in different taxa, which could have an effect on analytical assumptions.

-Development of out-group assumptions

Sequences were obtained from GenBank for non-lithodid anomuran genera *Emerita*, *Pagurus* and *Aegla*. From these, an out-group was chosen for use in this analysis. Five species of *Pagurus* (*P. criniticornis, P. longicarpus, P. brevidactylus, P. leptonyx, P. comptus*); three species of *Aegla* (*A. intercalata*, *A. platensis*, *A. neuquensis*); and three species of *Emerita* (*E. analoga, E. brasiliensis, E. benedicti*) were compared. A phylogenetic tree of aligned sequences (lithodid and non-lithodid) was selected by the minimum evolution (ME) criterion in <*MEGA*3.1> for 529 bp of the gene 16S. The ME criterion was used for such preliminary tests because searches are orders of magnitude faster than ML analyses. Trees for this analysis were rooted at the mid-point of maximum sequence divergence, so there was no initial out-group assumption. In this tree ($AT_{A,}$ standing for 'all taxa'), the lithodid taxon set is large and unresolved in comparison to the long branches of the out-groups; AT_A is figured with monophyletic groups of lithodids condensed to a single taxon label. From these, a monophyletic out-group genus was selected for use in further analyses, and this is discussed in the results (Section **A1**.3.9).

If the monophyly of the Lithodidae and each of the anomuran genera *Aegla*, *Pagurus*, and *Emerita* was supported by high confidence levels (bootstrap analysis, 1000 replicates), then an examination of the variability within these taxa was conducted. An enumeration of polymorphic loci in a trimmed alignment (all sequences of the same length except where there are internal insertions) was used as an approximate measure of variability. Insertions, point-mutations, and deletions were all given equal weighting. Scores for *Pagurus, Aegla* and *Emerita* were compared with levels of variability observed within the same set of loci in lithodid genera (*Paralomis* [16 species], *Lithodes* [9 species] and *Neolithodes* [3 species]). This aimed to provide a very conservative estimate of variation in homologous genes between closely related species of different taxa.

-Production of consensus sequences

For each species, at least 5 different individuals were sampled if these could be obtained. Often (because of the sporadic nature of sampling deep-sea organisms), this was not possible. Where sequences from the same morphological species were identical, these were condensed down to one sequence for analysis, because reducing taxon number substantially increases processing time. Where isolated autapomorphies existed within sequences of a species, a consensus was formed by retaining aligned bases where there was agreement between all specimens, and by indicating ambiguities using the IUPAC ambiguity codes (1986) where base identities disagree. In cases where sequences of the same morpho-species showed polymorphisms consistently at several loci or in more than one gene, these were treated as potential sub-populations and two consensus sequences were produced. For non-lithodid anomuran taxa, a generic 'consensus' was produced (Appendix B). This provides a conservative estimate of the ancestral gene sequence, as opposed to using the derived sequences from one species which will have mutated further since divergence. This also avoids, to some extent, problems with rooting alignments based on members of polyphyletic taxa (Fig **A1**.2b).

AM.5 Phylogenetic analysis methods

A molecular phylogenetic tree is a topological representation of sequence divergence within a hierarchically related lineage. A set of assumptions about the nature of sequence evolution, based on data gathered from extant taxa, was used to estimate ancestral events (Cavalli-Sforza & Edwards 1967, Page & Holmes 1998). The 'best' tree(s) were found using three different optimality criteria: minimum evolution (ME), maximum likelihood (ML) and Bayesian analysis (BAY). The aim was to obtain three independent estimates of phylogenetic topology from the data, to ensure that different assumptions inherent in the analytical methods did not skew the results.

AM.5.1 Phylogenetic analysis methods overview

1. Total evidence (TE_B) datasets were created using gene fragments 16S, COI, 28SB and ITS1; alignments contained 50 unique sequences of length (*l)* 2110 bp (ambiguous alignment in out-groups or missing data [N] were distinguished from insertion mutations [–]).
2. In <*PAUP*4.0b10*> (Swofford 2000), a partition homogeneity test (Farris et al 1995, command name <<HOMPART>>) examined whether ME trees generated for the single-gene (partition) datasets [16S, COI, ITS, 28S] varied significantly over 1000 replicates from those produced when the data are

combined as TE_B. This tested the hypothesis that a natural partition of TE_B (by genes) was significantly different from a random partition of the dataset.

3. For each gene and for the combined dataset (TE_B), the model of evolution most likely to account for the observed sequence divergence was assessed using <*Modeltest 3.7*> (hLRT).
4. The phylogenetic signal from each gene (COI, COII, ITS1, 16S, 28SB) was examined by creating ME and ML trees in <*MEGA3.1*> and <PHYLIP*DNAml*> respectively.
5. For TE_B, ML, ME and BAY trees were produced, and these are discussed in the text (Section **A1**.3.11).
6. For discussion, a schematic of relationships between the genera was taken from TE_B trees to form a single tree, TE_C. In TE_C, species within monophyletic genera were condensed to a single taxon label and polyphyletic or paraphyletic genera were indicated by multiple taxon labels. Less frequent alternative topologies were indicated by dotted lines on the same tree.

AM.5.2 Phylogenetic software

- Modeltest 3.7

The executable <*Modeltest 3.7*> uses hierarchical Likelihood Ratio Testing (hLRT) to examine 56 nested models of molecular evolution (14 basic models which can be modified to include between-site rate heterogeneity: Shoemaker & Fitch 1989, Posada & Crandall 1998, Posada & Buckley 2004)). The program works in sequence from the less complex to the more complex models, reflecting the trade-off between under-estimation of change, and over parameterisation (Posada & Crandall 1998).

-MEGA 3.1: Minimum Evolution criterion

Distance-based analyses of alignments were performed in <*MEGA3.1*> (Kumar et al 2004) using the ME optimality criterion (Saitou & Imanishi 1989, Rzhetsky & Nei 1992). Within the ME analysis, <*MEGA*> allows the use of several different GTR based models, incorporating prior knowledge about parameters (from <*Modeltest 3.7*>) or assumptions about the data in order to estimate evolutionary change. Searches were performed using a close-neighbour-interchange (CNI) algorithm to examine the neighborhood of an initial Neighbour Joining (NJ) tree (distance-based method in which the tree is produced by a clustering algorithm rather than a search-and-optimality method: Saitou & Nei 1987). The topology with the smallest total branch length was selected (Nei et al 1998, Takahashi & Nei 2000). The program was instructed to delete missing data from alignments for pair-wise comparisons only, rather than the default

setting, which completely deletes all missing data. With this exception, all other parameters were set to default. All trees were rooted at the midpoint of the maximum sequence divergence and no outgroup was formally assigned; although *Pagurus* and *Aegla* were included in the taxon set.

-PHYLIP:DNAml settings

Maximum likelihood analyses of datasets were performed using <PHYLIP*DNAml*> (Hasegawa & Yano 1984, Hasegawa et al 1991, Felsenstein 1993, Felsenstein & Churchil 1996). Parameters for relative rates of transition and transversion mutations and equilibrium base frequencies were calculated in <*Modeltest 3.7*> for each alignment (see Results Section **A1**.3). The Gamma function was used to infer different rates of evolution at different sites if this were required (Yang et al 1994, Yang 1994, 1995, 1996, Felsenstein & Churchill 1996). This effectively removes the artificial assumption that all sites have the same rate of change. Global rearrangements were applied, which means that for the 'best trees' found, each of the terminal branches were sequentially removed and replaced to test that no new trees could be found with a higher likelihood. The tree was rooted using the consensus sequence of the out-group genus chosen in preliminary analysis of tree AT_A (as detailed in Section **A1**.3.9).

For all ME and ML analyses, confidence in the selected topology was assessed with a bootstrap analysis. One thousand iterations of the search algorithm were performed on replicate datasets produced by sampling with replacement from the original dataset. The proportion of times each clade was retrieved over multiple iterations was reflected in the bootstrap value (Table **A3**, Figs **A1**.3a, b). In <*PHYLIP*>, bootstrap searches were performed using the executable <*Seqboot*> (Felsenstein 1985).

-Bayesian analysis using MrBayes

<*MrBayes3.1*> is a program for the Bayesian estimation of phylogeny (Huelsenbeck et al 2001, Senn 2003, Beaumont & Rannala 2004). Bayesian inference of phylogeny is similar in principle to a maximum likelihood analysis; however, it incorporates prior knowledge of the distribution of tree topologies, as estimated over 2 x 1,000,000 iterations by Markov chain Monte Carlo (MCMC) in two parallel runs (Huelsenbeck & Ronquist 2001). The TE_B dataset was partitioned four ways (by gene) in the input (*Nexus*) file prior to implementation, which allows unlinked models and model parameters to be calculated for the different partitions. Following the manual of <*MrBayes 3.1*> (http://mrbayes.csit.fsu.edu/wiki/index.php/Manual), the number of

parameters (<*Modeltest3.7*>) was specified, but the parameter values were allowed to vary during the initial iterations (Huelsenbeck & Ronquist 2001). This approach is thought to provide a more conservative but more realistic posterior probability of each node (Raupach et al 2009). A number of initial iterations were discarded, until it was determined by inspection that the two parallel runs had converged on a family of topologies (split standard deviation <0.05). Trees selected from the remaining MCMC iterations were pooled to indicate the most probable overall topology. Confidence values indicate the probability of a particular node given the prior assumptions, the model parameters and the observed data (Huelsenbeck & Ronquist 2001). As in the ML analysis, the tree was rooted using the consensus sequence of the out-group genus chosen in preliminary analysis (as detailed in Section **A1**.3.9).

CHAPTER A1: MOLECULAR PHYLOGENY OF THE LITHODIDAE

A1.1 Aims and context

The Lithodidae have an enigmatic evolutionary history. Molecular evidence obtained by other authors indicates a strong and recent (13 Ma-25 Ma BP) relationship between fully-carcinised lithodids and shell-dwelling members of the genus *Pagurus* (Cunningham et al 1992). From this, it has been hypothesised that the un-calcified abdomen uniting the subfamily Hapalogastrinae reflects the retention of a primitive condition, and that 'primitive' groups from the shallow north Pacific were the seeding populations for the global deep-water expansion of the Lithodinae. This hypothesis remains a source of controversy (McLaughlin et al 2007).

More than 100 species are recognised from the subfamily Lithodinae; the majority of these belong to the globally distributed, predominantly deep-sea genera *Paralomis, Lithodes* and *Neolithodes* (Appendix A). With the exception of the genus *Glyptolithodes* from South America, these are the only genera of Lithodidae that are not endemic to the North Pacific (Zaklan 2002b).

The objectives of this chapter are to use gene-sequence data to:

- assess the hypothesis that the Lithodinae arose from ancestors with uncalcified abdomens in shallow-water of the North-East Pacific.
- investigate the monophyly and interrelationships of genera within the Lithodinae, especially the larger lithodine taxa: *Paralomis*, *Lithodes*, *Neolithodes* and *Paralithodes*.
- estimate the scale and minimum number of transitions from the shallow environment to the deep sea and vice versa.

A1.2 Synopsis of methods

More than 200 tissue samples of 21 identified species (and several unidentified specimens) were obtained from a variety of preserved and fresh sources. These were supplemented with sequence data from a further 17 lithodid and non-lithodid anomurans from the NCBI GenBank database. Three mitochondrial genes (Cytochrome oxidase I [COI], Cytochrome oxidase II [COII] and ribosomal DNA [16S]) and three nuclear regions (small subunit rDNA [18S], large subunit rDNA [28S] and internally transcribed spacer 1 [ITS1]) were amplified and sequenced. Sequence data were algorithmically aligned and then optically examined within each gene. Minimum Evolution (ME), Maximum Likelihood (ML) and Bayesian (BAY) probability criteria were used to score phylogenetic tree topologies. Trees were rooted

with a consensus of three *Aegla* sequences as the result of a preliminary investigation into the position of the Lithodidae with respect to other anomuran taxa.

A1.3 Results

A1.3.1 Extraction and Amplification

PCR products of expected lengths were produced using the Qiagen DNeasy blood and tissue protocol (Appendix Ci) for approximately 80% of freshly sampled (non-museum) specimens, and around 5% of museum specimens preserved using an unknown medium or method.

Of the thirty formalin-fixed lithodid tissue samples from which DNA was extracted using critical point drying (Palero et al. 2010; Appendix Cii), 18 failed to produce amplicons, 5 produced PCR products but were not successfully sequenced and 7 samples (23%) produced fully-sequenced PCR products (GenBank accession numbers: EU493266-EU493270, EU493272-EU493275 and EU493277-EU493278). The results obtained from a database search on GenBank using Megablast (BLASTN v2.2.18) showed that the sequences from formalin-fixed specimens were homologous to the available lithodid sequences.

A1.3.2 Base frequency homogeneity

Base frequency homogeneity tests showed no significant variation in base frequencies between taxa for 16S ($p=1.000$), ITS ($p=1.000$), 28S ($p=0.9988$) and COI ($p=0.991$) datasets. Any minor deviations in base frequency are not expected to affect phylogenetic reconstructions.

A1.3.3 COI

621 sites were included in the final alignment of the COI gene. The reading frame began on the 3rd position of the alignment and did not include any termination codons. Including changes between the ingroup and outgroup, 230/621 sites were variable. As would be expected in a protein coding gene, mutations are heavily biased onto the third position of the codon: there are 39 1st position changes, 3 2nd position changes, and 188 3rd position changes. The translated protein structure was verified using the NCBI *<BLASTP>* algorithm and it matched the product of functional COI genes in other organisms. ME trees produced separately for the first and third codon positions of COI showed that a similar phylogenetic signal could be retrieved from both (Fig **A1**.1). No insertions or deletions were found in either the ingroup or the outgroup sequences and so the alignment was unambiguous when inspected manually.

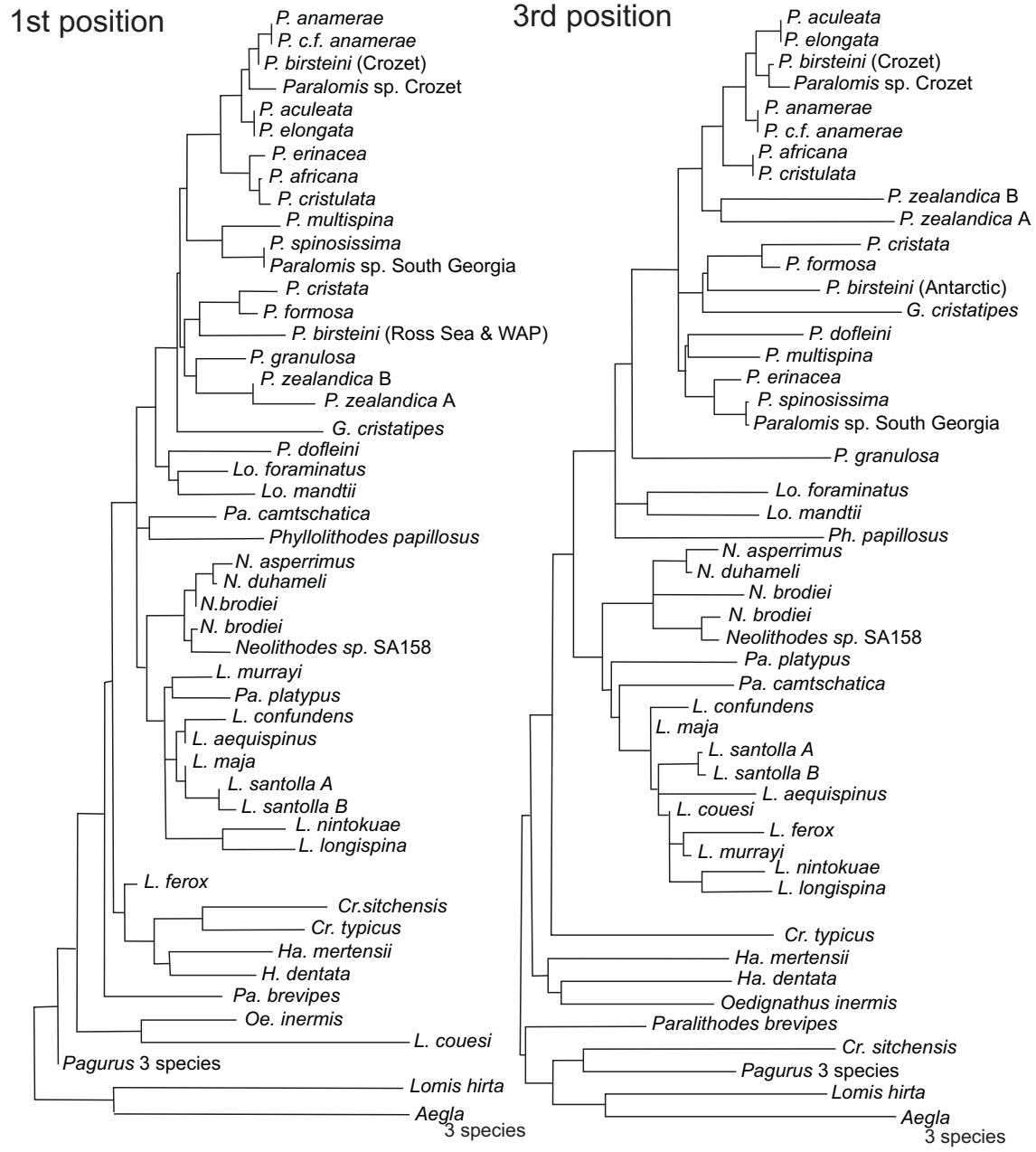

Figure A1.1 Minimum evolution trees produced in MEGA for COI codon positions 1 and 3. Trees were rooted at the mid-point of the maximum sequence divergence. Abbreviations: N= *Neolithodes,* L = *Lithodes* P= *Paralomis*, Pa = *Paralithodes*, Lo=*Lopholithodes*, Cr= *Cryptolithodes,* Ha= *Hapalogaster*, Oe= *Oedignathus,* G=*Glyptolithodes*, Ph= *Phyllolithodes*.

Analysis of the COI dataset in <*Modeltest 3*.7> indicated that a GTR model best describes the molecular evolution. Between-site rate heterogeneity was modelled by the Gamma function (shape parameter = 1.0879) with a proportion (0.5884) of invariable sites (GTR+I+G). Equilibrium base frequencies (A:0.3076 C:0.1676 G:0.1370 T:0.3878), number of substitution types = 6, Rate matrix = ([A:C 1.1574] [A:G 12.1127] [AT: 0.6581] [C:G 1.5420] [C:T 7.2343] [G:T 1.000]). For ME analysis, the best approximation to this model in <*MEGA 3.1*> is that of 6- parameter model, Tamura-Nei. The Gamma function with shape parameter 1.0 was used to model rate heterogeneity between sites. For ML analysis in <*PHYLIP DNAml*>, base frequencies, rate heterogeneity and Transition/Transversion (Ti/Tv) ratios are defined as above. Phylogenetic trees based on COI data alone are not figured, but confidence values for selected nodes are shown in Table **A3**.

A1.3.4 16S

16s amplicons were sequenced and aligned for 113 specimens. These were used directly in tree AT_A (Fig **A1**.2a) and then condensed into 48 consensus sequences, including those for out-group genera *Pagurus* and *Aegla*. When sequences were trimmed to the length of the shortest sequence, the resulting alignment was 402 bp; the longest sequence was 529 bp. Even though rDNA doesn't have the same reading-frame constraints as a protein coding gene, insertion mutations were absent from the in-group 16S sequences (except 2 single-base insertions in *Cryptolithodes sitchensis*). At least 7 separate regions of nucleotide insertion are present in outgroups, which added some ambiguity to the alignment process in some variable regions.

The model of evolution governing the 16S data for an alignment of all taxa (excluding *Emerita*) had two substitution parameters (HKY+I+G) with unequal base frequencies (A:0.3938 C:0.1067 G:0.1355) and between-site rate heterogeneity modelled by the Gamma function with a shape parameter of 0.2505, and a proportion (0.4282) of invariant sites. Ti/Tv Ratio=4.2248. In <*MEGA 3.1*>, this model is approximated by the Kimura 2-parameter model, with a Gamma function shape parameter of 0.2. In <PHYLIP*DNAml*>, parameters were defined as above. With the exception of the 'all-taxa' tree (AT_A, Fig **A1**.2a), confidence values for selected nodes on the 16S ME and ML trees are shown in Table A3.

A1.3.5 COII

Five out of 44 unique lithodid COII sequences had single frame-shift mutations and a number of stop-codons were produced when translating the alignment. These could have either been introduced through an error in sequencing (the polymerase adding

bases stochastically), or could indicate that this is not a functional copy of the gene. No frame-shift mutations were seen in the amplified copy of the COI gene: it is possible that these COII primers target analogous versions of the gene and potentially misleading phylogenetic signals are expected. 50 1st position changes, 15 (8 in ingroup) 2nd position, and 148 3rd position changes were seen in the alignment. Based on this evidence, COII was excluded from the 'total evidence' (TE_B) analysis.

The model most likely to explain the sequence evolution of the COII gene fragment is (HKY+I+G) selected by hLRT in <*Modeltest 3.7*>. It is a 2-parameter model (Ti/Tv Ratio = 4.3667) with unequal base frequencies (A:0.3498 C:0.1582 G:0.1228 T:0.3692) and between-site rate heterogeneity modelled by the Gamma function (Shape=0.6797) with a proportion (0.4661) of invariant sites. In <*MEGA 3.1*>, this model is approximated by the Kimura 2-parameter model, with a Gamma shape parameter of 0.5.

A1.3.6 ITS1

490 base pairs of ITS1 were amplified, and there was no ambiguity in the alignment process. Using <*Modeltest 3.7*>, the model most likely to reflect the molecular evolution of the lithodid ITS1 region was the single substitution rate model (Jukes-Cantor), which specifies equal base frequencies at equilibrium, equal probabilities of transition and transversion mutations and homogenous mutation rates across all sites in the amplified region. In the ME analysis in <*MEGA*>, the Jukes-Cantor model of evolution was used. In the ML analysis in <*PHYLIPDNAml*>, Ti/Tv was set to 1 and all other parameters were default.

A1.3.7 18S

In total, three point-mutations were observed in lithodids over 1836 bp of 18S rDNA. The V4 expansion segment (Fig **AM**.1b), was amplified in species from three lithodid genera (*Lithodes santolla*, *Paralomis formosa, P. elongata* and *Neolithodes brodiei*), but only a single point-mutation was observed. The low level of variation meant that the 18S rDNA gene was not targeted further for analysis.

A1.3.8 28S

An alignment of 28S gene fragments from 22 anomuran taxa, including 14 species of Lithodidae, indicated low levels of in-group variability in the 5' region (3/301 bp polymorphic: GenBank AF425344-59, Zaklan 2002a). Gene fragment 28SA (Fig **AM**.1a) includes the D1 expansion segment (Hancock et al 1988), and polymorphies occurred at 8/739 sites within four lithodine genera (GenBank AY596100.1,

AB193824.1, AB193821.1, HM020882-5). Fragment 28SB was variable at 25/683 positions, including base insertions in the sequence of *Lithodes santolla*. Gene fragment NURI had 3 polymorphic positions in 415 bp of the lithodine genome (GenBank HM020886-9).

60 specimens produced 30 unique sequences for the 28SB gene fragment, including 2 out-group consensus sequences (*Pagurus* & *Aegla*). No additional GenBank sequences for in-groups were available in this region, as this appears to be a novel use of these primers within the Lithodidae. The high degree of similarity between in-group sequences meant that the secondary structure of transcribed rRNA could be compared to the conserved arthropod structure. At least six regions of base insertion (or deletion) occur between the out-group and the in-group sequences, indicating a high level of divergence between these sequences in the anomura.

Using <*Modeltest 3.7*>, a 2 substitution type model (HKY+I, *Ti/Tv = 2.4685*) was the most likely to reflect the molecular evolution of the lithodid 28S gene fragment B. A high proportion (0.8484) of invariable sites and mutation rate homogeneity across the gene was indicated. Base frequencies= (*A:0.1984, C:0.2606, G:0.3160, T:0.2350)*. These parameters were then used where required for defining the model of evolution. In the ME analysis in <*MEGA*>, the Kimura 2-parameter model of evolution was assumed, and the Gamma function was not used to model inter-site rate heterogeneity.

A1.3.9 Out-groups

(Bootstrap values of tree AT_A [Fig **A1**.2a] indicated by *)

From the results of an ME analysis of all taxa for the 16S rDNA gene, a consensus of *Aegla* species *A. platensis*, *A. intercalata* and *A. neuquensis* was chosen to root subsequent ML and Bayesian analyses. Tree AT_A (Fig **A1**.2a) shows that *Pagurus* species, whilst being close to the monophyletic Lithodidae (*99), were themselves paraphyletic based on the 16S sequence. Results match with a hypothesised scenario (Fig **A1**.2b) in which a consensus sequence of *Pagurus* species should provide a good outgroup for this study. Nevertheless, a compromise was made in rooting the trees with *Aegla* species because of the less complicated relationship between them and the Lithodidae. The *Pagurus* consensus sequence was retained in all taxonomic sets and was used as a substitute to root analyses if no corresponding *Aegla* sequence was available. The *Emerita* sequences were particularly different from those of the Lithodidae, implying a distant relationship. *Emerita* was excluded from all other phylogenetic analyses to maximise graphical resolution for taxa within the Lithodidae.

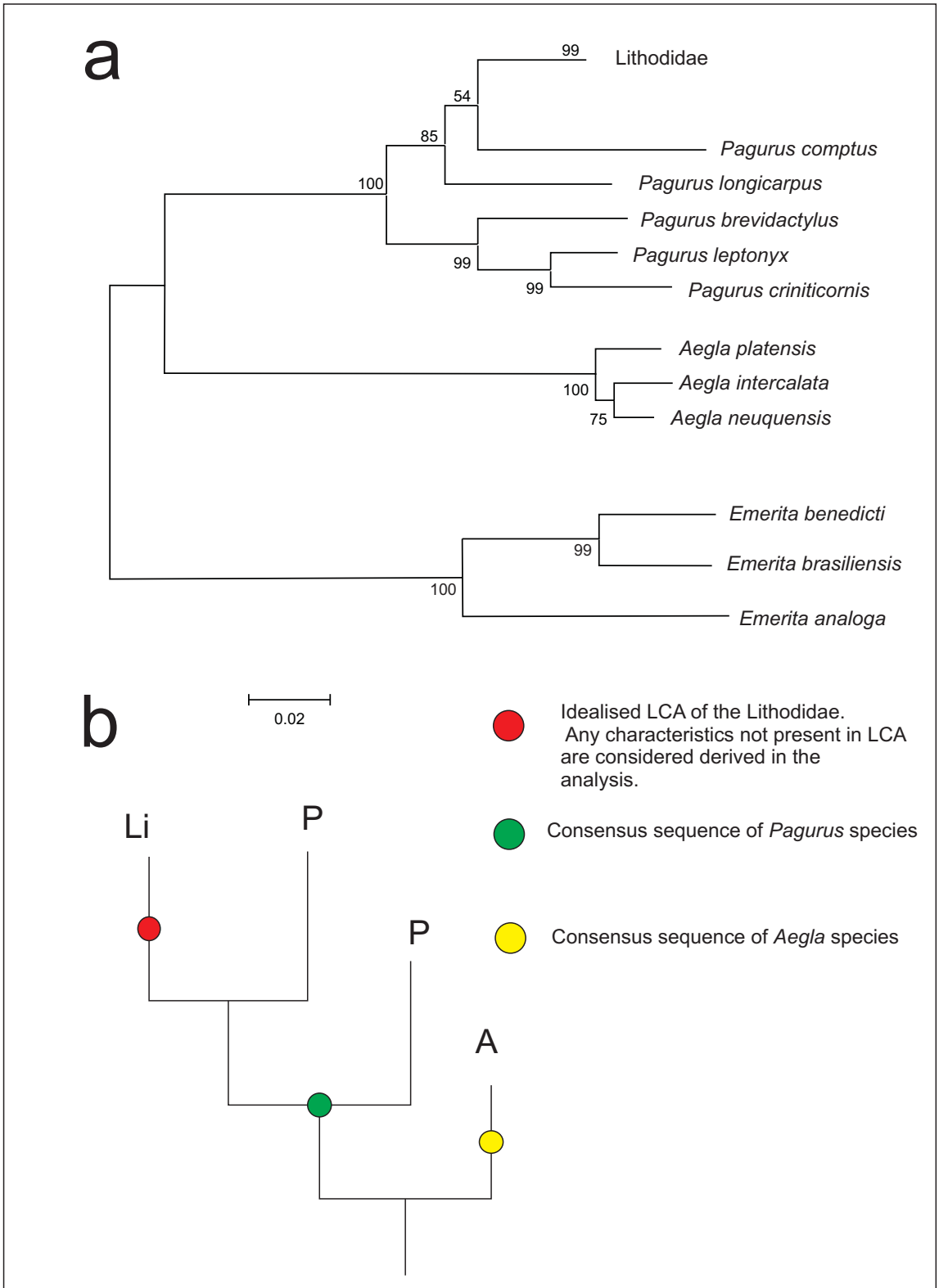

Figure A1.2 Preliminary investigation of out-groups using the 16S rDNA gene. **a)** AT_A tree. Produced using a close-neighbour interchange algorithm from an initial neighbour joining tree, using the minimum evolution (ME) optimality criterion. Analysis includes all taxa obtained for the 16S rDNA gene, but the lithodid lineage is condensed to a single taxon label. **b)** Schematic of a relationship between Lithodidae (Li), *Pagurus* (P) and *Aegla* (A), and the principle of producing an out-group consensus sequence.

A1.3.10 Genetic Variability within the Lithodidae

(Bootstrap values of tree AT_A [Fig **A1**.2a] indicated by *). The monophyly of clades within genera *Pagurus* (South American species *P. brevidactylus*, *P. criniticornis*, *P. leptonyx* *99), *Aegla* (*100) and *Emerita* (*100) was confirmed by the production of ME tree AT_A for the 16S gene (Fig **A1**.2a). Results for enumeration of polymorphic loci are summarised in Table A2.

Table A2. Number of single base polymorphisms between trimmed homologous alignments of parts of 5 genes (number of species in brackets).

Clade	**COI: 621 bp**	**16S: 402 bp**	**28SB: 582 bp**	**ITS1: 490 bp**	**COII: 570 bp**	**18S**
Pagurus: 3 South American species	N/A	53 (3)	N/A	N/A	N/A	N/A
Lithodidae: 40 species (10 genera)	219 (40)	68 (45)	N/A	57 (25)	181 (18)	N/A
Lithodinae (excluding *Cryptolithodes*): 35 species (7 genera)	198 (35)	53 (33)	19 (22)	46 (20)	158	3/1960 (3 genera: *Paralomis*, *Lithodes* and *Neolithodes*)
Neolithodes: 3 species	48 (3)	4 (3)	2 (3)	1 (3)	14 (2)	N/A
Lithodes: 9 species	48 (9)	17 (6)	0 (4)	17 (4)	68 (4)	N/A
Paralomis: 16 species	156 (16)	27 (15)	9 (13)	15 (8)	92 (9)	0/1960 (2)
Aegla: 3-8 species	74 (3)	25 (3)	17 (3)	N/A	N/A	6/1960(8)
Emerita: 3 species	135 (3)	61 (3)	N/A	N/A	N/A	11/1980 (*E. analoga, E. brasiliensis*)

A1.3.11 Total Evidence Trees [TE_B] = (16S+COI+ITS+28S)

Over 1000 replicates, ME trees generated for each gene independently did not yield a significantly different phylogenetic signal to that of the combined dataset ($p = 0.63$). This indicates that the data can be combined into a single alignment (TE_B) without introducing conflicting results.

When molecular evidence from fragments of COI, 16S, ITS1, 28SB were combined, <*Modeltest 3.7*> predicts the following model of molecular evolution (using hLRT): (HKY+I+G) is a 2-substitution rate model (Ti/Tv ratio = 3.7305) with unequal base frequencies (A:0.2862, C: 0.1995, G:0.1981, T:0.3162), and between-site rate heterogeneity modelled by the Gamma function (shape = 0.3470) and a proportion

(0.5318) of invariant sites. For the ME analysis in <*MEGA3.1*>, the Kimura 2-parameter model of evolution was assumed. For Maximum Likelihood analysis in <*PHYLIPDNAml*>, all parameters were taken from the above estimations. For Bayesian analysis, the number of substitution types, (COI:6, 16S:2, ITS:1, 28S:2) were indicated for each of 4 gene partitions (Bayes block included in Appendix D) values of model parameters were allowed to change during iterations of the algorithm (described in methods AM.5.1.5).

-Phylogeny results for analysis of the TE_B alignment

Confidence indicators (bootstrap values for ME and ML, posterior probabilities for BAY) from three analyses indicated are indicated by the bracket style (ME) [ML] {BAY}. Letters in bold square brackets refer to commonly resolved clades on the phylogenies: refer to figures (**A1**.3 a-c).

--Root of the tree

The ME tree (Fig **A1**.3a) is rooted at its mid-point, and so no outgroup is explicitly defined in the input data. In this case, *Lomis hirta* and *Aegla* species are paired (99) to the exclusion of the Lithodidae and *Pagurus*. The Lithodidae **[A]** are monophyletic in all topologies (93[100{0.89}]).

--Genera

Genera *Cryptolithodes* **[D]** (98[100{0.82}]), *Hapalogaster* **[E]** (82[95{0.92}], *Oedignathus inermis*, and *Paralithodes brevipes* are excluded from a clade **[G]** (67[90{0.61}]) containing the remaining *Lithodidae*. Relationships between these basal groups are ambiguous, because the ML, Bayesian and ME topologies do not agree whether the subfamily Hapalogastrinae **[C]** includes the (lithodine) genus *Cryptolithodes*. *Oedignathus* and *Hapalogaster* are sister taxa within clade **[C]** in the ME and Bayesian (51{0.81}) but not the ML topology, in which *Oedignathus* and *Cryptolithodes* are sister taxa [65]. *Paralithodes brevipes*, whilst being placed consistently outside a clade **[G]** uniting other lithodine genera, is placed alternately with the Hapalogastrinae **[B]** (63{0.81}) or at the base of the Lithodinae **[F]** [60] by different methods of analysis.

Monophyly of *Lithodes* **[K]** (55[72{0.97}]), *Neolithodes* **[J]** (99[99{1.0}]) and *Paralomis* (plus Glyptolithodes) **[M]** (98[56{1.0}]) are supported under all analytical methods. Support for a grouping of *Lithodes* with *Neolithodes* **[I]** (which is sometimes inclusive of *Paralithodes camtschatica* and *P. platypus*) is weak but present in all analyses (57[40{0.81}]). *Lopholithodes* is closely allied with

Paralomis+Glyptolithodes **[L]** in the ML and Bayesian analyses [99{1.00}], and is never included within the monophyletic *Paralomis* (+*Glyptolithodes*) taxon **[M]**.

The genus *Paralithodes* is represented by three species: *Paralithodes camtschatica, P. platypus* and *P. brevipes*. This genus is not supported as a monophyletic clade in any of the selected topologies. *P. platypus* and *P. camtschatica* are resolved as sister taxa in clade **[H]** under ML analysis [60]. *Neolithodes asperrimus* and *N. duhameli* are paired within clade **[N]** (99[99{0.98}]) to the exclusion of *N. brodiei*, and another Southern Pacific *Neolithodes* (species indeterminate) sample.

--Lithodes

Maximum Likelihood analysis resolves two groups within *Lithodes*; separating *L. maja, L. santolla* and *L.confundens* **[O]** [40{0.63}] from *L. murrayi*, *L. longispina*, and *L. nintokuae* **[Q]** (97[98{1.00}]). Within clade **[O],** South American species *L. santolla* and *L. confundens* are paired, forming clade **[P]** [99{1.00}]. *L. ferox, L. couesi, L. maja,* and *L. aequispinus* can not be resolved with confidence on the basis of these results, instead appearing in a polytomy at the base of the *Lithodes* clade **[K]** in both the ME and ML analyses. In the Bayesian analysis, *L. aequispinus* is allied with *L. nintokuae, L. longispina* and *L. murrayi* outside clade **[Q]** {0.85}; and *L. ferox, L. couesi* outside the clade of Atlantic *Lithodes*, **[O].**

--*Paralomis*

Paralomis elongata (paratype) is the sister group of *P. aculeata,* as indicated by clade **[R]** (100[100{1.00}]). There are no polymorphic sites in a comparison of 2110 bp of *P. elongata* and *P. aculeata* DNA. Clade **[R]** is nested within a larger clade of sub-Antarctic specimens **[S]** (99[99{1.00}]), including *P. anamerae* (caught by long-line fisheries in South Georgia); sample SA06 (morphological I.D. close to *P. anamerae*) in South Georgia; *P. birsteini* (sample SA147: Crozet); and *Paralomis* unidentified tissue sample (2 specimens: Crozet).

An 'African clade' of *Paralomis* (*P. elongata*, *P. africana*, *P. cristulata*) is supported by ME analysis **[Y[** (72), but not by other optimisation criteria. ML analysis and Bayesian inference, produce topologies in which *P. africana* (+*P. cristulata*) are the sister taxa of clade **[S]** within a larger clade **[T]** [98{1.00}]. Clade **[U]** (Figs **A1**.3 b, c) includes *P. erinacea* as sister taxon to clade **[T]** with a high degree of support in the ML and Bayesian analyses [80{0.99}].

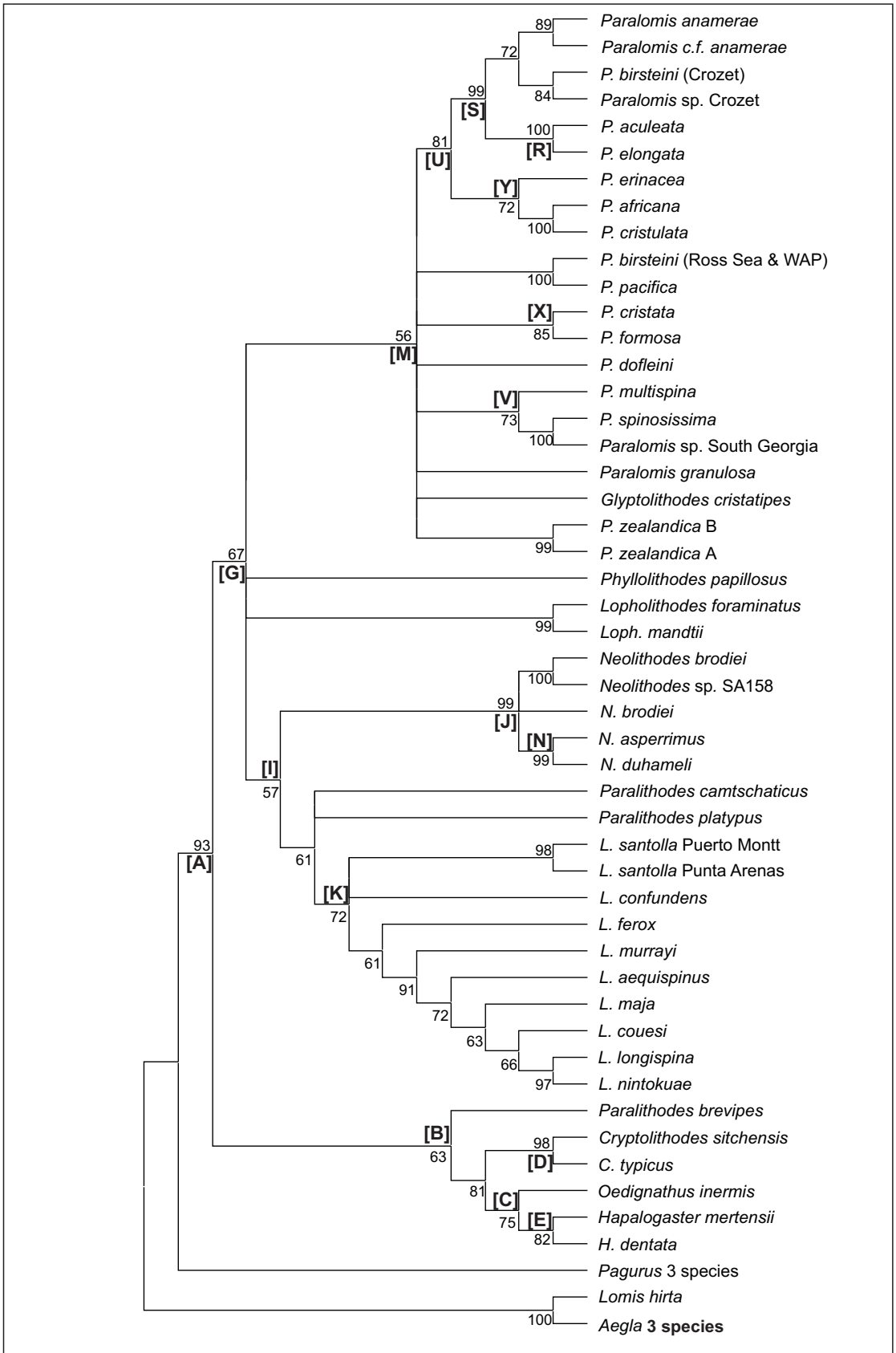

Figure A1.3 Trees produced from a total evidence alignment (TE_B) of genes ITS1, 16S, COI and 28SB. Terminal taxa are consensus sequences produced from multiple specimens using IUPAC ambiguity codes. Where sequences within species differ consistently at multiple loci species are split into multiple labels. Letters at nodes refer to clades discussed in the text. **a)** Minimum evolution tree produced in MEGA 3.1. Mid-point rooted. Numbers at nodes are bootstrap values (1000 replicates).

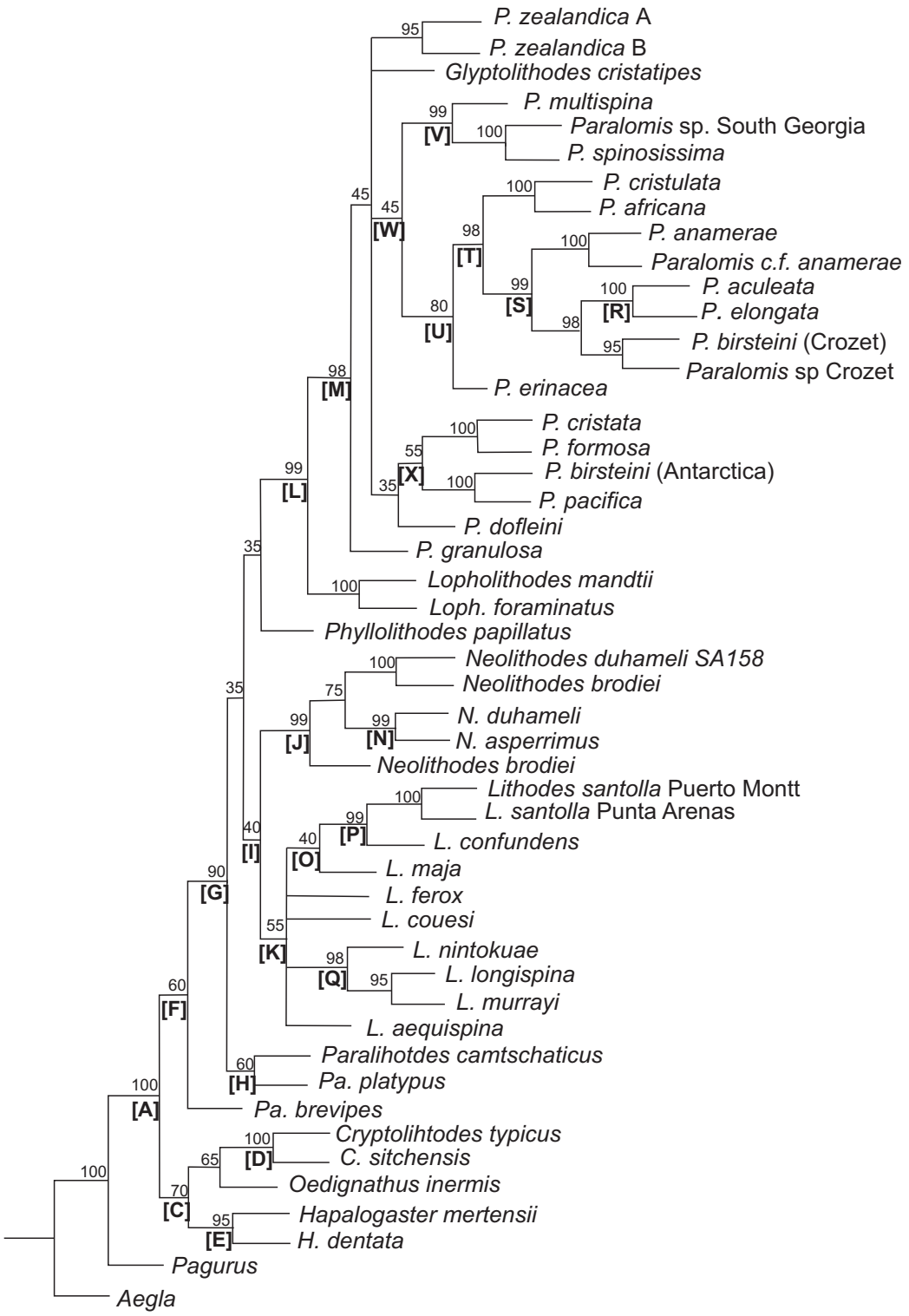

Figure A1.3 cont
b) Maximum likelihood tree produced in *PHYLIPDNAml*. Rooted using a consensus sequence of 3 *Aegla* species. Numbers at nodes are bootstrap values (1000 replicates).

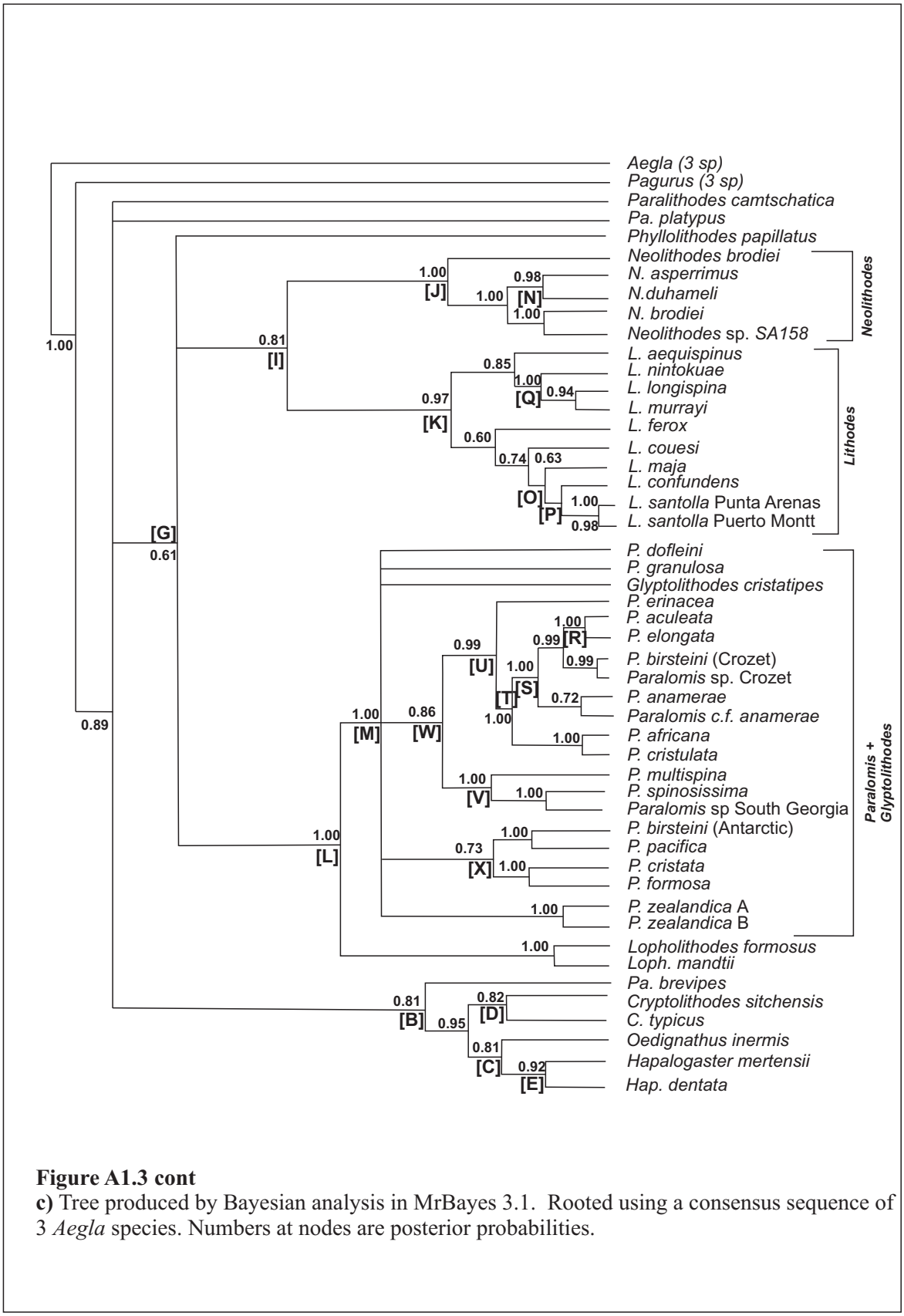

Figure A1.3 cont
c) Tree produced by Bayesian analysis in MrBayes 3.1. Rooted using a consensus sequence of 3 *Aegla* species. Numbers at nodes are posterior probabilities.

Paralomis spinosissima is the sister taxon of *Paralomis multispina* **[V]** (73[99{1.00}]), although the position of this clade is ambiguous within *Paralomis* as a whole. There is some indication that these species might be associated with clade **[U],** to form clade **[W]** [45{0.86}].

A derived relationship is indicated between *Paralomis formosa* and *P. cristata* in clade **[X]** (85[100{1.00}]), as well as a similarity between an Antarctic specimen of *Paralomis birsteini* and *P. pacifica* sequences from GenBank. Several other species, *Glyptolithodes cristatipes, P. dofleini, P. zealandica, P. granulosa,* are always included within *Paralomis* **[M]**; however, these species are never grouped with sufficient confidence alongside any of the other species included in the analysis.

64/1523 bp (4.2% of bases) are polymorphic when *P. birsteini* from the Crozet islands in the southern Indian Ocean, is compared with *P. birsteini* from the Ross Sea and Bellingshausen Sea (SA101+SA85). These two strains of the *P. birsteini* morphotype do not form a monophyletic clade based on the genes sampled. In fact, fewer loci are polymorphic (1.57% of bases) when *P. birsteini* from Crozet is compared with *P. aculeata* (also from Crozet).

A1.3.12 Overview of phylogenetic signal from individual genes

Analyses are heavily based on the models used, and many different assumptions must be incorporated into the models. Many trees were produced during this study: not all of which have had their results examined explicitly in the text, including those produced for individual genes. It is important to consider the effects of the assumptions, and of the difference in information provided by each gene as an evolutionary unit. An overview is provided in Table A3. The phylogenetic signal of the in the TE_B alignment (Fig **A1**.3) appears to be derived predominantly from the COI gene, which has the highest level of sequence divergence within the group. Other genes support some of the very strong divisions (between genera, or pairs of terminal taxa), but conflict exists at some of the intermediate nodes. Although there are gaps in species sampling and gene sampling, the topology of the tree should not change when more species are added, especially in well supported groupings.

Table A3. Confidence indicators at nodes for phylogenetic analysis of individual genes. KEY: (ME [ML]) **(-)** = unresolved; X = Rejected.

Clade labelled on Fig A1.3	**COI**	**16S**	**28SB**	**COII**	**ITS1**
[C] Clade containing *Oedignathus* and *Hapalogaster*: with or without *Cryptolithodes*.	(-[-])	(53[X])	N/A	N/A	N/A

[G] *Lithodinae* exclusive of *P. brevipes*	(91[38])	(-[X])	N/A	(X)	(71)
[I] *Lithodes* + *Neolithodes*: with or without *Paralithodes camtschatica* and *P. platypus*.	(75[-])	(-[-])	(58[60])	(X)	(X)
[J] *Neolithodes*	(98[81])	(-[45])	(98[88])	(99)	(98)
[K] *Lithodes* (and *P. camtschatica / P. platypus*)	(63[47])	(-[-])	(95[43])	(53)	(91)
[M] *Paralomis* (and *Glyptolithodes*)	(66[60])	(X)	(60[36])	(-)	(55)
[N] *N. asperrimus* + *N. duhameli*	(99[74])	(53[X])	(81[77])	(99)	(-)
[O] *L. maja* + *L. confundens* + *L. santolla*.	(-)	(X)	N/A	N/A	N/A
[P] *L.san*tolla + *L. confundens*	(-[34])	(79[83])	(-[-])	(60)	(97)
[Q] *L. nintokuae* + *L. longispina* + *L. murrayi*	(68)	N/A	N/A	N/A	N/A
[R] *P. elongata* + *P. aculeata*	(100[97])	(98[97])	(-[-])	(67)	(-)
[S] *P. elongata* + *P. aculeata* + *P. anamerae*.	(96[92])	(-[X])	(-[-])	(-)	(-)
[T] *P. elongata* + *P. aculeata* + *P. anamerae* + *P. africana* + *P. cristulata.*	(X[X])	(-[-])	N/A	(-)	(-)
[U] (**[T]** + *P. erinacea*)	(66[71])	(-[X])	N/A	(X)	(-)
[V] *P. multispina* + *P. spinosissima*	(53[29])	(99[93])	N/A	N/A	(81)
P. cristulata + *P. africana*	(99[79])	(96[98])	(-[-])	N/A	(64)
[W] ([U] + [V])	(-[-])	(-[-])	(-[-])	(X)	(55)
P. formosa + *P. cristata*	(99[97])	(-[-])	N/A	N/A	N/A
[X] *P. formosa* + *P. birsteini* + *P. cristulata* + *P. pacifica*	(46[-])	(-[-])	(-[-])	(X)	(92)
Lithodes + *Paralithodes camtschatica* + *P. platypus*	(63[-])	(-[-])	(-[X])	N/A	(-)
P.multispina + *P. spinosissima* + *P. erinacea*	(X[X])	(-[-])	N/A	N/A	X

A1.4 Discussion

A1.4.1 Mutations Rates within the Lithodidae

The number of polymorphic loci in the 5' half of the 28S gene, and the V4 region of the 18S gene was so low that the study of these genes was discontinued to economise on resources. A low level of sequence diversity within the Lithodidae is indicated; however, there is only incidental evidence to suggest that the expected levels of variation should be higher (Nelles et al 1984, Crease & Taylor 1998, Held 2000). A like-with-like comparison of mutation rates between different lineages is almost impossible without geological calibration for the age of the taxon (which we don't have for the Lithodidae).

For a homologous alignment of the 16S gene, a conservative estimate of expected amounts of variation was taken from monophyletic groups within the genera *Pagurus*, *Aegla* and *Emerita* (I emphasise the comparison of genus-level anomuran taxa with the **whole sub-family** Lithodinae). For 402 (in-group) bp of the 16S gene, the variation within a monophyletic clade of South American *Pagurus* was equal to that found within the whole Lithodine sub-family, and 10 times the variation found within genus *Neolithodes*. The same degree of disparity was found within three species of *Emerita*; however, three species of *Aegla* had the same number of variable sites as the 15 tested species of the genus *Paralomis*. In the 18S gene, there were 3 variable positions between three Lithodine genera, but 11 within *Emerita* and 6 within *Aegla*. Disparity was less marked in the COI gene and comparisons were not made for 28S, COII or ITS. These results are not conclusive, but there is an indication that the Lithodinae have an atypically low genetic variation for such a large (and diverse) anomuran taxon. This could be evidence of a number of scenarios:

- a low rate of molecular evolution as a product of temperature-related change decreased enzymatic activity, decreased or less efficient DNA replication rates, and increased generation times experienced at low temperatures (Bargelloni et al 1994, Martin 1999); alternatively, it could reflect a lineage-specific mutation rate that is not linked to temperature (Held 2001).
- a relatively recent radiation.
- a residual level of gene-flow tending to increase the homogeneity of related species.

A1.4.2 Relationships between lithodid genera

Of those studied, all lithodid genera are monophyletic as currently defined, with the exception of *Paralithodes* (see below), and *Paralomis*, which includes the single

species of genus *Glyptolithodes*. *Paralomis, Glyptolithodes* and *Lopholithodes* are all lithodids with compact, well calcified carapaces, and calcified plates on their abdominal segments (as opposed to nodules of calcification like in *Lithodes*, *Paralithodes* and *Neolithodes*; or uncalcified plates like those present in the Hapalogastrinae). *Glyptolithodes* occurs off the coast of Chile and has a known bathymetric range of 250-800 m. *Lopholithodes* species *L. mandtii* and *L. foraminatus* diverge outside, but close to the base of the clade containing all sampled *Paralomis* and *Glyptolithodes* species.

The arrangement of the genera does not provide conclusive evidence for or against the 'hermit to king' (Cunningham et al 1992, Zaklan 2002a) or 'king to hermit' (McLaughlin & Lemaitre 1997) theories, nor was that the aim of the study. The data indicate that under the strict definition of the Lithodinae (including genus *Cryptolithodes*), the subfamily is probably paraphyletic (Fig **A1**.3a-c). This is a tentative confirmation of the evidence given by McLaughlin et al (2004, 2007) that the soft abdomen of the Hapalogastrinae is not an ancestral feature (*Cryptolithodes* has a fully calcified abdomen with the fewest tergal plates of all Lithodidae). Nevertheless, *Cryptolithodes* and the Hapalogastrinae belong to a lineage that diverged from the other Lithodinae **[F]** at the base of the lithodid stem; these data indicate that a shallow water, North Pacific habitat and planktotrophic larval feeding mode are plesiomorphic features of the Lithodidae (Schematic tree TE_C, Fig **A1**.4).

A1.4.3 <u>*Paralithodes*</u>

There are six species included in the genus *Paralithodes* (Appendix A), three of which are sampled here: *P. brevipes*, *P. camtschatica*, *P. platypus*. The group is unified morphologically by having five plates rather than three on the 2nd segment of the abdomen, and has no reduction of the antennal acicles. Small eggs (indicative of planktotrophic larval development) are shared between *Paralithodes brevipes*, *P. camtschatica*, *P. platypus* and several other North Pacific genera and are probably a plesiomorphic feature. Any derived morphological similarities between *P. camtschatica*, *P. brevipes* and *P. platypus* are contradicted by the evidence from their genetics that they are paraphyletic. Data intriguingly corroborate pre-cladistic theories developed by Bouvier (1895) and Makarov (1938) that predict the paraphyletic status of the genus *Paralithodes*, and specifically the closer relationship of *P. camtschatica* to *Lithodes* than to *P. brevipes*. The results of this analysis show that *P. camtschatica* and *P. platypus* are weakly allied with the *Lithodes* and *Neolithodes* genera.

A1.4.4 *Neolithodes*

A markedly low within-genus mutation rate was observed for all genes sampled from specimens of *Neolithodes* (Table A2). This suggests that either the three species sampled in this study are, by chance, particularly closely related within *Neolithodes*; or that these genes evolve more slowly in *Neolithodes* than they do in other genera.

Neolithodes asperrimus occurs around the cape of Africa (from northern Namibia to Madagascar), at depths of 518-1050 m. Around 2000 km south of the cape, *N. duhameli* is known from the Crozet islands 620-1500 m. *N. brodiei* is known from the Pacific islands of Vanuatu 950-1250 m (Appendix E). All three of these species are characterised within *Neolithodes* by having a large number of spinules on the carapace and all appendages. It is notable that of these three species, the two that are geographically closest are the most closely related.

A1.4.5 *Lithodes*

The structure of the *Lithodes* clade is not well resolved. Analysis of the same dataset produces a number of contradicting topologies. *L. murrayi* and Pacific species *L. nintokuae* and *L. longispina* are typically separated from the Atlantic species *L. santolla, L. confundens, L. ferox* and *L. maja*. *L. murrayi* shares a morphological affinity with *Lithodes* species from the Central Pacific and Indian Oceans (*L. longispina, L. richeri*), rather than with those from the North East Pacific or Atlantic (*L. aequispinus, L. santolla*) (Section **B2**). *L. murrayi* is, however, currently considered to have a wide distribution around the Southern Ocean: reported from Crozet (as sampled here), as well as the Bellingshausen Sea (Garcia-Raso et al 2005), and morphological similarities are strong with *L. turkayi* from the Scotia Sea. *Lithodes ferox* is found off the coast of Namibia, and shares a number of morphological features with *L. murrayi* which are discussed elsewhere (Section **B2**). The separation of *Lithodes murrayi* and *Lithodes ferox* suggests that the common ancestor of these two groups possessed morphological characteristics that these two now share. It is noteworthy that *L. maja* is placed close to *L. santolla* and *L. confundens* in the TE_B ML and Bayesian trees, since these are all Atlantic species from northern and southern high latitudes respectively.

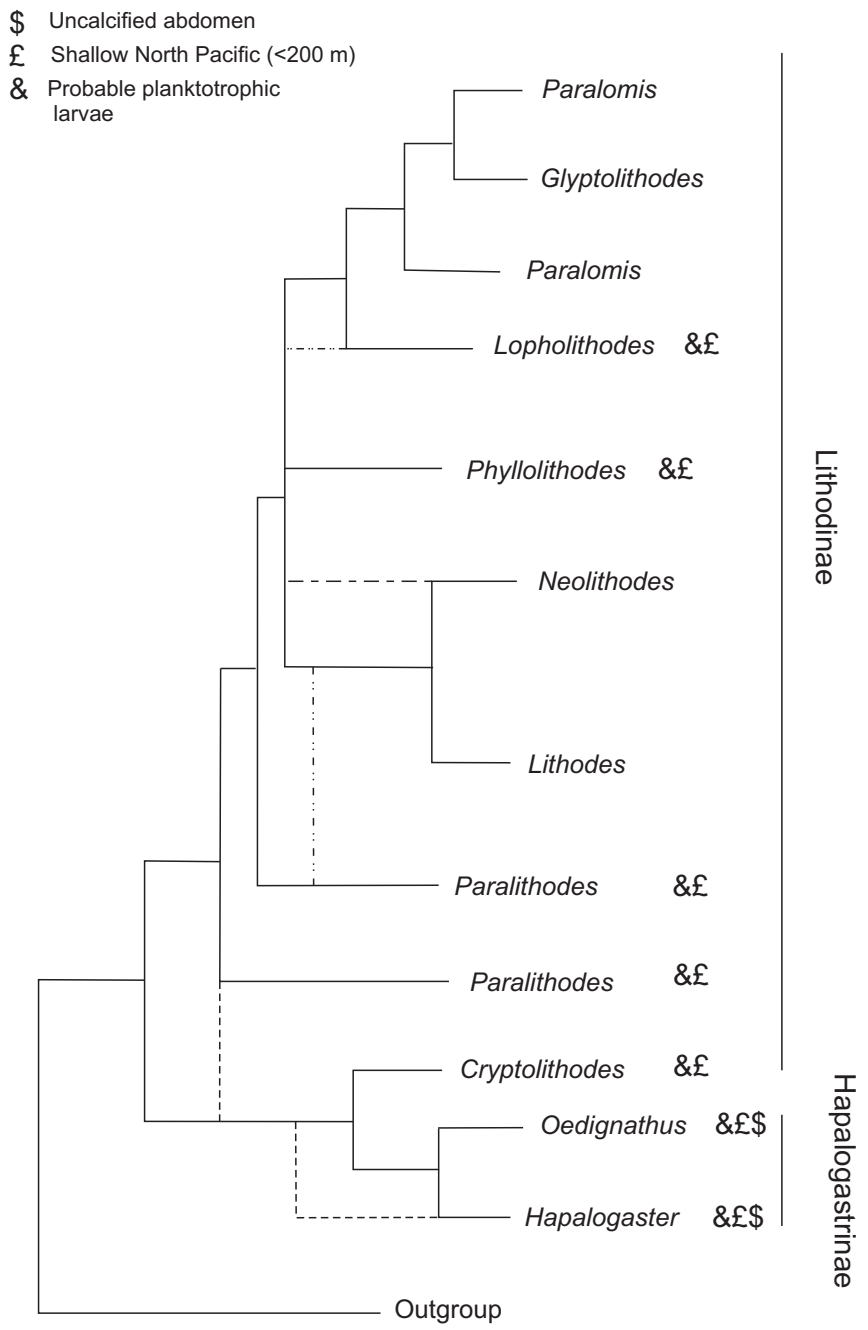

Figure A1.4 Schematic of the results of ML, ME and BAY analyses for alignment TE_B. In this tree, TE_C, species within monophyletic genera are condensed to a single taxon label, and polyphyletic or paraphyletic genera are indicated as such by multiple taxon labels. Less frequent alternative topologies are indicated by dotted lines on the same tree.

Lithodes santolla is morphologically similar to *L. confundens*, primarily based on the absence of a prominent mid-rostral spine, and this feature distinguishes them from many in the genus (Macpherson 1988a). The distinction between the species is based on the number and size of spines on the dorsal carapace and articles of the walking legs (which are larger and fewer in *L. santolla*). A survey of collected knowledge on the distribution of the two species (Appendix E) indicates that they have an overlapping distribution in and around Patagonia (South America). Information obtained in this study shows a consistent genetic difference between individuals belonging to the two species. There also appears to be two 'hapalotypes' of *Lithodes santolla*: one from individuals sampled around Puerto Montt (west coast Chile, 40° S), and one from individuals sampled at Punta Arenas (Straits of Magellan). The two strains of *Lithodes santolla* are more closely related to one another than either is to *Lithodes confundens*. The Straits of Magellan consist of several basins with hydrological and geological boundaries between them (Brambati et al 1991, Panella et al 1991, Antezana et al 1992). In several places, shallow sills constrain water exchange to the upper 40 m; it is possible that there is some restriction in the level of gene flow between the shallow water (10-212m) populations of *Lithodes santolla* from the West Coast and those in the central parts of the Straits of Magellan (Antezana 1999). Samples of *Lithodes confundens* were obtained from two locations (unfortunately neither of them the same as *L. santolla* sample sites): Cabo San Sebastian (0-10 m), on the Eastern coast of Argentina, and further (and deeper: 162 m) off shore on the Argentinean Plateau.

A1.4.6 *Paralomis*

61 species (including *Glyptolithodes cristatipes*) are currently recognised from within the genus *Paralomis*. Molecular data have been obtained for 16 of these species, broadly representing the total distribution of the genus throughout most of the world's oceans. Ancestral relationships at the base of the *Paralomis* clade have proved difficult to reconstruct based on these data. Pacific species *P. zealandica*, *Glyptolithodes cristatipes*, *P. dofleini*, and South Atlantic species *P. granulosa* in particular are not close enough to any other sampled species for ancestral similarities to be recognised. This perhaps reflects gaps in sampling in the Pacific region, which is known to have a high morphological diversity of Lithodidae (Appendix E, Section **B**). From this basal polytomy, two or three larger clades are resolved (**[V, U, X]** or **[W, X]**). Clade **[X]** contains an apparent assortment of North Pacific and South Atlantic *Paralomis*, and strongly implies a relationship between *P. formosa* and *P. cristata* that does not seem to reflect a distinct morphological or distributional similarity (although see Section **B3**).

West African species *P. erinacea*, *P. africana* and *P. cristulata* diverge at the base of a second clade, **[U]**. The recognised ranges of *P. africana* and *P. cristulata* have been recently expanded by explorations off the coast of Mauritania (courtesy of Ana Ramos, Vigo) and videos from the Serpent drilling projects off Nigeria (courtesy of Dan Jones, NOCS). Crabs with morphologies similar to *P. africana* and *P. cristulata* are now known from locations all along the coast around equatorial western Africa, around 1366 m deep off Nigeria, and 1500 m off Mauritania. This extends the previously recorded southern distribution of *P. africana* substantially. It also means that the two groups have an adjacent, if not overlapping distribution in this area. Molecular evidence supports a very close genetic relationship between these species, which can be distinguished by the form of lateral spines on the legs and carapace. These appear as strong crests in *P. cristulata* but several spines in *P. africana* (Macpherson 1988a).

Paralomis erinacea has a broadly overlapping range with *P. cristulata,* and was found alongside this species in Mauritania. It is morphologically quite different to the two other African species: most notably in the presence of spines uniformly covering the carapace, each with many long setae around the mid portion of the spines (Section **B1**). The original description (Macpherson 1988a) states that *P. erinacea* is close to *P. spinosissima* from the South Atlantic, with its carapace covered uniformly in large spines. *Paralomis erinacea*, however, does not have an obviously enlarged spine in the mid part of its gastric region, which (among other features) distinguishes it from *P. multispina* and *P. spinosissima.* In addition, the setae on the spines of *P. erinacea* are of a substantially different form to those in the later species (Section **B1**).

A consistently well resolved part of the tree, within clade **[U]** contains specimens exclusively from the sub-Antarctic region of the Atlantic and Indian Oceans at latitudes above 45° S **[S]**. *P. anamerae, P. aculeata* and *P. elongata* have distributions around isolated islands and seamounts at the latitudes associated with the eastward flowing Antarctic circumpolar current (Appendix E). The close genetic relationship between these groups suggests that they are not as isolated as their patchy distribution would suggest. No monophyletic group exists containing all southern high latitude *Paralomis* species; *P. formosa*, *P. granulosa* and *P. spinosissima* from sub-Antarctic waters all resolved elsewhere on the tree.

Known from opposite ends of the globe, *P. spinosissima* and *P. multispina* (clade **[V]**) certainly do not have an adjacent distribution (Appendix E). The tissue sample of *P. multispina* used in this study was taken from a preserved specimen found in waters off Japan (and also sequences from GenBank), although the species is known throughout the Bering Sea, and from the coast of North America between 600-1500 m. *P.*

spinosissima is known from the Scotia Sea and the South Atlantic, as well as from waters south of Cape Horn (162-1200 m), with distribution skewed towards the shallower end of this range (Purves et al 2003). Evidence suggests a close ancestral relationship between the two species.

P. multispina and *P. spinosissima* have a uniform coverage of spines across the carapace and legs, which in adults have an oblique face at the apex, with a ring of setae around the tip (Section **B1**). They both have 3-5 large, pointed spines without setae emanating from the gastric and branchial regions, and also from the lateral margins and legs. Tissue samples from preserved specimens of *P. phrixa* from the western coast of Peru (815-860 m) did not yield any good quality DNA, and no genetic data was obtained for this species. *P. phrixa* does, however, have spines and aspects of morphology of a similar form to *P. spinosissima* and *P. multispina*. Its intermediate distribution bridges the geographic gap between the North Pacific and the South Atlantic, and implies a radiation of this group along the western coast of the American continent.

-Spines: A plesiomorphy?

Presence or absence of a continuous coverage of spines is an obvious morphological trait by which *Paralomis* can be classified. There are several heavily spined *Paralomis* species in the global oceans, only three of which have been sampled for the genetic study, although most have been examined for morphological traits (Section **B3**). *P. bouvieri* from the Barents Sea, *P. hystrix* from Japan, and *P. aspera* (and similar species *P. makarovi* – described Hall & Thatje 2009b, Appendix F) are all distinguished based on many aspects of morphology, including spine form on a microscopic level (Section **B1**). If *P. erinacea* does have a monophyletic relationship with *P. anamerae* to the exclusion of *P. spinosissima* **[U]**, then either the common ancestor of this lineage **[W]** was covered in spines, or the condition has arisen separately in at least two lineages.

-Paralomis granulosa

On the strength of evidence from many genes, *P. granulosa* is distantly related to all of the other *Paralomis* species examined in the genetic study. The Magellanic fauna is thought to be relatively young, as until recently the area was glaciated and had no marine influence (McCulloch et al 2000, Hulton et al 2002). *P. granulosa* is also known from the Falkland islands, and from deeper waters (100-150 m) between the Falkland islands and the Straits of Magellan (Appendix E); however, it shares neither strong morphological nor genetic links, with any of the currently known Scotia Sea *Paralomis*. No west-coast *Paralomis* species were sampled for this study, but it might

be hypothesised that the ancestral links of *P. granulosa* are with deeper (400 m +) *Paralomis* on the continental slopes of northern Chile, where a wide variety of species are known. It should be mentioned, however, that the morphology of *P. granulosa* is strongly influenced by (or adapted to) the shallow water habitat in which it lives (Anger et al 2003).

-Paralomis birsteini

Specimens of *P. birsteini* have been sampled from populations in the Ross Sea, Bellingshausen Sea, and southern Indian Ocean. These specimens conform to the original species description (Macpherson 1988a, Ahyong & Dawson 2006), based on personal examination of 10 specimens covering these three locations.

Analysis of the COI, 16S, 28S, ITS genes in the a Bellingshausen sea specimen of *Paralomis birsteini* (SA101), and a Ross Sea specimen (SA85), in comparison with several Crozet specimens suggest that gene flow within this morphotype is limited or absent between the Southern Ocean and Crozet populations. Cryptic speciation has been previously discovered in other Antarctic taxa with limited dispersal potential (Held & Wägele 2005, Raupach & Wägele 2006); however, the level of variation between these populations seems to surpass a cryptic speciation event. Within the context of the global diversity of genus *Paralomis*, it seems that these populations are not closely related. The morphological similarities between Indian Ocean (Crozet) and Southern Ocean (Bellingshausen Sea, Ross Sea: similar to one another) examples of *Paralomis* are not reflected in genetic markers. It is possible that these populations have been mistakenly unified as a species, and are in fact similar by convergence. Otherwise, a study including greater sample numbers from each of these populations might be able to identify multiple genotypes at each location.

A1.5 Conclusions

- There are indications of lower than expected levels of mutation within the Lithodidae, and a thorough investigation of this phenomenon will be proposed for further work. This could indicate a recent common ancestor to the extant group, or a slow rate of molecular evolution in the Lithodidae.
- The Lithodinae as defined to include North Pacific genus *Cryptolithodes* may be paraphyletic, with the Hapalogastrinae and *Cryptolithodes* as sister taxa. This implies that the soft-bodied abdomen of the Hapalogastrinae might not be plesiomorphic for the Lithodidae.

- *Paralomis*, *Lopholithodes, Phyllolithodes, Lithodes* and *Neolithodes* share a common ancestor, from which the North Pacific Hapalogastrinae did not descend. Lithodid ancestors are likely to have had a north Pacific, shallow water distribution and to have had planktotrophic larvae.
- North Pacific genus *Paralithodes* is paraphyletic; *P. brevipes* is the most basal member of the genus (as sampled) while *P. camtshaticus* and *P. platypus* are more closely related to the genera *Lithodes* and *Neolithodes*.
- Genera *Lithodes*, *Neolithodes* and *Paralomis* (as sampled) are monophyletic if *Glyptolithodes* is included within *Paralomis*. *Lopholithodes* is closely related to, but not included within the *Paralomis* genus.
- *Paralomis* is divided into at least two major lineages: one containing South Atlantic, west African, and Indian Ocean species, and the other containing Pacific and South American species. Several species of *Paralomis* do not resolve consistently with any other groups sampled, implying a complex and possibly rapid global evolution early in the history of the genus.
- Relationships within the *Lithodes* genus vary between analytical methods, suggesting that conclusions may not be stable. Consistently, however, Indian Ocean and Pacific forms – *L. murrayi, L.longispina* and *L. nintokuae* form a group separated from Atlantic species such as *L. santolla*, *L. confundens, L. maja* and *L. ferox*.

Section B: Using morphology to delimit, identify and relate species

BO: SECTION INTRODUCTION AND DEVELOPMENT OF METHODS

BO.1 Defining and delimiting species

Huxley (1942), a pioneer of the 'Modern Synthesis' of evolutionary theory, describes the species problem succinctly: "although the degrees of discontinuity represented by good species are such that borderline cases are rare, there can not be any hard-and-fast distinction between a species and a subspecies, since in many instances one arises gradually out of another in the course of evolution; it is a matter of taste and convenience where the line is drawn." As discussed in the main introduction, the philosophy of the nature of species and speciation is complex; nevertheless, 'species' as cohesive units have an important practical role in biodiversity and biogeographical studies (Wheeler 1995, Carcraft 1997, Mace 2004). Therefore, it is important that species can be individually defined in an unambiguous way.

BO.1.1 The concept of a holotype

Practical definitions of zoological morphospecies assign a taxon name to a single specimen (holotype) or series of specimens (syntypes). This 'name-bearing type' is defined in the international code of zoological nomenclature as 'that which provides the objective standard of reference whereby the application of the name of a taxon can be determined' (ICZN 1985). As such, the holotype does not necessarily represent a 'typical' member of the species, nor does it have to delimit the total variation found within the taxon, which may not be known at the time of description. As species definitions refer formally to only a few individuals, it is important to recognise and describe the full scope of variation when further evidence becomes available.

BO.1.2 Characters variant within species: ontogeny

Significant changes with growth account for a major source of polymorphism within species. One example is a progressive change in carapace ornamentation, which has been noted by several authors for the Lithodidae (Haig 1974, Takeda 1974, Ingle & Garrod 1987, Macpherson 1988a, 1990, 2008). "The clear difference between juvenile and adult lithodids has been pointed out, and illustration is strongly recommended" Macpherson (2008). This phenomenon occurs in other decapod families, such as in *Cancer pagurus* Linnaeus, 1758, which displays progressively fewer features on its carapace in successive moults, from crab stage 1 to adults (Ingle 1981). Particularly in members of the lithodid genus *Neolithodes*, variation in spine length and density

between juveniles and adults makes identification to species level problematic – especially when a whole growth series isn't available for comparison. In descriptions of several species of the genus *Neolithodes*, the ontogenetic change itself is mentioned as a characteristic for identification (e.g. *N. agassizii* Smith 1882, *N. diomedeae* Benedict 1894, *N. asperrimus* Barnard 1947: in Macpherson 1988a). Differing growth stages can usually be unified as a single species using features other than the spines and tubercles; however, the microscopic changes often have substantial effects on the macroscopic appearance of a specimen. The identification process would be enhanced by increasing the available knowledge about variation within species.

BO.1.3 Characters variant within species: Environmental damage

Variation in carapace ornamentation within a moult stage caused by the erosion of spines, breakage and re-growth, or fouling of the surface, can hinder identification. The state of fouling on the carapace can assist in determining the age of a moult stage. Whereas juvenile and young reproductive adult stages have annual or semi-annual moult cycles, it is estimated that there can be several years between moulting stages of larger adults (McCaughran & Powell 1977). The effect of environmental attrition can therefore be assumed to be greater in larger adults.

BO.2 Handling continuity in phylogenetic analysis

Characters obtained for the production of a phylogeny have traditionally been omitted if it is not possible to code them discretely, and if they vary within a species (Wiens 2000). It can be argued that exclusion of continuous characters (if they are homologous to one another) is detrimental to the accuracy of the phylogeny (Kluge 1989, Campbell & Frost 1993, Wiens 2000).

There are two opposing considerations when coding continuous variation for phylogenetic analysis:

I) There is a trade-off in morphological phylogenetic analysis between incorporating a large amount of evidence (Kluge 1989), and maintaining the accuracy and mutual independence of the characters collected. Very often, there are few truly discrete and novel features separating closely related organisms (those in which the character is 'present' or 'absent'). In many cases, a modification of an ancestral characteristic is informative of inter-species difference, for example 'short setae' and 'long setae'. Where features are characterised in pseudo-discrete terms, such as 'long' and 'short', there is an

implicit description of a continuous range of values present within, and possibly between, taxa (Thiele 1993). The aim of morphological character coding is to select the maximum number of independent, homologous characters (both discrete and continuous) until the creation of further characters would be biologically tenuous (Kluge 1989).

II) The complexity of the process of gene expression (epigenetic, environmental effects) means that even in within one genotype, there might be variation in the expression of a character (Jaenisch & Bird 2003, Lamb & Jablonka 2005). Therefore, it is almost always simplistic to suggest that any character state is invariant. Phenotypic variation in this sense can be non-hereditary, and therefore confounding to a phylogenetic reconstruction. It is important to be able to separate random variation from underlying and hereditary gene expressions.

There are two different approaches that can be taken to code for continuous characters: Direct, continuous coding of measurements allows an unlimited number of different, ordered, states to be recorded without data loss (Rohlf & Marcus 1993). Importantly, continuous coding allows the statistical significance of intra-species vs inter-species variation to be incorporated into the analysis. Alternatively, pseudo-discrete coding divides a theoretically continuous dataset into discrete units based on a tendency for clustering in the data. Practically, this is done by assigning numerical limits to the cluster (e.g. short = 0-10 mm; long = 20-30 mm) (Wiens 2000). In any sense, it is desirable to be able to code inter-species variation in a way that allows us to analyse derived differences between both continuous and discrete character states.

BO.2.1 Morphometrics

Morphometrics is the study of measuring change in a complex shape; in this case the evolution of carapace shape in a lithodid crab. There are many branches to the field of morphometrics, including geometric morphometrics, in which the mapping of one shape onto another is investigated using multivariate analysis (Bookstein 1991, Rohlf & Marcus 1993). These methods preserve information about relative spatial arrangements of Cartesian coordinate (landmark) data (Rohlf 1998). Data are collected by recording multiple homologous landmarks in the same plane, and then scaling each shape to a unit size (Procrustes analysis: Hurley & Cattell 1962) before comparison (Bookstein 1991). Although ‘geometric morphometrics’ does provide the most up to date methods for analysing complex shapes, there are several problems which meant that a more simplistic approach to morphometrics was developed for this study.

- In 2-D geometric morphometrics, large amounts of data must be collected either by photography or by scanning. This technique was trialled for the dorsal carapace features in *Paralomis granulosa*, which are in a more-or-less 2-D plane and can be aligned to the camera using clamps. While this is technically possible for dorsal carapace features; legs and lateral features could not be analysed by two dimensional methods. Three-dimensional analysis would not have been possible because of the nature of sample collection in this study.
- When multiple landmarks are considered, average shape changes can be misleadingly dominated by characters for which homology is less certain, or for which measurement is difficult to place accurately (especially when perspective distorts the 2D plane in photographs). This probably non-biological variation affects the analysis more than do the smaller but consistent variations in other measured lengths – the techniques are prone to error.
- The aim of this study is primarily to produce a phylogeny of the Lithodinae and to maximise the confidence in the conclusions produced. Rohlf (In Wiens 2000) describes techniques for using 'partial warps' of shape-space (Fink & Zelditch 1995) to produce variables for use in phylogenetic study. There are, however, concerns about homology in comparing shape-space warps and their use in phylogenetic study is not fully established (Zelditch et al 1995, Rohlf 1998b, Monteiro et al 2002, Adams et al 2004). I have opted for a more simplistic method in which parameters are derived from basic biological principles, and the logical conclusions are less obscure.

"The complexity of morphological data means that we must dissect organisms into individual features. This dissection is often difficult and we rarely know *a priori* which lines of dissection correspond to evolutionary units. Yet this dissection is a crucial stage of character analysis. Morphometric data, because they are especially explicit about the features analysed, and because they force us to be explicit about our lines of dissection might be a useful general paradigm for complex data (Zelditch et al 1995, Zelditch: In Wiens 2000)".

BO.2.2 Landmark homologies in morphometric study

Establishing the homology of landmarks (points between which measurements are taken) underpins all morphometric and all phylogenetic study based upon it. Three

kinds of homology are defined in Rohlf's 'morphometric glossary' (1998a) and characters described by the first two are acceptable in this study.

Type I landmark: One whose homology is supported by anatomical or histological evidence.

Type II landmark: Homology is supported by geometric rather than anatomical evidence, for example, 'the tip of the rostrum'.

Type III landmark: At least one deficient dimension to the landmark, e.g. 'the longest diameter', or 'bottom of a concavity'. These are permitted in some multivariate techniques, but homology is not ascertainable.

BO.3 Background and theoretical derivation of morphometric methods used in this study

BO.3.1 Allometry: controlling for size

Allometry is a branch of morphometrics that investigates the change of shape as a function of size (Klingenberg 1996). If size can be removed as a variable, a meaningful comparison can be made between different lineages (Weston 2003).

Let character Y represent a linear difference between a pair of landmarks within an organism. If each landmark is biologically meaningful, we can assume that it is has a genetic origin and that the genetic basis for character Y is heritable.

Hypothesis $\mathbf{H_1}$ is that Y depends on functions of G (size), and Sp (a lineage-specific factor which varies because of changes in genes governing the position of the biological landmark).

$$Y = f(G,Sp)$$

In order to examine potential differences in measurement Y between species (Sp_1, Sp_2….Sp_n), it is necessary to remove all correlation between Y and size (G). The challenges with this are twofold:

i) Recognising the unknown function of G which is correlated with Y

ii) Ensuring that different species are governed by the same function of G.

Unless the data show otherwise, I will assume for simplicity that the function of G is the same for each of *n* species within character Y.

A not-exhaustive list of possibilities is

1) a linear relationship with growth: $Y=aG$
2) a polynomial relationship with growth: $Y= aG + bG^2\ldots$
3) an exponential relationship with growth: $Y = e^{aG}$

It makes biological sense for there to be no scalar element to the polynomial equation ($Y=aG$, not $Y=aG + b$) because very small values of G will have very small values of Y.

Individual phenotype does not only depend on heritable factors and size. The above calculations are made for an idealised population; however, measured data are expected to demonstrate an additional unpredictable variation. Statistical tests allow underlying parameters to be estimated from sampled data.

BO.3.2 Statistics

The r^2 statistic tests the appropriateness of a linear (or other) model for describing the relationship between two variables, such as Y and G in this case (Daly et al 1995). The value of r^2 describes the proportion of variability in Y that is explained by a change in G, given a model of linear regression. In practical terms, r^2 takes a value between 0 and 1, where 0 indicates no relationship, and 1 indicates a perfect relationship between Y and a linear function of G. An intermediate value, such as $r^2=0.7$ indicates that 30% of the variation in Y is derived from sources not related to a linear function of G. For the scenario described here, statistic r is also known as the Pearson product-moment correlation coefficient (Fisher 1921, Daly et al 1995).

If $Y= f(G,Sp)$ can be transformed such that $f(Y)=f(Sp)$, then it might be desirable to use further statistical tests to investigate the whether the value of Sp is the same in different lineages. A prerequisite for many tests of significance is to establish whether the sample is normally distributed and whether compared populations have an equal variance of the character measured (Daly et al 1995). Analysis of variance (ANOVA) is a method of examining variance within a population when the data are subdivided by different explanatory variables. In this case, there is one studied explanatory variable (species) with *n* different states, and *M* total observations. The ANOVA is performed in several steps to produce an F-statistic, which has a particular distribution (Fisher 1921) and probabilities can be calculated for obtaining certain values of F from two poplulations with equal variance. Very roughly, a large value of F indicates a

significant difference between intra-species means, although a probability of significance can be obtained from statistical tables (Daly et al 1995).

The Kruskal-Wallis test is a non-parametric version of the one-way ANOVA which can be used on ranked data if the condition of normality is not upheld (Kruskal & Wallis 1952). The result of ANOVA can determine whether there is significant inter-specific variance when compared to levels of intra-specific variance. ANOVA does not indicate which species are different to one another and which are indistinguishable.

BO.3.3 Size proxies

In work on lithodids, the standard linear size measurement is carapace length (CL). The segmental structure (Pilgrim 1973) and other aspects of thoracic anatomy (such as positions of the organs and the gills) can be used to demonstrate homology of this measurement when comparing members of the Lithodidae and other anomurans. There is no biological reason to think that CL should be dependent on any other measurements, with the exception of a mutual correlation with 'size'. The fact that CL is the standard measurement of size also means that data can be compiled for other studies as part of this work, and that data can be taken from the literature. Carapace width is rejected as an alternative to CL because no determination of homology can be made in this dimension. There is also no landmark on the branchiolateral margin that can be accurately and repeatably defined for comparison between all Lithodidae.

BO.4 Morphological Phylogeny

BO.4.1 Parsimony methods of phylogeny

The computer program <*PHYLIPpars*> uses the Wagner parsimony optimality criterion to select the tree topology that assumes the fewest changes (Eck & Dayhoff 1966; Kluge & Farris 1969). It allows an input of 8 discrete, unordered states for each character. Wagner parsimony is particular in its use of unknown ancestral states, so changes between all states are equally probable. The search algorithm considers both bifurcations and multifurcations of the tree. As the search algorithm is somewhat dependent on the species order in the input file, a 'Jumble' option in <*PHYLIP*> conducts multiple searches in which the input order is rearranged in a random order (Felsenstein 1993).

This test for maximum parsimony assumes (Felsenstein 1988):

1. Characters evolve independently.

2. Lineages evolve independently.
3. These changes are a priori improbable over the evolutionary time spans involved in the differentiation of the group in question.
4. Retention of polymorphism is far less probable than these state changes.
5. Rates of evolution in different lineages are sufficiently low that two changes in a long segment of the tree are far less probable than one change in a short segment.

BO.4.2 Distance methods of morphological phylogeny

Distance methods of phylogeny lend themselves to the investigation of continuous morphological data, since input values describe the pairwise distance between members of the input group. Distance algorithms select a single tree to represent the data, by minimising the disparity between observed values (in the input matrix) and distances obtained between nodes on the tree. It is useful that shape data from different parts of an organism can be assessed separately, and then combined into a single matrix for phylogenetic comparison (Adams et al 2002).

Fitch-Margoliash and <PHYLIPfitch>

An implicit assumption of the distance methods is that each distance is measured independently from the others, and that no item of data contributes to more than one distance. Felsenstein (1984), the author of *<PHYLIP>*, discusses that character independence is often not a valid assumption; he states that *<PHYLIPFitch>* should not give positively misleading results provided the assumption of additivity holds (Page & Holmes 1998).

The Fitch-Margoliash (1967) algorithm for fitting trees to distance matrices is one of several methods that select the tree which minimises the sum of squared differences between observed and expected data:

$$\text{Sum of Squares} = \Sigma_i \Sigma_j \left(\frac{n_{ij} (D_{ij} - d_{ij})^2}{D_{ij}^P} \right)$$

Where **D** is the measured distance between species *i* and *j*, and **d** is the sum of branch lengths joining *i* and *j* on the proposed tree. The set of distance methods which include Fitch-Margoliash assume that the measurement error varies with the P^{th} power of the

magnitude of the distance between species. In the Fitch-Margoliash algorithm, P=2 (Fitch & Margoliash 1967), which assumes that the error in measurement is nearly constant regardless of the magnitude of the evolutionary distance.

In the forthcoming sections, both parsimony and distance criteria will be used to investigate different aspects of morphological variation within groups of lithodids.

BM: SECTION METHODS

BM.1 Samples and scope of the section

Morphological sampling made use of preserved specimens curated by the following institutions: Natural History Museum, London; Senckenberg Museum, Frankfurt; Musée National d'Histoire Naturelle, Paris; Institut de Ciencies del Mar, Barcelona; United States National Museum of Natural History, Smithsonian Institute, Washington; the "Discovery Collection", National Oceanography Centre, Southampton; and un-deposited cruise materials (Mauritania: MAU 1107) at the Instituto Español de Oceanografica, Vigo. Species identities were verified with reference to type specimens and using comparative keys compiled by taxonomic specialists (Dawson 1985a, Macpherson 1988a). Examinations were made of more than 1000 specimens across the Lithodidae. Sample numbers, museum catalogue numbers, and location of capture are listed in chapters where relevant. For each specimen, the carapace was measured (CL), and photographs were taken of dorsal and ventral aspects of the carapace using the 'macro' setting of a Sony 8.2 megapixel digital camera; additional morphological data were collected as described in the following chapters.

This section contains three chapters describing how morphological variation poses challenges to species identification, but also how it can provide evidence of ancestral history. Variation with ontogeny, as well as variation within equivalent size-classes was assessed prior to phylogenetic analysis so that each species could be accurately delimited. Specifically, the dorsal carapace, abdomen and legs of each specimen were examined under a light microscope to assess the consistency of tubercle form within one specimen (Section **B1**). In Sections **B2** and **B3**, the parallel global radiations of two lithodid lineages (*Lithodes* and *Paralomis*) were examined by the production of morphological phylogenies using both continuous measurements and discrete morphological traits.

BM.2 Ornamentation terminology

The terminology used to describe ornamentation of *Paralomis* in this study (Fig. **B1**.1) were: 'tubercle', which replaced previously used synonyms: granule and papilla to describe structures that are not spines; and 'spine', which describes structures measuring more than 1.5 times as high as they are wide at the base. A distinction was then made between conical, flattened, pedunculate or rounded tubercles, and regular or irregular tubercles.

BM.3 Phylogenetics

Two large groups within the Lithodinae were considered separately, based on the results of the molecular study (Section **A1**). 24 *Paralomis* species, plus *Glyptolithodes cristatipes* and *Lopholithodes mandtii* were examined in the first study; 13 *Lithodes* species, and 4 *Paralithodes* species were examined for the second. Subdividing the Lithodinae allows the formation of different sets of characters to represent each lineage, without having to assert the homology of character origin between more distantly related groups.

Morphological variation was subdivided into two types for analysis: discrete-character data and morphometric data.

1. **Discrete-character analysis**. Truly discrete characters are those of novel generation, which appear in one species and not in another. These are very rare, especially within such closely related groups. Some morphological characters that were essentially continuous measurements were classified discretely if they formed clusters with no intermediates.
2. **Morphometric analysis.** Continuous characters, for which subdivision into state-categories would be arbitrary (Section **BM**.3.2.2), were examined using statistical methods to obtain quantitative figures for degrees of difference between species.

BM.3.1 Outgroup principles

Polarity of morphological change was derived from molecular evidence. In Section **A1**.4, it was shown that the genus *Lopholithodes* diverged close to the base of a strongly monophyletic *Paralomis* lineage. In parallel, it was shown that *Paralithodes* is paraphyletic with respect to *Lithodes* (with *P. brevipes* the most distantly related). In discrete-character based phylogenetic studies, polarity of each character was investigated independently. Character states observed in the designated outgroup (*Lopholithodes mandtii* and *Paralithodes brevipes* respectively) were assessed against

homologous characters in the Hapalogastrinae (*Oedignathus*, *Hapalogaster*, *Dermaturus*, *Placentron*), as well as the base of the other lineage (comparing *Lopholithodes* with *Paralithodes brevipes*). This is the outgroup comparison method (Watrous & Wheeler 1981). The process of assigning polarity for each discrete character is discussed in detail in sections **B2** and **B3**, with the outgroup state recorded as missing if polarity was ambiguous.

BM.3.2 Morphometrics

BM.3.2.1 *Sampling and data capture*

59 linear measurements between pairs of morphological landmarks (Bookstein 1991) were taken in a preliminary study of 21 specimens of *Parlomis granulosa* and 13 specimens of *Lithodes santolla.* Data capture was done using digital callipers, and recorded in millimetres to an accuracy of 2 decimal places. The homology of each landmark was derived from anatomy or comparative study.

For very small stages, measurements are prone to large percentage errors, so only specimens with CL> 20 mm were used in these analyses. Only species for which data had been collected for more than five specimens (m>5) were included in the final taxon set to increase the statistical significance of the analyses.

Based on preliminary data collection, the character set was refined to include only those which could be accurately defined and repeated with precision. 25 sex-specific characters were collected (chelipeds, abdomen), but not used for statistical analyses because of low sample sizes when species were further subdivided by reproductive stage and sex.

34 characters were collected for 25 species of *Paralomis, Lopholithodes mandtii*, *Glyptolithodes cristatipes* (Section **B3**), 13 species of *Lithodes,* and 4 species of *Paralithodes* (Section **B2**). Those characters that were considered to be unsuitable for further analysis after widening the sample set are italicised below:

1. (CL) Carapace length. The conventions described in Macpherson (1988a) are used to obtain this measurement of length from the midpoint of the orbital groove to the midpoint of the posterior margin excluding spines (Fig **BM**.1).
2. (CW) *Carapace Width: The width of the carapace at its widest point behind the major anterobranchial spine B2 (Fig **B2**.8). This is a type II landmark (Rohlf 1998a), and its definition, although unambiguous in most cases, has no homologous basis. CW was not analysed statistically.*
3. (LBH) Depth of the branchiostegite along the *sulcus verticalis* (Fig **BM**.3)
4. (LSH) Length from the base of the hepatic spine to the edge of the branchiostegite. (Fig **BM**.3)

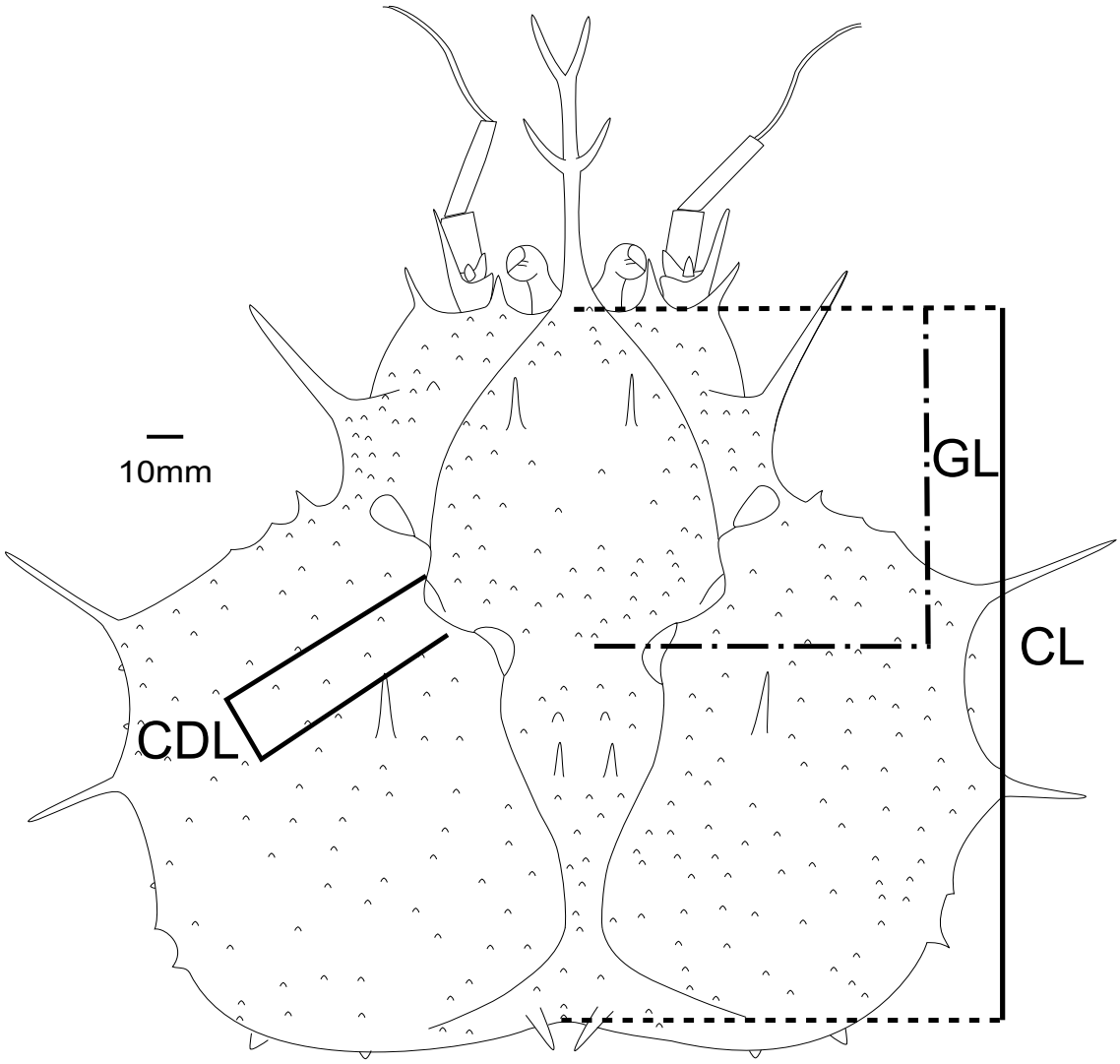

Figure BM.1 Carapace measurements in the Lithodinae 1: *Lithodes galapagensis* schematic with carapace length (CL), gastric length (GL) and cervical groove depression length (CDL) indicated.

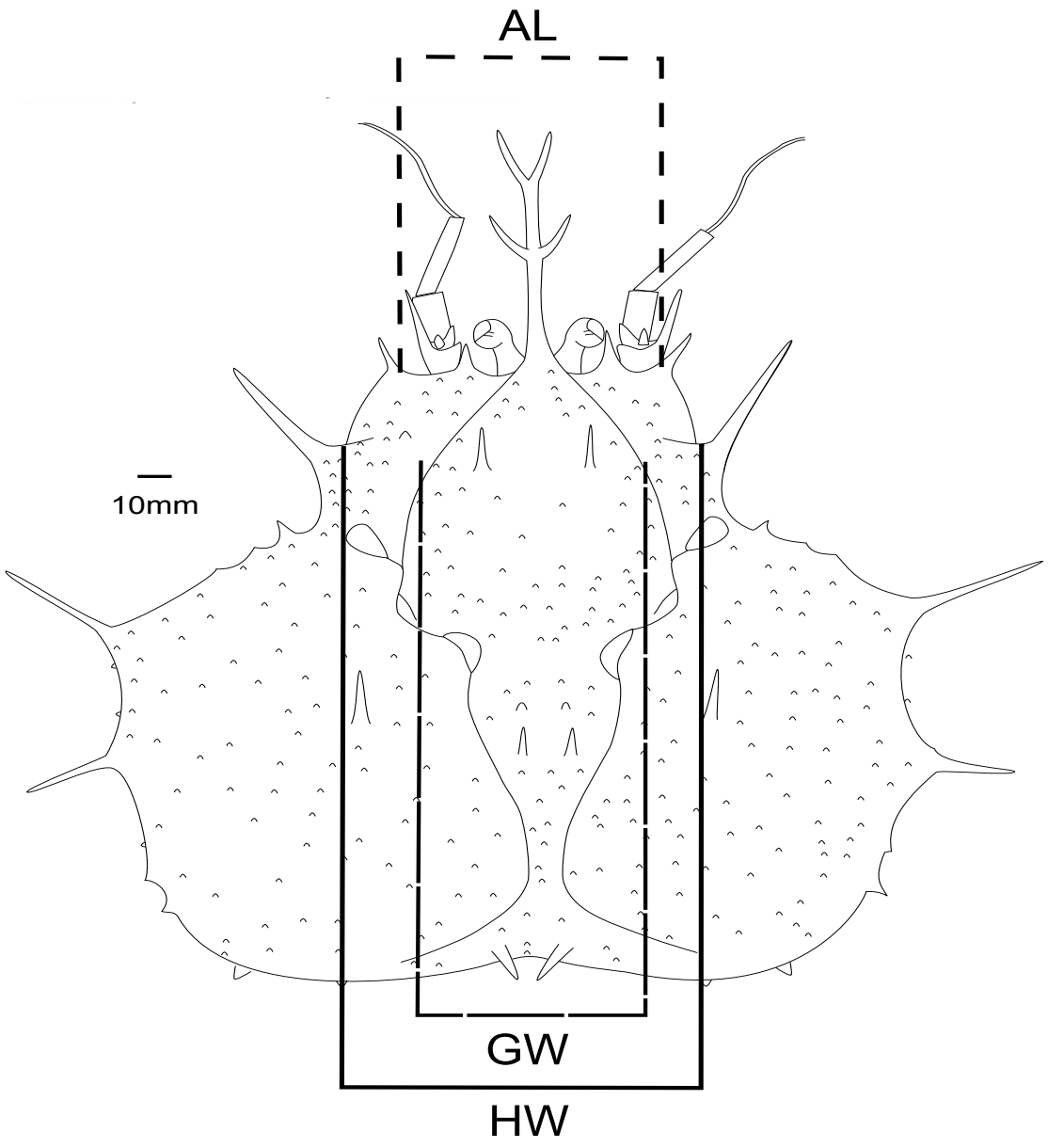

Figure BM.2 Carapace measurements in the Lithodinae 2. *Lithodes galapagensis* schematic with hepatic width (HW), gastric width (GW) and anterolateral width (AL) indicated.

5. (LHH) Length from the lateral edge of the cervical groove to the edge of the branchiostegite (Fig **BM**.3).
6. (AL) Anterolateral width. Internal width between the anterolateral spines (Fig **BM**.2).
7. (HW) Internal width between the base of the hepatic spines (Fig **BM**.2).
8. (HL) Length from orbit to anterior edge of hepatic spine. This character is too difficult to score accurately in many cases, since not all species have a prominent hepatic spine.
9. *Length, along the cervical groove of a homologous prominence* (Fig **M2**,vii) *termed the 'cervical knob'.* ***Judged too difficult to score accurately in Lithodes because the cervical knob is often reduced.***
10. *Length from the cervical knob to the hepatic margin.* ***Later judged too difficult to score accurately in Lithodes.***
11. (CDL) Length of depression at the posterior lateral side of the gastric region this is a type I homologous landmark (Rohlf 1998a) and present in all lithodids (Fig **BM**.1). Its size is related to the insertion area of the thoracic musculature (Pilgrim 1973).
12. (GCL) Length of the GC groove including lateral depressions. Homology can be verified by anatomical study, the lateral depressions being muscular insertions. Dixon et al (2003) emphasise the stability of such grooves as phylogenetic characters within the Anomura.
13. (GCW) Width of the GC groove (along the anteroposterior axis). Difficult to score accurately in some cases, especially in *Lithodes* because of a poorly defined limit to the groove in some s pecies (e.g. *Lithodes murrayi).*
14. (GW) Width of the gastric region between the midlateral gastric spines (always approximately at the level of the hepatic spines, and roughly the maximal width of the gastric region) (Fig **BM**.2).
15. (GL) Length of the gastric region along the midline from the orbit to the gastro-cardiac groove (Fig **BM**.1).
16. (VRL) Length of the ventral rostral spine from its dorsal convergence with the paired dorsal spines to the tip (Fig **BM**.3). There were concerns about this feature because of breakage of the spine in many cases, also that many ventral rostral spines are curved.
17. (RW)*Width of rostrum at the level of the orbits. There were difficulties with scoring this character because many species have several spines in this region which hinder accurate measurement.*

18. (DL) Length of the dactylus on pereiopod 3. Measured from the tip to the anterior articulation with the propodus (laterally).
19. (DH) Height of dactylus on pereiopod 3. Measured at the joint of the propodus.
20. (PL) Length of propodus on pereiopod 3. Measured along the dorsal edge from the articulation with the dactylus to the dorsal point of articulation with the carpus.
21. (CAL) Length of carpus on pereiopod 3. From the dorsal articulation with the propodus to the level of the anterior articulation of the merus.
22. (ML) Length of merus on pereiopod 3. From the anterior point of articulation with the coxa to the anterior articulation with the carpus.
23. (MH) Height of the merus at the joint with the carpus. Measured from the joint with the carpus to the dorsal face of the merus at the anterior edge.
24. (MW) Width of the merus at the joint with the carpus.
25. (OCW) Width of the cornea.
26. (OCL) Length of the cornea.
27. (ABW) Length of the 2nd abdominal segment at the midline. The first and second segments are almost always fused in the groups studied. If not, then ABW is the midline length of segment 1 plus segment 2.

The allometry of 20 characters (defined above) was analysed, from which quantitative inter-species differences were identified.

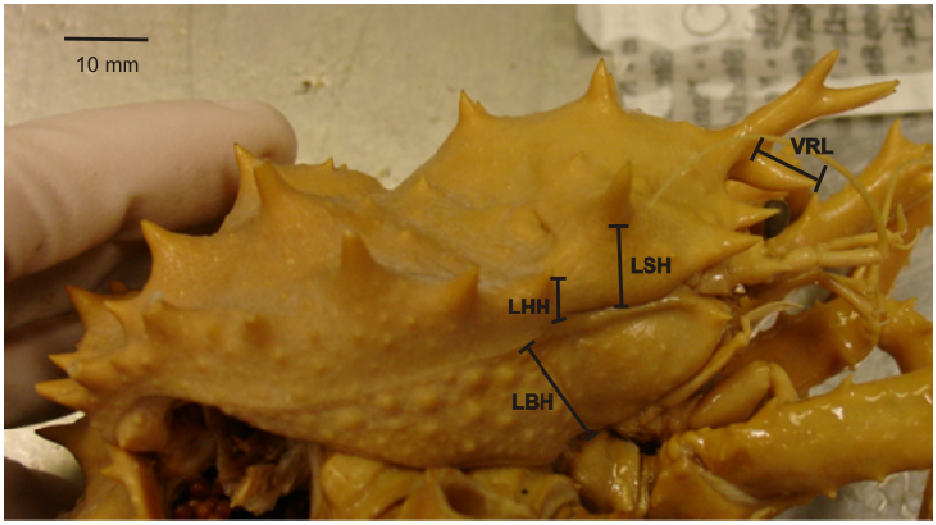

Figure BM.3. Lateral measurements of the carapace in the Lithodidae. Demonstrated for *Lithodes murrayi*. Ventral rostral length (VRL), Length of the *sulcus verticalis* (LBH), Length from the edge of the branchiostegite to the cervical groove (LHH), Length from the edge of the branchiostegite to the hepatic spine (LSH).

BM.3.2.2 *Graphical and statistical analysis of data*

A function of carapace length (CL) was used throughout this analysis to approximate growth. Character measurements are denoted Y_k, where k identifies a character (e.g. length between anterolateral spines [AL]). Each dataset (Y_{AL}, Y_{GW}…Y_k) consists of measurements from *m* specimens belonging to *n* species; $Y_{k,n}$ represents one such dataset subdivided by species.

-Reduction of the size-related variables governing Y_k

The form of $Y_k = f(CL)$ was examined in order of complexity of the function (from CL, CL^2, to e^{CL}), until all significant correlation of Y_k with f(CL) could be removed.

First, the nature of the polynomial function governing the raw dataset Y_k was investigated using polynomial regression. Four estimates of polynomial functions were produced, in which the highest terms were successively of the form x^0- x^3; the fit between the data and each of these functions (r^2) was calculated. In addition, a one-tailed t-test was conducted to examine the hypothesis that the coefficient of each term in the polynomial is significantly (99% confidence) different from zero. A t-statistic with a probability less than 0.01 is considered to indicate that the tested coefficient is not zero.

If the data were adequately described using a polynomial function of size, then Y_k/CL was examined for each species *n* to examine the possibility of eliminating CL as a variable.

- If no significant correlation was observed between $Y_{k,n}$/CL and CL ($r^2 < 0.4$), then it was concluded that $Y_{k,n}$ depended linearly on CL and not on any higher order function (such as CL^2, e^{CL}). [in this case, $Y_{k,n} = aCL$]
- If a significant correlation was observed between $Y_{k,n}$/CL and CL ($r^2 > 0.4$) and the probability that coefficient b = 0 is <0.01, it might be implied that $Y_{k,n} = aCL \pm bCL^2$.
    - If, in this case, the maximum measured value of **b** is less than 0.01 times the standard deviation of Y_k/CL (**a** and **b** determined by linear regression), then variation with size is responsible for less than 1% of the overall variation, and the CL^2 term was relatively insignificant in the size range considered. Under these circumstances, bCL^2 was not considered further. (N.B. If a significant component of the variability in Y_k/CL is governed by a function of CL [in addition to expected sources of

variability such as measurement error, individual variability, and species difference], then this has the effect of decreasing the statistical significance of any underlying inter-species difference - provided the sample size-range is similar for two species being compared. Simplification of variables in this way should lead to us falsely rejecting a character for analysis rather than accepting misleading results).

- Conversely, if b was found to be larger than 0.01 times the standard deviation of the Y_k/CL dataset, then coefficients **a** and **b** were estimated for each species ($b = Y_k/CL^2 - a_n/CL$), and these coefficients were considered separately in the following analyses.

If, after investigating polynomial functions of CL, a dataset without significant correlation to CL can not be produced, then logarithmic functions of CL ($Y_k = e^{aCL}$) were tested.

These above methods produce sets of approximately size-independent data, which are of the form: Y_k /CL; (Y_k /$CL^2 - a_{k,n}$/CL); $a_{k,n}$); or lnY_k/CL. Unless results showed otherwise, I assumed that within Y_k, all species are dependent on the same f(CL). For simplicity, I will refer to the transformed datasets as $f_{CL}(Y_k)$ in the forthcoming text.

$f_{CL}(Y_k)$ allows us to test the following hypotheses about inter-species differences-

H_0: variation in $f_{CL}(Y_k)$ is related only to individual variation, and measurement error.

H_1 : variation in $f_{CL}(Y_k)$ is additionally caused by significant inter-species variation (Sp).

-Tests of distribution and parameterisation

Normality of distribution and equal variance in the subdivided datasets ($f_{CL}(Y_{k,n})$) were tested using the Shapiro-Wilk test and the F-test, respectively (Shapiro & Wilk 1965, Shapiro et al 1968, Daly et al 1995). Probabilities of less than 0.01 indicated that there is 99% confidence of the population not being normally distributed or not having equal variance. It seems reasonable to assume that this test is appropriate for this set of linear measurements because they form a continuous, approximately symmetrical distribution with data clustering around the mean.

For all normally distributed populations $f_{CL}(Y_{k,n})$, a one-way analysis of variance (ANOVA; Daly et al 1995) was performed in <*Sigmaplot 11*>. In this case, (**p** < 0.01) indicates that there is a significant difference in the mean of $f_{CL}(Y_{k,n})$ between some

species. A significant ANOVA result indicates that the null hypothesis, $\mathbf{H_0}$ can be rejected with 99% confidence.

The Holm-Šidák method for multiple pair-wise comparisons (Šidák 1967, Holm 1979) was performed for each dataset subdivided by species with a confidence level of 99%. A **p**-value lower than the critical level (set by H-S correction) indicates a significant difference between the means of $f_{CL}(Y_{k,n})$ for two values of *n*. A **p**-value higher than the critical level indicates that any difference in the sample mean of $f_{CL}(Y_{k,n})$ for two species is based on random intra-species variation and measurement error.

Graphical methods illustrate how morphometric data could, and in some circumstances has been, coded discretely. Species were shaded red, green, or black based on the result of multiple pair-wise comparisons (compare Figs **BM**.4, 5). There is a statistically significant difference between the species shaded red and those species shaded black, and no significant difference between species of the same colour. The species shaded green are not significantly different from one another, and each was not significantly different from either the black or the red species. Where species were figured despite low sample sizes, and a t-test was not performed, they were shaded yellow. A character would not be used in further analysis if all species were shaded in green, since this would indicate that there were no two groups that were significantly different from one another. If a situation occurred where there were no green-shaded species and all were either black or red, then the characteristic could be coded discretely (0 and 1). The results of this graphical technique are not used directly in the construction of the phylogeny, but are used in decisions about character inclusion and interpretation of the results.

BM.3.2.3 *Morphometric phylogeny*

After the 20 morphometric characters were tested for patterns of inter-species variation, those selected were used in a phylogenetic analysis. Characters were useful if there was a rejection of H_0 in the analysis of variance (Section **BM**.3.2.2), and also if pair-wise comparisons revealed two or more pairs with significant differences between their means. By allowing statistical tests to select for useful levels of within/between species variation, it is hoped that the subjective character inclusion bias is minimised. Of those characters selected for further analysis, the datasets $f_{CL}(Y_k)$ were further transformed to produce inter-species distance statistics. These distances form the elements an $n \times n$ species comparison matrix that can be analysed by phylogenetic software <*PHYLIPFitch*>.

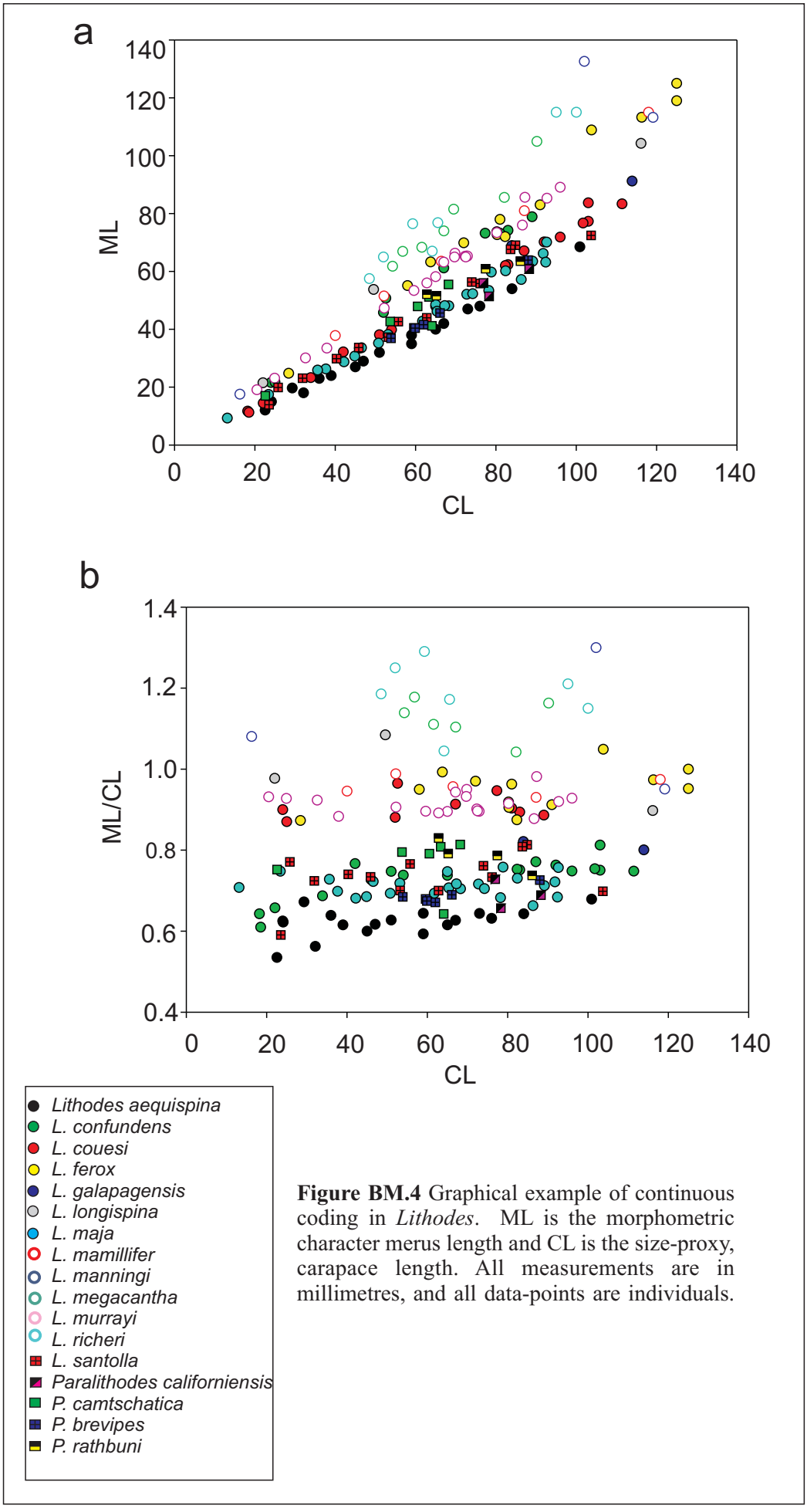

Figure BM.4 Graphical example of continuous coding in *Lithodes*. ML is the morphometric character merus length and CL is the size-proxy, carapace length. All measurements are in millimetres, and all data-points are individuals.

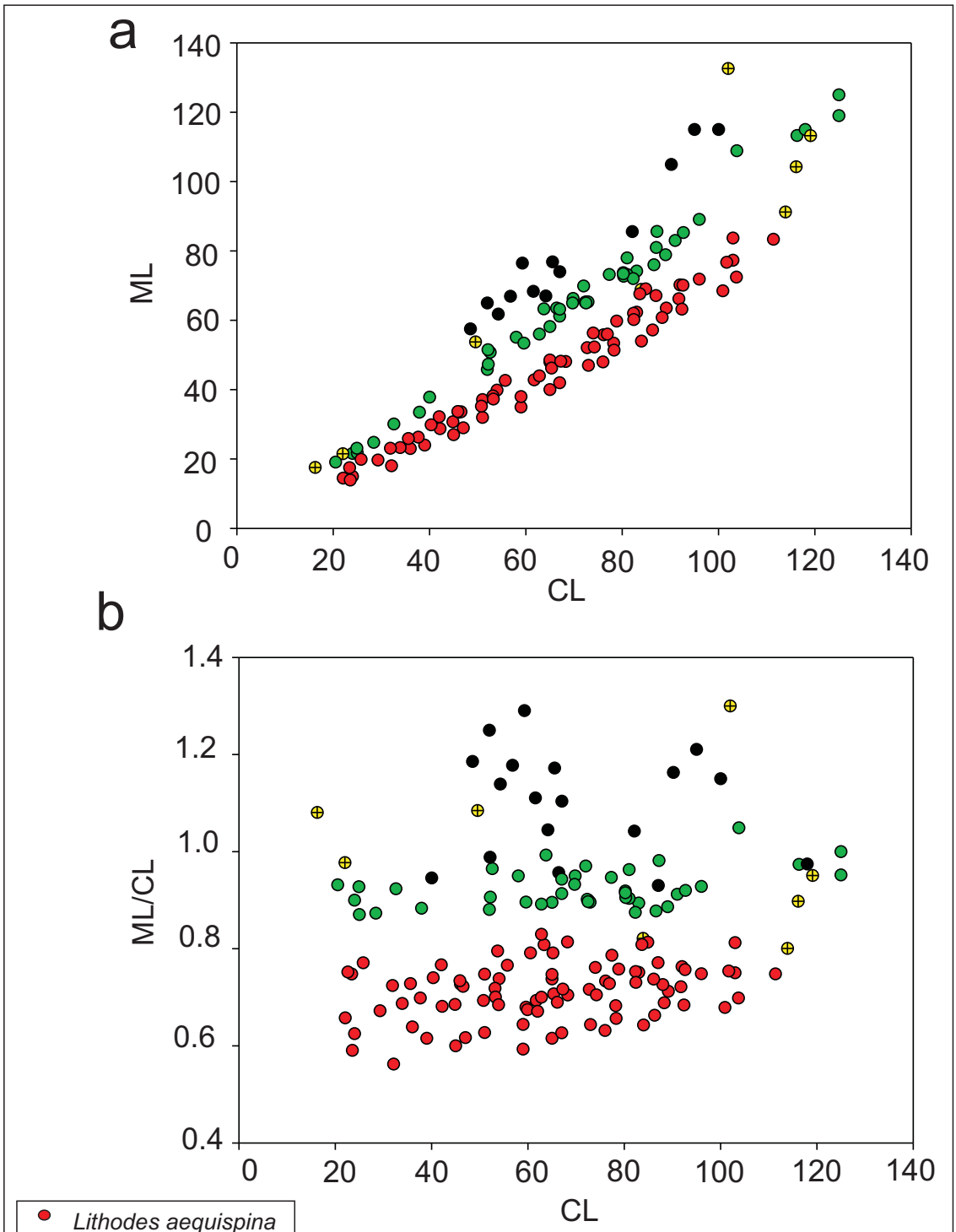

Figure BM.5 Graphical example of pseudo-discrete coding in *Lithodes*. ML is the morphometric character merus length, and all data are exactly the same as in Fig. BM.4. All measurements are in millimetres. Species shaded black and red are significantly different to one another in a statistical pairwise comparison of means (99% confidence). Green shading indicates species that are not necessarily significantly different from red or black species. This figure shows that, whereas there might be a difference in ML between species, it should not be coded discretely. Those shaded yellow represent species for which fewer than five samples were taken. Plotted points are measurements of individuals.

For any comparison or combination of *k* different characters, each set of measurements $f_{CL}(Y_k)$ must be scaled such that unit values represent their size and spread. If this were not done, large characters (merus length: ML) could not be meaningfully compared with small characters (gastric width: GW). The mean and standard deviation are useful indicators of scale and spread of distributions and datasets were standardised to centre the characters on a mean of 10 and a standard deviation of 1. Standardising to a mean of 10 is an arbitrary choice, which makes all values positive but doesn't affect the distributions.

$$U_{Ki} = \frac{f_{CL}(Y_k) - \text{mean}_k}{\text{standard deviation}_k} + 10$$

For each of the standardised datasets $U_{AL}, U_{GW} \ldots U_k$, a within-species mean and standard deviation are calculated. $\bar{U}_{k,n}$ is the arithmetic mean of the dataset U_k within species *n*. There are m_n sampled members of species *n,* and U_{Ki} is a member of dataset U_k. The sample standard deviation of species n for character k is calculated as

$$S_{k,n} = \sqrt{\frac{(\sum(U_{Ki} - \bar{U}_{k,n})^2}{(m-1)}}$$ (Daly et al 1995).

In normally distributed populations, 68% of data is expected to fall within 1 standard deviation of the mean (σ), and 90% within 1.64σ (Patel & Read 1982, Fig **BM**.6). In the context of a normally distributed sample, we can have 68% confidence that the true mean falls within 1 standard deviation ($S_{k,n}$) of the sample mean ($\bar{U}_{k,n}$) (Daly et al 1995).

For each character, two *n*×*n* pair-wise distance matrices were created, each element of which was an estimate of difference between two species for that character. Species were ordered by the value of the intra-specific mean ($\bar{U}_{k,n}$), and the pairwise distances for the first matrix were calculated as $[(\bar{U}_{(k,\ n=R)} - S_{(k\ ,\ n=R,)}) - (\bar{U}_{(k,\ n=C)} + S_{k,\ n=C,})]$ (where *R* and *C* are species in the row and column in the matrix, and $\bar{U}_{(k,\ \ n=R)} > \bar{U}_{(k,\ \ n=C)}$) (distance A on Fig **BM**.6). Where the resulting difference was positive, there is 68% confidence that the actual difference between species means was of that length or greater. A difference of less than zero indicates that the two species were not significantly different at this level of confidence. In the second matrix, there is 90% confidence that the true inter-species distance is of the stated length or greater.

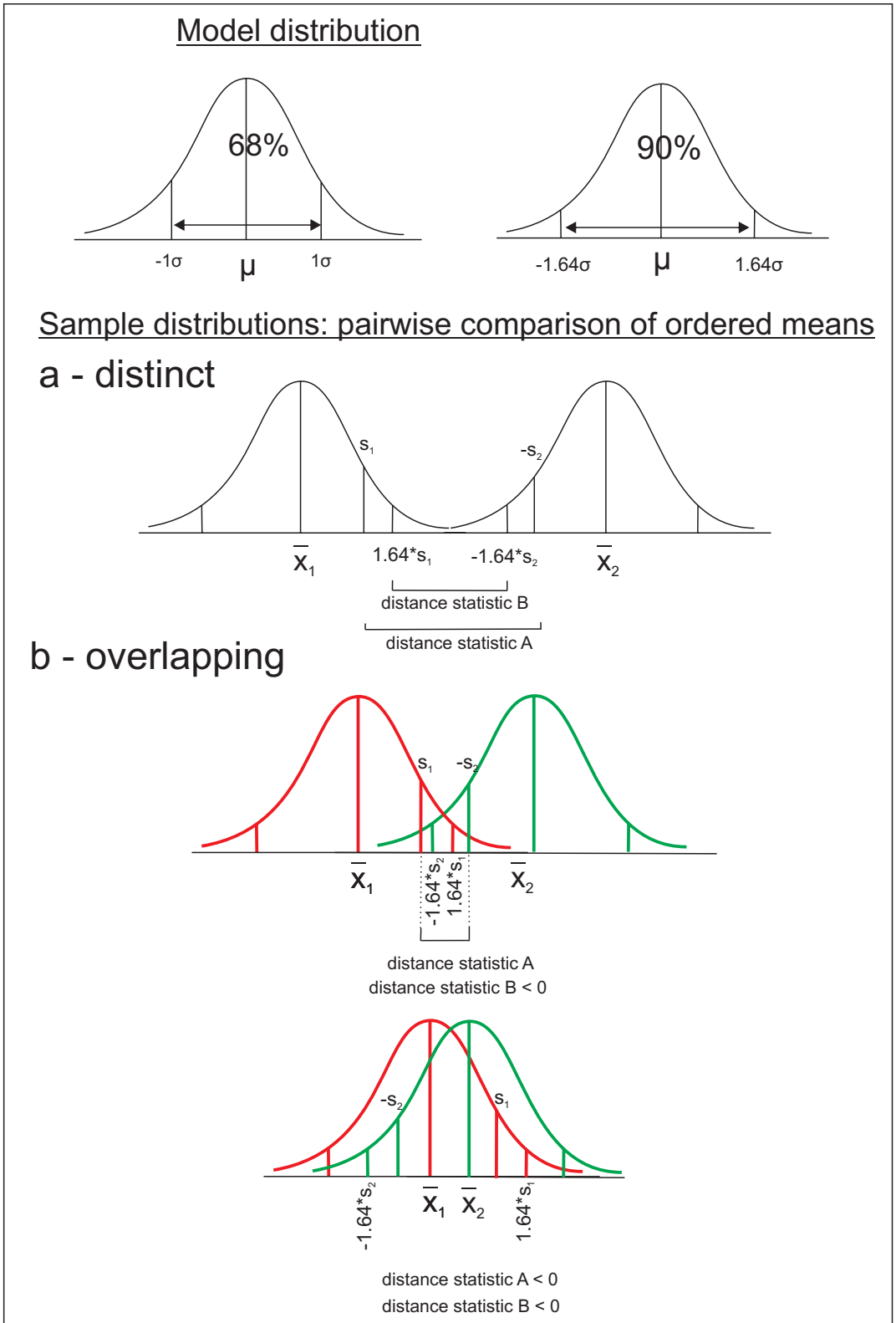

Figure BM.6 Pair-wise distance measurements between approximately normally distributed sample populations. Normally distributed populations are described by their mean (μ) and standard deviation (σ). In a sample of a nomally distributed population(s), the sample mean ($\bar{x}$) and standard deviation (**s**) can be used to calculate the likely magnitude of differences between population means. Populations 1 and 2 are different species measured for a normally distributed and standardised morphometric character. Distance statistic A is a minimum difference between the means for which there is 68% confidence; statistic B is a minimum difference with 90 % confidence.

Distances are calculated as in the first matrix [($\bar{U}_{(k,\ n=R)} - 1.64*S_{(k\ ,\ n=R,)}$) − ($\bar{U}_{(k,\ n=C)} + 1.64*S_{k,\ n=C,}$)] (where *R* and *C* are species in the row and column of the matrix, and $\bar{U}_{(n=R,\ k)} > \bar{U}_{(n=C,\ k)}$) (distance B on Fig **BM**.6). The second matrix will produce a very conservative tree that is unresolved at many of its internal nodes; however, this is a trade-off for increased confidence in the result.

Each character provides an insight into an aspect of morphological similarity between species or groups of species. In an isolated instance, morphological similarity can be incidental and harks back to days of classification before evolutionary theory (Goldstein & Desalle 2005). Suites of character data, however, can provide corroborative or contradictory data, which allow scenarios of nested hierarchy to be formulated. Addition of the corresponding elements of individual distance matrices produces a summed matrix of $n \times n$ species representing a total difference between species over all *k* characters. This method has an analogy with the distance methods of analysing molecular data, in which an observed difference per character is summed over many characters to produce a total inter-species difference (Rzetsky & Nei 1992).

BM.3.3 Discrete coding

Discrete characters are selected to reflect synapomorphies within each lineage and specifics of sampling will be discussed in the relevant chapter (Sections **B2** and **B3**). Each character has two or more character states (0, 1… 8), as well as an unknown/missing character state **X**. Ambiguous scores do not contribute to the final calculation of difference between species, and **X** is interchangeably used to show that the observed state is missing or irrelevant.

Character states are not ordered and not weighted, which means that a change 0→1 is worth the same as a change 1→0, or 0→2. '0' is not implicitly the ancestral state in the model, since the out-group is assigned in the input for the program. This allows the model to select more parsimonious polarities than 0→1 if they exist. Nevertheless, the designation of the binomial code (0 = ancestral, >1 = derived) makes it easier to organise the data. If there is reason to believe that characters are ordered, (e.g. 0→1→2 and 0→1→3) then these changes can be coded as such using multiple unordered characters so that in the above example: 1= 001, 2=101, 3=011 (Felsenstein 1979).

Polymorphic characters in which the change occurs predictably (i.e. with ontogeny, or sex) are coded using multiple characters, or the polymorphy itself is coded where homology applies. In the case of sexual polymorphisms, one character describes the case in males and the next in females (e.g. K_1=Abdomen asymmetry ♀, K_2=Abdomen asymmetry ♂). Polymorphisms, in which a proportion of the population displays

attribute A and a proportion attribute B are not used unless the character can be coded to encompass both varieties under a single state. Efforts are made to formulate codes in such a way that characters have some level of independence, and in which homology can be argued within the remit of the state definitions.

BM.3.3.1 *Phylogenetic analysis of discrete characters using the Parsimony criterion*

Phylogenetic analysis was conducted in <*PHYLIP_Pars*>, with 'thorough' search options employed. Trees were assessed on the criterion of Wagner Parsimony (Section **BO.**4.1). Trees were scored according to the number of observed state changes at the predicted internal nodes. Prior to assessment of most parsimonious trees, <*PHYLIPseqboot*> was used to create 1000 randomly sampled datasets (with replacement) for a bootstrap analysis (Felsenstein 1985) to provide confidence estimates to nodes on the final tree. If more than one topology is returned, it will be used to produce a majority-rule consensus tree (Margush & McMorris 1981), where nodes are represented on the consensus topology are those that are present in the majority of trees. The hypothetical out-group, based on comparison of *Lopholithodes mandtii* or *Paralithodes brevipes* with other Lithodidae was used to root these trees (Watrous & Wheeler 1981).

BM.3.3.2 *Phylogenetic analysis of discrete characters using Fitch-Margoliash distance methods*

Distance was calculated between pairs of species based on comparisons of their morphological character sets. Discrete character states are in all cases unordered, so all differences between numerical (non-**X**) scores were given a value of 1 and all identical characters were given a value of 0. Where one of the species had a missing entry (**X**) for a character, that comparison wasn't made. The total difference between each pair was divided by the number of comparisons and multiplied by the total number of characters. The resulting pair-wise distance represents the proportion of characters which differ between that pair of species.

The resulting $n \times n$ matrix was analysed using the Fitch-Margoliash distance algorithm in <Phylip*Fitch*>, in order to compare the distance-optimised tree with most parsimonious tree (methods differ fundamentally). Branch lengths on the output tree represent the 'length' (approximately the number of changes) between two nodes on the tree. Internode distances of approximately zero length are collapsed to form a polytomy on the tree. The hypothetical out-group was not used for this analysis; instead *Lopholithodes* or *Paralithodes* was set as the outgroup state as described in sections **B2** and **B3**.

BM.3.4 Combination of morphometric and discrete characters

Within *Lithodes* and *Paralomis*, the results for morphometric-character analysis and discrete-character analysis are independent of one another. This offers the opportunity for the results corroborate or refute one another, which is particularly important where the character numbers are small. The strongest interpretation occurs when characters are combined (Baum & Shaw 1995, Goldstein & DeSalle 2005) to produce a tree based upon a larger number of observations.

Two $n \times n$ pair-wise comparison matrices were produced by methods described in sections **BM**.3.2.3 and **BM**.3.3.2. The two matrices were weighted to reflect the number of characters they each contain (multiplying the smaller one by the number of characters in the larger and vice-versa), before being added together. The final matrix containing taxa common to both analyses (there is no possibility to include missing data in distance analyses) was combined for analysis in <PHYLIP_Fitch> (Section **BO.**4.2, Fitch & Margoliash 1967, Felsenstein 1993). Global branch rearrangement (GBR) is employed and the input order of species is jumbled randomly in 100 parallel runs. Bootstrap testing can not be performed on this type of data, so the results of the 100 parallel runs are condensed, with nodes only resolved on the final tree if they appear in more than 50% of the runs.

CHAPTER B1: ONTOGENETIC CHANGES IN CARAPACE ORNAMENTATION IN THE FAMILY LITHODIDAE, WITH A FOCUS ON THE GENUS *PARALOMIS*

B1.1 Rationale and context

The deep-water, patchy distribution of the subfamily Lithodinae (Hall & Thatje 2009a) means that many species are not commonly or easily targeted for sampling. Many species are based on a description of one or two specimens and are found infrequently after first publication (Macpherson 1988a, Spiridonov et al 2006, Hall & Thatje 2009b). One of the characters used to distinguish species of king crab is the size, position and form of dorsal carapace ornamentation (Macpherson 1988a). The 117 described lithodid species, particularly the 61 species of the genus *Paralomis,* display an array of distinctive spines and tubercles, which can aid diagnosis (Macpherson 2003, Spiridonov et al 2006, Takeda & Bussarawit 2007, Macpherson 2008, Hall & Thatje 2009b). Few authors have given images of these structures under magnification, but those that have (e.g. Haig 1974, Andrade 1980) reveal the intricate structures that adorn carapaces within this family. Ontogenetic changes in tubercle morphology are potential sources of confusion for diagnosis, especially when complete growth series are not on hand for comparison. The aims of this chapter are:

- to catalogue and describe the microscopic and macroscopic form of the spines and tubercles that can distinguish species, and to assess variability between similar sized specimens.
- to examine whether ontogenetic changes in carapace spines or tubercles can be diagnostic features of species, or whether there is a single pattern of change within the genus.

In scientific writing on the Lithodidae, the words used to describe carapace structures are various and sometimes vaguely defined. The word tubercle (Haig 1974, Macpherson 1988a) describes small protuberances, swellings or nodules, and is used interchangeably with the terms papillae (Faxon 1895, Haig 1974), granule (Macpherson 1988a, 1992), flattened spinules (Takeda 1974), areolations (Eldredge 1976), vesiculous granules (Takeda 1979). These terms actually describe a whole spectrum of morphological features (Table **B1**), but in an inconsistent way that can sometimes be unhelpful in diagnosis. If described in an unambiguous manner through the provision

of detailed drawing or photography, real differences could be used to identify species more accurately; to delimit lineages; and to allow non-specialists to make useful comparisons between the works of different authors.

A taxonomist attempting to identify a potentially novel species is unlikely to have a complete growth series of similar species available to refer to. I herein aim to look for common ontogenetic trajectories within *Paralomis*, and to provide the basis of a catalogue covering within-species variety.

B1.2 Synopsis of methods

For 32 species of *Paralomis*, adult specimens (larger than CL 50 mm) were illustrated under magnification (Figs **B1**.2–15; Table **B1**) in order to provide a reference for future descriptive works. Eight species of *Paralomis* with good representation in sample collections were also selected to illustrate the growth-related changes within the genus (*P. cubensis* Chace, 1939; *P. erinacea* Macpherson, 1988a; *P. granulosa* Jaquinot, 1847; *P. inca* Haig, 1974; *P. mendagnai*, Macpherson, 2003; *P. multispina* Benedict, 1894; *P. spinosissima*, Birstein & Vinogradov, 1972; *P. stella*, Macpherson, 2001). These sample species were chosen to cover a range of habitat depths and localities and so to reflect the global range of the genus (Appendix E).

Following the study by Ingle & Garrod (1987) on *Paralomis granulosa*, specimens from two or three size classes (CL 10–25mm, 30–50mm, 50+mm) were chosen for illustration. In all *Paralomis* species figured (except possibly *P. inca*), the 50+ size class typically contains reproductively active adults (Lovrich & Vinuesa 1993, Zaklan 2002b). Usual maximum sizes for *Paralomis* species range between 60 mm and 120 mm (Macpherson 1988a, Zaklan 2002b, S. Hall, pers. obs.). No juvenile specimens (<30 mm) of *Paralomis erinacea* are deposited in museums; however, the change in form between adults in the studied range warrants their inclusion in the growth series. Figured specimens were judged to be representative of their size class by microscopic and macroscopic comparison. Sample measurements are stated in the relevant sections, and there was no observed difference in the features to indicate a division between the sexes. Growth series specimens are obtained from as close to the type location as possible.

Photographs were taken under magnification in a light microscope, focussing on the mid-point of the right branchial region, unless otherwise stated in the figure legend. If the mid-branchial region was not representative of the entire dorsal carapace, exceptions are noted in the text.

B1.3 Sample data and results

B1.3.1 Growth Series

***Paralomis cubensis* Chace, 1939** (Fig **B1**.2)

Paralomis cubensis Chace, 1939: 49; Macpherson, 1988a: 97, Fig 44, pl. 22B, 23A.

Type locality: East of Havana, Cuba 23° 12' 30''N., 82° 12' W., 420–548 m; Also, 300–600 m Caribbean sea and Western Atlantic, from 1°N to 27°N.

Specimens examined: 5 ♀ (CL 25–52 mm), 13 ♂ (CL 23–85 mm) (including paratypes). Specimens figured: ♀ CL 26 mm (USNM 231310), R/V Miss Virginia 329–366 m, 21.III.1962 ; ♂ CL 45.8 mm (USNM 213542) 26°45'N, 84°55'W, 466–732 m, XII.1983 ; ♂ CL 79.6 mm (USNM 231312), Amazon River Mouth, 411 m, XI.1957.

In the original description of the 53.2 mm female holotype of *Paralomis cubensis,* Chace (1939) notes "the dorsal carapace crowded with tubercles of different sizes, low and rounded on most surfaces, becoming more acute towards the margins". This description matches the figured specimen (Fig **B1**.2d-e) in the CL 30–50 mm size class. Substantial ontogenetic change is seen in *P. cubensis*, with later growth stages bearing progressively flattened tubercles (Fig **B1**.2g). Specimens smaller than CL 30 mm bore pedunculate tubercles or spines with a bulbous swelling at the apex (Fig **B1**.2b,c). Setae are not found on the apices of these tubercles at any growth stage, instead tubercles are covered evenly in short setae. Macpherson (1988a) reports corroborating features in a CL 28 mm specimen, "granules very acute, forming small spines" but does not include a figure.

***Paralomis erinacea* Macpherson, 1988a** (Fig **B1**.3)

Paralomis erinacea Macpherson, 1988a: 82, figs 36A, 37, pl. 19A.

Type locality: Guinea Bissau and the Ivory Coast 251–900 m; recently found off Mauritania around 1500 m. (Ramos, unpublished).

Specimens examined: 9 ♀ (CL 44–66 mm), 8 ♂ (CL 61–83 mm) studied. Specimens figured (Fig **B1**.3): ♀ CL. 44.87 mm (MNHN Pg-2937); ♀ CL 59 mm; ♂ CL 83 mm (2 specimens in collection of A. Ramos, Vigo, Spain.), Mauritania 14.XII.07.

In the original description of this species (Macpherson 1988a), 9 adult specimens are examined, CL 46–78 mm. Our examination slightly extends this range, doubling the specimen count, and examining newly identified individuals from CL 44 mm to 83 mm. Macpherson (1988a: Fig 37G therein) shows spines similar to those that we found on the smaller size classes (40–50 mm: Fig **B1**.3b). These are large conical spines, of uniform size, bearing small setae. The larger specimen, at CL 83 mm (Fig **B1**.3e, f) has spines which are wider, lower and blunter than those originally figured specimens.
The macroscopic appearance of the larger adults is smoother than the spiny smaller adults, and can be a cause of misidentification. In *P. erinacea*, the lateral spines are similar in form to the dorsal spines.

***Paralomis granulosa* Jaquinot, 1847** (Fig **B1**.4)
Lithodes granulosa Jaquinot, 1847: figs 15–21, plate 8.
Lithodes granulosus White, 1847: 56.
Lithodes granulata Jaquinot, 1853: 94.
Lithodes verrucosa Dana, 1852: 428. — Dana, 1855: pl. 26, Fig 16 — Cunningham, 1871: 494.
Paralomis verrucosa Bouvier, 1895: 187, pl. 13, Fig 3 — Bouvier, 1896: 26.
Paralomis granulosa White, 1856: 134.

Distribution: 5–130 m Fjords of Patagonia, and the Falkland islands.

Specimens examined: 20 ♀ (CL 28–55 mm), ♂ (CL 13–90 mm). Specimens figured: ♂ CL 25.6 mm (USNM 231429) Strait of Le Maire, Tierra del Fuego, 25.IV.1971 ; ♀ CL 45.6 mm; ♂ CL 65.7 mm (2 specimens, NHM 152710), Tierra del Fuego, 10 m. (Fig **B1**.4)

P. granulosa, studied by Ingle & Garrod (1987), demonstrates the ontogenetic progression of tubercular flattening observed in *P. cubensis*. Small specimens (particularly those CL 10–25 mm) are covered with very distinctive pedunculated irregular tubercles (Fig **B1**.4a, b), sometimes described as 'boleate' (Ingle & Garrod 1987). These progressively become less pedunculated (Fig **B1**.4d) until they are reduced to low tubercles (Fig **B1**.4f). This reduction does not happen evenly across the carapace, with the more lateral tubercles tending to flatten first. The largest specimen that we found bearing pedunculated tubercles was CL 35 mm. In very large specimens of up to CL 90 mm (not mentioned in the 1987 work on this species), the tubercular cover can be quite sparse, and fouling or wear on the carapace can be substantial, as

moults become less frequent (McCaughran & Powell 1977). The 1987 study of Falklands populations, conducted by Ingle & Garrod, is supported by these results, and can be generalised over the wider geographic range of the species.

***Paralomis inca* Haig, 1974** (Fig **B1**.5)
Paralomis inca Haig, 1974: 157, figs 3, 4.

Type locality: Pacific coast of Ecuador and Peru, 06° 31.5' S, 81° 01.5' W 600–800 m.
Specimens examined: 5 ♀ (CL >90 mm). Information about smaller size classes comes from the original description (Haig, 1974). Specimen figured (Fig **B1**.5): ♀ CL 96 mm (USNM 259223) 7°49'00''S 80°38'00''W, 705–735 m.

No specimen of *Paralomis inca* (Fig **B1**.5) examined was smaller than CL 90 mm, and the smallest of the 'adult' type collection (Haig 1974) was CL 80 mm. In the original description (Haig 1974, Fig 4 therein), a figure of a juvenile CL 69 mm is double the normal minimum size of maturity for many species of the genus (Zaklan 2002b). Haig (1974) does illustrate a marked difference between juvenile and adult spines, as can be seen in Fig **B1**.5. In large specimens, tubercles are low, regular mounds, with a circular patch of short setae at the apex. In the small paratype, the dorsal ornamentation is much more spiniform, with long setae eminating from the apex.

***Paralomis mendagnai* Macpherson, 2003** (Fig **B1**.6)
Paralomis mendagnai Macpherson, 2003: p. 414, figs 1–3.

Type locality: Solomon Islands 9°06.9'S, 159°53.2'E, 869–912 m; also found 400–1200 m Solomon Islands.
Specimens examined: Examined 6 ♀ (CL 7–49.9 mm), 6 ♂ (CL 11–59 mm). Specimens figured (Fig **B1**.6): 2 ♂ CL 11 mm, 58.8 mm, ♀ CL 36 mm (MNHN Pg-6408), Solomon Islands 896–1012 m, 25-26.IX.2001.

From an ovigerous female found 700-800 m, they are known to be reproductively mature by at least CL 50 mm. *P. mendagnai* appears to be different from other South Pacific groups studied, (Figs **B1**.12, 14) in the smoothly rounded tubercles of the adults, which have pores (possibly minute setae) on the apex (not in a circular pattern) on the apex. Specimens in the CL 10–25 mm size class had conical, or spiniform tubercles, unlike anything found on specimens above CL 30 mm. The small paratype of *P. mendagnai,* (Fig **B1**.6a, b) has a spiniform enlargement (Fig **B1**.6b) of one of the

conical tubercles of the mid-branchial region; whereas the surrounding tubercles are much smaller. In positions on the carapace where juveniles have such enlarged conical tubercles, specimens larger than CL 30 mm have only wide (> 3 mm diameter, flat or rounded tubercles.)

***P. multispina* Benedict, 1894** (Fig **B1**.7)

Leptolithodes multispina Benedict 1894: 484. – Rathbun, 1904: 165.

Paralomis multispina Schmitt, 1921: 159, pl. 23; pl. 30, figs 7, 8. – Makarov 1962 (1938): 257, Fig 102. – Sakai, 1971: pl. 6, Fig 2; pl. 14, figs 1, 2.

Distribution: Approximately 500–1100 m North Pacific, particularly around Japan.

Specimens examined: 7 ♀ (CL 14–93 mm) 9 ♂ (CL 7–105 mm) were examined. Specimens figured (Fig **B1**.7): ♀ CL 17 mm (USNM 18591), Sea Lion rocks, WA, 1253 m ; ♀ CL 68 mm (USNM 18589) San Diego, CA, 1503 m.

In *P. multispina*, the spines in the larger size classes (> CL 50 mm) are stout, sharp-tipped, and conical, flattened at an oblique (posterior facing) angle, and with a circumference of short setae around that face (Fig **B1**.7e). Juveniles (CL 7–30 mm) of *P. multispina* have short, blunt, pedunculated tubercles, bearing a halo of short setae (Fig **B1**.7b, c). In specimens of around CL 30 mm, there is evidence for the tubercles becoming longer, and developing an acute tip, as in larger adults; however, the angle of the oblique, posterior directed face is smaller. In all specimens, one spine in the mid-gastric region is larger than the other spines or tubercles, which has no setae, nor does it have a flattened region posteriorly: this spine appears to be particularly large in relation to the lower tubercles on small specimens.

***Paralomis spinosissima*, Birstein & Vinogradov, 1972** (Fig **B1**.8)

Paralomis spinosissima Birstein & Vinogradov, 1972: 352, figs 1, 2.

Type locality: 53°37'S, 36°13'W, off South Georgia, 640–650 m; Also found: 150–800 m South Georgia and the southern and western coasts of Cape Horn.

Distribution: 8 ♀ (CL 17–56 mm), 10 ♂ (CL 28–80 mm) specimens examined. Specimens figured (Fig **B1**.8): ♀ CL 17.1 mm (USNM 154634) Drake's Passage, 384–394 m, .IX.1963 ; ♀ CL 55.6 mm (USNM 231422) South Georgia, 563–598 m, May 1975.

The spines in the larger size classes of *P. spinosissima* (CL >50 mm) appear to be almost identical to *P. multispina* previously examined. Spines in adult specimens are stout, sharp and conical, flattened apically at an oblique (posterior facing) angle, and with an apical circumference of short setae (Fig **B1**.7e; Fig **B1**.8d). Juveniles (CL 7–30 mm) of *P. spinosissima* have long, sharp spines with long setae (Fig **B1**.8b). Again, similar to *P. multispina*, one spine in the mid-gastric region on all sizes of specimen is prominent and without setae or a posterior face.

***P. stella* Macpherson, 1988c** (Fig **B1**.9)

Paralomis stella Macpherson, 1988c: p. 118, Fig 1; pl. 1 A-C.

Type locality: La Réunion, 350-937 m.

Specimens examined: 6 ♀ (CL 39–49 mm) 7 ♂ (CL 17–86 mm). Figured specimens (Fig **B1**.9) ♂ CL 24.5 mm (MNHN Pg-4257) Réunion Islands, 350–750 m, 28.VIII.1982 ; holotype ♂ 71.3 mm (MNHN Pg-4255).

P. stella, from the south-eastern Indian Ocean, has a very similar adult spine morphotype, and a comparable ontogenetic progression to *P. mendagnai*. In both groups, the CL 10–25 mm size class have conical, spiniform tubercles, although in *P. stella*, none of the spines on the carapace are consistently enlarged in comparison to others on the same specimen. Adults larger than CL 30 mm have regular, rounded tubercles with pores (possibly minute setae) dispersed across the apex.

B1.3.2 Additional adult morphologies

Images of 24 additional species of the genus *Paralomis* (Figs **B1**.10–15; Table B1) demonstrate the diversity of ornamentation within adults (and in two cases, of juveniles) of the Lithodidae, with a view to standardising terminology and aiding future identifications using carapace features.

B1.4 Discussion

B1.4.1 Ontogenetic Patterns

There appears to be no single function governing the ontogenetic change of carapace ornamentation across the genus *Paralomis*. In several of the groups (*P. cubensis* Fig **B1**.2*, P. erinacea* Fig **B1**.3, *P. granulosa* Fig **B1**.4*, P. inca* Fig **B1**.5*, P. stella* Fig **B1**.9), there is evidence for a progressive flattening of tubercles over subsequent moult stages. Additionally, in *P. africana* Macpherson, 1982 (Figs **B1**.10b, d), the juvenile paratype (CL 15.7 mm) has the ornamentation of the carapace “as in adults, but

proportionally longer" (Macpherson 1982). This is not the case for all species – with the large spines of adult *P. multispina* (Fig **B1**.7) developing contrary to this hypothesis from the pedunculated tubercles present in juveniles. It is clear, however, that significant and consistent changes do occur within species. If the ontogenetic progression for more species were recorded, it may also be possible to detect trends within lineages.

B1.4.2 Lineages and forms

Based on the carapace ornamentation, several basic forms of ornamentation appear to exist. Some vague geographical patterns are apparent, for example the similarity of *P. dofleini*, *P. haigae* and *P. ochthodes* from the Pacific and Indian Oceans, respectively. In general however, trying to make such links without knowing life histories might be flawed. In the 'western South America' region, ornamentation seem to be most similar to that from species from neighbouring biogeographic zones (e.g. *P. phrixa* is comparable to *P. spinosissima* (Southern Ocean, Fig **B1**.8) and *P. multispina* (North Pacific, Fig **B1**.7); *P. otsuae* (South Atlantic, Fig **B1**.12d) to *P. verrilli* (North Pacific, Fig **B1**.13f), suggesting a complex pattern of dispersal to or from this region.

B1.4.3 Functionality

Little is known about the significance of the setae and tubercles for camouflage or protection in different habitats. Migrations during development are recorded for many lithodid species (Miquel et al 1985, Abelló & Macpherson 1991, Stone et al 1992, Lovrich & Vinuesa 1995), and it seems reasonable to suggest the environmental pressures of changing habitats to explain a change in ornamentation. Thus, it is possible that changes in ornamentation are partially environmentally controlled. Juveniles are generally more densely ornamented than adults, and their spines tend to be proportionally longer. This may reflect the more vulnerable trophic position of the juveniles. Alternatively, the change in appearance may be a by-product of the mechanics of tubercle structure formation; whereby the feature-forming nuclei in the epidermis are spread apart as a result of growth. The mechanism by which spines and tubercles are formed at each moult, and the genetic or epigenetic mechanism that controls their form is unknown at present, and experimental work would need to be done to test this hypothesis.

B1.4.4 Application to other genera

This study could have been extended to encompass some of the other lithodid genera. *Paralomis* has 61 species (Appendix A), and as such is the most speciose genus of the Lithodidae. Species of this genus inhabit a wide variety of habitats, locations, and depths, and their identification can pose a challenge for field-ecologists. Ontogenetic changes are well documented for the 10 species of the deep-sea genus *Neolithodes*, as noted in many of their species descriptions (Benedict 1894, Barnard 1946, Macpherson 1988a). Spines in *Neolithodes* are long, thin and devoid of setae. The global, abyssal habitat of *Neolithodes* is more homogenous than that of *Paralomis* (Hall & Thatje 2009a), but it has been observed that those species of *Neolithodes* inhabiting shallower water have a spinier carapace and legs than those in deeper waters in the same region (Smith 1882, Benedict 1894, Stebbing 1905, Barnard 1946). This may be evidence of a higher predatory pressure in shallow seas.

The genus *Paralomis* is paraphyletic, but only with respect to *Glyptolithodes* (Section **A1**.4.2), and the forms of carapace ornamentation documented here, are not found in any of the other lithodid groups. Genera *Lithodes* Latreille, 1806, and *Neolithodes* have thin spines with no setae; Hapalogastrine have overlapping features, described as 'scales', which have setae on their anterior edges (Zaklan 2002a).

B1.4.5 Terminology

It is with particular difficulty that the tubercular stuctures of the Lithodidae are described. Aligning the descriptions in original works with pictures taken of adults (type specimens where possible: Table B1), highlights deficiencies in the current semantics (for example, where *P. aculeata* in Spiridonov (2006) [Fig **B1**.11a, b] is described in the same way as *P. pectinata* in Macpherson (1988a) [Fig **B1**.10f]). Ornamentational structures with different basic forms are not adequately differentiated in descriptions. While it might be possible to create a complex universal classification of carapace ornamentation for the Lithodidae, this would involve conjecture on the homology and the biological processes involved in tubercle development. In this thesis, the terminology used to describe ornamentation of *Paralomis* (Fig **B1**.1) is: 'tubercle', which replaces previously used synonyms: granule and papilla to describe structures less than 1.5 x as tall as wide; and 'spine' to describe structures more than 1.5 x as tall as wide. A distinction should then be made between conical, flattened, pedunculate or rounded tubercles, and regular or irregular tubercles (Fig **B1**.1 for details).

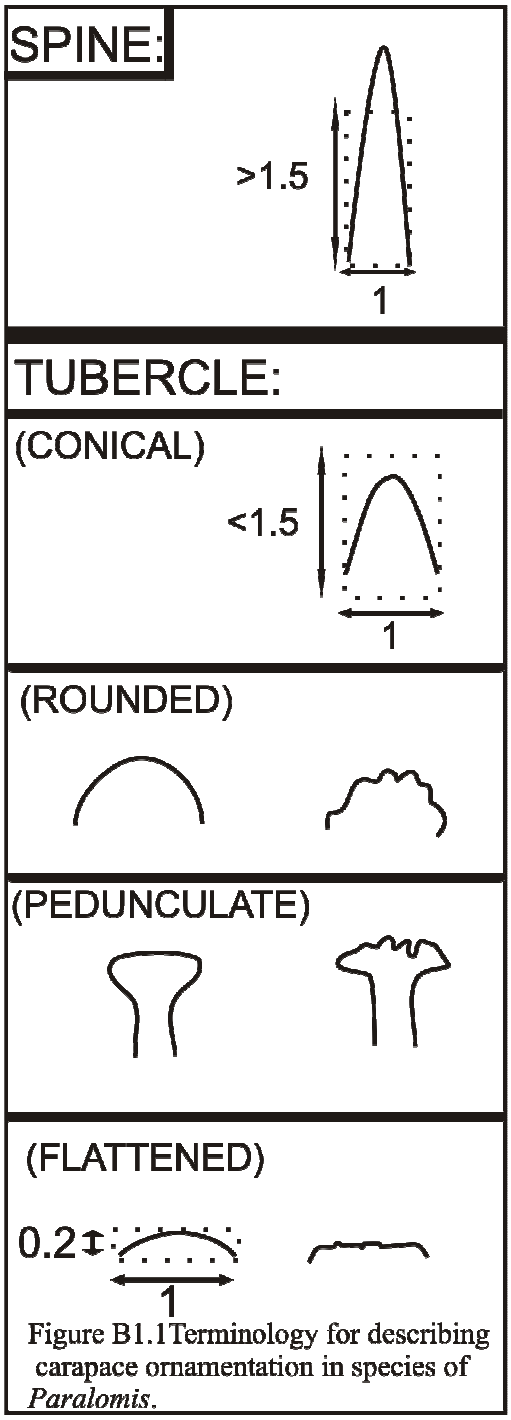

Figure B1.1Terminology for describing carapace ornamentation in species of *Paralomis*.

This emphasises the fact that tubercles may be able to change between these forms within an individual between moults. This standardisation of descriptive terms encourages the use of diagrams or photographs (which are lacking from most of the original descriptions) to illustrate the different forms of tubercles found in this genus.

B1.5 Conclusions

This work highlights the need for the entire growth spectrum to be taken into account when identifying species. The fact that many described lithodid species are represented by only a few specimens underlines the importance of this comparative approach, in which general patterns for the genus are sought.

- In *Paralomis*, particularly, dramatic changes in tubercle form can occur over a succession of moults.
- Tubercle variability within specimens and within size classes of the same species is low in comparison to ontogenetic variations.
- No single pattern could be found to describe the directionality of ontogenetic change within *Paralomis*, indicating that the trajectory of change itself might be a diagnostic character: potentially useful in morphological phylogeny.
- The most common trend within *Paralomis* was for a reduction in the height of ornamentation – from spines or conical tubercles to flattened tubercles. This was not universal.

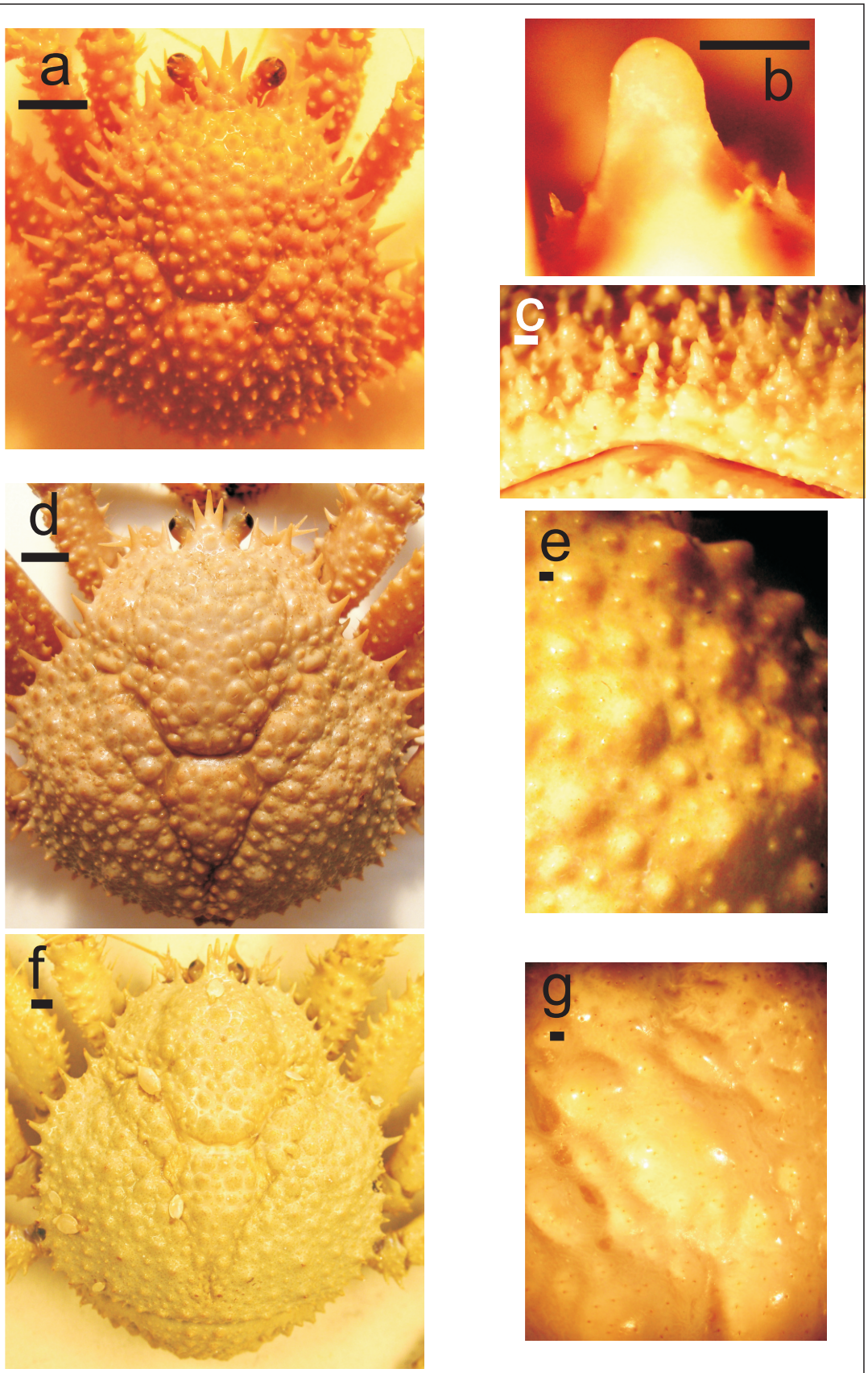

Figure B1.2 Carapace ornamentation of *Paralomis cubensis* Chace, 1939. **a, b, c)** Female CL 26 mm (USNM-231310), R/V Miss Virginia 329–366 m, 21.III.1962; **d, e)** Male CL 45.8 mm (USNM-213542) 26°45'N, 84°55'W, 466–732 m, XII.1983; **f, g)** Male CL 79.6 mm (USNM-231312), Amazon River Mouth, 411 m, XI.1957. **a)** carapace, dorsal view, scale: 5 mm; **b)** mid-branchial spines, posterio-lateral view, scale bar: 1 mm; **c)** branchial spines, posterior view, scale bar: 1 mm; **d)** carapace, dorsal view, scale bar: 5 mm; **e)** mid-branchial region, dorsal view, scale bar: 1 mm; **f)** carapace, dorsal view, scale bar: 5 mm; **g)** mid-branchial region, dorsal view, scale bar: 1 mm

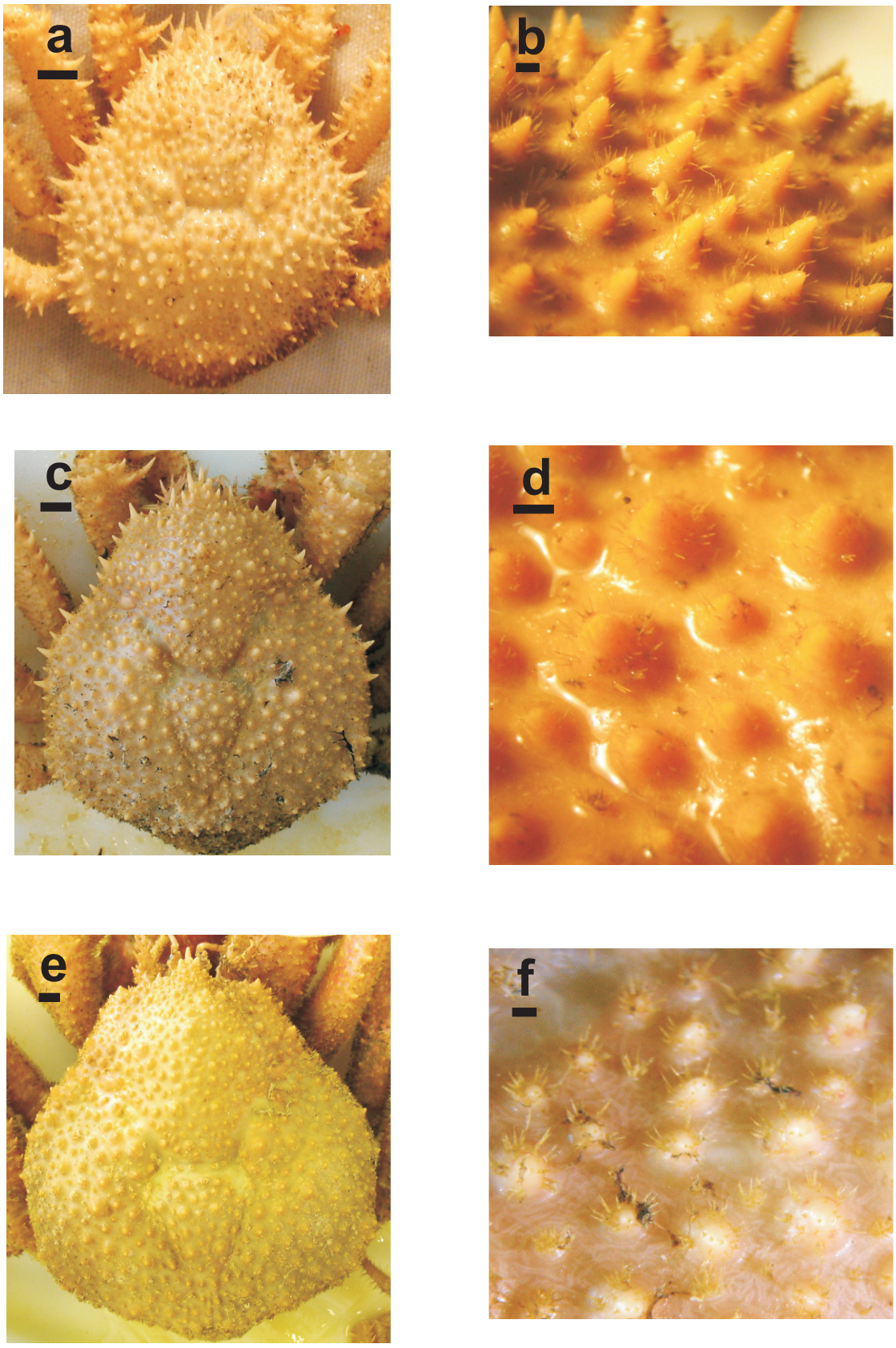

Figure B1.3 Carapace ornamentation of *Paralomis erinacea* Macpherson, 1988. **a, b)** Female CL 44.87 mm (MNHN Pg-2937); **c, d)** Female CL 59 mm (specimen in collection of A Ramos, Vigo), Mauritania 14.XII.07 **e, f)** Male CL 83 mm (specimen in collection of A Ramos, Vigo) Mauritania 14.XII.07. **a)** carapace, dorsal view, scale bar: 5 mm; **b)** dorsal spines, posterior view, scale bar: 1 mm; **c)** carapace, dorsal view, scale bar: 5 mm; **d)** dorsal spines, posterior view, scale bar: 1 mm; **e)** carapace, dorsal view, scale bar: 5 mm; **f)** dorsal tubercles, posterior view, scale bar: 1 mm.

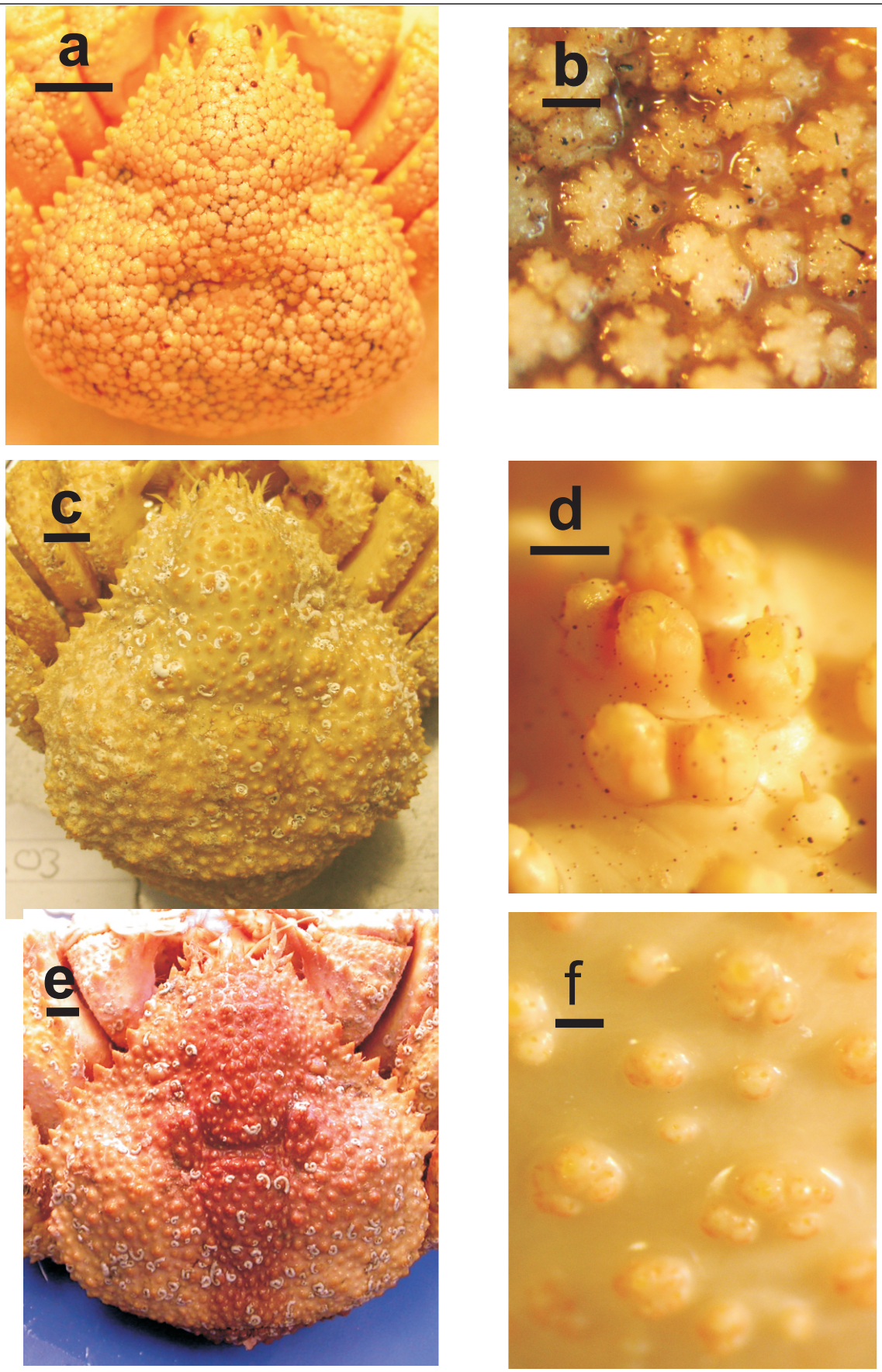

Figure B1.4 Carapace ornamentation of *Paralomis granulosa* Jaquinot, 1852. **a, b)**, Male CL 25.6 mm (USNM-231429) Strait of Le Maire, Tierra del Fuego, 25.IV.1971; **c, d)** Female CL 45.6 mm (NHM-152710); **e, f)** Male CL 65.7 mm (NHM-152710), Tierra del Fuego, 1939; **a)** carapace, dorsal view, scale bar: 5 mm; **b)** mid-branchial region pedunculated tubercles, dorsal view, scale bar: 0.5 mm; **c)** carapace, dorsal view, scale bar: 5 mm; **d)** mid-branchial tubercle, postero-lateral view, scale bar: 1 mm; **e)** carapace, dorsal view, scale bar: 5 mm; **f)** mid-branchial region, dorso-lateral view, scale bar: 1mm.

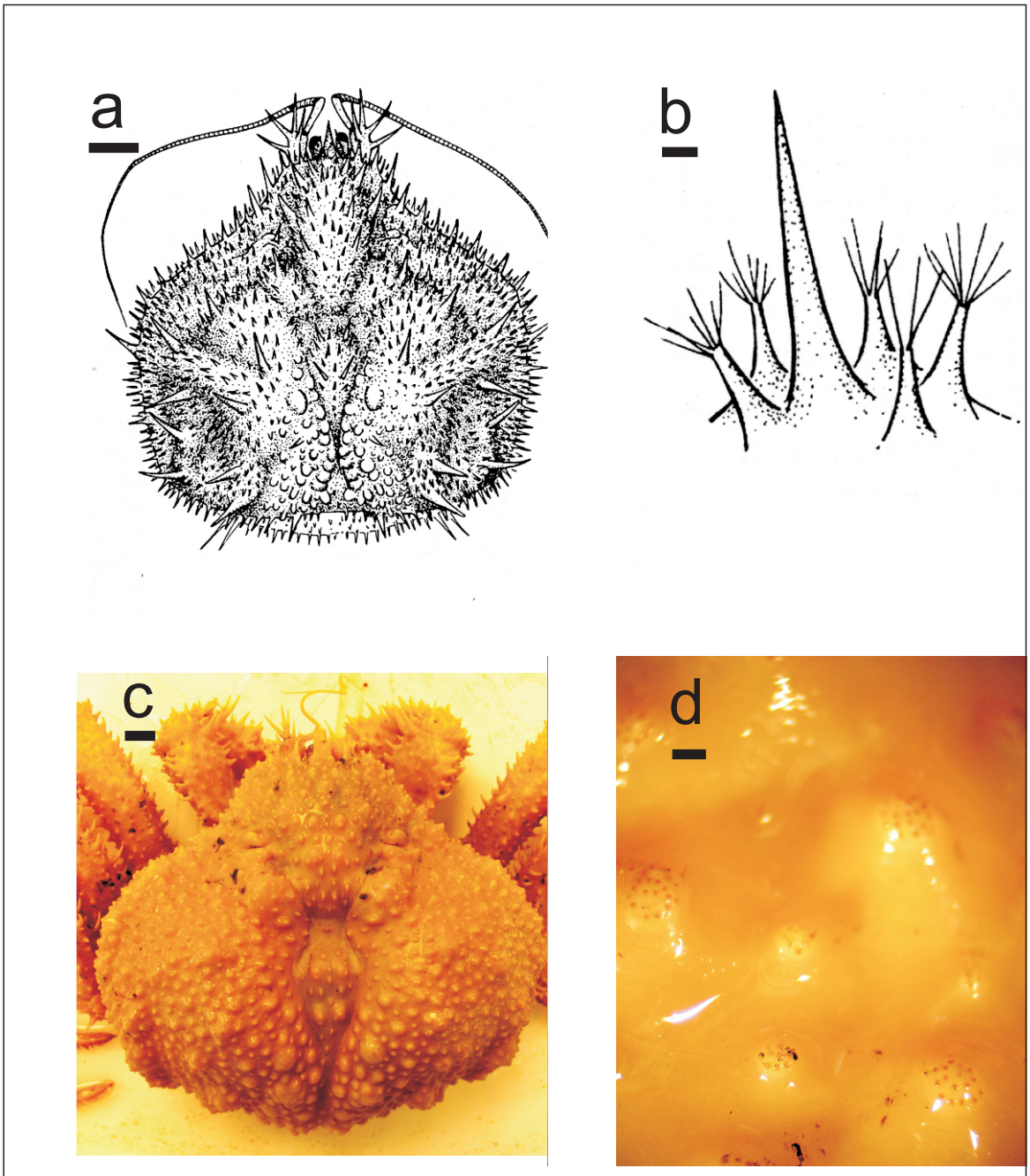

Figure B1.5 Carapace ornamentation of *Paralomis inca* Haig, 1974. **a, b)** Male CL 69 mm (image of paratype from Haig, 1974), 12 miles SW of Banco de Mancora, Peru, 620 m, III.1971 **c, d)** Female CL 96 mm (USNM-259223) 7°49'00"S 80°38'00"W, 705–735 m; **a)** carapace, dorsal view, scale bar: 10 mm; **b)** carapace spine, lateral view, scale bar: 1 mm; **c)** carapace, dorsal view, scale bar: 10 mm; **d)** mid-branchial tubercle, lateral view, scale bar: 1 mm.

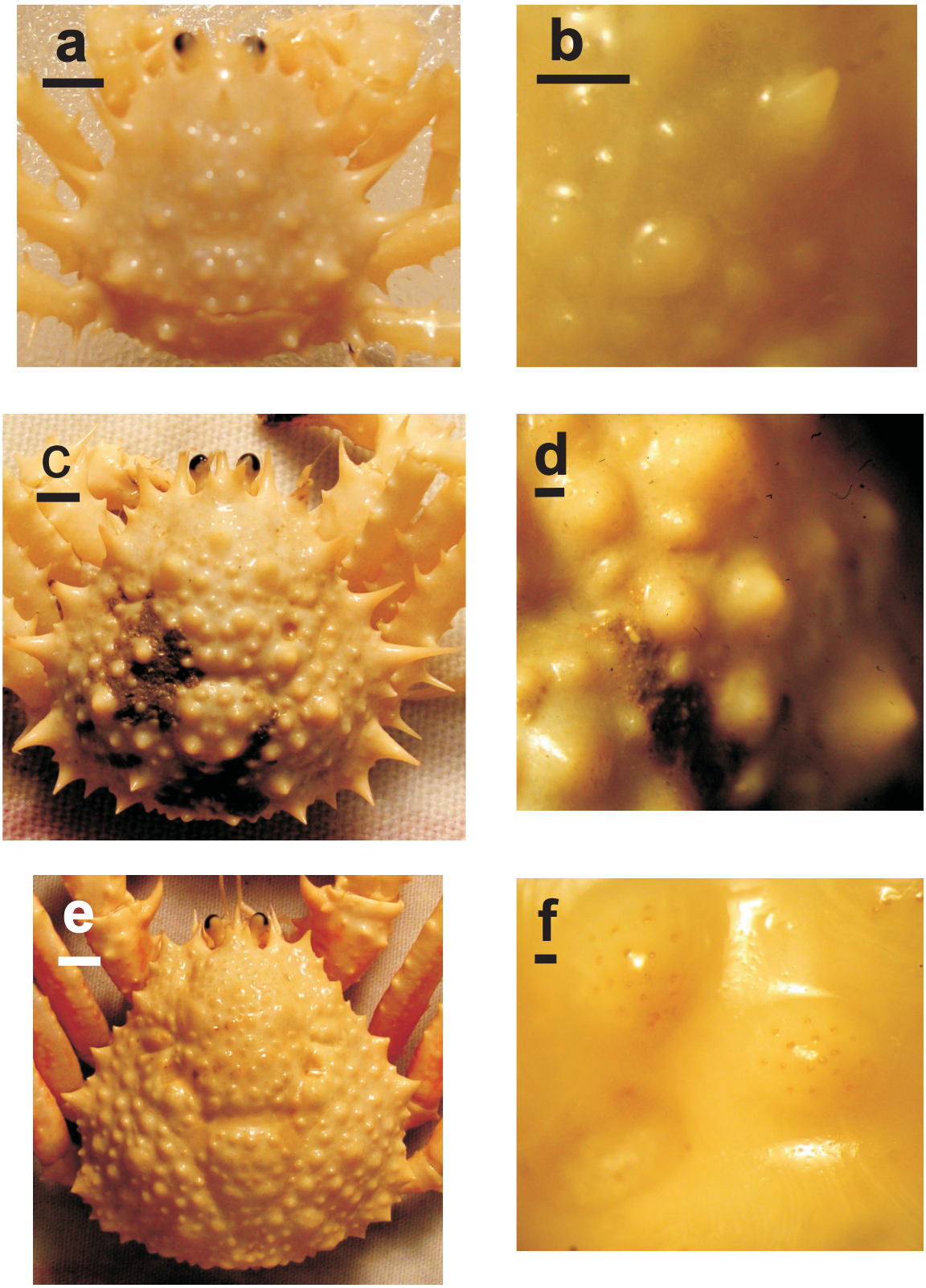

Figure B1.6 Carapace ornamentation of *Paralomis mendagnai* Macpherson, 2003. **a, b)** Male CL 11 mm (MNHN Pg-6408), Solomon Islands 1001–1012 m, 26.IX.2001 **c, d)** Female CL 36 mm (MNHN Pg-6408), Solomon Islands 896–912 m, 25.IX.2001 **e, f)** holotype Male 58.8 mm (MNHN Pg-6408) Solomon Islands 896–912 m, 25.IX.2001; **a)** carapace, dorsal view, scale : 2 mm; **b)** mid-branchial region, dorsal view, scale bar: 1 mm; **c)** carapace, dorsal view, scale bar: 5 mm; **d)** mid-branchial region, dorsal view, scale bar: 1 mm ; **e)** carapace, dorsal view, scale bar: 5 mm; **f)** mid-branchial flattened tubercle, scale bar: 1 mm.

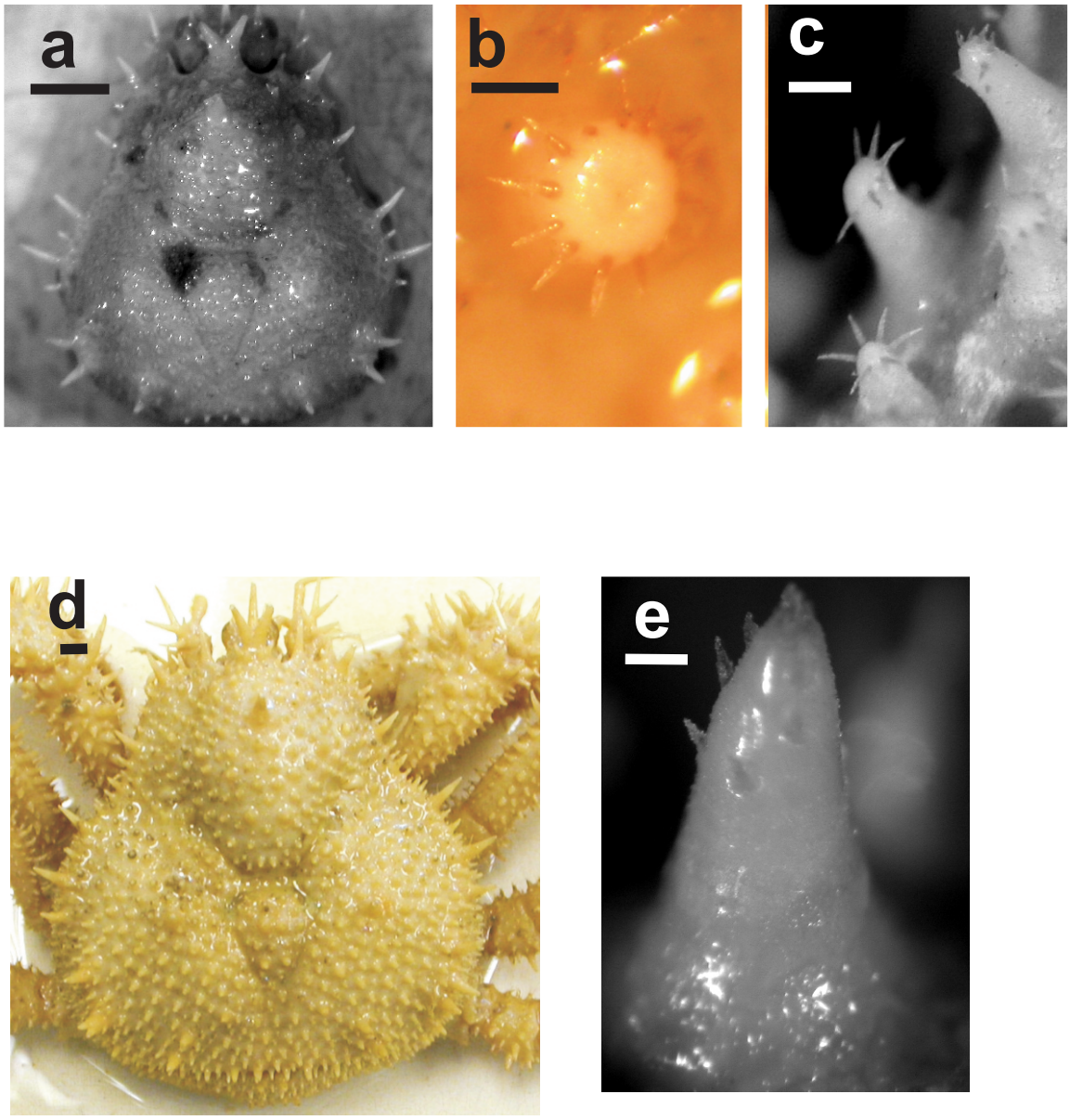

Figure B1.7 Carapace ornamentation of *Paralomis multispina* Benedict, 1895. **a, b, c)** Female CL 17 mm (USNM-18591), Sea Lion rocks, WA, 1253 m; **d, e)** Female CL 68 mm (USNM-18589); **a)** carapace, dorsal view, scale bar: 5 mm; **b)** mid-branchial spine, dorsal view, scale bar: 0.5 mm; **c)** mid-branchial spine, right lateral view, scale bar: 1 mm; **d)** carapace, dorsal view, scale bar: 5 mm; **e)** typical mid-branchial spine, right lateral view, scale bar: 1 mm.

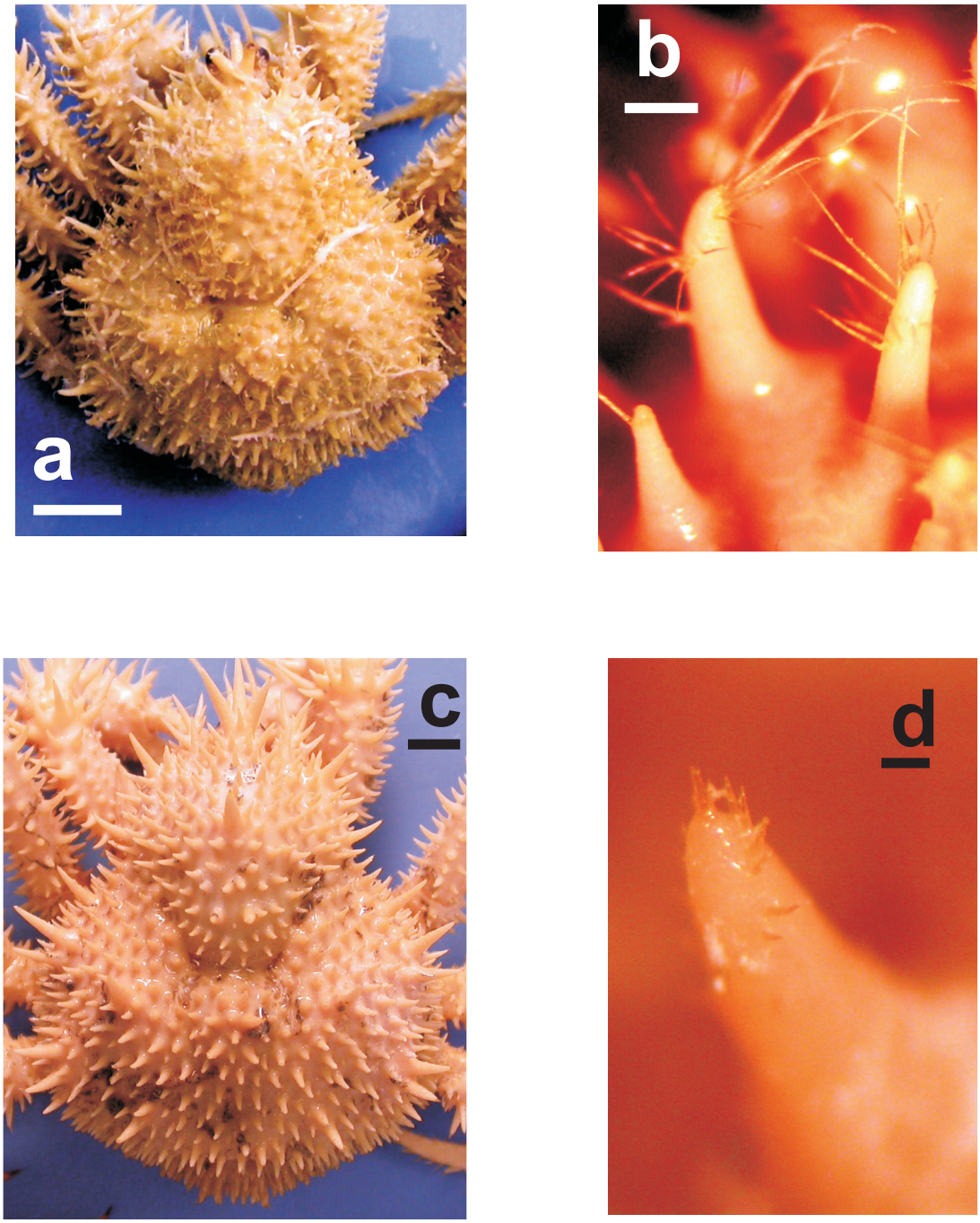

Figure B1.8 *Paralomis spinosissima.* Birstein & Vinogradov, 1972. **a, b)** Female CL 17.1 mm (USNM-154634) Drake Passage, 384–394 m, IX.1963; **c, d)** Female CL 55.6 mm (USNM-231422) South Georgia, 563–598 m, V.1975; **a)** carapace, dorsal view, scale bar: 5 mm; **b)** branchial spines, right lateral view, scale bar: 1 mm; **c)** carapace, dorsal view, scale bar: 5 mm; **d)** typical mid-branchial spine, right lateral view, scale bar: 1 mm.

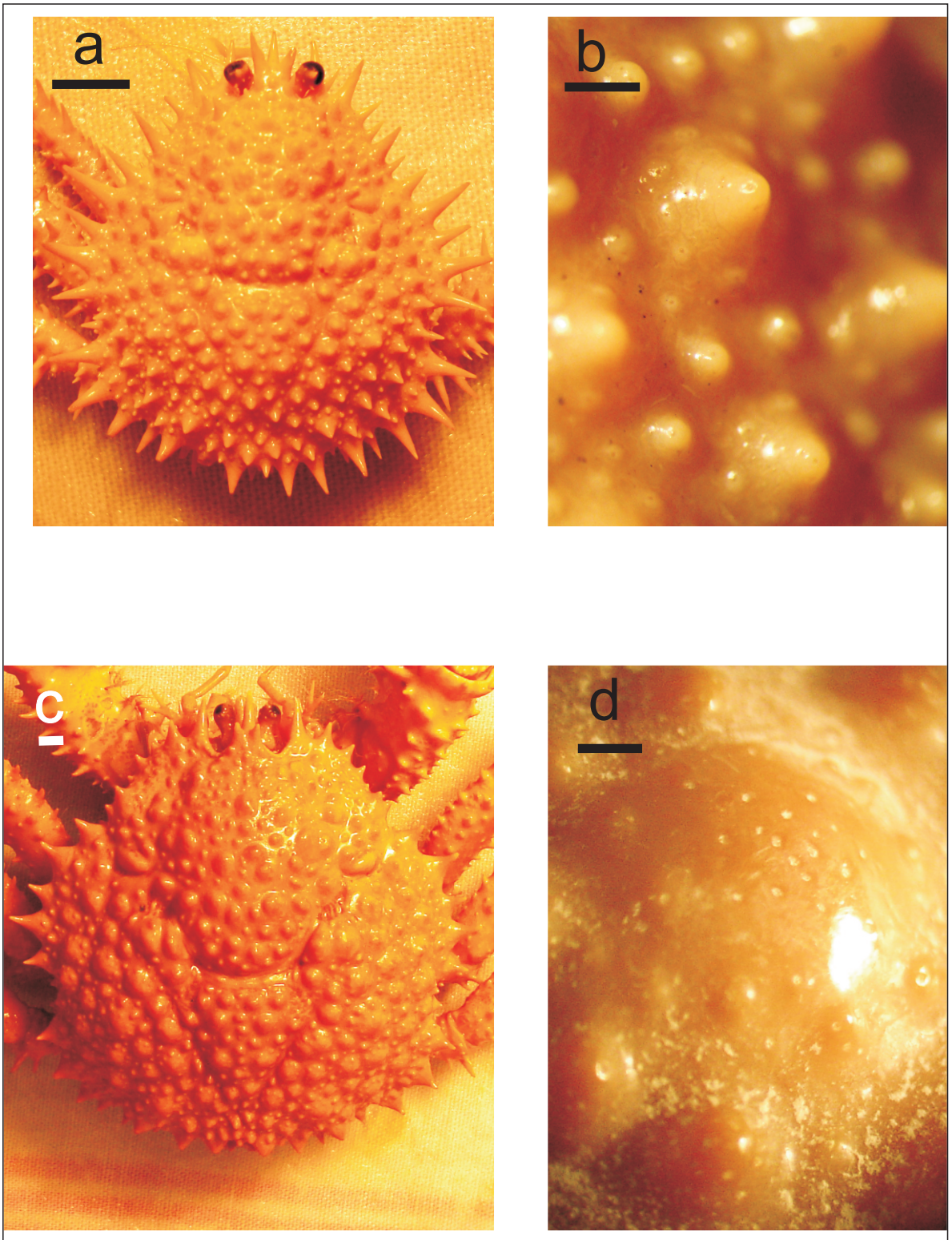

Figure B1.9 *Paralomis stella* Macpherson, 1988. **a, b)** Male CL 24.5 mm (MNHN Pg-4257) Réunion Islands, 350–750 m, 28.VIII.1982. **c, d)** holotype Male 71.3 mm (MNHN Pg-4255); **a)** carapace, dorsal view, scale bar: 5 mm; **b)** mid-branchial spines, left lateral view, scale bar: 0.5 mm ; **c)** carapace, dorsal view, scale bar: 5 mm; **d)** mid-branchial tubercle, left lateral view, scale bar: 1 mm .

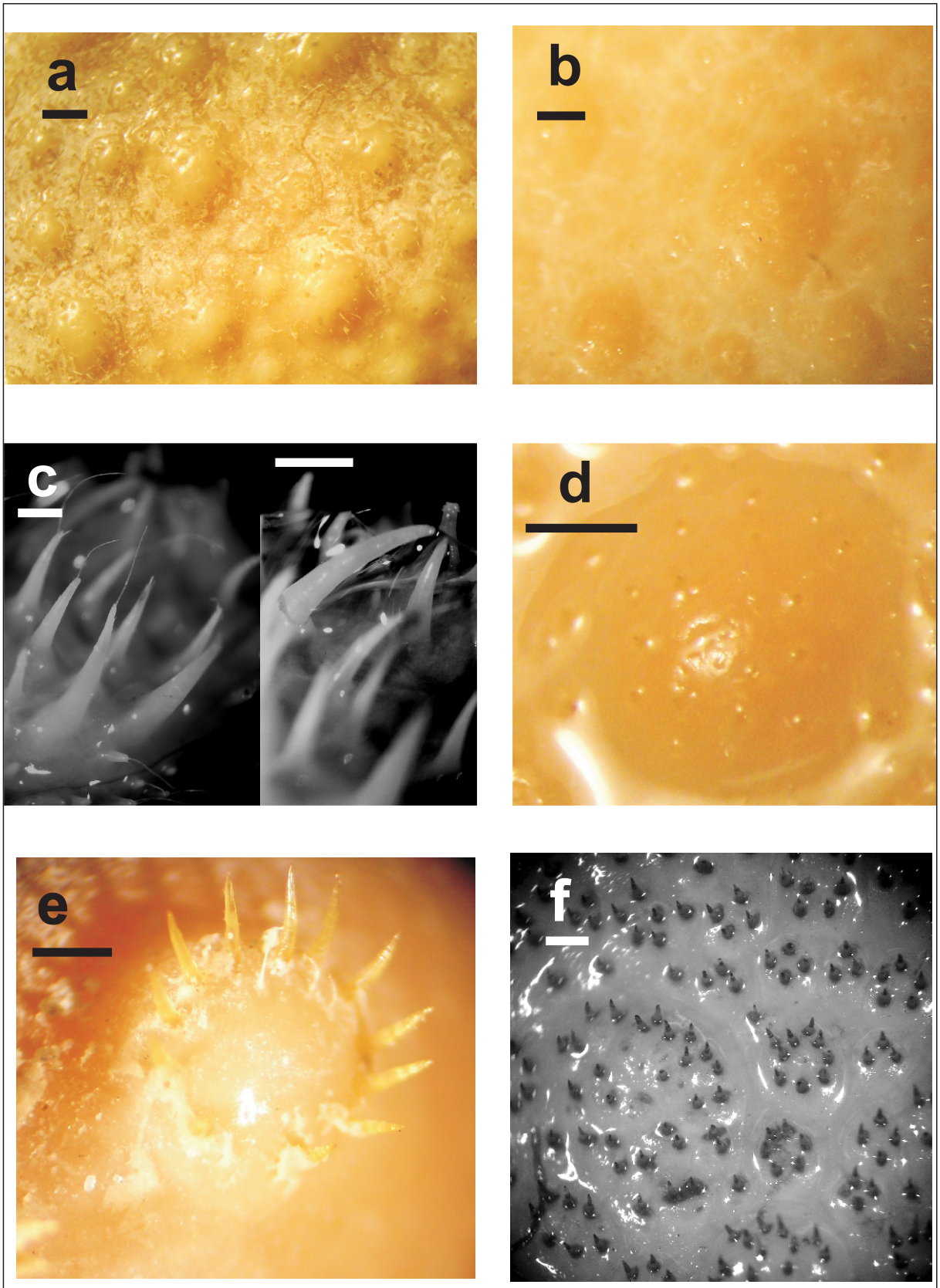

Figure B1.10 Carapace ornamentation of northern and central Atlantic species of *Paralomis*. Scales 1 mm. **a)** *P. cristulata* holotype Female CL 55 mm (MNHN Pg 3427) Senegal, 650 m, mid-branchial region, dorsal view; **b, d)** *P. africana* Male CL 68.4 mm (USNM 213153) mid-branchial region, dorsal view; **c)** *P. bouvieri* Male CL 17.7 (USNM 231209), dorsal carapace spines, lateral view; **e)** *P. grossmani* holotype Female CL 93.4 mm (USNM 228832) mid-branchial tubercle, dorsal view; **f)** *P. pectinata* holotype Female CL 96.4 mm (USNM 233599) mid-branchial region, dorsal view.

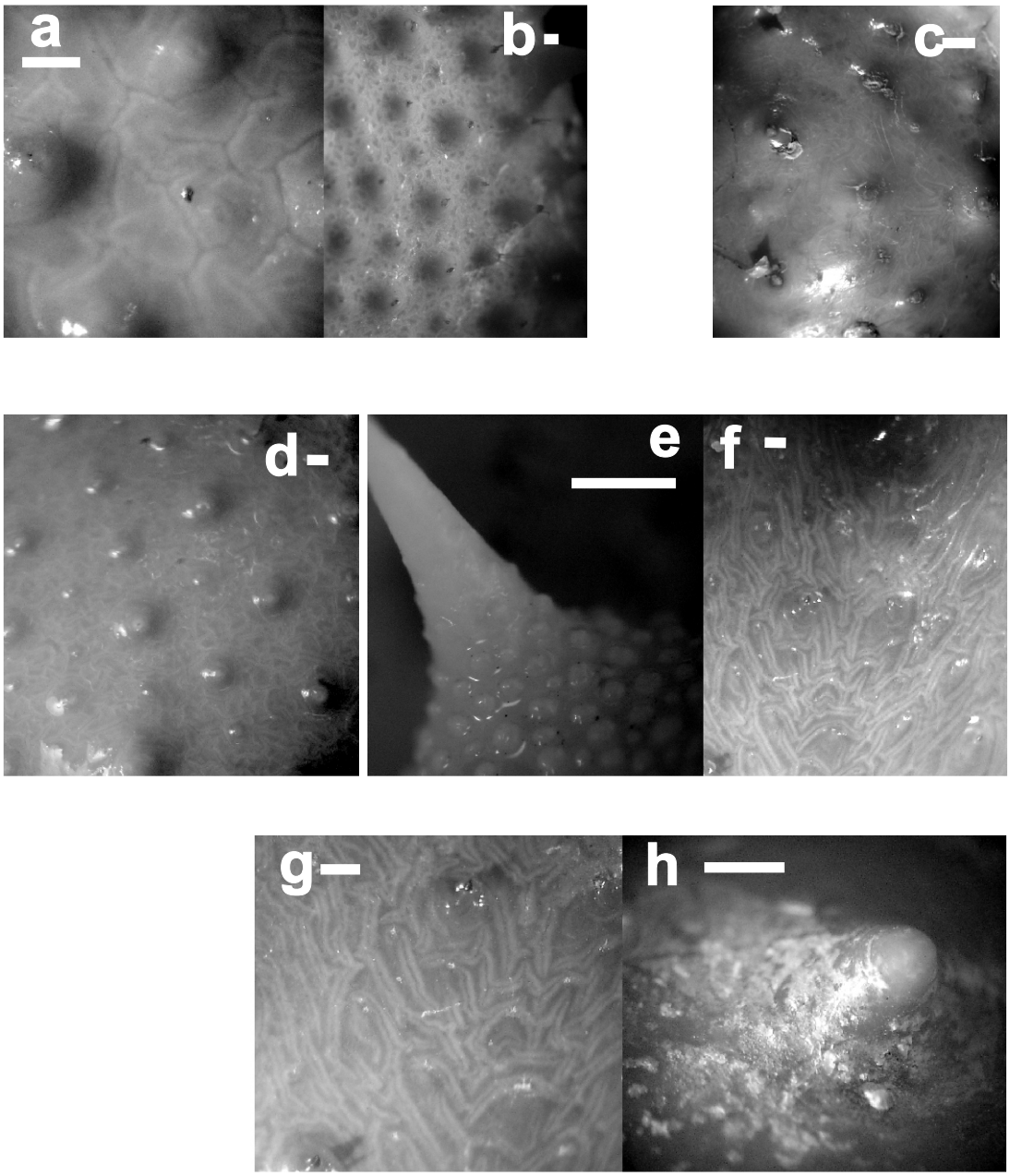

Figure B1.11 Carapace ornamentation of Southern Ocean *Paralomis* species. Scales 1 mm. **a, b)** *P. aculeata*, holotype Male CL 41 mm (NHM 88.33) Prince Edward Islands, **a)** mid-branchial region, dorsal view, **b)** antero-lateral carapace, dorsal view; **c)** *P. elongata* Female CL 65 mm (collection S. Thatje, NOCS) Bouvet Island, mid-branchial region, depicting significant intermoult wear on the tubercles, dorsal view; **d)** *P. anamerae* Female CL 72 mm (MD 24 Crozet Islands, 655—700 m, IX.1980) mid-branchial region, dorsal view; *P. formosa* **e)** paratype Male CL 16.4 mm (NHM 88.33), Rio Plata, base of a lateral spine, showing secondary tubercles in juvenile specimen, dorsal view; **f)** Male CL 72.6 mm (collection, S. Thatje, NOCS) South Georgia groundfish survey mid-branchial region, not showing main spines, which are up to 10 mm in length, dorsal view; **g, h)** *P. birsteini* holotype Female CL 54.7 mm (USNM 228830).

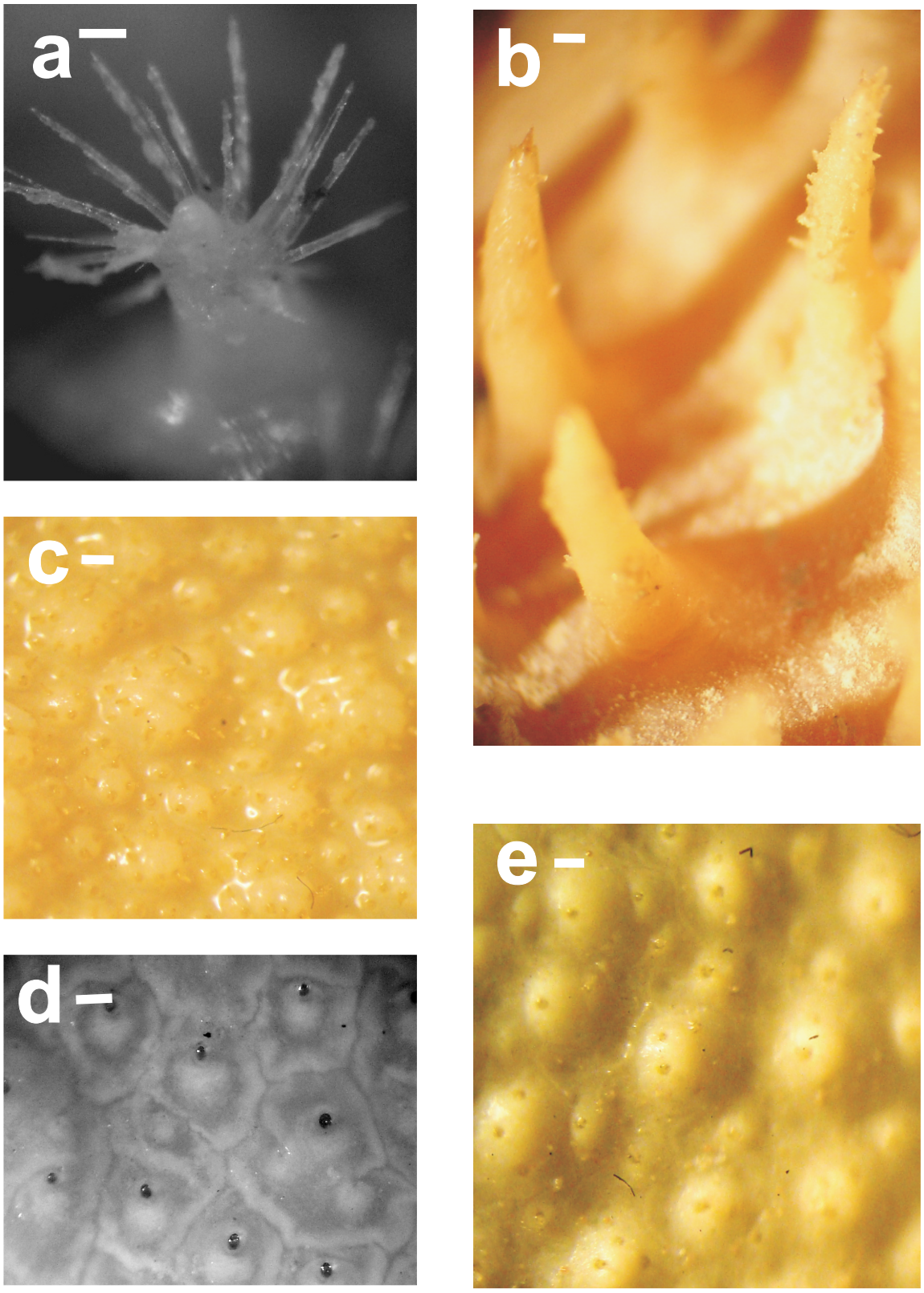

Figure B1.12 South Pacific *Paralomis* species 1. Scales 1 mm **a)** *P. aspera* Male CL 53 mm (NHM) Coquimbo, 560 m, VI.1971 mid-branchial spines, postero-lateral view; **b)** *P. phrixa* holotype Female CL 64.6 mm (USNM 259380) mid-branchial spines, lateral view; **c)** *P. arae* holotype Male CL 74.5 mm (MNHN Pg 5945) mid-branchial region, dorsal view; **d)** *P. otsuae* Female 73.4 mm (USNM 259219) mid-branchial region, dorsal view; **e)** *Glyptolithodes cristatipes* mid-branchial region, dorsal view.

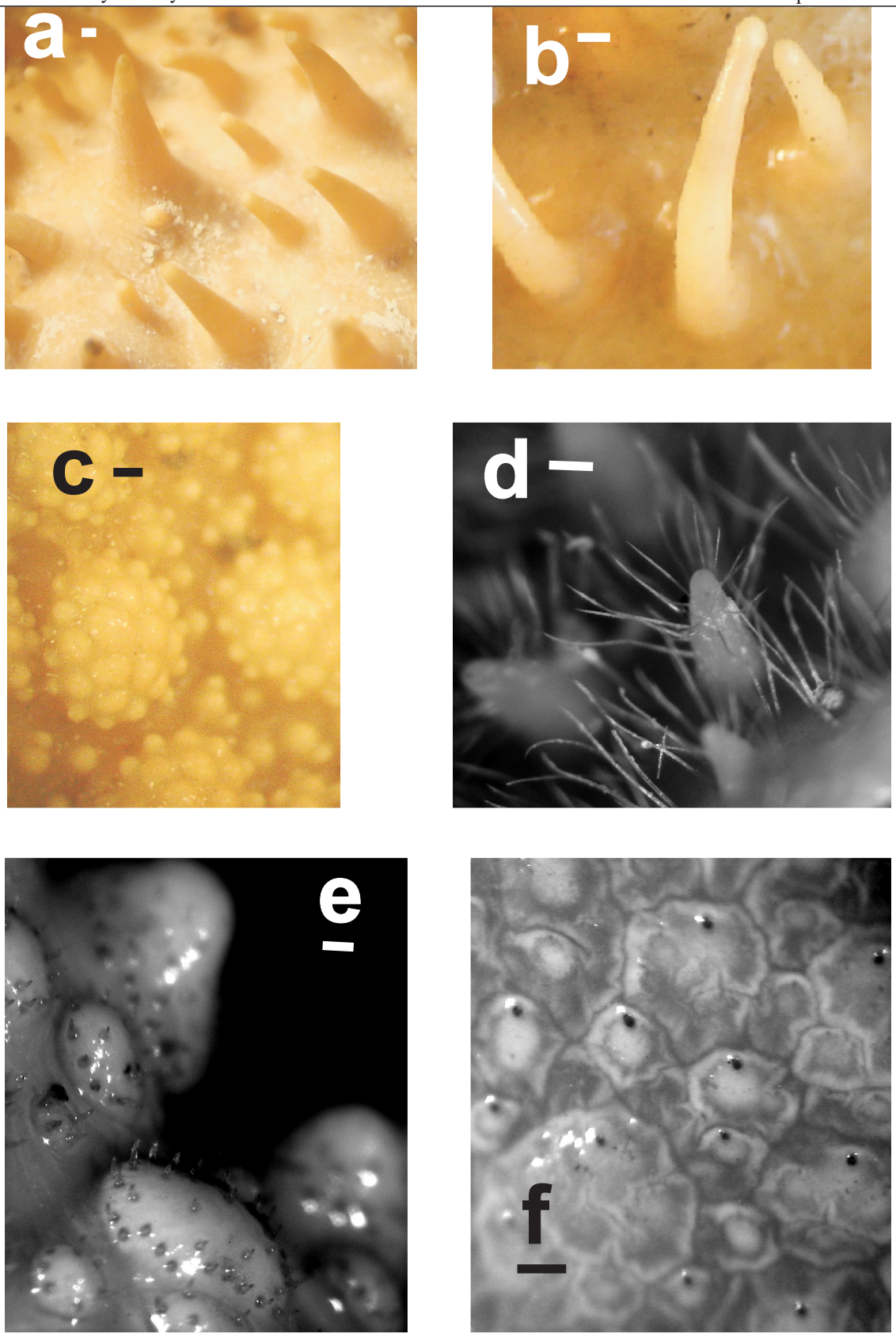

Figure B1.13 Japan and North Pacific species of *Paralomis*. Scales 1 mm **a, b)** *P. histrix* mid-branchial spines, lateral view **a)** Female CL 63.2 mm (NHM 1985.140), **b)** Male CL 34.9 mm (MNHN Pg 2212); **c)** *P. japonica* Male CL 46.7 mm (MNHN) mid-branchial tubercles, dorsal view; **d)** *P. makarovi* holotype Male CL 23 mm (USNM 1122582) mid-branchial carapace spine, lateral view; **e)** *P. cristata* Female 76.4 mm (USNM 229721) mid-branchial tubercle, dorso-lateral view; **f)** *P. verrilli* (Benedict, 1894) holotype Male CL 78 mm (USNM 18537) mid-branchial region, dorsal view.

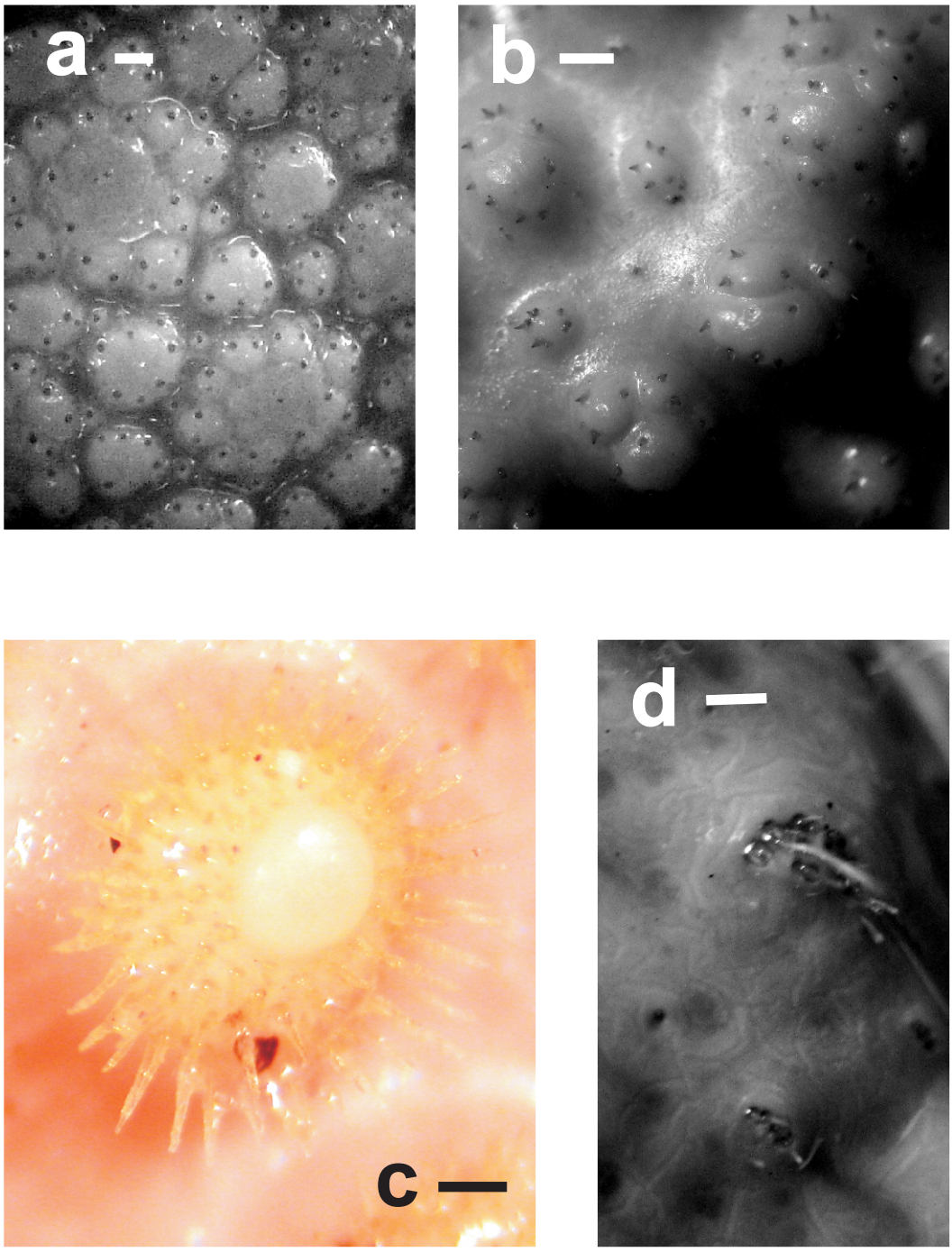

Figure B1.14 Central Pacific species of *Paralomis.* Scale 1 mm **a)** *P. seagranti* Eldredge, 1976, Male CL 74.7 mm (Pg 4265) mid-branchial region, dorsal view; **b)** *P. dawsoni* Female 57.3 mm (MNHN Pg-4279) mid-branchial tubercles, dorsal view; **c)** *P. haigae* Male CL 49.9 mm (MNHN Pg-4276) mid-branchial tubercle, dorsal view; **d)** *P. hirtella* Male CL 47 mm (MNHN Pg-4662) mid-branchial region, dorsal view.

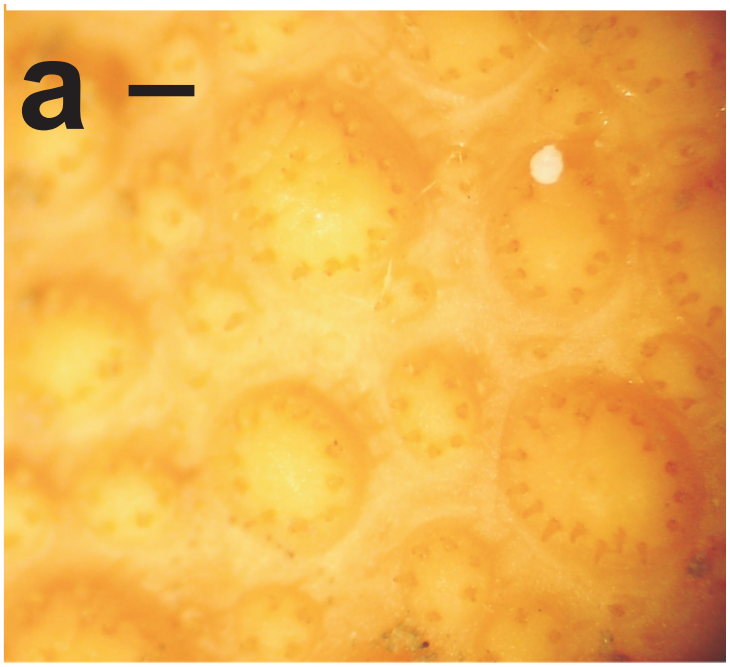

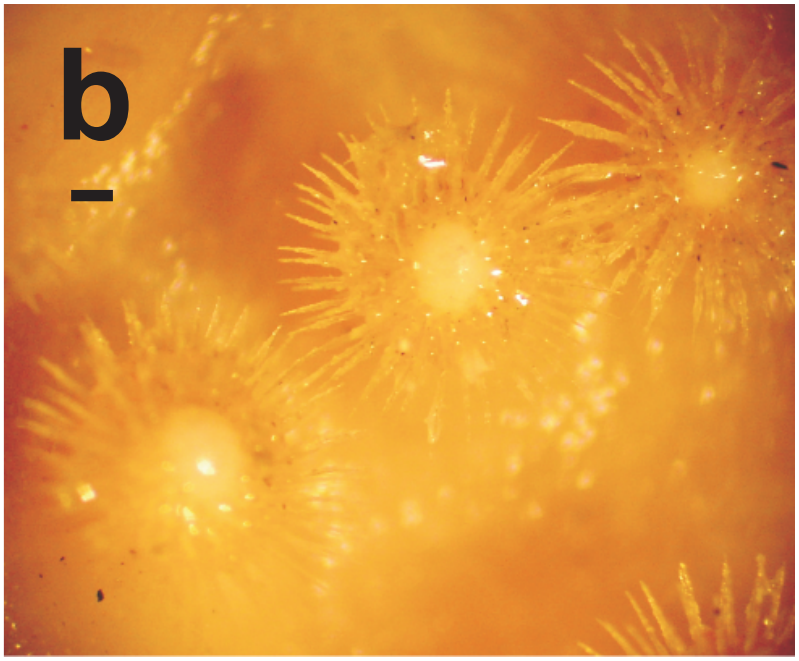

Figure B1.15 Indian Ocean species of *Paralomis*.Scale 1 mm. **a)** *P. ceres* holotype Male CL 58.1 mm (NHM 1989.926) mid-branchial region, dorsal view; **b)** *P. ochthodes* holotype Male CL 71.6 mm (USNM 228831) mid-branchial tubercles, dorsal view.

Table B1: Some descriptions of tubercular structures taken from the literature, alongside results from studies of adult forms using terminology set out in Figure **B1**.1. Both original descriptions and 'previous' publications (other than the original description) were used to compile this table.

Species and systematics	Material Examined	Previous and original descriptions by other authors compared with revised descriptions
P. aculeata Henderson, 1888 **Type locality:** Prince Edward Islands; also known from the Crozet Islands (300—approximately 1500m; Macpherson 2004, Spiridonov et al 2006).	30 specimens CL 25–74 mm.	**Previous:** Carapace dorsally covered with small granules (Spiridonov et al 2006) **Revised:** Sparsely covered with rounded tubercles less than 1 mm in diameter (Figs **B1**.11a, b). Some tubercles towards the anterior edge of the carapace are acute and conical, and some bear setae, especially in smaller adults (Fig **B1**.11b).
P. africana Macpherson, 1982 **Type locality:** off Namibia 550–750 m; also known from Mauritania (Ramos unpublished records).	7 ♀ CL 31-57 mm, 6 ♂ CL 62-78 mm.	**Original:** Covered in granules of variable but small size with stiff setae on the summit. (Macpherson 1982) **Revised:** Flattened to rounded tubercles, with several pores and very short setae scattered over the surface of the tubercle (Figs **B1**.10b, d). In smaller specimens of *P. africana*, around 30 mm, tubercles are more rounded; becoming flattened in larger adults.
P. anamerae Macpherson, 1988a. **Type locality:** North of the Falkland Islands, 132-135 m; now known from South Georgia, around 300-500 m.	4♀ 4♂CL 68-98 mm (USNM 1079617; collection of S. Thatje, NOCS).	
P. arae Macpherson, 2001 **Type locality:** Fiji 1058-1091 m.	Holotype ♂ CL 74.5 mm (MNHN Pg 5945).	**Original:** Granules usually with several setae. Dorsal surface covered with small granules of different sizes (Macpherson 2001). **Revised:** Carapace ornamentation is made up of irregularly rounded tubercles, tightly packed and clustered, with individual setae on some tubercles. (Fig **B1**.12c)
P. aspera Faxon, 1893	♂ Holotype CL 53	**Previous:** Whole surface of carapace and

Type locality: Off Ecuador and western Panama, 750-1200 m (Del Solar 1972, Haig, 1974)	mm (NHM) Coquimbo, 560 m, June 1971.	abdomen thickly beset with papillae or tubercles, each one of which is encircled with a crown of stiff setae (Faxon 1985). **Revised:** A dense coverage of spines or conical tubercles, each with a ring of stiff setae around the acute tip. (Fig **B1**.12a)
Paralomis birsteini Macpherson 1988b **Type locality:** Ross Sea; now known from the Bellingshausen Sea (Thatje, 2008) and Crozet Islands (Macpherson 2004).	5♀ 5♂ examined CL 46-99 mm. (USNM 228830; collection of S. Thatje, NOCS; MD08 1976 cruise to Crozet Islands, 1500 m).	**Original:** Covered with granules of small size, and several spines. **Revised:** Small rounded tubercles less than 1 mm in diameter, in addition to several much larger conical tubercles in consistent positions on the carapace. (Fig **B1**.11g, h)
P. bouvieri Hansen, 1908 **Type locality:** off Iceland, 1471 m; also found off south western Ireland (4152 m: Macpherson, 1988a) and the eastern seaboard of the USA and Canada (1460 m: Macpherson, 1988a).	2 ♂ juveniles, CL 13 mm (USNM 231309), 17 mm (MNHN: Geomanche, November 1985, 47°60'N, 12°19'W).	**Previous:** Dorsal surface covered with many long spines, without granules among them. Normally no setae on spines. Sizes of spines variable, some clearly longer than others. (Macpherson 1988a) **Revised:** All specimens caught to date are between 13 and 34 mm, and have several long spines on their carapace. Previous reports have stated that spines usually have no setae (Macpherson 1988a), but we find this not to be the case in the specimens examined (Figs **B1**.10c). Setae are long and apical, but not in the circumferential arrangement found in small specimens of *P. spinosissima* Birstein & Vinogradov 1972 (Fig **B1**.8b), or other similar species.
P. ceres Macpherson, 1989 **Type locality:** Ra's al Haad, Arabian Sea, 1189-1354 m.	♂ holotype, CL 58.1 mm (NHM 1989.926)	**Original:** Thickly covered with rounded prominent granules of varying sizes (Macpherson, 1989) **Revised:** Several rounded tubercles with a roughly defined ring of single setae towards the top. Lateral, tubercles are conical and which have many setae towards their base (Fig **B1**.15a).
Paralomis chilensis Andrade, 1980.	Not studied.	**Original:** Rows of spiniform tubercles of greater length with some smaller spiniform

Type locality: 420 m, off Chile, 40°S.		tubercles in the interspaces. Spines with a ring of several stiff setae around the tip, but the tip of spines not obliquely cut. (Andrade, 1980). See original description for diagram, in which it is described as having tubercles similar to *P. aspera* Faxon 1893 (Fig **B1**.12a) (Andrade 1980)
P. cristata Takeda & Ohta, 1979. **Distribution:** Around Sagami Bay, and the coast of Japan.	12 specimens, CL 74–96mm.	**Original:** Thickly covered with vesiculous granules of variable but small size, thus the carapace surface of scaly appearance. (Takeda & Ohta 1979). **Revised:** Covered with rounded tubercles (Fig **B1**.13e), each with a ring of short setae around the top. Often these tubercles are clustered into groups.
P. cristulata Macpherson, 1988 a. **Type locality:** Guinea Bissau, eastern Atlantic, 385 m.	2 ♀, including holotype. CL 55.5 (MNHN-Pg 3427), CL 48.34 (ICMD 130/1991).	**Revised:** Rounded or flattened tubercles in adults. Some pores visible across the apex, possibly bearing setae. (Fig **B1**.10a)
P. cubensis Chace, 1939	See text.	**Original:** Covered with crowded tubercles of different sizes, low and rounded on most surfaces, becoming more acute towards the margins (Chace, 1939). **Revised:** Fig **B1**.2 & discussion herein
P. dawsoni Macpherson, 2001 **Distribution:** Solomon Islands and New Caledonia 897—1057 m (Macpherson 2001, 2003).	4 specimens CL 57–77 mm.	**Original:** Rounded clustered granules of different sizes. Granules with short setae (Macpherson, 2001). **Revised:** Dorsal surface of the carapace covered with clusters of rounded or conical tubercles, each with a ring of setae around the apex (Fig **B1**.14b).
P. dofleini Balss, 1911. **Distribution:** Sagami Bay, and the coast of Japan.	3 ♂ CL 46-89mm. Mouth of Tokyo bay, off Tateyama 350-400m March 1991.	**Previous:** Studded with tubercles of varying sizes (Sakai, 1971). Ornamentation is very similar to that in *P. haigae* (Fig **B1**.14c) (Macpherson 2008)
P. elongata Spiridonov	Three paratypes.	**Original:** Carapace dorsally covered with

et al 2006 **Type locality:** Spiess seamount, Bouvet Island, South Atlantic, 300-900 m.		small granules (Spiridonov et al 2006). **Revised:** Sparsely covered with rounded tubercles less than 1 mm in diameter (Fig **B1**.11c). Larger specimens with evidence of environmental inter-moult wear on the tubercles.
Paralomis formosa Henderson 1888 **Distribution:** South East Atlantic, off the coast of Argentina, and South Georgia 400-1600 m.	4 ♀ inc. juv. paratypes, CL 14-85 mm, 3♂ 70-84 mm. (USNM 231436-231439; NHM 88.33; collection of S. Thatje, NOCS)	**Previous:** Entire surface covered with small granules, and a few spines. (Macpherson 1988a) **Revised:** Small rounded or conical tubercles less than 1 mm in diameter, in addition to several much larger conical tubercles or spines in consistent positions on the carapace. The smaller tubercles from juvenile specimens (Fig **B1**.11e) are very densely packed, and proportionally larger in relation to the conical tubercles than those in the adult form (Fig **B1**.11f).
P. grossmani Macpherson 1988a **Type locality:** off the coast of Suriname and Northern Brazil, 770 m.	2 ♀ov including holotype, CL 93, 97 mm (USNM 228832, 228833).	**Original:** Dorsum and sides covered with granules that are more or less acute, without forming spines. Granules bearing thin setae. **Revised:** Rounded (Fig **B1**.10e), or conical tubercles, bearing rings of short setae around the apex of individual tubercles.
P. haigae Eldredge, 1976 **Distribution:** Guam and the Solomon Islands (Eldredge 1976, Macpherson, 2008).	7 specimens CL 43–92 mm. Figured: ♂ CL 49.9 mm (MNHN Pg 4276)	**Original:** Covered with large and small round tubercles, each with a circlet of short setae near the uppermost portion (Eldredge, 1976). **Revised:** *P. haigae* (Fig **B1**.14c) has individual or clustered, rounded tubercles on its carapace and abdominal plates, with a thick ring of setae around the apex of each tubercle.
P. hirtella de Saint Laurent & Macpherson 1997 **Type locality:** Vent sites in Lau, and North Fiji Basins, South West Pacific.	4♀ CL 46-62 mm 3♂ CL 32-54 mm. (MNHN Pg-4658, 4659, 4661, 4662).	**Original:** Carapace devoid of granules, tubercules [sic], or spines, but sparsely covered by tufts of erect setae. (de Saint Laurent & Macpherson 1997). **Revised:** No raised tubercles on the carapace. It does, however, have long (possibly sensory) setae, in semicircular arrays across all surfaces of the carapace (Figs **B1**.14d).
Paralomis hystrix De	3♀ CL 63-96 mm 3♂	**Previous:** Spines very long and sharply

Haan 1849 **Distribution:** Around Sagami Bay, the coast of Japan, and Solomon Islands.	CL 16-98 mm (NHM 1894.7.8.7; 1985.40; USNM 1079610).	pointed. (Sakai 1971) **Revised:** Long, curved, round-tipped spines, without setae in any size of individual examined (Figs **B1**.13a, b). Spines are particularly densely packed in this species, covering all surfaces of the legs, abdomen, and dorsal carapace.
P. hystrixoides Sakai, 1980: 1. **Distribution:** Pacific coast of Japan, and Sagami Bay, Japan, 700-1100 m.	Not studied.	**Original:** Spines of the carapace are slender and sharp. In *P. hystrix*, they are basally swollen in the form of a bulb, especially in fully-grown specimens. In younger specimens, however, the spines are slender and not particularly swollen basally (Sakai, 1980). **Revised:** Compare with *P. hystrix* (Figs **B1**.13a, b)
P. inca Haig, 1974	See text.	**Original:** Covered in tubercles of different sizes, each bearing a cluster of very short, stiff setae over the summit. Juveniles sharp tipped spines with rudimentary setae at the apex. (Haig, 1974) **Revised:** Fig **B1**.5 & discussion herein.
P. indica Alcock & Anderson, 1899 **Type locality:** 800 m, off south-east India (Travancore coast).	Not studied.	**Original:** The surface of the carapace is studded with vesiculous, pustulous and conical tubercles of various sizes (Alcock & Anderson, 1899).
P. investigatoris Alcock & Anderson, 1899 **Type locality:** 800 m, off south-east India (Travancore coast).	Not studied.	**Original:** Closely covered with equal sized papilliform tubercles each with a crown of small stiff hairs (Alcock & Anderson, 1899). Ornamentation visible in original description (Alcock & Anderson 1899). *P. investigatoris* appears to have similar carapace ornamentation to *P. cristata* from Japan, and *P. ceres* Macpherson 1989 (Fig **B1**.15a) from the Arabian sea.
P. japonica Balss, 1911. **Distribution:** Around Sagami Bay, and the coast of Japan.	♂ CL 46.7 mm (MNHN)	**Original:** Carapace covered with conical processes of variable size, and the surfaces covered with tiny tubercles, thus the entire body [has a] frosted appearance (Sakai, 1971).

		Revised: Many large clusters of small, rounded tubercles (Fig **B1**.13c) arranged on ridges across the carapace, especially the branchial region.
P. longipes Faxon, 1893. **Type locality:** 1410 m, 6°S, 87°W; also known from off the coasts of Ecuador and Peru, 700-1800 m.	Not studied.	**Original:** Whole surface of the carapace thickly covered with blunt tubercles; viewed under a lens, each tubercle is seen to be encircled with a ring of short stiff setae (Faxon, 1895). Figured in Faxon (1895); appearance similar to ornamentation in *P. grossmani*, from Brazil in having rounded tubercles with a ring of short setae at the apex (Haig 1974) (Fig **B1**.10e)
P. mendagnai Macpherson, 2003	See text.	**Original:** Dorsal carapace surface densely covered with rounded, more or less prominent granules of different sizes (Macpherson, 2003). **Revised:** Fig **B1**.6 and discussion herein
P. multispina Benedict, 1894	See text.	**Previous:** Most of the spinules of the carapace are cut obliquely from behind or rectangularly, terminating in a round elliptical face. (Sakai, 1971) **Revised:** Fig **B1**.7 & discussion herein
P. ochthodes Macpherson, 1988b **Type locality:** Gulf of Boni, Indonesia, 1281 m	♂ holotype CL 71.6 mm (USNM 228831).	**Original:** Thickly covered with spinulous tubercles, with dense stiff setae on the summit (Macpherson, 1988b). **Revised:** Rounded tubercles, but with thick bands of stiff setae ringing the top of the tubercles, similar to *P. haigae* and *P. dofleini* (Figs **B1**.15b; 14c).
P. otsuae Wilson, 1990 **Type locality:** off the coast of Chile 800-1800 m.	8 specimens CL 52-110mm.	**Original:** Carapace covered with granules of small size (Wilson, 1990). **Revised:** Several flattened tubercles, sometimes clustered together, and usually quite sparsely covering the carapace. Sometimes very short setae are found on the tubercles in *P. otsuae* (Fig **B1**.12d).
P. pectinata Macpherson, 1998a **Type locality:** 1400-	♀ holotype CL 64.6 mm (USNM 259380).	**Original:** Covered with small granules of various sizes (Macpherson, 1988a). **Revised:** Flattened tubercles on the carapace

1600 m, off the coast of Venezuela.		of the holotype, bearing rings of short setae around individual tubercles. (Fig **B1**.10f).
P. phrixa Macpherson, 1992. **Type locality:** Ecuador and Peru, 1700-1900m.	5 ♀ CL 55–64 mm.	**Original:** Thickly covered with long spines Macpherson, 1992. **Revised:** A dense coverage of spines, each with an obliquely blunt tip, and the oblique face surrounded by a ring of setae (Fig **B1**.12b).
P. roeleveldae Kensley, 1981 **Type locality:** The cape of Africa, 625-900 m	Not studied.	**Original:** Short, rounded tubercles of varying sizes. (Kensley, 1981). Tubercles seem to be of a form very similar to *P. ceres* from the northern Indian Ocean (Fig **B1**.15a).
P. seagranti Eldredge, 1976 **Distribution:** Guam and Kiribati, Central Pacific.	2 specimens 46, 75mm.	**Original:** Carapace surface covered with low areolations, covered with minute bristles or setae arranged mostly in circular patterns at the bases of the areolateion, occasional shorter setae on the surface of the mounds. (Eldredge, 1976) **Revised:** *P. seagranti*, has densely setose legs and carapace edges. Its dorsal carapace surface has many flattened tubercles (Fig **B1**.14a), each with scattered setae on the surface. This gives the carapace a smooth appearance when viewed macroscopically, but is rough to the touch.
P. serrata Macpherson 1988a **Type locality:** 1100 m, off the coast of Colombia.	♂ holotype CL 104.8 mm (USNM 228836).	See *P. pectinata*, Fig **B1**.10f.
P. truncatispinosa Takeda, 1980 **Distribution:** Around Japan.	Not studied.	**Original:** Wart-like truncated tubercles of various size which are symmetrically disposed in basic pattern, some larger tubercles among them. (Takeda, 1980). For high resolution figure, see Macpherson 2008
P. tuberipes Macpherson, 1988b **Type locality:** Southern Chile, No depth	Not studied.	**Original:** Granules similar to *P. granulosa* but not clustered or pedunculated, and more prominent and numerous [than *P. granulosa* of a similar size]. Known only from the CL

recorded.		76 mm holotype in Macpherson (1988b), and figured therein.
Paralomis verrilli (Benedict, 1894). **Distribution:** Around the coast of Japan to the Bering sea. (Sakai, 1971).	7 specimens, CL 58-94mm.	**Previous:** Very thickly covered with flat tubercles (Sakai, 1971). **Revised:** Many flattened tubercles (Fig **B1**.13f), sometimes clustered together, and usually quite sparsely covering the carapace. Sometimes very short setae are found on the tubercles in *P. verrilli,* and its carapace ornamentation bears a strong resemblance to that of *P. otsuae* (Fig **B1**.12d) from the Pacific coast of South America.
P. zealandica Dawson & Yaldwin, 1971. **Type locality:** Chatham Rise, South of New Zealand, 640 m.	Not studied.	**Original:** Dorsal surface with numerous subequal conical blunt pointed short spines (Dawson & Yaldwin, 1971). Detailed figure unavailable. The original description suggests the closest allegiance is with adult *P. granulosa* (Fig **B1**.4)

CHAPTER B2: MORPHOLOGICAL PHYLOGENY OF THE GENUS *LITHODES*

B2.1 Context and objectives

The genus *Lithodes* contains 21 species (Appendix A) which are known to inhabit most of the world's oceans, including one representative (*L. murrayi*) in the Bellingshausen Sea, Southern Ocean (Klages et al 1995). *Lithodes* species typically inhabit depths greater than 200 m, although above 40 ° of latitude (north and south) some *Lithodes* species are found in shallower waters (Appendix E). *Paralithodes* contains 6 species, all of which are endemic to the North Pacific, above 30 °N, generally shallower than 300 m (Zaklan 2002b).

A close relationship between the genus *Lithodes* and the North Pacific group *Paralithodes* has been indicated in several studies (including Section **A1** herein). *Paralithodes* was shown to be paraphyletic and the divergence of species *Paralithodes brevipes* was closest to the base of the Lithodinae. *Paralithodes* and *Lithodes* genera both have their medial abdominal plates 3-6 constructed from numerous heavily calcified nodules.

From a North Pacific origin, it is hypothesised that the *Lithodes* genus made a transition into deeper waters in other oceans. Analysis of morphological traits shared uniquely between species of *Lithodes* can begin to elucidate pathways and links between different regions that may not be evident by examination of species outside of a phylogenetic context. The aims of this chapter are:

- to place species of *Lithodes* within a nested hierarchy of ancestry, in order to identify historically related groups.
- to examine the biogeographic distribution of closely related species.
- to provide an analysis in parallel to that of another globally distributed lineage, *Paralomis* (Section **B3**), so that comments can be made on the differences and similarities of these two radiations.

B2.2 Synopsis of methods

Linear measurements and multi-state discrete characters were collected for 158 specimens belonging to 17 species of *Lithodes* and *Paralithodes* (Appendix A for species list). These were used to produce two independent estimations of *Lithodes* phylogeny as follows:

For the linear-measurement data, analysis of variance (ANOVA) was used to test 20 growth-standardised character-measurements for significant levels of inter-species variation. Those character-measurements selected for further analysis were used to produce distance matrices that compared each pair of species in the taxon set. Each

element in these matrices was an estimate of the actual inter-species difference for that character, and was calculated using properties of the normal distribution. A sum of all distances matrices was analysed by Fitch-Margoliash least squares optimisation <PHYLIP*Fitch*> which produced an estimate of phylogeny to best describe the observed differences.
Additionally, 24 discrete characters were coded for 17 species of *Lithodes* and *Paralithodes*. These were analysed in <PHYLIP*Pars*> using the criterion of Wagner parsimony to select the tree topology that optimally described the observed data.

Analyses were based on the assumption that any features shared between the species *Paralithodes brevipes* and the genus *Lithodes* were present in their last common ancestor. Where possible, ancestral states for the analysis were produced from a comparison of *P. brevipes* with more distant groups, such as *Paralomis* (Lithodinae) and *Hapalogaster* (Hapalogastrinae). The comparison of multiple outgroups reduces the chance of being misled by autapomorphies within the *Paralithodes brevipes* lineage.

B2.3 Results

B2.3.1 Morphometry results

B2.3.1.1 *Morphometric sampling results and data inclusion*

The deep-water habitat of the *Lithodes* genus meant that sampling was sporadic; it was desirable to include some species in the taxon set for which five or fewer samples are available. This reduces the statistical power of some of the tests employed; however, it was important to include these species so that a global view of lithodid evolution could be examined (habitat-depth is an important factor governing how readily available sample specimens are). Such samples are included for distance analyses; however, they are not included in tests of regression or as part of the analysis of variance. This applies to *Lithodes manningi* (3 specimens), *L. galapagensis* (2 specimens), and *L. longispina* (3 specimens). These groups are coloured yellow on graphs (Figs **BM**.5, **B2**.1, **B2**.2). The other 14 species are more commonly encountered and larger sample sizes could be obtained.

B2.3.1.2 *Growth standardistation*

All of 20 morphometric characters (Y_k) have a demonstrably positive and approximately linear relationship with carapace length (CL). The first order (1°) polynomial regression indicates that CL is a good 'explanatory variable' for the change in all characters measured, as indicated by a high $\mathbf{r^2}$ value and a low probability that the

coefficient of the linear term (Y_k = **a**CL) is zero (Appendix **J**.a, Fig **BM**.5a). In most cases, there was no strong or significant relationship indicated between higher order functions of CL and measurements Y_k before data were subdivided by species.

An approximately linear relationship between CL and Y_k was tested further in species-subdivided datasets Y_{kn}. In all but a few cases, there was no significant relationship between $Y_{k,n}$/CL and CL, as indicated by a low $\mathbf{r^2}$ value when tested against a linear regression (Appendix **J**.b, Fig **BM**.5b). In most cases, there was a high probability that coefficient **B** was zero in the equation Y_k /CL= A + BCL. Wherever a relationship between $Y_{k,n}$/CL and CL existed (high r^2), the coefficient of CL in the linear regression ($Y_{k,n}$/CL = A + BCL) was less than 0.01 times the standard deviation of $Y_{k,n}$/CL (Appendix **J**.b). The size-specific variation of data Y_k/CL was so small that it should be expected to have a very small effect on overall variation. Y_k/CL was used as the size-standardised statistic in all cases for simplicity and consistency.

B2.3.1.3 *Parameter testing and analysis of variance*

F-statistics (Appendix **J**.a) indicated that measurements $Y_{k,n}$ did not come from species with significantly unequal variances (p(EV)>0.01). The majority of characters did not have a significantly non-normal distribution (p(N)>0.01) when considered as a single population. One-way analysis of Variance (ANOVA) indicated that 13 out of 20 characters (Highlighted, Appendix **J**) have significantly different inter-species means when compared with the total amount of variation present in the population. In the remaining character-sets, there is no evidence that species are significantly different from one another, and they were not analysed further.

For all subdivided datasets ($Y_{k,n}$), the assumption of normality was upheld (Appendix **J.**b), indicating that properties of normally distributed populations could be used to give confidence estimates for evolutionary distances calculated from these data. Pair-wise tests based on the t-statistic were used to indicate differences between species for each character The results of significance tests for some of the of pair-wise species differences are illustrated graphically (Figs **BM**.5, **B2**.1, **B2**.2).

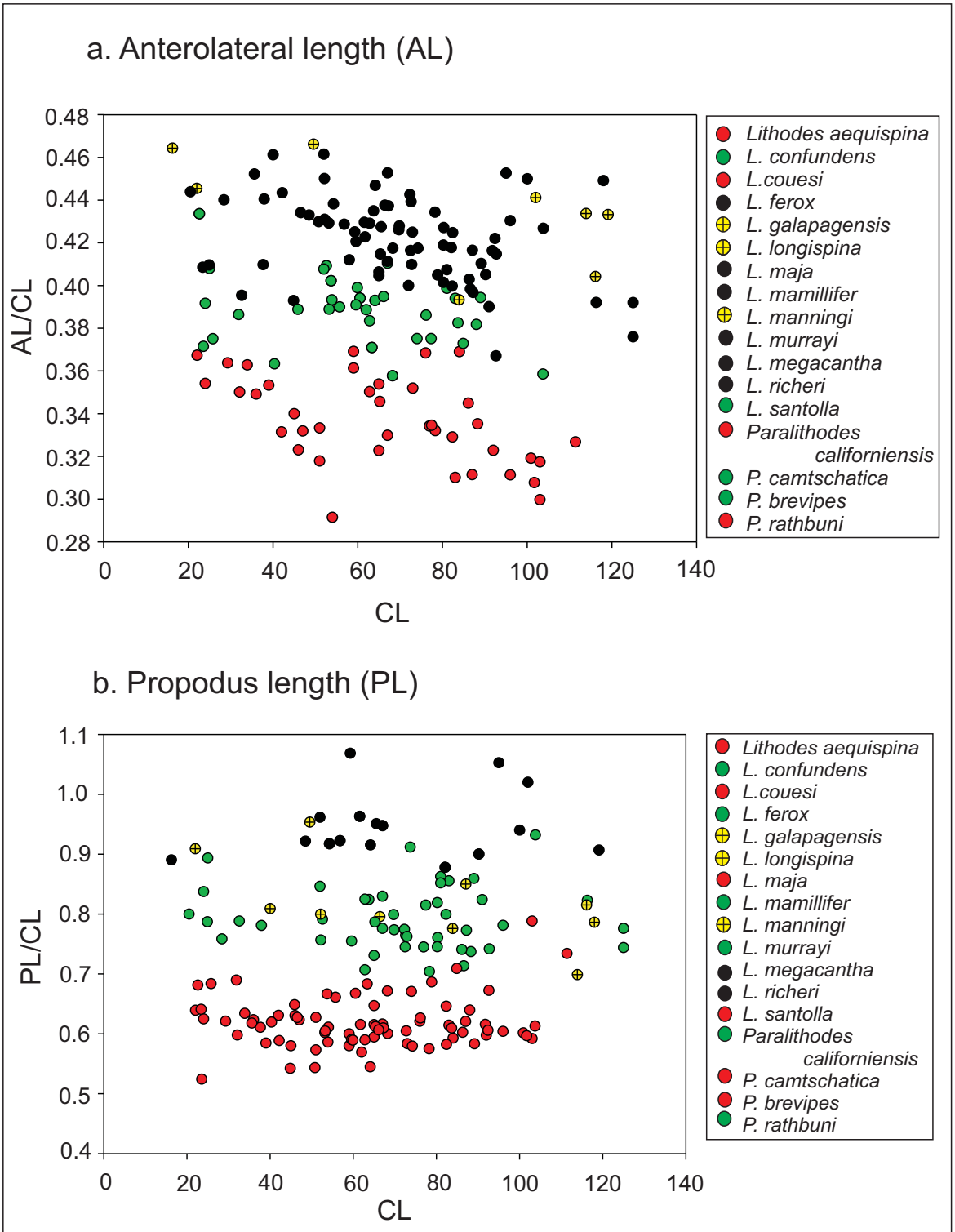

Figure B2.1 Standardised measurements of individual specimens from species of *Lithodes* and *Paralithodes.* Specimens shaded within species, based on the results of pair-wise significance testing, in which red and black groups are significantly different from one another. All measurements in millimetres. **a**) Anterolateral length (AL) standardised for size (CL). **b)** Propodus length (PL).

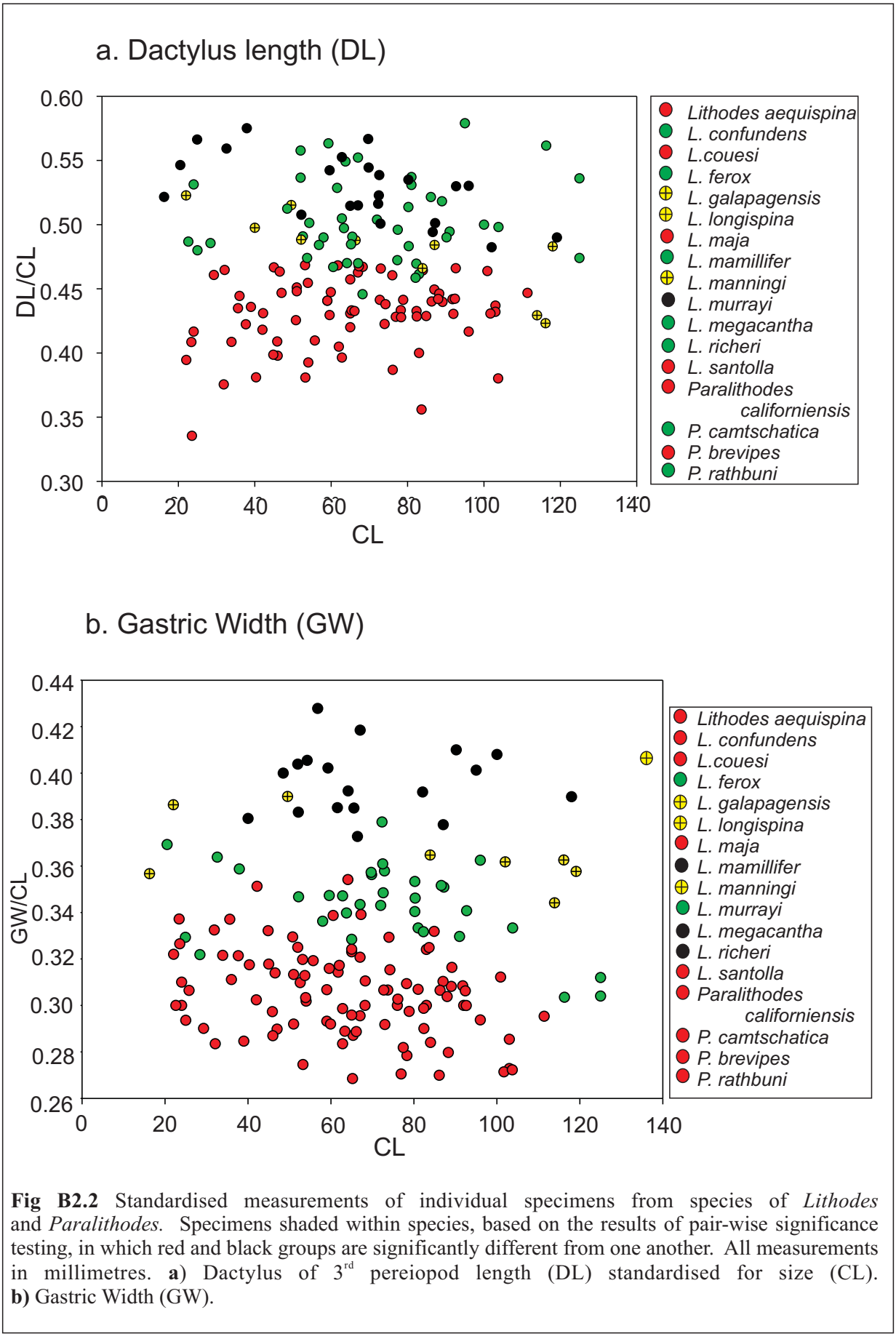

Fig B2.2 Standardised measurements of individual specimens from species of *Lithodes* and *Paralithodes.* Specimens shaded within species, based on the results of pair-wise significance testing, in which red and black groups are significantly different from one another. All measurements in millimetres. **a**) Dactylus of 3rd pereiopod length (DL) standardised for size (CL). **b)** Gastric Width (GW).

B2.3.1.4 *Morphometric distance phylogeny*

Size-standardised linear measurements from 13 characters (Appendix **J**.a) were used to estimate the mean and standard deviation of differences between 17 species. These differences were used to produce two distance matrices in which there is either 64% or 90% confidence that 'true' inter-species differences are as long or longer. Fitch-Margoliash distance methods were then used to select phylogenetic tree topologies that best represented the data. In these distance trees (Fig **B2**.3), nodes are described by letters e.g. **[Ф]** as discussed in the text.

*-TREE 1: Mean ± 1.64*standard deviation*

The more conservative of the two morphometric distance trees (Fig **B2**.3a) indicates the *Lithodes* lineage is split into two groups. The first, clade **[Б],** includes four North Pacific species belonging to the genera *Lithodes* and *Paralithodes*. The second group **[Ж]** contains South Atlantic, Indian Ocean, and Central Pacific species, with South Atlantic species *L. confundens* as a sister group to this clade. A monophyletic group **[Ф]** of central Pacific species: *L. longispina*, *L. megacantha*, and *L. richeri* is nested within clade **[Ж]**. The obelus symbol indicates species for which there is a low confidence in the values of the sample mean because of low sample size (e.g. *L. galapagensis*). The placement of these groups should be treated with caution.

-TREE 2: Mean ± 1 standard deviation

A tree based on data for which there is 68 % confidence of the minimum inter-species difference (Fig **B2**.3b) also splits into two lineages, with outgroup *Paralithodes brevipes* and North Pacific species *P. camtschatica* at its base. The first group includes shallow S. Atlantic species *Lithodes santolla* and *L. confundens* at its base and clade **[Б]** containing only North Pacific *Lithodes* species, *Paralithodes californiensis* and *P. rathbuni*. The second group **[Ж]** contains south Atlantic and Indian Ocean species *L. ferox*, *L. murrayi* and *L. mamillifer* as well as south/central Pacific species: *L. megacantha* and *L. richeri* and *L. longispina* (3 samples).

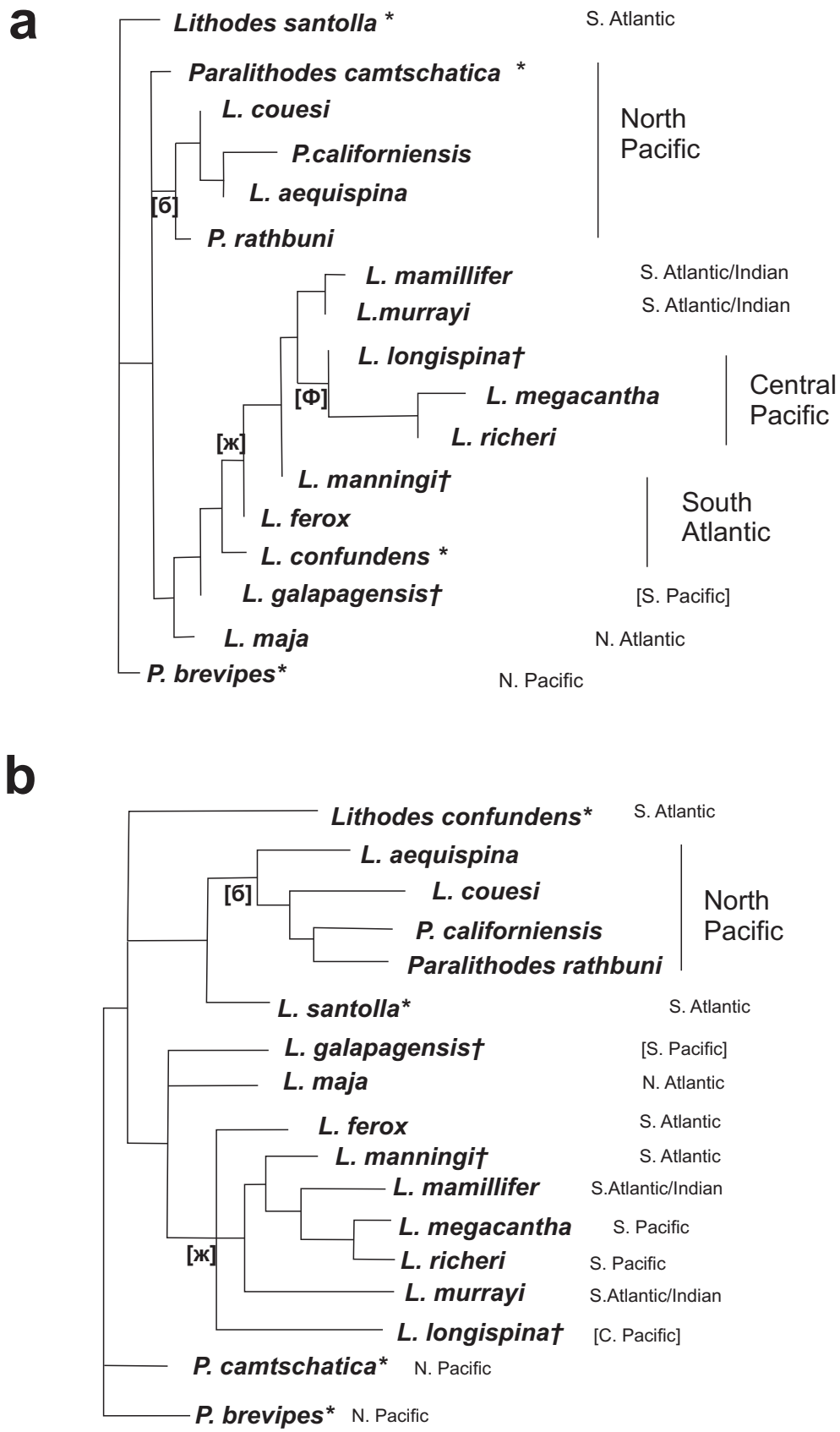

Figure B2.3 Morphometric trees produced for 17 species of *Lithodes* and *Paralithodes* using data from 13 characters. Trees are rooted using data collected for *Paralithodes brevipes*. Species based on the average of fewer than 5 specimens are indicated (†). Species typically inhabiting shallow water environments (< 100 m) are indicated (*). **a)**Distances calculated as pairwise differences between ordered means ± 1.64*standard deviation. **b)**Distances calculated as pairwise differences between ordered means ± 1 standard deviation.

B2.3.2 Formulation and scoring of discrete morphological characters

For results, refer to Table B2.

-Enlarged spines on the carpus of the walking legs

***--Ancestral state*:** No evidence of enlarged spines on the proximal and distal joints of the carpus is seen in any of the other lithodid genera (except *Neolithodes*, which may share some ancestral history with *Lithodes* but needs to be investigated further). No evidence of such spines is seen in *Paralithodes brevipes* or any other species of *Paralithodes* at any life-stage.

Characters 1&2. --Enlarged spines on the proximal and distal portions of the walking leg carpus and distal portion of walking leg merus in juveniles (CL < 30 mm) and adults (Fig B2.4).

(**0X**) No evidence of spines at these positions at any life stage (measured specimens 10-100 mm CL, Fig **B2**.4a, b).

(**10**) Long spines at these positions are found only in juvenile specimens (Fig **B2**.4c, d).

(11) Elongated spines on the merus and carpus joints, are found to be at least three times the size of other spines on the merus in adults and juveniles (Fig **B2**.4e).

-Rostrum spines

--Ancestral state: *Paralithodes brevipes, Paralomis* and *Neolithodes* all have a pair of dorsal spines and a prominent ventral rostral spine between the eyestalks. Common to *Paralithodes* and *Paralomis*, and therefore assumed to be ancestral, is a second pair of dorsal spines behind the first. A large, usually bifurcated mid-rostral spine is found in *Lithodes* and some *Paralithodes* only.

--**Characters:**

3.---Presence of an unpaired spine at the base of the rostrum (Fig B2.5a, b).

(0) No unpaired spine at the base of the rostrum

(1) Large unpaired spine medially and dorsally at the base of the rostrum

4.---Presence of a long pedunculation to the medial (mid-rostral) spine (Fig B2.5c).

(0) No elongated mid-rostral spine

(1) An unpaired mid-rostral spine (sometimes bifurcate at the tip)

Groups scoring **4:0** are recorded as (**6:X, 7:X**) in order to maintain character independence.

5.---Paired spines dorsally at the base of the rostrum (Fig B2.5).

(0) Spines at the base of the rostrum.

(1) Absence of spines at the base of the rostrum.

6.---Paired dorsal spines on the mid-rostral spine (after the divergence of the later from the ventral spine) (Fig B2.5c).

(0) Spines absent.

(1) Spines present.

7.---Rostral spine bent in the middle (always directly distal of the mid-rostral spines, Fig B2.6).

(0) Mid-rostral spine is not bent (where present).

(1) Rostrum is markedly bent approximately half way along the spine (often coinciding with the spines in [**6**]).

-Antennal Acicle

--Ancestral state: The scaphocerite, acicle or scale on the antenna is, in *Paralithodes brevipes*, large and with several (2-3) branches on the outer edge. All members of the genus *Paralomis*, *Lopholithodes* and the Hapalogastrine genus *Acantholithodes* have large acicles with several (>3) branches on their lateral aspect. *Oedignathus*, *Hapalogaster* and *Cryptolithodes* have large, plate-like acicles. The ancestral state for the Lithodinae is likely to have been a large, multi-branched antennal acicle.

--Characters (Fig B2.7):

8.---Un-branched antennal acicle.

(0) Multi-branched acicle.

(1) Un-branched acicle.

9.---Greatly reduced antennal acicle.

(0) Large antennal acicle.

(1) Acicle reduced to a size of <2 mm.

-Eyestalk

--Ancestral position: *Phyllolithodes, Paralithodes*, *Paralomis*, and some *Lithodes* have spines, often one large spine, on the dorsal portion of the ocular peduncle. *Paralithodes brevipes* has a small spine on the edge of the dorsal side of the cornea.

--Characters

10.---Large spine on cornea.

(**0**) A spine or spines on the dorsal surface of the ocular peduncle.

(1) A completely smooth dorsal surface of the ocular peduncle.

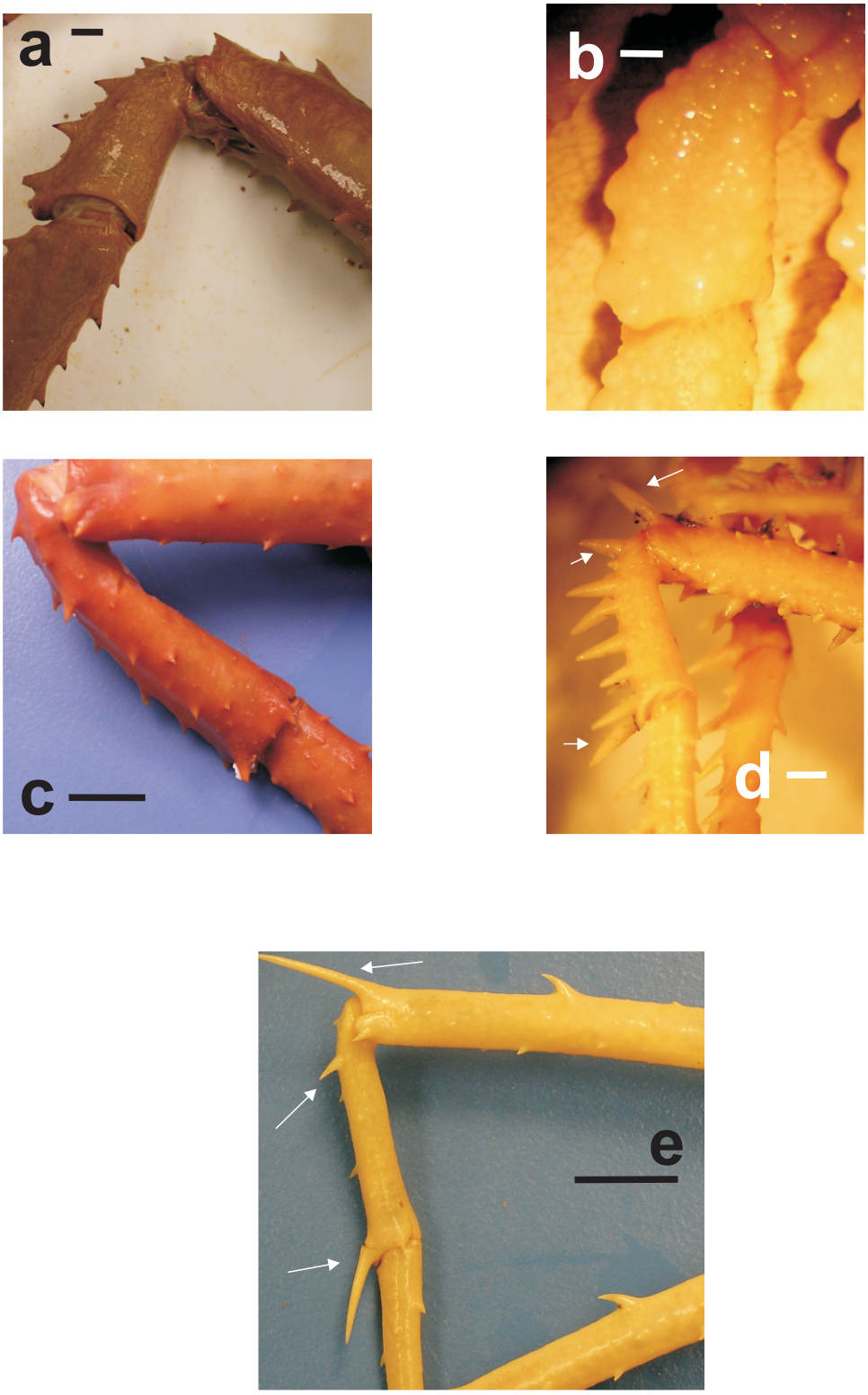

Figure B2.4 Walking leg spines in *Lithodes* **a)** Carpus of 3rd pereiopod *Paralithodes brevipes* USNM 18580 ♀ ov CL 103 mm scale 10 mm; **b)** Carpus of 3rd pereiopod *P. brevipes* USNM 18597 ♀ CL 17 mm scale 1 mm; **c)** *Lithodes couesi* USNM 52745 ♀ CL 103 mm scale 10 mm; **d)** *L. couesi* USNM 18532 ♀ CL 18.2 mm scale 1 mm **e)** *L. richeri* USNM 266470 ♀ CL 48.5 mm scale 10 mm.

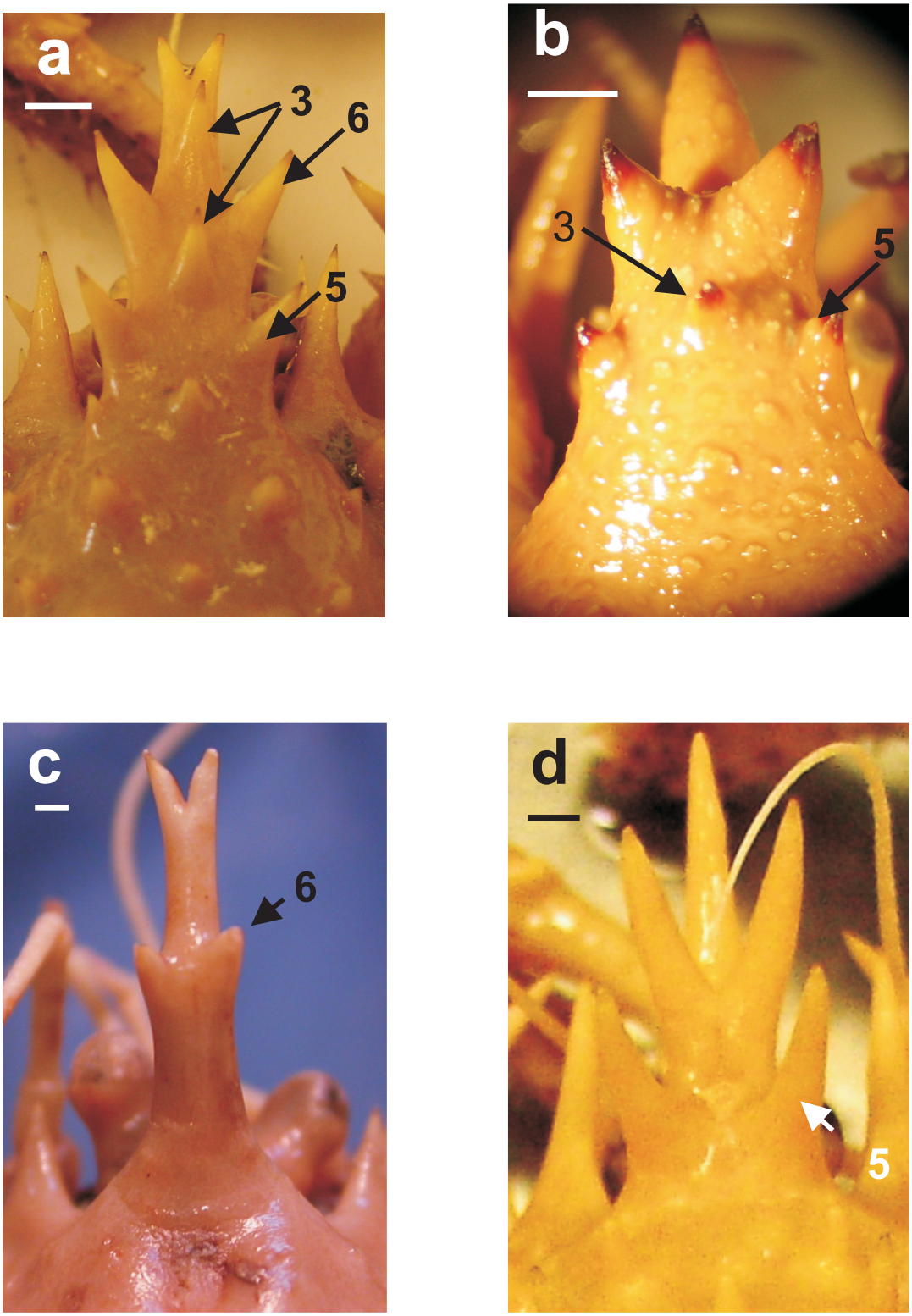

Figure B2.5 Dorsal view of the rostral spines in *Lithodes* **a)** *Lithodes aequispina* USNM 18528 ♀ CL 100.9 mm scale 5 mm; **b)** *Paralithodes brevipes* USNM 18580 ♀ ov CL 103 mm scale 2 mm; **c)** *L. murrayi* USNM 1027852 ♀ CL 52.2 mm scale 1 mm; **d)** *L. santolla* NHM 2004.3001 ♀ CL 76.1 mm scale 1 mm. *Lithodes* character **4** is present in its derived state in parts **a** and **c** of this figure. The 'primitive' state is shown in part **b**.

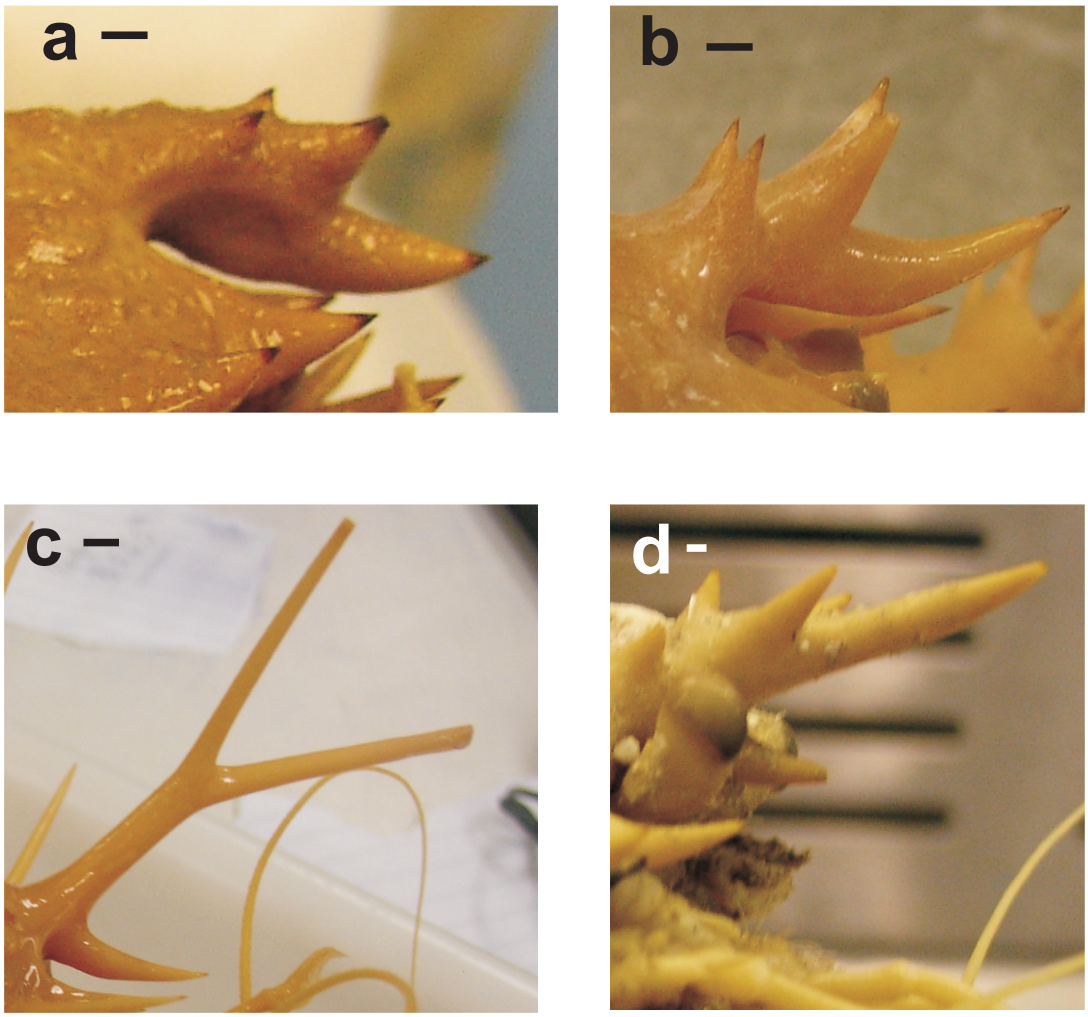

Figure B2.6 Lateral view of the rostral spines in *Lithodes*. **a)** *Paralithodes brevipes* USNM 18580 ♀ ov CL 103 mm scale 1 mm; **b)** *L. santolla* NHM 2004.3001 ♀ CL 76.1 mm scale 1 mm; **c)** *L. longispina* ♀ ov CL 116.13 mm scale 1 mm. **d)** *L. maja* ♀ CL 50.78 mm scale 1 mm. The mid-rostral spine is 'bent' in figured image **c** and is a derived state for *Lithodes* character **7**.

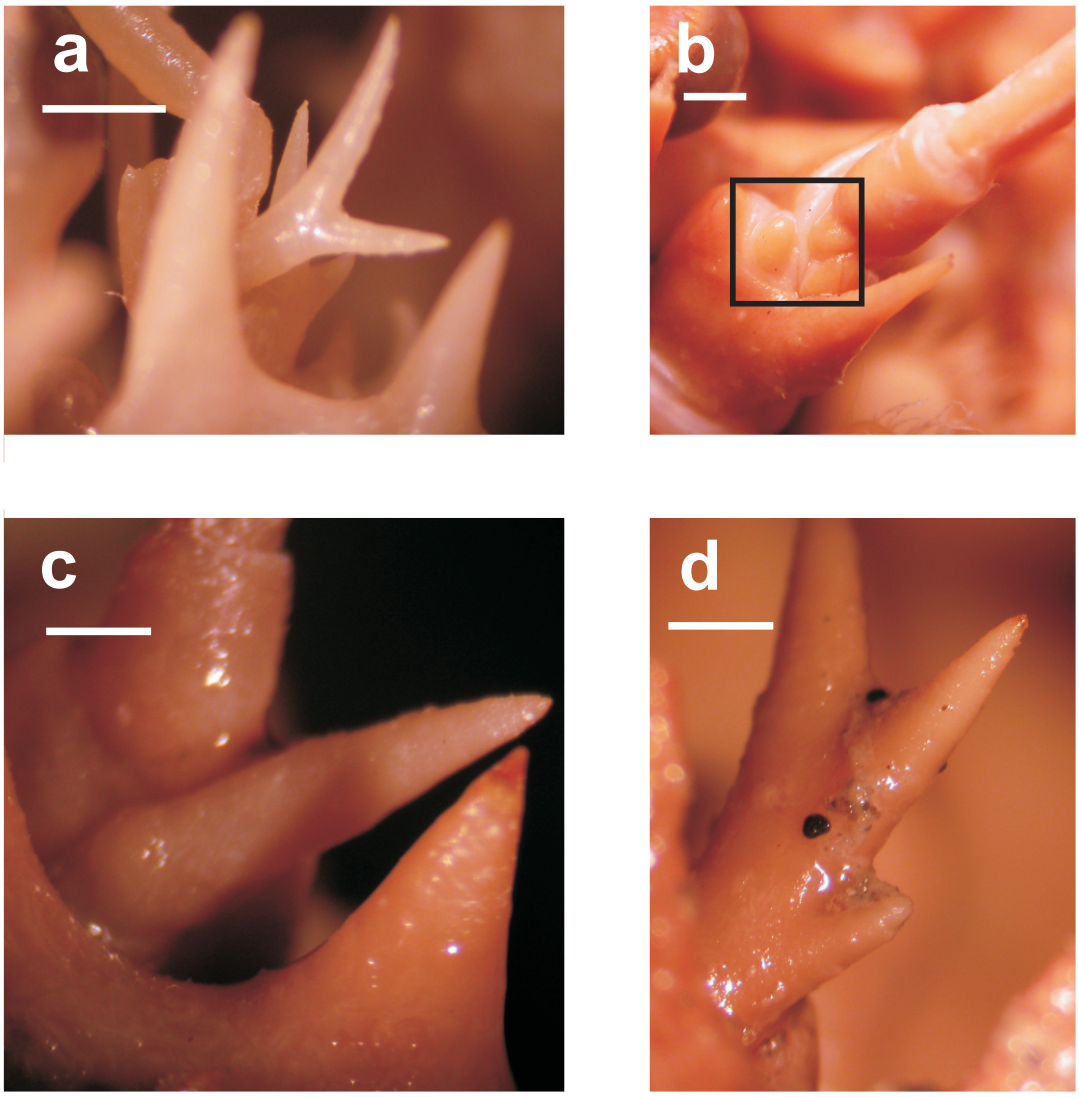

Figure B2.7 Antennal acicle of *Lithodes* **a)** *L. aequispina* antennal acicle and right antenna, partially obscured by external orbital spine USNM 259209 ♀ CL 32. 1 mm, scale 1 mm; **b)** *L. couesi* demonstrating much reduced antennal acicle, highlighted, USNM 52745 ♀ CL 103 mm, scale 1 mm; c) *Paralithodes camtschaticus* acicle and base of right antenna USNM 204290 ♀ CL 68.2 mm scale 1 mm. **d)** *Paralithodes brevipes* acicle only USNM 18580 ♀ ov CL 103 mm. Scale 1 mm.

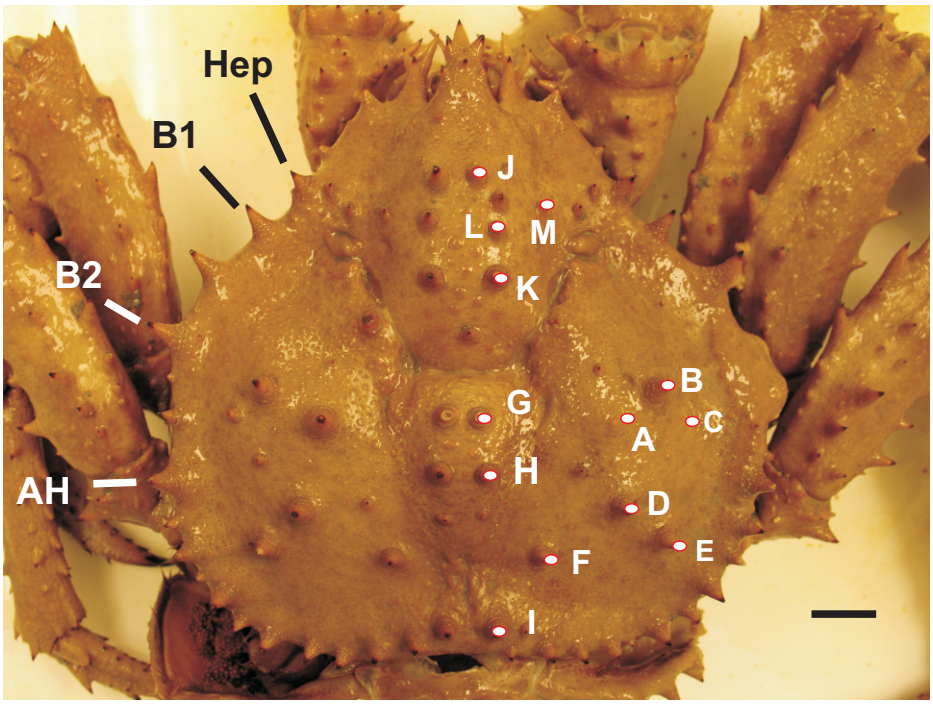

P. brevipes

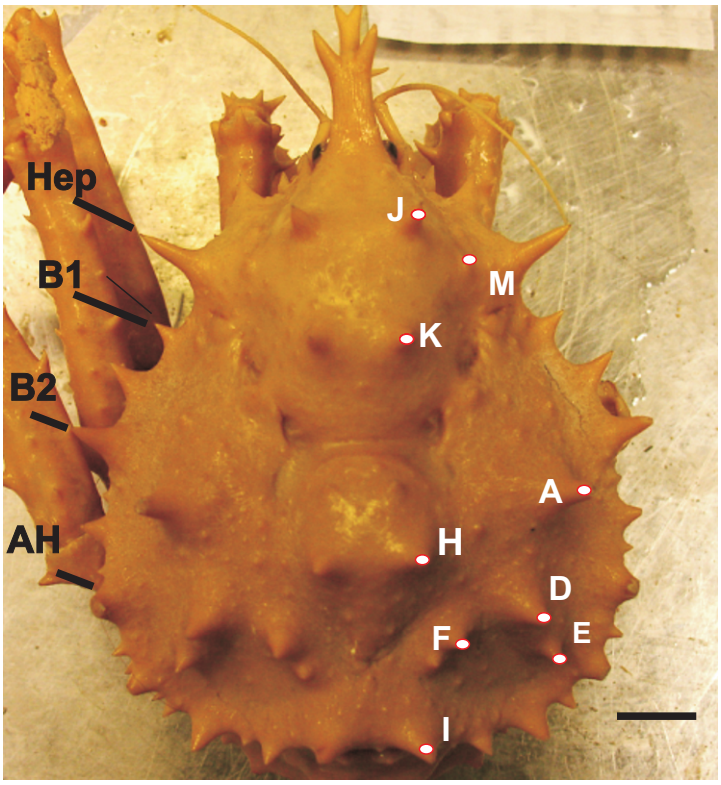

L. murrayi

Figure B2.8 Hypothesised homologies between spines in *Lithodes* and *Paralithodes*. The hepatic spine (Hep), anterior branchiolateral spines (B1 and B2) and the most anterior of the posterior branchiolateral spines (AH) is indicated. Scale = 10 mm

-*Carapace spines* (Fig **B2**.8)

The position, although not necessarily the size, of primary spines seems to be consistent within species of Lithodes (Macpherson 1988a). The size and position of the lateral spines are particularly consistent. It follows, then, that there should be some genetic basis for this spine pattern, and that it should be informative in phylogenetic analysis.

--Ancestral state: 12 spines were considered for this analysis, and are labelled on the figure of *Paralithodes brevipes* (Fig **B2.8**). These are also found in other *Paralithodes* species (e.g. *P. camtshcaticus*). Spines A-K& M can be compared to those found in *Neolithodes*, and spines A, D-I, K & M are found throughout *Paralomis.* A major problem with this analysis is that most of the other lithodid genera have complex ornamentation which obscures any 'major' spines. Within *Lithodes* and *Paralithodes*, a cursory examination of the anatomy underlying spine formation was unable to demonstrate a relationship between dorsal spine position and internal anatomy or muscular insertion. For this reason, assertion of homology between dorsal spines remains largely speculation.

Based on the similarities between *Paralomis, Neolithodes* and *Paralithodes*, the ancestral position is coded such that the loss of a spine is considered a derived character. Some species have multiple additional spines which make identification of homologous spines ambiguous. In most instances, this is handled by encoding ambiguities as 'missing data' (**X**).

--Characters (Fig B2.8):

11.---Spine A- posterior to the gastro-cardiac groove, mid-branchial.

(**0**) Spine **A** present.

(**1**) Absent.

12.---Spine B - spine on lateral side of branchial region, anterior one of two.

(**0**) Spine **B** present.

(**1**) Absent.

13.---Spine C - spine on lateral side of branchial region, posterior of two.

(**0**) Spine **C** present.

(**1**) Absent.

14.---Spine D - spine on mid-posterior third of branchial region, anterior on of two usually arranged obliquely.

(**0**) Spine **D** present.

(**1**) Absent.

15.---Loss of Spine E - spine on mid-posterior third of branchial region, posterior one of two usually arranged obliquely.

(**0**) Spine **E** present.

(**1**) Absent.

16.---Spine F - close to the convergence of the gastro-branchial grooves posteriorly.

(**0**) Spine **F** present.

(**1**) Absent.

17.---Spine G - anterior of two on the cardiac region (sometimes indicated by spinules).

(**0**) Spines **G** and **H** are of similar size to one another and to other major spines on the carapace.

(**1**) Absent. Spines **G** are sometimes spinules, but are coded as absent.

18.---Spine K, posterior pair of spines on the gastric region.

(**0**) Spines **K** present.

(**1**) Absent.

19.---Spines L: pair of tubercules directly between K and J.

(**0**) Spines **L** present.

(**1**) Absent.

-Lateral branchial spines (Fig **B2**.8)

--Ancestral states: Three spines are found on the anterior edge of the branchial region in *Paralithodes, Lithodes,* some specimens of *Paralomis* and several other genera. In *Paralithodes*, *Acantholithodes* and *Paralomis*, these spines are of roughly equal length. In *Neolithodes* and some *Lithodes*, the spines are markedly different, with some very reduced and some very long.

--Characters (Fig B2.8):

20.---Spine B1 is the more anterior of the three antero-branchial edge.

(0) Spine not substantially enlarged in comparison to other spines in the region.

(1) Spine enlarged more than twofold compared to the antero-lateral spine.

21.---Spine B2 is the more posterior of the three antero-branchial edge.

(0) Spine not substantially enlarged in comparison to other spines in the region.

(1) Spine enlarged more than twofold compared to the antero-lateral spine.

22.---Spine AH is the most anterior spine on the edge of the posterior-branchial region.

(0) Spine not substantially enlarged in comparison to other spines in the region.

(1) Spine enlarged more than twofold compared to the antero-lateral spine.

-2nd Abdominal segment

--Ancestral state*:* The definition of the genus *Paralithodes*, and the main way in which it is distinct from *Lithodes* is the presence of 5 plates rather than 3 plates on the 2nd

abdominal segment. The 2nd abdominal plate of *Lopholithodes* and *Paralomis* is composed of a single plate. McLaughlin et al (2004) present evidence that all lithodid megalopa have a single tergal plate on the 2nd segment. Division into multiple plates occurs at juvenile crab stages after metamorphosis, and the marginal plates of *Lithodes* are homologous to those in *Paralithodes*; however, marginal and lateral plates in *Lithodes* fuse into three plates at a later stage in development.

--***Characters:***

23.---Plates on abdominal tergite 2.

(1) 3 plates on the 2nd abdominal tergite.

(2) 5 plates on the 2nd abdominal tergite.

-Egg-size and/or reproductive strategy

--*Ancestral state:* Empirical studies (References in Section **O**.5.3) have shown that *Lithodes* species from around the world (*L. santolla*, *L. maja*, and *L. aequispina*) produce lecithotrophic larvae, whereas *Paralithodes camtschatica* and *P. brevipes* have planktotrophic larval stages. For 11 out of 17 species of *Lithodes* and *Paralithodes* here examined, I have been able to find ovigerous females in museum collections and/or fresh specimens. Although this is only a proxy for reproductive strategy, it is thought that the average size of the egg is an indication of maternal investment into food-independent larval development. When egg diameter is plotted for species of Lithodidae (Fig **B2**.9), there is a pseudo-discrete division between species with eggs larger than 1.5 mm and those smaller than 1.2 mm. Species *P. brevipes* and *P. camtschatica*, known to have planktotrophic larval development, have eggs smaller than 1.2 mm; those known to have lecithotrophic development have egg size around 2 mm diameter.

Paralithodes brevipes shares egg size <1.2 mm with lithodine genera *Lopholithodes*, *Rhinolithodes*, and hapalogastrine genera *Hapalogaster* and *Oedignathus*, building a fairly strong case that egg size smaller than 1.2 mm is the ancestral state for the Lithodinae.

--Characters (Fig B2.9):

24. ---Average egg diameter

(0) Egg diameter on average smaller than 1.2 mm (indicative of planktotrophic zoeal feeding modes).

(1) Egg diameter on average larger than 1.5 mm.

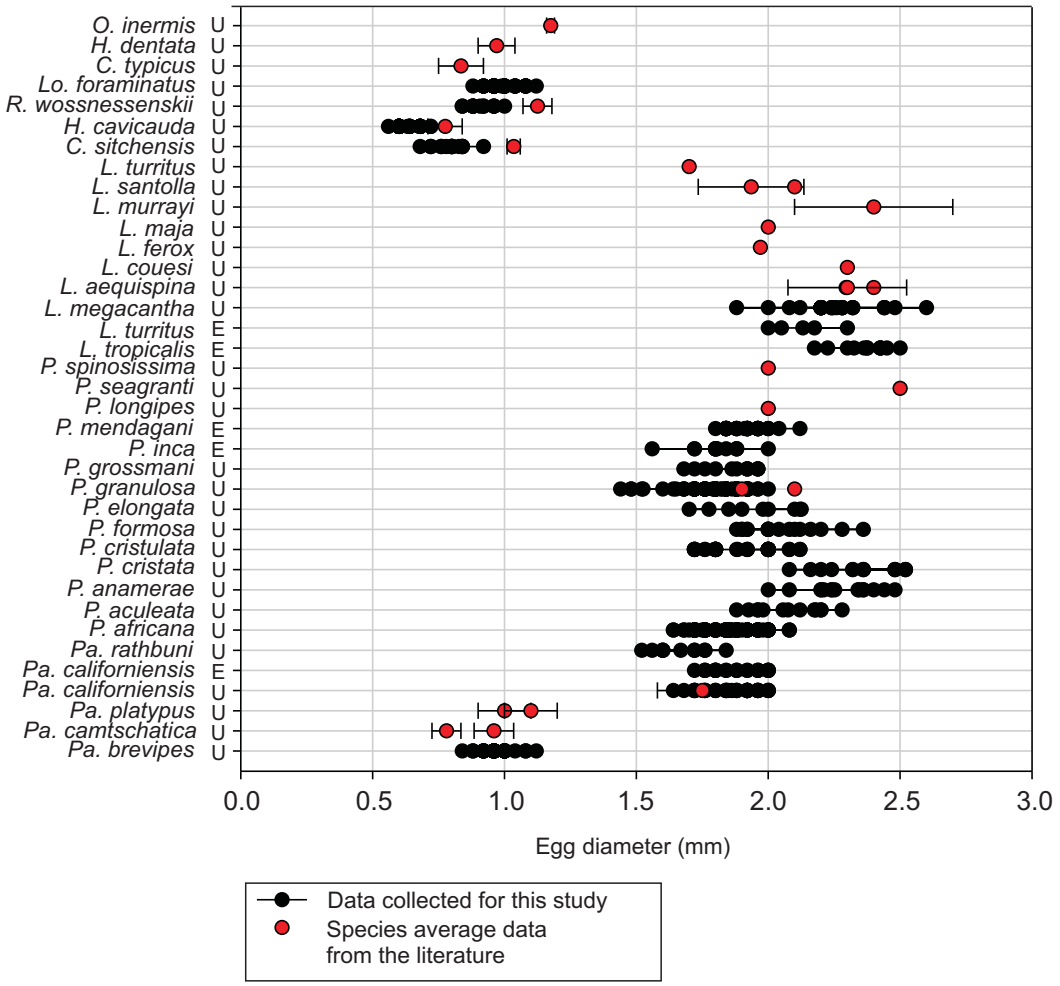

Figure B2.9 Egg size ranges in the Lithodidae. Average diameter (mm) of eggs obtained from ovigerous females of different species of Lithodidae. Each of the black points represents the average diameter of at least 30 eggs from a single ovigerous female. Red points are taken from Zaklan 2002a and references therein. Abbreviations: Pa= *Paralithodes* P= *Paralomis* L= *Lithodes* Lo = *Lopholithodes.* U indicates an uneyed embryonic stage and E indicates that an eyed embryo is visible. Note that developmental stage might affect egg size although the effect does not seem to be significant based on these data.

.

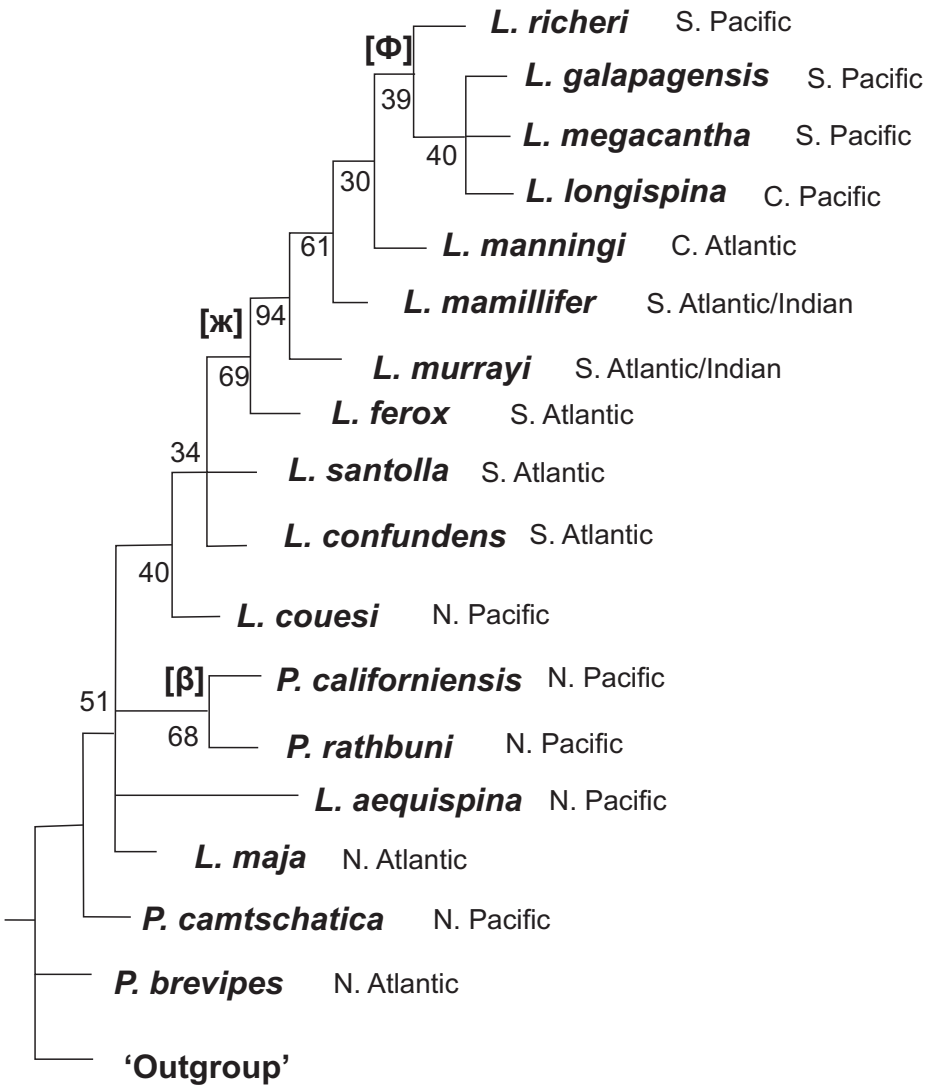

Figure B2.10 Discrete-character phylogeny for the *Lithodes* genus. Tree rooted with a hypothetical 'outgroup' based on a comparison of *Paralithodes brevipes* with other Lithodinae and Hapalogastrinae. Tree selected using Wagner Parsimony with 1000 replicates in a bootstrap analysis. Bootstrap confidence values are placed at nodes on the tree as percentages. Letters on the tree refer to the text.

	1	2	3	4	5	6	7	8	9	10	A	B	C	D	E	F	G	H	I	J	K	L	20	21	22	23	24
L. aequispina	0	x	1	1	0	1	0	0	0	1	x	x	x	x	x	x	x	x	x	x	x	x	x	x	x	2	1
P. californiensis	0	x	0	1	0	0	0	1	0	1	0	1	0	0	0	0	0	0	0	0	0	0	1	1	1	1	1
P. camtschatica	0	x	1	1	0	0	0	1	0	1	x	x	x	0	0	0	0	0	0	0	0	1	x	x	x	1	0
L. confundens	0	x	1	0	0	x	x	1	1	1	x	x	x	x	x	x	x	x	x	x	x	x	x	x	x	2	1
L. couesi	1	0	0	1	0	1	0	1	1	1	x	x	x	0	0	0	0	0	0	0	0	1	1	1	0	2	1
L. ferox	1	0	0	1	1	1	0	1	1	1	0	1	1	0	0	0	0	0	0	0	0	0	x	x	x	2	1
L. galapagensis	1	1	0	1	1	1	0	1	1	0	0	1	1	1	1	1	1	0	0	0	1	0	1	0	0	2	x
L. longispina	1	1	0	1	1	1	1	1	1	1	0	1	1	1	1	1	1	0	0	0	0	0	1	0	0	2	x
L. maja	0	x	1	1	0	1	0	1	1	1	0	0	0	0	0	0	0	0	0	0	0	1	x	x	x	2	1
L. mamillifer	1	1	0	1	1	1	1	1	1	1	0	1	1	0	1	0	1	0	0	0	0	0	1	1	0	2	x
L. manningi	1	1	0	1	1	1	1	1	1	0	0	1	1	0	1	0	1	0	0	0	0	0	1	0	0	2	x
L. megacantha	1	1	0	1	1	1	1	1	1	0	0	1	1	1	1	1	1	0	0	0	0	0	1	1	0	2	1
L. murrayi	1	1	0	1	1	1	0	1	1	0	0	1	1	0	0	0	1	0	0	0	0	0	x	x	0	2	1
P. brevipes	0	x	1	0	x	x	x	0	0	1	0	0	0	0	0	0	0	0	0	0	0	1	x	x	x	1	0
P. rathbuni	0	x	0	1	0	0	0	1	0	0	0	1	0	0	0	0	0	0	0	0	0	0	1	1	1	1	1
L. richeri	1	1	0	1	1	1	1	1	1	0	0	1	1	0	1	1	1	0	0	0	0	0	1	0	0	2	x
L. santolla	0	x	0	0	0	x	x	1	1	1	x	x	x	x	x	x	0	0	x	0	0	0	x	x	x	2	1
Outgroup	0	x	0	0	x	x	x	0	0	0	0	0	0	0	0	0	0	0	0	0	0	0	0	0	0	x	0

Table B2 Discrete character codes for phylogenetic analysis of *Lithodes* genus. Note that H-J (Fig B2.8) were invariable for all of the tested groups and were excluded.

B2.3.3 Discrete-character phylogeny results

Nodes e.g. **[Ж]** discussed in the following text refer to clades on a phylogenetic tree selected by the Wagner Parsimony criterion based on discrete-character data (Fig **B2**.10). In this analysis, the 'outgroup' sequence was broadly based upon *Paralithodes brevipes*; however, the position of *P. brevipes* was theoretically unconstrained if its basal position was not parsimonious. *Paralithodes* species, excluding *P. camtschatica* group into a clade **[β]**, which is nested within several 'unresolved' North Pacific and Atlantic species at the base of the tree.

A clade diverging at node **[Ж]** contains only South Atlantic, Indian Ocean and South/Central Pacific *Lithodes* species, with nested clades in this region supported by high bootstrap values (> 50). Species diverging at the base of clade **[Ж],** *L. ferox*, *L. murrayi* and *L. mamillifer* are known from the South Atlantic and Indian Ocean. A clade containing *L. richeri*, *L. galapagensis*, *L. megacantha*, *L. longispina* (all species from the Central and South Pacific) appears furthest from the base of the tree at node **[Φ]**.

B2.4 Discussion

The two methods of estimating phylogeny employed in this chapter are based on small, but independent character sets. It is significant that both discrete-character analysis and morphometric analysis converge upon very similar topologies:

- Relationships within Paralithodes

The effect of choosing a North Pacific species (*Paralithodes brevipes*) to indicate the 'primitive state' in the morphometric phylogeny perhaps has an effect of artificially centring the phylogeny on the North Pacific. I believe that this assumption is justified, based on molecular evidence for the whole family. It is also a prior assumption of this analysis that *Paralithodes* is paraphyletic with respect to *Lithodes* (as its name suggests). *Paralithodes* species have a close relationship in both analyses to one another and to *Lithodes aequispina*. Gross morphology indicates an important division within the genus *Paralithodes* (which are unified on the basis of sharing 5 tergal plates on their 2nd abdominal segment). *P. camtschatica*, *P. brevipes* and *P. platypus* have planktotrophic larval stages, a similar body shape, and are native to the Bering Sea from Kamtschatca, Russia to British Columbia, Canada. *P. rathbuni* and *P. californiensis* are found from Washington state, USA to Mexico and they both produce large eggs, indicative of lecithotrophic zoeal development. This division within *Paralithodes* is evident in the results of both the discrete **[Б]** and morphometric **[β]** analyses. The

morphometric analysis (Fig **B2**.3) indicates that the *Lithodes* genus is not monophyletic; however, this is not necessarily supported by the discrete-character analysis, in which the crucial node is unresolved (Fig **B2**.10).

- *Phylogenetic position of* Lithodes santolla *and* L. confundens

Lithodes santolla and *L. confundens* are the only species of *Lithodes* that are regularly found in shallow waters: up to the intertidal zone in the cold water around Patagonia (Appendix E). *L. confundens* confounds field scientists with its morphological similarities to *L. santolla*; however, in the morphometric analysis of the two species, they are placed quite far apart (Fig **B2**.3a, b). The separation of the two species is different at different levels of confidence in the morphometric analysis and it may be explained by a higher than usual variance of the characters measured in *L. santolla*. Habitat is almost unknown for the deep-water species of *Lithodes* and is something which has not been considered in this analysis. It is possible that a similarity in habitat between shallow/intertidal species *L. santolla, L. confundens* and *P. brevipes* has a convergent effect on morphometric variables such as leg length. This may reflect a tendency for morphometric data to group species by morphological similarity rather than ancestral history and as such is it not a fundamentally cladistic technique.

In the discrete-character analysis, *L. santolla* and *L. confundens* (S.W. Atlantic) are resolved within a clade containing *Lithodes ferox* (S.E. Atlantic). This type of analysis is unlikely to be affected by habitat in the same way as the morphometric analysis. In general, results (Fig **B2**.3a, Fig **B2**.10) indicate that *L. confundens* (at least) emerged into shallow water in the southern high latitudes following a deep-water ancestry.

- *Relationship between central Pacific species and Indian Ocean species*

Results presented here converge upon the conclusion that central and southern Pacific lineages of *Lithodes* are closely related to one another (clade **[Φ]**) and to the Indian Ocean and South Atlantic *Lithodes* species (clade **[Ж]**). *Lithodes murrayi* is perhaps typical of a basal Indian Ocean/Southern Pacific morphotype and it has a notably widespread southern distribution. The range of *L. murrayi* is thought to be almost, if not, circum-Antarctic: from the Crozet islands in the southern Indian Ocean, to the Macquarie islands south of New Zealand (Appendix E). Such widespread southern species distributions may have been typical throughout the evolutionary history of the clade labelled **[Ж]**.

The evidence from this study and from the literature suggests a shallow north Pacific ancestry for the *Lithodes* genus, sharing plesiomorphies including a planktotrophic

larval stage. From this hypothesised origin, a transition was made towards a more deep-sea life history, as displayed by basal north Pacific species *Lithodes aequispina*. Ancestors of Atlantic species *Lithodes maja, L. santolla* and *L. confundens* may have made the first 'escape' from the Pacific through an Arctic and/or Antarctic pathway into the Atlantic, as both groups occupy fairly basal (but unresolved) positions within the phylogeny of the genus. Subsequent radiations out of the Atlantic followed a deep-water pathway around southern Africa, through the southern Indian Ocean and into the central and southern Pacific. There is little or no evidence of a biogeographic link between the north Pacific and the central Pacific within the species tested. Deep, cold-water currents that connect the Atlantic sequentially with the Indian Ocean and the Pacific may have facilitated the circum-global pathway of dispersal indicated by these results.

17 species of *Paralithodes* and *Lithodes* were included in the taxonomic sample for these morphological analyses. Although an effort has been made to equally represent the morphotypes within this genus, the sample does not reflect the full diversity of the *Lithodes* genus (27 species if *Paralithodes* is included, Appendix A). Some notable gaps in sampling exist along the eastern Pacific margin, where *L. wiracocha* and *L. panamensis* inhabit depths from 600-1500 m; north/central Pacific island chains, where species such as *Lithodes nintokuae, L. longispina* may provide evidence of a link between the deep north Pacific and central Pacific as far south as 20 °N; and along the western Pacific margin from Japan to Indonesia, where some species of *Lithodes* of a central Pacific morphotype have been found (such as *Lithodes paulayi*, Appendix E). In theory, the topology of the trees produced in this analysis should not change when new species are added, provided that assumptions about the polarity of change (ancestral states) are correct.

B2.5 Summary of conclusions

- Those *Paralithodes* species with a more southerly distribution within the coastal North Pacific (*P. californiensis* and *P. rathbuni*) may represent a transitional state between ancestors close to *P. brevipes* and the genus *Lithodes*.
- Morphometric and discrete character analyses corroborate one another, with the exception of the placement of shallow southern species *L. santolla* and *L. confundens*. Morphometric techniques are useful in systematics, but a tendency to group on similarity rather than ancestry must be interpreted with caution.

- Atlantic species *L. maja* and *L. santolla* were amongst the earliest species to leave the ancestral region of the north Pacific. It is unclear whether these movements were linked, or whether they were independent.
- A clade containing species from southern African, Indian Ocean, and south Pacific waters indicates the importance of large scale dispersals in a west-east direction. This may be linked with west-east cold deep-water currents which connect the south Atlantic with the other major oceans.

CHAPTER B3: MORPHOLOGICAL PHYLOGENY OF THE GENUS *PARALOMIS*

B3.1 Rationale

Paralomis White, 1856 is a genus with a global distribution, found in waters deeper than 500 m and shallower at high latitudes (Hall & Thatje 2009a). The genus is the most speciose of the Lithodidae, currently including 61 species, and new descriptions have been frequent in recent decades (Macpherson 2003, Spiridonov et al 2006, Takeda & Bussarawit 2007, Macpherson 2008, Hall & Thatje 2009b). Molecular evidence (Section **A1**) has shown that *Paralomis* includes the single species described from the genus *Glyptolithodes* Faxon 1893. The presence of an undivided medial plate on the 3rd abdominal segment, and fusion of all plates of the 2nd abdominal segment unites *Paralomis* and *Glyptolithodes* to the exclusion of the other major groups of Lithodidae. In terms of abdominal morphology, the nearest genera to *Paralomis* are *Lopholithodes* and *Cryptolithodes*, which have additional medial accessory plates on the 3rd abdominal segment, and an undivided 2nd abdominal plate (Macpherson 1988a, Zaklan 2002a, McLaughlin et al 2004). Molecular data strongly suggest that *Lopholithodes* has a relatively recent ancestor in common with the monophyletic group containing *Paralomis* (+ *Glyptolithodes*) (Section **A1**). *Lopholithodes* contains two species (*L. mandtii* and *L. foraminatus*) in the north east Pacific, which have a distribution typically 20-300 m, and have been found no further south than the Baja California, Mexico.

The aim herein is to elucidate relationships within the *Paralomis* genus based on morphology to:

- examine the evolutionary context of a transition from the shallow north Pacific into the deep sea, independent from that in genus *Lithodes*.
- provide a basis for comparison of results with phylogenies based on molecular data (Synthesis D.3).
- map distinct lineages within the genus to biogeographic regions and pathways within its present and hypothesised past distribution.
- assess the phylogenetic position of the single shallow-water species *Paralomis granulosa* (Patagonia) within the deep-sea members of the genus.

B3.2 Synopsis of Methods

Twenty linear measurements and 31 multi-state discrete characters (defined in Section **BM**.3.2.1) were collected for 25 species of *Paralomis* and were used to produce two independent estimations of *Paralomis* phylogeny as follows:

For the linear measurement data, analysis of variance (ANOVA) was used to test 20 growth-standardised character-measurements for significant levels of inter-species variation. Those characters selected for further analysis were used to produce matrices that compared each pair of species in the taxon set. Each element in these matrices was an estimate of the actual inter-species difference for that character, and was calculated using properties of the normal distribution where appropriate. A sum of all distance matrices was analysed by Fitch-Margoliash least squares optimisation <PHYLIP*Fitch*> which produced an estimate of phylogeny to best describe the observed differences.

Additionally, 30 discrete characters, each with up to 4 states were coded for 25 species of *Paralomis*, *Glyptolithodes*, and *Lopholithodes*. These were analysed in <PHYLIP*Pars*> using the criterion of Wagner parsimony to select the optimal tree topology. These discrete characters were also transformed into a pseudo-continuous character set so that they could be combined with the results of the morphometric analysis.

Analyses were based on the assumption that any features shared between the species *Lopholithodes mandtii* and the genus *Paralomis* were present in their last common ancestor. Where possible, ancestral states for the analysis were produced from a comparison of *Lopholithodes* with more distant groups, such as *Lithodes* (Lithodinae) and *Hapalogaster* (Hapalogastrinae). The comparison of multiple outgroups reduces the chance of being misled by autapomorphies within the *Lopholithodes* lineage (Watrous & Wheeler 1981).

B3.3 Results

B3.3.1 Morphometry results

B3.3.1.1 *Growth standardistation*

All 20 morphometric character measurements (BM.3.2.1) have a demonstrably positive and approximately linear relationship with carapace length (CL, Appendix **K.**a). The first order (1°) polynomial regression indicates that CL is a good 'explanatory variable' for the change in all characters measured, as indicated by a high $\mathbf{r^2}$ value and a low probability that the coefficient (**a**) of the linear term ($Y_k = \mathbf{a}CL$) is zero (Appendix **K.**a, Fig **BM**.5a). In most cases, there was no strong or significant relationship indicated between higher order functions of CL and measurements Y_k before data were subdivided by species.

An approximately linear relationship between CL and Y_k was tested further in species-subdivided datasets Y_{kn}. In all but a few cases, there was no significant relationship between ($Y_{k,n}$/CL) and CL, as indicated by a low $\mathbf{r^2}$ between the data and the linear

regression (Appendix **K.**b, Fig **BM**.5b). There was in most cases, a high probability that the coefficient **B** is zero in the equation Y_k /CL= A + **B**CL.

Approximately one species per character does have a relationship between measured values $Y_{k,n}$ with CL^2 , as indicated by $\mathbf{r^2}$ ($Y_{k,n}$/CL, CL) > 0.4 (highlighted Appendix **K.**4b). Lateral branchial height (LBH/CL) in 8 specimens of *Paralomis anamerae*, for example, has a correlation with CL; however, in this and in all similar cases, the coefficient of CL in the linear regression ($Y_{k,n}$/CL = A + BCL) was less than 0.01 times the standard deviation of $Y_{k,n}$/CL (Appendix **K.**b). This size-specific variation was so small that should be expected to have a very small effect on overall variation. Y_k/CL was used as the size-standardised statistic in all cases for simplicity and consistency.

B3.3.1.2 *Parameter testing and analysis of variance*

F-statistics (Appendix **K.**b) indicated that measurements $Y_{k,n}$ did not come from species with significantly unequal variances (p(EV)>0.01). The majority of characters did not have a significantly non-normal distribution (p(N)>0.01) when considered as a single population. One-way analysis of Variance (ANOVA) indicated that seven out of 20 characters (HW, AL, ML, LBH, GL, GCL, DL) have significantly different intra-species means when compared with the total amount of variation present in the population. In the remaining character-sets, there was no evidence that species were significantly different from one another, and they were not analysed further.

For all subdivided datasets ($Y_{k,n}$), the assumption of normality was upheld, indicating that properties of normally distributed populations could be used to give confidence estimates for evolutionary distances calculated from these data. Pair-wise tests based on the t-statistic indicated differences between pairs of species samples for each character. The results of these significance tests are represented graphically (Figs **B3**.1-4).

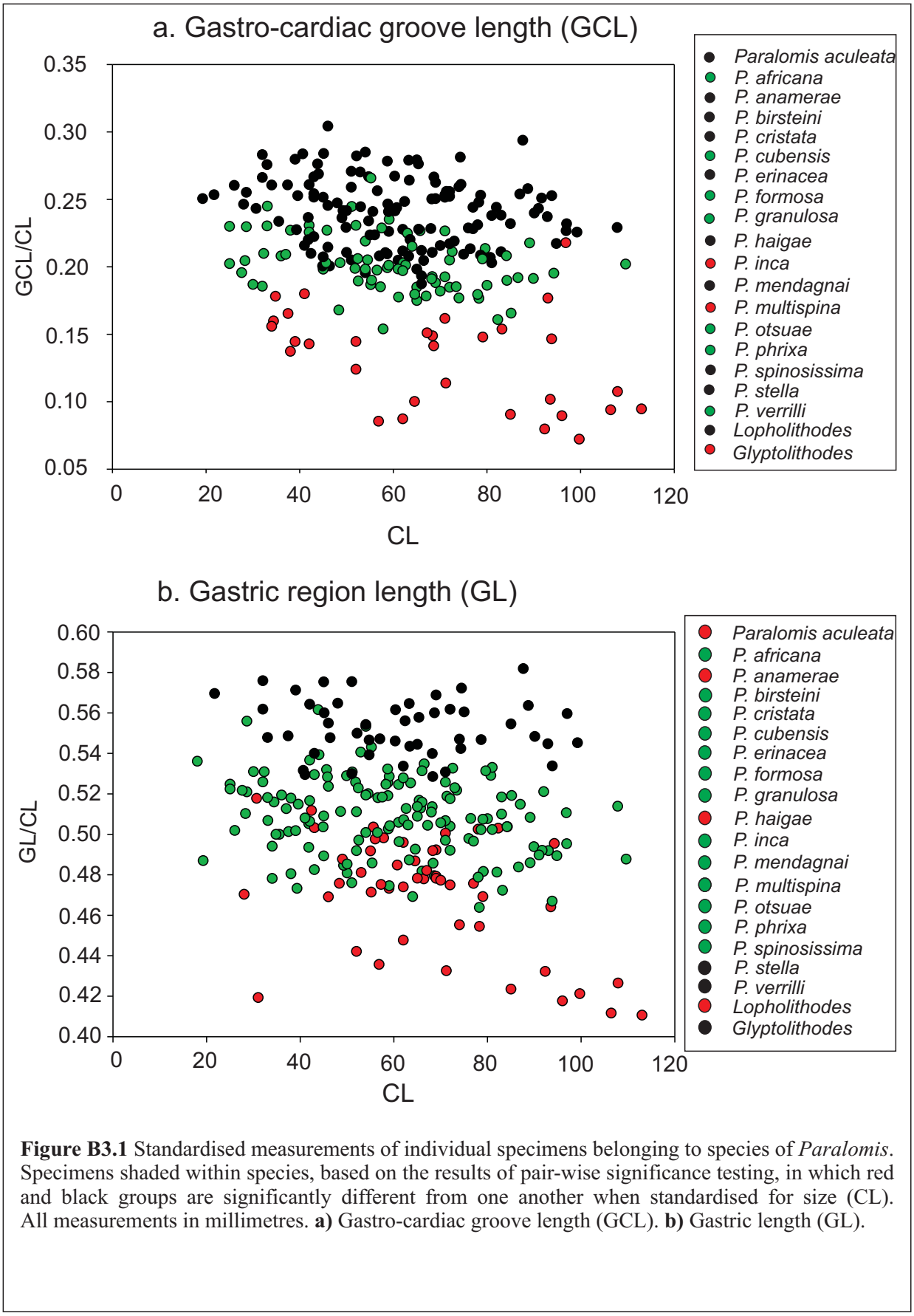

Figure B3.1 Standardised measurements of individual specimens belonging to species of *Paralomis*. Specimens shaded within species, based on the results of pair-wise significance testing, in which red and black groups are significantly different from one another when standardised for size (CL). All measurements in millimetres. **a)** Gastro-cardiac groove length (GCL). **b)** Gastric length (GL).

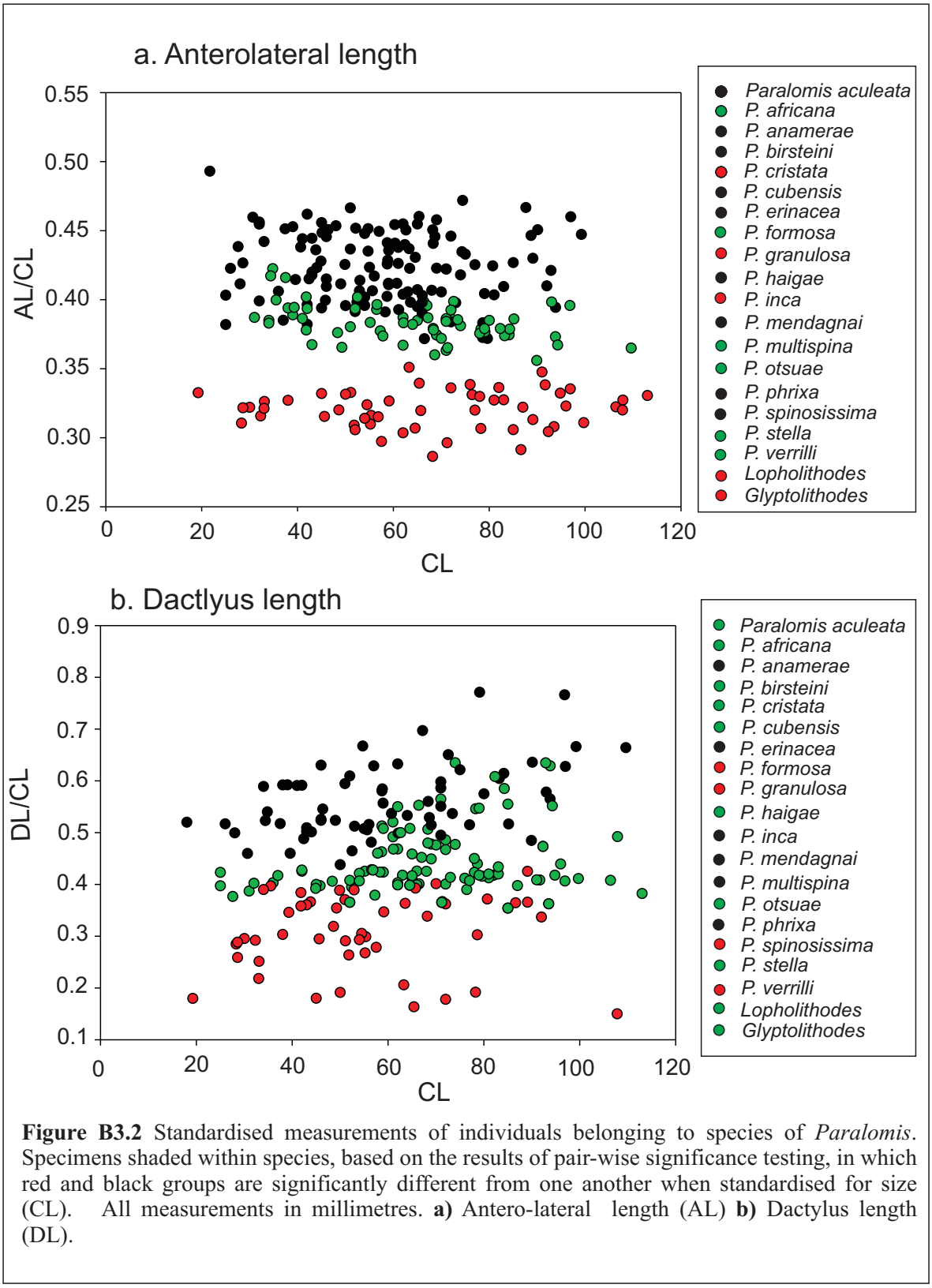

Figure B3.2 Standardised measurements of individuals belonging to species of *Paralomis*. Specimens shaded within species, based on the results of pair-wise significance testing, in which red and black groups are significantly different from one another when standardised for size (CL). All measurements in millimetres. **a)** Antero-lateral length (AL) **b)** Dactylus length (DL).

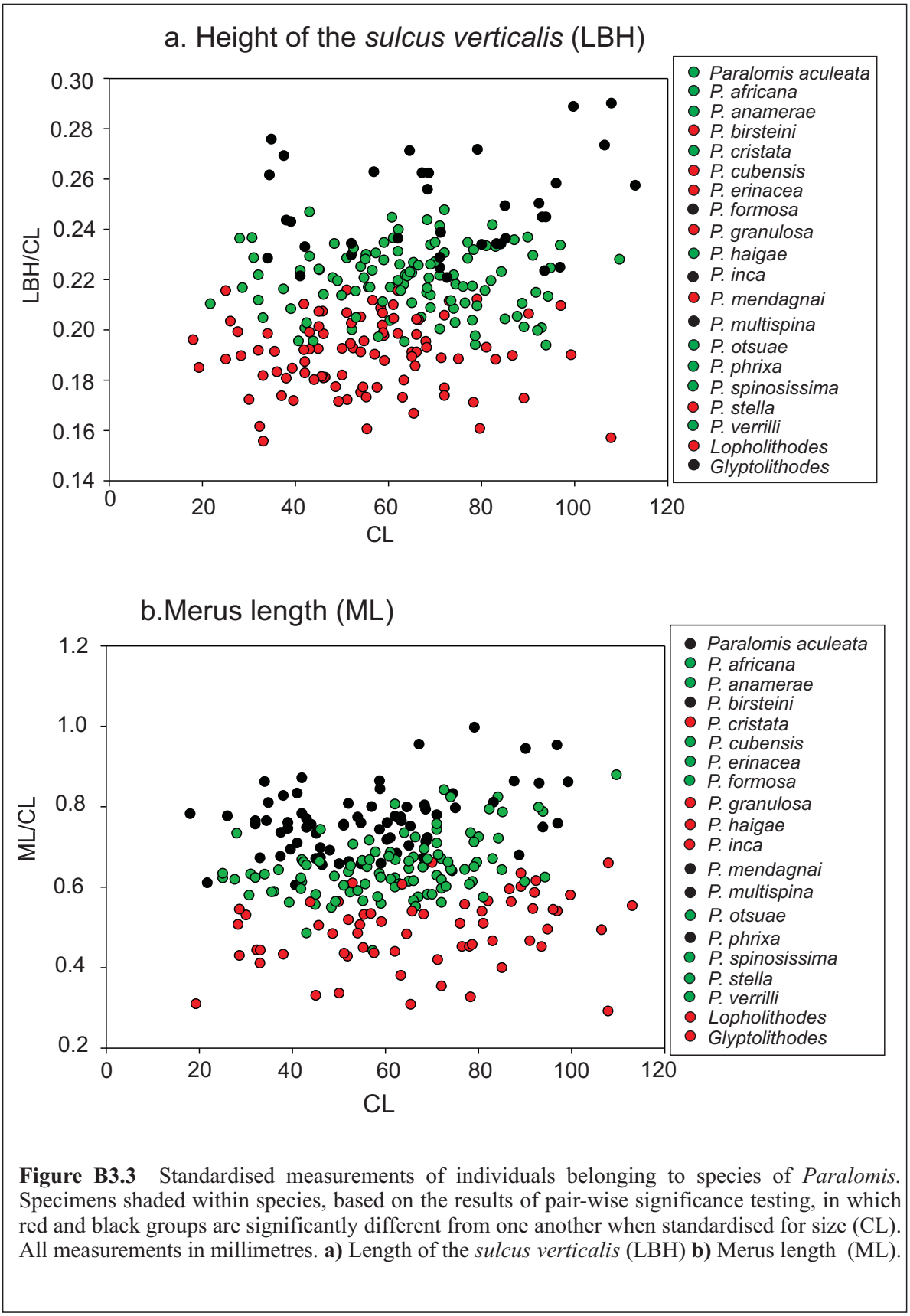

Figure B3.3 Standardised measurements of individuals belonging to species of *Paralomis*. Specimens shaded within species, based on the results of pair-wise significance testing, in which red and black groups are significantly different from one another when standardised for size (CL). All measurements in millimetres. **a)** Length of the *sulcus verticalis* (LBH) **b)** Merus length (ML).

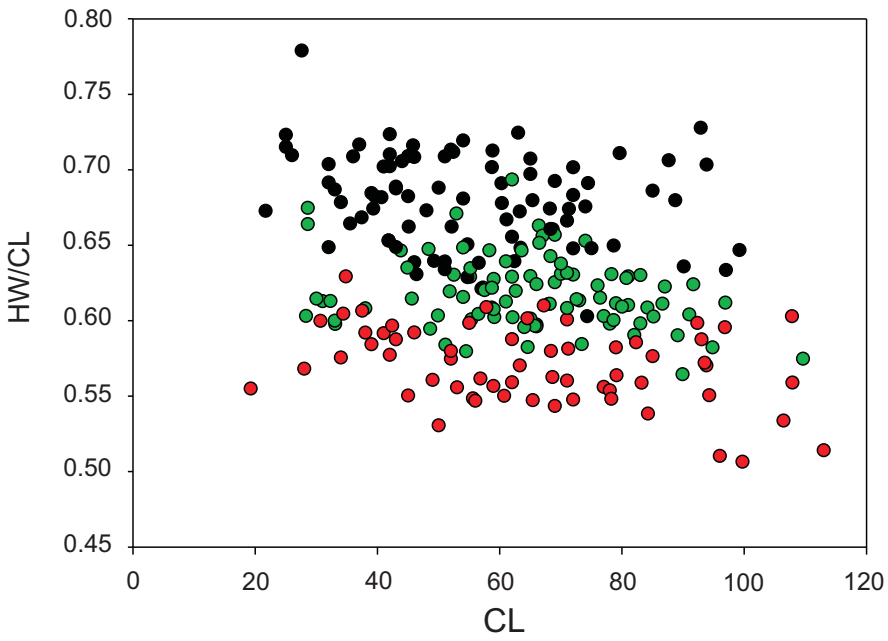

Figure B3.4 Standardised measurements of individuals belonging to species of *Paralomis*. Specimens shaded within species, based on the results of pair-wise significance testing, in which red and black groups are significantly different from one another when hepatic width (HW) is standardised for size (CL). All measurements in millimetres.

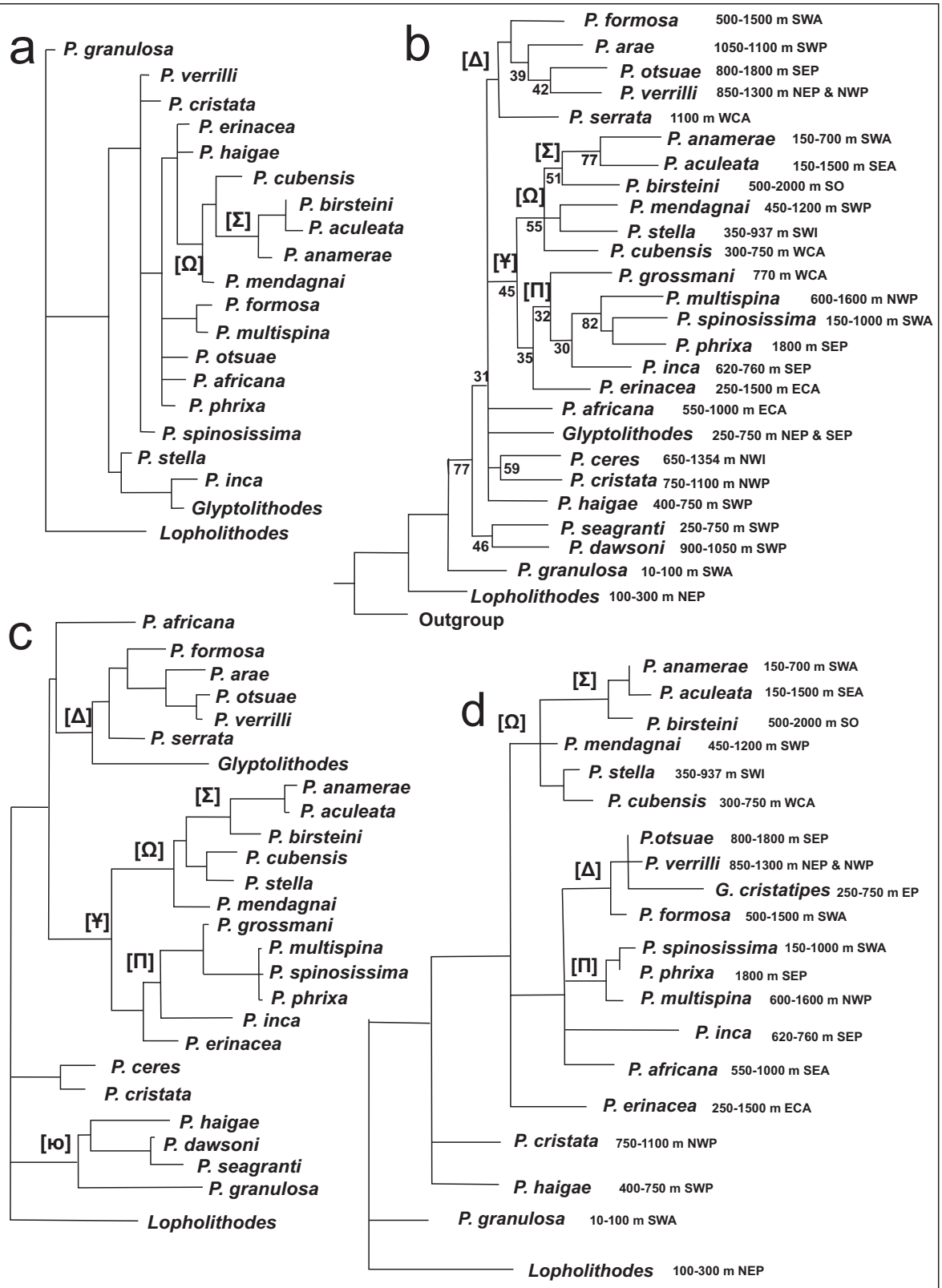

Figure B3.5 Phylogenetic trees based on: **a)**Morphometric analysis of the difference between the means of 20 species tested for 7 characters. Distances calculated using the mean +/- 1 standard deviation. **b)**Discrete character analysis of 27 *Paralomis* and outgroup taxa using 31 unordered, multi-state discrete characters. Tree selected using the criterion of wagner parsimony in <*PHYLIPpars*>. Node values indicate the results of a bootstrap analysis with 1000 replicates. **c)**Discrete character analysis of the same taxon set as in Fig 3.5b, with the same 31 unordered multi-state discrete characters converted into pair-wise distances: where a difference is scored 1, an identity is scored 0 and the totals summed. **d)**Morphometric and discrete-character distance matrices combined to produce a summed pair-wise distance matrix for 38 characters. Trees **a, c** and **d** selected using the Fitch-Margoliash least squares optimisation method (distance), and branch lengths indicate distance between nodes.

B3.3.1.3 *Morphometric distance phylogeny*

The set of 25 species of *Paralomis* examined was reduced to 20 commonly encountered species for which more than five specimens could be obtained. Seven size-standardised morphometric characters which displayed significant inter-specific variation were used to produce a pair-wise distance matrix for the taxon set. The difference between groups of species was not as clear as it was in *Lithodes* (Section B2) for the characters measured, so only the less conservative tree (difference of sample means modified by one standard deviation, as described in section **BM**.3.2.3) is presented (Fig **B3**.5a). Properties of the normal distribution mean there is 68% confidence that inter-species distances produced by these methods are at least as great as the true difference between populations.

Paralomis granulosa resolves nearest to the base of the tree in this analysis, which is rooted using *Lopholithodes mandtii*. Node **[Ω],** containing *P. birsteini*, *P. aculeata*, *P. anamerae*, *P. cubensis,* and *P. mendagnai* is the most clearly resolved clade. Many nodes are unresolved on the tree because the pair-wise distances were zero if no significant difference could be found between the species. Two south-east Pacific species, *P. inca* and *Glyptolithodes cristatipes*, resolve as sister taxa close to the base of the tree.

B2.3.2 Formulation and scoring of discrete morphological characters

Results of coding in Table B3.

-*Spine morphology*

Paralomis is peculiar amongst the Lithodinae in the great diversity of ornamentation found covering the carapace and legs (Section **B1**). As shown elsewhere in this thesis, ornamentation varies between life-stages, and can vary predictably within an individual. In many cases, spines in certain locations on the carapace (such as a single spine in the mid-gastric region) are different from the ornamentation 'uniformly' covering the rest of the carapace. The following characters refer only to the 'secondary' ornamentation cover, and not to lateral, mid-gastric, or mid-branchial spines, which are covered in later sections.

--***Ancestral state:*** Spine morphology in the last common ancestor of *Paralomis* is ambiguous, because there is little similarity between the different lithodine lineages. In *Lopholithodes* and *Phyllolithodes*, the carapace is covered with irregular clusters of circular, flattened tubercles of approximately 1 mm in diameter (Fig **B3**.6a, b). Short setae are found in *Lopholithodes*, but at a frequency of less than one per tubercle. Where *Lithodes*, *Paralithodes* and *Neolithodes* have anything analogous to secondary ornamentation, it is always in the form of acute spines or spinules and no setae are

found in any size-class. Hapalogastrinae, such as *Oedignathus* and *Dermaturus* have scale-like ornamentation, with a fringe of setae at the anterior edge; the hapalogastrine tubercles do not resemble anything found in *Paralomis* (Fig **B3**.6c, d). On balance, the intricate tubercle formations in *Paralomis* are likely to be of novel origin within the lineage, from a lithodine ancestor with few setae on the carapace.

--Characters (Fig B3.7):

A.---Tubercles evenly spaced across the carapace (not in clusters).

(0) Clusters of between one and ten tubercles across the carapace and sometimes legs (Fig **B3**.6a, Fig **B1**.12c, **B1**.13c).

(1) Evenly spaced spines or tubercles, never in clusters (e.g. Fig B1.12a, b, d, e).

The outgroup state is ambiguous (**X**) because of the substantial differences between *Lopholithodes* (**0**) and *Paralithodes* (**1**).

B1.---Ornamentation flattened/pointed in juveniles (<30mm CL).

Juvenile specimens usually have more acute or spiniform tubercles than adults of the same species. This character examines only secondary ornamentation, and not the mid-gastric or mid-branchial spines.

(0) Flattened tubercle.

(1) Conical tubercle or spine (Fig **B3**.7).

B2.---Ornamentation flattened/pointed in adults (>40 mm CL).

(0) Flattened tubercle (Fig **B3**.6a, **B3**.7).

(1) Conical tubercle or spine (e.g Fig B1.12a, **B3**.7).

C.---Spines as secondary ornamentation in adults.

(0) Tubercles are less than 1.5 times as high as wide at the base (Fig **B3**.6a). Spines can technically be either pointed or have flattened apices.

(1) Spines are defined as features of ornamentation in which height is more than 1.5 times width at the base (e.g. Fig B1.12a, b).

[*B and C coded in a way which allows a relationship between conical tubercles and spines to be recorded, but also taking account of changes with ontogeny* (Fig **B3**.7)]

D.---Posterior-directed oblique face to spine or tubercle in adults.

(**0**) No oblique face to spine or tubercle.

(**1**) Posterior-directed, oblique face to spines or tubercles (e.g. Fig B1.12b, **B3**.7)**.** This state was ambiguious in *P. grossmani*, which scored **D:X**.

E.---Setae isolated/multiple clusters on tubercles.

(**0**) Very few or no setae per unit of ornamentation (Fig **B3**.6a).

(**1**) Many setae in clusters on each tubercle.

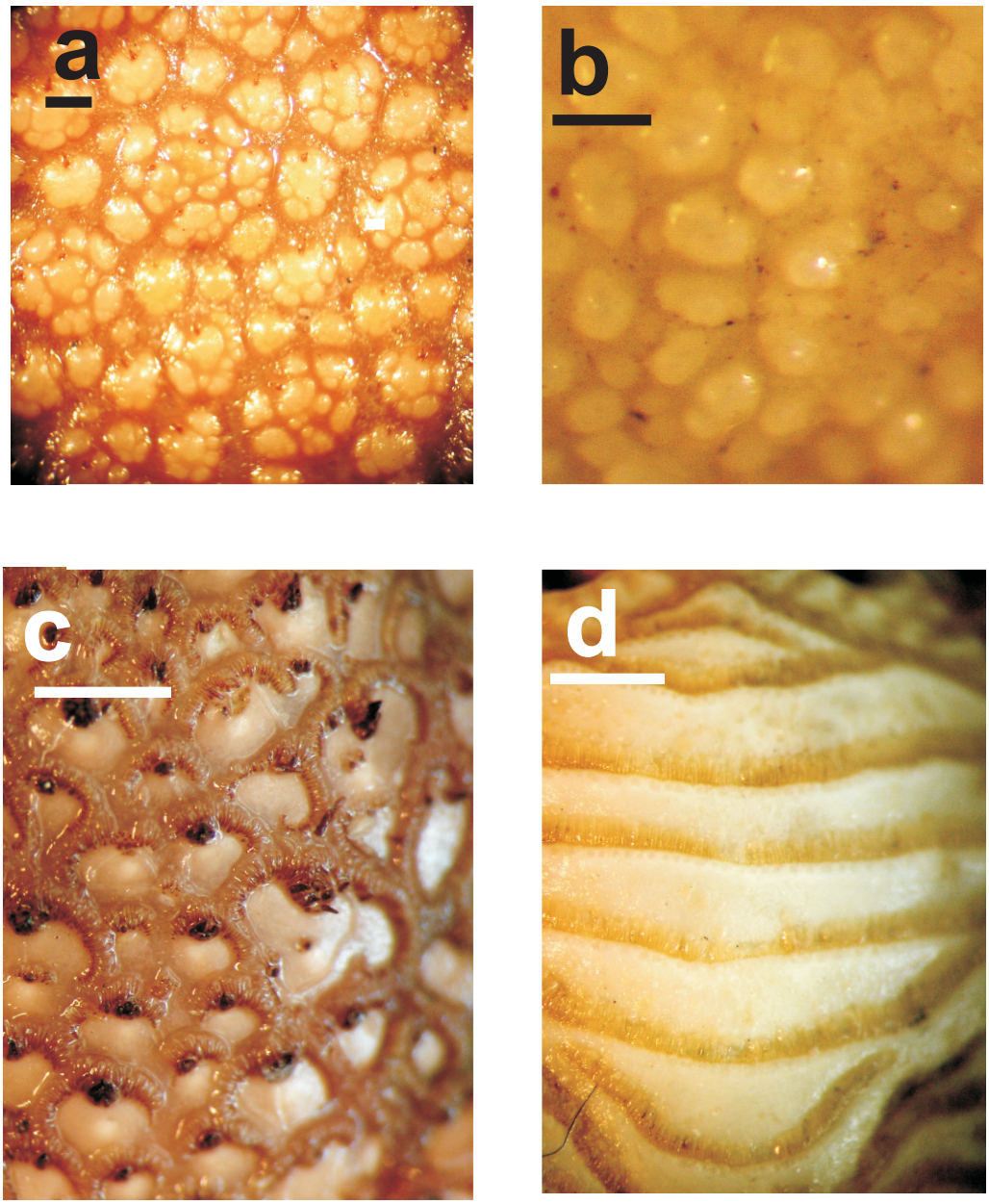

Figure B3.6 Spine morphology coding in *Lopholithodes* Scales 1mm. **a)** *Lopholithodes mandtii* ♀ CL 107.8 mm; **b)** *Phyllolithodes papillosus* ♀ CL 32.5 mm; **c)** *Oedignathus inermis*♀ CL 22.5; **d)** *Dermaturus mandtii* ♀ CL17 mm.

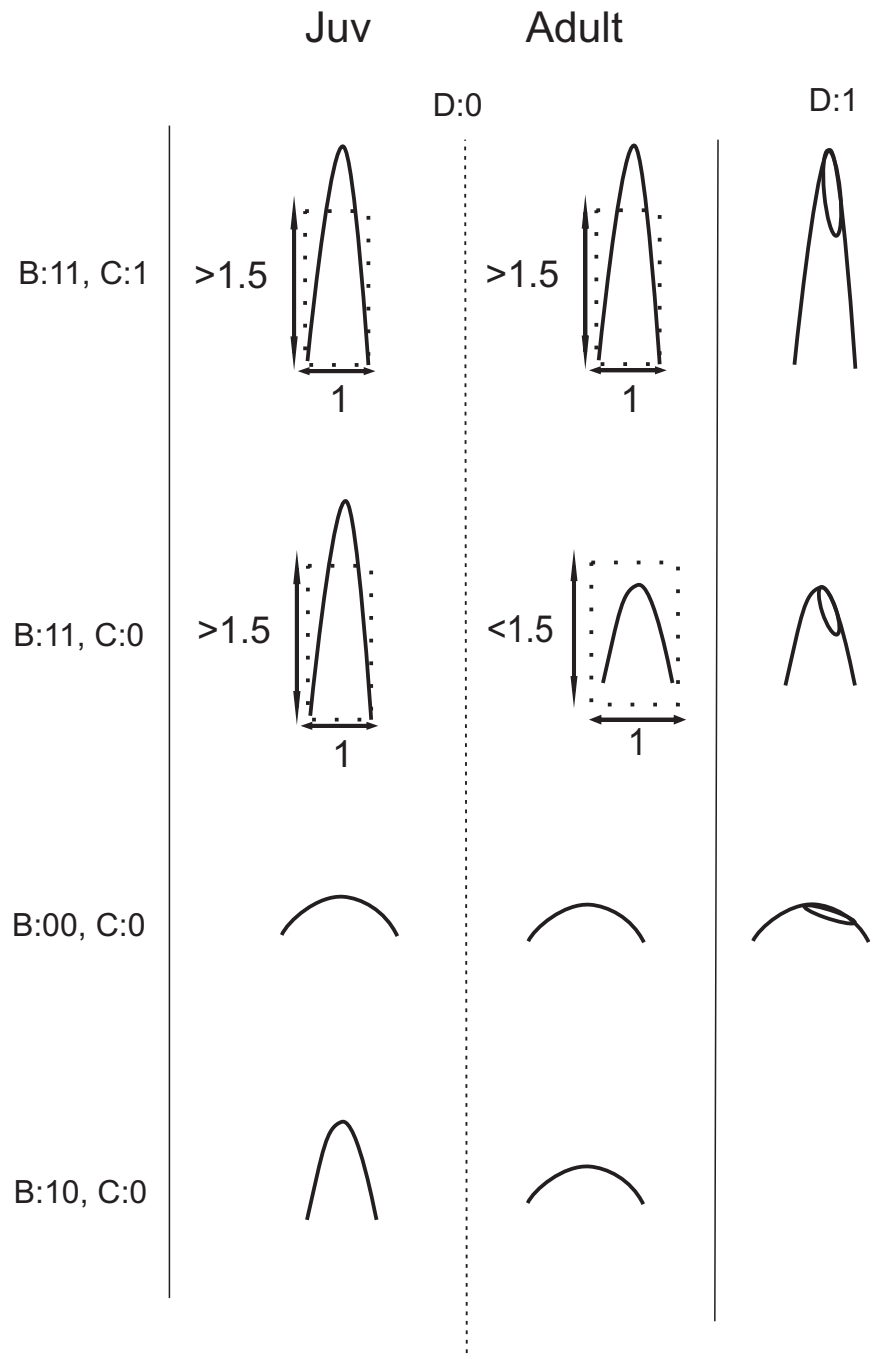

Figure B3.7 Schematic of spine coding for phylogeny characters B-D in *Paralomis*.

F.*---*Arrangement of setae on units of ornamentation. Only those scoring **E:1** are distinguished for the present character.

(1) Setae in a ring at or near the apex (Fig B1.12b, B1.14c).

(2) Setae in a tuft on the apex (Fig B1.11b).

(**3)** Setae distributed evenly over the surface (Fig B10.a,b,d).

***G.---Setae in 'single ring' or 'multiple ring'*:** Character divides **F:1** into two groups species scoring **F:2** or **F:3** score **G:X**.

(1) Setae in a single ring (Fig B1.12b)**.**

(2) Setae in multiple rings (Fig B1.14c).

-*Carapace spines*

The mid-gastric spine is peculiar in that its form does not vary to the same degree as the secondary ornamentation. To a lesser extent, this is true of a spine in the mid-branchial region and many spines on the lateral edges of the carapace. Several spine positions (e.g Fig **B2**.8), derived from similarities between *Lopholithodes, Lithodes* and *Paralithodes*, were assessed. The results indicated that whilst ornamentation at certain positions were different from the rest of the carapace, homologies were obscured by the nature of the secondary ornamentation. In *Paralomis*, it is often unclear whether a thickened tubercle can be equivalent to an enlarged spine where they appear at consistent locations on the carapace.

--Ancestral state: A spine in the middle of the gastric region is very pronounced in *Lopholithodes* (Fig **B3**.8) and *Phyllolithodes*. *Lithodes, Paralithodes, Neolithodes* and *Rhinolithodes* have four spines in a square on the gastric region and no mid-gastric spine. In general, the Hapalogastrinae have no prominent spines and the gastric region is flat.

--Characters:

***H.---Prominence of mid-gastric spine*.**

(0) Mid-gastric spine prominent, at the level of the anterior part of the hepatic region. The largest spine on the carapace (with possible exception of a single mid-branchial spine: Fig **B3**.8a, b, d).

(1) Mid-gastric spine reduced to spinule or the same size as all other spines, with little or no enlargement of the anterior part of the gastric region (Fig **B3**.8c).

In *P. aculeata* and *P. anamerae*, the gastric spine is not greatly enlarged; however, the gastric region is skewed anteriorly, with a small spine visible at the apex and so these cases are scored **(0)**.

In some cases, the nature of the secondary ornamentation makes this a difficult feature to score. In such cases, the 'ambiguity value' of **X** is recorded so that this character has no effect on the phylogenetic resolution of those species.

-Rostral spines

--Ancestral states: The form of the rostral spines in *Lopholithodes mandtii* (Fig **B3**.9e) matches the form in *Paralithodes*, and seems likely to be a symplesiomorphy of the Lithodinae. A ventral rostral spine (Macpherson 1988a) protrudes from between the ocular peduncles; dorsally, paired (primary) spines diverge from one another after a short anterior elongation of the carapace. Between the dorsal spines and the ventral spine there is an unpaired prominence in *Lopholithodes* and *Phyllolithodes*. Paired secondary dorsal spines behind the primary paired spines are found in *Lopholithodes, Paralithodes*, and some *Lithodes*. A single unpaired spine, with possible homology to the ventral rostral spine is found in the Hapalogastrinae.

*--**Characters:***

I.---Paired primary spines dorsally *(Fig **B3**.9).*

(0) Present

(1) Absent

(2) Unpaired spine

J.---Paired secondary spines dorsally.

(0) Pair of spines present behind the primary spines (Fig **B3**.9a, e).

(1) No pair of spines behind the primary spines (see Fig **B3**.9b-d).

K.---Unpaired spine dorsally at the base of the rostrum (typically between spines J).

(0) Present (see Fig **B3**.9a, e).

(1) Absent (see Fig **B3**.9b-d).

L.---Keeled rostrum*. A deep keel on the ventral-rostral spine.*

(0) Absent.

(1) Present.

M.---Medial-dorsal spine. *Spine or prominence between spines **I,** above the ventral rostral spine.*

(0) Absent (see Fig **B3**.9a-c).

(1) Present (see Fig **B3**.9d, e).

N.---Third paired spines dorsally, behind spines J.

(0) Absent.

(1) Present (see Fig **B3**.9a).

-Lateral spines

--Ancestral states: Comparing basal groups *Paralithodes* and *Lopholithodes*, and keeping the morphologies of other genera in mind, it is difficult to discern the ancestral shape of the carapace margin. The hepatic spine is of moderate in size in *Lopholithodes* and *Paralithodes brevipes,* as well as *Acantholithodes* (Hapalogastrinae) and *Rhinolithodes*. In *Lithodes* and *Neolithodes*, there is an enlargement of several lateral spines, including the hepatic spine, at consistent positions. In all Lithodinae, there is a point at the mid-branchial region where the dorsal carapace becomes flush with the lateral wall, and the dorsal aspect of the carapace is more or less 'pinched' in. At the posterior angle of the branchial region is a very large spine (and deformation of the carapace) in *Lopholithodes* (Fig **B3**.10e) and a smaller spine is present at this position in *Paralithodes*. On the posterior margin are several small spines, less significant than those on the anterior margins. *Lopholithodes* has 4-6 spines between the anterolateral spine and the mid-branchial region; most of these on the anterobranchial rather than hepatic region. Hapalogaster has 6 spines on the corresponding region anterobranchial region, although the carapace shape is much more rounded towards the posterior.

--Characters:

O.---Spines between the anterolateral and anterobranchial region.

(0)4-7 spines on the antero-lateral and antero-branchial regions (Fig **B3**.10c, e). These spines are found mostly on the anterobranchial region in *Lopholithodes, P. otsuae, P. formosa*, and others**.**

(1) Fewer than 4 spines on the anterolateral and anterobranchial regions. This is found in *P. ceres, P. haigae* and *P. cristata*, and these spines are found on the anterobranchial region, none on the hepatic margin of the carapace.

(2) More than 8 spines found on the anterolateral and anterobranchial regions (Fig **B3**.10a, b, d). In this case, more spines are found on the hepatic region, and there is little or no distinction between the hepatic and anterobranchial margins.

P.---Transition between the anterobranchial and posterobranchial margins.

(1) Expanded flange behind the mid-branchial region, and a marked angle at the.posterior margin (Fig **B3**.10c, e).

(2) No marked angle at the posterior branchial postion and a more or less continuous margin of spines (Fig **B3**.10a, d).

(3)A significant change between anterior and posterior branchial margins (notably, spines on the anterior but absent on the posterior margins) (Fig **B3**.10b).

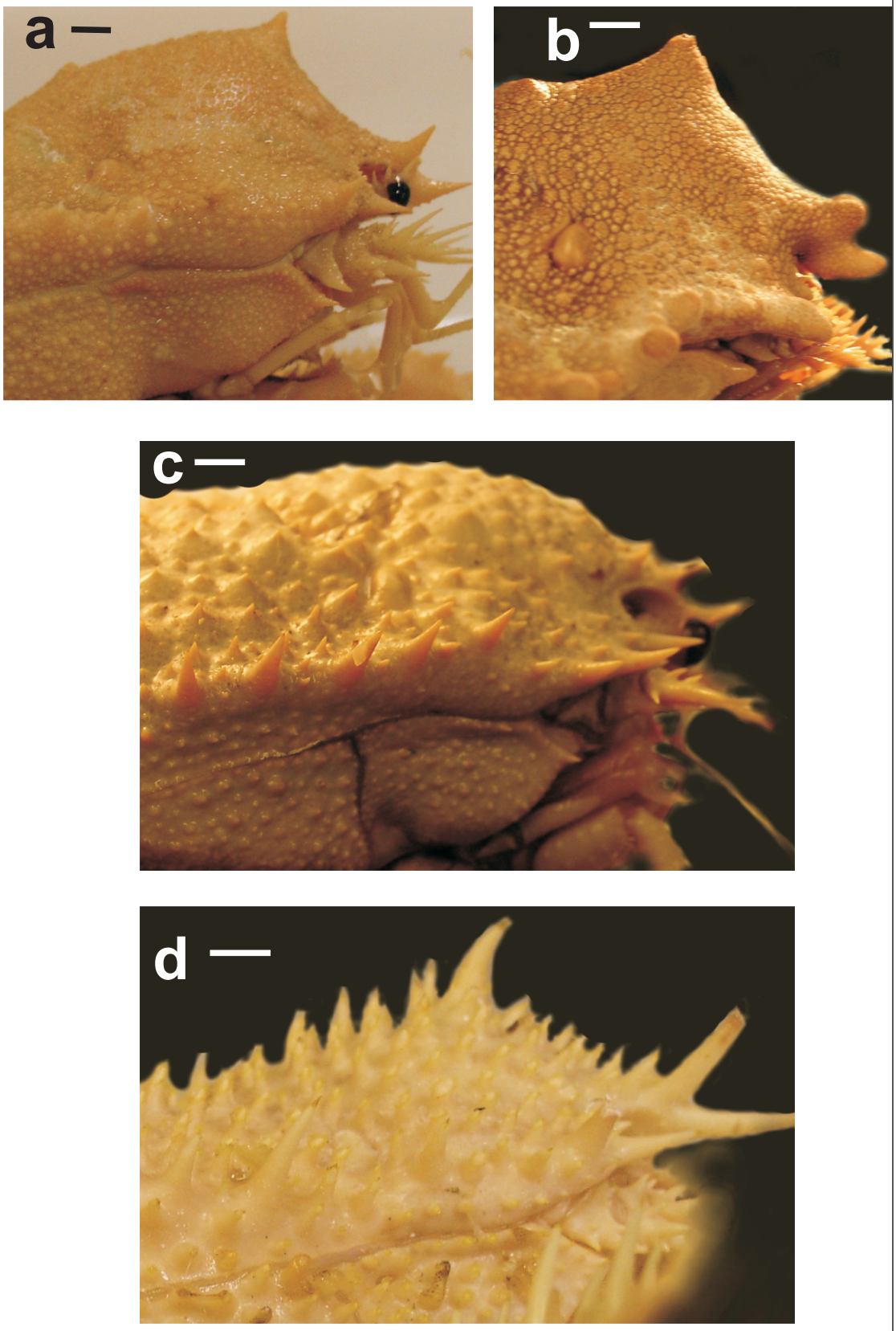

Figure B3.8 Gastric spines in *Paralomis* and *Lopholithodes*, lateral view of the anterior part of the carapace. Scales 5 mm. **a)***P. arae,* ♂ CL 74.5 mm (MNHN Pg 5945); **b)** *Lopholithodes mandtii* ♂ CL 107.8 mm (USNM 2103); **c)***P. cubensis* ♂ CL 61 mm **d)***P. spinosissima* ♂ CL 58.9 mm.

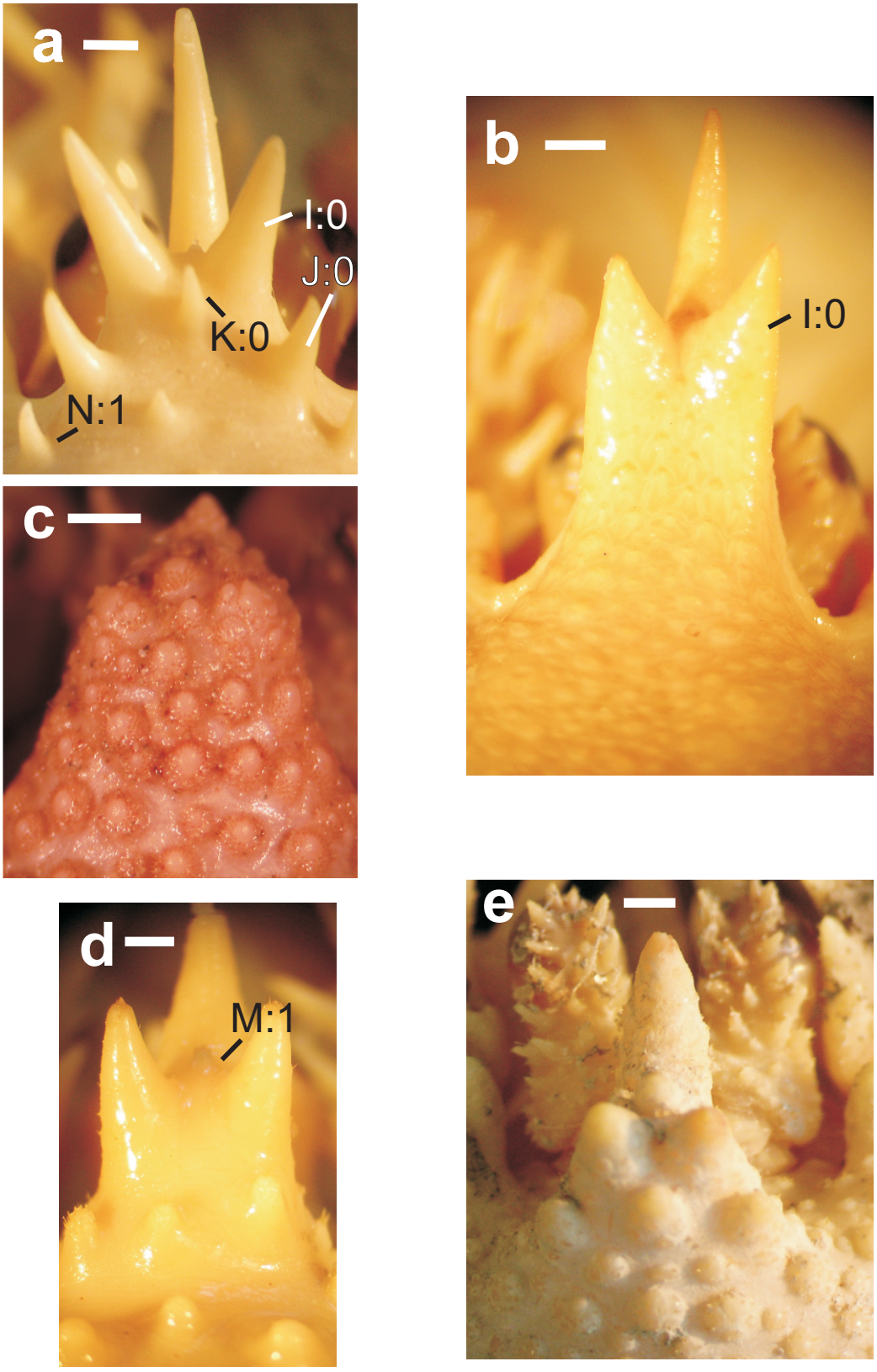

Figure B3.9 Rostrum. Scales 1 mm.
a)*P. aculeata* holotype ♂ CL 41 mm (coding *Paralomis* I:0; J:0 K:0 M:0 N:1).
b)*P. verrilli* ♂ 57.8 mm (coding *Paralomis* I:0; J:1 K:1 M:0 N:0).
c) *P. haigae* ♀ CL 52 mm (coding *Paralomis* I:1; J:1 K:1 M:0 N:0)
d) *P. inca* ♂ CL 99 mm (coding *Paralomis* I:0; J:0 K:1 M:1 N:0)
e) *Lopholithodes* ♂ CL 107.8 mm (coding *Paralomis* I:0; J:0 K:0 M:1 N:0).

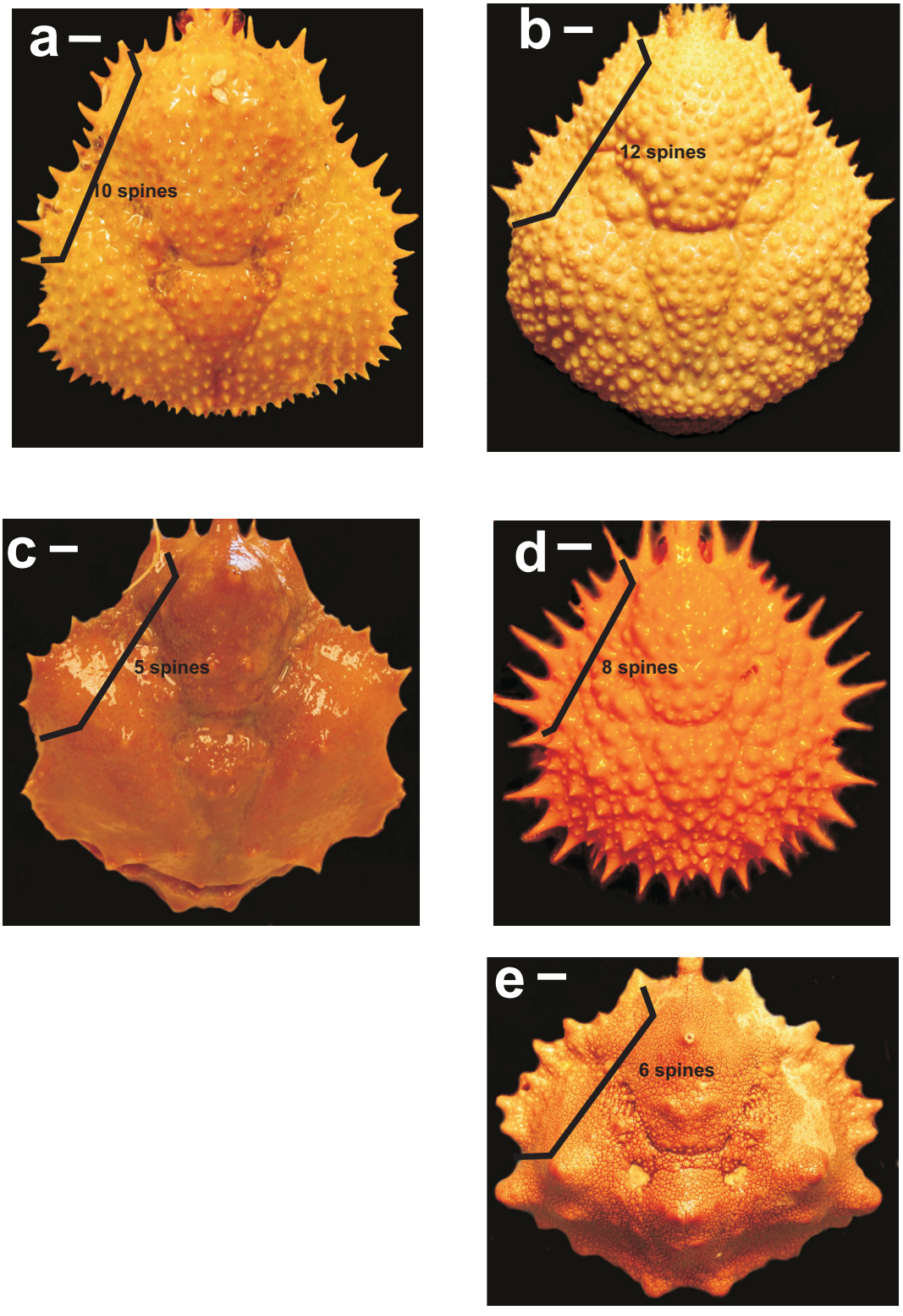

Figure B3.10 Lateral spines. Scales 5 mm
a) *P. aculeata* ♂ CL 62 mm (coding *Paralomis* O:2 P:2).
b) *P. dawsoni* ♂ CL 62 mm (coding *Paralomis* O:2 P:3).
c) *P. verrilli* ♂ 57.8 mm (coding *Paralomis* O:0 P:1),
d) *P. stella* ♂ 56.5 mm (coding *Paralomis* O:2 P:2)**.**
e) *Lopholithodes mandtii* ♀ CL 107.8 mm (coding *Paralomis* O:0 P:1).

-<u>*Walking legs*</u>

--Ancestral states: Short patches of setae at the dorsal tip of the dactylus are found in the outgroup *Lopholithodes,* and in the Hapalogastrinae. They are not found at all in *Lithodes*, *Neolithodes* and *Paralithodes*. Arrangement of spines in the walking legs is left as ambiguous for the out-group state.

*--**Character:***

Q.---Merus cross-section.

(1) Pereiopod 3 merus with an approximately triangular cross-section to the merus, skewed towards the anterior (Fig **B3**.11a, b).

(2) Distinctly quadrilateral cross section to the pereiopod 3 merus, with two dorsal edges usually but not necessarily with spines on each (Fig **B3**.11c, d).

(3) Closely tessellating and almost triangular merus of walking legs in dorsal view, with the thicker end distally (Fig **B3**.11e, f).

R.---Comb of curved spines along the anterior aspect of walking legs.

(0) Irregularly sized spines arranged more or less in rows along the merus, carpus and propodus of the walking legs (Fig **B3**.11c, d).

(1)A comb of strong, curved spines running in a continuous line along the anterior edge of the merus, carpus, and the dorsal edge of the propodus (Fig **B3**.11: **R:1**).

S.---Prominent rows of setae flanking the dorsal tip of the dactylus.

(0) Two rows of setae less than 1/6 (typically a lot less) of dactylus length at the tip of the walking leg dactylus (Fig **B3**.12a, c)**.**

(1) Two rows of setae extending for more than 1/5 of length of the dactylus on the walking legs (Fig **B3**.12b, d).

Variation occurs in such a way that the long and short patches can be coded with a lack of ambiguity in most cases.

T.---Dactyl lateral setae.

(0) The lateral faces of the walking leg dactyli free of setae (Fig **B3**.12a, b, d).

(1) Walking leg dactyli with setae on the dorsal, ventral and lateral faces (Fig **B3**.12c).

U.---Spines on proximal end of dactylus. *Importantly, this character is not dependent on the extent of the carapace spines.*

(1) 0-4 small spines present at the proximal end of the walking leg dactylus (Fig **B3**.12a, c, d).

(2) 5-8 large spines on the proximal portion of the walking leg dactyli (Fig **B3**.12b).

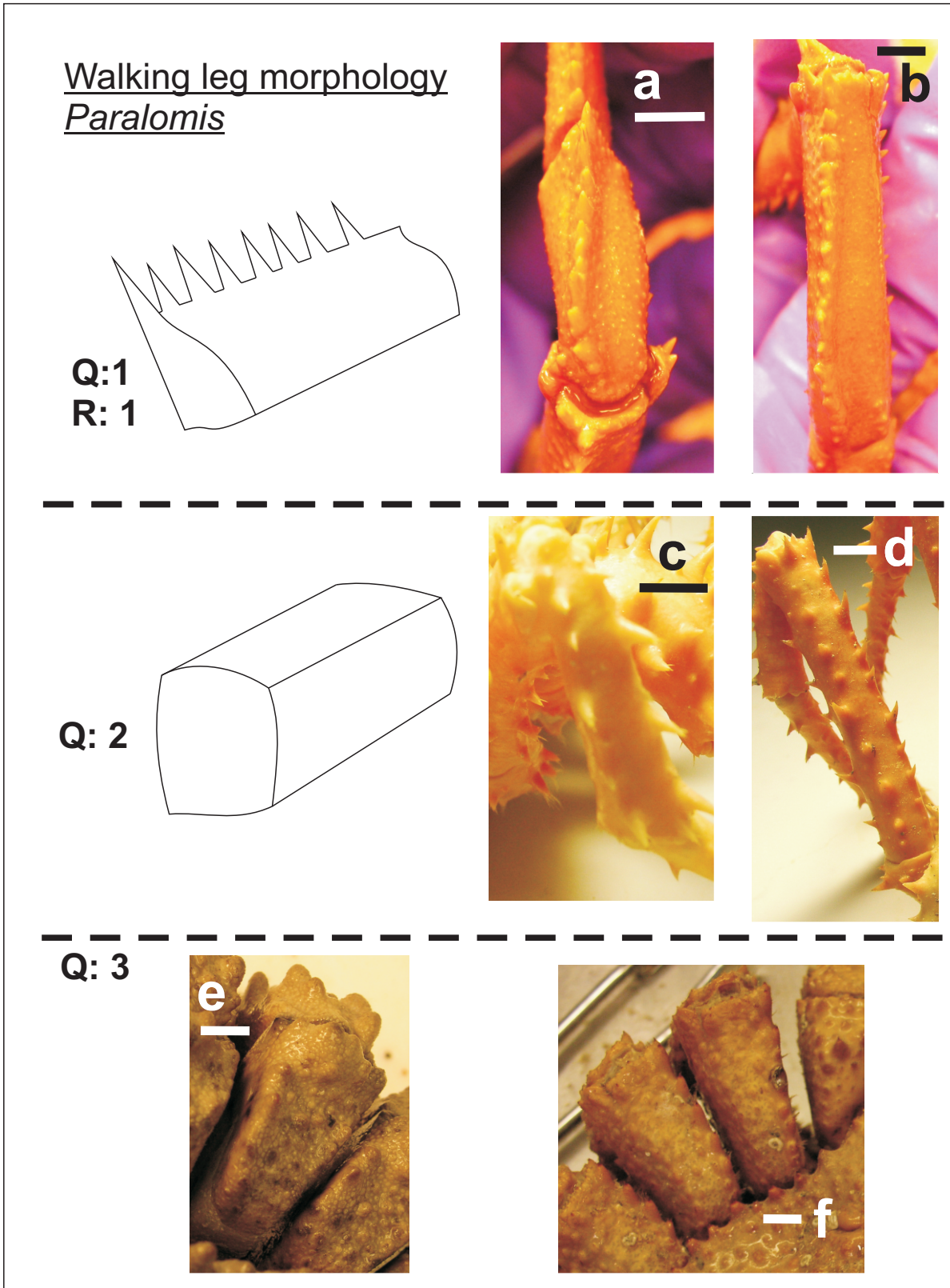

Figure B3.11 walking legs in *Paralomis* and *Lopholithodes* Scales 5 mm.
a, b) *P. verrilli* ♀ 57.8 mm pereiopod 3 (a) carpus (b) merus.
c, d) *P. aculeata* ♀ CL 62 mm pereiopod 3 (a) carpus (b) merus.
e) *Lopholithodes mandtii* ♀ CL 107.8 mm. Merus, dorsal view.
f) *P. granulosa* ♀ CL 65 mm. Merus, dorsal view.

-Abdominal segments

--Ancestral states: All examined *Paralomis*, *Glyptolithodes* and *Lopholithodes* have a single plate on 2nd abdominal segment; in all cases except some of the juveniles, the second and first segments are demonstrably fused. This fusion occurs by juvenile crab stage II in both *Lopholithodes* and *Paralomis* (McLaughlin et al 2004). Spines on the first abdominal segment, present in the outgroup are present to a variable extent in the ingroup with no discernable pattern.

Lopholithodes, Paralomis and several other genera have medial accessory plates on segments 3-6 of the abdomen, which form after the primary divisions of the megalopal tergites in juvenile crab stages (McLaughlin et al. 2004). Under schemes of evolution in which the Lithodidae evolved from pagurid ancestors with uncalcified abdomens (Boaz 1880, Richter & Scholtz 1994), the fusion of abdominal plates is a derived character (see Section **O**.2.2). Developmental studies, however, show that division of the medial and lateral plates, and the additional calcification of nodules at the abdominal margin and medial regions are novel within the Lithodidae (McLaughlin et al 2004). Up to 16 marginal plates are found in *Paralomis* species, although often these are secondarily fused into several larger units. *Neolithodes* has up to 21 marginal plates allied with segments 3-6, which makes homologies between the two groups difficult to determine without further comparative developmental studies. Fusion of marginal accessory plates to one another or to the lateral plates is likely to be a derived character within this group (McLaughlin et al 2004).

--Characters:

V.---Fusion of lateral and marginal plates on male abdominal segment 3.

(0): No fusion of marginal and lateral plates on the 3rd abdominal segment (Fig **B3**.13a, b)**.**

(1) Marginal segments at least partially fused to 3rd lateral plates (as identified by spines on the margin of the lateral plate) – partial fusion can not be distinguished from full fusion, because the positional homology of the 'unfused' plates can not currently be determined (Fig **B3**.13c).

W.---Fusion of the marginal plates associated with abdominal segments 4 and 5.

(**0**)At least two separate marginal plates associated with each of the lateral plates in abdominal segments 4 and 5 (Fig **B3**.13a-c).

(1) Marginal plates are fused into two blocks associated with the 4th and 5th lateral plates.

X.---Spines on the upper margin of the basis of pereiopod 2-4.

(0)A smooth upper margin to the basis on each of the walking legs (Fig **B3**.13a-c).

(1) Spines are present on the upper margin of each pereiopod (2-4) basis**.**

-Ocular peduncle

Y.---Large spine on the eyestalk.

(0) At least one large spine on the terminal dorsal part of the ocular peduncle (Fig **B3**.14a, c).

(1) No large spines on the dorsal portion of the eyestalk (Fig **B3**.14b).

-Antennal acicles

--*Ancestral state:* The antennal acicle in lithodids typically consists of a long central spine with a number of spines branching from its medial and lateral sides; however, many different forms exist. In *Cryptolithodes*, the acicle is flattened and large, with no spines. In *Lithodes* and *Neolithodes*, the acicle is substantially reduced in size. In *Paralithodes*, there are up to three spines on the external surface. In *Rhinolithodes, Phyllolithodes* and *Lopholithodes*, the acicle is large, with up to ten spines of similar sizes coming from either side, and several additionally from the central axis.

--*Characters*

***Z.---Form of the antennal acicle*:** The antennal acicle can vary slightly in the number of spines within a species; however, all variation is within the categories as they are formulated here (Fig **B3**.15).

(1) Acicles with 5-8 (or more) stout spines arranged in a comb like pattern on each side of a central spine, sometimes with several smaller spines along the central axis in addition (Fig B **B3**.15c, d).

(2)3-4 stout spines on each side of a stout central axis, the outer spines longer (Fig **B3**.15 b).

(3) Acicle with long, slender spines (Fig B **B3**.15a). Typically, two or three large spines on the outer side or towards midline and one or two smaller spines on the inner surface towards the base. Often, the inner spines are heavily reduced.

-*Secondary ornamentation covering accessory spines*

Lateral spines are usually consistent within *Paralomis*, even when the rest of the dorsal ornamentation varies substantially. Where tubercles cover the carapace, spines on the carapace and antennal acicle are almost always conical and prominent. In *Lopholithodes, Phyllolithodes* and *Rhinolithodes*, secondary ornamentation covers prominent, conical lateral spines. In *Lithodes*, *Paralithodes* and the Hapalogastrinae, the spines of the antennal acicle are smooth and free of secondary ornamentation and setae.

--***Characters:***

AA.---Lateral spine ornamentation.

(**0**)Setae and/or secondary carapace ornamentation along the length of lateral spines or crests.

(1) Lateral spines free of setae or tubercles from the base.

AB.---Secondary texture on spines of the antennal acicle.

(0) Antennal acicle spines with no setae or secondary tubercles (Fig **B3**.15a, d).

(1) Antennal acicle has many tubercles and setae in addition to the spines (Fig **B3**.15b, c).

-Chelae

AC♂, AD♀. --Ratio between cutting surface and crushing surface on the right cheliped of adults (CL > 50 mm).

There are some quantitative characters (like egg size in the *Lithodes* part) that I would like to incorporate into analyses, but do not have enough data to produce a statistical comparison of means for all species. Sexually dimorphic characters, such as the chela size, are also influenced by reproductive maturity. Subdividing the dataset by sex and stage dramatically reduces the sample size. Cutting (black sclerotised) vs crushing (white teeth) ratio of right chela on different reproductively mature *Paralomis* (> 50 mm CL) were examined in males and females (Fig **B3**.16). The measurement of cutting surface (black sclerotised surface) was made from the tip of the dactylus to the end of the cutting surface. The measurement of the whole dactylus length is made from the tip of the article to the articulation point with the propodus. It is estimated that the crushing surface is the part of the dactylus that is not sclerotised (Fig **B3**.16). For each distribution, a division of the dataset was done by inspection into a high ratio and a low ratio group. Coding used a value of **0** for those above a defined level for males or females and **1** for those above it. Any data within 0.05 units of the mean are coded as ambiguous (Fig **B3**.17). This is a very rough method for determining a difference between species and should be replaced by statistically rigorous techniques when sufficient data are available.

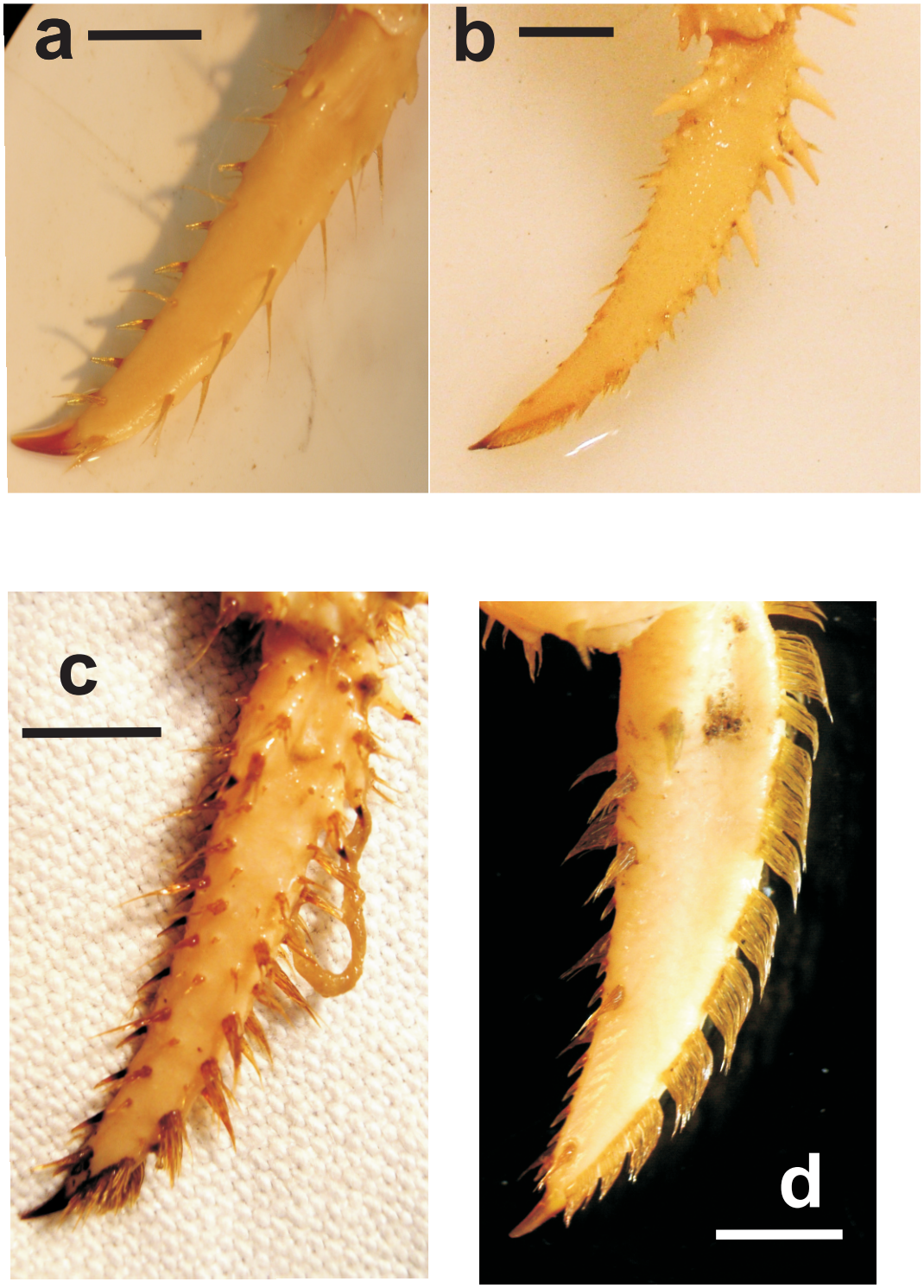

Figure B3.12 Dactylus of *Paralomis* species. Scales 5 mm.
a) *P. aculeata* holotype ♂ CL 41 mm (coding *Paralomis* S:0 T:0 U:1).
b) *P. arae* ♂ CL 74.5 mm (coding *Paralomis* S:1 T:0 U:2)
c) *P. dawsoni* ♂ CL 62 mm (coding *Paralomis* S:0 T:1 U:1)
d) *Glyptolithodes cristatipes* ♂ CL 71.2 mm (coding *Paralomis* S:1 T:0 U:1)

Abdominal characteristics in male *Paralomis*

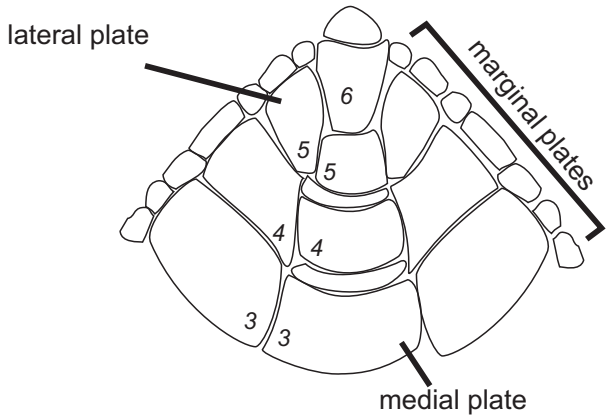

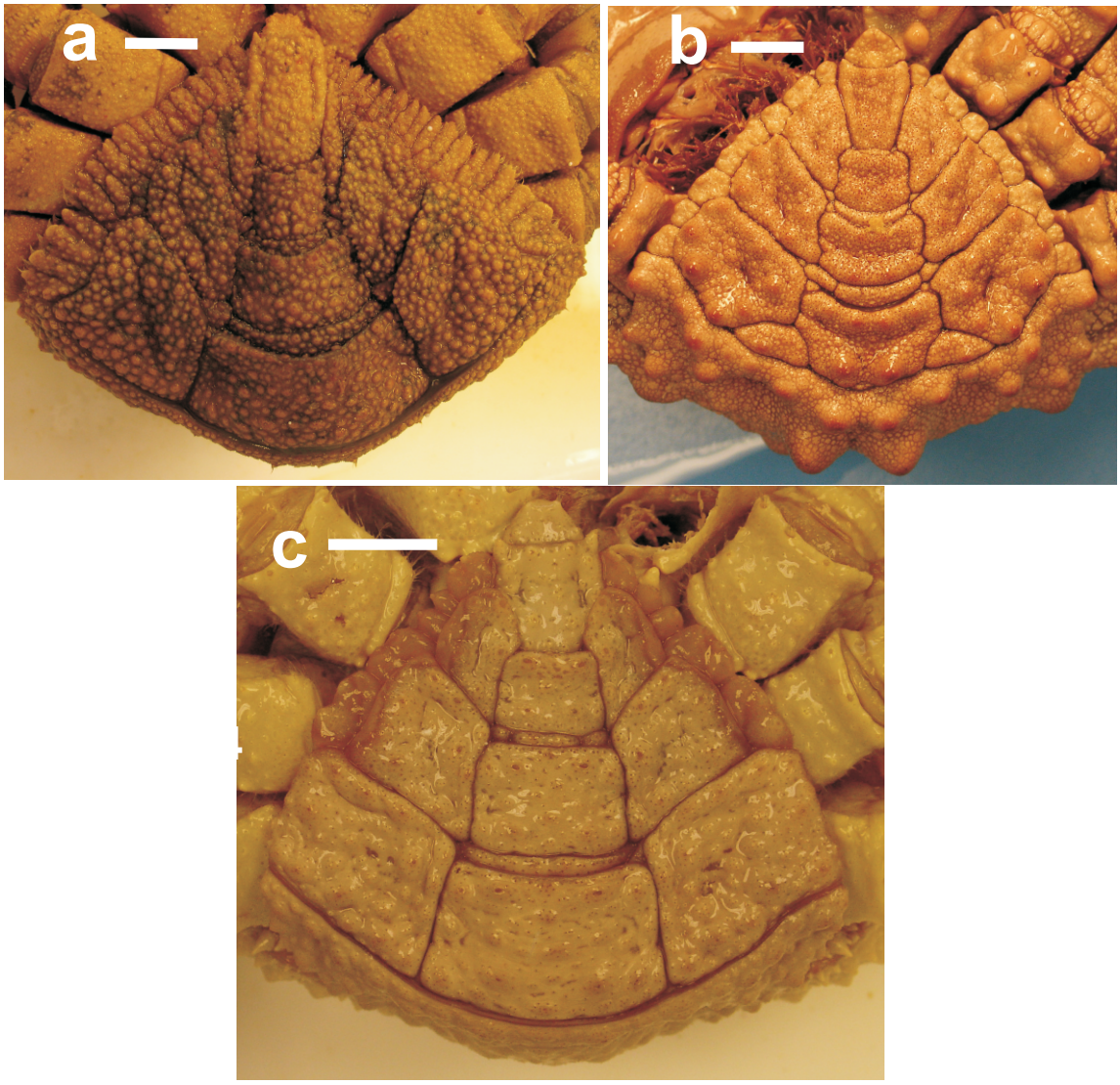

Figure B3.13 Abdominal tergites 3-5 in male *Paralomis*. Scales 5 mm.
a)*P. cristata* ♂ 96.9 mm (coding *Paralomis* V:0 W:0 X:0)
b)*Lopholithodes mandtii* ♂ 65 mm (coding *Paralomis* V:0 W:0 X:0).
c)*P. cubensis* ♂ 61 mm (coding *Paralomis* V:1 W:0 X:0)

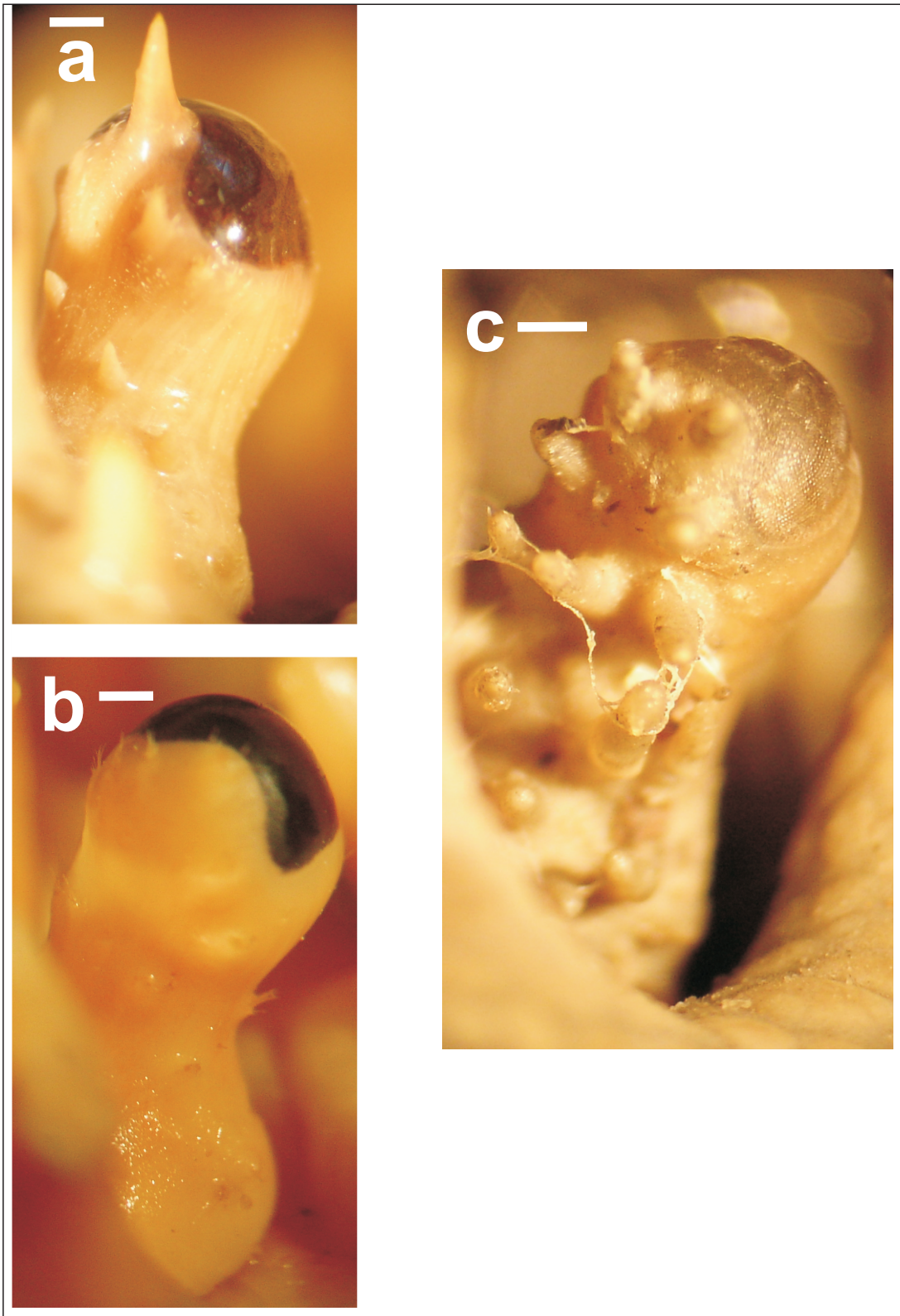

Figure B3.14 Eyestalk of *Paralomis* and *Lopholithodes* Scales 1 mm.
a)*P. cubensis* ♂ CL 61 mm (coding *Paralomis* Y:0).
b)*Lopholithodes mandtii* ♂ 65 mm (coding *Paralomis* Y:0).
c)*Paralomis aculeata* holotype ♂ CL 41 mm (coding *Paralomis* Y:1).

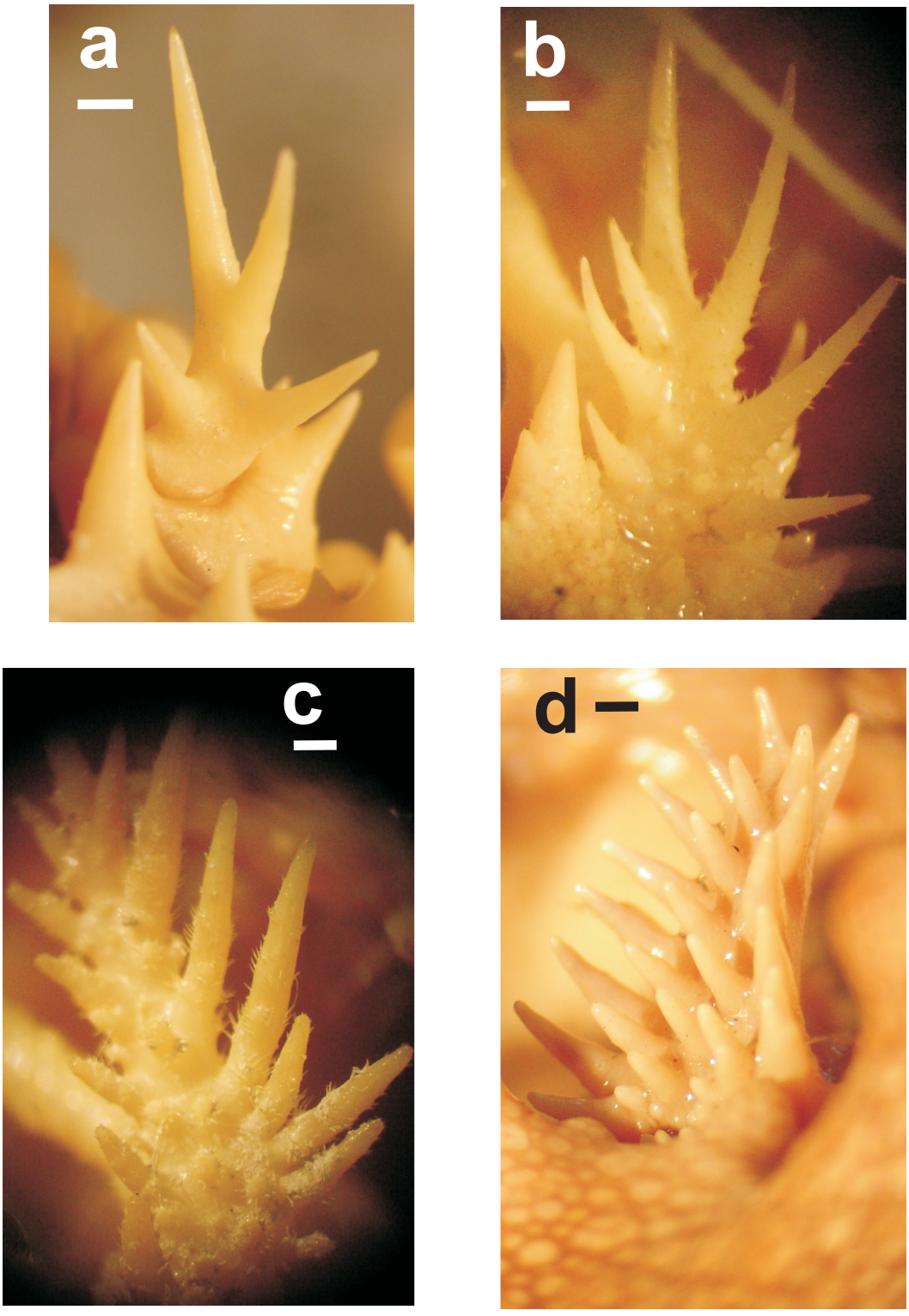

Figure B3.15 Antennal acicle of *Paralomis* and *Lopholithodes.* Scale 1 mm.
a)*P. aculeata* ♂ CL 41 mm (coding *Paralomis* Z:3 AB:0).
b)*P. arae* ♂ CL 74.5 mm (coding *Paralomis* Z:2 AB:1).
c)*P. haigae* ♂ CL 49.9 mm (coding *Paralomis* Z:1 AB:1).
d)*Lopholithodes mandtii* ♂ 65 mm (coding *Paralomis* Z:1 AB:0).

Figure B3.16 Right ♀ chelae. White line indicates sclerotised cutting surface; black line indicates dactylus length measurement. Scale 5 mm.
a)*P. inca* ♀ CL 99 mm (coding *Paralomis* AD: 1)
b)*P. mendagnai* ♀ CL 50 mm (coding *Paralomis* AD: 0).

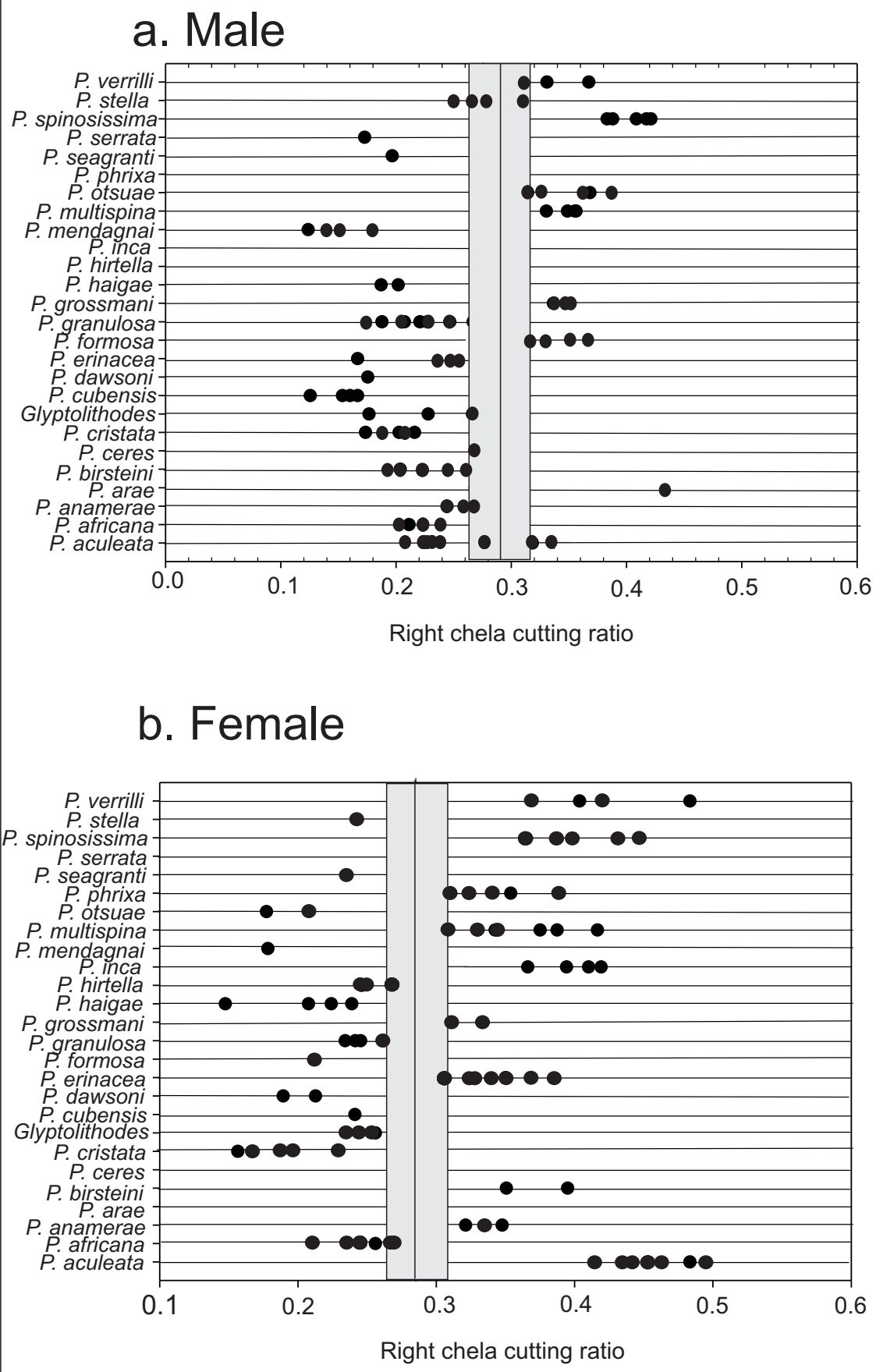

Figure B3.17 Graph of sizes of *Paralomis* cutting surface as a proportion of the right chela dactylus length. Grey box indicates the cut-off point, placed by eye in the middle of the distribution, and the 'ambiguous' region 0.05 units wide either side of it within which points aren't scored. **a)**Males with CL > 50 mm. **b)**Females with > 50 mm CL.

	A	B	B2	C	D	E	F	G	H	I	J	K	L	M	N	O	P	Q	R	S	T	U	V	W	X	Y	Z	AA	AB	AC	AD
P. aculeata	1	1	1	0	0	1	2	X	0	0	0	0	0	0	1	2	2	2	0	0	0	1	1	1	0	1	3	1	0	X	1
P. africana	1	0	0	0	0	1	3	X	1	0	1	1	0	0	0	2	1	1	0	1	0	1	1	0	0	0	2	0	1	0	0
P. anamerae	1	1	1	0	0	1	2	X	0	0	0	1	0	0	1	2	2	2	0	0	0	1	1	1	0	1	3	1	0	0	1
P. arae	0	0	0	0	X	0	X	X	0	0	1	1	0	0	0	0	1	1	1	1	0	2	1	0	0	0	2	0	1	1	X
P. birsteini	1	1	0	0	0	1	2	X	0	0	0	1	0	0	0	0	2	2	0	0	0	1	1	0	0	1	3	1	0	0	1
P. ceres	0	0	0	0	0	1	1	1	0	0	1	1	0	1	0	1	3	1	1	X	0	1	0	0	0	0	1	0	1	X	X
P. cristata	0	0	0	0	0	1	1	1	0	0	1	1	0	1	0	1	1	1	0	1	0	1	0	0	0	0	1	0	1	0	0
P. cubensis	1	1	0	0	0	1	3	X	1	0	0	0	0	0	0	2	2	2	0	0	0	1	1	0	0	0	3	1	0	0	0
P. dawsoni	0	0	0	0	0	1	1	1	1	0	1	1	0	0	0	2	3	3	0	0	1	1	1	0	0	0	1	0	X	0	0
P. erinacea	1	1	1	1	0	1	3	X	X	0	0	1	0	0	X	2	2	2	0	1	X	X	1	0	0	0	2	0	X	0	1
P. formosa	1	0	0	0	0	X	X	X	0	0	1	1	0	0	0	0	1	X	1	1	0	1	1	0	0	0	3	X	0	X	0
P. granulosa	0	1	0	0	0	0	X	X	1	0	0	0	0	1	0	2	3	3	0	0	1	2	1	0	0	0	2	0	X	0	0
P. grossmani	1	0	0	0	X	1	1	1	0	0	0	0	0	0	0	2	2	2	0	1	0	2	X	0	0	0	2	0	0	1	1
P. haigae	0	0	0	0	0	1	1	2	1	1	1	1	0	X	0	0	3	1	0	0	0	1	1	0	0	0	1	0	1	0	0
P. inca	1	1	0	0	0	1	2	X	X	0	X	1	0	1	0	X	2	2	0	1	0	2	X	0	1	0	2	0	0	X	1
P. mendagnai	1	1	0	0	0	1	3	X	1	0	1	1	0	0	0	2	2	X	0	X	0	1	1	0	0	1	3	1	0	0	0
P. multispina	1	0	1	1	1	1	1	1	0	0	0	X	0	0	0	2	2	2	0	1	0	2	1	0	X	0	3	0	0	1	1
P. otsuae	0	0	0	0	0	0	X	X	0	0	1	1	0	0	0	0	1	1	1	1	0	2	1	0	0	0	2	1	0	X	0
P. phrixa	1	1	1	1	1	1	1	1	0	0	0	0	0	0	0	2	2	2	0	1	0	2	1	0	1	0	3	0	0	X	1
P. seagranti	0	0	0	0	0	1	1	1	1	0	1	1	0	0	0	2	3	3	0	0	1	1	0	0	0	0	1	0	X	0	0
P. serrata	0	0	0	0	0	1	1	1	0	0	1	1	0	0	0	0	1	1	1	1	0	1	1	0	0	0	3	0	0	0	X
P. spinosissima	1	1	1	1	1	1	1	1	0	0	0	0	0	0	0	2	2	2	0	1	0	2	1	0	1	0	3	0	0	1	1
P. stella	1	1	0	0	0	1	3	X	1	0	0	1	0	0	0	2	2	2	0	0	0	1	1	1	0	0	3	1	0	0	X
P. verrilli	0	0	0	0	0	0	X	X	0	0	1	1	0	0	0	0	1	1	1	1	0	1	1	0	0	0	2	1	0	1	1
Lopholithodes	0	0	0	0	0	0	X	X	0	0	0	0	0	1	0	0	1	3	0	0	0	1	0	0	0	0	1	0	0	X	X
G. cristatipes	1	0	0	0	0	0	X	X	0	2	1	1	1	0	0	0	1	1	0	1	0	1	1	0	0	0	2	0	1	0	0
Outgroup	X	X	X	0	0	0	X	X	0	0	0	0	0	X	0	0	X	X	0	0	0	X	0	0	0	X	X	0	X	X	X

Table B3 Discrete character codes for phylogenetic analysis of *Paralomis* genus.

B3.3.3 Discrete-character phylogeny result

-Parsimony

The most parsimonious tree based on 31 characters for 27 taxa (Fig **B3**.5b) shows two well-resolved terminal clades (**[Δ]** and **[Ɣ]**) connected at an unresolved polychotomy. Close to the base of the tree, central Pacific species *P. seagranti*, *P. dawsoni* and South American (shallow-water) species *P. granulosa* resolve near to the outgroup and to *Lopholithodes*.

Clade **[Δ]** includes species from waters near the American continent(s), off both the Pacific and South Atlantic coasts (as well as *P. arae*, from the mid-Pacific). Within this clade, the Atlantic species *P. formosa* and *P. serrata* diverge near the base; a close relationship was indicated between *P. verrilli* and *P. otsuae* from the northern and southern Pacific Ocean respectively.

Clade **[Ɣ]** divides into two clades: one, labelled **[Ω],** containing three Southern Ocean and sub-Antarctic species (*P. aculeata, P. anamerae, P. birsteini*), as well as species from the Southern Indian, Atlantic and Pacific Oceans. A second clade **[Π]** contains 'spiney' species, also with a distribution throughout the eastern Pacific continental margin. Basal groups of clade **[Π]**, *P. inca* and *P. grossmani,* are found either side of the isthmus of Panama in the Pacific and Atlantic, respectively. *P. multispina*, *P. phrixa* and *P. spinosissima* appear as a strongly supported group (bootstrap value = 82) within clade **[Π]**.

-Fitch-Margoliash distance

In comparison to the parsimony-based tree (Fig **B3**.5b), there are fewer weak nodes (indicated by short branch length) in the tree produced from the same discrete-character data transformed into a distance matrix (Fig **B3**.5c). The designation of *Lopholithodes* as the out-group does not substantially affect the topology of the distance-based tree in comparison to the parsimony-based tree in which a hypothesised out-group state was used (Fig **B3**.5b,c). Nodes **[Δ, Π, Ω]** are present on both trees in more or less equivalent topologies (Fig **B3**.5b, c)**.** Clade **[Ю]** (Fig **B3**.5c) includes central Pacific species *P. haigae*, *P. dawsoni* and *P. seagranti*, along with South Atlantic species *Paralomis granulosa* and this clade is resolved close to the base of the *Paralomis* lineage as tested here.

B3.3.4 Combination of discrete-character and morphometric distance matrices

A distance-based tree (Fig **B3**.5d) was created for the 20 species of *Paralomis* for which both morphometric and discrete character data could be collected. *P. granulosa* was the most basal species on this topology, which was rooted with *Lopholithodes*.

Three well-resolved clades were labelled **[Δ]**, **[Π]** and **[Ω]**. Clade **[Π]** contains *P. spinosissima*, *P. phrixa* and *P. multispina*; species that share derived features such as spines with oblique faces uniformly covering the carapace; large gastric spines; relatively large merus compared to body length. Clade **[Δ]** includes species *P. otsuae, P. verrilli, Glyptolithodes cristatipes* and *P. formosa*; these share several derived characteristics such as the triangular cross-section of the walking-leg merus. Clade **[Ω]** contains species *P. stella, P. cubensis, P. mendagnai, P. anamerae, P. aculeata, P. birsteini*, with the later three appearing as an internal clade **[Σ]**: these groups share features such as relatively long GC groove; relatively large anterolateral lengths compared to body length, and the morphology of the tergites on the third abdominal segment.

B3.4 Discussion

The pattern of dispersal in *Paralomis* from their proposed origin close to *Lopholithodes* is one of radiations between the Pacific and other oceans; however, directionality of the radiations is not clear. Four groupings have emerged from this morphology-based analysis and are supported to a greater or lesser extent by evidence from both morphometrics and discrete character analysis. Several species don't resolve consistently within any group mentioned in the discussion so far, such as *P. africana, P. erinacea, P. cristata, P. ceres* and *P. haigae.* Just less than 50% of *Paralomis* species are included in this analysis and, despite attempts to include representatives of the key morphotypes of *Paralomis*, there are many areas which simply have not been covered. It is quite likely that those species which do not resolve well here could be allied with some of the missing groups.

Sometimes forming a clade (**Ю**, Fig **B3**.5), are a group of species from the mid-Pacific Ocean — *P. dawsoni* and *P. seagranti* — as well as *Paralomis granulosa* from the shallow waters of S. America. In the combined distance analysis (Fig **B3**.5d), most of these species are excluded because of small sample sizes, so *P. granulosa* resolves alone at the base of the tree. With the exception of aspects of stout leg morphology, the carapace of *P. granulosa* shares only a few features with *Lopholithodes* and in many ways (e.g tubercle structure) is quite derived in its morphology. *P. dawsoni* and *P. seagranti* are both found in the deep waters (to at least 1050 m) of the south west Pacific Ocean, whereas *P. granulosa* has the shallowest range of any in its genus (10-100 m). A south west/east Pacific radiation close to the base of the *Paralomis* lineage could fit with the only fossil evidence of the genus, *P. debodeorum* in New Zealand from the mid-late Miocene (Feldmann 1998).

The first well resolved group (Fig **B3**.5 **[Δ]**) contains *P. formosa*, *P. arae, P. otsuae, P. verrilli, P. serrata* and sometimes *Glyptolithodes cristatipes*. In general, *P. otsuae*, *P. verrilli* and *P. arae* are most closely allied within this clade, with the other three species resolved at the base of the clade. With the exception of *P. arae* (mid-Pacific), all of these species occupy water along the Pacific coast of the Americas, Japan, the Gulf of Mexico and the Patagonian continental shelf, predominantly between 800 and 2000 m (Appendix E). This distribution, despite being bipolar, is geographically limited to waters close to the American Pacific coast. *Glyptolithodes cristatipes* (Pacific coast, California to Chile) is often resolved within this clade, strongly implying that *Paralomis* — as currently defined — is paraphyletic.

A second clade (Fig **B3**.5 **[Π]**) includes *P. multispina*, *P. spinosissima*, *P. phrixa, P. grossmani*, and *P. inca*. The first three species almost always appear in a clade exclusive of the latter two. Again, a bipolar distribution along the eastern Pacific continental margin is implied by the exclusive relationship of these species. *P. multispina* is found in Japan and the Bering Sea; *P. phrixa*, *P. spinosissima, P. inca* and *P. grossmani* are from the western coast of South America or waters geographically close to South America (including the Gulf of Mexico).

A complex pattern of dispersal is indicated by these data, especially emphasising the importance of bipolar links between the north and south Pacific along the western coast of America. This potential dispersal pathway is indicated for least two lineages (**[Π], [Δ]**) although there is no evidence that it was a unidirectional (north→south) movement in either case. Both of these lineages include additional species from the Caribbean (*P. grossmani* and *P. serrata* respectively). There are no species in either of these lineages on the continental slope of eastern South America between Rio Plata 34 °S and 7 °N. Between these latitudes the only *Paralomis* species found are *P. shinkaimaruae* in the mid-Atlantic at 31 °S and *P. cubensis* at 2 °N (Appendix A,E). An absence of species in the present (identified) distribution doesn't mean that these lineages aren't or haven't been connected on the eastern continental slope of S. America; however, an uninterrupted distribution of *Paralomis* along the western continental slope of S. America suggests that this is the more likely route for dispersal along isobaths.

The third well-resolved group (Fig **B3**.5 **[Ω]**) containing *P. stella, P. mendagnai, P. cubensis* and *P. anamerae, P. birsteini* and *P. aculeata*, is furthest from the outgroup in the morphometric analysis and is well resolved based on discrete-character data. In all cases, *P. aculeata* and *P. anamerae* are allied with one another, and in most cases *P. birsteini* is a sister species to these. *P. birsteini* is a Southern Ocean species with a theoretically circum-Antarctic distribution. It has been found in the Ross Sea, the

Bellingshausen Sea, as well as in Crozet in the southern Indian Ocean. *P. anamerae* and *P. aculeata* have a demonstrably close relationship, despite a considerable geographic distance between *P. anamerae* populations in South Georgia (south-east Atlantic), and *P. aculeata* in the Southern Indian Ocean. *P. cubensis*, *P. stella*, *P. mendagnai* are native to the southern parts of the Atlantic, Indian and Pacific Oceans respectively. Circum-Antarctic gene-flow may have established this link between *Paralomis* species in the southern parts of the world oceans.

Paralomis species are found predominantly at slope rather than abyssal depths (<2000 m) and although some species can theoretically tolerate depths up to 4000 m, there is no evidence of this being a genus-wide trend. In reconstructions indicated here, pathways of dispersal largely follow continental margins. Species with trans-oceanic or mid-ocean distributions in *Paralomis* are not unknown (particularly in the Pacific), but dispersal patterns occur along island chains or along mid-oceanic ridges. The lecithotrophic larval stages of *Paralomis* are not recorded from pelagic environments; experimental observation (Lovrich 1999) indicates that they might have a demersally drifting habit. On the other hand, development is slow in low temperature environments and larval stages are likely to be long-lived. Deep ocean currents in addition to adult migration are perhaps the means by which dispersal occurs in this taxon.

B3. 5 Conclusions

- In a sample set of 25 out of 61 species of *Paralomis*, several do not resolve within these morphological phylogenies. Such groups may be closer to some of the non-sampled *Paralomis* lineages.
- *Glyptolithodes cristatipes* nests within *Paralomis* on the basis of morphology when *Lopholithodes* is assumed to be the outgroup.
- Shallow-water species *Paralomis granulosa* bears some (perhaps convergent) similarity to *Lopholithodes* in the morphometry of its walking legs and some aspects of discrete morphology. When *P. dawsoni* and *P. seagranti* are included in the taxon set, all three of these cluster close to the base of the *Paralomis* lineage.
- Meridional links between the north and south Pacific Oceans and South Georgia are evident in two lineages of *Paralomis*.
- Relatively recent circum-Antarctic interchange seems to link species on subAntarctic seamounts and island chains.

Section C: The Biogeography of the Lithodidae

CHAPTER C: TEMPERATURE CONSTRAINTS IN THE FAMILY LITHODIDAE

Sections from an article published in the Journal of Biogeography. Hall & Thatje (2009a), with additional data incorporated.

C.1 Introduction

Ten out of the 15 lithodid genera (Appendix A) are restricted to the coast of North America and linked island chains, at depths typically shallower than 200 m. The concept of a bottleneck in the radiation of lithodids, connected to their transition into the deep sea, has been proposed by several authors over the last 150 years (Bouvier 1896, Makarov 1938, Zaklan 2002a). They have hypothesized that, commencing from a shallow water origin, lithodids followed one route of radiation along the coastline of the North Pacific, and another through the deep water into adjacent oceans. Ecological or physiological factors have limited the range of the shallow-water lineage(s), resulting in an endemic North Pacific subfamily. Isothermal submergence at the poles is a phenomenon known from several other taxa with bipolar distributions (Andriashev 1986, Harrison & Crespi 1999, Briggs 2003, Raupach et al 2009). This principle may explain how some lineages followed a deep-sea route out of the North Pacific, and into other water bodies.

Despite the substantial evidence for cold water preferences or restrictions (Zaklan 2002a, Thatje et al 2004), the exact nature of the relationship between biogeography and temperature has not yet been examined in this group. This study tests the hypothesis that lineage-specific temperature tolerances influence the distribution of lithodid subfamilies.

C.2 Methods

C.2.1 Data sources

Data were gathered from three sources, as follows:

(1) 197 published records of lithodids were sourced from peer-reviewed journals and other literature. Identity was verified from descriptions and pictures, or by inspection where samples were deposited in museums. Data were included only for genus-level analyses if species identity was ambiguous.

(2) More than 1000 specimens (mostly unpublished records) were examined from museum collections in the Natural History Museum, London (NHM); Senckenberg Museum, Frankfurt; Musée National d'Histoire Naturelle, Paris (MNHN); Institut de

Ciencies del Mar, Barcelona; United States National Museum of Natural History, Smithsonian Institute, Washington (USNM); and the "Discovery Collection", National Oceanography Centre, Southampton (NOCS).

(3) 56 specimens with associated environmental data were obtained courtesy of commercial vessels or scientific cruises, from locations in the Southern Ocean, South America and un-deposited West African samples (Mauritania: MAU 1107) at the Instituto Español de Oceanografica, Vigo.

For each specimen studied, the depth, location and date of sample collection were noted. Most records were for crab stages; however, a few larval records were included. The study included 82% of the lithodid species (90 /117) described to date (Appendix **A**), with 65% of these species represented by more than 10 sample sites. Data from 871 worldwide sample locations (Fig **C.1**, Appendix **E**) were used.

Water temperature at the time of sampling was obtained from cruise reports where possible. Otherwise, temperatures were estimated, based on time of year, depth and location. The majority of the climatic data were taken from the National Oceanographic Data Centre <*World Ocean Atlas 2005*> (Locarnini et al 2006) and the National Oceanic and Atmospheric Administration – Earth System Research Laboratory (NOAA-ESRL), Physical Sciences Division (http://www.cdc.noaa.gov/). Southern Ocean data were obtained from the <Southern Ocean Atlas> (Olbers et al 1992) (http://odv.awi.de/en/data/ocean/southern_ocean_atlas/).

C.2.2 Phylogeny

The link between the habitat temperature range and the position of taxa within the lithodid phylogeny was examined. Molecular phylogenies were produced by Maximum Likelihood (ML) and Minimum Evolution (ME) criteria and Bayesian inference (BAY), using molecular alignment $\mathbf{TE_B}$ formed from parts of the COI, 16S, ITS and 28S genes (Section **A1**, Fig **A1.4**). A schematic of $\mathbf{TE_B}$ trees was produced for this chapter by condensing all monophyletic (or single species) genera to a single branch, and indicating the paraphyletic status and position of the other genera (Fig **C.2**). Where ML, ME and BAY $\mathbf{TE_B}$ trees disagree with one another, the conflict is indicated with a dashed line for the minority condition and solid line for the majority condition. Genera that include species with distributions outside the north Pacific were highlighted.

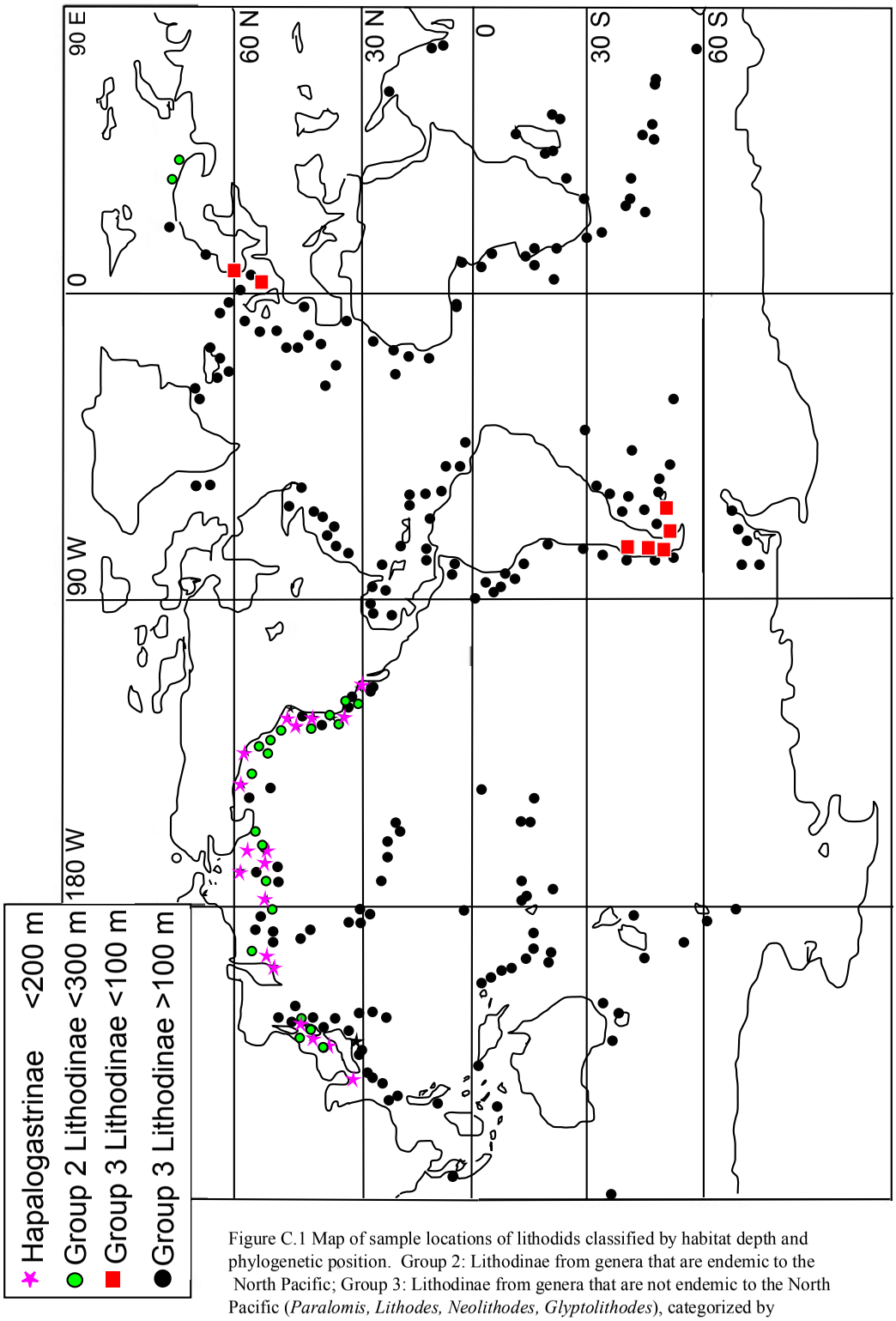

Figure C.1 Map of sample locations of lithodids classified by habitat depth and phylogenetic position. Group 2: Lithodinae from genera that are endemic to the North Pacific; Group 3: Lithodinae from genera that are not endemic to the North Pacific (*Paralomis, Lithodes, Neolithodes, Glyptolithodes*), categorized by habitat depth. Positions of markers represent sample sites. Markers falling within 50 km of another sample site of the same type were omitted for clarity.

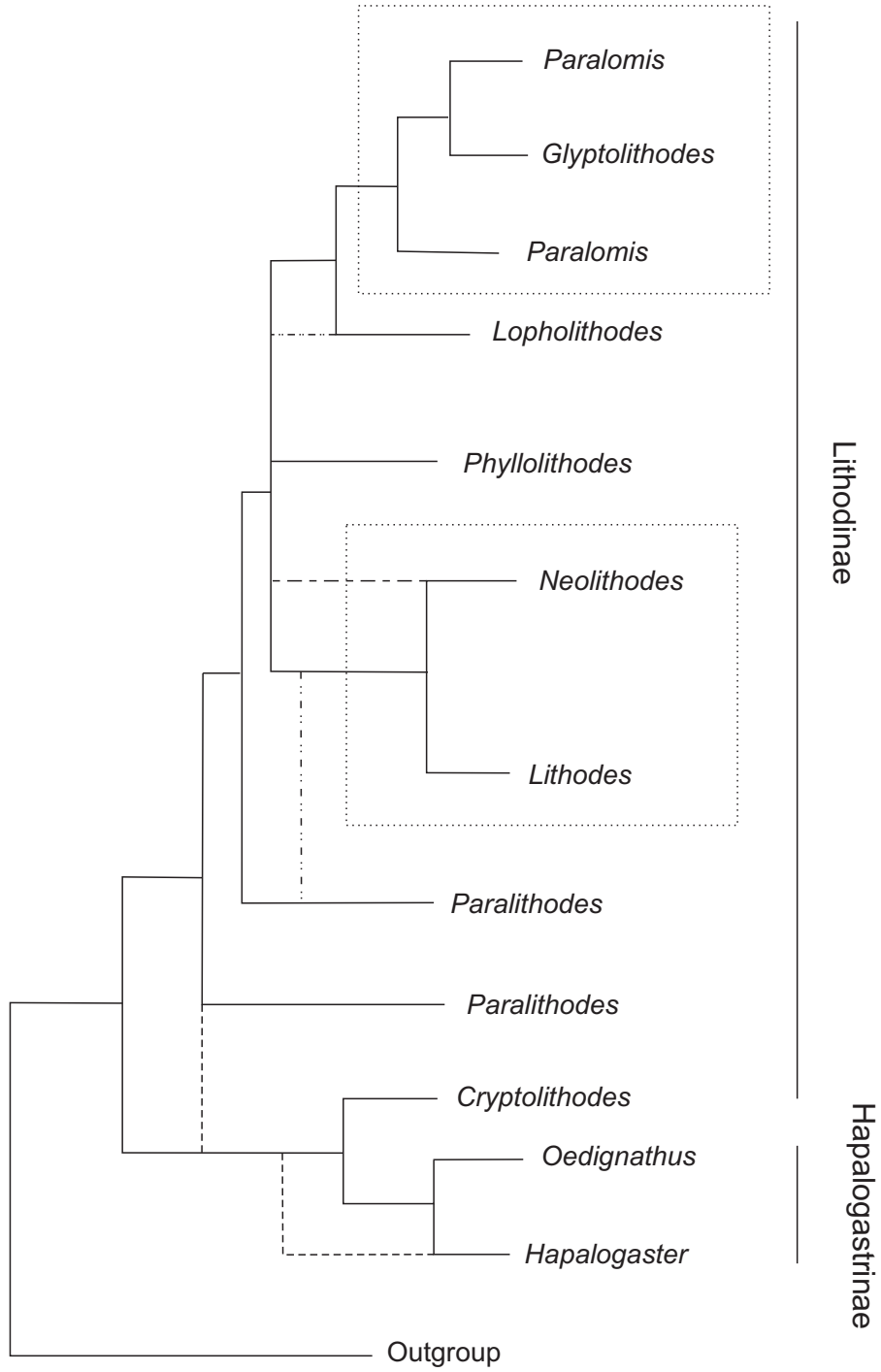

Figure C.2 Maximum likelihood tree created with <*PHYLIPdnaml*> for species representing 10 genera of Lithodidae. Analyses were conducted in Chapter 1 of this thesis (TE_B) based on sequences of ITS1, 16S, COI (mitochondrial), and 28S (nuclear) genes. Monophyletic genera were condensed to a single taxon label, and polyphyletic genera are indicated by multiple branches. Subfamilies Lithodinae and Hapalogastrinae are labelled. Genera, within which members occur below 200 m and/or outside the Pacific Ocean, are distinguished with a box. Outgroup genera from other anomuran families (*Pagurus* and *Aegla*) were used to root the tree.

C.2.3 Analysis

Latitudinal and bathymetric data

Records of shallowest specimen depth were compared with sample-site latitude. Most species had a range covering several tens of degrees of latitude; however, within species there was no significant ($\mathbf{r^2}$<0.05) difference in depth across sites of differing latitude. This observation justified the pooling of data from different sample locations into a mean latitude for each species. The shallowest depth was calculated as the 90th percentile of records within species groups (points, Fig **C.3**).

Depth, location and temperature data

Records of depth and local temperature for individual samples were compared – data were not pooled into species groups for this analysis. Mean seasonal variation in temperature was projected for each sample location (Fig **C.4**). Estimates of maximal and minimal global temperature profiles were taken from the <*World Ocean Atlas 2005*> (Locarnini et al 2006), excluding data from inland or sheltered shallow seas that have atypical temperature profiles, and in which lithodids have not been found. This provided a diagrammatic sense of the range of temperatures typically found at different depths in world oceans.

To investigate patterns of variation between lineages, data points were classified in all analyses according to their position in the molecular phylogeny (Fig **C.2**), as follows.

(1) Subfamily Hapalogastrinae.

(2) Members of genera within the subfamily Lithodinae, which share larval planktotrophy and shallow (<300 m) North Pacific habitats with the Hapalogastrinae.

(3) Lithodinae belonging to genera within which members are found deeper than 200 m and/or outside the North Pacific: *Paralomis, Lithodes, Neolithodes* and *Glyptolithodes*.

Southerly range boundaries and upper temperature limits for North Pacific subtidal populations

In order to examine the nature of the upper temperature thresholds in lithodids, the species tolerant of temperatures higher than 13°C were considered in further detail. All of these species occur exclusively in the North Pacific (Table C1). The most southerly populations of Lithodidae are found along the oceanic coast of Baja California, Mexico (29°47N; 15 m deep). Detailed weekly average temperature profiles are available for this region between August 1992 and 2008, courtesy of the NOAA-ESRL (http://www.cdc.noaa.gov/). For each month from 1992-2002, the temperature in the subtidal range (5–15 m) was recorded for latitudes 26, 30, 32, 34 and 36°N (Fig **C.5**). This enabled the seasonality of larval release to be examined with respect to water

temperature. Hatching seasons for North Pacific lithodids were similar throughout the group, occurring between February and May (Table C1, Zaklan, 2002b). Additionally, the locations of the coastal 15.5 °C isotherms between February and May in years 1996-2000 were calculated from the NOAA-ESRL (http://www.cdc.noaa.gov/) dataset for North America (Fig **C.6**). A comparison was then made between the latitude of the most southerly lithodid populations and the fluctuating positions of the subtidal 15.5°C isotherm.

Southern Ocean and sub-Antarctic range limits

The distribution of decapods in the southern hemisphere has been used to indicate a separation of the temperate/tropical fauna from the subAntarctic/Southern Ocean fauna (Gorny 1999). The subAntarctic/Southern Ocean region, which includes some of the coldest waters on earth (Barnes et al 2006), was divided into two groups for examination, based on latitude and oceanographic features. The range 45-60 °S includes locations within the Antarctic Circumpolar Current (ACC), from the sub-Antarctic front to the southern circum-Antarctic front (Antarctic divergence) and is split internally by the Polar Front (c. 50 °S; Section **O.**3.2.1). The ACC passes south of Patagonia before diverging across the Argentine continental shelf (Antezana 1999), so fauna in and around coastal South America are not included in this part of the study. The Scotia Arc is an array of trenches and elevations for 1500 km between the Antarctic Peninsula and Patagonia (Acosta et al 1989), which have previously been thought of as a possible route of faunal transmission into the Antarctic (although there is no direct evidence of this, Dayton 1990). The arc has a northern (South Georgia, c. 52 °S) and a southern arm (South Shetland, South Orkney, c. 59 °S) which have different temperature profiles and faunal distributions (Figs **C.8**i, iii), despite both being south of the Polar front (c. 50 °S; Section **O.**3.2.1, Lovrich et al 2005). Of the other circum-Antarctic islands included in the 45-60 °S range, Bouvet Island and the Kerguelen islands all lie south of the Polar Front; and the Falkland Islands, Prince Edward Islands, Crozet Islands, and the Macquarie Islands all lie north of the Polar Front (Eckmann 1953). Latitudinal variation of the polar currents within this range made it difficult to split the ACC graphically into sub-Antarctic and Polar water; however, the longitudinal location of these islands is indicated on temperature profiles (Fig **C.8**).

The second range (60-75 °S) approximately includes all waters south of the Antarctic divergence (the southern boundary of the ACC). Each oceanic front marks a transition in water density; often a notable change in temperature at the surface. Scott Island in

the Ross Sea, Peter I island in the Bellingshausen Sea, and the West Antarctic Peninsula (WAP) (all south of 60 °S) lie south of the Antarctic divergence (Section **O.**3.2.1).

Within each latitudinal range outlined above, the longitudinal and depth distributions are examined within and between species of lithodids (Fig **C.7**). The southern-most frontier of the lithodid distribution is examined by plotting water temperature variation with depth and longitude at 60 °S, 65 °S, 70 °S and 75 °S (Fig **C.8-10**). This was performed using data from <Southern Ocean Atlas> (Olbers et al 1992); each temperature estimate was taken by pooling all data within one degree of the stated latitude (e.g. 60 ± 1°S). Temperature at depths of 200 m, 500 m, 1000 m, and 2000 m were sampled, as they are relevant to the distribution of lithodids in this region.

C.3 Results

C.3.1 Latitudinal bathymetry clines

A distributional bottleneck (Bouvier 1896, Makarov 1938, Zaklan 2002a) separated 11 genera occurring at shallow northern latitudes from four deep-water genera: *Neolithodes, Lithodes, Paralomis* and *Glyptolithode*s. All lithodids appeared to be competitively or physiologically excluded from waters shallower than 400 m between 30°N and 40°S (Fig **C.3**). In addition, a pattern of emergence from the deep sea could be seen towards high southern latitudes (41-55°S) in the genera *Lithodes* and *Paralomis*.

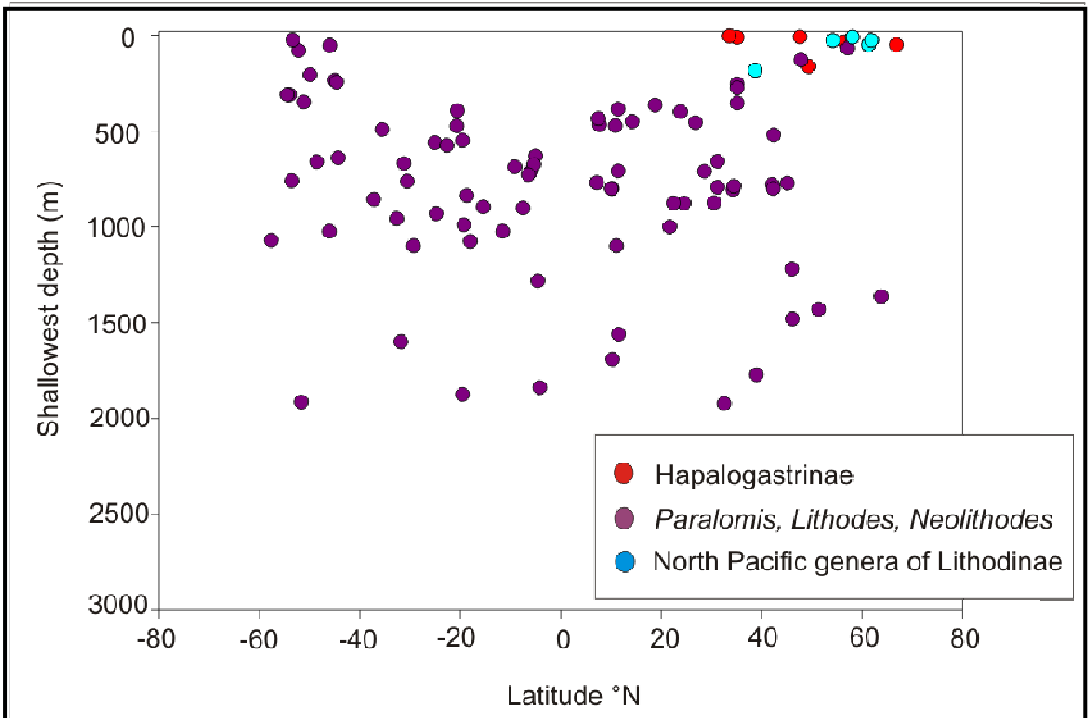

Figure C.3 Variation in the shallowest depth of lithodid species according to latitude. Data points represent the mean latitude and 90th percentile of depth for each of 90 lithodid species. Species are classified according to subfamily and habitat depth.

C.3.2 Temperature thresholds

GROUP 1: The Hapalogastrinae are predominantly non-migratory and endemic to the North Pacific intertidal/subtidal zones. This study confirmed that adults of the Hapalogastrinae inhabit water with a much larger range of temperatures (from 0°C in the northern Sea of Okhotsk to 25°C off the coast of California) than do the adults of the Lithodinae (Fig **C.4**). However, experimental evidence of defined temperature thresholds has only been shown for larval stages. Analyses of local temperature data (Figs **C.5** & **C.6**) indicated some range limitation in response to maximal water temperature during the larval hatching and development period. Over a sample period of 10 years, the water temperature at the most southerly subtidal sample locations dipped to 16.5°C (from summer maxima of 25°C) for the duration of hatching and larval development [67-87 days March – May (from Crain & McLaughlin 2000, Zaklan, 2002b)]. *Hapalogaster cavicauda* was the most southerly recorded species, inhabiting waters that were usually within 1°C of the spring 15.5°C isotherm (Fig **C.6**). The position of this isotherm varied by several degrees of latitude annually (Fig **C.6**), and most of the species were only found north of this fluctuation.

GROUP 2: The Lithodinae (including those not inhabiting the deep sea) have experimentally determined physiological temperature thresholds at 0.5 °C and 13-15 °C (Kurata 1960, Nakanishi 1981, 1985, Vinuesa et al 1985, Shirley & Shirley 1989, Calcagno et al 2005). Subtidal North Pacific species of Lithodinae have a similar distributional range to those shallow-water species of Hapalogastrinae (Table C1, Fig **C.6**). This may be an indication of a shared ancestral trait.

GROUP 3: For those genera occurring globally (highlighted, Fig **C.2**), there appeared to be little effect of temperature on range below depths of 1000 m. Most temperatures encountered at depth were within the predicted larval temperature thresholds for the subfamily. At depths shallower than 500 m, distributions were restricted at both ends of the temperature scale, with limits at 0.5° and 13°C. At the shallowest, warmest locations in which these groups were found, seasonal temperature fluctuations occurred (Fig **C.4**). At some sample locations, temperature would be expected to approach a maximum of 15°C over the course of a typical year. Vertical migratory behaviour (Miquel et al 1985, Abelló & Macpherson 1991, Paul & Paul 2001) in relation to the reproductive cycle might be linked to the narrower temperature tolerances of early life-stages.

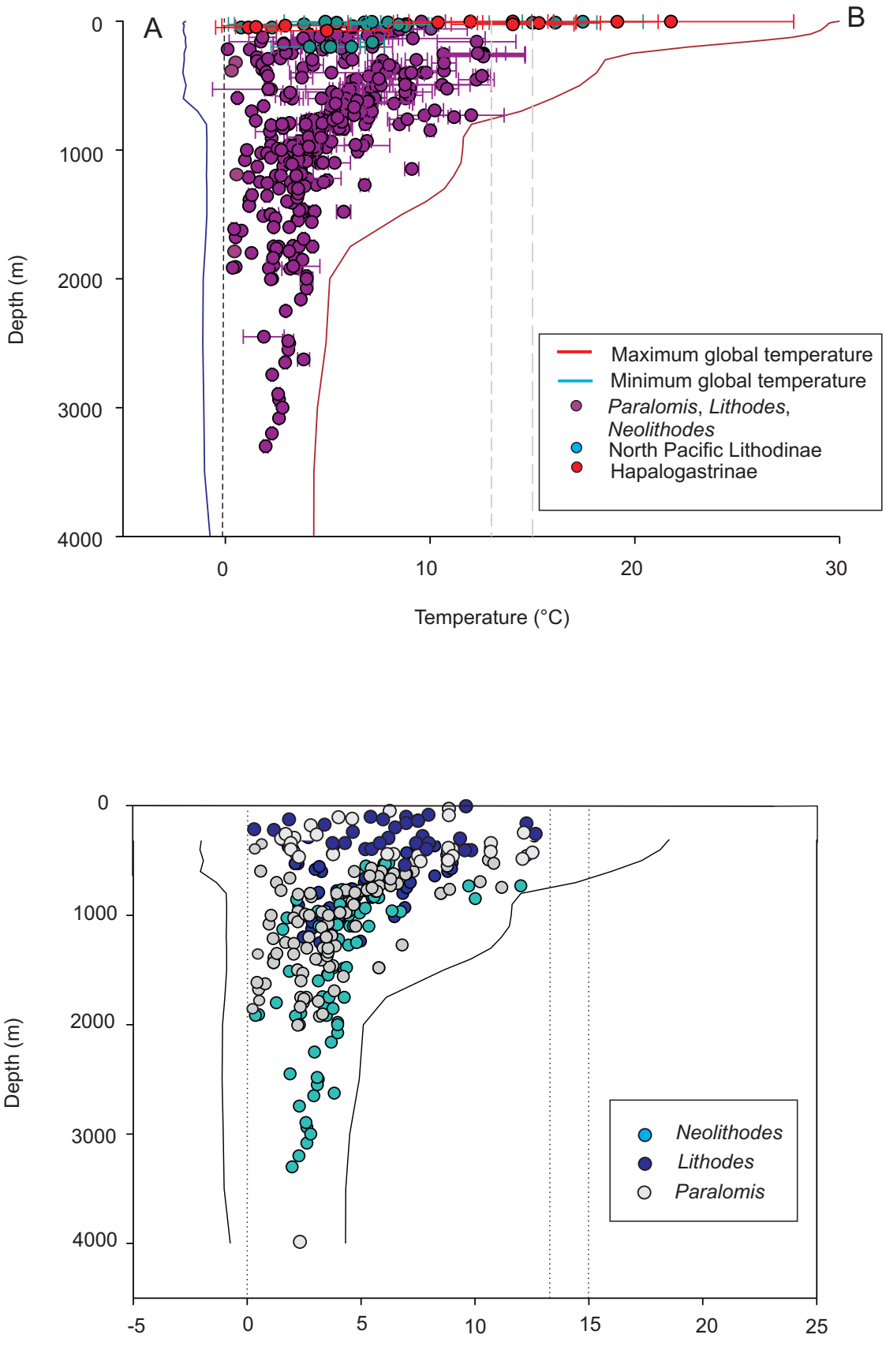

Figure C.4

i: The effect of temperature on the depth distribution of the two subfamilies of Lithodidae.

ii: The relationship between temperature and depth for genera of 'deep-sea' Lithodinae.

Dashed lines at 0, 13 and 15 degrees indicate possible temperature thresholds as determined experimentally for lithodid larvae.

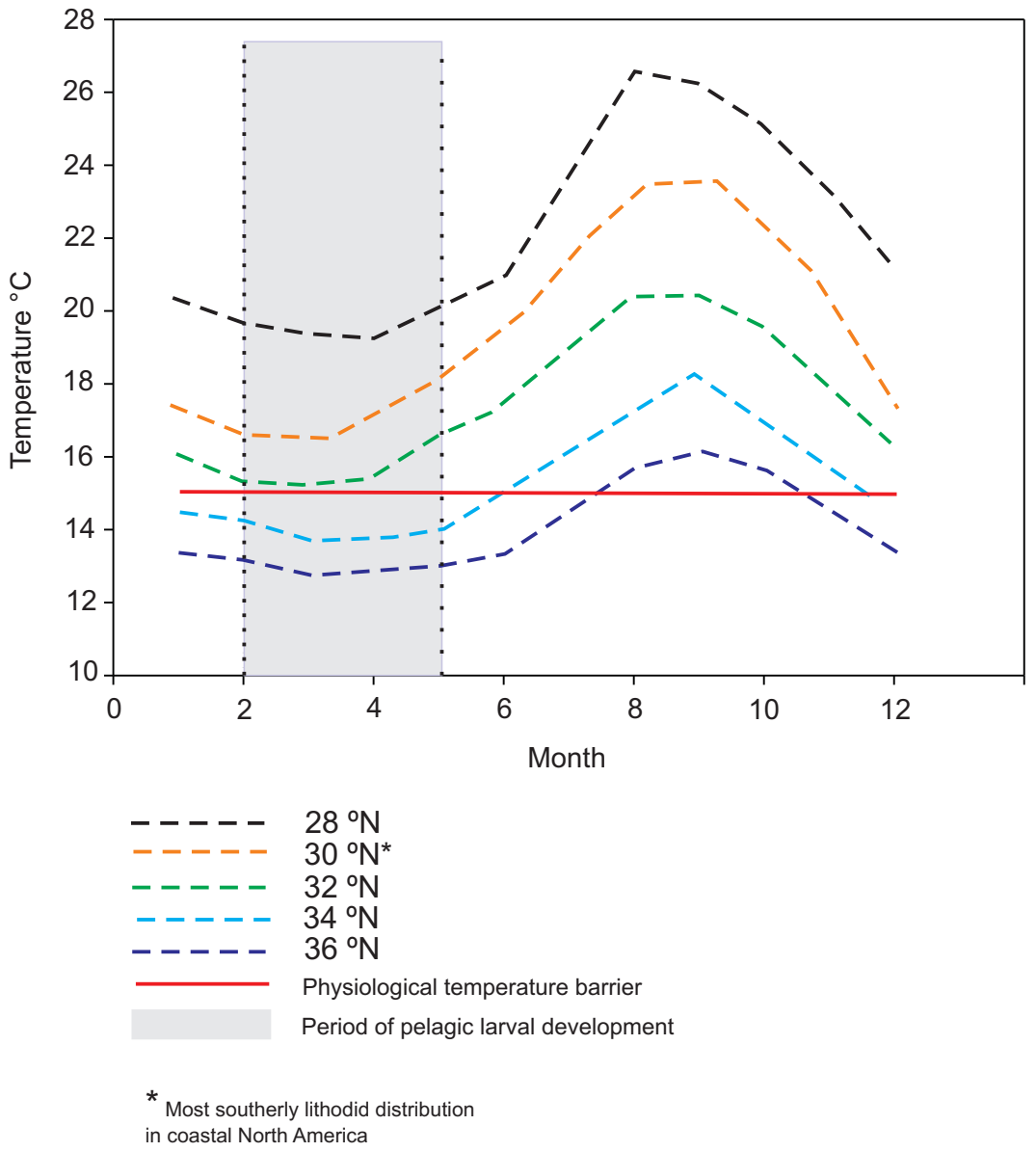

Figure C.5 Subtidal temperatures along the coast of California. For each month from 1992 –2002, the average temperature in the subtidal range (5–15 m) was recorded for latitudes 26, 30, 32, 34 and 36°N (NOAA-ESRL). A projection at a temperature of 15.5°C indicates the maximum, empirically predicted, larval survival threshold. Shading blocks out the months February to May, which represent an estimate of the period during which lithodid larvae would hatch and develop to the megalopal stage at 9°C (from Crain & McLaughlin, 2000; Zaklan 2002b). This period may be shorter at the elevated temperatures considered here.

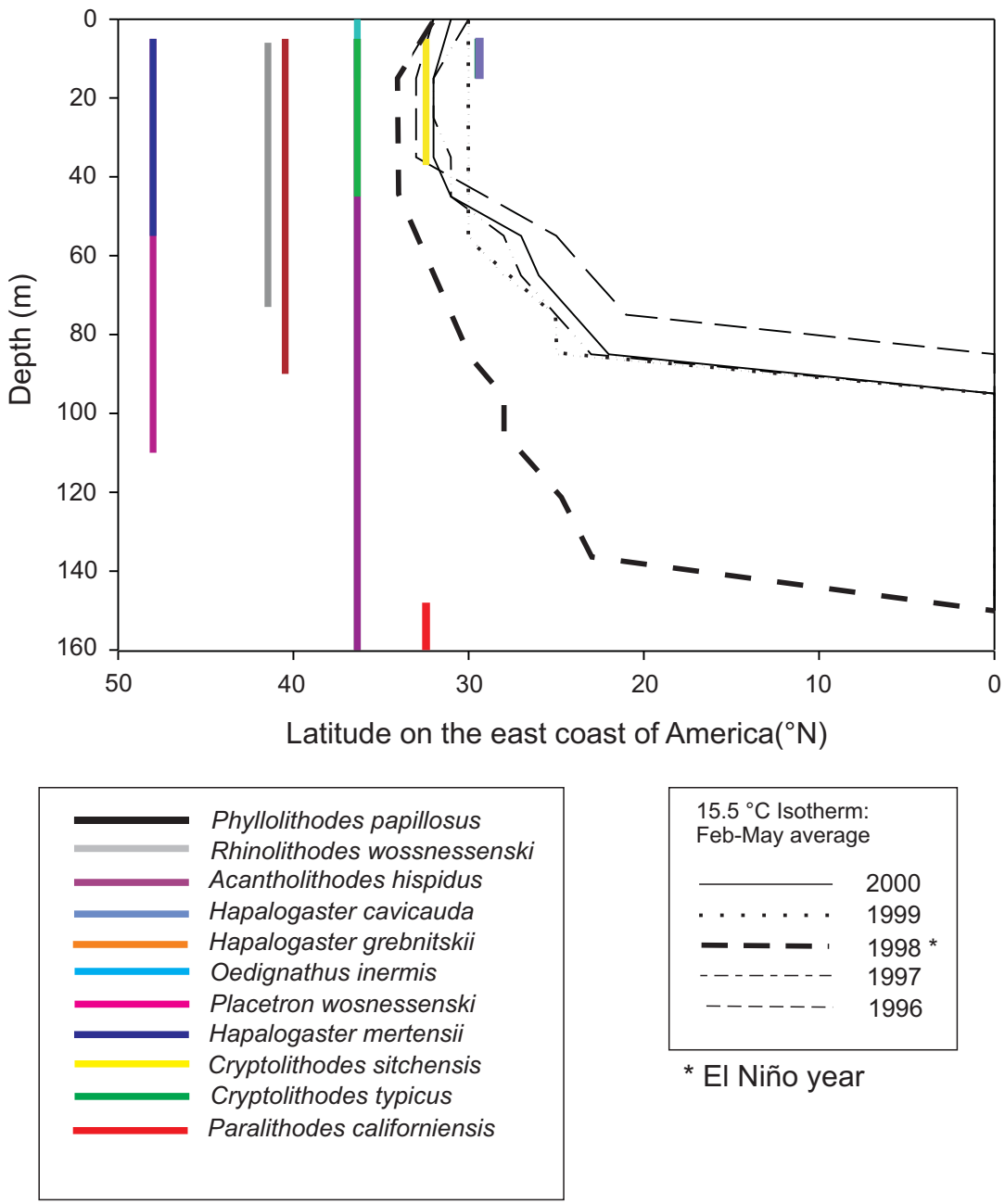

Figure C.6 The most southerly records of subtidal Lithodidae on the North American Pacific coastline in relation to the spring 15.5°C isotherm. Dashed line-plots represent the location, to the nearest 0.5° latitude, of the 15.5°C isotherm (NOAA-ESRL) between February and May within 100 km of the west coast of North America. One plot per year from 1996 to 2000 is displayed. In addition, the location of the most southerly sample sites and depth ranges of species (Table 1) along the west coast of North America are indicated with coloured blocks. Please note that some of these overlap on the diagram.

C.3.3 Antarctic and Subantarctic distribution of 'Group 3 Lithodinae'

At the lower end of the temperature scale, it has been reported that members of the subfamily Lithodinae inhabit some of the relatively warmer waters around Antarctica (Klages et al 1995, Arana & Retamal 1999, Garcia-Raso et al 2004, Thatje et al 2008). No lithodids are found at water temperatures colder than 0.5 °C (Fig **C.7**), and median temperatures for lithodids in Antarctic/sub-Antarctic waters are between 1 and 4 °C.

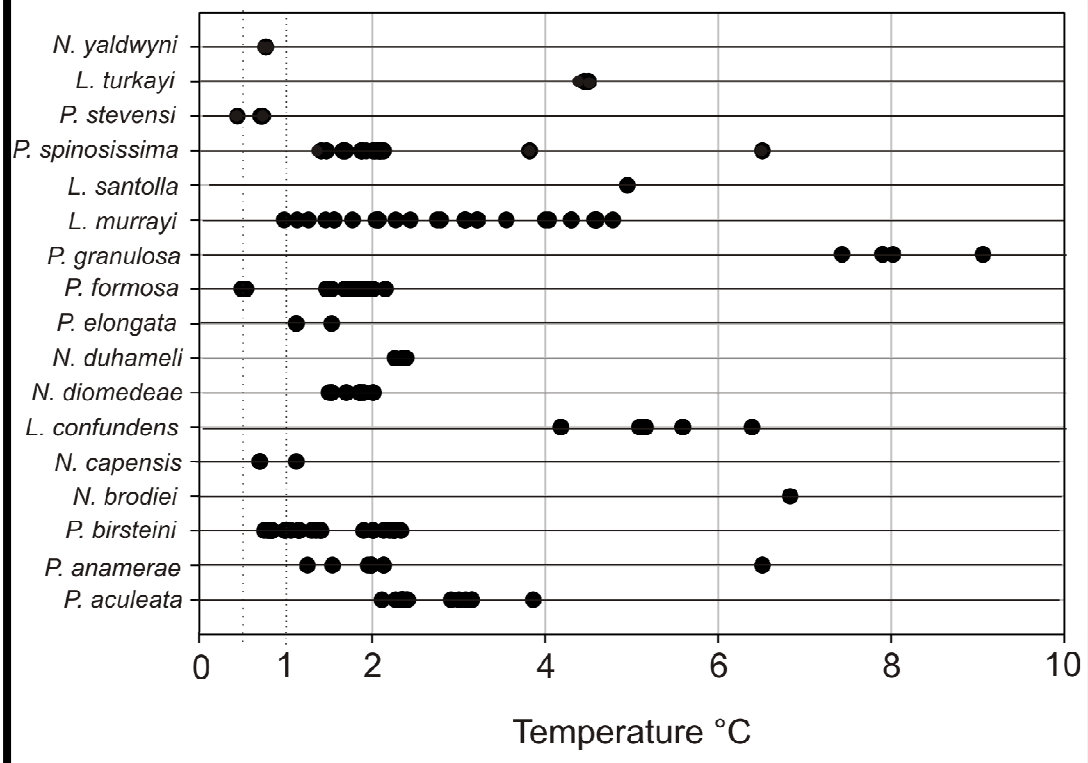

Figure C.7 Temperature at sample location for species of Lithodinae south of the sub-Antarctic front (approx 45 °S, excluding Patagonia). Temperature data obtained either at the time of capture or from the <*Southern Ocean Atlas*> (Olbers et al 1992). A dashed line at 0.5 °C represents the coldest waters in which lithodids have been found in this region.

45-60 °S

13 species of lithodids are found between 45 and 60 °S (*Paralomis aculeata, P. anamerae, P. birsteini, P. elongata, P. formosa*, *P. granulosa, P. spinosissima, Lithodes confundens, L. murrayi, L. santolla, L. turkayi, Neolithodes diomedae, N. duhameli, N. capensis*). *P. spinosissima*, *P. formosa* and *P. anamerae* have overlapping distributions, and high concentrations of these species have been found around South Georgia (Fig **C.8**ii). Exploratory fisheries (63-643 m) in the area have shown that *P. spinosissima* is encountered regularly in waters between 200-800 m around Shag Rocks

and South Georgia (López Abellán & Balguerías 1993, Purves et al 2003); however, *P. formosa* was not found often within that range (600-1600 m: Purves et al 2003) and adults tolerate temperatures at least between 0.5 and 2.1 °C (Fig **C.7**). In the southern islands of the Scotia Arc (60 °S, 25-60 °W: 0.5 - -1°C, Fig **C.8**i), no populations of *Paralomis* have been identified above 500 m, despite a significant sampling effort (López Abellán & Balguerías 1993). *P. aculeata* was described at 600 m off the Prince Edward Islands (45 °S), and is known also from the Crozet Islands in the southern Indian Ocean (46 °S, Miquel et al 1985). It has a wide bathymetric range, approximately 150 to 1500 m, and a recorded temperature range from 1 to 2 °C (Figs **C.7**, **C.8**). Between 25 °W and 30 °E, no records of any lithodids exist with the exception of *P. elongata* at 300 m close to Bouvet Island (54 °S, 2°E; 0.5-3 °C, Fig **C.8**iii). This gap in distribution coincides with a plunge in water temperatures in the mid-Atlantic at 55 °S in comparison to the South American continental slope (1.5-0°C, Fig **C.8**iii); bottom temperatures in this void are not far outside the normal range for several species of lithodid (e.g. *Neolithodes yaldwyni*, *P. stevensi*, *P. formosa,* Fig **C.7**).

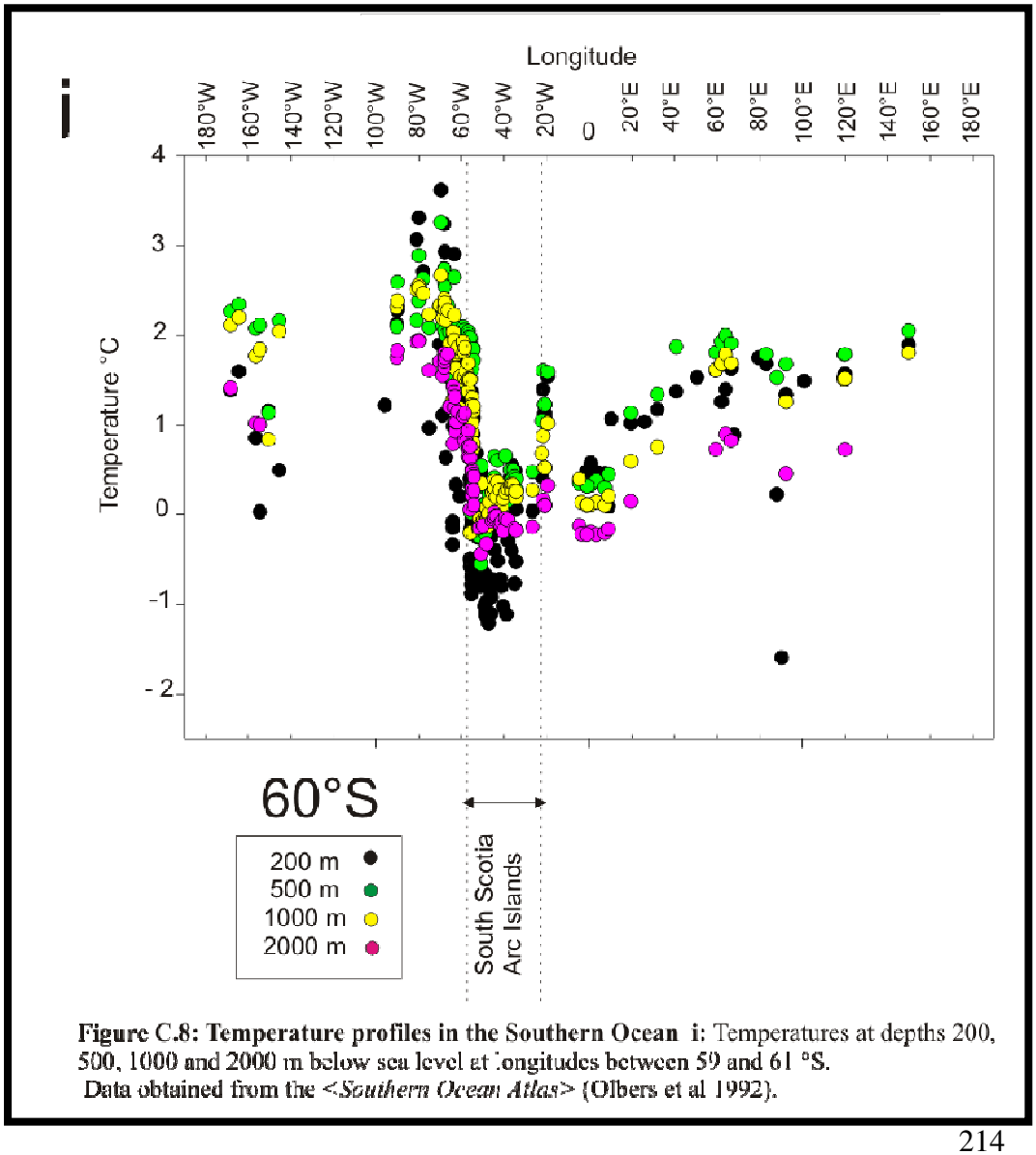

Figure C.8: Temperature profiles in the Southern Ocean i: Temperatures at depths 200, 500, 1000 and 2000 m below sea level at longitudes between 59 and 61 °S. Data obtained from the <*Southern Ocean Atlas*> (Olbers et al 1992).

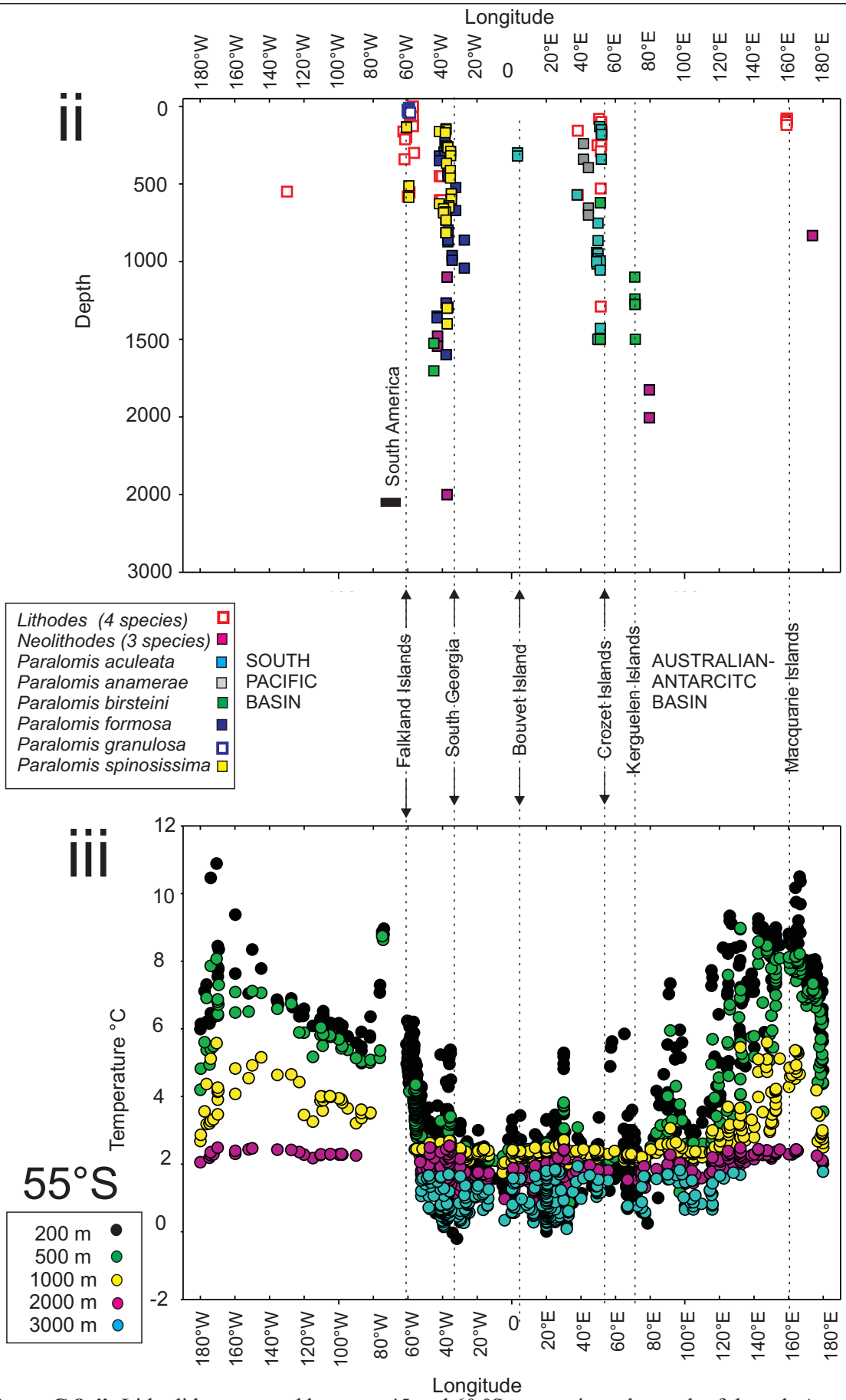

Figure C.8. **ii:** Lithodidae captured between 45 and 60 °S, approximately south of the sub-Antarctic front and north of the Antarctic divergence. Represented by depth and longitude. To increase graphical clarity, species *Lithodes murrayi, L. santolla, L. confundens* and *L. turkayi* are pooled; as are species *Neolithodes diomedae* (50-30 °W) , *N. duhameli* (60-80 °E) and *N. brodiei* (170 °E). *Paralomis elongata* (3 °E) and *P. aculeata* (30-60 °E) were shown to be more or less equivalent in molecular studies (Chapter 1). **iii:** Temperatures at depths 200, 500, 1000, 2000 and 3000 m below sea level at longitudes between 54 and 56 °S. Data obtained from the <*Southern Ocean Atlas*> (Olbers et al 1992)

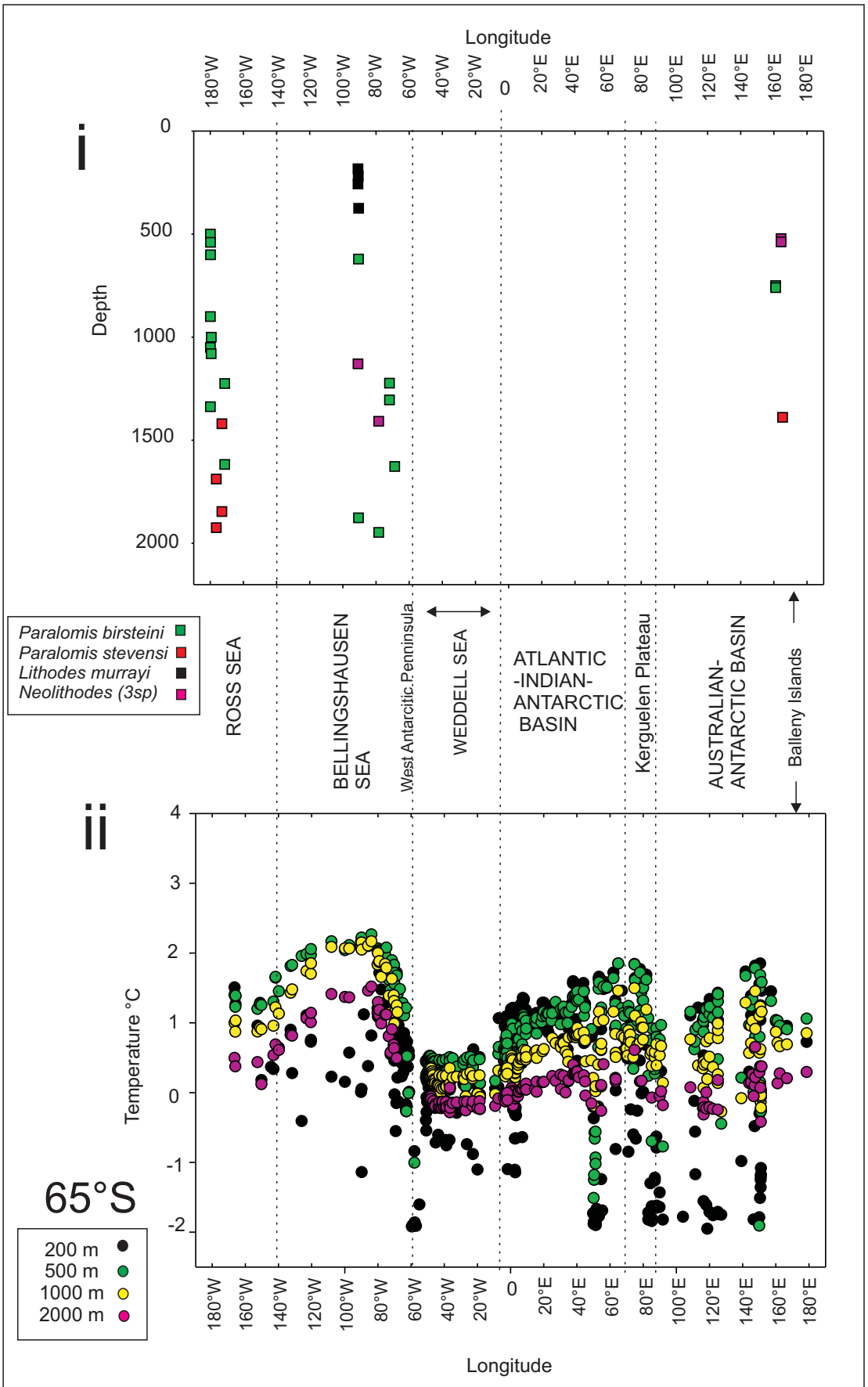

Figure C.9
i: Lithodidae captured south of 60 °S, approximately south of the Antarctic circumpolar current. Most southerly records were north of 70 °S. Represented by depth and longitude. *Neolithodes* species are *N. yaldwyni* (160 °E), *N. capensis* and *N. diomedae* (60-100 °W).
ii: Temperatures at depths 200, 500, 1000 and 2000 m below sea level at longitudes between 64 and 66 °S. Data obtained from the <*Southern Ocean Atlas*> (Olbers et al 1992).

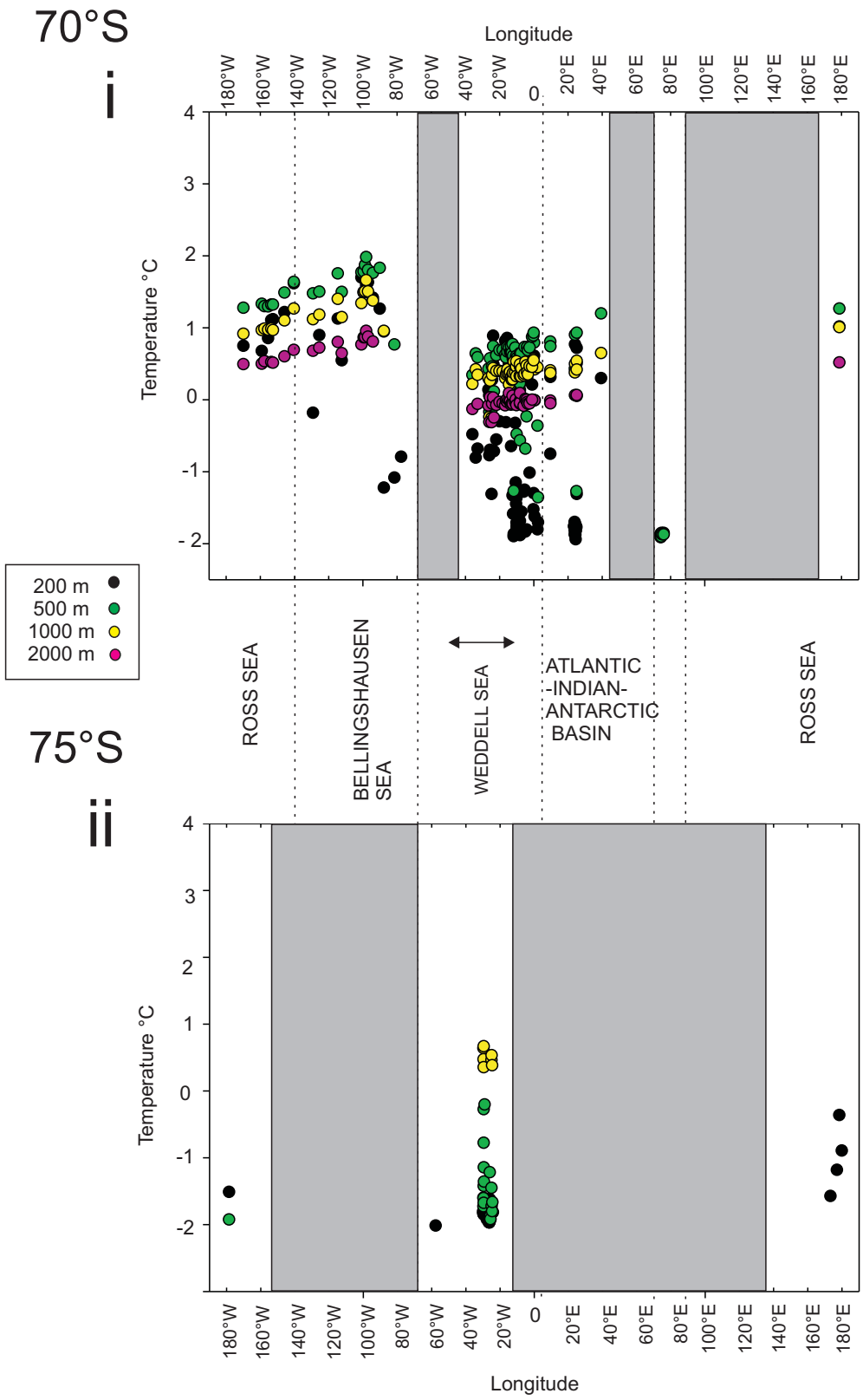

Figure C.10 i: Temperatures at depths 200, 500, 1000 and 2000 m below sea level at longitudes between 69 and 71 °S. Data obtained from the <*Southern Ocean Atlas*> (Olbers et al 1992). **ii:** Temperatures at depths 200, 500 and 1000 m below sea level at longitudes between 73 and 76 °S. Data obtained from the <*Southern Ocean Atlas*> (Olbers et al 1992). Grey blocks represent landmass above sea-level.

60+ °S

Within high Antarctic waters above 60 °S, lithodid diversity declines substantially to include species *Paralomis birsteini, P. stevensi, Lithodes murrayi*, *Neolithodes diomedae, Neolithodes yaldwyni* (Fig **C.9**). At 65 °S, temperature dips substantially below zero in the Weddell Sea and in the Australian-Antarctic basin (Fig **C.9**). The areas between 60-70 °S in which lithodids are found are those with particular peaks in temperature (0.5-2.5 °C, Figs **C.9-10**), such as the Bellingshausen Sea and Ross Sea (north of 70 °S). Lithodids are present on the continental slope of the West Antarctic Penninsula but not on the continental shelf, where temperatures are around 1 °C (60 °W, Fig **C.9**). No lithodids have been found below 70 °S and they are absent at all latitudes from the Weddell Sea. The Southern Ocean below 70 °S is not a continuous body of water, and is divided by the continent into a Weddell Sea section (-2 to 1 °C), and a Ross Sea section (0.5 to 1.5 °C). Below 75 °S, both the Weddell Sea and the Ross Sea (continental shelf) are colder than 0.5 °C (Fig **C.10**).

C.4 Discussion

The molecular phylogeny (Fig **C.2**, Section **AO**) indicates that the lithodid ancestors were shallow/subtidal animals in the North Pacific with planktotrophic larvae. This substantiates the hypothesis (Bouvier 1896, Makarov 1938) that a movement from the North Pacific to the global deep sea and the associated transition to a lecithotrophic larval feeding mode was important in lithodid evolutionary history.

Protracted larval hatching (Section **O**.5) and a cold-tolerant physiology are shared by all Lithodidae. These features are likely to be the result of a common adaptive history in a cold and unpredictable environment. From such a common ancestor, the subfamilies Hapalogastrinae and Lithodinae progressed along diverging evolutionary pathways.

C.4.1 Subtidal groups

The Hapalogastrinae inhabit a wide range of shallow water environments. The results here indicate that adult Hapalogastrinae tolerate higher temperatures than do the adults of the Lithodinae. Despite the wider range of temperature tolerance, the Hapalogastrinae and some genera of the Lithodinae are restricted to the North Pacific. Data presented here show that non-migratory adults are tied to areas where seasonal temperature drops (or rises) to a level optimal for larval survival (at least during the months of hatching and larval development; Crain & McLaughlin 2000, Zaklan 2002, shaded area, Fig **C.5**).

It is conceivable that the North Pacific Hapalogastrinae were once more widespread and were subject to a subsequent range-restriction. However, the lack of present or fossil

populations of Hapalogastrinae in the Atlantic suggests that they did not pass through the Arctic Ocean, or through the Panama seaway before it closed 3.5–13 Ma BP (Schneider & Schmittner 2006, Section **O.**3.3). In this case, distribution-limiting barriers (geographical or physiological) must have isolated the North Pacific population since the divergence of the family. Dates for the divergence of lithodids from their most recent ancestors suggest that North Pacific populations have existed for 13–25 Myr (Cunningham et al 1992). The only fossil evidence is from a deep-sea lithodid of the genus *Paralomis*, 10 Ma BP in New Zealand (Feldmann 1998). Without substantial fossil evidence or updated molecular clock estimates (McLaughlin et al 2007), it is difficult to speculate further, but this study may eventually help to impose some limiting dates on the timescale of divergence in this family.

C.4.2 Vertically migrating North Pacific Lithodinae

The lithodine genus *Paralithodes* is known experimentally to have increased larval mortality above 15°C (Kurata 1960, Shirley & Shirley 1989). Unlike the small Hapalogastrinae, which have uncalcified abdomens and a range tied to protective kelp forests or rocks (Zaklan 2002a), *Paralithodes* species are anatomically capable of migrating very large distances (Jørgensen et al 2005). Their sampled range (Table C1) indicates that they are able to survive in waters deep enough to avoid seasonally-influenced temperature fluctuations, but their planktotrophic larval phase (of at least *P. camtschatica, P. brevipes* and *P. platypus*) links them to surface waters. In these circumstances, range expansion south of the spring 15°C isotherm (Fig **C.6**) would not be possible (Somerton 1985).

C.4.3 Submergence

Each of the three deep-sea genera (*Lithodes*, *Neolithodes*, and *Paralomis* + *Glyptolithodes*) had distinct distributional characteristics (Fig **C.4**ii), and the molecular phylogeny (Fig **C.2**) suggested that at least two deep-sea radiations were independent.

Several advantages may be associated with an increase in habitat depth, including a lowered metabolic energy consumption and an increase in environmental stability – especially in areas where surface waters are affected by seasonal fresh water influx (Shirley & Shirley 1989).

In the deeper regions of the sea, there is increased difficulty in coordinating spawning with favourable surface temperature, as the cues are more remote (Stevens 2006). A (at least) facultative lecithotrophic larval mode of development allows some independence from seasonal variations in primary productivity. Experimentally determined lecithotrophy is known from zoeal stages of the genera *Lithodes* and *Paralomis* (Anger

1996, Shirley & Zhou 1997, Kattner et al 2003, Calcagno et al 2003, 2005, Watts et al 2006, Thatje & Mestre 2010) in geographically disparate species. This higher maternal investment might have become a feature of deep-sea lithodids because of the mismatch between prolonged embryo/larval developmental times at low temperatures and unpredictable pulses of primary production coming from the surface (Shirley & Zhou 1997, Thatje et al 2005, Morley et al 2006).

C.4.4 Emergence

Polar emergence (actually, subAntarctic emergence 40-50 °S) is a trend within species of both *Paralomis* and *Lithodes* genera (Fig **C.3**). There is no such trend in the genus *Neolithodes*, possibly because of its abyssal specializations. In Patagonia, where members of the deep-sea genera of Lithodinae have emerged into a subtidal or intertidal environment (Lovrich et al 2002), they retain full and apparently obligatory lecithotrophy in all larval stages (Kattner et al 2003, Saborowski et al 2006). Adults of these groups (*P. granulosa, Lithodes santolla, L. confundens,* Fig **C.4**) seem to have lower maximum temperature tolerances (12-13 °C) than do confamilial North Pacific genera; this may be a retention of adaptations to the cold-stenothermal environment of the deep-sea. The possibility of a transition from larval lecithotrophy back to planktotrophy is doubted by larval ecologists and physiologists (Strathman 1978). If this viewpoint is accepted, then the observation of lecithotrophy in *Paralomis granulosa* and *Lithodes santolla* represents further support for a deep-sea emergence pattern in the Southern Hemisphere, and furthermore refutes the possibility of North Pacific populations originating in the deep sea.

C.4.5 Lower temperature limits in the deep-water Lithodinae

Temperatures in the Southern Ocean are low, but stable; seasonal temperatures only fluctuate by a few degrees Celsius (Foster 1984). Diversity of lithodids in the region 45-60 °S is higher than 60-70 °S, and species *Neolithodes yaldwyni* and *Paralomis stevensi* are both endemic to waters south of 60 °S. This indicates that some adaptations to very low temperatures are present in lithodids living at the lowest end of the family's temperature range.

A limit to the southern distribution of the Lithodidae coincides with regions where water temperature is colder than 0.5 °C (Fig **C.7**): at locations including the Weddell Sea (Fig **C.9**-**10**); waters shallower than 500 m on the southern Scotia arc islands (Fig **C.8**i); and on the Antarctic continental shelf (from 70 °S) in all longitudes (Fig **C.10**). Temperature inversion in the surface waters of the Southern Ocean mean that often the shallower waters are colder than the surrounding deeper waters (Figs **C.8**-**10**, Section

O.3). Close to the Antarctic continent, particularly in the Weddell Sea, extremely dense, cold Antarctic Bottom water (AABW) sinks from the surface to the deep sea. This makes the water of the Weddell Sea and south-east Scotia Ridge (Figs **C.9**-**10**) particularly cold and is a possible reason for the exclusion of the Lithodidae from these regions.

The correlation between lithodid distribution and temperatures greater than 0.5 °C is not perfect. At 55 °S in the mid-Atlantic (25-30 °S, Fig **C.8**iii), water temperatures are between 0 and 1.5 °C; similarly at 70 °S in the Ross Sea, temperatures are greater than 0.5 °C (Fig **C.10**i); and the continental shelf of the WAP has temperatures only slightly lower than the continental slope, where lithodids are present (1-1.5°C, Fig **C.10**) (Thatje et al 2008). Several reasons could be proposed to explain this:

- It is possible that those species present at temperatures lower than 1 °C (Fig **C.7**) might have lower (colder) temperature thresholds than congeneric species from lower latitudes
- Adult specimens found in the very coldest water temperatures might be migrant rather than reproductive populations – adults may tolerate temperatures lower than do larvae or juveniles, so reproductive populations can not establish at the frontier of the lithodid range.
- Warming of the polar oceans might be gradually opening up new habitats to the Southern Ocean lithodids (Aronson et al 2007), and these data could be evidence of a range-expansion in progress.

Thirteen specimens of *P. birsteini*, including juveniles, were video recorded between 1123 m and 1394 m water depths on the Antarctic continental slope/rise in the Bellingshausen Sea (Thatje et al. 2008) and an individual from this population was sampled by ROV for the present study (*P. birsteini*_SA101, Section **A1**). This, as well as the presence of ovigerous females of *P. stevensi*, and *P. birsteini* (Ross Sea: Ahyong & Dawson 2006; Bellingshausen Sea: Arana & Retamal 1999) above 60 °S, indicates that reproductive populations of lithodids do in fact exist south of the Antarctic divergence.

C.4.6 Implications

The changing thermal structure of oceans may play an important role in patterns of lithodid biogeography. This could be an increasingly important phenomenon in consideration of climate change and oscillations in oceanic upwelling zones (Thatje et al 2005). Species of the genera *Paralomis, Lithodes* and *Neolithodes* are among the few anomuran taxa found at high latitudes in the Southern Ocean and it seems likely

that a history of deep-sea adaptation, particularly of life history (Thiel et al 1996, Thatje 2004), has been associated with their successful colonization of Polar regions.

In the Antarctic particularly, lithodids in the Bellingshausen Sea have the potential to threaten the isolated shelf communities (Thatje et al 2005, Aronson et al 2007), which have evolved in the absence of crushing predators such as crabs, lobsters, sharks and rays that would be found in shelf ecosystems at lower latitudes (Dayton et al 1974, Feldmann & Tshudy 1989, Crame 1994, Arntz et al 1994, McClintock & Baker 1997). Here, where lithodids seem to be living at the lower boundary of their physiological threshold, even a slight increase in temperature might open up new habitats.

C.5 Conclusions

- Distributional traits, shared between paraphyletic members of the Lithodinae and the Hapalogastrinae, suggest an ancestral population of shallow-water anomurans in the North-East Pacific Ocean, which were cold-eurythermal.
- Some shallow-water populations of Lithodidae (those with no ancestral link to the deep sea) are tied to waters north of 30°N because of the restricted thermal tolerance of larval stages.
- At least two lineages from within the subfamily Lithodinae (Fig **C.2**) have an expanded bathymetric range and widespread distribution. These groups are limited to greater depths, except at high latitudes, and have narrower adult temperature tolerance as an adaptation to the cold stenothermal deep sea.
- Lithodids of the subfamily Lithodinae are living at the frontier of their lower temperature threshold in the Southern Ocean. They have the potential to expand into previously uninhabitable regions of polar seas if water temperatures continue to increase, with potentially devastating effects for the Antarctic shelf fauna.

Table C1 Table of distributional data for species belonging to genera of Lithodidae endemic to the North Pacific Ocean. These data were obtained predominantly from Zaklan (2002b) and the collections of the United States National Museum of Natural History (USNM).

Species	**Most southerly range extent along west coast America**	**Depth Range (metres)**	**Hatching Period**
Subfamily Lithodinae			
Phyllolithodes papillosus	Monterey, CA 36.35°N	0-183	March – May
Rhinolithodes wosnessenskii	Crescent city, CA 41.45°N	6-73	March
Sculptolithodes derjugini	N/A	20-35	
Cryptolithodes expansus	British Columbia	50-60	
Cryptolithodes sitchensis	San Diego, CA 32.43°N	0-37	
Cryptolithodes typicus	Monterey, CA 36.35°N	0-45	March – April
Paralithodes brevipes	N/A	0-66	March – April
Paralithodes camtschatica	N/A	5-200	February-May
Subfamily Hapalogastrinae			
Acantholithodes hispidus	Monterey, CA 36.35°N	0-245	
Dermaturus mandtii	N/A	0-72	
Hapalogaster cavicauda	Isla San Jeronimo, Mexico 29.47°N	0-15	
Hapalogaster dentata	N/A	0-180	February – March
Hapalogaster grebnitzkii	Humboldt bay, CA 40.46°N	0-90	
Hapalogaster mertensii	Puget Sound, WA 48°N	0-55	February – March
Oedignathus inermis	Pacific Grove, CA 36.35°N	0-15	February – March
Placetron wosnessenskii	Puget Sound, WA 48°N	0-110	March

Section D. SYNTHESIS

D.1 Comparison of main aims and conclusions

At the beginning of this thesis, I set out three aims by which to examine the origins, environmental adaptations and distributional limits of the deep-sea Lithodinae. In this section, I will revisit those original aims and discuss how the results of the research chapters have addressed them.

Aim 1: Investigate the origins of the deep-sea Lithodinae within the family Lithodidae, including the monophyly and interrelationships of the major deep-sea genera; specifically to look at the minimum number of interchanges between the deep and shallow seas.

Conclusions

- Lithodid ancestors are likely to have had a North Pacific, shallow water distribution and planktotrophic larvae; however, the soft-bodied abodomen of the Hapalogastrinae might not be plesiomorphic for the Lithodidae.
- At least two monophyletic lineages from within the subfamily Lithodinae (*Paralomis* and *Lithodes* (+ *Neolithodes*)) have an expanded bathymetric range and widespread distribution. These groups are limited to greater depths, except at high latitudes, and have narrower adult temperature range (0.5–13°C) as an adaptation to the cold-stenothermal deep sea.
- The North Pacific genus *Paralithodes* is paraphyletic; those *Paralithodes* species with a more southerly distribution within the coastal North Pacific (*P. californiensis* and *P. rathbuni*) may represent a transitional state between ancestors close to *P. brevipes* and the genus *Lithodes*.
- There may be indications of lower than expected levels of mutation within the Lithodidae, and a thorough investigation of this phenomenon will be proposed for further work.

Aim 2

Aim 2: To elucidate phylogenetic relationships and indications of environmental adaptation within deep-sea lithodine genera *Paralomis* and *Lithodes*.

Conclusions

- Clades of *Lithodes* and *Paralomis* containing species from southern African, Indian Ocean, and south Pacific waters indicates the importance of large scale dispersals in a

west-east direction. This may be linked with west-east cold deep-water currents, which connect the south Atlantic with the other major oceans.

- Indian Ocean and Pacific forms – *L. murrayi, L. longispina* and *L. nintokuae* form a group separated from Atlantic species such as *L. santolla*, *L. confundens, L. maja* and *L. ferox*.
- Ancestors of Atlantic species *L. maja* and *L. santolla* were amongst the earliest to leave the ancestral region of the North Pacific. It is unclear whether these movements were linked, or whether they were independent.
- Meridional links between the north and south-east of the Pacific Ocean are evident in two lineages of *Paralomis*.
- The shallow-water species *Paralomis granulosa* bears some (perhaps convergent) similarity to *Lopholithodes* in the morphometry of its walking legs and some aspects of discrete morphology. When central Pacific species are included in the taxon set, these cluster close to the base of the *Paralomis* lineage.
- In *Paralomis*, particularly, dramatic changes in tubercle form can occur over a succession of moults indicating differential adaptation of different life stages to their environment.

Aim 3: Comparison of geographical and physiological boundaries with the present distribution of the deep-sea Lithodidne and the species that have secondarily emerged into shallow waters.

Conclusions

- Some shallow-water populations of Lithodidae (those with no ancestral link to the deep sea) are tied to waters north of 30°N, because of the restricted thermal tolerance of larval stages.
- Lithodids of the subfamily Lithodinae are living at the frontier of their lower temperature threshold in the Southern Ocean. They are currently excluded from some regions with low water temperature, but they have the potential to expand into previously uninhabitable regions of polar seas if water temperatures continue to increase. This could have potentially devastating effects on the Antarctic shelf fauna.

D.2 Origins

The origin of large deep-sea Lithodinae from within shallow-water ancestral populations in the North Pacific is incredible given the ecology and morphology of extant species. The timescale

and mechanism by which the very diverse subfamilies Hapalogastrinae and Lithodinae evolved has incited much debate in the past 150 years (Bouvier 1895, Cunningham et al 1992, Richter & Scholtz 1994, McLaughlin et al 2007). Evidence presented in this thesis is consistent with a North Pacific, shallow-water ancestry for deep-sea lineages of the Lithodinae, but it does not resolve the arguments about the position of the family within the Anomura based on morphology. Ancestral features such as larval planktotrophy and cold-eurythermal shallow-water ecology are retained by the majority of lithodid genera, including all of the subfamily Hapalogastrinae.

The genus *Paralithodes* may retain transitional features, critical to the emigration taxa from the North Pacific. Of five out of six species of *Paralithodes* examined using phylogenetic methods, *P. brevipes*, *P. platypus* and *P. camtschatica* represent lineages that diverged early in the history of the subfamily Lithodinae (Fig **A1**.3). Like many others of the same rank (e.g. *Lopholithodes*, *Phyllolithodes*) *Paralithodes* remains endemic to the cold/temperate continental shelf of the North Pacific (Butler & Hart 1962). A switch in reproductive strategy (as approximated by egg size) appears to have taken place between species of the North Pacific genus *Paralithodes* (Fig D.1). A binary mode of reproduction observed in the Lithodidae (Fig D.1) probably represents two adaptive strategies which make trade-offs between fecundity and maternal energy investment into individual offspring (Thorson 1950, Mileikovsky 1971). Morphological examination and systematics linked *P. californiensis* and *P. rathbuni* with the global deep-sea genus, *Lithodes* (Section **B2**; Figs **B2**.3, **B2**.10 **[Б, β]**). Where they are found on the coast of California, *Paralithodes californiensis* and *P. rathbuni* inhabit depths far below the 15.5 °C spring isotherm (34 °N, Fig C.6); maternal investment into lecithotrophic larval development may have broken the link between life-history cycles and seasonal primary production in the euphotic zone.

The focus of this thesis was to examine the conditions and constraints of the dispersal of lithodids from the north Pacific into the global deep ocean. Compared to other genera, *Paralomis*, *Lithodes* and *Neolithodes* have an expanded distribution, both in terms of bathymetry (0–3500 m, Fig C.4) and geographical range (Fig C.1). Each genus has a characteristic bathymetric range (Fig C.4), possibly indicating that they occupy different ecological niches (Gage & Tyler 1991).

- The *Lithodes* genus has the shallowest and smallest range and, in general, species within this genus are found at upper continental-slope depths (200–1000 m). Species-specific variations from this pattern exist, with some *Lithodes* species found at shelf depths in the NE and NW Atlantic as well as the large continental shelf east of Argentina (0–200 m, Lovrich et al 2002).

- Species of *Paralomis* are normally found at continental slope depths, between 200 and 2000 m. *Paralomis granulosa* is anomalous in its shallow-water distribution around Patagonia; and a single juvenile specimen of *P. microps* has been reported from abyssal depths of 4000 m in the Bay of Biscay (Macpherson 1988a).
- The genus *Neolithodes* has a depth range around 600 – 3500 m; containing the only species of Lithodidae that can be thought of as habitually abyssal (e.g. *Neolithodes grimaldii*, mid Atlantic ≈1000–3200 m). There is depth zonation of species within genera; however, the bathymetric range of species is often in excess of 1000 m (Appendix E).

Distributions of the globally occurring Lithodinae largely follow slope-depths on continental margins (Appendix E). Species with trans-oceanic or mid-ocean distributions are not unknown (particularly in the Pacific), but proposed dispersal events could more or less follow isobaths along island chains or along mid-oceanic ridges. Major oceans are connected at depths of around 2000 m by relatively homogenous environments; below depths of 4000 m, the oceans are divided into discrete basins (Allen & Sanders 1996). Deeper seas are somewhat insulated from fluctuations in physical conditions such as temperature and salinity. All of the globally distributed genera have an approximate in-situ temperature range from 0.5–12.5 °C; although temperatures are usually between 0 and 5 °C at depths below 1000 m (Locarnini et al 2006). Species are likely to have different 'preferred' temperature ranges within these limits (Fig C.5), although experimental evidence is limited to those shallow-water species that can be maintained in aquaria (Anger et al 2003).

D.3 Dispersal routes and timescale

The major challenge in the interpretation of phylogenetic data within the Lithodidae is that the timescale and chronology of events that led to modern distributions can only be very roughly estimated. Using a geologically calibrated molecular clock, Cunningham et al (1992) estimated that the divergence of the family Lithodidae is millions of years younger (13–25Ma BP) than the Paguridae, which are known from fossils in the Cretaceous (113 Ma BP). What that study actually estimated was time since the divergence of *Lithodes aequispina* and *Paralithodes camtschatica*, which was an event occurring close to the first deep-sea radiations of the extant *Lithodes* lineage (Fig **A1**.3). Deep-water decapods are under represented in paleontological studies (Feldmann 2003) and the only lithodid fossil record is *Paralomis debodeorum* Feldmann (1998) from the mid–late Miocene (10–15 Ma BP) in New Zealand. The age of the other anomuran families (Feldmann 1984) suggests that the Lithodidae may have been present in the North Pacific for a period prior to the worldwide radiation(s) of the extant taxa. A lithodid molecular clock was not produced in this study, both because no geological calibration

could be justified and because the low rates of molecular divergence observed within extant deep-sea genera warrants more detailed consideration (Section A.1, Table A2; Held 2001). The limited and preliminary evidence from fossil and molecular data indicate that deep-sea lithodine radiations are likely to have occurred predominantly during the Cenozoic era (0–65 Ma BP).
Within the paeleo-oceanological framework of the Cenozoic, common geographical pathways of global radiation were suggested for the lineages *Lithodes* and *Paralomis* using cladistic methods (Fig D.2). The Eocene to late Miocene spans a period of global cooling and significant shifts in ocean circulation, particularly affecting the bathymetric and latitudinal temperature gradient (Flower & Kennett 1994, Nikolaev et al 1998, Lear et al 2000, Von der Heydt & Dijkstra 2006). The gradual opening of deep circum-Antarctic pathways throughout the early Cenozoic had a significant impact on global oceanic circulation (Deacon 1937, Shackleton & Kennett 1974, Sykes et al 1998), and is implicated as an important pathway for inter-oceanic dispersal in southern *Lithodes* and *Paralomis* lineages (Figs D.2, **A1**.3 **[U]**, **B2**.10 **[Ж]**, **B3**.5 **[Ω]**). Specifically, a directional west-east pathway of dispersal from the Atlantic to the Pacific, through the southern Indian Ocean, is indicated in the genus *Lithodes* (Fig **B2**.10 **[Ж])** when systematic studies are rooted with North Pacific species *Paralithodes brevipes*. Directionality of dispersal can not be inferred from similar studies of *Paralomis*, but closely related sub-Antarctic species *P. anamerae, P. aculeata* and *P. elongata* (Fig **A1**.3 **[S], B3**.5 **[Σ]**) are distributed near to the pathway of west-east circum-Antarctic currents (Deacon 1984).

The nature of early faunal links between the Pacific and the Atlantic are not clear. In the *Lithodes* lineage, some of the most basal morphological alliances were indicated between North Atlantic *L. maja* and North Pacific *L. aequispina* (Fig **B2**.10). Around the Arctic Ocean, *Paralithodes* species are found in shallow waters of the Bering Sea and Barents Sea (c. 50 m) to 70 °N; although anthropogenic manipulation is responsible for this particular circum-Arctic distribution (Jørgensen et al 2005). Arctic-Pacific marine links did not exist between the end of the Cretaceous and the late Pliocene (65–3.5 Ma BP, Zenkevitch 1963, Dunton 1992), making an Arctic faunal link unlikely in the timeframe discussed here. Since the Pliocene, biogeographic links between the North Atlantic and Pacific are evident in molluscs (Marincovich et al 1990); however, there is no distributional evidence to indicate that lithodid dispersal through the Arctic routes would be possible in modern climatic conditions.

In the early Miocene (25–13 Ma BP), hydrological interchange between Atlantic and Pacific tropical oceans occurred through the deep Panamanian seaway. Depth-stratified water masses would have affected faunal transfer differently depending on habitat depth: at 3000 m, deep North Atlantic water is thought to have flowed into the Pacific; at 500 m, low salinity intermediate water passed from the Pacific into the Atlantic; and at the surface, warm, tropical

Atlantic water influenced the shallow Pacific coastline (Lunt et al 2008). High seasonal temperatures in shallow waters seem to limit the modern distribution of some Hapalogastrinae and Lithodinae to Pacific latitudes higher than 30 °N, because of temperature sensitive planktotrophic larval stages (Fig C.9). Even before the closure of tropical links between the Atlantic and Pacific (13–2.6 Ma BP, Haug & Tiedemann 1998), it may be that the warm Caribbean surface waters would have been an impediment to the range expansion of the shallow water Lithodidae. At the greater depths observed in the genera *Lithodes* and *Paralomis*, water was colder and transfer between the intermediate or deep Pacific and Atlantic may have occurred. Two lineages from within *Paralomis* (Fig **B3**.5 **[Δ] [II]**) show evidence of a tropical faunal link between the Pacific and Atlantic, although the directionality of this movement is not clear.

The most southerly point of confluence between the Atlantic and Pacific, Drake Passage, opened before 37 Ma BP (Lawver et al 1992, Crame 1999) and substantial tectonic activity proceeded to create a deep-water pathway c.28–32.5 Ma BP (Barker & Burrell 1977, Barker et al 1991). Historical links between west-coast South American and South Georgian (S. Atlantic) species are indicated for two separate lineages of *Paralomis* (Fig **B3**.5 **[Δ] [II]**). This fits partially with the pattern of biogeography within the extant southern Decapoda, where there is a link between fauna on the southern tip of the South American continent with the sub-Antarctic islands (such as South Georgia, Gorny 1999). Cold-water currents in the Cape Horn region may have an important role in facilitating such transport (Antezana 1999). At present, with the exception of three species inhabiting the marine waterways of Patagonia, there are no lithodid species with a distribution both west and east of Cape Horn (Appendix E). It is possible that the sampling record is patchy in this region and that the western range extent for South Atlantic species isn't yet known.

D.4 Dispersal and speciation mechanisms

Long-distance dispersal is implied by the close relationships of geographically disparate deep-water Lithodinae (Sections A1, B2, B3). Mechanisms of dispersal in the Lithodinae are adult migration and swimming or drifting in larval stages. As a result, characteristics of life history affect dispersal distances. Within the normal habitat range of species of the Lithodinae (a subset of 0-12°C: Fig C.4, C.5), temperature can have a substantial effect on the duration of larval development (Kurata 1960, Nakanishi 1985, Shirley et al 1990, Anger et al 2003, 2004). In *Lithodes maja,* development from larval hatching to megalopa takes around 49 days at 9 °C (Anger 1996); however, the duration of the larval stage more than doubles at temperatures

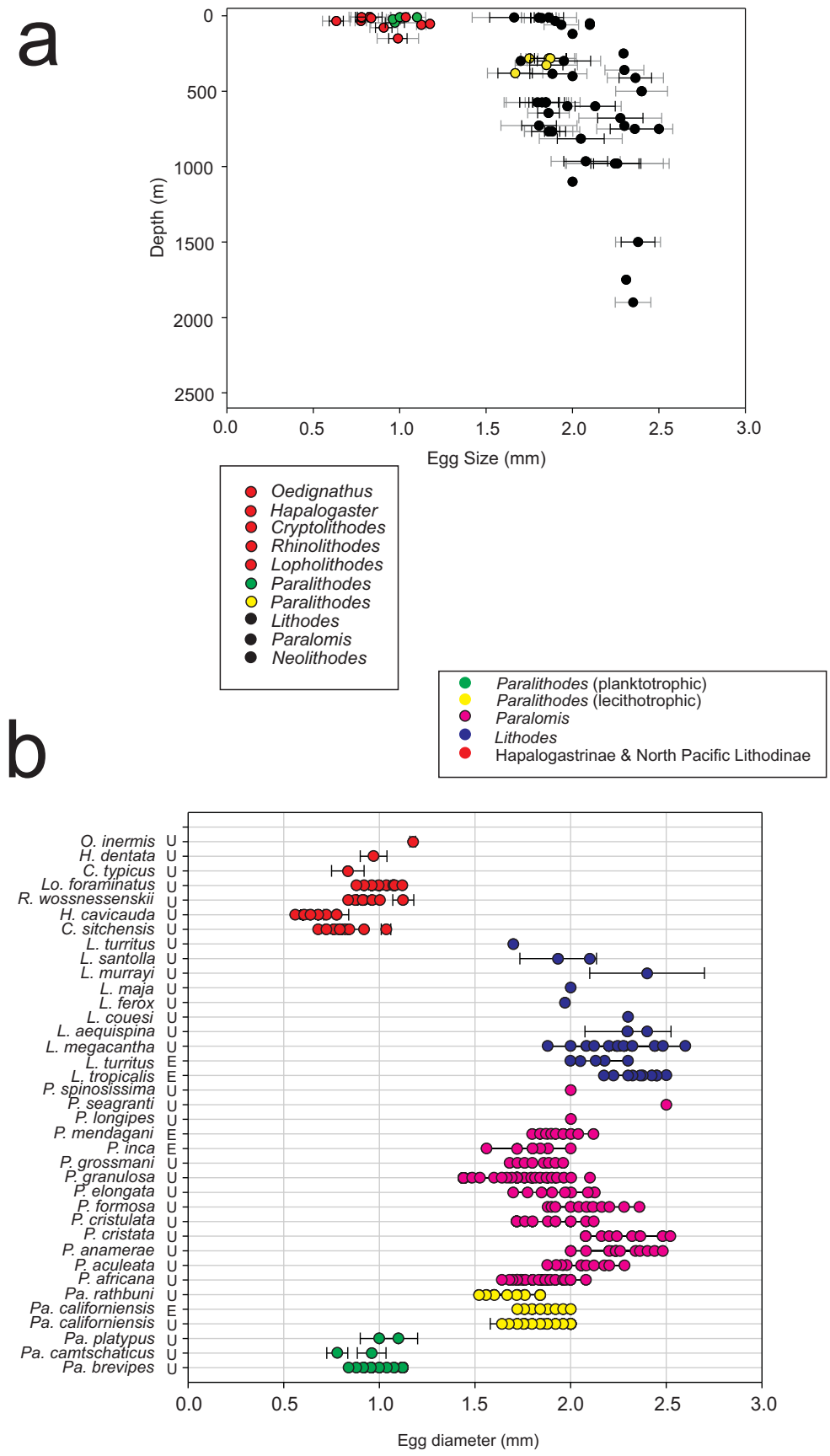

Figure D.1 Egg Size in the Lithodidae. Graphs show the variation in egg size with **a)** depth and **b)** lineage. Lecithotrophic larval development, as indicated by yolk volume, divides the genus *Paralithodes* into two groups. Pa = *Paralithodes*. U= uneyed embryonic stage, E= eyed embryos and a late developmental stage. In **a)**, points are the average of at least 30 eggs from a single ovigerous female.

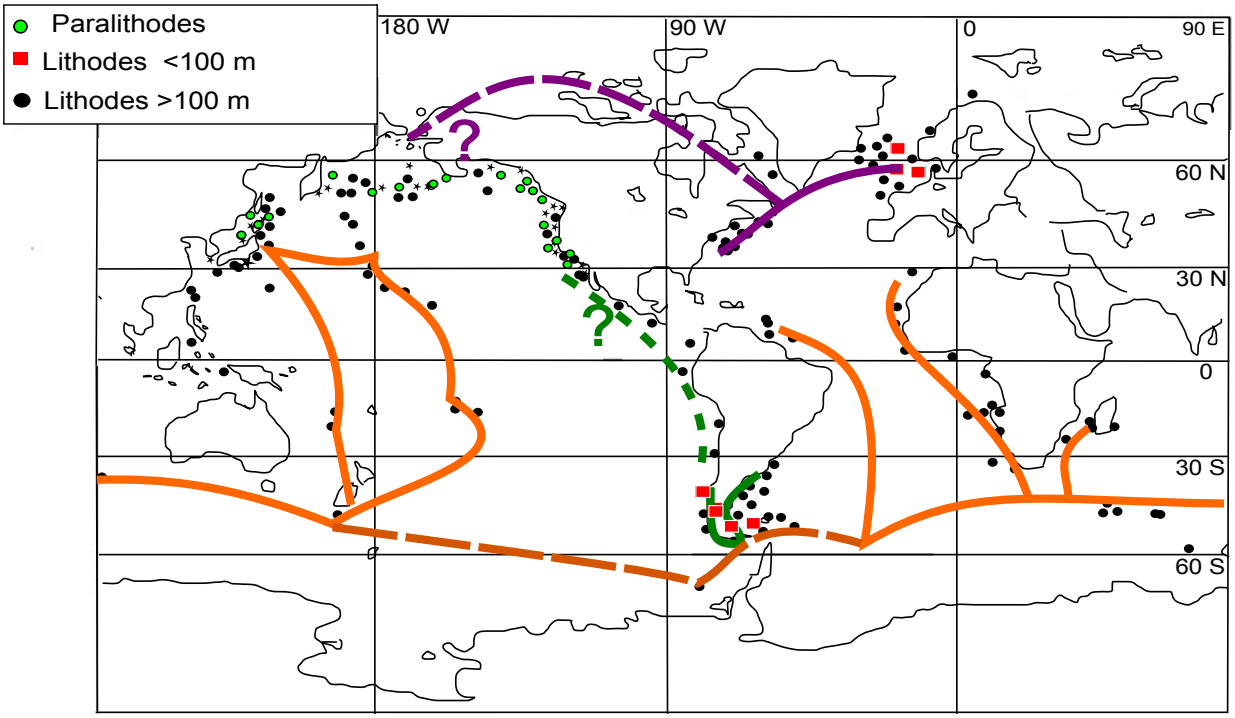

Figure D.2a Hypothesis of radiation during the Cenozoic (0-65 Ma BP) for the genus *Lithodes* Map represents roughly the position of the continents during the Eocene and Miocene. Distributional pathways are referred to in the text. Broken lines represent pathways only weakly implied by the data. Different colours represent different lineages. The main interpretation of the data is shown by the orange line, connecting *L. ferox*, *L. murrayi*, *L. mamillifer*, *L. longispina* and *L. richeri*, to the exclusion of the lineages represented by the purple (*L. maja*) and green (*L. santolla*) pathways.

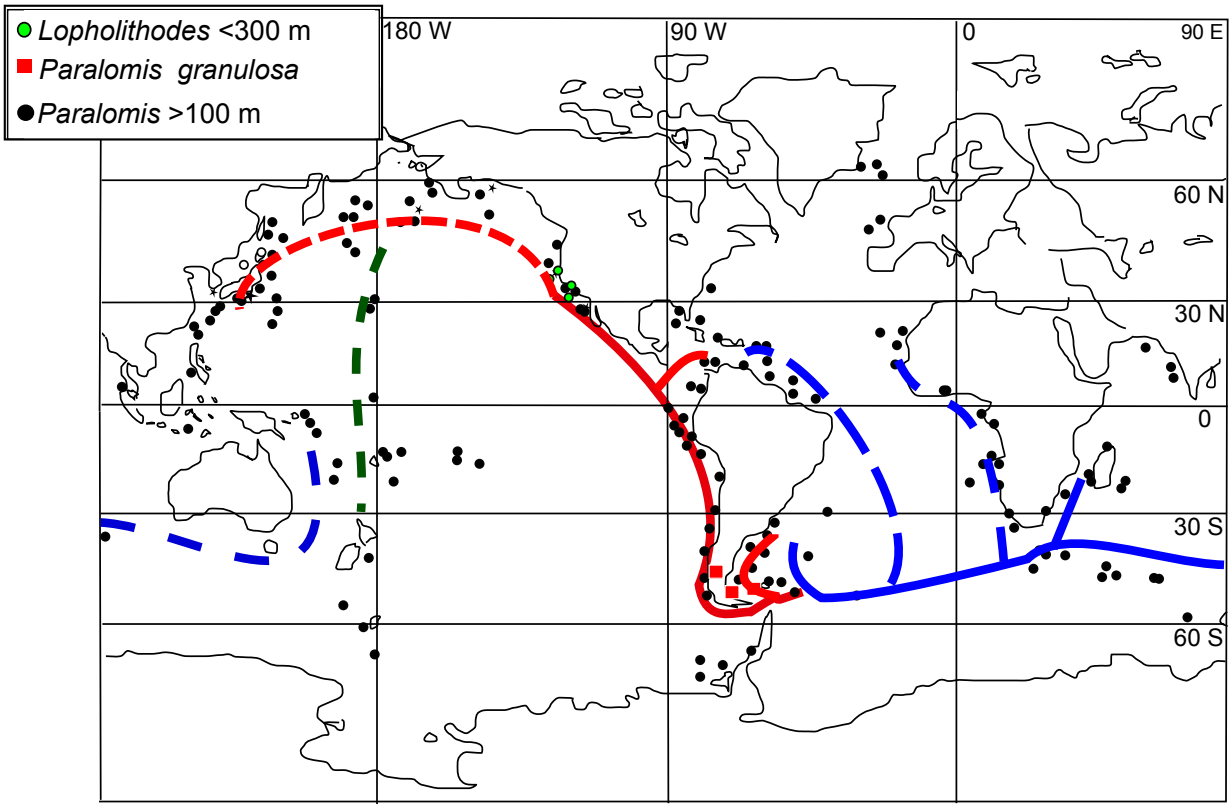

Figure D.2b Hypothesis of distributional pathways during the Cenozoic (0-65Ma BP) for the genus *Paralomis* Map represents the roughly the position of the continents during the Eocene and Miocene (50-20 Ma BP). Distributional pathways are referred to in the text. Broken lines represent pathways weakly implied by the data. Different colours represent different lineages, for example the blue pathway indicates the relationship between *P. aculeata*, *P. anamerae* and *P. elongata*, and their more distant relationship with *P. cubensis*, and *P. stella.* The red line shows the relationship between *Paralomis formosa, P. otsuae and P. verilli* as well as that of *P. spinosissima* and *P. multispina.*

typical of deep-sea and subpolar environments (0–5 °C Fig C.4, C.5, Kurata 1960, Watts et al 2006). Non-feeding zoeae of species including *Lithodes aequispina* (Jewett et al 1985, Shirley & Zhou 1997), *Lithodes maja*, *Lithodes santolla* and *Paralomis granulosa* (Vinuesa et al 1985, 1999) do not have active swimming behaviour in experimental conditions. Larvae of these species are not found in pelagic zooplankton samples and these stages are thought to have an epibenthic, demersally drifting habit (Lovrich 1999). Currents just above the sea floor in the deep ocean are typically a few cm/sec (Eckman & Thistle 1991); however, they can be persistent enough to provide a conduit for long-distance transport. A demersally drifting habit may not be as conducive to long-range dispersal as pelagic development; however, the protracted development times of cold-water lithodids mean that larval stages have a higher chance of being transported by epibenthic currents.

Adults of *Paralithodes camtschatica* have a body shape and long walking legs that are not dissimilar in proportion to many of the deep-water Lithodinae (Section **B2**). This relatively shallow-water species is known to migrate long distances as part of their reproductive cycle (13 km/day Jørgensen et al 2005). Migration is also observed in *Lithodes confundens*, which migrates from deeper water to the intertidal regions of Patagonia, despite having non-feeding larval stages (Lovrich et al 2002). A migratory habit is common amongst these genera of Lithodinae and it seems reasonable to extrapolate a long-distance adult dispersal potential for lesser known deep-sea species (Abelló & Macpherson 1991, Hoggarth 1993, Loher & Armstrong 2000, Pereladov & Miljutin 2002). Despite a tolerance of high pressure, there may be physiological or ecological reasons why lithodids are rarely, if ever, found at the greatest oceanic depths between 3,500 and 10,000 m. Adult migration provides part of the explanation for the widespread occurrence of the Lithodidae, but does not indicate that they roam the ocean depths unconstrained.

-*Dispersal into and within the deep sea*

Evidence presented here indicates at least two transitions from the shallow North Pacific into the deep-sea. Such events are known to have occurred in other deep-sea fauna, including several parallel submergence events within the crustacean group Asellota (Raupach et al 2009). Like temperature, pressure has a physical effect on chemical reactions at a very basic level and can affect all biological processes (Angilletta 2009). Acclimatisation or adaptation to pressure is a unique challenge of the deep sea environment and can govern bathymetric range limits in both directions (Marsland 1938, 1950, Young & Cameron 1989, Mestre et al 2009). Large bathymetric ranges of species indicate that lithodids are not only tolerant of high pressures but also of differences in pressure. Many theories of distributional submergence, however, consider temperature to be the main constraining factor (Tyler & Young 1998), relying on the

observation that temperature tolerance ranges compared to bathymetric temperature gradients are often larger than the equivalent effects of gradual increases in pressure (Mestre et al 2009). Isothermal submergence at the poles is a mechanism by which cold-adapted organisms in high latitudes might have been pre-adapted to temperatures found in the deep sea since the Miocene (Kussakin 1973, Menzies et al 1973). This principle is used to explain the bipolar distribution of deep-sea organisms in several taxa (Andriashev 1986, Harrison & Crespi 1999, Briggs 2003, Raupach et al 2008), and could be extended to the Lithodidae.

-Adaptation to environmental niches and speciation

The deep sea is characterised by a high degree of genetic similarity within species distributed over large distances (Gardner 1997) as well as ecological homogeneity and environmental stability (Gage & Tyler 1991). Although there are exceptions to this rule, (Miya & Nishida 1997, Etter et al 1999, Raupach & Wägele 2006) this characterisation appears to be valid for the Lithodidae. Molecular results are not conclusive for the Lithodidae, but they do indicate a low level of genetic variation for such a large and diverse anomuran taxon.

Little is known about the ecology of the deep-sea Lithodidae; as is the case for many deep-sea organisms, they are rarely observed in-situ. Environmental adaptation is inferred from their distribution, their morphology and from the rare occasions when they have been successfully maintained in laboratory environments (Anger et al 2003, Reid et al 2007). Remote technology for observing organisms in their natural environment continues to improve, but still only provide a snapshot of population dynamics and behaviour (Thatje et al 2008). Some morphological properties, such as the locomotory mechanics of the walking legs have an obvious adaptive significance: those with long legs (*Neolithodes* species) can efficiently cover long distances of homogenous sea-floor, whereas those with short and compact legs (e.g. *Paralomis granulosa*) can resist tidal motion in kelp hold-fasts close to the surface (Lovrich & Vinuesa 1995). The adaptive significance of the carapace setae, spines and tubercles in different habitats is unknown, although it they seem likely to afford some camouflage or protection. Ontogenetic shifts in ornamentation, particularly, may reflect adaptive changes to defined ecological niches throughout the life cycle (Benedict 1894, Barnard 1946, Macpherson 1988a, Lovrich & Vinuesa 1995). Speciation theorists struggle to explain the great morphological diversity (Rex 1981, Grassle & Maciolek 1992) in the deep ocean in the absence of discernable barriers to gene flow (Wilson & Hessler 1987). The Lithodidae provide at least two examples of deep-sea genera in which a great diversity of morphology is found to have arisen entirely within the deep sea (i.e., not seeded from several shallow-water radiations).

The Strait of Magellan and Beagle Channel are two major marine inlets in southern Patagonia, which harbour shallow-water lithodids in the Southern Hemisphere (Lovrich & Vinuesa 1993).

These inlets consist of several basins with hydrological and topographical boundaries between them (Brambati et al 1991, Panella et al 1991, Antezana et al 1992). Unlike the deeper environment inhabited by congeneric species, *P. granulosa, L. santolla* and *L. confundens* occupy a disjoint environment which has been disturbed over time by glacial processes (McCulloch et al 2000). Throughout the late Cenozoic, glacial periods have been associated with low sea levels and it is only in the last 5 ka that there have been marine incursions into the Strait of Magellan (Hulton et al 2002). Morphological evidence indicates that *Lithodes santolla*, *L. confundens* and *P. granulosa* all emerged at some point from within deep-water lineages (Figs **B2**.10, **B3**.5c); this conclusion is also supported for the *Lithodes* species by molecular evidence (Fig **A1**.3). Molecular samples taken from specimens of Patagonian *Lithodes* suggest that these recent colonisers of shallow waters already have morphological differences consistent with their molecular divergence. Additionally, there are consistent molecular differences between western and south eastern populations of *L. santolla* indicating reduced gene flow. Physically disjoint habitats, periodic habitat disturbance and perhaps higher temperatures (Fig C.5) could contribute to a faster rate of mutation, adaptation and speciation in such shallow-water species (Erlich & Raven 1969, Bargelloni et al 1994, Martin 1999).

D.5 Constraints to dispersal throughout the Cenezoic

Within deep-sea lineages of the Lithodidae, distribution is constrained to a large extent by the topology and pressure within the ocean basins, which change slowly (Gage & Tyler 1991). A major theme of this work was to examine the frontiers of the lithodid distribution in order to predict and explain shifting patterns of biogeography (Thatje et al 2005, Jørgensen et al 2005).

As ectothermic organisms, the distribution of the Lithodidae is influenced by water temperature (Section C, Fig C.4). Basic chemical processes in eukaryotes occur from -2 to 60 °C (Tansey & Brock 1972), but complex organisms have a narrower tolerance within this range because of the cost of a complex system and trade offs in specific adaptation to high or low temperatures (Angilletta 2009). Different life stages and different individuals have unique sets of reactions and reaction rates that define the limits of their temperature tolerance, although those with a genetic basis are constrained additionally by ancestral history (Fig C.5; Fields 2001). Experimentally determined optimal temperatures for larval survival (5–10 °C, Vinuesa et al 1985, Calcagno et al 2005) in lithodids indicate that species in the Southern Ocean do not always live within a temperature range that maximises their theoretical fitness. Some species can both survive and reproduce in temperatures as low as 0.5 °C (Fig C.7, Section C.4.5, Klages et al 1995, Thatje et al 2005). There is an imperfect match between fitness-maximising selective pressure and environmental adaptation, especially in a fluctuating or changing environment (Aronson et al 2007).

Temperature thresholds, beyond which long-term survival is impossible, exist for a variety of biochemical and physiological reasons (Cossins & Bowler 1987, Pörtner 2002). If species in the Southern Ocean are living outside their optimal temperature range but within their physiological thresholds, then this environment represents a frontier of survival. For species, the geographic location of frontiers can be fluid, both because of continual but imperfect adaptation of species to the environment (Angilletta 2009) and because the frontier can physically move.

Climate change has occurred throughout the Cenozoic, from a hot-house Cretaceous to the ice-ages of the Quaternary and has substantially altered the marine environment (Zachos et al 2001). Anthropogenic effects on the climate may not be larger than changes witnessed over geological time, but they are pertinent, measurable and like all climatic events, difficult to predict (Oreskes 2004). Linked climatic and tectonic events in the recent millennia have shaped the distribution and radiation of the extant Lithodidae, producing such diversity as the intertidal umbrella crab *Cryptolithodes* and the deep-sea predators *Paralomis*, *Lithodes* and *Neolithodes*. At frontiers all over the world, measurable changes in ocean temperature, ocean currents and benthic habitat in the forthcoming years will change the distribution of the lithodids and other marine biota as they have in the past.

D.6 Future perspectives

This thesis leaves open several questions which can be addressed in future work:

A first line of investigation might examine the plasticity of egg size in Lithodidae varying with depth, temperature and maternal size. For this study, I have collected and measured a large number of eggs from ovigerous females (Fig D1) in different genera of Lithodidae. There seems to be some trend with depth although only a few ovigerous specimens of the abyssal genus *Neolithodes* were found. An expanded dataset might provide insights into variation in maternal investment in relation to multiple physical factors.

This study did not set out to examine properties of mutation rates within the Lithodidae, the effect of mutation rates in deep sea organisms and particularly the effect of temperature on the efficiency and speed of DNA replication. An apparently low mutation rate hindered the gathering of variable sequences for the Lithodidae, to the detriment of resolution in molecular phylogenies. Experimental design is difficult, because to test the effect of the deep-sea environment on mutation rate all other variables need to be controlled and the taxon selected needs to:

a) be of a similar age and size (number of species) to the Lithodidae

b) have similar ancestry, ideally from within the Decapoda

c) have evolved in a similar temperature regime but in shallow water

The first constraint is perhaps the greatest, since the age of the Lithodidae is not known. This work perhaps can not be done until more fossil evidence is collected, or until a clearer idea is formed about the position of the Lithodidae within the Anomura, for which fossil records exist. If such conditions can be satisfied, then statistical tests to examine the significance of various environmental effects on mutation rate could be conducted. To this end, it would be interesting to compare the mutation rate in secondarily shallow species of Lithodidae (*Paralomis granulosa*, *Lithodes confundens*) with that of congeneric deep-sea groups.

REFERENCES

Nomenclature Committee of the International Union of Biochemistry (NC-IUB). (1986) Nomenclature for incompletely specified basis in nucleic acid sequences. Recommendations 1984. *Proceedings of the National Academy of Science USA* 83:4-8.

A

Abelló P, Macpherson E (1991) Distribution patterns and migration of *Lithodes ferox* Filhol (Anomura: Lithodidae) off Namibia. *Journal of Crustacean Biology* 11(2): 261-268.

Abdi H (2007) The Bonerferonni and Šidák corrections for multiple comparisons. In: N Salkind (Ed) *Encyclopedia of measurement and Statistics*. Thousand Oaks (CA) 1-9 pp.

Abrunhosa FA, Kittaka J (1997) Functional morphology of the mouthparts and foregut of the last zoea, glaucothoe and first juvenile of king crabs *Paralithodes camtschaticus, P. brevipes* and *P. platypus*. *Fisheries Science*. 63: 923-930.

Acosta J, Canals M, Herranaz P, Sans JL (1989) Investigacion geologica-geofisica y sedimentologica en el arco de Escocia y peninsula Antartica. In: MAPA (Ed) *Resultados de la campagna "ANTARTIDA 8611" Publ. Espec. Inst. Esp. Oceanogr. No2,* Madrid. 9-82 pp.

Adams DC, Rohlf FJ, Slice DE (2004) Geometric morphometrics: Ten years of progress following the 'revolution'. *Italian Journal of Zoology* 71: 5-16.

Ahyong ST, Dawson EW (2006) Lithodidae from the Ross Sea, Antarctica, with descriptions of two new species (Crustacea: Decapoda: Anomura). *Zootaxa* 1303: 45-68.

Alcock A, Anderson ARS (1899) Natural history notes from H. M. Royal Indian marine survey ship <<Investigator>>. Commander T. H. Hemming, R.N. commanding series III, No.2. An account of the deep-sea Crustacea dredged during the surveying season of 1897-1898. *Annals of the Magazine of Natural History, series 7* 3: 1-27.

Allen GJ, Sanders D (1996) Control of ionic currents in guard cell vacuoles by cytosolic and luminal calcium Source. *Plant Journal* 10: 1055-1069.

Altschul SF, Miller GW, Myers EW, Lipman DJ (1990) Basic local alignment search tool. *Journal of Molecular Biology* 129:97-102.

Andrade HV (1980) Nueva especie de *Paralomis* en aguas de Chile: *Paralomis chilensis* n. sp.. *Boletín del museo nacional de historia natural. Santiago, Chile* 37: 269-273.

Andriashev AP (1986) *Review of the snailfish genus Paraliparis (Scorpaeniformes, Liparididae) of the Southern Ocean*. Theses Zool. Vol. 7. Koenigstein Koelts Sci. 204 pp.

Anger K (1989) Growth and exuvial loss during larval and early larval development of the hermit crab *Pagurus bernhardus* reared in the laboratory. *Marine Biology* 103: 503-511.

Anger K (1996) Physiological and biochemical changes during lecithotrophic larval development and early juvenile growth in the northern stone crab, *Lithodes maja* (Decapoda: Anomura). *Marine Biology* (1996) 126: 283-296.

Anger K, Thatje S, Lovrich G, Calcagno J (2003) Larval and early juvenile development of *Paralomis granulosa* reared at different temperatures: tolerance of cold and food limitation in a lithodid crab from high latitudes. *Marine Ecology Progress Series* 253: 243-251.

Anger K, Lovrich GA, Thatje S, Calcagno JA (2004) Larval and early juvenile development of Lithodes santolla (Molina, 1782) (Decapoda: Anomura: Lithodidae) reared at different temperatures in the laboratory. *Journal of Experimental Marine Biology and Ecology* 306: 217-230.

Angilletta MJ (2009) *Thermal Adaptation: A theoretical and empirical synthesis*. Oxford University Press, Oxford. 289 pp.

Anikouchine WA, Sternberg RW (1973) The world ocean. An introduction to oceanography. Prentice-Hall, Englewood Cliffs, NJ. 338 p.

Antezana T, Guglielmo L, Ghirardelli E (1992) Microbasins within the Strait of Magellan affecting zooplankton distribution. In: Gallardo VA, Ferretti O, Moyano HI (Eds) *Oceanografia en Antartica*, Ediciones Documentas, Santiago. 453-458 pp.

Antezana T (1999) Plankton of the southern Chilean fjords: trends and linkages. *Scientia Marina* 63 (supp 1): 69-80.

Arana EP, Retamal MA (1999) New distribution of *Paralomis birsteini* Macpherson, 1988 in Antarctic waters (Anomura, Lithodidae, Lithodinae). *Investigaciones Marinas Universidad Catolica de Valparaíso* 27: 101-110.

Armbruster GF J, Korte A (2006) Genomic nucleotide variation in the ITS1 rDNA spacer of land snails. *Journal of Molluscan Studies* 72(2):211-213.

Armistead C, Bowers F, Gish R, Harrington G, Jones W, Kruse GH, Mabry K, Morrison R, Otto RS, Palach B, Stevens BG, Wilson E, Witherell D, Zheng J (2000) Crab SAFE. Stock assessment and fishery evaluation report for the king and

tanner crab fisheries of the Bering Sea and Aleutian Islands. North Pacific Fishery Management Council, Ancorage, AK. 15 p.

Arnaud PM, Do-Chi T (1979) *Résultats préliminaries obtenus sur les lithodes aux iles Crozet, Marion et Prince Edward, pendant la campagne océanographique MD.08.* C.N.F.R.A. (Comité nat. franç. Rech. antarct.) 44: 135-136.

Arntz W, Brey T, Gallardo VA (1994) Antarctic zoobenthos. *Oceanography and Marine Biology Annual Review* 32: 241-304.

Aronson RB, Blake DB (2001) Global climate change and the Antarctic Benthos. *American Zoologist* 41:27-39.

Aronson RB, Thatje S, Clarke A, Peck LS, Blake DB, Wilga CD, Seibel BA (2007) Climate change and invasibility of the Antarctic benthos. *Annual Review of Ecology Evolution and Systematics* 38: 129-154.

Atkins P, De Paula J (2006) *Physical chemistry* (8th ed) WH Freeman & Company 212 p.

Atkinson D, Morley SA, Weetman D, Hughes RN (2001) Offspring size responses to maternal temperature in ectotherms. In: Atkindson D, Thorndyke M (Eds) *Environment and animal development: Genes, Life histories and plasticity*. Oxford Bios Scientific Publishers 265-285 pp.

Averof M, Patel N (1997) Crustacean appendage evolution associated with changes in Hox gene expression. *Nature* 388: 682-686.

Avise JC, Ball RM Jr (1990) Principles of genealogical concordance in species concepts and biological taxonomy. *Oxford Survey of Evolutionary biology* 7: 45-67.

B

Báez RP, Bahamonde NN, Sanhueza SA (1986) *Neolithodes diomedeae* (Benedict 1894) en Chile (Crustacea, Decapoda, Lithodidae). *Investigacion Pesquera* (Chile) 33: 105-110.

Bahamonde NN (1961) Crustáceos en la obra de Molina. *Noticario Mensual Museo Nacional de Historica Natural*, *Santiago* (Chile) 136: 3-7.

Balss H (1911) Neue Paguriden aus den Ausbeuten der Deutchen Tiefsee-Expedition 'Valdivia' und der Japanischen Expedition Prof. Dofleins. *Zoologischer Anzeiger* 38: 1-9.

Baraclough TG, Vogler AP (2000) Detecting the geographic pattern of speciation from species-level phylogenies. *The American Naturalist* 155(4): 420-434.

Barker PF, Burrell J (1977) The opening of Drake Passage. *Marine Geology* 25: 15-34.

Barker PF, Dalziel IWD, Storey BC (1991) Tectonic evolution of the Scotia Arc region. In: Tingey RJ (Ed) *Antarctic Geology*. Oxford University Press 215-248 pp.

Barker PF, Thomas E (2004) Origin, signature and palaeoclimatic influence of the Antarctic Circumpolar Current. *Earth Science Reviews* 66(1-2): 143-162.

Bargelloni L, Ritchie PA, Patarnello T, Battaglia B, Lambert DM, Meyer A (1994) Molecular evolution at subzero temperatures: mitochondrial and nuclear phylogenies of fishes from Antarctica (Suborder Notothenioidei) and the evolution of antifreeze glycopeptides. *Molecular Biology and Evolution* 11: 854-863.

Barnard KH (1946) Descriptions of new species of South African decapod Crustacea, with notes on synonomy and new records. *Annals of the Magazine of Natural History* 102(11) 13: 361-392.

Barnard KH (1950) Descriptive catalogue of South African Decapod Crustacea (Crabs and Shrimps). *Annals of the South African Museum* 28:1-837.

Barnes DA, Fuentes V, Clarke A, Schloss IR, Wallace MI (2006) Spatial and temporal variation in shallow seawater temperatures around Antarctica. *Deep Sea Research II: Topical studies in Oceanography* 53(8-10): 853-865.

Barr N (1973) Extension of the known range of the crab, *Cryptolithodes typicus* Brandt, to Amchitka Island, Alaska (Decapoda, Anomura, Lithodidae). *Crustaceana* 25: 320.

Barría EM, Jara CG (2005) New record of *Paralomis otsuae* Wilson 1990 (Decapoda, Anomura, Lithodidae) en la costa centro-sur de Chile. *Investigaciones Marinas* 33(1) 115-120.

Barton NH (1989) The divergence of a polygenic system under stabilizing selection, mutation and drift. *Genetic Research* 54: 59-77.

Baum DA, Shaw KL (1995) Genealogical perspectives on the species problem. In Hoch PC, Stephenson AG (Eds) *Molecular and experimental approaches to plant biosystematics.* Missouri Botanical Garden, St. Louis. 289-303 pp.

Beaumont MA, Rannala B (2004) The bayesian revolution in genetics. *Nature Reviews Genetics* 5: 251-261.

Benedict JE (1894) Scientific results of explorations by the U.S. Fish Commission steamer Albatross. No. XXXI. Descriptions of new genera and species of crabs of the family Lithodidae, with notes on the young of *Lithodes camtschaticus* and *Lithodes brevipes*. *Proceedings of the United States National Museum* 17: 479-488.

Bensasson D, Zhang D-X, Hartl DL, Hewitt GM (2006) Mitochondrial Pseudogenes: evolution's misplaced witness. *Trends in Ecology and Evolution* 16(6): 314-321.

Birstein YA, Vinogradov LG (1967) Occurrence of *Paralomis spectabilis* Hansen

(Crustacea, Decapoda, Anomura) in the Antarctic. Explorations of the fauna of the sea. IV (XII). *Biological Research in the Soviet Antarctic Expedition* 3: 390–398 (Israel Program for Scientific Translations).

Birstein YA, Vinogradov LG (1972) Craboids (Decapoda: Anomura: Lithodidae) of the Atlantic sector of the Antarctic, South America, and South Africa. *Zoologichesky Zhurnal* 51: 351-363.

Boas JEV (1880) Studier over Decapodernes Slaegtskabsforhold. *Vidensk. Selsk Skr., 6 Raekke natur. Mathem Afd.* I: 25-210.

Bookstein FL (1991) *Morphometric tools for landmark data. Geometry and biology*. Cambridge University Press: New York..

Boone L (1926) A new family of Crustacea. Preliminary technical description. *New York Zoological Society Bulletin* 29:73.

Bosch I, Beauchamp KB, Steele ME, Pearse JS (1987) Development, metamorphosis, and seasonal abundance of embryos and larvae of the antarctic sea urchin *Sterechinus neumayeri*. *Biological Bulletin* 173: 126-135.

Boschi EE (1979) Geographic distribution of Argentinian marine decapod crustaceans. *Bulletin of the Biological society of Washington* 3:134-143.

Bouvier EL (1895) Recherches sur les affinités des *Lithodes* et des Lomis avec les Pagurides. *Annales des Science Naturelles, Zoologie* 7: 157-213.

Bouvier EL (1896) Sur la classification des Lithodinés et sur leur distribution dans les ocans. *Anales Scien Natur.* Zoologie (8) 1:1-46.

Bowman D (1972) A new range record for the Umbrella crab, *Cryptolithodes sitchensis* Brandt. *California Fish and Game* 58(3) 240-243.

Boyle EE, Zardus JD, Chase MR, Etter RJ, Rex MA (2004) Strategies for molecular genetic studies of preserved deep-sea macrofauna. *Deep Sea Research Part 1: Oceanographic Research Papers* 51(10): 1319-1336.

Brambati A, Fontolan G, Simeoni U (1991) Recent sediments and sedimentological processes in the Strait of Magellan. *Mem. Biol. Mar. Ocean.* 19: 217-259.

Branch ML, Griffiths CL, Kensley B, Sieg J (1991) The benthic Crustacea of subantarctic Marion and Prince Edward Islands: Illustrated keys to the species and results of the 1982-1989 Universtiy of Cape Town Surveys. *South African Journal of Antarctic Research* 1: 3-44.

Brandini FP, Boltovskoy D, Piola A, Kocmur S, Rottgers R, Abreu PC, Lopes RM, (2000) Multiannual trends in fronts and distribution of nutrients and chlorophyll in the southwestern Atlantic (30-62 ° S). *Deep-Sea Research Part I* 47: 1015-1033.

Brandt JF (1848) Die Gattung *Lithodes* Latreille nebst vier neuen ihr verwandten von Wosnesenski entdekten, als Typen einer besondern Unterabtheilung (Tribus

Lithodea) der Edwards'schen Anomuren. *Bulletin de la Classe Physico-mathematique de l'Academie Imperiale des Sciences de St-Petersburg* 7: 171-176.

Brandt JF (1850). Bericht uber die fur die Reisebeschreibung des Herrn von Middendorff von J.F. Brandt bearbeiden Krebsthiere aus den Abtheilungen der Brachyuren (Krabben), Anomuren und Makrouren (Krebse). *Bulletin de la Classe Physico-mathematique de l'Academie Imperiale des Sciences de St-Petersburg* 8: 234-238.

Breslauer KJ, Frank R, Blöcker H, Marky LA (1986) Predicting DNA duplex stability from the base sequence. *Proceedings of the National Acadademy of Sciences* 83(11): 3746–3750.

Brey T, Dahm C, Gorny M, Klages M, Stiller M, Arntz WE (1996) Do Antarctic invertebrates show an extended level of eurybathy? *Antarctic Science* 8:3-6.

Briggs JC (1991) Global species diversity. *Journal of Natural History* 25: 1403-1406.

Briggs JC (2003) Marine centres of origin as evolutionary engines. *Journal of Biogeography* 30: 1-18.

Brito MJL (2001) *Paralomis otsuae* Wilson 1990 (Crustacea: Lithodidae) en la costa central de Chile. *Estudias Oceanologica.* 20: 29-32.

Brito MJL (2002) Lithodidae off San Antonio, central Chile (Crustacea: Anomura) *Investigaciones Marinas Universidad Catolica de Valparaíso* 30(1): 57-62.

Britten RJ (1986) Rates of DNA Sequence Evolution differ between taxonomic groups. *Science* 231(4744): 1393-1398.

Bromham L, Penny D (2003) The modern molecular clock.. *Nature Reviews Genetics* 4(2003): 216-224.

Brown WM, George M, Wilson AC (1979) Rapid evolution of animal mitochondrial DNA. *Proceedings of the National Academy of Science* USA 76(4): 1967-1971.

Butler TH, Hart JFL (1962) The occurrence of the King crab, *Paralithodes camtschatica* (Tilesius) and of *Lithodes aequispina* (Benedict) in British Columbia. *Journal of Fisheries Research Board Canada* 19: 401-408.

C

Calcagno JA, Thatje S, Anger K, Lovrich GA, Kaffenberger A (2003) Changes in biomass and chemical composition during lecithotrophic larval development of the Southern stone crab, *Paralomis granulosa* (Jacquinot). *Marine Ecology Progress Series* 257: 189-196.

Calcagno JA, Lovrich GA, Thatje S, Nettelmann U, Anger K (2005) First year growth in the lithodids *Lithodes santolla* and *Paralomis granulosa* reared at different temperatures. *Journal of Sea Research* 54(3): 221-230.

Campbell JA, Frost DR (1993) Anguid lizards of the genus Abronia: revisionary notes, descriptions of four new species, a phylogenetic analysis, and key. *Bulletin of the American Muserum of Natural History* 216: 1-121.

Campodonico I, Guzman L (1972) *Lithodes murrayi* Henderson 1888, Nuevo Litodido para la patagonia austral de Chile (Crustacea, Decapoda, Anomura). *Annales de Institut de la Patagonia, Punta Arenas* (Chile) 3(1-2):221-231.

Carcraft J (1983) Species concepts and speciation analysis *Current Ornithology* 1: 159-187.

Carcraft J (1989) Speciation and its ontology: The empirical consequences of alternative species concepts for understanding patterns and processes of differentiation. In (D Otte and JA Endler Eds.) *Speciation and its consequences* Sinauer Associates, Sunderland MA. 28-57 pp.

Carcraft J (1997) Species concepts in systematics and conservation biology – an ornithological viewpoint. In Claridge MF, Dawah HA, Wilson MR (Eds) *Species: the units of biodiversity* Chapman & Hall, NY. 325-339 pp.

Cavalli-Sforza LL, Edwards SV (1967) Phylogenetic Analysis: Models and Estimation Procedures. *Evolution* 21(3): 550-570.

Chace FA Jr (1939) Reports on the scientific results of the first Atlantis expedition to the West Indies, under the joint auspices of the University of Havana and Harvard. Preliminary descriptions of one new genus and seventeen new species of decapod and stomatopod crustaceans. *Memórias de al Sociedad Cubana de Historica Natural* 13: 31-54.

Chow S, Ueno Y, Toyokawa M, Oohara I , Takeyama H (2009) Preliminary Analysis of Length and GC Content Variation in the Ribosomal First Internal Transcribed Spacer (ITS1) of Marine Animals. *Marine Biotechnology* 11(3): 301-306.

Chu KH, Li CP, Ho HY (2001) The First Internal Transcribed Spacer (ITS-1) of Ribosomal DNA as a Molecular Marker for Phylogenetic and Population Analyses in Crustacea. *Marine Biotechnology* 3(4): 355-361.

Chuang JH, Li H (2004) Functional bias and spatial organisation of genes in mutational hot and cold regions in the human genome. *PloS Biology* 2(2): e29.

Clarke A (2003) The Deep Sea Floor: an overview. In: P Tyler (Ed) *Ecosystems of the world.* 2nd edition. Chapter 8: 241-262 pp.

Clary DO, Wolstenholme DR (1984) The Drosophila mitochondrial genome. *Oxford Survey of Eukaryotic Genes.* 1:1-35.

Collins DW, Jukes TH (1994) Rates of transition and transversion in coding sequences since the human-rodent divergence. *Genomics* 20(3): 386-396.

Cooke MS, Evans MD, Dizdaroglu M, Lunec J (2003) Oxidative DNA damage:

mechanisms, mutation, and disease. *The FASEB Journal* 17: 1195-1214.

Cossins AR, Bowler K (1987) *Temperature biology of animals.* Chapman and Hall, London 339 pp.

Crain JA (1999) Functional Morphology of prey ingestion by *Placetron wosnessenskii* Schalfeew zoeae (Crustacea: Anomura: Lithodidae). *Biological Bulletin. Marine Biological Laboratory, Woods Hole*. 197: 1899-1999.

Crain JA, McLaughlin PA (2000) Larval and early juvenile development in the Lithodidae (Decapoda: Anomura: Paguroidea) reared under laboratory conditions. *Invertebrate reproduction and development* 37 (2): 43-59, 113-127.

Crame JA (1994) The evolutionary history of Antarctica. In: Hempel G *Antarctic Science- Global Concerns* Springer, Berlin 188-214 pp.

Crame JA (1999) An evolutionary perspective on marine faunal connections between southernmost South america and Antarctica. *Scientia Marina* 63: 1-14.

Crease TJ, Taylor DJ (1998) The origin and evolution of variable-region helices in V4 and V7 of the small-subunit ribosomal RNA of branchiopod crustaceans. *Molecular Biology and Evolution* 15: 1430–1446.

Cunningham CW, Blackstone NW, Buss LW (1992) Evolution of king crabs from hermit crab ancestors. *Nature* 355: 539-542.

D

da Silva JL, Anderson JB, Stravers J (1997) Seismic facies changes along a nearly continuous 24° latitudinal transect: the fjords of chile and the northern Antarctic Peninsula. *Marine Geology* 143: 103-123.

Daly F, Hand DJ, Jones MC, Lunn AD, McConway KJ (1995) *Elements of Statistics*. The Open University, 682 pp.

Daniel RM, Peterson ME, Danson MJ, Price NC, Kelly SM, Monk CR, Weinberg CS, Oudshoorn ML, Lee CK (2009) The molecular basis of the effect of temperature on enzyme activity. *Biochemical Journal* 425(2): 353–60.

Darwin C (1859[1964]) *On the Origin of Species: A Facsimile of the First Edition*, Cambridge, MA: Harvard University Press. 495 pp.

Dawson EW, Yaldwyn JC (1970) Diagnosis of a new species of *Neolithodes* (Crustacea: Anomura: Lithodidae) from New Zealand (Note). *New Zealand journal of marine and freshwater Research.* 4: 227-228.

Dawson EW, Yaldwyn JC (1971) Diagnosis of a new species of *Paralomis* (Crustacea: Anomura: Lithodidae) from New Zealand. *Records of the Dominion Museum* 7: 51-54.

Dawson EW, Yaldwyn JC (1985a) King crabs of the world or the world of king crabs: an overview of identity and distribution with illustrated diagnostic keys to the

genera of the Lithodidae and to the species of *Lithodes*. *Proceedings of the International King Crab Symposium* Anchorage. Alaska: 69-106 pp.

Dawson EW & Yaldwyn JC (1985b) *Lithodes nintokuae* Sakai: A Deep-water King Crab (Crustacea, Anomura, Lithodidae) Newly Recorded from Hawaii. *Pacific Science* 39(1):16-23.

Dayton PK, Robillard GA, Paine RT, Dayton LB (1974) Biological accommodation in the benthic community at McMurdo Sound, Antarctica. *Ecological Monographs* 44: 105-128.

Dayton PK (1990) Polar benthos. In: Smith WO (Ed) *Polar Oceanography*. Academic Press. London. 631-685 p.

de Haan W (1833-1850) *Crustacea. Fauna Japonica sive descriptio animalium, quae in itinere per Japoniam, jussu et auspiciis superiorum, qui summum in India Batava Imperium tentent, suscepto, annis 1823-1830 collegit, notis, observationibus et adumbretionibus illustravit.* d. Siebold. Leiden. ix-iv + vii-xvii +i-xxxi + 1-243 + plates 1-55 +A-Q + circ 2.

de Quieroz K, Donoghue MJ (1988) Phylogenetic systematics and the species problem. *Cladistics* 4: 37-338.

de Queiroz K, Gauthier J (1994) Toward a phylogenetic system of biological nomenclature. *Trends in Ecology and Evolution* 9: 27-31.

de Queiroz K (2007) Species concepts and species delimitation. *Systematic Biology* 56(6): 879-886.

de Saint Laurent M, Macpherson E (1997) *Paralomis* White, 1856, a new species from south west Pacific hydrothermal vents (Crustacea: Decapoda). *Zoosystema* 19(4): 721-727.

del Solar EM (1972) Addenda al catalogo de crustaceos del Peru. *Informe Instituto del Mar del Peru* 38: 1-21.

Deacon GER (1937) The Hydrology of the Southern Ocean. *Discovery Reports* 15: 3-122.

Deakon G (1984) *The Antarctic Circumpolar Ocean*. Cambridge University Press. 180p.

DiVenere VJ, Kent DV, Dalziel IWD (1994) Mid-Cretaceous paleomagnetic results from Marie Byrd Land, West Antarctica: a test of post-100 Ma relative motion between East and West Antarctica, Journal of Geophysical Research, 99, 15115-15139.

Dixon CJ, Ahyong ST, Schram FR (2003) A new hypothesis on decapod phylogeny. *Crustaceana* 76(8): 935-975.

Dobzhansky (1936) Studies on hybrid sterility II. Localization of sterility factors in

Drosophila pseudoobscura hybrids. *Genetics* 21: 113-135.

Draper I, Hedenäs L, Grimm GW (2007) Molecular and morphological incongruence in European species of *Isothecium* (Bryophyta). *Molecular Phylogenetics and Evolution* 42(3): 700-716.

Drummond AJ, Pybus OG, Rambaut A, Forsberg R, Rodrigo AG (2003) Measurably evolving populations. *Trends in Ecology and Evolution* 18(9): 481-488.

Drummond AJ, Ho SYW, Phillips MJ, Rambaut A (2006). Relaxed phylogenetics and dating with confidence. *Plos Biology* 4(5): 699-710.

Duguid WDP, Page LR (2009) Larval and early post-larval morphology, growth and behaviour of laboratory reared *Lopholithodes foraminatus* (brown box crab). *Journal of the Marine Biological Association of the United Kingdom*. 89(8): 1607-1626.

Dunton K (1992) Arctic biogeography: The paradox of the marine benthic fauna and flora. *Trends in Ecology and Evolution* 7(6): 183-189.

Dupré J (2001) In defense of classification. *Studies in the History and Philosophy of Biology and the Biomedical Sciences* 32: 203–219.

Durand D, Hoberman R (2006) Diagnosing duplications- can it be done? *Trends in Genetics* 22: 156-164.

E

Eck RV, Dayhoff MO (1966) *Atlas of protein sequences and structure.* National Biomedical Research Foundation, Silver Springs, Maryland.

Eckman JE, Thistle D (1991) Effects of flow about biologically produced structure on harpacticoid copepods in San Diego Trough. *Deep-Sea Research* 38: 1397-1416.

Edgar RC (2004), MUSCLE: multiple sequence alignment with high accuracy and high throughput. *Nucleic Acids Research* 32(5): 1792-97.

Edgar RC (2004) MUSCLE: a multiple sequence alignment method with reduced time and space complexity. *BMC Bioinformatics* 5(1): 113.

Eldredge LG (1976) Two new species of lithodid crabs from Guam. *Micronesica* 12: 309-315.

Epelbaum AB, Borisov R (2006). Feeding behaviour and functional morphology of the feeding appendages of red king crab *Paralithodes camtschaticus* larvae. *Marine Biology Research* 2(2): 77-88.

Ereshefsky M (1998) Species pluralism and anti-realism. *Philosophy of Science* 65: 103-120.

Ereshefsky M (2009) Darwin's Solution to the Species Problem *Synthese* In press. DOI 10.1007/s11229-009-9538-4.

Erlich PR, Raven PH (1969) Differentiation of Populations. *Science* 165:1228.

Etter RJ, Rex MA, Chase MC, Quattro JM (1999) A genetic dimension to deep-sea biodiversity. *Deep Sea Research I* 46: 1095-1099.

F

Fang SG, Wan QH, Fujihara N (2002) Formalin removal from archival tissue by critical point drying. *Biotechniques* 33: 604–611.

Faxon W (1893) Reports on the dredging operations off the west coast of Central America to the Galapagos by the U.S. Fish Commission steamer Albatross VI. Preliminary descriptions of new species. *Bulletin of the Museum of Comparative Zoology, Harvard College* 24: 149-220.

Faxon W (1895) XV The stalk-eyed Crustacea. Reports of the exploration off the west coast of Mexico, Central and South America, and the Galapagos Islands by the U.S. Fish Commission steamer "Albatross" during 1891. *Memoires of the Museum of Comparative Zoology, Harvard College* 18: 42-52.

Feldmann RM (1984) *Haumuriaegla glaessnei* n. gen. and sp. (Decapoda; Anomura; Aeglidae) from Haumurian (Late Cretaceous) rocks near Cheviot, New Zealand. *New Zealand Journal of Geology and Geophysics* 27: 379-385.

Feldmann RM, Tshudy DM (1989) Evolutionary patterns in macrurous decapod crustaceans from Cretaceous to early Cenozoic rocks of the James Ross Island region, Antarctica. In: Crame JA (Ed) *Origins of the Antarctic Biota*, Geological Society, London, Special Publications 183-195 pp.

Feldmann RM (1998) *Paralomis debodeorum*, a new species of decapod crustacean from the Miocene of New Zealand: first notice of the Lithodidae in the fossil record. *New Zealand Journal of Geology and Geophysics* 41: 35-38.

Feldmann RM (2003) The Decapoda: New initiatives and novel approaches. *Journal of Paleontology* 77(6): 1021-1039.

Felsenstein J (1979) Alternative methods of phylogenetic inference and their interrelationship. Systematic Zoology 28: 49-62.

Felsenstein J (1984) Distance methods for inferring phylogenies: a justification. *Evolution* 38: 16-24.

Felsenstein J (1985) Confidence limits on phylogenies: an approach using the bootstrap. *Evolution* 39: 783-791.

Felsenstein J (1988) Phylogenies from molecular sequences: inference and reliability. *Annual Review of Genetics* 22: 521-565.

Felsenstein J (1993) PHYLIP (Phylogeny Inference Package) version 3.5c. Department of Genetics, University of Washington, Seattle.

Felsenstein J, Churchill GA (1996) A Hidden Markov Model approach to variation among sites in rate of evolution. *Molecular Biology and Evolution* 13(1): 93-104.

Fields PA (2001) Protein function at thermal extremes: balancing stability and flexibility. *Comparative Biochemistry and Physiology* A. 129: 417-431.

Filhol H (1884) Explorations sous marines. Voyages du Talisman. *La Nature (Paris)* 12: 326-330.

Fink WL, Zelditch ML (1995) Phylogenetic analysis of ontogenetic shape transformations: a reassessment of the piranha genus *Pygocentrus* (Teleostei). *Systematic Biology*. 44: 343-360.

Fisher RA (1921) On the probable error of a coefficient of correlation deduced from a small sample. *Metron* 1(4): 3–32.

Fitch WM (1971) Toward defining the course of evolution: minimum change for a specified tree topology. *Systematic Zoology* 20: 406-416.

Fitch WM, Margoliash E (1967) Construction of phylogenetic trees. *Science* 155:279-284.

Flower B, Kennett JP (1994) The middle Miocene climatic transistion: East Antarctic ice sheet development, deep ocean circulation and global carbon cycling. Palaeogeography, Palaeoclimatology, Palaeoecology 108:537-555.

Folmer O, Black M, Hoeh W, Lutz R, Vrijenhoek R (1994) DNA primers for amplification of mitochondrial cytochrome C oxidase subunit I from metazoan invertebrates. *Molecular Marine Biology and Biotechnology* 3:294-299.

Forster A, Schouten S, Baas M, Sinninghe Damsté JS (2007) Mid-Cretaceous (Albian–Santonian) sea surface temperature record of the tropical Atlantic Ocean. *Geology* 35(10): 919-922.

Forward RB (1987) Larval release rhythms of decapod crustaceans: an overview. *Bulletin of Marine Science* 41: 165-176.

Foster TD (1984) The marine environment. In: Laws RM (Ed) *Antarctic Ecology* 2. Academic Press, London. 345-371 pp.

France SC, Kocher TD (1996) DNA sequencing of formalin-fixed crustaceans from archival research collections. *Molecular Marine Biology and Biotechnology* 5(4): 304-313.

Frederich M, Sartoris FJ, Arntz WE, Pörtner HO (2000) Haemolymph Mg^{2+} regulation in decapod crustaceans: physiological correlates and ecological consequences in polar areas. *The Journal of Experimental Biology* 203: 1383-1393.

Frederich M, Sartoris FJ, Pörtner HO (2001) Distribution patterns of decapod crustaceans in polar areas: a result of magnesium regulation? *Polar Biology* 24: 719-723.

G

Gage JD, Tyler PA (1991) *Deep Sea Biology: A natural history of organisms at the deep-sea floor*. Cambridge University Press, UK. 504 p.

Galtier N, Jobson RW, Nabholz B, Glémin S, Blier PU (2009) Mitochondrial whims: metabolic rate, longevity and the rate of molecular evolution. *Biology Letters* doi: 10.1098/rsbl.2008.0662.

García Raso JE, Manjón-Cabeza ME, Ramos A, Olasi I (2005) New record of Lithodidae (Crustacea, Decapoda, Anomura) from the Antarctic (Bellingshausen Sea). *Polar Biology* 28: 642-646.

Gardner JPA (1997) Hybridisation in the Sea. *Advances in Marine Biology* 31: 1-55.

Gillespie JH (1998) *Population Genetics. A concise guide.* The Johns Hopkins University Press, Maryland. 165 p.

Greene CN, Jinks-Robertson S (2001) Spontaneous frameshift mutations in *Saccharomyces cerevisiae*: accumulation during DNA replication and removal by proofreading and mismatch repair activities. *Genetics* 159(1): 65–75.

Grether GF (2005) Environmental change, Phenotypic plasticity and genetic compensation. *The American Naturalist* 166(4): e116-e123.

Goldman N, Yang Z (1994) A codon-based model of nucleotide substitution for protein coding DNA sequences. *Molecular Biology and Evolution* 11(5): 725-736.

Goldstein PZ, DeSalle R (2005) Phylogenetic Species, Nested Hierarchies, and Character Fixation. *Cladistics* 16(4): 364-384.

Gordon AL, Greengrove CL (1986) Geostrophic circulation of the Brazil-Falkland Confluence. *Deep Sea Research* 33: 573-585.

Gorny M, Arntz WE, Clarke A, Gore DJ (1992) Reproductive biology of caridean decapods from the Weddell Sea. *Polar Biology* 12: 111–120.

Gorny M (1999) On the biogeography and ecology of the Southern Ocean decapod fauna. *Scientia Marina* 63(S1): 367-382.

Goshima S, Ito K, Wada S, Shimizu M, Nakao S (1995) Reproductive biology of the stone crab *Hapalogaster dentata*. *Crustacea Research* 24: 8-18.

Gouretski VV, Danilov AI (1994) Characteristics of warm rings in the African sector of the Antarctic Circumpolar Current. *Deep Sea Research Part I: Oceanographic Research Papers*. 41(8): 1131-1157.

Grant WS, Duffy DC, Leslie RW (1994) Allozyme phylogeny of *Spheniscus* penguins. *The Auk* 111(3): 716-720.

Grassle JF, Maciolek NJ (1992) Deep-sea species richness: regional and local diversity estimates from quantitative bottom samples. *Deep Sea Research Part I: Oceanographic Research Papers* 48: 1709-1739.

H

Haig J (1974) Observations on the lithodid crabs of Peru, with description of two new species. *Bulletin of the Southern California Academy of Science* 73: 152-164.

Hain S, Melles M (1994) Evidence for marine molluscan fauna beneath ice shelves in the Lazarev and Weddell Seas, Antarctica. *Polar Biology* 11: 169-177.

Hall S, Thatje S (2009a) Global bottlenecks in the distribution of marine Crustacea: temperature constraints in the family Lithodidae. *Journal of Biogeography* 36(11): 2125-2135.

Hall S, Thatje S (2009b) Four new species of the family Lithodidae (Decapoda: Anomura) from collections of the National Museum of Natural History, Smithsonian Institution. *Zootaxa* 2302: 31-47.

Hancock JM, Tautz D, Dover GA (1988) Evolution of Secondary Structures and compensatory mutations in the Ribosomal RNAs of *Drosophila Melanogaster*. *Molecular Biology and Evolution* 5(4): 393-414.

Hancock JM (1995) The contribution of DNA slippage to eukaryotic nuclear 18S rRNA evolution. Journal of Molecular Evolution. 40(6): 629-639.

Hansen HJ (1908) *Crustacea Malacostraca I. The Danish Ingolf Expedition* Bianco Luno, Copenhagen 3(2): 1-120.. Translated by H.M.Kyle.

Harkema R, Weatherly GL (1989) A compilation of moored current meter data in the Argentine Basin: April 25 1987 - March 14 1988. *Technical Report CMF-89-01*. Florida State University 64 p.

Harrison RG (1990) Hybrid zones*:* windows on evolutionary process. *Oxford Survey of Ecology and Biology* 7: 69-128.

Harrison MK, Crespi BJ (1999) Phylogenetics of *Cancer* crabs (Crustacea: Decapoda: Brachyura). *Molecular Phylogenetics and Evolution* 12**:** 186–199.

Hasegawa M, Yano T (1984a) Maximum likelihood method of phylogenetic inference from DNA sequence data. *Bulletin of the Biometric Society of Japan* 5: 1-7.

Hasegawa M, Kishino H, Saitou N (1991) On the Maximum Likelihood method in molecular phylogeny. *Journal of Molecular Evolution* 32: 443-445.

Haug GH, Tiedemann R (1998) On Atlantic Ocean thermohaline circulation. *Nature* 393: 673.

Hazel JR (1995) Thermal adaptation in biological membranes: Is homeoviscous adaptation the explanation? *Annual review of Physiology* 57: 19-42.

Hebling NJ, Rieger PJ (1986) Os ermitões (Crustacea Decapoda: Paguridae e Diogenidae) do litoral do Rio Grande do Sul, Brasil. *Atlântica* 8: 63–77.

Held C (2000) Phylogeny and Biogeography of Serolid Isopods (Crustacea, Isopoda, Serolidae) and the Use of Ribosomal Expansion Segments in Molecular Systematics. *Molecular Phylogenetics and Evolution* 15(2): 165-178.

Held C (2001) No evidence for slow-down of molecular substitution rates at subzero temperatures in Antarctic serolid isopods. (Crustacea, Isopoda, Serolidae). *Polar Biology* 24: 497-501.

Held C, Wägele JW (2005) Cryptic speciation in the giant Antarctic isopod *Glyptonotus antarcticus* (Isopoda: Valvifera: Chaetiliidae). *Scientia Marina* 69: 175-181.

Henderson JR (1888) The voyage of H.M.S. Challenger. Report on the Anomura collected by H.M.S. Challenger during the Years 1873-76. *Reports on the scientific results of the Voyage of H.M.S Challenger during the years 1873-76. Zoology*. 27: 1-221.

Hennig W (1966) *Phylogenetic Systematics.* University of Illinois Press, Urbana, Chicago & London. 263 pp.

Henze K, Martin W (2003) Evolutionary biology: Essence of mitochondria. *Nature* 426:127-128.

Hessler RR, Sanders HL (1967) Faunal diversity in the deep-sea. In: *Deep-sea research and oceanographic abstracts* 65 p.

Hey J (2001) The mind of the species problem. *Trends in Ecology and Evolution* 16: 326–329.

Hochachka PW, Somero GN (1984) *Biochemical adaptations*. Princeton University Press, USA 355 p.

Hoggarth DD (1993) The life history of the lithodid crab, *Paralomis granulosa,* in the Falkland Islands. *ICES J. Mar. Sci.* 50: 405-424.

Hollister CD, Nowell ARM, Jumars PA (1984) The dynamic abyss. *Scientific American* 250: 42-53.

Holm S (1979) A simple sequentially rejective multiple test procedure. Skandinavian Journal of Statistics 6: 65-70.

Holm-Hansen O (1985) Nutrient cycles in Antarctic marine ecosystems. In: Siegfried WR, Condy RR, Laws RM (Eds) *Antarctic nutrient cycles and food webs* Springer-Verlag, Berlin. 6-10 pp.

Hong SY, Perry RI, Boutillier JA, Kim MH (2005) Larval development of *Acantholithodes hispidus* Stimpson (Decapoda: Anomura: Lithodidae) reared in the laboratory. *Invertebrate reproduction and development* 47: 101-110.

Huber M, Sloan LC (2001) Heat transport, deep waters, and thermal gradients: Coupled simulation of an Eocene greenhouse climate. *Geophysical Research Letters* 28(18): 3481–3484.

Huelsenbeck JP, Ronquist F (2001) MRBAYES: Bayesian inference of phylogeny. *Bioinformatics* 17: 754-755.

Huelsenbeck JP, Ronquist F, Nielsen R Bollback JP (2001) Bayesian inference of phylogeny and its impact on evolutionary biology. *Science* 294: 2310-2314.

Hull D (1965) The Effect of Essentialism on Taxonomy: Two Thousand Years of Stasis. *British Journal for the Philosophy of Science* 15: 314–326, 16: 1–18.

Hulton NRJ, Purves RS, McCulloch RD, Sugden DE, Bentley MJ (2002) The last glacial maximum and deglaciation in southern South America. *Quaternary Science Reviews* 21: 233-241.

Hurley JR, Cattell RB (1962) The Procustes program: Producing direct rotation to test a hypothesized factor structure. *Behavioral Science* 7: 258-262.

Huxley JS (1942) *Evolution: the modern synthesis*. Allen & Unwin, London. 2nd ed 1963; 3rd ed 1974.

I

Ingle RW (1981) The larval and post larval development of the edible crab Cancer pagurus Linnaeus (Decapoda: Brachyura). *Bulletin of the British Museum* (Natural History). (Zoology). London 40(5): 211-236.

Ingle RW, Garrod C (1987) Ornamentation changes associated with growth of Falkland Island populations of *Paralomis granulosa* (Jacquinot, 1842-1847) (Decapoda: Lithodidae). *Crustaceana* 52: 220-224.

J

Jacobs SS, Amos AF, Bruchhausen PM (1970) Ross Sea oceanography and Antarctic Botton Water formation. *Deep-Sea Research* 17: 935-962.

Jaenisch R, Bird A (2003) Epigenetic regulation of gene expression: how the genome integrates intrinsic and environmental signals. *Nature Genetics* 33(Suppl): 245–54.

Jaquinot H (1842-1853) Crustacea. Zoologie. III. In Jaquinot H, Lucas H (Eds) *Voyage au Pôle sud et dans l'Oceanie sur les corvettes L'Astrolabe et la Zelee, exécuté pendant les annees 1837-1840 sous le commandement de M. J. Dumont d'Urville, Capitaine de vaisseau, publié par ordre du Gouvernment et sous la direction superieure de M. Jaquinot & c.* Gide et Baudry, Paris, 107 p.

Jensen GC (1995) *Pacific coast crabs and shrimps*. Monterey, California: Sea Challengers.

Jewett SC, Onuf CP (1988) Habitat suitability models: red king crab. *US Fish and Wildlife Service Biology Report* 82(10.153) Washington DC.

Jørgensen LL, Manushin I, Sundet JH, Birkely SR (2005) *The intentional introduction of the marine red king crab Paralithodes camtschaticus into the southern Barents Sea.* ICES Cooperative Research Report No. 277: 18 p.

Jukes TH (1987) Transitions, transversions, and the molecular evolutionary clock. *Journal of Molecular Evolution* 26(1-2): 87-98.

K

Kattner G, Graeve M, Calcagno JA, Lovrich GA, Thatje S, Anger K (2003) Lipid, fatty acid and protein utilization during lecithotrophic larval development of *Lithodes santolla* (Molina) and *Paralomis granulosa* (Jaquinot). *Journal of Experimental and Marine Biology and Ecology* 292 61-74.

Keeling PJ, Palmer JD (2008) Horizontal gene transfer in eukaryotic evolution. *Nature Reviews Genetics* 9:605-618.

Kelchner SA, Thomas MA (2006) Model use in phylogenetics: nine key questions. *Trends in Ecology and Evolution* 22(2): 87-94.

Kensley B (1977) The South African Meiring Naude cruises Pt 2: Crustacea, Decapoda, Anomura and Brachyura. *Annals of the South African museum* 72(9): 161-188.

Kensley B (1981) The South African Museum's Meiring Naude cruises Pt 12: Crustacea Decapoda of the 1977, 1978, 1979 cruises (Description of *Paralomis roelveldae*). *Annals of the South African Museum* 83: 49-78.

Kim MH, Hong SY (2000) Larval development of *Cryptolithodes expansus* Miers (Decapoda: Anomura: Lithodidae) reared in the laboratory. *Proceedings of the Biological Society of Washington* 113: 54-65.

Kimura M (1980) A simple method for estimating evolutionary rate of base substitutions through comparative studies of nucleotide sequences. *Journal of Molecular Evolution* 16:111-120.

Kitcher P (1984) Species. *Philosophy of Science* 51: 308–333.

Klages M, Gutt J, Starmans A, Bruns T (1995) Stone crabs close to the Antarctic continent: *Lithodes murrayi* Henderson, 1888 (Crustacea; Decapoda; Anomura) off Peter I Island (68°51′ S, 91°51′ W). *Polar Biology* 15: 73-75.

Klingenberg CP (1998) Heterochrony and allometry: the analysis of evolutionary change in ontogeny. *Biological Review* 73: 79-123.

Kluge AG, Farris JS (1969) Quantitative phyletics and the evolution of anurans. *Systematic Zoology* 18: 1-32.

Kluge AG (1989) A concern for evidence and phylogenetic hypothesis of relationships among *Epicrates* (Boidae, Serpentes). *Systematic Zoology* 38: 7-25.

Kluge AG (1990) Species as historical individuals. *Biological Philosophy* 5: 417-431.

Knowlton N (2000) Molecular genetic analyses of species boundaries in the sea. *Hydrobiologica* 420: 73-90.

Knox GA (1960) Littoral ecology and biogeography of the southern oceans. *Proceedings of the Royal society of London (ser B)* 152(949): 577-624.

Konishi K (1986) Larval devleopment of the stone crab, *Hapalogaster dentata* (De Haan 1844) (Crustacea: Decapoda: Anomura: Lithodidae) reared in the laboratory.

Journal of the Faculty of Science Hokkaido University, (4) *Zoology* 24:155-172.

Konishi K, Taishaku H (1994) Larval development in *Paralomis hystrix* (De Haan 1846) (Crustacea, Anomura, Lithodidae) under laboratory conditions. *Bulletin for the National Research Institute for Aquaculture* 23: 43-54.

Kruskal WH, Wallis WA (1952) Use of ranks in one-criterion variance analysis. *Journal of the American Statistical Association* 47(260): 583–621.

Kumar S, Tamura K, Nei M (2004) MEGA3: Integrated software for Molecular Evolutionary Genetics Analysis and sequence alignment. *Briefings in Bioinformatics* 5:150-163.

Kurata H (1960) Studies on the larva and post-larva of *Paralithodes camtschatica* III. The influence of temperature and salinity on the survival and growth of the larva. *Bulletin of the Hokkaido Region Fisheries Research Laboratory* 21: 9-14.

Kussakin OG (1973) Peculiarities of the geographical and vertical distribution of marine isopods and the problem of deep-sea fauna origin. *Marine Biology* 23(1): 19-34.

L

Lamb HH (1977) Climatic Instabilities: Climate: Past, Present and Future. 2 *Climatic History and the Future*. London: Methuen. 835 p.

Lamb MJ, Jablonka E (2005) *Evolution in four dimensions: genetic, epigenetic, behavioral, and symbolic variation in the history of life*. MIT Press Cambridge, MA.

Lear CH, Elderfield H, Wilson PA (2000) Cenozoic Deep-Sea Temperatures and Global Ice Volumes from Mg/Ca in Benthic Foraminiferal Calcite. *Science* 287(5451): 269-272.

Larkin MA, Blackshields G, Brown NP (2007) Clustal W and Clustal X version 2. *Bioinformatics* 23(21): 2947-2948.

Larsson SL, Nygård O (2001) Proposed Secondary Structure of Eukaryote Specific Expansion Segment 15 in 28S rRNA from Mice, Rats, and Rabbits. *Biochemistry* 40 (10): 3222–3231.

Latreille PA (1806) *Genera Crustaceorum et Insectorum secundum ordinem naturalem in familias doisposita, iconibus exemplurisque plurimis explicata*. Paris et Argentorati, Amand Koenig, Bibliopolam I: i-xviii, 1-280..

Lawver LA, Gahagan LM, Coffin MF (1992) The development of palaeoseaways around Antarctica. In: Kennett JP, Warnke DA (Eds) *The Antarctic Palaeoenvironment: a perspecitive on global climate change, Antarctic Research Series*. 56. AGU, Washington DC, 7-30 pp.

Levin LA, Etter RJ, Rex MA, Gooday AJ, Smith CR, Pineda J, Stuart CT, Hessler RR, Pawson D (2001) Environmental influences on regional deep-sea species diversity. *Annual review of Ecology and Systematics*. 32: 51-93.

Levinton JE (2001) *Marine Biology. Function, diversity, ecology.* Second Edition. Oxford university press, NY 515 p.

Lilliendhal K, Einarsson ST, Palsson J (2005) Two species of rare crabs, *Paralomis spectabilis* and *Paralomis bouvieri* (Crustacea: Decapoda), in Icelandic waters. *Natturufraedingurinn* 73(3-4): 89-94.

Lin JJ, Somero GN (1994) Temperature-dependent changes in expression of thermostable and thermolabile isozymes of cytosolic malate dehydrogenase in the eurythermal goby fish *Gillichthys mirabilis*. *Physiological Zoology* 68: 114-128.

Linnaeus C (1758, 1767) *Systema Naturae per regna tria naturae, secundum classes, ordines, genera, species, cum characteribus, differentiis, synonymis, locis.* Laurentii Salvii Holmiae [=Stockholm], vol I, 894 p; pt 2: 1069-1327.

Locarnini RA, Mishonov AV, Antonov JI, Boyer TP, Garcia HE (2006) *World Ocean Atlas 2005,* Volume 1*: Temperature. NOAA Atlas NESDIS 61* (S. Levitus [Ed]). US Government Printing Office, Washington, DC.

Loher T, Armstrong DA (2000) Effects of habitat complexity and relative larval supply on the establishment of early benthic phase red king crab (*Paralithodes camtschaticus* Tilesius 1815) populations in Auke Bay, Alaska. *Journal of Experimental Marine Biology and Ecology* 245: 83-109.

López Abellán LJ, Balguerías JA (1993) On the presence of *Paralomis spinosissima* and *P. formosa* in catches taken during the Spanish survey Antartida 8611. *CCAMLR Science* 1:165-173.

Lovrich GA, Vinuesa JH (1993) Reproductive biology of the false southern king crab (*Paralomis granulosa*, Lithodidae) in the Beagle Channel, Argentina. *Fishery Bulletin* 91(4): 664-675.

Lovrich GA, Vinuesa JH (1995) Growth of immature false southern king crab*, Paralomis granulosa* (Anomura: Lithodidae) in the Beagle Channel, Argentina. *Scientia Marina* 59(1): 87-94.

Lovrich GA (1999) Seasonality of larvae of Brachyura and Anomura (Crustacea, Decapoda) in the Beagle Channel, Argentina. *Scientia Marina* 63(Suppl 1): 347-354.

Lovrich GA, Perroni M, Vinuesa JH, Tapella F, Chizzini A, Romero MC (2002) Occurrence of *Lithodes confundens* (Decapoda: Anomura) in the intertidal of the southwestern Atlantic. *Journal of Crustacean Biology,* 22: 894-902.

Lovrich GA, Romero MC, Tapella F, Thatje S (2005) Distribution, reproductive and energetic conditions of decapod crustaceans along the Scotia Arc (Southern Ocean). *Scientia Marina* 69(S2): 183-193.

Lovrich GA, Thatje S (2006) Reproductive and larval biology of the sub-Antarctic hermit crab *Pagurus comptus* reared in the laboratory. *Journal of the Marine Biological Association of the United Kingdom* 86: 743-749.

Lunt DJ, Valdes PJ, Haywood A, Rutt AC (2008) Closure of the Panama Seaway during the Pliocene: implications for climate and Northern Hemisphere glaciation 30(1): 1-18.

M

Mace GM (2004) The role of taxonomy in species conservation. *Philosophical tranactions of the Royal Society of London B Biological Sciences* 359(1444): 711-719.

MacDonald JD, Pike RB, Williamson DI (1957) Larvae of the British species of *Diogenes, Pagurus, Anapagurus* and *Lithodes* (Crustacea, Decapoda). *Proceedings of the zoological Society of London.* 128: 209-257.

MacLeay WS (1838) On the brachyurous decapod Crustacea brought from the Cape by Dr Smith: Illustrations of the Annulosa of South Africa; being a portion of the objects of Natural History chiefly collected during an expedition to the interior of South Africa under the direction of Dr Andrew Smith in the years 1834, 1835, and 1836; fitted out by the "Cape of good hope association for exploring central Africa". Smith, Elder and Co., London, 53-71 pp.

Mackay DCG (1932) Description of a new species of crab of the genus *Paralithodes*. *Contributions to Canadian Biology and Fisheries* 27: 337-340.

Macpherson E (1982) A new species of *Paralomis* (Decapoda: Anomura) from the south eastern Atlantic. *Crustaceana* 43(2): 142-146.

Macpherson E (1984) Crustaceos Decapodos del Banco Valdivia (Atlantico sudoriental). *Res. Exp. Cient.* 12: 39-105.

Macpherson E (1988a) Revision of the Family Lithodidae Samouelle, 1819 (Crustacea: Decapoda: Anomura) in the Atlantic Ocean. *Monografias de Zoologia Marina* 2: 9-153.

Macpherson E (1988b) Three new species of *Paralomis* (Crustacea: Decapoda: Anomura: Lithodidae) from the Pacific and Antarctic Oceans. *Zoologica Scripta* 17(1): 69-75.

Macpherson E (1988c) Lithodid crabs from Madagascar and La Reunion (SW Indian Ocean) with descriptions of two new species. *Bulletin du Muséum national d'Histoire naturelle, section A* 10: 117-133.

Macpherson E (1989) A new species of the genus *Paralomis* from the Indian Ocean. *Scientia Marina* 53: 117-120.

Macpherson E (1990) Crustacea Decapoda: On some species of Lithodidae from the western Pacific. In Croznier A (Ed), Résultats des Campagnes MUSORSTOM, Volume 6. *Mémoires. Muséum National d'Histoire Naturelle* 145: 217-226.

Macpherson E (1991) A new species of the genus *Lithodes* (Crustacea: Decapoda: Lithodidae) from French Polynesia. *Muséum National d'Histoire Naturelle. Zoosystema* 13(1-2): 153-158.

Macpherson E (1992) *Paralomis phrixa* (Decapoda: Anomura: Lithodidae), a new species from northern Peru, and a key to the eastern Pacific species of the genus. *Crustaceana* 63: 313-317.

Macpherson E (1994) Occurrence of two lithodid crabs (Crustacea: Decapoda: Lithodidae) in the cold seep zone of the South Barbados accretionary prism. *Proceedings of the Biological Society of Washington* 107(3): 465-468.

Macpherson E (2001) New Species and new records of lithodid crabs (Crustacea, Decapoda) from the south western and central Pacific. *Zoosystema* 23(4): 797-805.

Macpherson E (2003) Some lithodid crabs (Crustacea: Decapoda: Lithodidae) from the Solomon Islands (SW Pacific Ocean), with the description of a new species. *Scientia Marina* 67(4): 413-418.

Macpherson E (2004) A new species and new records of lithodid crabs (Crustacea: Decapoda: Lithodidae) from the Crozet and Kerguelen Islands area (Subantarctica). *Polar Biology* 27(7): 418-422.

Macpherson E, Chan T-Y (2008) Some lithodid crabs (Crustacea: Decapoda: Lithodidae) from Taiwan and adjacent waters, with the description of one new species from Guam. *Zootaxa* 1924: 43-52.

Macpherson E, Wehrtmann IS (2010) Occurrence of lithodid crabs (Decapoda, Lithodidae) on the Pacific coast of Costa Rica, Central America. *Crustaceana* 83(2): 143-151

Maddison DR, Swofford DL, Wayne PM (1997) NEXUS: An Extensible File Format for Systematic Information. *Systematic Biology* 46(4): 590-621.

Makarov VV (1938) *in Fauna of the USSR (Crustacea).* pp.1-283 Israel Program for Scientific Translations. Jerusalem (1962).

Mallet J (1995) A species definition for the Modern Synthesis. *Trends in Ecology and Evolution* 10(7): 294-299.

Mallet J (2008) Mayr's view of Darwin: was Darwin wrong about speciation? *Biological Journal of Linnaean Society* 95: 3–16.

Margush T, McMorris FR (1981) Consensus n-trees. *Bulletin of Mathematical Biology* 43: 239-244.

Marincovich L, Brouwers EM, Hopkins DM, McKenna MC (1990) Late Mesozoic and Cenozoic paleogeographic and paleoclimatic history of the. Arctic Ocean Basin, based on shallow-water marine faunas and terrestrial vertebrates. In: Grantz A, Johnson L, Sweeney JF (Eds) *The Arctic Ocean region*. Geological Society of America, The Geology of North America, v. L, 403-426 pp.

Marsland DA (1938) The effects of high hydrostatic pressure upon cell division in *Arbacia* eggs. *Journal of Cellular and Comparative Physiology* 12: 57-70.

Marsland DA (1950) The mechanisms of cell division*;* temperature-pressure experiments on the cleaving eggs of *Arbacia punctulata. Journal of Cellular and Comparative Physiology* 36: 205-227.

Martin AP, Kessing BD, Palumbi SR (1990) Accuracy of Estimating Genetic Distance between species from short sequences of Mitochondrial DNA. *Molecular Biology and Evolution* 7(5): 485-488.

Martin AP (1999) Substitution rates of organelle and nuclear genes in sharks: implicating metabolic rate (again). *Molecular Biology and Evolution* 16: 996-1002.

Martin JW, Abele LG (1986) Phylogenetic relationships of the genus *Aegla* (Decapoda: Anomura: Aeglidae), with comments on Anomuran phylogeny. *Journal of Crustacean Biology* 6(3): 576-616.

Martin JW, Sánchez CA, Pereyra R (1997) Notes on the distribution of two lithodid crabs (Crustacea: Decapoda: Anomura) from off the coast of Baja California Sur, Mexico. *Bulletin of the Southern California Academy of Sciences* 96(2): 78-86.

Martin JW, Davis GE (2001) An updated classification of the recent Crustacea. *Contributions in Science* 39: 1-124

Martin JM (2005) Crustacean glossary **http://crustacea.nhm.org/glossary**

Masson DG (1996) Catastrophic collapse of the volcanic island of Hierro 15 ka ago and the history of landslides in the Canary Islands. *Geology* 24: 231-34.

Mayr E (1957) Species concepts and definitions. In: Mayr E (Ed) *The Species Problem*.

American Association for the Advancement of Science Publication No. 50.

Mayr E (1963) *Animal species and evolution.* Harvard University Press, Cambridge, MA 797 p.

Mayr E, Ashlock PD (1991) *Animal Species and Evolution.* Harvard University Press, Cambridge, MA.

McCaughran DA, Powell GC (1977) Growth model for Alaska king crab *Paralithodes camtschatica*. *Journal of the Fiseries. Research. Board Canada* 34: 989-995.

McClintock JB, Baker BJ (1997) A review of the chemical ecology of Antarctic marine invertebrates. *American Zoologist* 37:329–342.

McCulloch RD, Bentley MJ, Purves RS, Hulton NRJ, Sugden DE, Clapperton CM (2000) Climatic inferences from glacial and palaeoecological evidence at the last glacial termination, southern South America. *Journal of Quaternary Science* 15: 409-147.

McLaughlin PA (1983a) Hermit Crabs - are they really polyphyletic? *Journal of Crustacean Biology* 3: 608-621.

McLaughlin P (1983b). Internal Anatomy. In: Bliss (Ed) *The Biology of Crustacea volume* 5.

McLaughlin PA, Holthuis LB (1985) Anomura versus Anomala. *Crustaceana* 49: 204-209.

McLaughlin PA Lemaitre R (1997) Carcinization in the Anomura - fact or fiction*? Contributions to Zoology*. 67: 79-123.

McLaughlin PA, Anger K, Kaffenberger A, Lovrich G (2001) Megalopal and early juvenile development in *Lithodes santolla* (Molina 1782) (Decapoda: Anomura: Paguroidea:Lithodidae, with notes on zoeal variations. *Invertebrate Reproduction and Development* 40: 53-67.

McLaughlin PA, Lemaitre R, Tudge CC (2004) Carcinisation in the Anomura – fact or fiction? Evidence from larval, megalopal and early juvenile morphology. *Contributions to Zoology* 73(3): 1-49.

McLaughlin PA, Lemaitre R, Sorhannus U (2007) Hermit crab phylogeny: A reappraisal and its "fall-out". *Journal of Crustacean Biology* 27: 97-115.

McLaughlin PA, Lemaitre R (2009) A new classification for the Pylochelidae (Decapoda: Anomura: Paguroidea) and Description of New Taxa, *Raffles Bulletin of Zoology* S20: 159-231.

McTaggart S, Crease T (2009) Length Variation in 18S rRNA Expansion Segment 43/e4 of *Daphnia obtusa*: Ancient or Recurring Polymorphism? *Journal of Molecular Evolution* 69 (2):142-149.

Medlin LK, Elwood HJ, Stickel S, Sogin ML (1988) The charectarization of enzymatically amplified eukaryotic 16S-like rRNA coding regions. *Gene* 71: 491-499.

Medwar PB, Medwar JS (1983) *Aristotle to Zoos*. Harvard University Press, Cambridge MA.

Menzies RJ, George RY, Rowe GT (Eds, 1973) *Abyssal environment and ecology of the world oceans*. Wiley-Inter-science, New York and London 488 p.

Meredith MP, King JC (2005) Rapid climate change in the ocean west of the Antarctic Peninsula during the second half of the 20th century. *Geophysical Research Letters* 32: L19604.

Mestre NC, Thatje S, Tyler P (2009) The ocean is not deep enough: Pressure tolerances during the early ontogeny of the blue mussel, *Mytilus edulis*. *Proceedings of the Royal. Society B* 276: 717-726.

Metz EC, Palumbi SR (1996) Positive selection and sequence rearrangements generate extensive polymorphism in the gamete recognition protein bindin. *Molecular Biology and Evolution* 13: 397-406.

Miers EJ (1881) Account of the zoological collections made during the survey of HMS Alert in the straits of Magellan and the coast of Patagonia. Crustacea. *Proceedings of the Zoological Society of London.* 1881: 61-79.

Mickevich MF (1978) Taxonomic Congruence. *Systematic Biology* 27(2): 143-158.

Mileikovsky SA (1971) Types of larval development in marine bottom invertebrates, their distribution and ecological significance: a re-evaluation. *Marine Biology* 10: 193-213.

Miller P, Coffin H (1961) A laboratory study of the developmental stages of *Hapalogaster mertensii* (Brandt), Crustacea, Decapoda. *P.ublications, Department of Biological Scences, Walla Walla College*. 30: 1-18.

Milne-Edwards H, Lucas H (1841) Déscription des Crustacés nouveau ou peu connu. *Archives Mus. Hist. Nat. Paris* 2: 463-472, pls 24-27.

Milne-Edwards A, Bouvier EL (1894) Crustaces decapodes provenant des campagnes du yacht l'hirondelle. Premiere partie Brachyures et Anomures. *Résultats des Campagnes Scientifiques accomplies sur son yacht par Albert 1er Prince Souverain de Monaco* 7**:** 1-112.

Miquel JC, Arnaud PM, Dochi T (1985) Population structure and migration of the stone crab *Lithodes murrayi* in the Crozet Islands, sub-Antarctic Indian Ocean. *Marine Biology* 89(3): 263-269.

Miya M, Nishida M (1997) Speciation in the open ocean. *Nature* 389: 803-804.

Monteiro LR, Diniz-Filho AF, dos Reis SF, Araújo ED (2002) Geometric estimates of

heritability in biological shape. *Evolution* 56(3): 563-572.

Moore JK, Abbott MR, Richman JG (1999) Location and dynamics of the Antarctic Polar front from satellite sea surface temperature data. *Journal of Geophysics Research* 104: 3059-3073.

Morley SA, Belchier M, Dickson J, Mulvey T (2006) Reproductive strategies of sub-Antarctic lithodid crabs vary with habitat depth. *Polar Biology* 29: 581-584.

Morrison CL, Harvey AW, Lavery S, Tieu K, Huang Y, Cunningham CW (2002) Mitochondrial gene rearrangements confirm the parallel evolution of the crab-like form. *Proceedings of the Royal Society of London B* 269: 345-350.

Mullis KB, Falloma F, Scharf S, Saiki R, Horn G, Erlich H (1986) Specific enzymatic amplification of DNA in vitro: the polymerase chain reaction. *Cold Spring Harbor Symposia on Quantitative Biology* 51: 263-273.

N

Nakanishi T (1981) The effect of temperature on growth, survival and oxygen consumption of larvae and post larvae of *Paralithodes brevipes*. *Bulletin of the Japanese Sea Region Fisheries Research Laboratory* (Nissuiken Hokoku). 32: 49-56.

Nakanishi T (1985) The effects of the environment on the survival rate, growth and respiration of eggs, larvae and post larvae of king crab (*Paralithodes camtschatica*). *International King Crab Symposium*. Alaska Sea Grant Ankorage, Alaska. 167-185 pp.

Nei M, Kumar S, Takahashi K (1998) The optimization principle in phylogenetic analysis tends to give incorrect topologies when the number of nucleotides or amino acids used is small. *Proceedings of National Academy of Sciences* (*USA*) 95:12390-12397.

Nei M, Kumar S (2000) *Molecular Evolution and Phylogenetics*. Oxford University Press, New York.

Nelles L, Fang BL, Volckaert G, Vandenberghe A, and De Wachter R (1984) Nucleotide sequence of a crustacean 18S ribosomal RNA gene and secondary structure of eukaryotic small subunit ribosomal RNAs. *Nucleic Acids Research* 12: 8749–8876.

Nikolaev SD, Oskina NS, Blyum NS, Bubenshchikova NV (1998) Neogene–Quaternary variations of the 'Pole–Equator' temperature gradient of the surface oceanic waters in the North Atlantic and North Pacific. *Global and Planetary Change* 18(3-4): 85-111.

Nosil P, Crespi BJ (2006) Ecological divergence promotes the evolution of cryptic reproductive isolation. *Proceedings of the royal society of London B* 273: 991-997.

Nowlin WD, Klink JM (1986) The physics of the Antarctic Circumpolar Current. *Reviews of Geophysics* 24: 489-491.

O

Olivero EB, Martinioni DR (1996) Late Albian inoceramid bivalves from the Andes of Tierra del Fuego; age implications for the closure of the Cretaceous marginal basin. *Journal of Paleontology* 70(2): 272-274.

Omta AW, Dijkstra HA (2003) A physical mechanism for the Atlantic-Pacific flow reversal in the early Miocene. *Global and Planetary Change* 36: 265-276.

Oreskes N (2004) Beyond the Ivory Tower: The Scientific Consensus on Climate Change *Science* 306(5702): 1686.

Orlov Y, Ivanov B (1978) On the Introduction of the Kamchatka King Crab *Paralithodes camtschatica* (Decapoda: Anomura: Lithodidae) into the Barents Sea. *Marine Biology* 48: 373-375.

Orsi AH, Whitworth TW, Nowlin WD (1995) On the meridional extent and fronts of the Antarctic Circumpolar Current. *Deep-Sea Research* 42: 641-673.

Ortmann AE (1892) Die Decapoden-Krebse des Strassburger Museums, 4. Die Abteilungen Galatheidea und Paguridea. *Zoologisches Jarbuch* 6: 241-326.

P

Page RDM, Holmes EC (1998) *Molecular Evolution – A Phylogenetic Approach.* Blackwell Science Ltd. 346 p.

Palero F, Hall S, Clark PF, Johnston D, Mackenzie-Dodds J, Thatje S (2010) DNA extraction from formalin-fixed tissue: new light from the deep sea. *Scientia Marina* 74(3) in press.

Palumbi SR, Metz EC (1991) Strong reproductive isolation between closely related tropical sea urchins (genus *Echinometra*). *Molecular Biology and Evolution* 8(2):227-239.

Panella S, Michelato A, Perdicaro R, Magazzù G, Decembrini S, Scarazzato P (1991) A preliminary contribution to understanding the hydrological characteristics of the Strait of Magellan: Austral spring 1989. *Boll. Ocean. Teor. Appl.* 9:107-126.

Patel JK, Read CB (1982) *Handbook of the Normal Distribution.* Decker New York, NY.

Paterson HEH (1985) The recognition concept of species In: Vrba ES (Ed) *Species and Speciation* Transvaal Museum Monograph 4 Transvaal Museum, Pretoria. 21-29 pp.

Patterson C (1988). Homology in classical and molecular biology. *Molecular Biology and Evolution* 5: 603-625.

Patterson SL, Whitworth T (1990) Physical Oceanography. In: Glasby GP (Ed) *Antarctic Sector of the Pacific*. Elsevier Oceanographic Series, vol 51. Elsevier,

Amsterdam. 55-93 pp.

Paul AJ, Paul JM (1980) The effect of early starvation on later feeding success of king crab zoeae. *Journal of Experimental Marine Biology and Ecology* 44: 247-251.

Paul AJ, Paul JM, Coyle KO (1989) Energy sources for first feeding zoeae of king crab *Paralithodes camtschatica* (Tilesius) (Decapoda: Lithodidae). *Journal of Experimental Marine Biology and Ecology.* 130: 55-69.

Paul AJ, Paul JM (2001) The reproductive cycle of Golden King crab *Lithodes aequispinus* (Anomura: Lithodidae) *Journal of shellfish research* 20 (1): 369-371.

Pearse JS, McClintock JB, Bosch I (1991) Reproduction of Antarctic benthic marine invertebrates: tempos, modes and timing. *American Zoologist* 31: 65-80.

Peck LS, Conway LZ (2000) The myth of metabolic cold adaptation: oxygen consumption in stenothermal Antarctic bivalves. In Harper E, Taylor JD, Crame JA (Eds) *Evolutionary biology of the bivalvia* Vol 177 Geological society special publications London 441-450 pp.

Pereladov MV, Miljutin DM (2002) Population structure of Blue King Crab (*Paralithodes platypus*) in the North western Bering Sea. *Crabs in Cold Water Regions: Biology, Management, and Economics.* Alaska Sea Grant College Program 511-520.

Pérez-Losada M, Bond-Buckup G, Jara CG, Crandall KA (2004) Molecular Systematics and Biogeography of the Southern South American freshwater "Crabs" *Aegla* (Decapoda: Anomura: Aeglidae) using multiple heuristic tree search approaches. *Systematic Biology* 53(5): 767-780.

Peterson PA (1985) Virus-induced mutations in maize: on the nature of stress-induction of unstable loci. *Genetical Research* 46:207-217.

Pilgrim P (1973) Axial skeleton and musculature in the thorax of Hermit Crab *Pagurus bernhardus*. *Journal of the Marine Biological Association of the United Kingdom* 53: 363-396.

Pisani D, Benton MJ, Wilkinson M (2007) Congruence of Morphological and Molecular Phylogenies. *Acta Biotheoretica* 55(3):269-281.

Plotnick RE (1986) Taphonomy of a modern shrimp: implications for the arthropod fossil record. *PALAIOS* 1:286–293.

Pohle G (1989) Gill and embryo grooming in lithodid crabs: Comparative functional morphology based on *Lithodes maja*. In: Felgenhauer BE, Watling L, Thistle AB *Functional morphology of feeding and grooming in Crustacea*. 75-94 pp.

Poore HRR, Samworth NJ, White S, Jones M, McCave IN (2006) Neogene overflow of Northern Component Water at the Greenland-Scotland Ridge. *Geochemistry Geophysics. Geosystems*. 7: Q06010, doi:10.1029/2005GC001085.

Porter ML, Pérez-Losada M, Crandall KA (2005) Model-based multi-locus estimation of decapod phylogeny and divergence times. *Molecular Phylogenetics and Evolution.* 37(2):355-369.

Pörtner HO (2002) Climate variations and the physiological basis of temperature dependent biogeography: systemic to molecular hierarchy of thermal tolerance in animals. *Comparative Biochemistry and Physiology Part A* 132: 739-761.

Posada D, Crandall KA (1998) Modeltest: testing the model of DNA substitution. *Bioinformatics* 14 (9): 817-818.

Posada D, Buckley TR (2004) Model Selection and Model Averaging in Phylogenetics: Advantages of Akaike Information Criterion and Bayesian Approaches over likelihood ratio tests. *Systematic Biology* 53(5): 793-808.

Purves MG, Agnew DJ, Moreno G, Daw T, Yau C, Pilling G (2003) Distribution, demography, and discard mortality of crabs caught as bycatch in an experimental pot fishery for toothfish *Dissostichus eleginoides* in the South Atlantic. *Fisheries Bulletin* 101: 874-888.

R

Ramsey ATS, Smart CW, Zachos JC (1998) A model of early to mid-Miocene deep ocean circulation for the Atlantic and Indian Oceans. In Cramp A MacLeod CJ, Lee SV & Jones EJW (Eds) *Geological Evolution of Ocean Basins: Results from the Ocean drilling program.* Geological society, London. Special Publications. 131: 55-70.

Raupach MJ, Mayer C, Malyutina M, Wägele JW (2009) Multiple origins of deep-sea Asellota (Crustacea: Isopoda) from shallow waters revealed by molecular data. *Proceedings of the Royal Society B.* 276:799-808.

Raupach MJ, Wägele JW (2006) Distinguishing cryptic species in Antarctic Asellota (Crustacea: Isopoda) - a preliminary study of mitochondrial DNA in *Acanthaspidia drygalskii*. *Antarctic Science* 18:191-198.

Reid W, Watts J, Clarke S, Belchier M, Thatje S (2007) Egg development, hatching rhythm and moult patterns in reared *Paralomis spinosissima* (Decapoda: Anomura: Paguroidea: Lithodidae) from South Georgia waters (Southern Ocean). *Polar Biology* 30:1213-1218.

Retamal MA, Soto R (1993) Decapodos abisales de la zona Arica Iquique. *Estúdios Oceanológicos* 12: 111-129.

Retamal MA (1994) Los Lithodidae Chilenos. *Ans. Inst. Pat. Ser. Cs. Nts., Punta Arenas* (Chile). 21: 111-129.

Revuelta AG, Andrade VH (1978) Nueva localidad para *Lithodes murrayi* Henderson en el Pacifico Sud Oriental (Crustacea, Decapoda, Anomura, Lithodidae). *Noticario Mensual Mus. Nac. Hist. Nat. Chile.* 22: 2-4.

Rex MA (1981) Community structure in the deep-sea benthos. *Annual Review of Ecology and Systematics* 12: 331-351.

Rex MA, Stuart CT, Hessler RR, Allen JA, Sanders HL, Wilson GDF (1993) Global scale latitudinal patterns of species diversity in the deep-sea benthos. *Nature* 365: 636-639.

Richter S, Scholtz G (1994) Morphological evidence for a hermit crab ancestry of lithodids (Crustacea, Decapoda, Anomala, Paguroidea). *Zoologischer Anzeiger* 233: 187-210.

Ridley M (2004) *Evolution* Blackwell Science 3rd Edition 751 p.

Rintoul S R, Hughes CW, Olbers D (2001) The Antarctic Circumpolar Current system. In: Siedler G, Church J, Gould J (Eds) *Ocean Circulation and Climate*, London Academic Press 271-302 pp.

Robertson JD (1953) Further studies on ionic regulation in marine invertebrates. *Journal of Experimental Biology* 20:277-296.

Rohlf FJ, Marcus LF (1993) A revolution in morphometrics. *Trends in Ecology and Evolution* 8:129-132.

Rohlf FJ (1998a) Geometric morphometrics glossary. http:// life.bio.sunysb.edu/morph/glossary/gloss2.html.

Rohlf FJ (1998b) On applications of geometric morphometrics to studies of ontogeny and phylogeny. *Systematic Biology* 47:147-158.

Ronquist F, Huelsenbeck JP (2003) MRBAYES 3: Bayesian phylogenetic inference under mixed models. *Bioinformatics* 19:1572-1574.

Rzhetsky A, Nei M (1992) A simple method for estimating and testing minimum evolution trees. *Molecular Biology and Evolution* 9:945-967.

S

Saborowski R, Thatje S, Calcagno JA, Lovrich GA, Anger K (2006) Digestive enzymes in the ontogenetic stages of the southern king crab, *Lithodes santolla*. *Marine Biology* 149: 865-873.

Saiki R, Gelfand DH, Stoffel S, Scharf SJ, Higuchi R, Horn GT, Mullis KB, Erlich HA (1988) Primer directed enzymatic amplification of DNA with a thermostable DNA polymerase. *Science* 239: 487-491.

Sakai T (1971) Illustrations of 15 species of crabs of the family Lithodidae, two of which are new to science. *Researches on Crustacea* 4-5: 1-491.

Sakai T (1978) Decapod Crustacea from the Emperor Seamount chain. *Researches on Crustacea* 8(supplement): 1-39.

Sakai T (1980) New species of crabs of the families Lithodidae and Calappidae. *Researches on Crustacea* 10: 1-11.

Sakai K (1987) Biogeographical records of five species of the family Lithodidae from the abyssal valley off Gamoda-Misaki, Tokushima, Japan. *Researches on Crustacea* 16: 19–24.

Sakai K (1988) Record of *Neolithodes nipponensis* Sakai, 1971 (Lithodidae, Decapoda, Crustacea) from off cape Gamouda (Anan city, Tokushima). *Naturalists* 2:15-17.

Saitou N, Imanishi T (1989) Relative efficiencies of the Fitch-Margoliash, maximum-parsimony, maximum-likelihood, minimum-evolution and neighbour joining methods of phylogenetic tree construction and obtaining the correct tree. *Molecular Biology and Evolution* 6(5) 514-525.

Saitou N, Nei M (1987) The neighbour-joining method: a new method for reconstructing phylogenetic trees. *Molecular Biology and Evolution* 4: 406-425.

Sambrook J, Fritsch EF, Maniatis T (1989) *Molecular cloning. A laboratory manual.* 2nd edition. Cold Spring Harbor Laboratory Press, New York.

Samouelle G (1819) *The entemologist's useful compendium, or an introduction to the knowledge of British Insects.* London. 496 pp.

Sanger F, Nicklen S, Coulson AR (1977) DNA sequencing with chain-terminating inhibitors. Proceedings of the Nationall Academy of Sciences USA. 74(12): 5463-5467.

Schander C, Halanych KM (2003) DNA, PCR and formalinized animal tissue- a short review and protocols. *Organisms Diversity and Evolution* 3: 195-205.

Schmidt WL (1921) The marine decapod crustacea of California. *University of California Publications in Zoology.* 23: 1-470.

Schmidt-Nielsen K (1997) *Animal Physiology. Adaptation and Environment*. Fifth ed. Cambridge University Press, Cambridge 607 pp.

Schneider B, Schmittner A (2006) Simulating the impact of the Panamanian seaway closure on ocean circulation, marine productivity and nutrient cycling. *Earth and Planetary Science Letters* 246: 367-380.

Schnitker D (1980) Global paleoceanography and its deep water linkage to the Antarctic glaciation. *Earth-Science Reviews* 16: 1-20.

Schram FR (1986) *Crustacea*. Oxford University Press, Oxford. 606 p.

Senn S (2003) Bayesian, Likelihood and frequentist approaches to statistics. A comparison of methods. *Applied Clinical Trials* 2003: 35-38.

Shackleton NJ, Kennett JP (1974) Paleotemperature history of the Cenozoic and the initiation of Antarctic glaciation: oxygen and carbon isotope analyses at DSDP sites 277, 279 and 281. In: Kennett JP, Houtz RE et al (Eds) *Initial Reports of the Deep Sea Drilling Program* 29. US Govt Printing Office, Washington 743-755 pp.

Shapiro SS, Wilk MB (1965) An analysis of variance test for normality (complete samples). *Biometrika* 52: 591-611.

Shapiro SS, Wilk MB, Chen HJ (1968) An comparative study of various tests of normality. *Journal of the American Statistical Association* 63: 1343-1372.

Shikama K (1965) Effect of freezing and thawing on the stability of double helix DNA. *Nature* 207: 529-530.

Shirley TC, Shirley SM (1989) Temperature and salinity tolerances and preferences of red king crab larvae. *Marine Behaviour and Physiology* 16: 19-30.

Shirley TC, Shirley SM, Korn S (1990) Incubation period, molting and growth of female red king crabs: effects of temperature. Pp. 51-64. In Meltef B (Ed) *Proceedings of the International Symposium on King and Tanner Crabs.* Anchorage, Alaska USA. University of Alaska Sea Grant Program. Report No. AK-SK-90-4.

Shirley TC, Zhou S (1997) Lecithotrophic development of the golden king crab *Lithodes aequispinus* (Anomura: Lithodidae). *Journal of Crustacean Biology* 17(2): 207-216.

Shoemaker JS, Fitch WM (1989) Evidence from nuclear sequences that invariable sites should be considered when sequence divergence is calculated. *Molecular Biology and Evolution* 6(3):270-89.

Šidák Z (1967) Rectangular confidence region for the means of multivariate normal distributions. *Journal of the American Statistical Association* 62: 626-633.

Simpson GG (1961) Principles of Animal Taxonomy. Columbia University Press, NY.

Skroch P, Nienhuis J (1995) Impact of scoring error and reproducibility RAPD data on RAPD based estimates of genetic distance. *Theoretical and applied genetics* 91(6-7): 1086-1091.

Slatkin M (1987) Gene flow and the geographic structure of natural populations. *Science* 236: 787-792.

Sloan NA (1985) Distribution by depth of *Lithodes aequispina* and *Paralithodes camtschatica* confined in northern British Columbia fjords. *International King Crab Symposium*, Ancorage, Alaska 63 p.

Smetacek V, de Baar HJW, Bathmann UV, Lochte K, Rutgers Van der Loeff MM (1997) Ecology and biogeochemistry of the antarctic circumpolar current during

austral spring: a summary of southern ocean JGOFS cruise AnT X/6 of R.V. *Polarstern*. *Deep Sea Research* II: *Topical Studies in Oceanography* 44(1-2): 1-21.

Smith SI (1882) Report on the Crustacea. Part I. Decapoda. Reports on the results of dredging, under the supervision of Alexander Agassiz, on the east coast of the United States, during the summer of 1880, by the U.S. coast Survey Steamer <<Blake>>. *Bulletin of the Museum of Comparative Zoology, Harvard College.* 10: 1-108.

Sober E, (1980) Evolution, Population Thinking and Essentialism. *Philosophy of Science* 47: 350–383.

Sokal RR, Crovello TJ (1970) The biological species concept: A critical evaluation. *The American Naturalist* 104 (936): 127-153.

Somero GN (1992) Adaptations to high hydrostatic pressure. *Annual Review of Physiology* 54: 557-577.

Somerton DA (1985) The disjunct distribution of the blue king crab, *Paralithodes platypus*, in Alaska: some hypotheses. *Proceedings of the International King Crab Symposium* Anchorage, Alaska. 13-14 pp.

Spiridonov V, Türkay M, Arntz W, Thatje S (2006) A new species of the genus *Paralomis* from the Spiess seamount near Bouvet Island (Southern Ocean), with notes on habitat and ecology. *Polar Biology* 29: 137-146.

Starr M, Therriault J-C, Conan GY, Comeau M, Robichaud G (1994) Larval release in a sub-euphotic zone invertebrate triggered by sinking phytoplankton particles. *Journal of Plankton Research* 16: 1137-1147.

Stebbing TRR (1905) *South African Crustacea.* Part 3. Marine Investigations in South Africa IV: 21-123, pls, 10.

Stevens BG (1990) Temperature-dependent growth of juvenile red king crabs (*Paralithodes camtschatica*) and its effects on size-at-age and subsequent recruitment in the eastern Bering Sea. *Canadian Journal of Fisheries and Aquatic Science* 47: 1307-1317.

Stevens BG (2003) Settlement, substratum preference, and survival of red king crab *Paralithodes camtschaticus* (Tilesius, 1815) glaucothoe on natural substrata in the laboratory. *Journal of Experimental Marine Biology and Ecology* 283: 63-78.

Stevens BG (2006) Timing and duration of larval hatching for blue king crab *Paralithodes platypus* Brandt 1850, held in the Laboratory. *Journal of Crustacean Biology* 26(4): 495-502.

Stevens JR, Schofield CJ (2003) Phylogenetics and sequence analysis – some problems for the unwary. *Trends in Parasitology* 19(12): 582-588.

Stiassny MLJ (1992) Atavisms, phylogenetic character reversals, and the origin of evolutionary novelties. *Netherlands Journal of Zoology* 42 (2-3): 260-276.

Stone RP, Oclair CE, Shirley T (1992) Seasonal migration and distribution of female red king crabs in a south east Alaskan estuary. *Journal of Crustacean Biology* 12(4): 546-560.

Stone RP, Oclair CE, Shirley TC (1992) Seasonal migration and distribution of female red king crabs in a southeast Alaskan estuary. *Journal of Crustacean Biology* 12: 546-560.

Strathman RL (1978) The evolution and loss of feeding stages in marine invertebrates. *Evolution* 32: 894-906.

Sverdrup HU, Johnson MW, Fleming RH (1942) *The Oceans, Their Physics, Chemistry, and General Biology*. Prentice Hall, New York, 1087 pp.

Swindell SR, Plasterer TN (1997) SEQMAN Find Similar Sequence Data Analysis Guidebook 75-89 pp.

Swofford DL (2000) PAUP*. Phylogenetic Analysis Using Parsimony (*and Other Methods). Version 4 beta 10. Sinauer Associates, Sunderland, Massachusetts.

Sykes TJS, Ramsay ATS, Kidd RB (1998) Southern hemisphere Miocene bottom-water circulation: a palaeobathymetric analysis. In: Cramp A, Macleod CJ, Lee SV, Jones EJW (Eds) *Geological evolution of ocean basins*: *Results from the Ocean drilling program*. Geological Society, London, Special Publications 131: 43-54.

T

Takahashi K, Nei M (2000) Efficiencies of fast algorithms of phylogenetic inference under the criteria of maximum parsimony, minimum evolution, and maximum likelihood when a large number of sequences are used. *Molecular Biology and Evolution* 17:1251-1258.

Takeda M (1974) On three species of the Lithodidae from the central Pacific. *Bulletin of the National Museum of Nature and Science Series A - Zoology* 17: 200-212.

Takeda M, Ohta S (1979) A new species of the Lithodidae from Suruga Bay, central Japan. *Bulletin of the National Museum of Nature and Science Series A-Zoology* 5: 195-200.

Takeda M (1980) A new species of *Paralomis* from the East China Sea. *Annotated Zoology, Japan* 53: 42-45.

Takeda M, Hiramoto K, Suzuki Y (1984) Additional material of *Paralomis cristata* Takeda et Ohta (Crustacea, Decapoda) from Suruga Bay, Japan. *Bulletin of the Biogeographical Society of Japan*. 39(5): 27-31.

Takeda M, Hatanaka H (1984) Records of Decapod crustaceans from the Southwestern Atlantic collected by the Japanese fisheries research trawlers. *Bulletin of the National Science Museum Tokyo, Series A*. 10(1): 11-17.

Takeda M (1985) A new species of *Paralomis*, the crab-shaped anomura from the Kyushu-Palu submarine ridge. *Bulletin of the National Science Museum Tokyo Series A (Zoology)*, 11: 137–140.

Takeda M, Hashimoto J (1990) A new species of the genus Paralomis from Minami-Ensei Knoll in the Mid Okinawa Trough. *Bulletin of the National Science Museum Tokyo Series A* (*Zoology*) 16: 79–88.

Takeda M, Nagai S (2004) Four species of giant crustaceans from the Indonesian depths, with description of a new species of the family Lithodidae. *Bulletin of the National Science Museum Series A (Zoology)* 30(1): 9–21.

Takeda M, Bussarawit S (2007) A new species of the genus *Paralomis* White, 1856 (Crustacea: Decapoda: Anomura: Lithodidae) from the Andaman Sea. *Bulletin of the National Museum of Nature and Science Series A-Zoology* 33(2): 51-59.

Tamura K, Nei M (1993) Estimation of the number of nucleotide substitutions in the control region of mitochondrial DNA in humans and chimpanzees. *Molecular Biology and Evolution* 10: 512-526.

Tamura K, Kumar S (2002) Evolutionary distance estimation under heterogeneous substitution pattern among lineages. *Molecular Biology and Evolution* 19: 1727-1736.

Tansey MR, Brock TD (1972) The upper temperature limit for eukaryotic organisms. *Proceedings of the National Academy of Science USA*. 69: 2426-2428.

Tavaré S (1986) Some Probabilistic and Statistical Problems in the Analysis of DNA Sequences. *American Mathematical Society: Lectures on Mathematics in the Life Sciences* 17: 57–86.

Tavares MS (1990) *Paralomis formosa* Henderson 1888 from off southeastern Brazilian coast (Crustacea, Decapoda, Lithodidae). *Zoologica* 340: 1-3.

Templeton AR (1989) The meaning of species and speciation: A genetic perspective. In Otte D, Endler JA (Eds) *Speciation and its consequenses* Sinauer Associates, Sunderland MA. 3-27 pp.

Thackray GD (2001) Extensive Early and Middle Wisconsin Glaciation on the Western Olympic Peninsula, Washington, and the Variability of Pacific Moisture Delivery to the Northwestern United States. *Quaternary Research* 55 (3): 257-270.

Thatje S, Calcagno JA, Lovrich GA, Sartoris FJ, Anger K (2003) Extended hatching periods in the Subantarctic lithodid crabs *Lithodes santolla* and *Paralomis granulosa* (Crustacea: Decapoda). *Helgoland Marine Research* 57: 110-113.

Thatje S, Fuentes V (2003) First record of anomuran and brachyuran larvae from Antarctic waters. *Polar Biology* 26: 279-282.

Thatje S (2004) Reproductive trade offs in benthic decapod crustaceans of high southern latitudes: tolerance of cold and food limitation. *Berichte zur Polar- und Meeresforschung* 483: 1-183.

Thatje S, Arntz WE (2004) Antarctic reptant decapods: more than a myth? *Polar Biology* 27:195-201.

Thatje S, Anger K, Calcagno JA, Lovrich GA, Pörtner HO, Arntz WE (2005) Challenging the cold: crabs reconquer the Antarctic. *Ecology* 86 (3): 619-625.

Thatje S, Lörz AN (2005) First record of lithodid crabs from Antarctic waters off the Balleny Islands. *Polar Biology* 28: 334-337.

Thatje S, Hall S, Held C., Hauton C, Tyler P (2008) Encounter of *Paralomis birsteini* on the continental slope of Antarctica, sampled by ROV. *Polar Biology* 31(9): 1143-1148.

Thatje S, Mestre NC (2010) Energetic changes throughout lecithotrophic larval development in the deep-sea lithodid crab *Paralomis spinosissima* from the Southern Ocean. *Journal of Experimental Marine Biology and Ecology* (doi:10.1016/j.jembe.2010.02.015).

Thistle D (2003) The Deep Sea Floor: an overview. In P Tyler (Ed) *Ecosystems of the world*. 2nd edition. 5-37 pp.

Thiel H, Pörtner HO, Arntz WE (1996) Deep-sea and extreme shallow-water habitats: affinities and adaptations. In: Uiblein F, Ott J, Stachowitsch M (Eds) *Deep-sea and extreme shallow-water habitats: affinities and adaptations.* Biosystematics and Ecology Series 11: 183-219.

Thiele K (1993) The holy grail of the perfect character: the cladistic treatment of morphometric data. *Cladistics* 9: 275-304.

Thomas DJ (2004) Evidence for deep-water production in the North Pacific Ocean during the early Cenozoic warm interval. *Nature* 430: 65-68.

Thompson JD, Higginsand, DG, Gibson TJ (1994) Clustal W. *Nucleic Acids Research.* 22: 4673–4680.

Thorson G (1950) Reproduction and larval ecology of marine bottom invertebrates. *Biological Reviews* 25(1):1-45.

Toggweiler JR, Samuels B (1995) Effect of Drake Passage on the global thermohaline circulation. *Deep-Sea Research I* 42: 477-500.

Toggweiler JR, Bjornsson H (1999) Drake Passage and palaeoclimate. *Journal of Quaternary Science* 15:319-328.

Tomczak M, Godfrey SJ (1994) *Regional Oceanography: an Introduction*. Pergamon

Press, New York, 422 p.

Truesdale GA, Downing AL, Lowden GF (1955) The solubility of oxygen in pure water and sea water. *Journal of Applied Chemistry* 5: 53-62.

Tudge CC, Jamieson BGM, Sandberg L, Erséus C (1998) Ultrastructure of the mature spermatozoon of the king crab *Lithodes maja* (Lithodidae, Anomura, Decapoda): further confirmation of a lithodid-pagurid relationship. *Invertebrate Biology* 117(1): 57-66.

Turelli M, Barton NH, Coyne JA (2001) Theory and Speciation. *Trends in Ecology and Evolution* 16(7): 330-343.

Tweedie S, Ashburner M, Falls K, Leyland P, McQuilton P, Marygold S, Millburn G, Osumi-Sutherland D, Schroeder A, Seal R, Zhang H, and The FlyBase Consortium (2009) FlyBase: enhancing Drosophila Gene Ontology annotations. *Nucleic Acids Research* 37: D555-D559; doi:10.1093/nar/gkn788.

Tyler PA, Young CM (1998) Temperature and pressure tolerances in dispersal stages of the genus *Echinus* (Echinodermata: Echinoidea): prerequisites for deep-sea invasion and speciation.*Deep-Sea Research II* 45: 253-277.

Tyler PA, and participants (2007) NERC Cruise report. James Clark Ross Cruise No. 166 (in association with JCR cruise no. 157). 18pp (unpublished report).

U

Ubero-Pascal N, Fortuño J, Puing M (2005) New application of air-drying techniques for studying Ephermeroptera and Plecoptera eggs by scanning electron microscopy. *Microscopy Research and Techniques* 68: 264-271.

V

Van Dover CL, Factor JR, Gore RH (1982) Developmental patterns of larval scaphognathites: an aid to the classification of anomuran and brachyuran Crustacea. *Journal of Crustacean Biology* 2(1): 48-53.

Van Dover CL (2000) *The ecology of deep-sea hydrothermal vents*. Princeton University Press 424 p.

Vinuesa JH, Ferrari L, Lombardo RJ (1985) Effect of temperature and salinity on larval development of the southern king crab (*Lithodes antarcticus*). *Marine Biology* 85: 83-87.

Vinuesa JH, Lovrich GA, Tapella F (1999) New localities for Crustacea: Decapoda in the Magellan region, southern South America. *Scientia Marina* 63(Supp. 1): 321-323.

Vivek BS, Simon PW (1999) Phylogeny and relationships in Daucus based on restriction fragment length polymorphisms (RFLPs) of the chloroplast and mitochondrial genomes. *Euphytica* 105(3): 183-189.

Von der Heydt A, Dijkstra HA (2006) Effect of ocean gateways on the global ocean circulation in the late Oligocene and early Miocene. *Palaeoceanography* 21: 18.

W

Wägele J-W (1987) On the reproductive biology of *Ceratoserolis trilobitoides* (Crustacea: Isopoda): Latitudinal variation of fecundity and embryonic development. *Polar Biology* 7: 11-24.

Waide RB, Willig MR, Steiner CF, Mittelback G, Gough L (1999) The relationship between productivity and species richness. *Annual Review of Ecology, Evolution and Systematics* 30: 257-300.

Watrous LE, Wheeler QD (1981) The outgroup comparison method of character analysis. *Systematic Zoology* 30(1): 1-11.

Watts J, Thatje S, Clarke S, Belchier M (2006) A description of larval and early juvenile development in *Paralomis spinosissima* (Decapoda: Anomura: Paguroidea: Lithodidae) from South Georgia waters (Southern Ocean). *Polar Biology* 29: 1028-1038.

Wei W, Wise SW Jr (1992) Selected Neogene calcarious nanofossil index taxa of the Southern Ocean: biochronology, biometrics and paleooceanography. In: Wise SW, Schilich R et al. (Eds.) *Proceedings of the Ocean drilling program. Scientific Results. 120.* Ocean Drilling Program, College Station, TX 523-537 pp.

Weston EM (2003) Evolution of ontogeny in the hippopotamus skull: using allometry to dissect developmental change. *Biological Journal of the Linnean Society* (2003) 80: 625-638.

Wheeler (1995) Systematics, the scientific basis for inventories of biodiversity. *Biomedical and Life Sciences* 4(5): 476-489.

White A (1856) Some remarks on Crustacea of the genus *Lithodes*, with a brief description of a species apparently hitherto unrecorded. *Proceedings of the Zoological Society of London* 24: 132–135.

Whittaker ET, Robinson G (1967) The normal frequency distribution. In *The Calculus of Observation: A treatise on Numerical Mathematics* 4th Ed. New York: Dover, 164-208 pp.

Wiens JJ (Ed, 2000) *Phylogenetic analysis of morphological data*. Smithsonian Institution press. Washington DC 220 pp. ISBN 1-56098-816-9

Williams JG, Kubelik AR, Livak KJ, Rafalski JA, Tingey SV (1990) DNA polymorphisms amplified by arbitrary primers are useful as genetic markers. *Nucleic Acids Research* 25 18(22): 6531-6535.

Williams AB, Smith CR, Baco AR (2000) New species of *Paralomis* (Decopoda, Anomura, Lithodidae) from a sunken whale carcass in the San Clemente basin off

southern California. *Journal of Crustacean Biology* 20(S2): 281-285.

Wilson GDF, Hessler RR (1987) Speciation in the Deep Sea. *Annual Review of Ecology and Systematics* 18: 185-207.

Wilson R (1990) Paralomis otsuae, a new species of (Decapoda: Anomura) from deep water off the Chilean coast. Crustaceana 58: 130-135.

Wishner KF, Ashjian CJ, Gelfman C, Gowing MM, Kann L, Levin LA, Mullineaux LS, Saltzman J (1995) Pelagic and benthic ecology of the lower interface of the Eastern Tropical Pacific oxygen minimum zone. *Deep Sea Research Part I: Oceanographic Research Papers* 42(1): 93-115.

Wolfe KH, Sharp PM, Li WH (1989) Mutation rates differ among regions of the mammalian genome. *Nature* 337: 283-285.

Woll AK, Burmeister A (2002). Occurance of Northern Stone Crab (*Lithodes maja*) at Southeast Greenland. *Crabs in Cold Water Regions: Biology, Management and Economics.* Alaska Sea Grant College Program AK-SG-02-01. 733-748 pp.

Woodruff F, Savin SM (1989) Miocene deep-water oceanography. *Palaeooceanography* 4: 87-140.

Wright JD, Miller KG, Fairbanks RG (1992) Early and middle Miocene stable isotopes: Implications for deep water circulation. *Palaeoceanography* 7: 357-389.

Wu S-H, Chan T-Y, Yu H-P (1998) First record of the King Crab *Lithodes turritus* Ortmann 1892 (Decapoda, Lithodidae) in Taiwanese waters. *Crustaceana* 71(7): 818-823.

Wu C-I (2001) The genic view of the process of speciation. *Journal of Evolutionary Biology* 14: 851-865, 899-891.

Y

Yaldwyn JC (1970) The stone crab *Lithodes murrayi* Henderson: the first New Zealand record. *Records of the Dominion Museum* 6(17):275-284.

Yang Z, Goldman N, Friday A (1994) Comparison of models for nucleotide substitution used in maximum likelihood phylogenetic estimation. *Molecular Biology and Evolution* 11: 316-324.

Yang Z (1994) Maximum likelihood phylogenetic estimation from DNA sequences with variable rates over sites: approximate methods. *Journal of Molecular Evolution* 39: 306-314.

Yang Z (1995) A space-time process model for the evolution of DNA sequences. *Genetics* 139: 993-1005.

Yang Z (1996) Among-site rate variation and its impact on phylogenetic analysis. *Trends in Ecology and Evolution* 11: 367-324.

Young CM, Cameron JL (1989) Developmental rate as a fuction of depth in the bathyal echinoid *Linopneustes longispinus* In: Ryland JS, Tyler PA (Eds) *Reproduction, genetics and distribution of marine organisms.* Olsen & Olsen 225-231 pp.

Young JS, Peck LS, Matheson T (2006) The effects of temperature on walking and righting in temperate and Antarctic crustaceans. *Polar Biology* 29(11) 978-987.

Yumao TWF, Zhicheng L (1984) A new species of Lithodidae (Crustacea, Anomura) from the east China sea. *Zoological Research* 4: 331-332.

Z

Zachos J, Pagani M, Sloan L, Thomas E, Billups K (2001) Trends, rhythms, and aberrations to global climate 65 Ma to Present. *Science* 292: 686-693.

Zaklan SD (2000) A case of reversed asymmetry in *Lithodes maja* (Linnaeus, 1758) (Decapoda, Anomura, Lithodidae). *Crustaceana* 73: 1019-1022.

Zaklan SD (2002a) *Evolutionary History and Phylogeny of the Family Lithodidae*. PhD Thesis, University of Alberta

Zaklan SD (2002b) Review of the family Lithodidae (Crustacea: Anomura: Paguroidea): Distribution, biology, and fisheries. In: Paul AJ, Dawe EG, Elner R, Jamieson GS, Kruse GH, Otto RS, Sainte-Marie B, Shirley TC, Woodby D (Eds) *Crabs in cold water regions: biology, management, and economics.* University of Alaska Sea Grant College Program AK-SG-02–01, Fairbanks, pp 751–845.

Zelditch ML, Fink WL, Swiderski DL. (1995) Morphometrics, homology and phylogenetics: Quantified characters as synapomorphies. *Systematic Biology* 44(2): 179-189.

Zenkevitch L (1963) *Biology of the Seas of USSR*. George Allen and Unwin Ltd, London.

Ziegler TA, Forward RB (2005) Larval release rhythm of the mole crab *Emerita talpoida* (Say). *Biological Bulletin* 209: 194-203.

Zhou S, Shirley TC, Kruse GH (1998) Feeding and growth of the red king crab *Paralithodes camtschaticus* under laboratory conditions. *Journal of Crustacean Biology* 18(2): 337-345.

APPENDICES

Appendix A: Taxonomic list of lithodid species.

The Hapalogastrinae contain genera *Dermaturus* Brandt 1850, *Hapalogaster* Brandt 1850, *Oedignathus* Benedict 1894, *Acantholithodes* (Stimpson) and *Placetron* Schalfeew 1892; a total of 9 species. The Lithodinae contain genera *Lithodes* Latreille 1806, *Lopholithodes* Brandt 1848, *Paralithodes* Brandt 1848, *Cryptolithodes* Brandt 1848, *Rhinolithodes* (1 species: *R. wosnessenski*) Brandt 1848, *Phyllolithodes* Brandt 1848, *Paralomis* White 1856, *Neolithodes* A. Milne Edwards & Bouvier 1894, *Glyptolithodes* Faxon 1895, and *Sculptolithodes* Makarov 1934; a total of 108 species.

Lithodidae 117 species
***= used only in molecular studies**
^= used only in morphological phylogeny
****= used in both molecular and morphological studies**

Hapalogastrinae: 9 species
Oedignathus inermis Stimpson 1860
Acantholithodes hispidus Stimpson 1860
Dermaturus mandtii Brandt 1850
Placetron wosnessenskii Schalfeew 1892
Placetron forcipatus Benedict 1895
Hapalogaster dentata Haan 1849
H. mertensii Brandt 1850
H. grebnitzkii Schalfeew 1892
H. cavicauda Stimpson 1859

Lithodinae: 108
(10 below) + 21 *Lithodes*, 61 extant *Paralomis,* 6 *Paralithodes*, 10 *Neolithodes*.
Glyptolithodes cristatipes Faxon 1893
Lopholithodes mandtii Stimpson 1859
Lopholithodes foraminatus Brandt 1848
Phyllolithodes papillosus Brandt 1848
Sculptolithodes derjugini Makarov 1934
Rhinolithodes wosnessenskii Brandt 1848
Cryptolithodes typicus Brandt 1848
C. sitchensis Brandt 1853
C. expansus Miers 1879

C. brevifrons

21 species *Lithodes* Latreille 1806

****Lithodes aequispina***
Benedict 1894
=*Paralithodes longirostris* (Navosov Lavroff 1929)

Lithodes ceramensis Takeda & Nagai 2004

****Lithodes confundens*** Macpherson 1988
Macpherson 1988a, fig 24, pls 11, 12.

****Lithodes couesi*** Benedict 1894

****Lithodes ferox***
Filhol 1885
=Pseudolithodes pyriformis Birstein & Vinogradov 1972
=Lithodes murrayi in Kensley 1980 p. 22 (not Henderson 1888)
=*Lithodes tropicalis* A. Milne Edwards 1833, p. 13

Lithodes formosae Ahyong & Chan 2010
Lithodes sp. Macpherson & Chan 2008: 47-48; Ahyong & Chan 2010, figs 1-4.

^***Lithodes galapagensis*** Hall & Thatje 2009

****Lithodes longispina*** Sakai 1971

****Lithodes maja*** Linnaeus 1758
Cancer maja Linnaeus 1758, p. 269
Lithodes maia Samouelle 1819, p. 90
Lithodes maja Ortmann 1898 pl. 52; Holthuis 1950, figs 51-53; Williams 1984 fig 166; Macpherson 1988a figs 25, 26, pl. 13.

^***Lithodes mamillifer*** Macpherson 1988
= *Lithodes murrayi* Kensley 1976 off Natal

^*Lithodes manningi* Macpherson 1988
Macpherson 1988a figs 27, 28, pl. 14.

^*Lithodes megacantha* Macpherson 1991

****Lithodes murrayi*** Henderson 1888

Lithodes nintokuae Sakai 1978

Lithodes panamensis Faxon 1893
Faxon 1895, 50 pl. 10 figs. 1 a-c; Macpherson & Wehrtmann 2010 fig. 1
=*Phyester macrocephalus* Linnaeus

Lithodes paulayi Macpherson & Chan 2008

^*Lithodes richeri* Macpherson 1990

****Lithodes santolla*** Molina 1782
Cancer santolla Molina 1782 p. 207
Lithodes antarctica Jaquinot 1844, pls 7, 8, figs 9-14
Lithodes antarcticus White 1847, p. 56
Pseudolithodes zenkevitchi Birstein & Vinogradov 1972, p. 356, figs 5, 6.
Lithodes santolla Philippi 1867, p. 777; Macpherson 1988a figs 21-23, pls. 9, 10.

Lithodes turkayi Macpherson 1988
=*Lithodes murrayi* Campodicono 1972; Revuelta & Andrade 1978; Retamal 1981; Takeda 1984 (not Henderson 1888).

Lithodes turritus Ortmann 1892

Lithodes unicornis Macpherson 1984
Macpherson 1984 figs 20-23; Macpherson 1988a, fig 32, plate 17D.

Lithodes wiracocha Haig 1974
Haig 1974, fig.1; Macpherson & Wehrtmann 2010, fig. 2

6 species *Paralithodes* Brandt 1848

****Paralithodes brevipes*** A. Milne Edwards & Lucas 1841
=*Lithodes brevipes* Milne Edwards & Lucas 1841, Benedict 1894,
=*Lithodes camtschaticus* Richters p404 fig 9 and 10

****Paralithodes camtschatica*** Tilesius 1815
=*Maja camtschatica* Tilesius 1815
=*Lithodes camtschaticus* Latreille, Benedict
=*Lithodes spinosissimus* Brandt 1857

^***Paralithodes californiensis*** Benedict 1895

****Paralithodes platypus*** Brandt 1850

^***Paralithodes rathbuni*** Benedict 1895

Paralithodes rostrofalcatus MacKay 1932

10 species *Neolithodes* A. Milne Edwards & Bouvier 1894

Neolithodes agassizii Smith 1882
Lithodes agassizii Smith 1882, p. 8 pl 1, fig. 1 (not fig 2, = *N. grimaldii*)
Not Smith 1884, p 54; Smith 1886, p. 34, pl. 3, Figs 1, 2; Henderson 1888 p. 42 (= *N. grimaldii*)
Neolithodes agassizii Macpherson 1988a figs 13, 14, 15A, plate 2C.

****Neolithodes asperrimus*** Barnard 1947
Barnard 1950 p. 411, Figs 77d-77f; Macpherson 1983 p. 5, figs 1,2; Macpherson 1988a figs 15D, 16, plates 3, 4.

****Neolithodes brodiei*** Dawson & Yaldwyn 1970

Neolithodes capensis Stebbing 1905
Stebbing 1905 pls. 19,20; Barnard 1950 figs 77a-77c; Macpherson 1988 fig 17, pl. 5.

Neolithodes diomedeae Benedict 1894
Lithodes diomedeae Benedict 1894

Neolithodes diomedeae Baez et al 1986 p 106, fig.1; Macpherson 1988a figs 12, 15c, plates 1, 2A,B.
= *Neolithodes martii* Birstein & Vinogradov 1972 p361, Figs 8, 9.

Neolithodes duhameli

Neolithodes grimaldii A. Milne Edwards & Bouvier 1894
Lithodes agassizii Smith 1882, p. 8 pl. I, fig. 2 (juvenile only); Smith 1886 p. 34, pl. 3, figs 1, 2 (not *N. agassizii* Smith 1882).
Lithodes goodei Benedict 1894, p. 479.
Neolithodes grimaldii Macpherson 1988a figs 15B, 18, pl. 6, 7.

Neolithodes nipponensis Sakai 1971

Neolithodes vinogradovi Macpherson 1988a
Macpherson 1988a, fig. 19, pl. 8.

Neolithodes yaldwyni Ahyong & Dawson 2006

62 species *Paralomis* (61 extant)

****Paralomis aculeata*** Henderson 1888
Paralomis aculeatus Henderson 1888: p. 45, pl 5, fig. 1.
Paralomis aculeata Spiridonov et al 2006, p. 144 fig. 6

****Paralomis africana*** Macpherson, 1982

Paralomis alcockiana Hall & Thatje 2009

****Paralomis anamerae*** Macpherson, 1988a

^***Paralomis arae*** Macpherson, 2001

Paralomis arethusa Macpherson, 1994

Paralomis aspera Faxon, 1893

Paralomis aspera Faxon, 1893, p. 164; Faxon, 1895, pl. 8; Bouvier, 1896, p. 26; del Solar, 1972, p. 5,14.

Leptolithodes asper Faxon, 1895, p. 47.

****Paralomis birsteini*** Macpherson 1988b

Paralomis spectabilis; Birstein & Vinogradov, 1967 p. 390, figs 1, 2 (not Hansen 1908).

Paralomis birsteini Macpherson, 1988b, p. 72, figs 4, 5a-e; Macpherson 2004, p. 421; Ahyong & Dawson 2006; Thatje et al 2008, p. 1146.

Paralomis bouvieri Hansen 1908

Paralomis bouvieri Hansen, 1908, p. 24, pl. 2, figs 2a-f; Stephensen, 1912, p. 578; Birstein & Vinogradov, 1967 (in list); Takeda, 1974 (in list); Takeda et al 1984, (in list); Dawson & Yaldwyn, 1985 (in list); Macpherson, 1988, p. 85, fig. 38.

****Paralomis ceres*** Macpherson 1989

Paralomis ceres Macpherson, 1989, p. 117, figs 1-2.

Paralomis chilensis Andrade 1980

****Paralomis cristulata*** Macpherson 1988a

*****Paralomis cristata*** Takeda & Ohta 1979

Paralomis cristata Takeda & Ohta 1979, p. 195, pls 1-3.

****^Paralomis cubensis*** Chace 1939

Paralomis danida Takeda 2007

****^Paralomis dawsoni*** Macpherson 2001

Paralomis debodeorum † Feldmann 1998

Paralomis diomedeae Faxon, 1893

Faxon 1893, 1895 pl. 7 figs 3, 3a, b; Bouvier 1896; Haig 1974; Macpherson, 1992 313; Macpherson, 2010 fig. 3.

***Paralomis dofleini** Balss 1911

Paralomis dofleini Balss 1911, p. 8, figs. 16, 17; Sakai 1971, p.18, pl. 7, fig. 1; pl 12.

***Paralomis elongata** Spiridonov 2006

Paralomis elongata Spiridonov, 2006, p. 138, figs 1-5.

****Paralomis erinacea** Macpherson 1988

Macpherson, 1988a: p. 82, figs 36A, 37; plate 19A.

****Paralomis formosa** Henderson 1888

Paralomis formosus Henderson, 1888, p. 46, pl. 5, fig. 2

Paralomis formosa Bouvier, 1896, p. 26; Boschi et al 1981, p. 244; Macpherson, 1988a, p. 88, figs 36B, 40, pl. 20.

Paralomis spectabilis Birstein & Vinogradov, 1972, p. 352 (not Hansen, 1908)

*** Paralomis granulosa** Jaquinot 1847

Lithodes granulosa Jaquinot, 1847: figs 15-21, pl. 8.

Lithodes granulosus White, 1847: p. 56.

Lithodes granulata Jaquinot, 1853: p. 94.

Lithodes verrucosa Dana, 1852: p. 428; Dana, 1855: plate 26, fig. 16; Cunningham, 1871: p. 494.

Paralomis verrucosa Bouvier, 1895: p. 187, plate 13, fig. 3; Bouvier, 1896: p. 26.

Paralomis granulosa White, 1856: p. 134.

^Paralomis grossmani Macpherson 1988

^Paralomis haigae Eldredge 1976

Paralomis hirtella de Saint Laurent & Macpherson 1997

Paralomis hystrixoides Sakai 1980

Paralomis histrix De Haan 1849

Lithodes histrix De Haan 1849, p. 218, pl. 48, figs. 1a-c.

Acantholithus hystrix Strimpson 1858, p. 231; Bouvier 1894, p. 182, pl. 11: figs 8, 14, pl.12: figs 9, 20; Stimpson, 1896, p. 25; Doflein 1902, p. 948; Doflein, 1906, p. 236; Balss, 1913, p. 75; Yokoya, 1933, p. 95; Miyake, 1965, p. 650, fig. 1104.
Paralomis hystrix Ortman, 1892, p. 321, pl. 12, fig. 27; Sakai 1971, p. 17.

^*Paralomis inca* Haig 1974

Paralomis indica Alcock & Anderson 1899

Paralomis investigatoris Alcock & Anderson 1899

Paralomis jamsteci Takeda & Hashimoto 1990

Paralomis japonica Balss 1911

Paralomis kyushupalauensis Takeda 1985

Paralomis longidactyla Birstein & Vinogradov 1972

Paralomis longipes Faxon 1893
Paralomis longipes Faxon 1893 p. 165; Faxon 1895, pl. 9; Bouvier, 1896, p. 25; del Solar, 1972, p. 5, 14; Haig 1974, p. 155.
Leptolithodes longipes Faxon 1895, p. 48.

Paralomis makarovi Hall & Thatje 2009

Paralomis manningi Williams 2000

Paralomis medipacifica Takeda 1974

^*Paralomis mendagnai* Macpherson 2003

Paralomis microps Filhol 1884
Paralomis microps Filhol 1884, p. 330, fig p. 329.
Rhinolithodes biscayensis A. Milne Edwards & Bouvier, 1894; Bouvier, 1895, p. 187, 199, pl. 11: fig 10, 18; pl 12: figs 12, 23, 30, 32; pl. 13: fig. 5; Bouvier, 1896, p. 26; A.

Milne Edwards & Bouvier, 1900, p. 269, pl 27, fig 21; Macpherson, 1988, p. 113, fig 52.

****Paralomis multispina*** Benedict 1894
Leptolithodes multispina Benedict 1894: p. 484; Rathbun, 1904: p. 165
Paralomis multispina Schmitt, 1921: p. 159, pl. 23; pl. 30, figs 7, 8; Makarov 1962 (1938), p. 257, fig. 102; Sakai, 1971: pl. 6, fig. 2; pl 14, figs 1, 2.

Paralomis nivosa Hall & Thatje 2009

Paralomis ochthodes Macpherson 1988b

Paralomis odawari Sakai 1980
Lopholithodes odawarai Sakai 1980
Paralomis odawarai Macpherson 1988a

****^Paralomis otsuae*** Wilson 1990

Paralomis pacifica Sakai 1978

Paralomis papillata Benedict 1895
Leptolithodes papillatus Benedict, 1895 p. 485.
Paralomis papillata Bouvier, 1896, p. 25; Haig, 1974 p. 157, fig. 2; del Solar 1981.

Paralomis pectinata Macpherson 1988a

****^Paralomis phrixa*** Macpherson 1992

Paralomis roeleveldae Kensley 1981

****^Paralomis seagranti*** Eldredge 1976

****^Paralomis serrata*** Macpherson 1988a

Paralomis shinkaimaruae Takeda 1984

Paralomis spectabilis Hansen 1908

Paralomis spectabilis Hansen, 1908, p. 22, pl. I, figs. 3a-d. Pl. II, figs 1a, b;
Stephensen, 1912, p. 577; Heegaard, 1941, p. 15; Birstein & Vinogradov 1967 (in list);
Takeda, 1974 (in list).
Not *Paralomis spectabilis* Birstein & Vinogradov, 1967, p. 390, figs 1, 2; Zarenkov,
1970, p. 184 (= *P. birsteini*, Macpherson 1988b).
Not *Paralomis spectabilis* Birstein & Vinogradov, 1972, p. 352 (= *P. formosa*
Henderson 1888).

****Paralomis spinosissima*** Birstein & Vinogradov 1972
Birstein & Vinogradov, 1972: p. 352, figs 1, 2.

Paralomis stevensi Ahyong & Dawson 2006

^*Paralomis stella* Macpherson 1988c

Paralomis truncatispinosa Takeda & Miyake 1980
Paralomis truncatispinosa Takeda & Miyake 1980, p. 42 figs 1-4.
= *Paralomis heterotuberculata* Yumao & Zhicheng 1984, p. 331

Paralomis tuberipes Macpherson 1988b

^*Paralomis verrilli* Benedict 1864

Paralomis zealandica Dawson & Yaldwyn 1971

Name of consensus sequence	Sample location	Sample number	COI alignment position	COI GenBank accession	16S alignment position	16S GenBank accession	ITS1 alignment position	ITS1 accession	28SB amplicon length	28SB accession
N. asperrimus	Mauritania L36	SA310	642-1325	HM020891	13-567	HM020938	12-496	HM021016		
N asperrimus	Mauritania L3	SA324	685-1279	HM020890	13-568	HM020937				
N. asperrimus	Mauritania L3	SA319			1-569	N/S	10-496	HM021019		
N. asperrimus	Mauritania L9	SA312			1-569	N/S	7-496	HM021018	1-598	HM020848
N. asperrimus	Mauritania L9	SA320					14-496	HM021020		
N. asperrimus	Mauritania L36	SA311			13-567	N/S	7-496	HM021017	1-598	HM020847
Neolithodes sp 158	1446-1466 m Crozet 50°41S-69°22'E	SA158	643-1325	HM020895	156-558	HM020948			1-598	
N. brodiei 1	NIWA02	SA86 (H)	707-1220	HM020893	158-515	HM020944			1-598	HM020851
N. brodiei 1	NIWA	SA95 (C) 1	648-1323	HM020894	158-515	FJ462644			1-598	HM020852
N. brodiei 1	NIWA01	SA 95 (C) 2							1-598	
N. brodiei 2	964-1036m 14°44'48S 167°8'40E CP2312 Vanuatu	SA159	687-1277	EU493263	158-515	HM020942				
N. brodiei 2	NIWA07	SA 83 (I)	704-1260	N/S	158-515	HM020943			1-598	HM020853
N. duhameli	1297-853 m 45°32.64S 51°2.84E Crozet	SA 202	656-1279	N/S	156-558	HM020945	12-496	HM021021	1-598	HM020849
N. duhameli	1297-853 m	SA 203	673-1279	HM020896	156-558	HM020946	12-496	HM021022	1-598	HM020850

	45°32.64S 51°2.84E Crozet									
Paralithodes brevipes		GBK	665-1305	AB211297.1 AB211298.1 AB211299.1 AB211300.1	8-875	AF425337.1			1-598	AB211308.1
Paralithodes platypus		GBK	685-1330	AB211448.1 AB211301.1 AB211302.1 AB211447.1 AB211444.1					1-598	AB193822.1 AB193821.1
Paralithodes camtschaticus		GBK	643-1329	AF425376	8-879	AF425338.1			1-598	AB193824 AB193823
Lithodes longispina		GBK	778-1330	AB476813 AB476814 AB476815						
L. aequispina		GBK	4-1334	AF425308	2-878	N/S				
L. couesi		GBK	675-1314	DQ882086 DQ882085						
L. maja		GBK	556-1314	FJ581742 FJ581745	8-844	AF425330.1				
L. santolla A	Puerto Montt 41°36'40.86''S 72°53'45.61''W	SA213	656-1279	HM020897	156-557	HM020955	13-494	HM021015	1-598	HM020861
L. santolla A		GBK			48-823	AY595927.1			1-598	AY596100
L. santolla B	Punta Arenas	SA211			156-557	HM020955			1-598	HM020860
L. santolla B	Punta Arenas 15-30 m 54°53'8.94''S	SA215	722-1279	HM020898					1-598	HM020859

	68°17'0.14''W									
L. santolla B		GBK			93-560	AF425331.1				
L. nintokuae		GBK	675-1293	AB375135 AB375146 AB375137						
L. murrayi		SA208					8-496	HM021014		
L. murrayi	1289-529 m 46°49.05S 51°28E Crozet	SA 204	837-1279	HM020899	157-557	HM020953	14-496	HM021012	1-598	HM020857
L. murrayi	662-570 m 46°49.26S 51°29.96E Crozet	SA 207	691-1279	HM020899	157-557	HM020953	8-496	HM021013	1-598	HM020858
L. confundens	53°9'48.52''S 68°28'19.96''W St 10T1.	SA15	642-1322	EU493257	155-535	EU493273				
L. confundens	119-124 m 53°32'60.00"S 64°55'60.00"W	SA14 Lcon	636-1341	HM020901	155-557	HM020949	48-477	HM021008		
L. confundens	Chile	SA216	655-1279	HM020900	155-557	FJ464648			1-598	HM020855
L. ferox	ICMD 331/2000 23°03'S 12°55'E	SA125	726-1232	HM020903	156-546	HM020952	7-486	HM021009	1-598	HM020856

	607-615 m 21/04/1981									
L. ferox	ICMD 112/1991 32-A A-15	SA130	726-1232	N/S	157-557	HM020950	8-496	N/S		
L. ferox	Mauritania L2	SA318	726-1232	N/S	1-496	HM021011	8-496	N/S		
L. ferox	Mauritania L2	SA317	726-1232	N/S	9-571	HM020951	8-496	HM021010		
P. aculeata	570-662 m 46° 49.26S 51° 29.96E Crozet	SA 205	656-1279	HM020904	156-557	HM020957	8-496	HM020984	1-598	HM020862
P. aculeata	865-752 m 45°31.69S 49°49.72E	SA 201	701-1279	HM020904	156-557	HM020958	12-496	HM020985	1-598	HM020862
P. aculeata	949-981 m 45°30.27S 49°59.3E	SA 206	656-1279	HM020904			58-465	HM020983	1-598	N/S
P. anamerae	KEP aquarium, died 3.1.04. crab number 404 Male, caught during 2003 toothfish season	SA01 Extraction D200	635-1325	HM020905	157-557	HM020959			1-598	N/S
P. anamerae	KEP aquarium,	SA01	621-1341	HM020905	157-557	HM020959			1-598	HM020866

	died 3.1.04. crab number 404 Male, caught during 2003 toothfish season	Extraction D204								
P. anamerae	EVT 18 Male, KEP. Date 16.01/04	SA02 D201	597-1327	HM020906	157-530	HM020960	8-484	HM020987	1-598	HM020865
P. anamerae	EVT 18 Male, KEP. Date 16.01/04	SA02 D205	641-1343	HM020906	156-534	N/S			1-598	
P. africana	ICMD 302/2000 Namibia 24°40S 13°20E 571-578m 23/04/1983	SA116	588-1343	HM020907	157-482	EU493272			1-598	HM020864
P. africana	3A A-1-6-ICMD81/1991	SA 134			157-369	EU493275	8-485		1-598	
P. cristulata	ICMD 130/1991 11° 22'N 17°22W 13/01/1985 385m	SA141	597-1343	HM020908	156-483	EU493271			1-598	HM020870
P. birsteini 1	1300m JCR crab	SA101	700-1326	EU493260	157-557	N/S	8-496	HM020988	1-598	HM020867

	25.01.07 JCR 157 1300m									
P. birsteini 1	Scott Islands, Ross Sea	SA85 (A)	642-1324 644-1324	HM020909	157-525	N/S				
P. birsteini 2	1240-1275m Kerguelen St Pal. 60 16.12.1999	SA147	641-1322	HM020910	157-557	N/S	75-238		1-598	HM020868
P. indet 1	Crozet Islands	SA91 (G)	706-1260	N/S	157-520	N/S			1-598	HM020869
P. indet 1	Crozet Islands	SA92 (B)	649-1256	N/S	157-557	HM020961			1-598	
P. cristata	22530 900m Japan shikoku Tokushima ken Gamoda Misaki 900m	SA112	732-1331	HM020911	156-557	EU493267				
P. dofleini	SKG 31816 340-360m Japan, Tochyo Bucht im Suden von Sunosaki 340-360 Tiefe 10.02.97 Jan O5	SA104	645-1327	HM020912					1-598	HM020871
P. dofleini	SKG 31816	SA109	747-1303	HM020913	156-540	HM020962				

	340-360m Japan, Tochyo Bucht im Suden von Sunosaki 340-360 Tiefe 10.02.97 Jan O5									
P. elongata	300m 54°44.4 S 0°8.13E Syntype 300m 11.01.04 Polarstern	Sa96	645-1324	HM020914	156-558	N/S	10-494	HM020989	1-598	HM020872
P. erinacea	L56 Mauritania	SA305	596-1324	HM020917	13-570	HM020965	13-496	HM020991	1-598	HM020873
P. erinacea	L29 Mauritania	SA306			2-580	HM020966	8-486	HM020992	1-598	HM020873
P. erinacea	L56 Mauritania	SA307			2-569	HM020967	8-496	HM020993	1-598	HM020873
P. erinacea	L56 vile Mauritania	Sa303	597-1344	HM020916	13-567	HM020964	12-484	HM020990	1-598	HM020873
P. erinacea	Mauritania L39	SA322	588-1342	HM020915	15-566	N/S	14-482	HM020994	1-598	HM020873
P. erinacea	Mauritania L29	SA321			14-566	HM020963	10-490	HM020995	1-598	HM020873
P. formosa	KCF 400 Aquarium Death 02/03/04	SA08 D211	601-1327	HM020918	157-557	N/S				
P. formosa	KCF event ID 1304 TMP51.	SA71	643-1324	HM020919	157-557	HM020973	48-484	HM020998	1-598	HM020875

P. formosa	KCF event ID 1298 TMP51 Tierra del fuego haul 99	SA72	642-1321	HM020920	157-557	HM020972	9-484	HM020999	1-598	HM020874
P. formosa	KCF leg event ID 1295 TMP 51 T d F haul 35	SA73	643-1324	HM020921	157-557	HM020974	12-485	HM021000	1-598	
P. formosa	KCF leg, event ID 1303 TMP 51 Polar pesca haul 106	SA75 2109	644-1323	HM020922	157-557	HM020975			1-598	
P. formosa	Long line South Georgia	SA102	705-1263	EU493262	156-556	FJ462645			1-598	HM020876
P. formosa	L013701 Atlantis 08	SA309			13-567	HM020970	12-496	HM021001		
Paralomis sp. c.f. anamerae	Longline South Georgia	SA06	620-1343	N/S	157-557	N/S				
P. granulosa		GBK			10-859	AF425339.1				
P. granulosa	Punta Arenas, Lovrich	SA 174	656-1279	EU493264.1 HM020925	157-558	HM020976	12-284	HM021004		
P. granulosa	Punta Arenas, Lovrich	SA 212					48-283	HM021003	1-598	HM020877
P. granulosa	From Sven's Box 3733. No Claw	SA20	645-1323	EU493264 HM020926	157-558	EU493274.1	49-283	HM021002	1-598	
P. granulosa	From Sven's Box 3733. Small sp	SA19			157-558	EU493278.1				
P. spinosissima	Event 14 Cruise DOS GO1O4	SA03	588-1343	EU493258	156-557	N/S				

	Species KCV									
P. spinosissima	Event 14 Cruise DOS GO1O4 Species KCV	SA03 ExD206	597-1343	HM020927	156-557	N/S			1-598	HM020879
P. spinosissima	DOS GO104 Frozen sample. Event 20 Date 17.01.04. KCV	SA04 Ex D203	596-1323	EU493259	156-557	HM020982			1-598	
P. spinosissima	Longline South Georgia	Sa04 Ex D207	680-1324	HM020928	156-557	EU493259			1-598	HM020880
P. spinosissima	Cruise DOS GO1O4, Event 3, KCV	SA10 D217	601-1331	HM020931	156-557	N/S	8-496	HM021007	1-598	
P. spinosissima	Cruise DOSGO104 Event 20 Date 17/01/04 Sp KCV1	SA09 D216	641-1330	HM020932	156-557	N/S	48-286	HM021005	1-598	
P. spinosissima	Cruise DOS GO1O4 Event 14, KCV	SA05 D208	627-1327	HM020933	156-557	N/S	8-490	HM021006	1-598	
P. indet SA11	Longline South Georgia	SA11	705-1279	HM020930	156-557	N/S			1-598	HM020881
P. indet SA11	Longline South Georgia	SA11 Ex2	656-1342	N/S	156-557	N/S			1-598	
P. indet SA11	Longline South Georgia	SA11 ExD219	624-1343	N/S	156-557	N/S			1-598	
P. indet SA11	Longline South	SA11	601-1343		156-557	N/S			1-598	

	Georgia	Ex218								
P. pacifica		GBK	675-1330	AB476747 AB476748 AB476749						
P. multispina	SKG 30854 Japan	SA099	642-1293	N/S						
P. multispina		GBK	642-1293	AB375545 AB428440 AB428440 AB428437						
P. zealandica 1	NIWA17	SA87 (F)	705-1257	HM020935	156-491	HM020981				
P. zealandica 1	NIWA 21	SA93 (E)	760-1170	HM020936	156-557	HM020980				
P. zealandica 2	NIWA18	SA 82 (D)	726-1234	N/S	156-482	N/S				
Lopholithodes foraminatus		GBK	654-1314	DQ882089.1 DQ882087.1						
Loph. mandtii		GBK	1-1299	AF425372	47-869	AF425333.1				
Phyllolithodes papillosus		GBK	22-1330	AF425378	69-872	AF425340.1				
Cryptolithodes sitchensis		GBK	55-1311	AF425363	51-818	AF425324.1				
C. typicus		GBK	51-1299	AF425364	23-846	AF425325.1				
Glyptolithodes cristatipes		GBK	2-1319	AF425365	132-872	AF425326.1				
Hapalogaster mertensi		GBK	1-1299	AF425367	2-879	AF425328.1				
H. dentata		GBK	10-1299	AF425366	12-871	AF425327.1				

Oedignathus inermis		GBK	915-1299	EU329164.1						
Oedignathus inermis		GBK	7-1446	AF425373	12-871	AF425334.1	275-496	Z14062.1		
Lomis hirta		GBK		AY595672.1 AF436035.1	8-571	AY595928.1 AF436052.1			1-598	AF435993.1
Aegla lingulata		GBK					309-496			
Aegla uruguayana		GBK					295-496			
Aegla intercalata		GBK		AY595666.1 AY595665.1 AY595664.1	78-560	AY595920.1 AY595919.1 AY595918.1			1-598	AY596091.1 AY596090.1 AY596089.1
Aegla neuquensis		GBK		AY595668.1	78-560	AY595922.1 AY595921.1			1-598	AY596093.1 AY596092.1
Aegla platensis		GBK		AY595663.1 AY595662.1 AY595644.1 AY595643.1	78-560	AY595917.1 AY595916.1 AY595898.1 AY595897.1			1-598	AY596088.1 AY596087.1 AY596069.1 AY596068.1
Aegla longorostri		GBK		AY595608.1 AY595609.1						

				1,009 bp linear DNA AY595610.1						
Pagurus comptus		GBK				FJ869144.1 FJ869142.1 FJ869145.1				
Pagurus pollicaris		GBK		AF483171.1 AF483170.1 AF483169.1	25-565	FJ869152.1 U96089.1				
Pagurus longicarpus		GBK		FJ581826.1 FJ581825.1 FJ581824.1 FJ581823.1		AF150756.1			1-598	AY739185.1 NC_003058.1
Pagurus bernhardus		GBK		AF483157.1						
Emerita analoga		GBK		L43101.1 L43099.1		L43108.1 AF246154.1 AF246153.1 L43107.1				
Emerita brasiliensis		GBK		L43151.1		DQ079712.1 L43110.1				DQ079786.1
Emerita talpoida		GBK		L43106.1 L43105.1 L43104.1		AF246152.1 AF246151. AF246150.1				

Pagurus brevidactylus		GBK			25-565	DQ369945				
Pagurus leptonyx		GBK			77-565	DQ369946.1				

N/S = non-submitted to GenBank either because of ambiguous species ID or because of an exact duplicate of one previously submitted.
GBK= data from GenBank, not obtained in this study.

APPENDIX B

Molecular sample data and GenBank accession numbers.

13 pages.

July 2006

DNeasy® Blood & Tissue Handbook

DNeasy Blood & Tissue Kit
DNeasy 96 Blood & Tissue Kit

For purification of total DNA from

- animal blood
- animal tissue
- rodent tails
- ear punches
- cultured cells
- fixed tissue
- bacteria
- insects

QIAGEN

Contents

Kit Contents

DNeasy Blood & Tissue Kit	(50)	(250)
Catalog no.	**69504**	**69506**
Number of preps	**50**	**250**
DNeasy Mini Spin Columns (colorless) in 2 ml Collection Tubes	50	250
Collection Tubes (2 ml)	100	500
Buffer ATL	10 ml	50 ml
Buffer AL*	12 ml	54 ml
Buffer AW1 (concentrate)*†	19 ml	95 ml
Buffer AW2 (concentrate)†‡	13 ml	66 ml
Buffer AE	22 ml	2 x 60 ml
Proteinase K	1.25 ml	6 ml
Handbook	1	1

* Contains a chaotropic salt. Not compatible with disinfecting agents containing bleach. See page 8 for safety information.

† Buffer AW1 and Buffer AW2 are supplied as concentrates. Add ethanol (96–100%) according to the bottle label before use to obtain a working solution.

‡ Contains sodium azide as a preservative.

DNeasy 96 Blood & Tissue Kit	(4)	(12)
Catalog no.	**69581**	**69582**
Number of preps	**4 x 96**	**12 x 96**
DNeasy 96 Plates	4	12
S-Blocks*	2	2
Collection Microtubes, 1.2 ml (racked)	4 x 96	12 x 96
Collection Microtube Caps	2 x (120 x 8)	5 x (120 x 8)
Elution Microtubes RS (racked) and caps	4 x 96	12 x 96
AirPore Tape Sheets	25	3 x 25
Buffer AL[†]	86 ml	247 ml
Buffer ATL	80 ml	3 x 80 ml
Buffer AW1 (concentrate)[†‡]	98 ml	3 x 98 ml
Buffer AW2 (concentrate)[‡§]	68 ml	3 x 68 ml
Buffer AE	2 x 110 ml	500 ml
Proteinase K	2 x 7 ml	5 x 7 ml
96-Well-Plate Register	4	12
Handbook	1	1

* Reusable; see Appendix B (page 54) for cleaning instructions.

† Contains a chaotropic salt. Not compatible with disinfectants containing bleach. See page 8 for safety information.

‡ Buffer AW1 and Buffer AW2 are supplied as concentrates. Add ethanol (96–100%) according to the bottle label before use to obtain a working solution.

§ Contains sodium azide as a preservative.

Storage

DNeasy spin columns, DNeasy 96 plates, and all buffers should be stored dry, at room temperature (15–25°C) and are stable for 1 year under these conditions.

DNeasy Blood & Tissue Kits contain a ready-to-use proteinase K solution, which is supplied in a specially formulated storage buffer. Proteinase K is stable for at least 1 year after delivery when stored at room temperature. For storage longer than one year or if ambient temperatures often exceed 25°C, we suggest storing proteinase K at 2–8°C.

Product Use Limitations

DNeasy Blood & Tissue Kits and DNeasy 96 Blood & Tissue Kits are intended for research use. No claim or representation is intended to provide information for the diagnosis, prevention, or treatment of a disease.

All due care and attention should be exercised in the handling of the products. We recommend all users of QIAGEN® products to adhere to the NIH guidelines that have been developed for recombinant DNA experiments, or to other applicable guidelines.

Product Warranty and Satisfaction Guarantee

QIAGEN guarantees the performance of all products in the manner described in our product literature. The purchaser must determine the suitability of the product for its particular use. Should any product fail to perform satisfactorily due to any reason other than misuse, QIAGEN will replace it free of charge or refund the purchase price. We reserve the right to change, alter, or modify any product to enhance its performance and design. If a QIAGEN product does not meet your expectations, simply call your local Technical Service Department or distributor. We will credit your account or exchange the product — as you wish. Separate conditions apply to QIAGEN scientific instruments, service products, and to products shipped on dry ice. Please inquire for more information.

A copy of QIAGEN terms and conditions can be obtained on request, and is also provided on the back of our invoices. If you have questions about product specifications or performance, please call QIAGEN Technical Services or your local distributor (see back cover).

Technical Assistance

At QIAGEN we pride ourselves on the quality and availability of our technical support. Our Technical Service Departments are staffed by experienced scientists with extensive practical and theoretical expertise in molecular biology and the use of QIAGEN products. If you have any questions or experience any difficulties regarding DNeasy Blood & Tissue Kits or QIAGEN products in general, please do not hesitate to contact us.

QIAGEN customers are a major source of information regarding advanced or specialized uses of our products. This information is helpful to other scientists as well as to the researchers at QIAGEN. We therefore encourage you to contact us if you have any suggestions about product performance or new applications and techniques.

For technical assistance and more information please call one of the QIAGEN Technical Service Departments or local distributors (see back cover).

Quality Control

In accordance with QIAGEN's ISO-certified Quality Management System, each lot of DNeasy Blood & Tissue Kits and DNeasy 96 Blood & Tissue Kits is tested against predetermined specifications to ensure consistent product quality.

Safety Information

When working with chemicals, always wear a suitable lab coat, disposable gloves, and protective goggles. For more information, please consult the appropriate material safety data sheets (MSDSs). These are available online in convenient and compact PDF format at www.qiagen.com/ts/msds.asp where you can find, view, and print the MSDS for each QIAGEN kit and kit component.

CAUTION: DO NOT add bleach or acidic solutions directly to the sample-preparation waste.

Buffer AL and Buffer AW1 contain guanidine hydrochloride, which can form highly reactive compounds when combined with bleach. If liquid containing this buffer is spilt, clean with suitable laboratory detergent and water. If the spilt liquid contains potentially infectious agents, clean the affected area first with laboratory detergent and water, and then with 1% (v/v) sodium hypochlorite.

The following risk and safety phrases apply to components of DNeasy Blood & Tissue Kits and DNeasy 96 Blood & Tissue Kits.

Buffer AL and Buffer AW1 (concentrate)

Contains guanidine hydrochloride: harmful, irritant. Risk and safety phrases:* R22-36/38, S13-26-36-46

Proteinase K

Contains proteinase K: sensitizer, irritant. Risk and safety phrases:* R36/37/38-42/43, S23-24-26-36/37

24-hour emergency information

Emergency medical information in English, French, and German can be obtained 24 hours a day from:

Poison Information Center Mainz, Germany

Tel: +49-6131-19240

* R22: Harmful if swallowed; R36/37/38: Irritating to eyes, respiratory system and skin; R36/38: Irritating to eyes and skin; R42/43: May cause sensitization by inhalation and skin contact; S13: Keep away from food, drink, and animal feedingstuffs; S23: Do not breathe spray; S24: Avoid contact with skin; S26: In case of contact with eyes, rinse immediately with plenty of water and seek medical advice; S36: Wear suitable protective clothing; S36/37: Wear suitable protective clothing and gloves; S46: If swallowed, seek medical advice immediately, and show container or label.

Introduction

DNeasy Blood & Tissue Kits are designed for rapid purification of total DNA (e.g., genomic, mitochondrial, and pathogen) from a variety of sample sources including fresh or frozen animal tissues and cells, blood, or bacteria. DNeasy purified DNA is free of contaminants and enzyme inhibitors and is highly suited for PCR, Southern blotting, RAPD, AFLP, and RFLP applications.

Purification requires no phenol or chloroform extraction or alcohol precipitation, and involves minimal handling. This makes DNeasy Blood & Tissue Kits highly suited for simultaneous processing of multiple samples. For higher-throughput applications, the DNeasy 96 Blood & Tissue Kit enables simultaneous processing of 96 or 192 samples.

The buffer system is optimized to allow direct cell lysis followed by selective binding of DNA to the DNeasy membrane. After lysis, the DNeasy Blood & Tissue spin-column procedure can be completed in as little as 20 minutes. Using the DNeasy 96 Blood & Tissue Kit, 96 or 192 samples can be processed in just 1 hour after lysis.

Simple centrifugation processing completely removes contaminants and enzyme inhibitors such as proteins and divalent cations, and allows simultaneous processing of multiple samples in parallel. In addition, DNeasy Blood & Tissue procedures are suitable for a wide range of sample sizes.

Purified DNA is eluted in low-salt buffer or water, ready for use in downstream applications. DNeasy purified DNA typically has an A_{260}/A_{280} ratio between 1.7 and 1.9, and is up to 50 kb in size, with fragments of 30 kb predominating. The DNeasy procedure also efficiently recovers DNA fragments as small as 100 bp.

Principle and procedure

DNeasy Blood & Tissue procedures are simple (see flowchart). Samples are first lysed using proteinase K.* Buffering conditions are adjusted to provide optimal DNA-binding conditions and the lysate is loaded onto the DNeasy Mini spin column or the DNeasy 96 plate. During centrifugation, DNA is selectively bound to the DNeasy membrane as contaminants pass through. Remaining contaminants and enzyme inhibitors are removed in two efficient wash steps and DNA is then eluted in water or buffer, ready for use. DNeasy purified DNA has A_{260}/A_{280} ratios of 1.7–1.9, and absorbance scans show a symmetric peak at 260 nm confirming high purity.

* Lysis efficiency can be improved by cell disruption using a rotor–stator homogenizer, such as the QIAGEN TissueRuptor, or a bead mill, such as the QIAGEN TissueLyser. A supplementary protocol allowing the simultaneous disruption of up to 48 tissue samples using the QIAGEN TissueLyser is available from QIAGEN Technical Services.

The DNeasy membrane combines the binding properties of a silica-based membrane with simple microspin technology or with the QIAGEN 96-Well-Plate Centrifugation System. DNA adsorbs to the DNeasy membrane in the presence of high concentrations of chaotropic salt, which remove water from hydrated molecules in solution. Buffer conditions in DNeasy Blood & Tissue procedures are designed to enable specific adsorption of DNA to the silica membrane and optimal removal of contaminants and enzyme inhibitors.

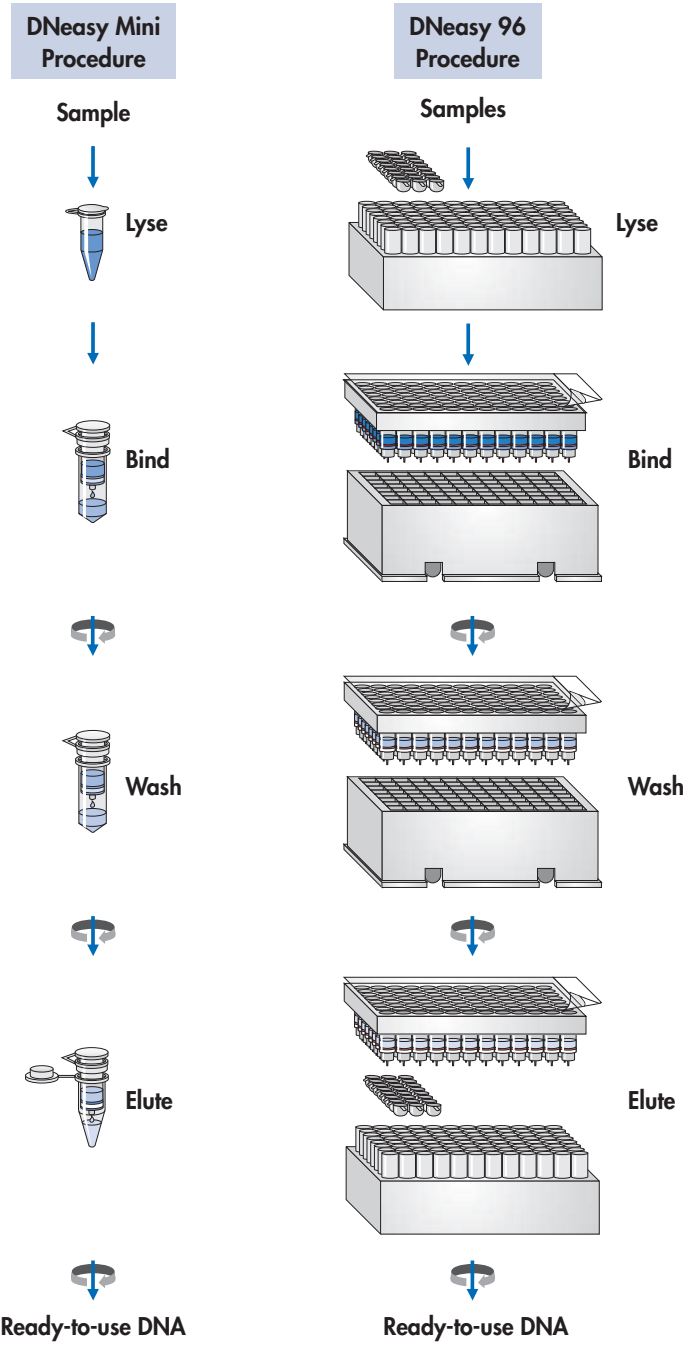
DNeasy Mini Procedure
Sample
Lyse
Bind
Wash
Elute
Ready-to-use DNA
DNeasy 96 Procedure
Samples
Lyse
Bind
Wash
Elute
Ready-to-use DNA

Description of protocols

Different protocols in this handbook provide detailed instructions to use DNeasy Kits for purification of total DNA.

The protocol "**Purification of Total DNA from Animal Blood or Cells (Spin-Column Protocol)**", page 25, is for use with the DNeasy Blood & Tissue Kit, for purification of DNA from animal blood (with nucleated or nonnucleated erythrocytes) or from cultured animal or human cells.

The protocol "**Purification of Total DNA from Animal Tissues (Spin-Column Protocol)**", page 28, is for use with the DNeasy Blood & Tissue Kit, for purification of DNA from animal tissues, including rodent tails.

The protocol "**Purification of Total DNA from Animal Blood or Cells (DNeasy 96 Protocol)**", page 31, is for use with the DNeasy 96 Blood & Tissue Kit, for high-throughput purification of DNA from animal blood (with nucleated or nonnucleated erythrocytes) or from cultured animal or human cells.

The protocol "**Purification of Total DNA from Animal Tissues (DNeasy 96 Protocol)**", page 35, is for use with the DNeasy 96 Blood & Tissue Kit, for high-throughput purification of DNA from animal tissues, including rodent tails.

Pretreatment and specialized protocols

There are several pretreatment protocols included in this handbook, which are optimized for specific sample types. These pretreatment protocols are used in conjunction with one of the DNA purification protocols described above.

The following pretreatment protocols are included in this handbook.

- Pretreatment for Paraffin-Embedded Tissue, page 41
- Pretreatment for Formalin-Fixed Tissue, page 43
- Pretreatment for Gram-Negative Bacteria, page 44
- Pretreatment for Gram-Positive Bacteria, page 45

Additional optimized protocols for purification of DNA from yeast, hair, insects, crude lysates, bone, saliva, and other specialized sample types are available online at www.qiagen.com/literature/protocols/DNeasyTissue.aspx or from QIAGEN Technical Services (see back cover).

Equipment and Reagents to Be Supplied by User

When working with chemicals, always wear a suitable lab coat, disposable gloves, and protective goggles. For more information, consult the appropriate material safety data sheets (MSDSs), available from the product supplier.

For all protocols

- Pipets and pipet tips
- Vortexer
- Ethanol (96–100%)*
- Optional: RNase A (100 mg/ml; cat. no. 19101)

For DNeasy Blood & Tissue Kit (spin column) protocols

- Microcentrifuge tubes (1.5 ml or 2 ml)
- Microcentrifuge with rotor for 1.5 ml and 2 ml tubes
- Thermomixer, shaking water bath, or rocking platform for heating at 56°C

For DNeasy 96 Blood & Tissue Kit protocols

- Centrifuge 4-15C or 4K15C with Plate Rotor 2 x 96 (see page 20)
- Multichannel pipet with extended tips
  For efficient processing , we recommend the use of an electric multichannel pipet with a capacity of at least 1 ml per pipet tip. Options include the Matrix Impact® cordless electronic multichannel pipet, which has a unique, adjustable tip-spacing system allowing the user to transfer liquid directly from sample tubes to 96-well plates.
  We recommend using extended tips with a maximum volume of 1250 µl with the Matrix multichannel pipet (available from Matrix, cat. no. 8255 for tips with filters or 8252 for tips without filters).
  These multichannel pipets and pipet tips can be purchased from Matrix Technologies Corporation (www.matrixtechcorp.com).†
- Reagent reservoirs for multichannel pipets
- Heavy plate or similar object to place on top of collection microtubes during incubation
- Oven or incubator for heating at 56°C

* Do not use denatured alcohol, which contains other substances such as methanol or methylethylketone.

† This is not a complete list of suppliers and does not include many important vendors of biological supplies.

For blood and cultured cells

- PBS, pH 7.2 (50 mM potassium phosphate, 150 mM NaCl)

For pretreatment of paraffin-embedded tissue (page 41)

- Xylene

For pretreatment of formalin-fixed tissue (page 43)

- PBS, pH 7.2 (50 mM potassium phosphate, 150 mM NaCl)

For pretreatment of gram-positive bacteria (page 45)

- Enzymatic lysis buffer:
  - 20 mM Tris·Cl, pH 8.0
  - 2 mM sodium EDTA
  - 1.2% Triton® X-100
  - Immediately before use, add lysozyme to 20 mg/ml

Important Notes

Sample collection and storage

Best results are obtained with fresh material or material that has been immediately frozen and stored at –20°C or –70°C. Repeated freezing and thawing of stored samples should be avoided, since this leads to reduced DNA size. Use of poor-quality starting material will also lead to reduced length and yield of purified DNA.

After proteinase K digestion, tissue samples can also be stored in Buffer ATL for up 6 months at ambient temperature without any reduction in DNA quality.

For certain bacterial cultures that accumulate large amounts of metabolites and/or form very dense cell walls, it is preferable to harvest cells in the early log phase of growth. Fresh or frozen cell pellets can be used in the procedure.

Starting amounts of samples

DNeasy Blood & Tissue procedures give DNA yields that increase linearly over a wide range, for both very small and large sample sizes (e.g., from as little as 100 cells up to 5 x 10^6 cells).

Maximum amount of starting material

In order to obtain optimum DNA yield and quality, it is important not to overload the DNeasy spin column or DNeasy 96 plate, as this can lead to significantly lower yields than expected (see Figure 1). For samples with very high DNA contents (e.g., spleen, which has a high cell density, and cell lines with a high degree of ploidy), less than the recommended amount of sample listed in Table 1 should be used. If your starting material is not shown in Table 3 (page 23) and you have no information regarding DNA content, we recommend beginning with half the maximum amount of starting material indicated in Table 1. Depending on the yield obtained, the sample size can be increased in subsequent preparations.

Very small sample sizes

DNeasy Blood & Tissue procedures are also suitable for purifying DNA from very small amounts of starting material. If the sample has less than 5 ng DNA (<10,000 copies), 3–5 µg carrier DNA (a homopolymer such as poly-dA, poly-dT, or gDNA) should be added to the starting material. Ensure that the carrier DNA does not interfere with your downstream application. In order to prevent any interference of the carrier with the downstream application, an RNA carrier can be used. This can be removed later by RNase digestion. DNA or RNA homopolymers can be purchased from various suppliers.

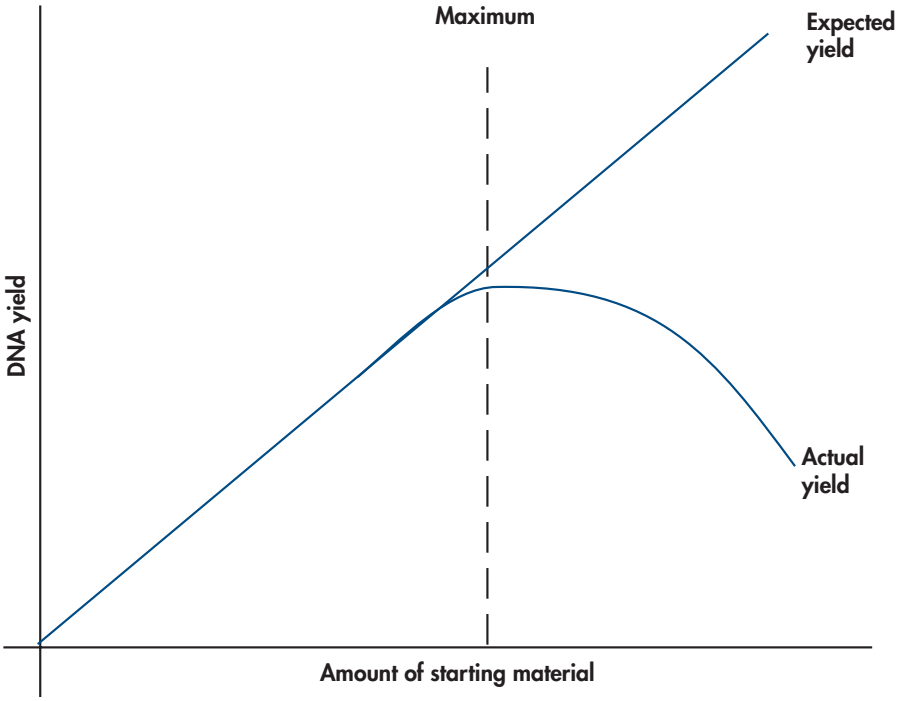

Figure 1 Schematic diagram of effect of sample size on DNA yield. If more than the maximum amount of starting material is used, DNA yield will be lower than expected.

Table 1. Maximum Amounts of Starting Material

Sample	Amount
Animal tissue (see Table 3, page 23)	25 mg (spin-column protocols) 20 mg (DNeasy 96 protocols)
Mammalian blood (see Table 4, page 23)	100 µl
Bird or fish blood (with nucleated erythrocytes)	10 µl
Mouse tail	0.6–1.2 cm
Rat tail	0.6 cm
Cultured cells	5×10^6
Bacteria	2×10^9

Quantification of starting material

Weighing tissue or counting cells is the most accurate way to quantify starting material. However, the approximate guidelines given below can also be followed.

Animal tissue

A 2 mm cube (approximately this size: ■; volume, approximately 8 mm^3) of most animal tissues weighs approximately 10–15 mg.

Animal cells

The number of HeLa cells obtained in various culture dishes after confluent growth is given in Table 2.

Table 2. Growth Area and Number of HeLa Cells in Various Culture Dishes

Cell culture vessel	Growth area* (cm^2)	Number of cells†
Multiwell plates		
96-well	0.32–0.6	4–5 x 10^4
48-well	1	1 x 10^5
24-well	2	2.5 x 10^5
12-well	4	5 x 10^5
6-well	9.5	1 x 10^6
Dishes		
35 mm	8	1 x 10^6
60 mm	21	2.5 x 10^6
100 mm	56	7 x 10^6
145–150 mm	145	2 x 10^7
Flasks		
40–50 ml	25	3 x 10^6
250–300 ml	75	1 x 10^7
650–750 ml	162–175	2 x 10^7

* Per well, if multiwell plates are used; varies slightly depending on the supplier.

† Cell numbers given are for HeLa cells (approximate length = 15 µm) assuming confluent growth. Cell numbers vary since animal cells can vary in length from 10 to 100 µm.

Bacteria

Bacterial growth is usually measured using a spectrophotometer. However, it is very difficult to give specific and reliable recommendations for the correlation between OD values and cell numbers in bacterial cultures. Cell density is influenced by a variety of factors (e.g., species, media, and shaker speed) and OD readings of cultures measure light scattering rather than absorption. Measurements of light scattering are highly dependent on the distance between the sample and the detector and therefore readings vary between different types of spectrophotometer. In addition, different species show different OD values at defined wavelengths (e.g., 600 or 436 nm).

We therefore recommend calibrating the spectrophotometer used by comparing OD measurements at appropriate wavelengths with viable cell densities determined by plating experiments (e.g., see Ausubel, F.M. et al., eds. [1991] *Current Protocols in Molecular Biology*, New York: John Wiley & Sons, Inc.). OD readings should be between 0.05 and 0.3 to ensure significance. Samples with readings above 0.3 should be diluted so that the readings fall within this range and the dilution factor used in calculating the number of cells per milliliter.

The following calculation can be considered as a rough guide, which may be helpful. An *E. coli* culture of 1 x 10^9 cells per milliliter, diluted 1 in 4, gives OD600 values of 0.25 measured using a Beckman DU®-7400 or 0.125 using a Beckman DU-40 spectrophotometer. These correspond to calculated OD values of 1.0 or 0.5 respectively for 1 x 10^9 cells per milliliter.

Preparation of Buffer AW1 and Buffer AW2

Buffer AW1 and Buffer AW2 are supplied as concentrates. Before using for the first time, add the appropriate volume of ethanol (96–100%) as indicated on the bottle and shake thoroughly. Buffer AW1 and Buffer AW2 are stable for at least 1 year after the addition of ethanol when stored closed at room temperature (15–25°C).

Buffer AL

Purification of DNA from animal blood, cultured cells, or Gram-positive bacteria

Buffer AL must be added to the sample and incubated at 56°C before ethanol is added. Ensure that ethanol has not been added to Buffer AL beforehand. Buffer AL can be purchased separately (see page 56 for ordering information).

Purification of DNA from animal tissues

Buffer AL and ethanol (96–100%) are added in the same step. Buffer AL and ethanol can be premixed and added together in one step to save time when processing multiple samples.

For the protocol "Purification of Total DNA from Animal Tissues (DNeasy 96 Protocol)": Add 90 ml ethanol (96–100%) to the bottle containing 86 ml Buffer AL or 260 ml ethanol to the bottle containing 247 ml Buffer AL and shake thoroughly. Mark the bottle to indicate that ethanol has been added. (Please note that, for purification of DNA from animal blood, Buffer AL must be used without ethanol. Buffer AL can be purchased separately if the same kit will be used for purification of DNA from animal blood.)

Buffer AL is stable for 1 year after the addition of ethanol when stored closed at room temperature.

Proteinase K

DNeasy Blood & Tissue Kits contain ready-to-use proteinase K supplied in a specially formulated storage buffer. The activity of proteinase K is 600 mAU/ml solution (or 40 mAU/mg protein), and has been chosen to provide optimal results.

Also included in the kits is an optimized buffer for tissue lysis, Buffer ATL. To enable efficient lysis, it is advisable to cut animal tissue into small pieces. If desired, lysis time can be reduced to 20 minutes by grinding the sample in liquid nitrogen* before addition of Buffer ATL and proteinase K. Alternatively, tissue samples can be effectively disrupted before proteinase K digestion using a rotor–stator homogenizer, such as the QIAGEN TissueRuptor, or a bead mill, such as the QIAGEN TissueLyser. A supplementary protocol for simultaneous disruption of up to 48 tissue samples using the TissueLyser can be obtained by contacting QIAGEN Technical Services (see back cover).

Proteinase K is stable for at least one year after delivery when stored at room temperature (15–25°C). To store for more than one year or if ambient temperature often exceeds 25°C, we suggest keeping proteinase K at 2–8°C.

Please contact QIAGEN Technical Services or your local distributor if you have any questions about the use of proteinase K (see back cover).

Copurification of RNA

DNeasy Blood & Tissue Kits copurify DNA and RNA when both are present in the sample. Transcriptionally active tissues such as liver and kidney contain high levels of RNA, which will be copurified. RNA may inhibit some downstream enzymatic reactions, although it does not affect PCR. If RNA-free genomic DNA is required, RNase A should be added to the sample before addition of Buffer AL, to digest the RNA. DNeasy protocols describe the use of an RNase A stock solution of 100 mg/ml. However, the amounts of RNase can be adjusted with less concentrated stock solutions, but not more than 20 µl of RNase solution should be used. Refer to the protocols for details.

* When working with chemicals, always wear a suitable lab coat, disposable gloves, and protective goggles. For more information, consult the appropriate material safety data sheets (MSDSs), available from the product supplier.

Centrifugation (DNeasy 96 procedures)

Centrifuges 4-15C and 4K15C

DNeasy 96 spin protocols use a streamlined centrifugation procedure that enables purification of DNA from up to 2 x 96 samples in parallel for direct use in any downstream application. The DNeasy 96 Blood & Tissue procedure requires use of the QIAGEN 96-Well-Plate Centrifugation System, comprising the Plate Rotor 2 x 96 and the table-top Centrifuge 4-15C or the refrigerated table-top Centrifuge 4K15C (see page 55 for ordering information). In addition to the Plate Rotor 2 x 96, a wide range of other rotors can be used with these centrifuges.

Standard table-top centrifuges and microtiter plate rotors are not suitable for the DNeasy 96 protocol for 2 reasons: the microtiter plate buckets are either not deep enough for the complete DNeasy 96 package or they will not swing out properly, and furthermore, high g-forces (>5500 x *g*) are required for optimal performance of the DNeasy 96 procedure. The speed limit of the Centrifuge 4-15C and the Centrifuge 4K15C (6000 rpm; 5796 x *g*) is programmed so that the given *g*-force will not be exceeded. All centrifugation steps are performed at room temperature.

IMPORTANT: Centrifuges must be properly maintained for optimal performance. It is particularly important that the buckets and rotor pins are routinely greased to prevent suboptimal running conditions that may lead to cracking of DNeasy 96 plates.

For further information about QIAGEN Centrifuges and the Plate Rotor 2 x 96, contact QIAGEN Technical Services or your local distributor (see back cover for contact information).

Note: If the Centrifuge 4K15C is used, set the temperature to 40°C for all centrifugation steps.

Note: Use AirPore Tape Sheets (provided) to seal DNeasy 96 plates during all centrifugation steps to prevent cross-contamination between samples.

Abbreviated instructions for using the Centrifuge 4-15C and Centrifuge 4K15C

Warning: Never run the centrifuge with empty plate carriers placed inside the buckets, that is, without the collection microtubes or DNeasy 96 plates and S-Blocks. If unsupported, the carriers will collapse under high *g*-forces. Therefore, remove the carriers during test runs. Standard microtiter plates may be centrifuged in the same carriers if the g-force does not exceed 500 x *g*.

1. Switch on the centrifuge by pressing the main switch on the back.
2. Select the rotor selection list in the display field by turning the knob. After pressing the knob, turn the knob again to select the rotor/bucket combination "09100/09158" for the Plate Rotor 2 x 96. Confirm entry by pressing the knob. Entering the rotor number automatically sets the time and speed limits for centrifugation for that particular rotor, thus eliminating the danger of the centrifuge over-speeding.

3. Select "Speed" by turning the knob. Press the knob and by turning the knob again, set the speed to "6000". Confirm entry by pressing the knob. The corresponding relative centrifugal force (RCF) is calculated from the rotor number and speed and appears automatically in the RCF field. It is also possible to enter the RCF value "5796 x *g*" manually in the RCF field after selecting "RCF" in the same way.
4. Select "Time" by turning the knob. Press once and by turning the knob again, set the time as recommended in the particular protocol step. Confirm entry by pressing the knob.
5. For the Centrifuge 4K15C, set the temperature to 40°C.
6. Open the lid, place the 96-well plates with the metal carriers in the buckets then close the lid. The start and lid keys light up.
7. Push "Start" to start the centrifuge. When the centrifuge is running the lid key will not be lit. Each run can be interrupted by pushing "Stop".
8. At the end of the run, the lid key will light up. Open the centrifuge lid by pressing the lid key. Remove the plates. All preset parameters remain after a run has finished.

Elution of pure nucleic acids

Purified DNA is eluted from the DNeasy Mini spin column or DNeasy 96 plate in either Buffer AE or water. For maximum DNA yield, elution is performed in two successive steps using 200 µl Buffer AE each. For more concentrated DNA, elution can be performed in two successive steps of 100 µl each. Keep in mind that elution volume and number of elution steps depends on the amount of DNA bound to the DNeasy membrane (see Figure 2).

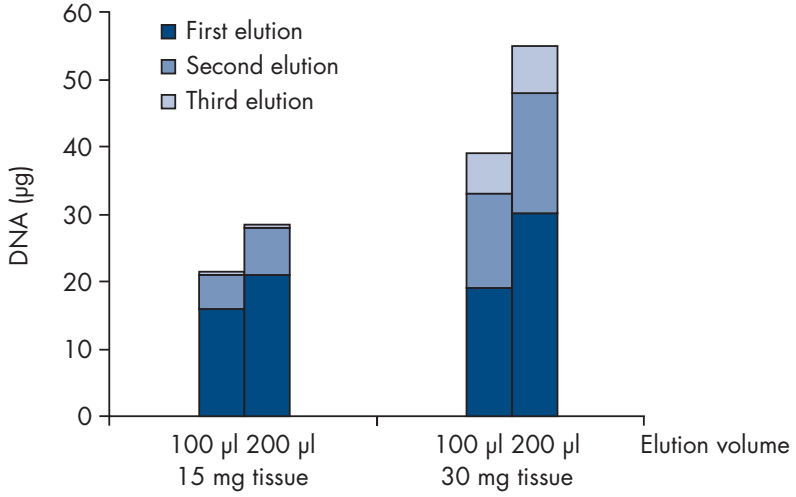

Figure 2 Yields of total nucleic acids in successive elutions of 100 or 200 µl.

For samples containing up to 10 µg DNA, a single elution step using 200 µl is sufficient. For samples containing more than 10 µg DNA, a second elution step with another 200 µl Buffer AE is recommended. Approximately 60–80% of the DNA will elute in the first elution. If >30 µg DNA is bound to the DNeasy membrane, elution in 3 x 200 µl may increase yield (see below).

Elution in 100 µl increases the DNA concentration in the eluate, but reduces overall DNA yield. To prevent dilution of the first eluate, the subsequent elution step can be performed using a fresh 1.5 ml microcentrifuge tube. More than 200 µl should not be eluted into a 1.5 ml microcentrifuge tube because the spin column will come into contact with the eluate, leading to possible aerosol formation during centrifugation.

For very small samples (containing less than 1 µg DNA), only one elution in 50 µl of Buffer AE or water is recommended.

Buffer AE is 10 mM Tris·Cl, 0.5 mM EDTA, pH 9.0. Elution with Buffer AE guarantees optimal recovery and stability of eluted DNA. However, if you wish to elute DNA with water please ensure that the pH of the water is at least 7.0 (deionized water from certain sources can be acidic). For long-term storage of DNA, elution in Buffer AE is strongly recommended since DNA stored in water is subject to acid hydrolysis. Buffer AE should be used at room temperature (15–25°C). Heating Buffer AE before elution is not necessary.

Expected yields

Yields of genomic DNA will vary from sample to sample depending on the amount and type of material processed. In addition, the quality of starting material will affect DNA yield.

Tables 3 and 4 can be used to provide an estimate of expected yield.

Table 3. Typical DNA Yields from Animal Tissues Using DNeasy Blood & Tissue Kits

Source	Amount	DNA (µg)
Mammalian blood (see Table 4)	100 µl	3–6
Bird blood	5 µl	9–40
Lymphocytes	5×10^6	15–25
HeLa cells	2×10^6	15–25
Liver	25 mg	10–30
Brain	25 mg	15–30
Lung	25 mg	5–10
Heart	25 mg	5–10
Kidney	25 mg	15–30
Spleen	10 mg	5–30
Mouse tail	1.2 cm (tip)	10–25
Rat tail	0.6 cm (tip)	20–40
Pig ear	25 mg	10–30
Horse hair	10 hairs	2–4
Fish fin	20 mg	10–20
Fish spawn (mackerel)	10 mg	5–10

Table 4. Typical DNA Yields from Animal Blood Using DNeasy Blood & Tissue Kits

Animal	Amount (µl)	DNA (µg)
Cattle	100	4–5
Horse	100	3–5
Pig	100	3–6
Sheep	100	3–6
Dog	100	4–5
Cat	100	3–6
Goat	50*	3
Chicken†	5	9–15

* Using more than 50 µl goat blood gave no significant increase in DNA yield.

† Bird blood contains nucleated erythrocytes, giving higher DNA yields than mammalian blood.

Purification of high-molecular-weight DNA

QIAGEN Genomic-tips and Blood & Cell Culture DNA Kits are recommended for large-scale purification of high-molecular-weight DNA (see page 56 for ordering information). QIAGEN Genomic-tips are available for purification of up to 500 µg of genomic DNA ranging in size from 50 to 150 kb. They are highly suited for use in Southern blotting, library construction, genome mapping, and other demanding applications. Please contact QIAGEN Technical Services or your local distributor for more information (see back cover).

Protocol: Purification of Total DNA from Animal Blood or Cells (Spin-Column Protocol)

This protocol is designed for purification of total DNA from animal blood (with nucleated or nonnucleated erythrocytes) or from cultured animal or human cells.

Important points before starting

- If using the DNeasy Blood & Tissue Kit for the first time, read "Important Notes" (page 15).
- All centrifugation steps are carried out at room temperature (15–25°C) in a microcentrifuge.
- Vortexing should be performed by pulse-vortexing for 5–10 s.
- PBS is required for use in step 1 (see page 14 for composition). Buffer ATL is not required in this protocol.
- Optional: RNase A may be used to digest RNA during the procedure. RNase A is not provided in the DNeasy Blood & Tissue Kit (see "Copurification of RNA", page 19).

Things to do before starting

- Buffer AL may form a precipitate upon storage. If necessary, warm to 56°C until the precipitate has fully dissolved.
- Buffer AW1 and Buffer AW2 are supplied as concentrates. Before using for the first time, add the appropriate amount of ethanol (96–100%) as indicated on the bottle to obtain a working solution.
- Preheat a thermomixer, shaking water bath, or rocking platform to 56°C for use in step 2.

Procedure

1. **For blood with nonnucleated erythrocytes, follow step 1a; for blood with nucleated erythrocytes, follow step 1b; for cultured cells, follow step 1c.**

   Blood from mammals contains nonnucleated erythrocytes. Blood from animals such as birds, fish, or frogs contains nucleated erythrocytes.

1a. **Nonnucleated: Pipet 20 µl proteinase K into a 1.5 ml or 2 ml microcentrifuge tube (not provided). Add 50–100 µl anticoagulated blood. Adjust the volume to 220 µl with PBS. Continue with step 2.**

   Optional: If RNA-free genomic DNA is required, add 4 µl RNase A (100 mg/ml) and incubate for 2 min at room temperature before continuing with step 2.

1b. Nucleated: Pipet 20 µl proteinase K into a 1.5 ml or 2 ml microcentrifuge tube (not provided). Add 5–10 µl anticoagulated blood. Adjust the volume to 220 µl with PBS. Continue with step 2.

Optional: If RNA-free genomic DNA is required, add 4 µl RNase A (100 mg/ml) and incubate for 2 min at room temperature before continuing with step 2.

1c. Cultured cells: Centrifuge the appropriate number of cells (maximum 5 x 10^6) for 5 min at 300 x g. Resuspend the pellet in 200 µl PBS. Add 20 µl proteinase K. Continue with step 2.

When using a frozen cell pellet, allow cells to thaw before adding PBS until the pellet can be dislodged by gently flicking the tube.

Ensure that an appropriate number of cells is used in the procedure. For cell lines with a high degree of ploidy (e.g., HeLa cells), it is recommended to use less than the maximum number of cells listed in Table 1, page 16.

Optional: If RNA-free genomic DNA is required, add 4 µl RNase A (100 mg/ml), mix by vortexing, and incubate for 2 min at room temperature before continuing with step 2.

2. Add 200 µl Buffer AL (without added ethanol). Mix thoroughly by vortexing, and incubate at 56°C for 10 min.

Ensure that ethanol has not been added to Buffer AL (see "Buffer AL", page 18). Buffer AL can be purchased separately (see page 56 for ordering information).

It is essential that the sample and Buffer AL are mixed immediately and thoroughly by vortexing or pipetting to yield a homogeneous solution.

3. Add 200 µl ethanol (96–100%) to the sample, and mix thoroughly by vortexing.

It is important that the sample and the ethanol are mixed thoroughly to yield a homogeneous solution.

4. Pipet the mixture from step 3 into the DNeasy Mini spin column placed in a 2 ml collection tube (provided). Centrifuge at ≥6000 x *g* (8000 rpm) for 1 min. Discard flow-through and collection tube.*

5. Place the DNeasy Mini spin column in a new 2 ml collection tube (provided), add 500 µl Buffer AW1, and centrifuge for 1 min at ≥6000 x *g* (8000 rpm). Discard flow-through and collection tube.*

6. Place the DNeasy Mini spin column in a new 2 ml collection tube (provided), add 500 µl Buffer AW2, and centrifuge for 3 min at 20,000 x *g* (14,000 rpm) to dry the DNeasy membrane. Discard flow-through and collection tube.

It is important to dry the membrane of the DNeasy Mini spin column, since residual ethanol may interfere with subsequent reactions. This centrifugation step ensures that no residual ethanol will be carried over during the following elution.

* Flow-through contains Buffer AL or Buffer AW1 and is therefore not compatible with bleach. See page 8 for safety information.

Following the centrifugation step, remove the DNeasy Mini spin column carefully so that the column does not come into contact with the flow-through, since this will result in carryover of ethanol. If carryover of ethanol occurs, empty the collection tube, then reuse it in another centrifugation for 1 min at 20,000 x *g* (14,000 rpm).

7. **Place the DNeasy Mini spin column in a clean 1.5 ml or 2 ml microcentrifuge tube (not provided), and pipet 200 µl Buffer AE directly onto the DNeasy membrane. Incubate at room temperature for 1 min, and then centrifuge for 1 min at ≥6000 x *g* (8000 rpm) to elute.**

   Elution with 100 µl (instead of 200 µl) increases the final DNA concentration in the eluate, but also decreases the overall DNA yield (see Figure 2, page 21).

8. **Recommended: For maximum DNA yield, repeat elution once as described in step 7.**

   This step leads to increased overall DNA yield.

   A new microcentrifuge tube can be used for the second elution step to prevent dilution of the first eluate. Alternatively, to combine the eluates, the microcentrifuge tube from step 7 can be reused for the second elution step.

   Note: Do not elute more than 200 µl into a 1.5 ml microcentrifuge tube because the DNeasy Mini spin column will come into contact with the eluate.

Protocol: Purification of Total DNA from Animal Tissues (Spin-Column Protocol)

This protocol is designed for purification of total DNA from animal tissues, including rodent tails.

Important points before starting

- If using the DNeasy Blood & Tissue Kit for the first time, read "Important Notes" (page 15).
- For fixed tissues, refer to the pretreatment protocols "Pretreatment for Paraffin-Embedded Tissue", page 41, and "Pretreatment for Formalin-Fixed Tissue", page 43.
- All centrifugation steps are carried out at room temperature (15–25°C) in a microcentrifuge.
- Vortexing should be performed by pulse-vortexing for 5–10 s.
- Optional: RNase A may be used to digest RNA during the procedure. RNase A is not provided in the DNeasy Blood & Tissue Kit (see "Copurification of RNA", page 19).

Things to do before starting

- Buffer ATL and Buffer AL may form precipitates upon storage. If necessary, warm to 56°C until the precipitates have fully dissolved.
- Buffer AW1 and Buffer AW2 are supplied as concentrates. Before using for the first time, add the appropriate amount of ethanol (96–100%) as indicated on the bottle to obtain a working solution.
- Preheat a thermomixer, shaking water bath, or rocking platform to 56°C for use in step 2.
- If using frozen tissue, equilibrate the sample to room temperature. Avoid repeated thawing and freezing of samples since this will lead to reduced DNA size.

Procedure

1. **Cut up to 25 mg tissue (up to 10 mg spleen) into small pieces, and place in a 1.5 ml microcentrifuge tube. For rodent tails, place one (rat) or two (mouse) 0.4–0.6 cm lengths of tail into a 1.5 ml microcentrifuge tube. Add 180 µl Buffer ATL. Earmark the animal appropriately.**

   Ensure that the correct amount of starting material is used (see "Starting amounts of samples", page 15). For tissues such as spleen with a very high number of cells for a given mass of tissue, no more than 10 mg starting material should be used.

We strongly recommend to cut the tissue into small pieces to enable more efficient lysis. If desired, lysis time can be reduced by grinding the sample in liquid nitrogen* before addition of Buffer ATL and proteinase K. Alternatively, tissue samples can be effectively disrupted before proteinase K digestion using a rotor–stator homogenizer, such as the QIAGEN TissueRuptor, or a bead mill, such as the QIAGEN TissueLyser (see page 56 for ordering information). A supplementary protocol for simultaneous disruption of up to 48 tissue samples using the TissueLyser can be obtained by contacting QIAGEN Technical Services (see back cover).

For rodent tails, a maximum of 1.2 cm (mouse) or 0.6 cm (rat) tail should be used. When purifying DNA from the tail of an adult mouse or rat, it is recommended to use only 0.4–0.6 cm.

2. **Add 20 µl proteinase K. Mix thoroughly by vortexing, and incubate at 56°C until the tissue is completely lysed. Vortex occasionally during incubation to disperse the sample, or place in a thermomixer, shaking water bath, or on a rocking platform.**

   Lysis time varies depending on the type of tissue processed. Lysis is usually complete in 1–3 h or, for rodent tails, 6–8 h. If it is more convenient, samples can be lysed overnight; this will not affect them adversely.

   After incubation the lysate may appear viscous, but should not be gelatinous as it may clog the DNeasy Mini spin column. If the lysate appears very gelatinous, see the "Troubleshooting Guide", page 47, for recommendations.

   Optional: If RNA-free genomic DNA is required, add 4 µl RNase A (100 mg/ml), mix by vortexing, and incubate for 2 min at room temperature before continuing with step 3.

   Transcriptionally active tissues such as liver and kidney contain high levels of RNA, which will copurify with genomic DNA. For tissues that contain low levels of RNA, such as rodent tails, or if residual RNA is not a concern, RNase A digestion is not necessary.

3. **Vortex for 15 s. Add 200 µl Buffer AL to the sample, and mix thoroughly by vortexing. Then add 200 µl ethanol (96–100%), and mix again thoroughly by vortexing.**

   It is essential that the sample, Buffer AL, and ethanol are mixed immediately and thoroughly by vortexing or pipetting to yield a homogeneous solution. Buffer AL and ethanol can be premixed and added together in one step to save time when processing multiple samples.

* When working with chemicals, always wear a suitable lab coat, disposable gloves, and protective goggles. For more information, consult the appropriate material safety data sheets (MSDSs), available from the product supplier.

A white precipitate may form on addition of Buffer AL and ethanol. This precipitate does not interfere with the DNeasy procedure. Some tissue types (e.g., spleen, lung) may form a gelatinous lysate after addition of Buffer AL and ethanol. In this case, vigorously shaking or vortexing the preparation is recommended.

4. **Pipet the mixture from step 3 (including any precipitate) into the DNeasy Mini spin column placed in a 2 ml collection tube (provided). Centrifuge at ≥6000 x *g* (8000 rpm) for 1 min. Discard flow-through and collection tube.***

5. **Place the DNeasy Mini spin column in a new 2 ml collection tube (provided), add 500 µl Buffer AW1, and centrifuge for 1 min at ≥6000 x *g* (8000 rpm). Discard flow-through and collection tube.***

6. **Place the DNeasy Mini spin column in a new 2 ml collection tube (provided), add 500 µl Buffer AW2, and centrifuge for 3 min at 20,000 x *g* (14,000 rpm) to dry the DNeasy membrane. Discard flow-through and collection tube.**

   It is important to dry the membrane of the DNeasy Mini spin column, since residual ethanol may interfere with subsequent reactions. This centrifugation step ensures that no residual ethanol will be carried over during the following elution.

   Following the centrifugation step, remove the DNeasy Mini spin column carefully so that the column does not come into contact with the flow-through, since this will result in carryover of ethanol. If carryover of ethanol occurs, empty the collection tube, then reuse it in another centrifugation for 1 min at 20,000 x g (14,000 rpm).

7. **Place the DNeasy Mini spin column in a clean 1.5 ml or 2 ml microcentrifuge tube (not provided), and pipet 200 µl Buffer AE directly onto the DNeasy membrane. Incubate at room temperature for 1 min, and then centrifuge for 1 min at ≥6000 x *g* (8000 rpm) to elute.**

   Elution with 100 µl (instead of 200 µl) increases the final DNA concentration in the eluate, but also decreases the overall DNA yield (see Figure 2, page 21).

8. **Recommended: For maximum DNA yield, repeat elution once as described in step 7.**

   This step leads to increased overall DNA yield.

   A new microcentrifuge tube can be used for the second elution step to prevent dilution of the first eluate. Alternatively, to combine the eluates, the microcentrifuge tube from step 7 can be reused for the second elution step.

   Note: Do not elute more than 200 µl into a 1.5 ml microcentrifuge tube because the DNeasy Mini spin column will come into contact with the eluate.

* Flow-through contains Buffer AL or Buffer AW1 and is therefore not compatible with bleach. See page 8 for safety information.

Protocol: Purification of Total DNA from Animal Blood or Cells (DNeasy 96 Protocol)

This protocol is designed for high-throughput purification of total DNA from animal blood (with nucleated or nonnucleated erythrocytes) or from cultured animal or human cells.

Important points before starting

- If using the DNeasy 96 Blood & Tissue Kit for the first time, read "Important Notes" (page 15).
- All centrifugation steps are carried out at room temperature (15–25°C).
- PBS is required for use in step 1 (see page 14 for composition). Buffer ATL is not required in this protocol.
- Ensure that ethanol has not been added to Buffer AL (see "Important Notes", page 15). Buffer AL can be purchased separately (see page 56 for ordering information).
- Optional: RNase A may be used to digest RNA during the procedure. RNase A is not provided in the DNeasy 96 Blood & Tissue Kit (see "Copurification of RNA", page 19).

Things to do before starting

- Buffer ATL and Buffer AL may form precipitates upon storage. If necessary, warm to 56°C for 5 min until the precipitates have fully dissolved.
- Buffer AW1 and Buffer AW2 are supplied as concentrates. Before using for the first time, add the appropriate amount of ethanol (96–100%) as indicated on the bottle to obtain a working solution.
- Mix Buffer AW1 before use by inverting several times.
- Preheat an incubator to 56°C for use in step 2.

Procedure

1. For blood with nonnucleated erythrocytes, follow step 1a; for blood with nucleated erythrocytes, follow step 1b; for cultured cells, follow step 1c.

Blood from mammals contains nonnucleated erythrocytes. Blood from animals such as birds, fish, or frogs contains nucleated erythrocytes.

1a. Nonnucleated: Pipet 20 µl proteinase K into each collection microtube. Add 50–100 µl anticoagulated blood per collection microtube. Use a 96-Well-Plate Register (provided) to identify the position of each sample. Adjust the volume to 220 µl each with PBS. Continue with step 2.

Optional: If RNA-free genomic DNA is required, add 4 µl RNase A (100 mg/ml) and incubate for 5 min at room temperature before continuing with step 2.

Keep the clear covers from the collection microtube racks for use in step 3.

1b. Nucleated: Pipet 20 µl proteinase K into each collection microtube. Add 5–10 µl anticoagulated blood. Use a 96-Well-Plate Register (provided) to identify the position of each sample. Adjust the volume to 220 µl each with PBS. Continue with step 2.

Optional: If RNA-free genomic DNA is required, add 4 µl RNase A (100 mg/ml) and incubate for 5 min at room temperature before continuing with step 2.

Keep the clear covers from the collection microtube racks for use in step 3.

1c. Cultured cells: Centrifuge the appropriate number of cells (maximum 5 x 10^6 each) for 5 min at 300 x *g*. Use a 96-Well-Plate Register (provided) to identify the position of each sample. Resuspend the pellets in 200 µl PBS each. Add 20 µl proteinase K each. Continue with step 2.

When using a frozen cell pellets, allow cells to thaw before adding PBS until the pellet can be dislodged by gently flicking the tube.

Ensure that an appropriate number of cells is used in the procedure. For cell lines with a high degree of ploidy (e.g., HeLa cells), it is recommended to use less than the maximum number of cells listed in Table 1, page 16.

Optional: If RNA-free genomic DNA is required, add 4 µl RNase A (100 mg/ml). Seal the collection microtubes properly using the caps provided, mix by vortexing, and incubate for 5 min at room temperature before continuing with step 2.

Keep the clear covers from the collection microtube racks for use in step 3.

2. Add 200 µl Buffer AL (without added ethanol) to each sample.

Ensure that ethanol has not been added to Buffer AL (see "Buffer AL", page 18). Buffer AL can be purchased separately (see page 56 for ordering information).

3. Seal the collection microtubes properly using the caps provided. Place a clear cover (saved from step 1) over each rack of collection microtubes, and shake the racks vigorously up and down for 15 s. To collect any solution from the caps, centrifuge the collection microtubes. Allow the centrifuge to reach 3000 rpm, and then stop the centrifuge.

Do not prolong this step.

IMPORTANT: The rack of collection microtubes must be vigorously shaken up and down with both hands to obtain a homogeneous lysate. Inverting the rack of collection microtubes is not sufficient for mixing. The genomic DNA will not be sheared by vigorous shaking. The lysate and Buffer AL should be mixed immediately and thoroughly to yield a homogeneous solution.

Keep the clear covers from the collection microtube racks for use in step 6.

4. **Incubate at 56°C for 10 min. Place a weight on top of the caps during the incubation. Mix occasionally during incubation to disperse the sample, or place on a rocking platform.**

   Note: Do not use a rotary- or vertical-type shaker as continuous rotation may release the caps. If incubation is performed in a water bath make sure that the collection microtubes are not fully submerged and that any remaining water is removed prior to removing the caps in step 5.

5. **Carefully remove the caps, and add 200 µl ethanol (96–100%) to each sample.**

6. **Seal the collection microtubes properly using the caps provided. Place a clear cover over each rack of collection microtubes, and shake the racks vigorously up and down for 15 s. To collect any solution from the caps, centrifuge the collection microtubes. Allow the centrifuge to reach 3000 rpm, and then stop the centrifuge.**

   Do not prolong this step.

   IMPORTANT: The rack of collection microtubes must be vigorously shaken up and down with both hands to obtain a homogeneous lysate. Inverting the rack of collection microtubes is not sufficient for mixing. The genomic DNA will not be sheared by vigorous shaking. The lysate and ethanol should be mixed immediately and thoroughly to yield a homogeneous solution.

7. **Place two DNeasy 96 plates on top of S-Blocks (provided). Mark the DNeasy 96 plates for later sample identification.**

8. **Remove and discard the caps from the collection microtubes. Carefully transfer the lysis mixture (maximum 900 µl) of each sample from step 6 to each well of the DNeasy 96 plates.**

   Take care not to wet the rims of the wells to avoid aerosols during centrifugation. Do not transfer more than 900 µl per well.

   Note: Lowering pipet tips to the bottoms of the wells may cause sample overflow and cross-contamination. Therefore, remove one set of caps at a time, and begin drawing up the samples as soon as the pipet tips contact the liquid. Repeat until all the samples have been transferred to the DNeasy 96 plates.

9. **Seal each DNeasy 96 plate with an AirPore Tape Sheet (provided). Centrifuge for 4 min at 6000 rpm.**

   AirPore Tape prevents cross-contamination between samples during centrifugation.

   After centrifugation, check that all of the lysate has passed through the membrane in each well of the DNeasy 96 plates. If lysate remains in any of the wells, centrifuge for a further 4 min.

10. **Remove the tape. Carefully add 500 µl Buffer AW1 to each sample.**

    Note: Ensure that ethanol has been added to Buffer AW1 prior to use.

11. **Seal each DNeasy 96 plate with a new AirPore Tape Sheet (provided). Centrifuge for 2 min at 6000 rpm.**

12. **Remove the tape. Carefully add 500 µl Buffer AW2 to each sample.**

    Note: Ensure that ethanol has been added to Buffer AW2 prior to use.

13. **Centrifuge for 15 min at 6000 rpm.**

    Do not seal the plate with AirPore Tape.

    The heat generated during centrifugation ensures evaporation of residual ethanol in the sample (from Buffer AW2) that might otherwise inhibit downstream reactions.

14. **Place each DNeasy 96 plate in the correct orientation on a new rack of Elution Microtubes RS (provided).**

15. **To elute the DNA, add 200 µl Buffer AE to each sample, and seal the DNeasy 96 plates with new AirPore Tape Sheets (provided). Incubate for 1 min at room temperature (15–25°C). Centrifuge for 4 min at 6000 rpm.**

    200 µl Buffer AE is sufficient to elute up to 75% of the DNA from each well of the DNeasy 96 plate.

    Elution with volumes less than 200 µl significantly increases the final DNA concentration of the eluate but may reduce overall DNA yield. For samples containing less than 1 µg DNA, elution in 50 µl Buffer AE is recommended.

16. **Recommended: For maximum DNA yield, repeat step 15 with another 200 µl Buffer AE.**

    A second elution with 200 µl Buffer AE will increase the total DNA yield by up to 25%. However due to the increased volume, the DNA concentration is reduced. If a higher DNA concentration is desired, the second elution step can be performed using the 200 µl eluate from the first elution. This will increase the yield by up to 15%.

    Use new caps (provided) to seal the Elution Microtubes RS for storage.

Protocol: Purification of Total DNA from Animal Tissues (DNeasy 96 Protocol)

This protocol is designed for high-throughput purification of total DNA from animal tissues, including rodent tails.

Important points before starting

- If using the DNeasy 96 Blood & Tissue Kit for the first time, read "Important Notes" (page 15).
- All centrifugation steps are carried out at room temperature (15–25°C).
- Optional: RNase A may be used to digest RNA during the procedure. RNase A is not provided in the DNeasy 96 Blood & Tissue Kit (see "Copurification of RNA", page 19).

Things to do before starting

- Buffer AL should be premixed with ethanol before use. Add 90 ml ethanol (96–100%) to the bottle containing 86 ml Buffer AL or 260 ml ethanol to the bottle containing 247 ml Buffer AL and shake thoroughly. Mark the bottle to indicate that ethanol has been added. (Please note that, for purification of DNA from animal blood, Buffer AL must be used without ethanol. Buffer AL can be purchased separately if the same kit will be used for purification of DNA from animal blood.)
- Buffer AW1 and Buffer AW2 are supplied as concentrates. Before using for the first time, add the appropriate amount of ethanol (96–100%) as indicated on the bottle to obtain a working solution.
- Buffer ATL and Buffer AL may form precipitates upon storage. If necessary, warm to 56°C for 5 min until the precipitates have fully dissolved.
- Mix Buffer AW1 before use by inverting several times.
- Preheat an incubator to 56°C for use in step 4.
- If using frozen tissue, equilibrate the sample to room temperature. Avoid repeated thawing and freezing of samples since this will lead to reduced DNA size.

Procedure

1. **Cut up to 20 mg tissue (up to 10 mg spleen) into small pieces. For rodent tails, place one (rat) or two (mouse) 0.4–0.6 cm lengths of tail into a collection microtube. Earmark the animal appropriately. Use a 96-Well-Plate Register (provided) to identify the position of each sample.**

Ensure that the correct amount of starting material is used (see "Starting amounts of samples", page 15). For tissues such as spleen with a very high number of cells for a given mass of tissue, no more than 10 mg starting material should be used.

We strongly recommend to cut the tissue into small pieces to enable more efficient lysis. If desired, lysis time can be reduced by disrupting the sample using a bead mill, such as the QIAGEN TissueLyser (see page 56 for ordering information), before addition of Buffer ATL and proteinase K. A supplementary protocol for simultaneous disruption of up to 48 tissue samples using the TissueLyser can be obtained by contacting QIAGEN Technical Services (see back cover).

For rodent tails, a maximum of 1.2 cm (mouse) or 0.6 cm (rat) tail should be used. When purifying DNA from the tail of an adult mouse or rat, it is recommended to use only 0.4–0.6 cm.

Store the samples at –20°C until a suitable number has been collected (up to 192 samples). Samples can be stored at –20°C for several weeks to months without any reduction in DNA yield. DNA yields will be approximately 10–30 µg, depending on the type, length, age, and species of sample used (see "Expected yields", page 22).

Keep the clear covers from the collection microtube racks for use in step 3.

2. **Prepare a proteinase K–Buffer ATL working solution containing 20 µl proteinase K stock solution and 180 µl Buffer ATL per sample, and mix by vortexing. For one set of 96 samples, use 2 ml proteinase K stock solution and 18 ml Buffer ATL. Immediately pipet 200 µl working solution into each collection microtube containing the tail sections or tissue samples. Seal the microtubes properly using the caps provided.**

   Note: Check Buffer ATL for precipitate. If necessary, dissolve the precipitate by incubation at 56°C for 5 min before preparing the working solution.

   IMPORTANT: After preparation, the proteinase K–Buffer ATL working solution should be dispensed immediately into the collection microtubes containing the tail or tissue samples. Incubation of the working solution in the absence of substrate for >30 min reduces lysis efficiency and DNA purity.

3. **Ensure that the microtubes are properly sealed to avoid leakage during shaking. Place a clear cover (saved from step 1) over each rack of collection microtubes, and mix by inverting the rack of collection microtubes. To collect any solution from the caps, centrifuge the collection microtubes. Allow the centrifuge to reach 3000 rpm, and then stop the centrifuge. It is essential that the samples are completely submerged in the proteinase K–Buffer ATL working solution after centrifugation.**

If the proteinase K–Buffer ATL working solution does not completely cover the sample, increase the volume of the solution to 300 µl per sample (additional reagents are available separately; see page 56 for ordering information). Do not increase volumes above 300 µl as this will exceed the capacity of the collection microtubes in subsequent steps.

Keep the clear covers from the collection microtube racks for use in step 5.

4. **Incubate at 56°C overnight or until the samples are completely lysed. Place a weight on top of the caps during the incubation. Mix occasionally during incubation to disperse the sample, or place on a rocking platform.**

   Lysis time varies depending on the type, age, and amount of tail or tissue being processed. Lysis is usually complete in 1–3 h or, for rodent tails, 6–8 h, but optimal results will be achieved after overnight lysis.

   After incubation the lysate may appear viscous, but should not be gelatinous as it may clog the DNeasy 96 membrane. If the lysate appears very gelatinous, see the "Troubleshooting Guide", page 47, for recommendations.

   Note: Do not use a rotary- or vertical-type shaker as continuous rotation may release the caps. If incubation is performed in a water bath make sure that the collection microtubes are not fully submerged and that any remaining water is removed prior to centrifugation in step 5.

5. **Ensure that the microtubes are properly sealed to avoid leakage during shaking. Place a clear cover over each rack of collection microtubes and shake the racks vigorously up and down for 15 s. To collect any solution from the caps, centrifuge the collection microtubes. Allow the centrifuge to reach 3000 rpm, and then stop the centrifuge.**

   IMPORTANT: The rack of collection microtubes must be vigorously shaken up and down with both hands to obtain a homogeneous lysate. Inverting the rack of collection microtubes is not sufficient for mixing. The genomic DNA will not be sheared by vigorous shaking.

   Keep the clear covers from the collection microtube racks for use in step 7.

   Ensure that lysis is complete before proceeding to step 6. The lysate should be homogeneous following the vigorous shaking. To check this, slowly invert the rack of collection microtubes (making sure that the caps are tightly closed) and look for a gelatinous mass. If a gelatinous mass is visible, lysis needs to be extended by adding another 100 µl Buffer ATL and 15 µl proteinase K, and incubating for a further 3 h. It is very important to ensure that samples are completely lysed to achieve optimal yields and to avoid clogging of individual wells of the DNeasy 96 plate.

Optional: If RNA-free genomic DNA is required, add 4 µl RNase A (100 mg/ml). Close the collection microtubes with fresh caps, mix by shaking vigorously, and incubate for 5 min at room temperature. To collect any solution from the caps, centrifuge the collection microtubes. Allow the centrifuge to reach 3000 rpm, and then stop the centrifuge. Remove the caps, and continue with step 6.

Transcriptionally active tissues such as liver and kidney contain high levels of RNA, which will copurify with genomic DNA. For tissues that contain low levels of RNA, such as rodent tails, or if residual RNA is not a concern, RNase A digestion is usually not necessary.

6. **Carefully remove the caps. Add 410 µl premixed Buffer AL–ethanol to each sample.**

   Note: Ensure that ethanol has been added to Buffer AL prior to use (see "Buffer AL", page 18).

   Note: A white precipitate may form upon addition of Buffer AL–ethanol to the lysate. It is important to apply all of the lysate, including the precipitate, to the DNeasy 96 plate in step 9. This precipitate does not interfere with the DNeasy procedure or with any subsequent application.

   If the volumes of Buffer ATL and proteinase K were increased in steps 3 or 5, increase the volume of Buffer AL and ethanol accordingly. For example, 300 µl proteinase K–Buffer ATL working solution will require 615 µl Buffer AL–ethanol.

7. **Ensure that the microtubes are properly sealed to avoid leakage during shaking. Place a clear cover over each rack of collection microtubes and shake the racks vigorously up and down for 15 s. To collect any solution from the caps, centrifuge the collection microtubes. Allow the centrifuge to reach 3000 rpm, and then stop the centrifuge.**

   Do not prolong this step.

   IMPORTANT: The rack of collection microtubes must be vigorously shaken up and down with both hands to obtain a homogeneous lysate. Inverting the rack of collection microtubes is not sufficient for mixing. The genomic DNA will not be sheared by vigorous shaking. The lysate and Buffer AL–ethanol should be mixed immediately and thoroughly to yield a homogeneous solution.

8. **Place two DNeasy 96 plates on top of S-Blocks (provided). Mark the DNeasy 96 plates for later sample identification.**

9. **Remove and discard the caps from the collection microtubes. Carefully transfer the lysate (maximum 900 µl) of each sample from step 7 to each well of the DNeasy 96 plates.**

   Take care not to wet the rims of the wells to avoid aerosols during centrifugation. Do not transfer more than 900 µl per well.

Note: Lowering pipet tips to the bottoms of the wells may cause sample overflow and cross-contamination. Therefore, remove one set of caps at a time, and begin drawing up the samples as soon as the pipet tips contact the liquid. Repeat until all the samples have been transferred to the DNeasy 96 plates.

Note: If the volume of proteinase K–Buffer ATL working solution was increased in steps 3 or 5, transfer no more than 900 µl of the supernatant from step 7 to the DNeasy 96 plate. Larger amounts will exceed the volume capacity of the individual wells. Discard any remaining supernatant from step 7 as this will not contribute significantly to the total DNA yield.

10. **Seal each DNeasy 96 plate with an AirPore Tape Sheet (provided). Centrifuge for 10 min at 6000 rpm.**

    AirPore Tape prevents cross-contamination between samples during centrifugation.

    After centrifugation, check that all of the lysate has passed through the membrane in each well of the DNeasy 96 plates. If lysate remains in any of the wells, centrifuge for a further 10 min.

11. **Remove the tape. Carefully add 500 µl Buffer AW1 to each sample.**

    Note: Ensure that ethanol has been added to Buffer AW1 prior to use.

    It is not necessary to increase the volume of Buffer AW1 if the volume of proteinase K–Buffer ATL working solution was increased in steps 3 or 5.

12. **Seal each DNeasy 96 plate with a new AirPore Tape Sheet (provided). Centrifuge for 5 min at 6000 rpm.**

13. **Remove the tape. Carefully add 500 µl Buffer AW2 to each sample.**

    Note: Ensure that ethanol has been added to Buffer AW2 prior to use.

    It is not necessary to increase the volume of Buffer AW2 if the volume of proteinase K–Buffer ATL working solution was increased in steps 3 or 5.

14. **Centrifuge for 15 min at 6000 rpm.**

    Do not seal the plate with AirPore Tape.

    The heat generated during centrifugation ensures evaporation of residual ethanol in the sample (from Buffer AW2) that might otherwise inhibit downstream reactions.

15. **Place each DNeasy 96 plate in the correct orientation on a new rack of Elution Microtubes RS (provided).**

16. **To elute the DNA, add 200 µl Buffer AE to each sample, and seal the DNeasy 96 plates with new AirPore Tape Sheets (provided). Incubate for 1 min at room temperature (15–25°C). Centrifuge for 2 min at 6000 rpm.**

    200 µl Buffer AE is sufficient to elute up to 75% of the DNA from each well of the DNeasy 96 plate.

Elution with volumes less than 200 µl significantly increases the final DNA concentration of the eluate but may reduce overall DNA yield. For samples containing less than 1 µg DNA, elution in 50 µl Buffer AE is recommended.

17. **Recommended: For maximum DNA yield, repeat step 16 with another 200 µl Buffer AE.**

    A second elution with 200 µl Buffer AE will increase the total DNA yield by up to 25%. However due to the increased volume, the DNA concentration is reduced. If a higher DNA concentration is desired, the second elution step can be performed using the 200 µl eluate from the first elution. This will increase the yield by up to 15%.

    Use new caps (provided) to seal the Elution Microtubes RS for storage.

Protocol: Pretreatment for Paraffin-Embedded Tissue

This protocol is designed for purification of total DNA from fixed, paraffin-embedded tissues using the DNeasy Blood & Tissue Kit. The protocol describes the preliminary removal of paraffin by extraction with xylene.

Important points before starting

- The length of DNA purified from fixed tissues is usually <650 bp, depending on the type and age of the sample and the quality of the fixative used.
- Use of fixatives such as alcohol and formalin is recommended. Fixatives that cause cross-linking, such as osmic acid, are not recommended as it can be difficult to obtain amplifiable DNA from tissue fixed with these agents.
- Lysis time will vary from sample to sample depending on the type of tissue processed.
- Yields will depend both on the size and the age of the sample processed. Reduced yields compared with fresh or frozen tissues are to be expected. Therefore, eluting purified DNA in 50–100 µl Buffer AE is recommended.
- This pretreatment protocol has not been thoroughly tested and optimized for high-throughput DNA purification using the DNeasy 96 Blood & Tissue Kit. As a general guideline, we recommend to decrease the amount of starting material when using this protocol with the DNeasy 96 Blood & Tissue Kit.

Things to do before starting

- Preheat a heating block, incubator, or water bath to 37°C for use in step 9.

Procedure

1. **Place a small section (not more than 25 mg) of paraffin-embedded tissue in a 2 ml microcentrifuge tube (not provided).**
2. **Add 1200 µl xylene. Vortex vigorously.**
3. **Centrifuge in a microcentrifuge at full speed for 5 min at room temperature (15–25°C).**
4. **Remove supernatant by pipetting. Do not remove any of the pellet.**
5. **Add 1200 µl ethanol (96–100%) to the pellet to remove residual xylene, and mix gently by vortexing.**
6. **Centrifuge in a microcentrifuge at full speed for 5 min at room temperature.**
7. **Carefully remove the ethanol by pipetting. Do not remove any of the pellet.**
8. **Repeat steps 5–7 once.**

9. **Incubate the open microcentrifuge tube at 37°C for 10–15 min until the ethanol has evaporated.**
10. **Resuspend the tissue pellet in 180 µl Buffer ATL, and continue with step 2 of the protocol "Purification of Total DNA from Animal Tissues (Spin-Column Protocol)", page 29.**

Protocol: Pretreatment for Formalin-Fixed Tissue

This protocol is designed for purification of total DNA from fixed, paraffin-embedded tissues. The protocol describes the preliminary washing with PBS to remove the fixative.

Important points before starting

- The length of DNA purified from fixed tissues is usually <650 bp, depending on the type and age of the sample and the quality of the fixative used.
- Use of fixatives such as alcohol and formalin is recommended. Fixatives that cause cross-linking, such as osmic acid, are not recommended as it can be difficult to obtain amplifiable DNA from tissue fixed with these agents.
- Lysis time will vary from sample to sample depending on the type of tissue processed.
- Yields will depend both on the size and the age of the sample processed. Reduced yields compared with fresh or frozen tissues are to be expected. Therefore, eluting purified DNA in a total volume of 50–100 µl Buffer AE is recommended.
- This pretreatment protocol has not been thoroughly tested and optimized for high-throughput DNA purification using the DNeasy 96 Blood & Tissue Kit. As a general guideline, we recommend to decrease the amount of starting material when using this protocol with the DNeasy 96 Blood & Tissue Kit.

Procedure

1. **Wash the sample (not more than 25 mg) twice in PBS to remove the fixative.**
2. **Discard the PBS and continue with step 1 of the protocol "Purification of Total DNA from Animal Tissues (Spin-Column Protocol)", page 28.**

Protocol: Pretreatment for Gram-Negative Bacteria

This protocol is designed for purification of total DNA from Gram-negative bacteria, such as *E. coli*. The protocol describes the preliminary harvesting of bacteria before DNA purification.

Important points before starting

- See "Quantification of starting material", page 17, for details of how to collect and store samples, and how to determine the number of cells in a bacterial culture.
- This pretreatment protocol has not been thoroughly tested and optimized for high-throughput DNA purification using the DNeasy 96 Blood & Tissue Kit. As a general guideline, we recommend to decrease the amount of starting material when using this protocol with the DNeasy 96 Blood & Tissue Kit.

Procedure

1. **Harvest cells (maximum 2 x 10^9 cells) in a microcentrifuge tube by centrifuging for 10 min at 5000 x *g* (7500 rpm). Discard supernatant.**
2. **Resuspend pellet in 180 µl Buffer ATL.**
3. **Continue with step 2 of the protocol "Purification of Total DNA from Animal Tissues (Spin-Column Protocol)", page 29.**

Protocol: Pretreatment for Gram-Positive Bacteria

This protocol is designed for purification of total DNA from Gram-positive bacteria, such as *Corynebacterium* spp. and *B. subtilis*. The protocol describes the preliminary harvesting of bacteria and incubation with lysozyme to lyse their cell walls before DNA purification.

Important points before starting

- See "Quantification of starting material", page 17, for details of how to collect and store samples, and how to determine the number of cells in a bacterial culture.
- Ensure that ethanol has not been added to Buffer AL (see "Buffer AL", page 18). Buffer AL can be purchased separately (see page 56 for ordering information).
- This pretreatment protocol has not been thoroughly tested and optimized for high-throughput DNA purification using the DNeasy 96 Blood & Tissue Kit. As a general guideline, we recommend to decrease the amount of starting material when using this protocol with the DNeasy 96 Blood & Tissue Kit.

Things to do before starting

- Prepare enzymatic lysis buffer as described in "Equipment and Reagents to Be Supplied by User", page 14.
- Preheat a heating block or water bath to 37°C for use in step 3.

Procedure

1. **Harvest cells (maximum 2 x 10^9 cells) in a microcentrifuge tube by centrifuging for 10 min at 5000 x g (7500 rpm). Discard supernatant.**
2. **Resuspend bacterial pellet in 180 µl enzymatic lysis buffer.**
3. **Incubate for at least 30 min at 37°C.**

   After incubation, heat the heating block or water bath to 56°C if it is to be used for the incubation in step 5.
4. **Add 25 µl proteinase K and 200 µl Buffer AL (without ethanol). Mix by vortexing.**

   Note: Do not add proteinase K directly to Buffer AL.

   Ensure that ethanol has not been added to Buffer AL (see "Buffer AL", page 18). Buffer AL can be purchased separately (see page 56 for ordering information).
5. **Incubate at 56°C for 30 min.**

   Optional: If required, incubate at 95°C for 15 min to inactivate pathogens. Note that incubation at 95°C can lead to some DNA degradation.

6. **Add 200 µl ethanol (96–100%) to the sample, and mix thoroughly by vortexing.**

   It is important that the sample and the ethanol are mixed thoroughly to yield a homogeneous solution.

   A white precipitate may form on addition of ethanol. It is essential to apply all of the precipitate to the DNeasy Mini spin column. This precipitate does not interfere with the DNeasy procedure.

7. **Continue with step 4 of the protocol "Purification of Total DNA from Animal Tissues (Spin-Column Protocol)", page 30.**

Troubleshooting Guide

This troubleshooting guide may be helpful in solving any problems that may arise. The scientists in QIAGEN Technical Services are always happy to answer any questions you may have about either the information and protocols in this handbook or molecular biology applications (see back cover for contact information).

		Comments and suggestions
Low yield		
a)	Storage of starting material	DNA yield is dependent on the type, size, age, and storage of starting material. Lower yields will be obtained from material that has been inappropriately stored (see "Sample collection and storage", page 17).
b)	Too much starting material	In future preparations, reduce the amount of starting material used (see "Quantification of starting material", page 16).
c)	Insufficient mixing of sample with Buffer AL and ethanol before binding	**DNeasy spin-column protocols**: In future preparations, mix sample first with Buffer AL and then with ethanol by pulse vortexing for 15 s each time before applying the sample to the DNeasy Mini spin column. **DNeasy 96 protocols**: In future preparations, ensure that samples are mixed by vigorous shaking, as described in the protocols, before applying the sample to the DNeasy 96 plate.
d)	DNA inefficiently eluted	Increase elution volume to 200 µl and perform another elution step. See also "Elution of pure nucleic acids", page 21. Check that ethanol was added before applying the sample to the DNeasy Mini spin column. Check that any precipitate in Buffer ATL and/or Buffer AL was dissolved before use.
e)	Buffer AW1 or Buffer AW2 prepared incorrectly	Make sure that ethanol has been added to Buffer AW1 and Buffer AW2 before use (see "Things to do before starting", pages 25, 28, 31, and 35).

		Comments and suggestions
f)	Water used instead of Buffer AE for elution	The low pH of deionized water from some water purifiers may reduce DNA yield. When eluting with water, ensure that the pH of the water is at least 7.0.
g)	**Animal tissue**: Insufficient lysis	In future preparations, reduce the amount of starting material used (see "Quantification of starting material", page 17). Cut tissue into smaller pieces to facilitate lysis. After lysis, vortex sample vigorously; this will not damage or reduce the size of the DNA. If a substantial gelatinous pellet remains after incubation and vortexing, extend incubation time at 56°C for proteinase K digest and/or increase amount of proteinase K to 40 µl. (For DNeasy 96 protocols, always check that the sample is completely lysed before addition of Buffer AL and ethanol. If a gelatinous mass is still present after the overnight incubation, lysis needs to be extended.) Ensure that the sample is fully submerged in the buffer containing proteinase K. If necessary, double the amount of Buffer ATL and proteinase K, and use a 2 ml microcentrifuge tube for lysis. Remember to adjust the amount of Buffer AL and ethanol proportionately in subsequent steps. (For example, a lysis step with 360 µl Buffer ATL plus 40 µl proteinase K will require 400 µl Buffer AL plus 400 µl ethanol to bind DNA to the DNeasy membrane). **DNeasy spin-column protocols**: Pipet the sample into the DNeasy Mini spin column in two sequential loading steps. Discard flow-through between these loading steps. **DNeasy 96 protocols**: Transfer a maximum of 900 µl of each sample to the DNeasy 96 plate.

		Comments and suggestions
h)	**Bacteria**: Insufficient lysis	In future preparations, extend incubation with cell-wall–lysing enzyme and/or increase amount of lysing enzyme. Harvest bacteria during early log phase of growth (see "Sample collection and storage", page 15).
i)	**DNeasy spin-column protocols**: DNA not bound to DNeasy Mini spin column	Check that ethanol was added before applying the sample to the DNeasy Mini spin column.
j)	**DNeasy 96 protocols**: Inefficient DNA elution	Repeat elution with Buffer AE preheated to 70°C. After addition of Buffer AE preheated to 70°C, the DNeasy 96 plate should be incubated at room temperature for 1 min. To increase elution efficiency, extend the incubation to 5 min at 70°C.
k)	**DNeasy 96 protocols**: Unequal volumes of Buffer AE or water delivered by the multichannel pipet	Ensure that all tips are firmly fitted to the pipet. Check liquid levels in tips before dispensing.
DNeasy Mini spin column or DNeasy 96 plate clogged		
	Too much starting material and/or insufficient lysis	Increase *g*-force and/or duration of centrifugation step. In future preparations, reduce the amount of starting material used (see "Quantification of starting material", page 17). For rodent tails or bacteria, see also "Insufficient lysis" in the "Low yield" section above.
Low concentration of DNA in the eluate		
	Second elution step diluted the DNA	Use a new collection tube for the second eluate to prevent dilution of the first eluate. Reduce elution volume to 50–100 µl. See "Elution of pure nucleic acids", page 21.
A_{260}/A_{280} ratio of purified DNA is low		
a)	Water used instead of buffer to measure A_{260}/A_{280}	Use 10 mM Tris·Cl, pH 7.5 instead of water to dilute the sample before measuring purity. See "Appendix A: Determination of Yield, Purity, and Length of DNA", page 52.
b)	Inefficient cell lysis	See "Low yield", above.

		Comments and suggestions
A_{260}/A_{280} ratio of purified DNA is high		
	High level of residual RNA	Perform the optional RNase treatment in the protocol.
DNA does not perform well in downstream applications		
a)	Salt carryover	Ensure that Buffer AW2 has been used at room temperature (15–25°C). Ensure that Buffer AW1 and Buffer AW2 were added in the correct order.
b)	Ethanol carryover	**DNeasy spin-column protocols**: Ensure that, when washing with Buffer AW2, the column is centrifuged for 3 min at 20,000 x *g* (14,000 rpm) to dry the DNeasy membrane. Following the centrifugation step, remove the DNeasy Mini spin column carefully so that the column does not come into contact with the flow-through. If ethanol is visible in the DNeasy Mini spin column (as either drops or a film), discard the flow-through, keep the collection tube, and centrifuge for a further 1 min at 20,000 x *g*. **DNeasy 96 protocols**: Incubate the DNeasy 96 plate, uncovered, in an oven or incubator for 10 min at 80°C after the second wash to remove all traces of Buffer AW2.
c)	Too much DNA used	For PCR applications, a single-copy gene can typically be detected after 35 PCR cycles with 100 ng template DNA.
DNA sheared		
a)	Sample repeatedly frozen and thawed	Avoid repeated freezing and thawing of starting material.
b)	Sample too old	Old samples often yield only degraded DNA.
White precipitate in Buffer ATL or Buffer AL		
	White precipitate may form at low temperature after prolonged storage	Any precipitate formed when Buffer ATL or Buffer AL are added must be dissolved by incubating the buffer at 56°C until it disappears.

	Comments and suggestions
Discolored membrane after wash with Buffer AW2, or colored eluate	
a) **Rodent tails**: Hair not removed from rodent tails during preparation	DNeasy spin-column protocols: In future preparations, centrifuge lysate for 5 min at 20,000 x *g* after digestion with proteinase K. Transfer supernatant into a new tube before proceeding with step 3. **DNeasy 96 protocols**: In future preparations, centrifuge the rack of collection microtubes containing the lysates for 5 min at 6000 rpm at step 5. Remove the caps. Carefully transfer the lysates, without disturbing the pelleted debris, to another rack of collection microtubes. Continue the protocol at step 6.
b) **Animal blood**: Contamination with hemoglobin	Reduce amount of blood used and/or double the amount of proteinase K used per preparation. Try using buffy coat instead of whole blood.

Appendix A: Determination of Yield, Purity, and Length of DNA

Determination of yield and purity

DNA yield is determined by measuring the concentration of DNA in the eluate by its absorbance at 260 nm. Absorbance readings at 260 nm should fall between 0.1 and 1.0 to be accurate. Sample dilution should be adjusted accordingly. Measure the absorbance at 260 nm or scan absorbance from 220–330 nm (a scan will show if there are other factors affecting absorbance at 260 nm; for instance, absorbance at 325 nm would indicate contamination by particulate matter or a dirty cuvette). An A_{260} value of 1 (with a 1 cm detection path) corresponds to 50 µg DNA per milliliter water. Water should be used as diluent when measuring DNA concentration since the relationship between absorbance and concentration is based on extinction coefficients calculated for nucleic acids in water.* Both DNA and RNA are measured with a spectrophotometer at 260 nm; to measure only DNA in a mixture of DNA and RNA, a fluorimeter must be used.

An example of the calculations involved in DNA quantification is shown below.

Volume of DNA sample	=	100 µl
Dilution	=	20 µl of DNA sample + 180 µl distilled water (1/10 dilution)

Measure absorbance of diluted sample in a 0.2 ml cuvette

A_{260}	=	0.2
Concentration of DNA sample	=	50 µg/ml x A_{260} x dilution factor
	=	50 µg/ml x 0.2 x 10
	=	100 µg/ml
Total amount	=	concentration x volume of sample in milliliters
	=	100 µg/ml x 0.1 ml
	=	10 µg DNA

The ratio of the readings at 260 nm and 280 nm (A_{260}/A_{280}) provides an estimate of the purity of DNA with respect to contaminants that absorb UV, such as protein. However, the A_{260}/A_{280} ratio is influenced considerably by pH. Since water is not buffered, the pH and the resulting A_{260}/A_{280} ratio can vary greatly. Lower pH results in a lower A_{260}/A_{280} ratio and reduced sensitivity to protein contamination. For accurate values, we recommend measuring absorbance in 10 mM Tris·Cl, pH 7.5, in which pure DNA has an A_{260}/A_{280} ratio of 1.8–2.0. Always be sure to calibrate the spectrophotometer with the same solution.

* Wilfinger, W.W., Mackey, M., and Chomcynski, P. (1997) Effect of pH and ionic strength on the spectrophotometric assessment of nucleic acid purity. BioTechniques **22**, 474.

Determination of length

The precise length of genomic DNA should be determined by pulse-field gel electrophoresis (PFGE) through an agarose gel. To prepare the sample for PFGE, the DNA should be concentrated by alcohol precipitation and the DNA pellet dried briefly at room temperature (15–25°C) for 5–10 minutes. Avoid drying the DNA pellet for more than 10 minutes since overdried genomic DNA is very difficult to redissolve. Redissolve in approximately 30 µl TE buffer, pH 8.0,* for at least 30 minutes at 60°C. Load 3–5 µg of DNA per well. Standard PFGE conditions are as follows:

- 1% agarose gel in 0.5 x TBE electrophoresis buffer*
- switch intervals = 5–40 seconds
- run time = 17 hours
- voltage = 170 V

* When working with chemicals, always wear a suitable lab coat, disposable gloves, and protective goggles. For more information, please consult the appropriate material safety data sheets (MSDSs), available from the product supplier.

Appendix B: Cleaning S-Blocks

Cleaning S-Blocks

To avoid cross-contamination, after each use rinse the S-Blocks thoroughly in tap water, incubate for 1 min at room temperature in 0.4 M HCl,* empty, and wash thoroughly with distilled water. Used S-Blocks can also be autoclaved after washing. Additional S-Blocks can be ordered separately (see page 55 for ordering information).

* When working with chemicals, always wear a suitable lab coat, disposable gloves, and protective goggles. For more information, please consult the appropriate material safety data sheets (MSDSs), available from the product supplier.

Ordering Information

Product	Contents	Cat. no.
DNeasy Blood & Tissue Kit (50)	50 DNeasy Mini Spin Columns, Proteinase K, Buffers, Collection Tubes (2 ml)	69504
DNeasy Blood & Tissue Kit (250)	250 DNeasy Mini Spin Columns, Proteinase K, Buffers, Collection Tubes (2 ml)	69506
DNeasy 96 Blood & Tissue Kit (4)*	For 4 x 96 DNA minipreps: 4 DNeasy 96 Plates, Proteinase K, Buffers, S-Blocks, AirPore Tape Sheets, Collection Microtubes (1.2 ml), Elution Microtubes RS, Caps, 96-Well Plate Registers	69581
DNeasy 96 Tissue Kit (12)*	For 12 x 96 DNA minipreps: 12 DNeasy 96 Plates, Proteinase K, Buffers, S-Blocks, AirPore Tape Sheets, Collection Microtubes (1.2 ml), Elution Microtubes RS, Caps, 96-Well Plate Registers	69582
QIAGEN 96-Well Plate Centrifugation System		
Centrifuge 4-15C	Universal laboratory centrifuge with brushless motor	Inquire
Centrifuge 4K15C	Universal refrigerated laboratory centrifuge with brushless motor	Inquire
Plate Rotor 2 x 96	Rotor for 2 QIAGEN 96-well plates, for use with QIAGEN Centrifuges	81031
Accessories		
Collection Tubes (2 ml)	1000 Collection Tubes (2 ml)	19201
Collection Microtubes (racked, 10 x 96)	Nonsterile polypropylene tubes (1.2 ml), 960 in racks of 96	19560
Collection Microtube Caps (120 x 8)	Nonsterile polypropylene caps for collection microtubes (1.2 ml) and round-well blocks, 960 in strips of 8	19566
S-Blocks (24)	96-well blocks with 2.2 ml wells, 24 per case	19585

* Larger kit sizes and/or formats available; please inquire.

Ordering Information

Product	Contents	Cat. no.
AirPore Tape Sheets (50)	Microporous tape sheets for covering 96-well blocks: 50 sheets per pack	19571
TissueRuptor	Handheld rotor–stator homogenizer	Inquire
TissueRuptor Disposable Probes (25)	25 nonsterile plastic disposable probes for use with the TissueRuptor	990890
TissueLyser	Universal laboratory mixer-mill disruptor	Inquire
TissueLyser Adapter Set 2 x 24	2 sets of Adapter Plates and 2 racks for use with 2.0 ml microcentrifuge tubes on the TissueLyser	69982
TissueLyser Adapter Set 2 x 96	2 sets of Adapter Plates for use with Collection Microtubes (racked) on the TissueLyser	69984
Stainless Steel Beads, 5 mm (200)	Stainless Steel Beads, suitable for use with the TissueLyser system	69989
QIAGEN Proteinase K (2 ml)	2 ml (>600 mAU/ml, solution)	19131
QIAGEN Proteinase K (10 ml)	10 ml (>600 mAU/ml, solution)	19133
RNase A (17,500 U)	2.5 ml (100 mg/ml; 7000 units/ml, solution)	19101
Buffer AL (216 ml)	216 ml Lysis Buffer	19075
Buffer ATL (200 ml)	200 ml Tissue Lysis Buffer for 1000 preps	19076
Buffer AW1 (Concentrate, 242 ml)	242 ml Wash Buffer (1) Concentrate	19081
Buffer AW2 (Concentrate, 324 ml)	324 ml Wash Buffer (2) Concentrate	19072
Buffer AE (240 ml)	240 ml Elution Buffer	19077
Related products		
QIAGEN Genomic-tip 20/G	25 columns	10223
QIAGEN Genomic-tip 100/G	25 columns	10243
QIAGEN Genomic-tip 500/G	10 columns	10262
Blood & Cell Culture DNA Mini Kit (25)	25 QIAGEN Genomic-tip 20/G, QIAGEN Protease, Buffers	13323

Ordering Information

Product	Contents	Cat. no.
Blood & Cell Culture DNA Midi Kit (25)	25 QIAGEN Genomic-tip 100/G, QIAGEN Protease, Buffers	13343
Blood & Cell Culture DNA Maxi Kit (10)	10 QIAGEN Genomic-tip 500/G, QIAGEN Protease, Buffers	13362
BioSprint 15 DNA Blood Kit (45)*	For 45 preps on the BioSprint 15 workstation: 5-Rod Covers, 5-Tube Strips, MagAttract Suspension G, Buffers and Reagents	940014
BioSprint 96 DNA Blood Kit (48)*	For 48 preps on the BioSprint 96 workstation: Large 96-Rod Covers, 96-Well Microplates MP, S-Blocks, MagAttract Suspension G, Buffers and Reagents	940054
RNeasy® Mini Kit (50)*	For 50 RNA minipreps: 50 RNeasy Mini Spin Columns, Collection Tubes (1.5 ml and 2 ml), RNase-free Reagents and Buffers	74104
RNeasy Midi Kit (10)*	For 10 RNA midipreps: 10 RNeasy Midi Spin Columns, Collection Tubes (15 ml), RNase-free Reagents and Buffers	75142
RNeasy Maxi Kit (12)	For 12 RNA maxipreps: 12 RNeasy Maxi Spin Columns, Collection Tubes (50 ml), RNase-free Reagents and Buffers	75162
RNeasy Protect Mini Kit (50)*	For RNA stabilization and 50 RNA minipreps: RNA*later*® RNA Stabilization Reagent (50 ml), 50 RNeasy Mini Spin Columns, Collection Tubes (1.5 ml and 2 ml), RNase-free Reagents and Buffers	74124

* Larger kit sizes and/or formats available; please inquire.

Ordering Information

Product	Contents	Cat. no.
RNeasy Fibrous Tissue Mini Kit (50)*	For 50 RNA minipreps: 50 RNeasy Mini Spin Columns, Collection Tubes (1.5 ml and 2 ml), Proteinase K, RNase-free DNase I, RNase-free Reagents and Buffers	74704
RNeasy Lipid Tissue Mini Kit (50)*	For 50 RNA minipreps: 50 RNeasy Mini Spin Columns, Collection Tubes (1.5 ml and 2 ml), QIAzol Lysis Reagent, RNase-free Reagents and Buffers	74804

* Larger kit sizes and/or formats available; please inquire.

QIAGEN Distributors and Importers

Please see the back cover for contact information for your local QIAGEN office.

Argentina
Tecnolab S.A.
Tel: (011) 4555 0010
Fax: (011) 4553 3331
E-mail: info@tecnolab.com.ar

Bangladesh
GeneTech Biotechnology
Tel: +880-2-8624304
Fax: +880-2-9568738
E-mail: info@genebiotechbd.com

Bosnia-Herzegovina
MEDILINE d.o.o.
Tel.: +386 1 830-80-40
Fax: +386 1 830-80-70
+386 1 830-80-63
E-mail: info@mediline.si

Brazil
Uniscience do Brasil
Tel: 011 3622 2320
Fax: 011 3622 2323
E-mail: info@uniscience.com

Chile
Biosonda SA
Tel: +562 209 6770
Fax: +562 274 5462
E-mail: ventas@biosonda.cl

China
Eastwin Scientific, Inc.
Order: +86-400-8182168
Tel: +86-10-51663168
Fax: +86-10-82898283
E-mail: laborder@eastwin.com.cn

Gene Company Limited
Tel: +86-21-64951899
Fax: +86-21-64955468
E-mail:
info_bj@genecompany.com (Beijing)
info_sh@genecompany.com (Shanghai)
info_cd@genecompany.com (Chengdu)
info_gz@genecompany.com
(Guangzhou)

Genetimes Technology, Inc.
Order: 800-820-5565
Tel: +86-21-54262677
Fax: +86-21-64398855
E-mail: order@genetimes.com.cn

Colombia
GENTECH – Genetics & Technology
Tel: (+57)(4)2519037
Fax: (+57)(4)2516555
E-mail:
gerencia@gentechcolombia.com
soporte@gentechcolombia.com

Croatia
INEL Medicinska Tehnika d.o.o.
Tel: (01) 2984-898
Fax: (01) 6520-966
E-mail:
inel-medicinska-tehnika@zg.htnet.hr

Cyprus
Scientronics Ltd
Tel: +357 22 467880/90
Fax: +357 22 764614
E-mail: a.sarpetsas@biotronics.com.cy

Czech Republic
BIO-CONSULT spol. s.r.o.
Tel/Fax: (+420) 2 417 29 792
E-mail: info@bioconsult.cz

Ecuador
INMUNOCHEM S.A.C.
Tel: +51 1 4409678
Fax: +51 1 4223701
E-mail: inmunochem@terra.com.pe

Egypt
Clinilab
Tel: 52 57 212
Fax: 52 57 210
E-mail: Clinilab@link.net

Estonia
Quantum Eesti AS
Tel: +372 7301321
Fax: +372 7304310
E-mail: quantum@quantum.ee

Greece
BioAnalytica S.A.
Tel: (210)-640 03 18
Fax: (210)-646 27 48
E-mail: bioanalyt@hol.gr

Hong Kong SAR
Gene Company Limited
Tel: +852-2896-6283
Fax: +852-2515-9371
E-mail: info@genehk.com

Genetimes Technology International Holding Ltd.
Tel: +852-2385-2818
Fax: +852-2385-1308
E-mail: hongkong@genetimes.com.hk

Hungary
BioMarker Kft.
Tel: +36 28 419 986
Fax: +36 28 422 319
E-mail: biomarker@biomarker.hu

India
Genetix
Tel: +91-11-51427031
Fax: +91-11-25419631
E-mail: genetix@genetixbiotech.com

Indonesia
PT Research Biolabs
Tel: +62 21 5865357
E-mail:
indonesia@researchbiolabs.com

Israel
Eldan Electronic Instruments Co. Ltd.
Tel: +972-3-937 1133
Fax: +972-3-937 1121
E-mail: bio@eldan.biz

Jordan
SAHOURY GROUP
Tel: +962 6 4633290-111
Fax: +962 6 4633290-110
E-mail: info@sahoury.com

Korea
LRS Laboratories, Inc.
Tel: (02) 924-86 97
Fax: (02) 924-86 96
E-mail: webmaster@lrslab.co.kr

Philekorea Technology, Inc.
Tel: 1544-3137
Fax: 1644-3137
E-mail: support@philekorea.co.kr

Latvia
SIA "J.I.M."
Tel: 7136393
Fax: 7136394
E-mail: jim@mednet.lv

Lithuania
INTERLUX
Tel: +370-5-2786850
Fax: +370-5-2796728
E-mail: spirit@interlux.lt

Malaysia
RESEARCH BIOLABS SDN. BHD.
Tel: (603)-8070 3101
Fax: (603)-8070 5101
E-mail: biolabs@tm.net.my

Mexico
Quimica Valaner S.A. de C.V.
Tel: (55) 55 25 57 25
Fax: (55) 55 25 56 25
E-mail: ventas@valaner.com

New Zealand
Biolab Ltd
Tel: (09) 980 6700
0800 933 966
Fax: (09) 980 6788
E-mail:
biosciences@nzl.biolabgroup.com

Oman
Al Mazouri Medical & Chemical Supplies
Tel: +971 4 266 1272
(ext. 301, 310, 311)
Fax: +971 4 269 0612
(ATTN: LAB DIVISION)
E-mail: shaji@almaz.net.ae

Pakistan
Pakistan Microbiological Associates
Tel: +92-51-5567953
Fax: +92-51-5514134
E-mail: orderpma@comsats.net.pk

Peru
INMUNOCHEM S.A.C.
Tel: +51 1 4409678
Fax: +51 1 4223701
E-mail: inmunochem@terra.com.pe

Poland
Syngen Biotech Sp.z.o.o.
Tel: (071) 798 58 50 - 52
Fax: (071) 798 58 53
E-mail: info@syngen.pl

Portugal
IZASA PORTUGAL, LDA
Tel: (21) 424 7312
Fax: (21) 417 2674
E-mail: consultasbiotec@izasa.es

Romania
Zyrcon Medical S. R. L.
Tel: +40 21 2245607
Fax: +40 21 2245608
E-mail:
virgil.dracea@zyrconmedical.ro
secretariat@zyrconmedical.ro

Saudi Arabia
Abdulla Fouad Holding Company
Tel: (03) 8324400
Fax: (03) 8346174
E-mail:
sadiq.omar@abdulla-fouad.com

Singapore
Research Biolabs Pte Ltd
Tel: 6777 5366
Fax: 6778 5177
E-mail: sales@researchbiolabs.com

Slovak Republic
BIO-CONSULT Slovakia spol. s.r.o.
Tel/Fax: (02) 5022 1336
E-mail: bio-cons@cdicon.sk

Slovenia
MEDILINE d.o.o.
Tel: (01) 830-80-40
Fax: (01) 830-80-70
(01) 830-80-63
E-mail: info@mediline.si

South Africa
Southern Cross Biotechnology (Pty) Ltd
Tel: (021) 671 5166
Fax: (021) 671 7734
E-mail: info@scb.co.za

Spain
IZASA, S.A.
Tel: (93) 902.20.30.90
Fax: (93) 902.22.33.66
E-mail: consultasbiotec@izasa.es

Taiwan
TAIGEN Bioscience Corporation
Tel: (02) 2880 2913
Fax: (02) 2880 2916
E-mail: order@taigen.com

Thailand
Theera Trading Co. Ltd.
Tel: (02) 412-5672
Fax: (02) 412-3244
E-mail: theetrad@samart.co.th

Turkey
Medek Medikal Ürünler
ve Saglik Hizmetleri A. S.
Tel: (216) 302 15 80
Fax: (216) 302 15 88
E-mail: makialp@med-ek.com

United Arab Emirates
Al Mazouri Medical & Chemical Supplies
Tel: +971 4 266 1272
(ext. 301, 310, 311)
Fax: +971 4 269 0612
(ATTN: LAB DIVISION)
E-mail: shaji@almaz.net.ae

Uruguay
Bionova Ltda
Tel: +598 2 6130442
Fax : +598 2 6142592
E-mail: bionova@internet.com.uy

Venezuela
SAIXX Technologies c.a.
Tel: +58212 3248518
+58212 7616143
+58212 3255838
Fax: +58212 7615945
E-mail: ventas@saixx.com
saixxventas@cantv.net

Vietnam
Viet Anh Instruments Co., Ltd.
Tel: +84-4-5119452
Fax: +84-4-5119453
E-mail: VietanhHN@hn.vnn.vn

All other countries
QIAGEN GmbH, Germany

Australia ▪ Orders 03-9840-9800 ▪ Fax 03-9840-9888 ▪ Technical 1-800-243-066

Austria ▪ Orders 0800/28-10-10 ▪ Fax 0800/28-10-19 ▪ Technical 0800/28-10-11

Belgium ▪ Orders 0800-79612 ▪ Fax 0800-79611 ▪ Technical 0800-79556

Canada ▪ Orders 800-572-9613 ▪ Fax 800-713-5951 ▪ Technical 800-DNA-PREP (800-362-7737)

China ▪ Orders 021-51345678 ▪ Fax 021-51342500 ▪ Technical 021-51345678

Denmark ▪ Orders 80-885945 ▪ Fax 80-885944 ▪ Technical 80-885942

Finland ▪ Orders 0800-914416 ▪ Fax 0800-914415 ▪ Technical 0800-914413

France ▪ Orders 01-60-920-920 ▪ Fax 01-60-920-925 ▪ Technical 01-60-920-930

Germany ▪ Orders 02103-29-12000 ▪ Fax 02103-29-22000 ▪ Technical 02103-29-12400

Ireland ▪ Orders 1800 555 049 ▪ Fax 1800 555 048 ▪ Technical 1800 555 061

Italy ▪ Orders 02-33430411 ▪ Fax 02-33430426 ▪ Technical 800 787980

Japan ▪ Telephone 03-5547-0811 ▪ Fax 03-5547-0818 ▪ Technical 03-5547-0811

Luxembourg ▪ Orders 8002-2076 ▪ Fax 8002-2073 ▪ Technical 8002-2067

The Netherlands ▪ Orders 0800-0229592 ▪ Fax 0800-0229593 ▪ Technical 0800-0229602

Norway ▪ Orders 800-18859 ▪ Fax 800-18817 ▪ Technical 800-18712

Sweden ▪ Orders 020-790282 ▪ Fax 020-790582 ▪ Technical 020-798328

Switzerland ▪ Orders 055-254-22-11 ▪ Fax 055-254-22-13 ▪ Technical 055-254-22-12

UK ▪ Orders 01293-422-911 ▪ Fax 01293-422-922 ▪ Technical 01293-422-999

USA ▪ Orders 800-426-8157 ▪ Fax 800-718-2056 ▪ Technical 800-DNA-PREP (800-362-7737)

QIAGEN

WWW.QIAGEN.COM

1037951 07/2006

Bench Protocol: Animal Blood (Spin-Column Protocol)

Note: Before using this bench protocol, you should be completely familiar with the safety information and detailed protocols in the *DNeasy Blood & Tissue Handbook*.

Please tear off here

Important points before starting

- Perform all centrifugation steps at room temperature (15–25°C).
- If necessary, redissolve any precipitates in Buffer AL.
- Ensure that ethanol has been added to Buffers AW1 and AW2.
- Preheat a thermomixer, shaking water bath, or rocking platform for heating at 56°C.

Procedure

1a. Nonnucleated blood: Pipet 20 µl proteinase K into a 1.5 ml or 2 ml microcentrifuge tube. Add 50–100 µl anticoagulated blood. Adjust the volume to 220 µl with PBS.

1b. Nucleated blood: Pipet 20 µl proteinase K into a 1.5 ml or 2 ml microcentrifuge tube. Add 5–10 µl anticoagulated blood. Adjust the volume to 220 µl with PBS.

1c. Cultured cells: Centrifuge maximum 5 x 10^6 cells for 5 min at 300 x *g*. Resuspend in 200 µl PBS. Add 20 µl proteinase K.

2. Add 200 µl Buffer AL. Mix by vortexing. Incubate at 56°C for 10 min.

3. Add 200 µl ethanol (96–100%). Mix thoroughly by vortexing.

4. Pipet the mixture into a DNeasy Mini spin column in a 2 ml collection tube. Centrifuge at ≥6000 x *g* (8000 rpm) for 1 min. Discard flow-through and collection tube.

5. Place the spin column in a new 2 ml collection tube. Add 500 µl Buffer AW1. Centrifuge for 1 min at ≥6000 x *g*. Discard flow-through and collection tube.

6. Place the spin column in a new 2 ml collection tube, add 500 µl Buffer AW2, and centrifuge for 3 min at 20,000 x *g* (14,000 rpm). Discard flow-through and collection tube.

Remove the spin column carefully so that it does not come into contact with the flow-through.

7. Transfer the spin column to a new 1.5 ml or 2 ml microcentrifuge tube, and add 200 µl Buffer AE for elution. Incubate for 1 min at room temperature. Centrifuge for 1 min at ≥6000 x *g*.
Recommended: Repeat this step for maximum yield.

Bench Protocol: Animal Tissues (Spin-Column Protocol)

Note: Before using this bench protocol, you should be completely familiar with the safety information and detailed protocols in the *DNeasy Blood & Tissue Handbook*.

Please tear off here

Important points before starting

- Perform all centrifugation steps at room temperature (15–25°C).
- If necessary, redissolve any precipitates in Buffers ATL and AL.
- Ensure that ethanol has been added to Buffers AW1 and AW2.
- Preheat a thermomixer, shaking water bath, or rocking platform for heating at 56°C.
- If using frozen tissue, equilibrate the sample to room temperature.

Procedure

1. **Cut tissue (up to 25 mg; up to 10 mg spleen) into small pieces, and place in 1.5 ml microcentrifuge tube. For rodent tails, use one (rat) or two (mouse) 0.4–0.6 cm lengths of tail. Add 180 µl Buffer ATL.**
2. **Add 20 µl proteinase K. Mix by vortexing, and incubate at 56°C until completely lysed. Vortex occasionally during incubation, or place in a thermomixer, in a shaking water bath, or on a rocking platform.**

   Lysis is usually complete in 1–3 h or, for rodent tails, 6–8 h. Samples can be lysed overnight.
3. **Vortex for 15 s. Add 200 µl Buffer AL to the sample. Mix thoroughly by vortexing. Then add 200 µl ethanol (96–100%). Mix again thoroughly.**

   Alternatively, premix Buffer AL and ethanol, and add together.
4. **Pipet the mixture into a DNeasy Mini spin column in a 2 ml collection tube. Centrifuge at ≥6000 x *g* (8000 rpm) for 1 min. Discard flow-through and collection tube.**
5. **Place the spin column in a new 2 ml collection tube. Add 500 µl Buffer AW1. Centrifuge for 1 min at ≥6000 x *g*. Discard flow-through and collection tube.**
6. **Place the spin column in a new 2 ml collection tube. Add 500 µl Buffer AW2. Centrifuge for 3 min at 20,000 x *g* (14,000 rpm). Discard flow-through and collection tube.**

   Remove the spin column carefully so that it does not come into contact with the flow-through.
7. **Transfer the spin column to a new 1.5 ml or 2 ml microcentrifuge tube, and add 200 µl Buffer AE for elution. Incubate for 1 min at room temperature. Centrifuge for 1 min at ≥6000 x *g*.**
   Recommended: Repeat this step for maximum yield.

Appendix Cii

From: Palero, Hall et al 2010

PROTOCOL FOR:
DNA extraction from formalin-fixed tissue

LEGEND

⇨ *ATTENTION*

* *HINT*

REST

REAGENTS

Tetramethylsilane (TMS) (Fluka-Riedel de Haën, Seelze, Germany, cat. no. 87920)
Tris base (Trizma)-Molecular Biology Grade (Calbiochem, San Diego, CA, USA)
HCl- sp. g. 1.18 (Analar, VWT Int Ltd, Poole Dorset, UK)
EDTA-disodium salt dihydrate (Sigma Chemical Co., St Louis, MO, USA)
Chelex 100 Resin-sodium form (Bio-Rad, Hemel Hemstead, Herts, UK)
Proteinase K-from Tritirachium album (Roche Diagnostics GmbH, Mannheim, Germany)

PROCEDURE

⇨ USE DNA-FREE AUTOCLAVED SOLUTIONS AND USE ONLY DISPOSABLE EQUIPMENT TO WEIGHT CHEMICALS AND PREPARE BUFFERS.

⇨ TMS IS A STRONG DEHYDRATOR AND IT SHOULD BE MANIPULATED CAREFULLY. PREFERENTIALLY IN A LAMINAR FLOW HOOD PREVIOUSLY STERILISED.

DEHYDRATION

1. Cut off a piece of the specimen (2mm3).
2. Squeeze tissue sample in a piece of absorbant paper.
3. Transfer tissue sample to the TMS solution (50-100ul).
4. Incubate with gentle agitation for 1h.

THIS INCUBATION MAY BE CARRIED OUT OVERNIGHT, EVEN THOUGH A SHORTER TIME IS RECOMMENDED TO REDUCE CONTAMINATION.

5. Open cap and let TMS evaporate in a flow chamber.

⇨ FILTER TIPS ARE RECOMMENDED TO MINIMIZE THE RISK OF CROSS-CONTAMINATION DUE TO DNA AEROSOLS.

TISSUE DIGESTION

6. Transfer tissue to a new 1.5mL eppendorf tube with 200uL of 10% Chelex solution in TE pH 8.0
7. Add 20uL of proteinase K (20mg/ml stock solution).
8. Incubate for 2-3h at 55ºC in a thermomixer.


THIS INCUBATION MAY BE CARRIED OUT OVERNIGHT.

9. Centrifuge for 5-10 minutes at 10,000 rpm.
10. Heat-shock at 95ºC for 15 minutes in a thermomixer.
11. Keep at 4ºC for 10 minutes.
12. Vortex tube and short-centrifuge (10sec-10,000 rpm) before transferring 100uL of the supernatant into a fresh tube.

* TRY TO AVOID TRANSFERRING ANY CHELEX PARTICLES, AS THIS MAY INTERFERE WITH PCR.

13. Centrifuge for 5 minutes at 12,000 rpm before use.
14. Take 1-2uL of the supernantant for a 25uL total volume PCR reaction.

RECIPES

⇨ HYDROGEN CHLORIDE CAN CAUSE SEVERE SKIN BURNS.

Tris-HCl 1M, pH 8 (1 L)

* MAKE SURE SOLUTION IS AT ROOM TEMPERATURE BEFORE MAKING FINAL PH ADJUSTMENTS.

Tris base 121.1 g
HCl approx. 42 ml
First dissolve 121g Tris base in 800 ml of water and adjust pH to the desired value by adding approximately 42 ml of concentrated HCl. Bring final volume to 1 liter. Sterilize by autoclaving.

EDTA 0.5M, pH 8 (1 L)

* EDTA WILL NOT GO INTO SOLUTION UNTIL THE PH IS ADJUSTED TO APPROX. 8.0 BY THE ADDITION OF NAOH.

EDTA 186.1g 0.5M
NaOH approx. 10g

Add EDTA to 800 ml of H2O. Stir vigorously on a magnetic stirrer. Adjust the pH to 8.0 with NaOH pellets. Dispense into aliquots and sterilize by autoclaving.

TE buffer, pH 8.0 (1 L)

Tris-HCl (1M) 10mL 10mM
EDTA (0.5M) 2mL 1mM

Add indicated volumes and water up to 1L. Set pH to 8 with NaOH pellets if needed. NaOH is caustic, so it should be handled with care.

EQUIPMENT

Flow chamber (Penryn Labspace Special Products, Basildon Essex, UK)

Microcentrifuge (Eppendorf Model 5415D, VWR Int Ltd, Poole Dorset, UK)

Thermomixer (Eppendorf Thermomixer Compact, VWR Int Ltd, Poole Dorset, UK)

Standard laboratory equipment such as different sized tubes, freezer and refrigerator for storing extracts and chemicals.

March 2008

QIAquick® Spin Handbook

QIAquick PCR Purification Kit
For purification of PCR products, 100 bp to 10 kb

QIAquick Nucleotide Removal Kit
For oligonucleotide (17-40mers) and DNA
(40 bp to 10 kb) cleanup from enzymatic reactions

QIAquick Gel Extraction Kit
For gel extraction or cleanup of DNA
(70 bp to 10 kb) from enzymatic reactions

Sample & Assay Technologies

QIAGEN Sample and Assay Technologies

QIAGEN is the leading provider of innovative sample and assay technologies, enabling the isolation and detection of contents of any biological sample. Our advanced, high-quality products and services ensure success from sample to result.

QIAGEN sets standards in:

- Purification of DNA, RNA, and proteins
- Nucleic acid and protein assays
- microRNA research and RNAi
- Automation of sample and assay technologies

Our mission is to enable you to achieve outstanding success and breakthroughs. For more information, visit www.qiagen.com .

Contents

Kit Contents

QIAquick PCR Purification Kits Catalog no.	(50) 28104	(250) 28106
QIAquick Spin Columns	50	250
Buffer PB*	30 ml	150 ml
Buffer PE (concentrate)	2 x 6 ml	55 ml
Buffer EB	15 ml	55 ml
pH Indicator I	800 µl	800 µl
Collection Tubes (2 ml)	50	250
Loading Dye	110 µl	550 µl
Handbook	1	1

QIAquick Nucleotide Removal Kits Catalog no.	(50) 28304	(250) 28306
QIAquick Spin Columns	50	250
Buffer PN*	30 ml	140 ml
Buffer PE (concentrate)	2 x 6 ml	55 ml
Buffer EB	15 ml	55 ml
Collection Tubes (2 ml)	100	500
Loading Dye	110 µl	550 µl
Handbook	1	1

QIAquick Gel Extraction Kits Catalog no.	(50) 28704	(250) 28706
QIAquick Spin Columns	50	250
Buffer QG*	2 x 50 ml	2 x 250 ml
Buffer PE (concentrate)	2 x 10 ml	2 x 50 ml
Buffer EB	15 ml	2 x 15 ml
Collection Tubes (2 ml)	50	250
Loading Dye	110 µl	550 µl
Handbook	1	1

* Buffers PB, PN, and QG contain chaotropic salts which are irritants. Take appropriate laboratory safety measures and wear gloves when handling.

Storage

QIAquick Spin Kits should be stored dry at room temperature (15–25°C). Under these conditions, QIAquick Spin Kits can be stored for up to 12 months without showing any reduction in performance and quality. Check buffers for precipitate before use and redissolve at 37°C if necessary. The entire kit can be stored at 2–8°C, but in this case the buffers should be redissolved before use. Make sure that all buffers and spin colums are at room temperature when used.

Product Use Limitations

QIAquick PCR Purification, QIAquick Nucleotide Removal, and QIAquick Gel Extraction Kits are intended for research use. No claim or representation is intended to provide information for the diagnosis, prevention, or treatment of a disease.

Product Warranty and Satisfaction Guarantee

QIAGEN guarantees the performance of all products in the manner described in our product literature. The purchaser must determine the suitability of the product for its particular use. Should any product fail to perform satisfactorily due to any reason other than misuse, QIAGEN will replace it free of charge or refund the purchase price. We reserve the right to change, alter, or modify any product to enhance its performance and design. If a QIAGEN product does not meet your expectations, simply call your local Technical Service Department or distributor. We will credit your account or exchange the product — as you wish. Separate conditions apply to QIAGEN scientific instruments, service products, and to products shipped on dry ice. Please inquire for more information.

A copy of QIAGEN terms and conditions can be obtained on request, and is also provided on the back of our invoices. If you have questions about product specifications or performance, please call QIAGEN Technical Services or your local distributor (see back cover or visit www.qiagen.com).

Quality Control

In accordance with QIAGEN's ISO-certified Quality Management System, each lot of QIAquick PCR Purification, QIAquick Nucleotide Removal, and QIAquick Gel Extraction Kits is tested against predetermined specifications to ensure consistent product quality.

Technical Assistance

At QIAGEN we pride ourselves on the quality and availability of our technical support. Our Technical Service Departments are staffed by experienced scientists with extensive practical and theoretical expertise in molecular biology and the use of QIAGEN products. If you have any questions or experience any problems regarding any aspect of QIAquick Spin Kits, or QIAGEN products in general, please do not hesitate to contact us.

QIAGEN customers are also a major source of information regarding advanced or specialized uses of our products. This information is helpful to other scientists as well as to the researchers at QIAGEN. We therefore also encourage you to contact us if you have any suggestions about product performance or new applications and techniques.

For technical assistance and more information please call one of the QIAGEN Technical Service Departments or local distributors (see back cover or visit www.qiagen.com).

Safety Information

When working with chemicals, always wear a suitable lab coat, disposable gloves, and protective goggles. For more information, please consult the appropriate material safety data sheets (MSDSs). These are available online in convenient and compact PDF format at www.qiagen.com/ts/msds.asp where you can find, view, and print the MSDS for each QIAGEN kit and kit component.

CAUTION: DO NOT add bleach or acidic solutions directly to the sample-preparation waste.

Buffer PB contains guanidine hydrochloride, which can form highly reactive compounds when combined with bleach.

In case liquid containing this buffer is spilt, clean with suitable laboratory detergent and water. If the spilt liquid contains potentially infectious agents, clean the affected area first with laboratory detergent and water, and then with 1% (v/v) sodium hypochlorite.

The following risk and safety phrases apply to the components of the QIAquick system.

Buffer PB

Contains guanidine hydrochloride and isopropanol: harmful, irritant, flammable. Risk and safety phrases*: R10-22-36/38. S23-26-36/37/39-46

Buffer PN

Contains sodium perchlorate and isopropanol: harmful, highly flammable. Risk and safety phrases*: R11-22. S13-16-23-26-36-46

Buffer QG

Contains guanidine thiocyanate: harmful. Risk and safety phrases*: R20/21/22-32. S13-26-36-46

24-hour emergency information

Emergency medical information in English, French, and German can be obtained 24 hours a day from:

Poison Information Center Mainz, Germany
Tel: +49-6131-19240

* R10: Flammable. R11: Highly Flammable. R22: Harmful if swallowed. R20/21/22: Harmful by inhalation, in contact with skin and if swallowed. R32: Contact with acids liberates very toxic gas. R36/38: Irritating to eyes and skin. S13: Keep away from food, drink and animal feedingstuffs. S16: Explosive when mixed with oxidizing substances. S23: Do not breathe vapour/spray. S26: In case of contact with eyes, rinse immediately with plenty of water and seek medical advice. S36: Wear suitable protective clothing. S36/37/39: Wear suitable protective clothing, gloves and eye/face protection. S46: If swallowed, seek medical advice immediately and show the container or label.

Product Specifications

	QIAquick PCR Purification Kit	QIAquick Nucleotide Removal Kit	QIAquick Gel Extraction Kit
Maximum binding capacity	10 µg	10 µg	10 µg
Maximum weight of gel slice	—	—	400 mg
Minimum elution volume	30 µl	30 µl	30 µl
Capacity of column reservoir	800 µl	800 µl	800 µl
Typical recoveries			
Recovery of DNA	90–95% (100 bp – 10 kb)	80–95% (40 bp – 10 kb)	70–80% (70 bp – 10 kb)
Recovery of oligonucleotides (17–40mers)	0	60–80%	10–20%
Recovered			
Oligonucleotides	—	17–40mers	—
dsDNA	100 bp – 10 kb	40 bp – 10 kb	70 bp – 10 kb
Removed			
<10mers	**YES**	**YES**	**YES**
17–40mers	**YES**	no	no

Introduction

The QIAquick system, designed for rapid DNA cleanup, includes:

- **QIAquick PCR Purification Kits** for direct purification of double- or single-stranded PCR products (100 bp – 10 kb) from amplification reactions and DNA cleanup from other enzymatic reactions.
- **QIAquick Nucleotide Removal Kits** for general cleanup of oligonucleotides and DNA up to 10 kb from enzymatic reactions (e.g., labeling, dephosphorylation, restriction, and tailing).
- **QIAquick Gel Extraction Kits** for extraction of DNA fragments (70 bp – 10 kb) from standard, or low-melt agarose gels in TAE (Tris·acetate/EDTA) or TBE (Tris·borate/EDTA) buffer and DNA cleanup from enzymatic reactions.

QIAquick PCR Kits are also available in multiwell format for preparation of 8 to 96 samples (see page 37 for ordering information).

Enzymatic reaction cleanup using QIAquick Kits

The QIAquick system is suitable for fast cleanup of up to 10 µg of DNA fragments from enzymatic reactions and agarose gels (Table 1). Enzyme contamination of DNA samples can interfere with subsequent downstream applications. QIAquick Spin Kits can be used for highly efficient removal of a broad spectrum of enzymes widely used in molecular biology. In addition, QIAGEN offers the MinElute® Reaction Cleanup Kit, which is specially designed for fast and easy DNA cleanup from all enzymatic reactions. Using proven microspin technology, the MinElute Reaction Cleanup Kit delivers highly concentrated purified DNA by using an elution volume of only 10 µl (see ordering information, page 37).

Table 1. QIAquick DNA Cleanup Guide

	From solutions			From gels
	QIAquick PCR Purification Kit	QIAquick Nucleotide Removal Kit	QIAquick Gel Extraction Kit	QIAquick Gel Extraction Kit
Alkaline phosphatase	**YES**	**YES**	**YES**	**YES**
cDNA synthesis	**YES**	no	no	**YES**
DNase, nuclease digestion	**YES**	**YES**	**YES**	**YES**
Kinase:				
DNA fragments	**YES**	**YES**	**YES**	**YES**
Oligonucleotides	no	**YES**	no	no
Ligation	**YES**	**YES**	**YES**	**YES**
Nick translation	**YES**	**YES**	**YES**	**YES**
PCR	**YES**	no	no	**YES**
Random priming	**YES**	**YES**	**YES**	**YES**
Restriction digestion	**YES**	**YES**	**YES**	**YES**
Tailing:				
DNA fragments	**YES**	**YES**	**YES**	**YES**
Oligonucleotides	no	**YES**	no	no

QIAquick Kits provide high yields of pure nucleic acids, for direct use in applications such as:

- Fluorescent and radioactive sequencing
- Restriction
- Labeling
- Hybridization
- Ligation and transformation
- Amplification
- In vitro transcription
- Microinjection

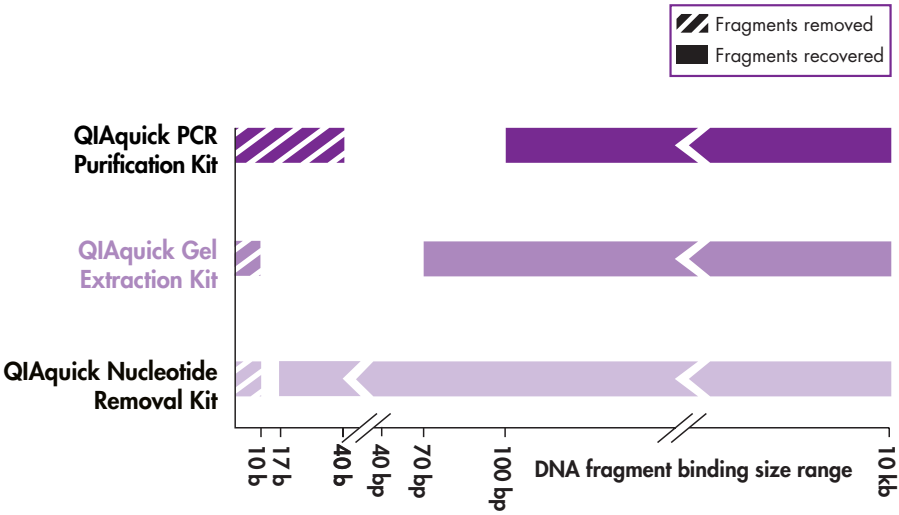

Figure 1. DNA fragment binding-size range. Recoveries of DNA fragments in the size range between "removed" and "recovered" are not defined.

Automated DNA cleanup

The QIAquick PCR Purification Kit and QIAquick Gel Extraction Kit can be fully automated on the QIAcube. The innovative QIAcube uses advanced technology to process QIAGEN spin columns, enabling seamless integration of automated, low-throughput sample prep into your laboratory workflow. Sample preparation using the QIAcube follows the same steps as the manual procedure (i.e., bind, wash, and elute) enabling purification of high-quality DNA.

The QIAcube is preinstalled with protocols for purification of plasmid DNA, genomic DNA, RNA, viral nucleic acids, and proteins, plus DNA and RNA cleanup. The range of protocols available is continually expanding, and additional QIAGEN protocols can be downloaded free of charge at www.qiagen.com/MyQIAcube .

A detailed protocol for using QIAquick spin columns on the QIAcube is provided with the QIAcube.

Note: It is not necessary to add pH indicator I to Buffer PB when using the QIAcube.

The QIAquick Principle

The QIAquick system combines the convenience of spin-column technology with the selective binding properties of a uniquely designed silica membrane. Special buffers provided with each kit are optimized for efficient recovery of DNA and removal of contaminants in each specific application. DNA adsorbs to the silica membrane in the presence of high concentrations of salt while contaminants pass through the column. Impurities are efficiently washed away, and the pure DNA is eluted with Tris buffer or water (see page 17). QIAquick spin columns offer 3 handling options — as an alternative to processing the spin columns in a microcentrifuge, they can now also be used on any commercial vacuum manifold with luer connectors (e.g., QIAvac 6S or QIAvac 24 Plus with QIAvac Luer Adapters) or automated on the QIAcube.

Adsorption to QIAquick membrane — salt and pH dependence

The QIAquick silica membrane is uniquely adapted to purify DNA from both aqueous solutions and agarose gels, and up to 10 µg DNA can bind to each QIAquick column. The binding buffers in QIAquick Spin Kits provide the correct salt concentration and pH for adsorption of DNA to the QIAquick membrane. The adsorption of nucleic acids to silica surfaces occurs only in the presence of a high concentration of chaotropic salts (1), which modify the structure of water (2).

Adsorption of DNA to silica also depends on pH. Adsorption is typically 95% if the pH is ≤7.5, and is reduced drastically at higher pH (Figure 1). If the loading mixture pH is >7.5, the optimal pH for DNA binding can be obtained by adding a small volume of 3 M sodium acetate, pH 5.0.

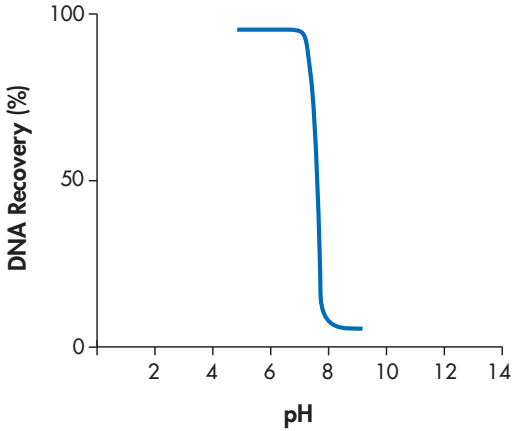

Figure 2. pH dependence of DNA adsorption to QIAquick membranes. 1 µg of a 2.9 kb DNA fragment was adsorbed at different pHs and eluted with Buffer EB (10 mM Tris·Cl, pH 8.5). The graph shows the percentage of DNA recovery, reflecting the relative adsorption efficiency, versus pH of adsorption.

Optimized binding buffers for every DNA cleanup task

All QIAquick Spin Kits contain identical QIAquick spin columns but different binding buffers optimized for each specific application:

- Buffer PB in the QIAquick PCR Purification Kit allows the efficient binding of single- or double-stranded PCR products as small as 100 bp and the quantitative (99.5%) removal of primers up to 40 nucleotides. This kit can therefore be used to remove oligo-dT primers after cDNA synthesis or to remove unwanted linkers in cloning experiments.
- Buffer PN in the QIAquick Nucleotide Removal Kit promotes the adsorption of both oligonucleotides ≥17 bases and DNA fragments up to 10 kb to the membrane.
- Buffer QG in the QIAquick Gel Extraction Kit solubilizes the agarose gel slice and provides the appropriate conditions for binding of DNA to the silica membrane.

All of these buffers are available separately (see ordering information, page 37).

pH indicator

Binding buffer PB and binding and solubilization buffer QG are specially optimized for use with the QIAquick silica membrane. Buffer QG contains an integrated pH indicator, while an optional pH indicator can be added to Buffer PB allowing easy determination of the optimal pH for DNA binding. DNA adsorption requires a pH ≤7.5, and the pH indicator in the buffers will appear yellow in this range. If the pH is >7.5, which can occur if during agarose gel electrophoresis, the electrophoresis buffer had been used repeatedly or incorrectly prepared, or if the buffer used in an enzymatic reaction is strongly basic and has a high buffering capacity, the binding mixture turns orange or violet (Figure 2). This means that the pH of the sample exceeds the buffering capacity of Buffer PB or QG and DNA adsorption will be inefficient. In these cases, the pH of the binding mixture can easily be corrected by addition of a small volume of 3 M sodium acetate*, pH 5.0, before proceeding with the protocol. In addition, in the QIAquick Gel

Figure 3. Indicator enables easy checking of the optimal pH. Indicator dye in solubilization and binding Buffers QG and PB identifies optimal pH for DNA binding.

* When working with chemicals, always wear a suitable lab coat, disposable gloves, and protective goggles. For more information, please consult the appropriate material safety data sheets (MSDSs) available from the product supplier.

Extraction Kit procedure, the color of the binding mixture allows easy visualization of any unsolubilized agarose, ensuring complete solubilization and maximum yields. The indicator dye does not interfere with DNA binding and is completely removed during the cleanup procedure. Buffers PB and QG do not contain sodium iodide (NaI). Residual NaI may be difficult to remove from DNA samples, and reduces the efficiency of subsequent enzymatic reactions such as blunt-end ligation.

Washing

During the DNA adsorption step, unwanted primers and impurities, such as salts, enzymes, unincorporated nucleotides, agarose, dyes, ethidium bromide, oils, and detergents (e.g., DMSO, Tween® 20) do not bind to the silica membrane but flow through the column. Salts are quantitatively washed away by the ethanol-containing Buffer PE. Any residual Buffer PE, which may interfere with subsequent enzymatic reactions, is removed by an additional centrifugation step.

Elution in low-salt solutions

Elution efficiency is strongly dependent on the salt concentration and pH of the elution buffer. Contrary to adsorption, elution is most efficient under basic conditions and low salt concentrations. DNA is eluted with 50 or 30 µl of the provided Buffer EB (10 mM Tris·Cl, pH 8.5), or water. The maximum elution efficiency is achieved between pH 7.0 and 8.5. When using water to elute, make sure that the pH is within this range. In addition, DNA must be stored at –20°C when eluted with water since DNA may degrade in the absence of a buffering agent. Elution with TE buffer (10 mM Tris·Cl, 1 mM EDTA, pH 8.0) is possible, but not recommended because EDTA may inhibit subsequent enzymatic reactions.

DNA yield and concentration

DNA yield depends on the following three factors: the volume of elution buffer, how the buffer is applied to the column, and the incubation time of the buffer on the column. 100–200 µl of elution buffer completely covers the QIAquick membrane, ensuring maximum yield, even when not applied directly to the center of the membrane. Elution with ≤50 µl requires the buffer to be added directly to the center of the membrane, and if elution is done with the minimum recommended volume of 30 µl, an additional 1 minute incubation is required for optimal yield. DNA will be up to 1.7 times more concentrated if the QIAquick column is incubated for 1 minute with 30 µl of elution buffer, than if it is eluted in 50 µl without incubation (Figure 4, page 14).

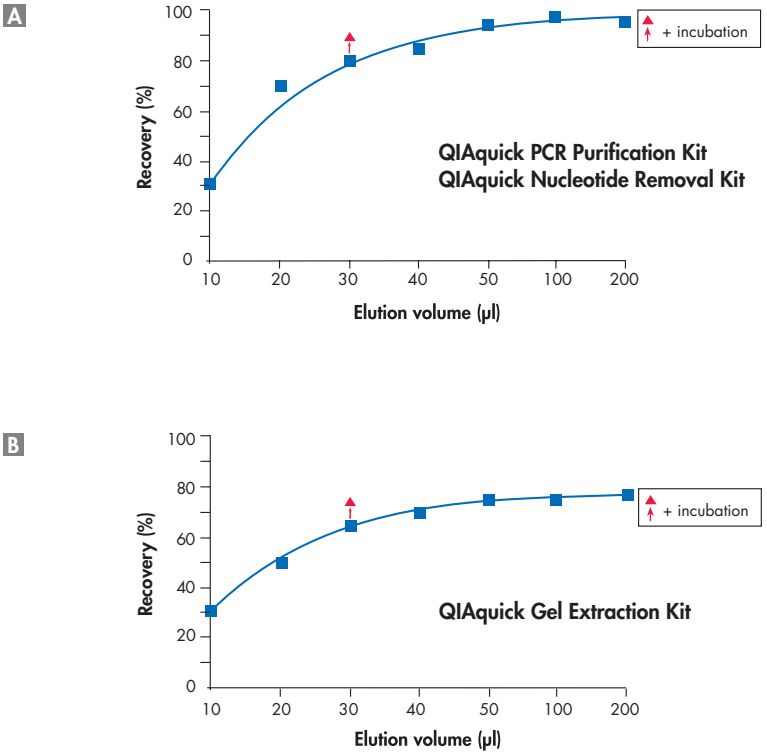

Figure 4. Highly concentrated DNA. Effect of elution buffer volume on DNA yield for A the QIAquick PCR Purification and QIAquick Nucleotide Removal Kit; B the QIAquick Gel Extraction Kit. 5 µg of a 2.9 kb DNA fragment were purified and eluted with the indicated volumes of Buffer EB. 30 µl plus 1 minute incubation on the QIAquick column gives DNA yields similar to 50 µl without incubation, but at a concentration 1.7 times greater.

Loading dye

Loading dye is provided for analysis of purified DNA samples using electrophoresis. It contains 3 marker dyes (bromophenol blue, xylene cyanol, and orange G) that facilitate estimation of DNA migration distance and optimization of agarose gel run time. Refer to Table 2 (page 15) to identify the dyes according to migration distance and agarose gel percentage and type. Loading dye is supplied as a 5x concentrate; thus 1 volume of loading dye should be added to 5 volumes of purified DNA.

Table 2. Migration Distance of Gel Tracking Dyes

%TAE (TBE) agarose gel	Xylene cyanol (light blue)	Bromophenol blue (dark blue)	Orange G (orange)
0.8	5000 bp (3000 bp)	800 bp (400 bp)	150 bp (<100 bp)
1.0	3000 bp (2000 bp)	400 bp (250 bp)	<100 bp (<100 bp)
1.5	1800 bp (1100 bp)	250 bp (100 bp)	<100 bp (<100 bp)
2.0	1000 bp (600 bp)	200 bp (<100 bp)	<100 bp (<100 bp)
2.5	700 bp (400 bp)	100 bp (<50 bp)	<50 bp (<50 bp)

Agarose gel analysis of yield

Yields of DNA following cleanup can be determined by agarose gel analysis. Table 3 shows the total yield obtained following extraction of 1 µg or 0.5 µg starting DNA from an agarose gel with a recovery of 80% or 60% using the QIAquick Gel Extraction Kit. The corresponding amount of DNA in a 1 µl aliquot from 50 µl eluate is indicated. Quantities of DNA fragment corresponding to these 1 µl aliquots are shown on the agarose gel in Figure 4.

Table 3. Amount of DNA in 1 µl aliquots of a 50 µl eluate following QIAquick purification

Starting DNA	Recovery	Total yield (50 µl eluate)	Amount of DNA in 1 µl
1 µg	80%	0.8 µg	16 ng
	60%	0.6 µg	12 ng
0.5 µg	80%	0.4 µg	8 ng
	60%	0.3 µg	6 ng

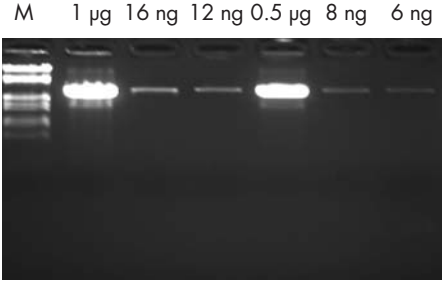

Figure 5. High DNA recovery. Quantities of purified 2.7 kb DNA fragment corresponding to 1/50 of the DNA obtained following purification from 1 µg or 0.5 µg starting DNA with a recovery of 80% or 60% (see Table 1). Samples were run on a 1% TAE agarose gel. **M**: lambda–EcoRI-HindIII markers.

Quantification of DNA fragments

DNA fragments can be quantified by running a sample alongside standards containing known quantities of the same-sized DNA fragment. The amount of sample DNA loaded can be estimated by visual comparison of the band intensity with that of the standards (Figure 5).

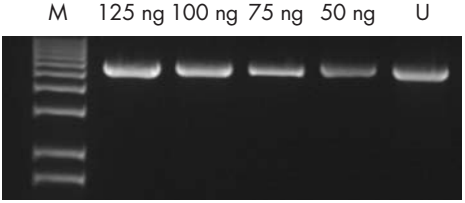

Figure 6. Agarose gel analysis. An unknown amount of a 5.5 kb DNA fragment (**U**) was run alongside known quantities (as indicated in ng) of the same DNA fragment. The unknown sample contained 75–100 ng DNA, as estimated by visual comparison with the standards. **M**: 1 kb DNA ladder.

Applications using QIAquick purified DNA

DNA purified with QIAquick is suitable for any subsequent application, such as restriction, labeling, hybridization, PCR, ligation and transformation, radioactive and fluorescent sequencing, in vitro transcription, or microinjection.

The QIAquick Procedure

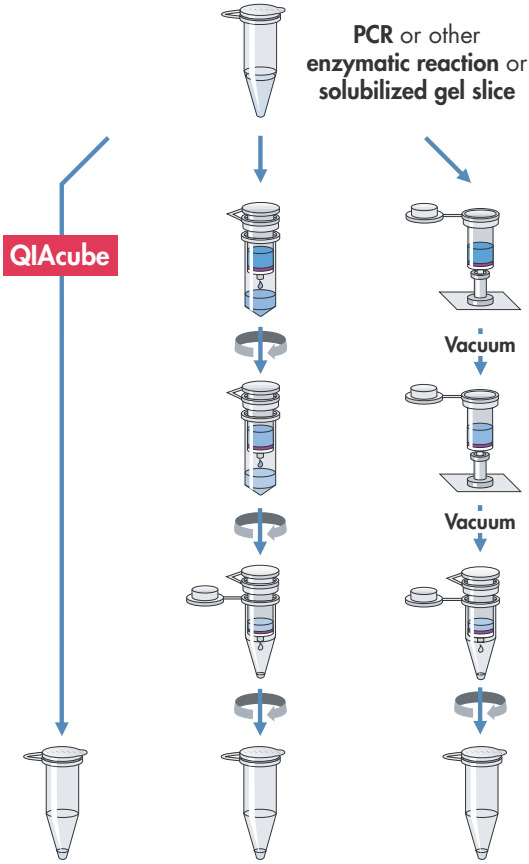

Equipment and Reagents to Be Supplied by User

When working with chemicals, always wear a suitable lab coat, disposable gloves, and protective goggles. For more information, please consult the appropriate material safety data sheets (MSDSs) available from the product supplier.

For all protocols

- Ethanol (96–100%)*
- Microcentrifuge
- 1.5 or 2 ml microcentrifuge tubes
- 3 M sodium acetate, pH 5.0, may be necessary for PCR purification and gel extraction protocols.
- Optional: Distilled water or TE buffer (10 mM Tris·Cl. 1 mM EDTA, pH 8) for elution of DNA.

Vacuum protocols

- Vacuum manifold (e.g., QIAvac 24 Plus or QIAvac 6S)
- Vacuum pump (e.g., QIAGEN Vacuum Pump, see ordering information).

Gel extraction protocols

- Isopropanol (100%)
- Heating block or water bath set at 50°C

* Do not use denaturated alcohol, which contains other substances such as methanol or methylethylketone.

QIAquick PCR Purification Kit Protocol

using a microcentrifuge

This protocol is designed to purify single- or double-stranded DNA fragments from PCR and other enzymatic reactions (see page 8). For cleanup of other enzymatic reactions, follow the protocol as described for PCR samples or use the MinElute Reaction Cleanup Kit. Fragments ranging from 100 bp to 10 kb are purified from primers, nucleotides, polymerases, and salts using QIAquick spin columns in a microcentrifuge.

Important points before starting

- Add ethanol (96–100%) to Buffer PE before use (see bottle label for volume).
- All centrifugation steps are carried out at 17,900 x *g* (13,000 rpm) in a conventional tabletop microcentrifuge at room temperature.
- Add 1:250 volume pH indicator I to Buffer PB (i.e., add 120 µl pH indicator I to 30 ml Buffer PB or add 600 µl pH indicator I to 150 ml Buffer PB). The yellow color of Buffer PB with pH indicator I indicates a pH of ≤7.5.
- Add pH indicator I to entire buffer contents. Do not add pH indicator I to buffer aliquots.
- If the purified PCR product is to be used in sensitive microarray applications, it may be beneficial to use Buffer PB without the addition of pH indicator I.

Procedure

1. **Add 5 volumes of Buffer PB to 1 volume of the PCR sample and mix. It is not necessary to remove mineral oil or kerosene.**

   For example, add 500 µl of Buffer PB to 100 µl PCR sample (not including oil).

2. **If pH indicator I has beein added to Buffer PB, check that the color of the mixture is yellow.**

   If the color of the mixture is orange or violet, add 10 µl of 3 M sodium acetate, pH 5.0, and mix. The color of the mixture will turn to yellow.

3. **Place a QIAquick spin column in a provided 2 ml collection tube.**
4. **To bind DNA, apply the sample to the QIAquick column and centrifuge for 30–60 s.**
5. **Discard flow-through. Place the QIAquick column back into the same tube.**

   Collection tubes are re-used to reduce plastic waste.

6. **To wash, add 0.75 ml Buffer PE to the QIAquick column and centrifuge for 30–60 s.**
7. **Discard flow-through and place the QIAquick column back in the same tube. Centrifuge the column for an additional 1 min.**

   IMPORTANT: Residual ethanol from Buffer PE will not be completely removed unless the flow-through is discarded before this additional centrifugation.

8. **Place QIAquick column in a clean 1.5 ml microcentrifuge tube.**

9. **To elute DNA, add 50 µl Buffer EB (10 mM Tris·Cl, pH 8.5) or water (pH 7.0–8.5) to the center of the QIAquick membrane and centrifuge the column for 1 min. Alternatively, for increased DNA concentration, add 30 µl elution buffer to the center of the QIAquick membrane, let the column stand for 1 min, and then centrifuge.**

   IMPORTANT: Ensure that the elution buffer is dispensed directly onto the QIAquick membrane for complete elution of bound DNA. The average eluate volume is 48 µl from 50 µl elution buffer volume, and 28 µl from 30 µl elution buffer.

   Elution efficiency is dependent on pH. The maximum elution efficiency is achieved between pH 7.0 and 8.5. When using water, make sure that the pH value is within this range, and store DNA at –20°C as DNA may degrade in the absence of a buffering agent. The purified DNA can also be eluted in TE buffer (10 mM Tris·Cl, 1 mM EDTA, pH 8.0), but the EDTA may inhibit subsequent enzymatic reactions.

10. **If the purified DNA is to be analyzed on a gel, add 1 volume of Loading Dye to 5 volumes of purified DNA. Mix the solution by pipetting up and down before loading the gel.**

    Loading dye contains 3 marker dyes (bromophenol blue, xylene cyanol, and orange G) that facilitate estimation of DNA migration distance and optimization of agarose gel run time. Refer to Table 2 (page 15) to identify the dyes according to migration distance and agarose gel percentage and type.

QIAquick PCR Purification Kit Protocol

using a vacuum manifold

QIAquick spin columns can now be used on any vacuum manifold with luer connectors (e.g., QIAvac 6S or QIAvac 24 Plus with Luer Adapters). The following protocol is designed to purify single- or double-stranded DNA fragments from PCR and other enzymatic reactions (see page 8). For cleanup of other enzymatic reactions, follow the protocol as described for PCR samples or use the MinElute Reaction Cleanup Kit. Fragments ranging from 100 bp to 10 kb are purified from primers, nucleotides, polymerases and salts using vacuum-driven sample processing.

Important points before starting

- Add ethanol (96–100%) to Buffer PE before use (see bottle label for volume).
- Switch off vacuum between steps to ensure that a consistent, even vacuum is applied during manipulations.
- Add 1:250 volume pH indicator I to Buffer PB (i.e., add 120 µl pH indicator I to 30 ml Buffer PB or add 600 µl pH indicator I to 150 ml Buffer PB). The yellow color of Buffer PB with pH indicator I indicates a pH of ≤7.5.
- Add pH indicator I to entire buffer contents. Do not add pH indicator I to buffer aliquots.
- If the purified PCR product is to be used in sensitive microarray applications, it may be beneficial to use Buffer PB without the addition of pH indicator I.

Procedure

1. **Add 5 volumes of Buffer PB to 1 volume of the PCR sample and mix. It is not necessary to remove mineral oil or kerosene.**

   For example, add 500 µl of Buffer PB to 100 µl PCR sample (not including oil).

2. **If pH indicator I has beein added to Buffer PB, check that the color of the mixture is yellow.**

   If the color of the mixture is orange or violet, add 10 µl of 3 M sodium acetate, pH 5.0, and mix. The color of the mixture will turn to yellow.

3. **Prepare the vacuum manifold and QIAquick columns according to step 3a, 3b, or 3c.**

3a. QIAvac 24 Plus (see page 33, and Figure 7):

Insert up to 24 QIAquick spin columns into the luer extensions of the QIAvac 24 Plus. Close unused positions with luer caps and connect QIAvac 24 Plus to a vacuum source.

3b. QIAvac 6S manifold (see page 34, and Figure 8):

Open QIAvac 6S lid. Place QIAvac Luer Adapter(s), or blanks to seal unused slots, into the slots of QIAvac top plate, and close the QIAvac 6S lid. Place the waste tray inside the QIAvac base, and place the top plate squarely over the base. Attach the QIAvac 6S to a vacuum source.

Insert each QIAquick column into a luer connector on the Luer Adapter(s) in the manifold. Seal unused luer connectors with plugs provided with the QIAvac Luer Adapter Set.

3c. Other vacuum manifolds: follow the supplier's instructions. Insert each QIAquick column into a luer connector.

4. To bind DNA, load the samples into the QIAquick columns by decanting or pipetting, and apply vacuum. After the samples have passed through the column, switch off the vacuum source.

The maximum loading volume of the column is 800 µl. For sample volumes greater than 800 µl simply load again.

5. To wash, add 0.75 ml of Buffer PE to each QIAquick column and apply vacuum.

6. Transfer each QIAquick column to a microcentrifuge tube or the provided 2 ml collection tubes. Centrifuge for 1 min at 17,900 x *g* (13,000 rpm).

IMPORTANT: This spin is necessary to remove residual ethanol (Buffer PE).

7. Place each QIAquick column into a clean 1.5 ml microcentrifuge tube.

8. To elute DNA, add 50 µl of Buffer EB (10 mM Tris·Cl, pH 8.5) or water (pH 7.0–8.5) to the center of each QIAquick membrane, and centrifuge the columns for 1 min at 17,900 x *g* (13,000 rpm). Alternatively, for increased DNA concentration, add 30 µl elution buffer to the center of each QIAquick membrane, let the columns stand for 1 min, and then centrifuge.

IMPORTANT: Ensure that the elution buffer is dispensed directly onto the QIAquick membrane for complete elution of bound DNA. The average eluate volume is 48 µl from 50 µl elution buffer volume, and 28 µl from 30 µl elution buffer.

Elution efficiency is dependent on pH. The maximum elution efficiency is achieved between pH 7.0 and 8.5. When using water, make sure that the pH value is within this range, and store DNA at –20°C as DNA may degrade in the absence of a buffering agent. The purified DNA can also be eluted in TE (10 mM Tris·Cl, 1 mM EDTA, pH 8.0), but the EDTA may inhibit subsequent enzymatic reactions.

9. If the purified DNA is to be analyzed on a gel, add 1 volume of Loading Dye to 5 volumes of purified DNA. Mix the solution by pipetting up and down before loading the gel.

Loading dye contains 3 marker dyes (bromophenol blue, xylene cyanol, and orange G) that facilitate estimation of DNA migration distance and optimization of agarose gel run time. Refer to Table 2 (page 15) to identify the dyes according to migration distance and agarose gel percentage and type.

QIAquick Nucleotide Removal Kit Protocol

using a microcentrifuge

This protocol is designed for cleanup of radioactive-, biotin-, or DIG-labeled DNA fragments and oligonucleotides ≥17 nucleotides from enzymatic reactions (see page 8). The protocol ensures removal of primers <10 bases, enzymes, salts, and unincorporated nucleotides. It is possible to use this kit with a vacuum manifold as well as with a microcentrifuge, and a protocol for vacuum processing is available on request from QIAGEN Technical Services or your local distributor. However, we do not recommend processing radioactive samples with a vacuum manifold.

Important points before starting

- Add ethanol (96–100%) to Buffer PE before use (see bottle label for volume).
- All centrifugation steps are in a conventional tabletop microcentrifuge at room temperature.

Procedure

1. **Add 10 volumes of Buffer PN to 1 volume of the reaction sample and mix.**

   For example, add 500 µl Buffer PN to a 50 µl reaction sample. For DNA fragments ≥100 bp, only 5 volumes of Buffer PN are required.
2. **Place a QIAquick spin column in a provided 2 ml collection tube.**
3. **To bind DNA, apply the sample to the QIAquick column and centrifuge for 1 min at 6000 rpm.**
4. **For radioactive samples:**
   Place the QIAquick column into a clean 2 ml collection tube and discard the tube containing the radioactive flow-through appropriately.

   For non-radioactive samples:
   Discard the flow-through and place QIAquick column back into the same tube.

   Collection tubes are reused to reduce plastic waste.
5. **For radioactive samples:**
   To wash QIAquick column, add 500 µl of Buffer PE and centrifuge for 1 min at 6000 rpm. Discard the flow-through appropriately and repeat wash with another 500 µl of Buffer PE.

   For non-radioactive samples:
   To wash QIAquick column, add 750 µl of Buffer PE and centrifuge for 1 min at 6000 rpm.

6. **Discard the flow-through and place the QIAquick column back in the same tube, which should be empty. Centrifuge for an additional 1 min at 13,000 rpm (17,900 x *g*).**

   IMPORTANT: Residual ethanol from Buffer PE will not be completely removed unless the flow-through is discarded before this additional centrifuge.

7. **Place the QIAquick column in a clean 1.5 ml microcentrifuge tube.**

8. **To elute DNA, add 100–200 µl of Buffer EB (10 mM Tris·Cl, pH 8.5) or water (pH 7.0–8.5) to the center of the QIAquick membrane and centrifuge the column for 1 min at 13,000 rpm (17,900 x *g*). Alternatively, for increased DNA concentration, add 30–50 µl elution buffer to the center of the QIAquick membrane, let the column stand for 1 min, and then centrifuge.**

   IMPORTANT: Ensure that the elution buffer is dispensed directly onto the QIAquick membrane for complete elution of bound DNA.

   Elution efficiency is dependent on pH. The maximum elution efficiency is achieved between pH 7.0 and 8.5. When using water, make sure that the pH value is within this range, and store DNA at –20°C as DNA may degrade in the absence of a buffering agent. The purified DNA can also be eluted in TE (10 mM Tris·Cl, 1 mM EDTA, pH 8.0), but the EDTA may inhibit subsequent enzymatic reactions.

9. **If the purified DNA is to be analyzed on a gel, add 1 volume of Loading Dye to 5 volumes of purified DNA. Mix the solution by pipetting up and down before loading the gel.**

   Loading dye contains 3 marker dyes (bromophenol blue, xylene cyanol, and orange G) that facilitate estimation of DNA migration distance and optimization of agarose gel run time. Refer to Table 2 (page 15) to identify the dyes according to migration distance and agarose gel percentage and type.

QIAquick Gel Extraction Kit Protocol

using a microcentrifuge

This protocol is designed to extract and purify DNA of 70 bp to 10 kb from standard or low-melt agarose gels in TAE or TBE buffer. Up to 400 mg agarose can be processed per spin column. This kit can also be used for DNA cleanup from enzymatic reactions (see page 8). For DNA cleanup from enzymatic reactions using this protocol, add 3 volumes of Buffer QG and 1 volume of isopropanol to the reaction, mix, and proceed with step 6 of the protocol. Alternatively, use the MinElute Reaction Cleanup Kit.

Important points before starting

- The yellow color of Buffer QG indicates a pH ≤7.5.
- Add ethanol (96–100%) to Buffer PE before use (see bottle label for volume).
- All centrifugation steps are carried out at 17,900 x *g* (13,000 rpm) in a conventional table-top microcentrifuge at room temperature.

Procedure

1. **Excise the DNA fragment from the agarose gel with a clean, sharp scalpel.**

   Minimize the size of the gel slice by removing extra agarose.

2. **Weigh the gel slice in a colorless tube. Add 3 volumes of Buffer QG to 1 volume of gel (100 mg ~ 100 µl).**

   For example, add 300 µl of Buffer QG to each 100 mg of gel. For >2% agarose gels, add 6 volumes of Buffer QG. The maximum amount of gel slice per QIAquick column is 400 mg; for gel slices >400 mg use more than one QIAquick column.

3. **Incubate at 50°C for 10 min (or until the gel slice has completely dissolved). To help dissolve gel, mix by vortexing the tube every 2–3 min during the incubation.**

   IMPORTANT: Solubilize agarose completely. For >2% gels, increase incubation time.

4. **After the gel slice has dissolved completely, check that the color of the mixture is yellow (similar to Buffer QG without dissolved agarose).**

   If the color of the mixture is orange or violet, add 10 µl of 3 M sodium acetate, pH 5.0, and mix. The color of the mixture will turn to yellow.

   The adsorption of DNA to the QIAquick membrane is efficient only at pH ≤7.5. Buffer QG contains a pH indicator which is yellow at pH ≤7.5 and orange or violet at higher pH, allowing easy determination of the optimal pH for DNA binding.

5. **Add 1 gel volume of isopropanol to the sample and mix.**

   For example, if the agarose gel slice is 100 mg, add 100 µl isopropanol. This step increases the yield of DNA fragments <500 bp and >4 kb. For DNA fragments between 500 bp and 4 kb, addition of isopropanol has no effect on yield. Do not centrifuge the sample at this stage.

6. **Place a QIAquick spin column in a provided 2 ml collection tube.**
7. **To bind DNA, apply the sample to the QIAquick column, and centrifuge for 1 min.**

   The maximum volume of the column reservoir is 800 µl. For sample volumes of more than 800 µl, simply load and spin again.
8. **Discard flow-through and place QIAquick column back in the same collection tube.**

   Collection tubes are reused to reduce plastic waste.
9. **Recommended: Add 0.5 ml of Buffer QG to QIAquick column and centrifuge for 1 min.**

   This step will remove all traces of agarose. It is only required when the DNA will subsequently be used for direct sequencing, in vitro transcription, or microinjection.
10. **To wash, add 0.75 ml of Buffer PE to QIAquick column and centrifuge for 1 min.**

    Note: If the DNA will be used for salt-sensitive applications, such as blunt-end ligation and direct sequencing, let the column stand 2–5 min after addition of Buffer PE, before centrifuging.
11. **Discard the flow-through and centrifuge the QIAquick column for an additional 1 min at 17,900 x *g* (13,000 rpm).**

    IMPORTANT: Residual ethanol from Buffer PE will not be completely removed unless the flow-through is discarded before this additional centrifugation.
12. **Place QIAquick column into a clean 1.5 ml microcentrifuge tube.**
13. **To elute DNA, add 50 µl of Buffer EB (10 mM Tris·Cl, pH 8.5) or water (pH 7.0–8.5) to the center of the QIAquick membrane and centrifuge the column for 1 min. Alternatively, for increased DNA concentration, add 30 µl elution buffer to the center of the QIAquick membrane, let the column stand for 1 min, and then centrifuge for 1 min.**

    IMPORTANT: Ensure that the elution buffer is dispensed directly onto the QIAquick membrane for complete elution of bound DNA. The average eluate volume is 48 µl from 50 µl elution buffer volume, and 28 µl from 30 µl.

    Elution efficiency is dependent on pH. The maximum elution efficiency is achieved between pH 7.0 and 8.5. When using water, make sure that the pH value is within this range, and store DNA at –20°C as DNA may degrade in the absence of a buffering agent. The purified DNA can also be eluted in TE (10 mM Tris·Cl, 1 mM EDTA, pH 8.0), but the EDTA may inhibit subsequent enzymatic reactions.
14. **If the purified DNA is to be analyzed on a gel, add 1 volume of Loading Dye to 5 volumes of purified DNA. Mix the solution by pipetting up and down before loading the gel.**

    Loading dye contains 3 marker dyes (bromophenol blue, xylene cyanol, and orange G) that facilitate estimation of DNA migration distance and optimization of agarose gel run time. Refer to Table 2 (page 15) to identify the dyes according to migration distance and agarose gel percentage and type.

QIAquick Gel Extraction Kit Protocol

using a vacuum manifold

QIAquick spin columns can now be used on any vacuum manifold with luer connectors (e.g., QIAvac 6S or QIAvac 24 Plus with Luer Adapters). The following protocol is designed to extract and purify DNA of 70 bp to 10 kb from standard or low-melt agarose gels in TAE or TBE buffer using vacuum-driven processing. Up to 400 mg agarose can be processed per spin column. This kit can also be used for DNA cleanup from enzymatic reactions (see page 8). For DNA cleanup from enzymatic reactions using this protocol, add 3 volumes of Buffer QG and 1 volume of isopropanol to the reaction and mix. Set up the vacuum manifold as described in step 4 and then and proceed with step 7 of the protocol. Alternatively, use the new MinElute Reaction Cleanup Kit.

Important points before starting

- The yellow color of Buffer QG indicates a pH ≤7.5.
- Add ethanol (96–100%) to Buffer PE before use (see bottle label for volume).
- Switch off vacuum between steps to ensure that a consistent, even vacuum is applied during manipulations.

Procedure

1. **Excise the DNA fragment from the agarose gel with a clean, sharp scalpel.**

   Minimize the size of the gel slice by removing extra agarose.

2. **Weigh the gel slice in a colorless tube. Add 3 volumes of Buffer QG to 1 volume of gel (100 mg or approximately 100 µl).**

   For example, add 300 µl of Buffer QG to each 100 mg of gel. For >2% agarose gels, add 6 volumes of Buffer QG. The maximum amount of gel slice per QIAquick column is 400 mg; for gel slices >400 mg use more than one QIAquick column.

3. **Incubate at 50°C for 10 min (or until the gel slice has completely dissolved). To help dissolve gel, mix by vortexing the tube every 2–3 min during the incubation.**

   IMPORTANT: Solubilize agarose completely. For >2% gels, increase incubation time.

4. **During the incubation, prepare the vacuum manifold and QIAquick columns according to steps 4a, 4b, or 4c.**

4a. **QIAvac 24 Plus (see page 33, and Figure 7):**

   Insert up to 24 QIAquick spin columns into the luer extensions of the QIAvac 24 Plus. Close unused positions with luer caps and connect QIAvac 24 Plus to a vacuum source.

4b. QIAvac 6S manifold (see page 34, and Figure 8):

Open QIAvac 6S lid. Place QIAvac Luer Adapter(s), or blanks to seal unused slots, into the slots of QIAvac top plate, and close the QIAvac 6S lid. Place the waste tray inside the QIAvac base, and place the top plate squarely over the base. Attach the QIAvac 6S to a vacuum source.

Insert each QIAquick column into a luer connector on the Luer Adapter(s) in the manifold. Seal unused luer connectors with plugs provided with the QIAvac Luer Adapter Set.

4c. Other vacuum manifolds: follow the suppliers instructions. Insert each QIAquick-column into a luer connector.

5. After the gel slice has dissolved completely, check that the color of mixture is yellow (similar to Buffer QG without dissolved agarose).

Note: If the color of the sample is orange or violet, add 10 µl of 3 M sodium acetate, pH 5.0, and mix. The color of the mixture will turn to yellow.

The adsorption of DNA to the QIAquick membrane is efficient only at pH ≤7.5. Buffer QG contains a pH indicator that is yellow at pH ≤7.5 and orange or violet at higher pH, allowing easy determination of the optimal pH for DNA binding.

6. Add 1 gel volume of isopropanol to the sample and mix by inverting the tube several times.

For example, if the agarose gel slice is 100 mg, add 100 µl isopropanol. This step increases the yield of DNA fragments <500 bp and >4 kb. For DNA fragments between 500 bp and 4 kb, addition of isopropanol has no effect on yield. Do not centrifuge the sample at this stage.

7. To bind DNA, pipet the sample onto the QIAquick column and apply vacuum. After the sample has passed through the column, switch off vacuum source.

The maximum volume of the column reservoir is 800 µl. For sample volumes of more than 800 µl, simply load again.

8. Recommended: Add 0.5 ml of Buffer QG to QIAquick column and apply vacuum.

This step will remove all traces of agarose. It is only required when the DNA will subsequently be used for direct sequencing, in vitro transcription, or microinjection.

9. To wash, add 0.75 ml of Buffer PE to QIAquick column and apply vacuum.

Note: If the DNA will be used for salt-sensitive applications, such as blunt-end ligation and direct sequencing, let the column stand 2–5 min after addition of Buffer PE before applying vacuum.

10. **Transfer QIAquick column to a clean 1.5 ml microcentrifuge tube or to a provided 2 ml collection tube. Centrifuge for 1 min at 17,900 x *g* (13,000 rpm).**

    IMPORTANT: This spin is necessary to remove residual ethanol (Buffer PE).

11. **Place QIAquick column in a clean 1.5 ml microcentrifuge tube.**

12. **To elute DNA, add 50 µl of Buffer EB (10 mM Tris·Cl, pH 8.5) or water (pH 7–8.5) to the center of the QIAquick membrane and centrifuge the column for 1 min at 17,900 x *g* (13,000 rpm). Alternatively, for increased DNA concentration, add 30 µl elution buffer, let stand for 1 min, and then centrifuge for 1 min.**

    IMPORTANT: Ensure that the elution buffer is dispensed directly onto the QIAquick membrane for complete elution of bound DNA. The average eluate volume is 48 µl from 50 µl elution buffer volume, and 28 µl from 30 µl.

    Elution efficiency is dependent on pH. The maximum elution efficiency is achieved between pH 7.0 and 8.5. When using water, make sure that the pH value is within this range, and store DNA at –20°C as DNA may degrade in the absence of a buffering agent. The purified DNA can also be eluted in TE buffer (10 mM Tris·Cl, 1 mM EDTA, pH 8.0), but the EDTA may inhibit subsequent enzymatic reactions.

13. **If the purified DNA is to be analyzed on a gel, add 1 volume of Loading Dye to 5 volumes of purified DNA. Mix the solution by pipetting up and down before loading the gel.**

    Loading dye contains 3 marker dyes (bromophenol blue, xylene cyanol, and orange G) that facilitate estimation of DNA migration distance and optimization of agarose gel run time. Refer to Table 2 (page 15) to identify the dyes according to migration distance and agarose gel percentage and type.

Troubleshooting Guide

This troubleshooting guide may be helpful in solving any problems that may arise. For more information, see also the Frequently Asked Questions page at our Technical Support Center: www.qiagen.com/FAQ/FAQList.aspx . The scientists in QIAGEN Technical Services are always happy to answer any questions you may have about either the information or protocols in this handbook or sample and assay technologies (for contact information, see back cover or visit www.qiagen.com).

		Comments and Suggestions
Low or no recovery		
a)	Buffer PE did not contain ethanol	Ethanol must be added to Buffer PE (concentrate) before use. Repeat procedure with correctly prepared Buffer PE.
b)	Inappropriate elution buffer	DNA will only be eluted efficiently in the presence of low-salt buffer (e.g., Buffer EB: 10 mM Tris·Cl, pH 8.5) or water. See "Elution in low-salt solutions", page 13.
c)	Elution buffer incorrectly dispensed	Add elution buffer to the center of the QIAquick membrane to ensure that the buffer completely covers the membrane. This is particularly important when using small elution volumes (30 µl).
Gel		
d)	Gel slice incompletely solubilized	After addition of Buffer QG to the gel slice, mix by vortexing the tube every 2–3 min during the 50°C incubation. DNA will remain in any undissolved agarose.
e)	pH of electrophoresis buffer too high (binding mixture turns orange or violet)	The electrophoresis buffer has been repeatedly used or incorrectly prepared, resulting in a sample pH that exceeds the buffering capacity of Buffer QG and leads to inefficient DNA binding. Add 10 µl of 3 M sodium acetate, pH 5.0, to the sample and mix. The color of the mixture will turn yellow indicating the correct pH for DNA binding. Even for binding mixtures with only small color changes (slight orange color), add the 10 µl sodium acetate.
f)	Gel slice was too large (>400 mg)	70–80% recovery can only be obtained from ≤400 mg gel slice per QIAquick column. For gel slices >400 mg, use multiple QIAquick columns.

Gel: refers to QIAquick Gel Extraction Kits only.

PCR: refers to QIAquick PCR Purification Kits only.

Other notes refer to all kits.

		Comments and Suggestions
PCR		
g)	Insufficient/no PCR product	Estimate DNA recovery by running 10% of PCR product before and after purification on an agarose gel.
PCR/Gel		
h)	Cloudy and gelatinous appearance of sample mixture after addition of isopropanol	This may be due to salt precipitation, and will disappear upon mixing the sample. Alternatively, the gel slice may not be completely solubilized. In this case, apply the mixture to the QIAquick column, centrifuge, and then add 0.5 ml Buffer QG to the column. Let stand for 1 min at room temperature, and then centrifuge and continue with the procedure. This additional wash will solubilize remaining agarose.
i)	Binding mixture turns orange or violet	The pH in the sample exceeds the buffer capacity of Buffer QG or PB respectively. Add 20 µl of 3 M sodium acetate, pH 5.0, to the sample and mix. The color of the mixture will turn yellow indicating the correct pH for DNA binding. Even for samples with slight color changes (orange color), add 10 µl sodium acetate.
DNA does not perform well (e.g., in ligation reactions)		
a)	Salt concentration in eluate too high	Modify the wash step by incubating the column for 5 min at room temperature after adding 750 µl of Buffer PE, then centrifuge.
b)	Eluate contains residual ethanol	Ensure that the wash flow-through is drained from the collection tube and that the QIAquick column is then centrifuged at 17,900 x *g* (13,000 rpm) for an additional 1 min.
Gel		
c)	Eluate contaminated with agarose	The gel slice is incompletely solubilized or weighs >400 mg. Repeat procedure, including the optional Buffer QG column-wash step.
PCR		
d)	Eluate contains primer-dimers	Primer-dimers formed are >20 bp and are not completely removed. After the binding step, wash the QIAquick column with 750 µl of a 35% guanidine hydrochloride aqueous solution (35 g in 100 ml). Continue with the Buffer PE wash step and the elution step as in the protocol.

		Comments and Suggestions
e)	Eluate contains denatured ssDNA, which appears as smaller smeared band on an analytical gel	Use the eluted DNA to prepare the subsequent enzymatic reaction but omit the enzyme. To reanneal the ssDNA, incubate the reaction mixture at 95°C for 2 min, and allow the tube to cool slowly to room temperature. Add the enzyme and proceed as usual. Alternatively, the DNA can be eluted in 10 mM Tris buffer containing 10 mM NaCl. The salt and buffering agent promote the renaturation of DNA strands. However the salt concentration of the eluate must then be considered for subsequent applications.

Appendix: QIAvac Vacuum Manifolds

Handling guidelines for QIAvac 24 Plus

- Always place the QIAvac 24 Plus on a secure bench top or work area. If dropped, the QIAvac 24 Plus manifold may crack.
- Always store the QIAvac 24 Plus clean and dry. For cleaning procedures see the *QIAvac 24 Plus Handbook*.
- The components of the QIAvac 24 Plus are not resistant to certain solvents (Table 4). If these solvents are spilled on the unit, rinse it thoroughly with water.
- To ensure consistent performance, do not apply silicone or vacuum grease to any part of the QIAvac 24 Plus manifold.
- Always use caution and wear safety glasses when working near a vacuum manifold under pressure.
- Contact QIAGEN Technical Services or your local distributor for information concerning spare or replacement parts.

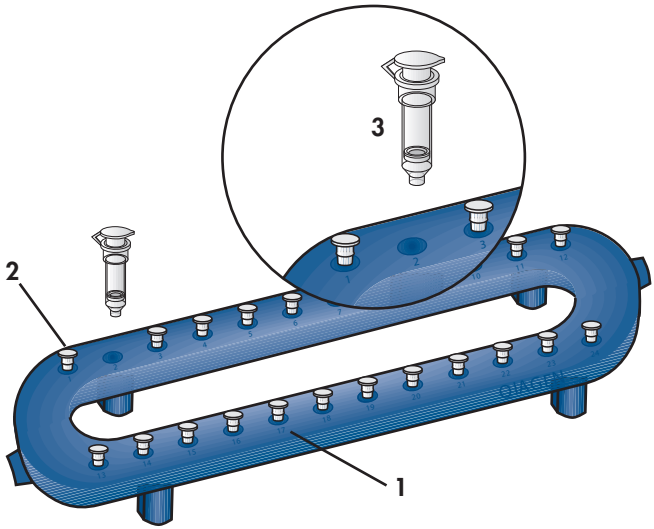

Figure 7. QIvac 24 Plus. Setting up the QIAvac 24 Plus with QIAprep®, QIAquick, MinElute, or RNeasy® Mini Spin Columns.

1. QIAvac 24 Plus vacuum manifold
2. Luer slot closed with luer plug
3. Spin column*

* Not included with the QIAvac 24 Plus. Included in appropriate purification kits.

Table 4. Chemical Resistance Properties of the QIAvac 24 Plus

Resistant to:		
Acetic acid	Chaotropic salts	Chlorine bleach
Chromic acid	Hydrochloric acid	SDS
Sodium chloride	Sodium hydroxide	Tween 20
Urea		
Not resistant to:		
Benzene	Chloroform	Ethers
Phenol	Toluene	

Handling guidelines for QIAvac 6S

QIAvac 6S facilitates DNA cleanup with QIAquick by providing a convenient modular vacuum manifold, which, in combination with QIAvac Luer Adapters, allows easy processing of QIAquick spin columns as an alternative to centrifugation. The following recommendations should be followed when handling the QIAvac 6S vacuum manifold.

- Always store the QIAvac 6S vacuum manifold clean and dry. To clean, simply rinse all components with water and dry with paper towels. Do not air-dry, as the screws may rust and need to be replaced. Do not use abrasives or solvents.
- Always place the QIAvac 6S vacuum manifold on a secure bench top or work area. If dropped, the manifold may crack.
- The components of QIAvac manifolds are not resistant to ethanol, methanol, or other organic solvents (Table 5). Do not bring solvents into contact with the vacuum manifold. If solvents are spilled on the unit, rinse thoroughly with distilled water, and do not incubate acrylic components in alcohol-containing reagents for long periods of time. Ensure that no residual Buffer PE remains in the vacuum manifold.
- To ensure consistent performance, do not apply silicone or vacuum grease to any part of the QIAvac 6S manifold. The spring lock on the top plate and the self-sealing gasket provide an airtight seal when vacuum is applied to the assembled unit. To maximize gasket lifetime, rinse the gasket free of salts and buffers after each use and dry with paper towels before storage.
- Remove blanks from the slots of the top plate after use and store them under the manifold.

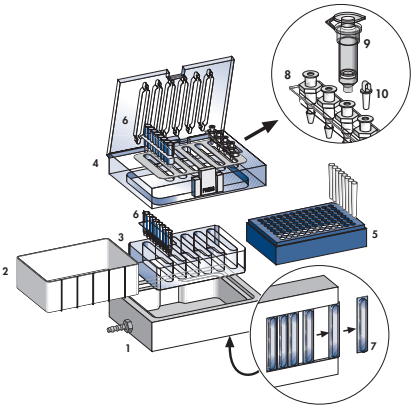

Figure 8. QIAvac 6S. Components of the QIAvac 6S manifold.

1. QIAvac base, which holds a waste tray, a strip holder, or a microtube rack
2. Waste tray
3. QIAvac strip holder to hold 8-well strips
4. QIAvac top plate with slots for 8-well strips or QIAvac Luer Adapters
5. Microtube rack
6. 8-well strip*
7. Blanks to seal unused slots
8. QIAvac Luer Adapter†
9. QIAquick spin column*
10. Plug to seal unused luer connectors†

* Not included with QIAvac Manifold. Included in appropriate kits.
† Not included with QIAvac 6S. Must be purchased separately.

Table 5. Chemical Resistance Properties of the QIAvac 6S

Resistant to:		
Chlorine bleach (12%)	Diluted alcohol	Hydrochloric acid
Sodium chloride	Sodium hydroxide	Urea
Not resistant to:		
Acetone	Benzene	Chloroform
Chromic acid	Ethers	Phenol
Toluene		

References

1. Vogelstein, B. and Gillespie, D. (1979) Preparative and analytical purification of DNA from agarose. Proc. Natl. Acad. Sci. USA ***76***, 615.
2. Hamaguchi, K. and Geiduschek, E.P. (1962) The effect of electrolytes on the stability of deoxyribonucleate helix. J. Am. Chem. Soc. ***84***, 1329.

Ordering Information

Product	Contents	Cat. no.
QIAquick Spin Kits		
QIAquick PCR Purification Kit (50)	50 QIAquick Spin Columns, Buffers, Collection Tubes (2 ml)	28104
QIAquick PCR Purification Kit (250)	250 QIAquick Spin Columns, Buffers, Collection Tubes (2 ml)	28106
QIAquick Nucleotide Removal Kit (50)	50 QIAquick Spin Columns, Buffers, Collection Tubes (2 ml)	28304
QIAquick Nucleotide Removal Kit (250)	250 QIAquick Spin Columns, Buffers, Collection Tubes (2 ml)	28306
QIAquick Gel Extraction Kit (50)	50 QIAquick Spin Columns, Buffers, Collection Tubes (2 ml)	28704
QIAquick Gel Extraction Kit (250)	250 QIAquick Spin Columns, Buffers, Collection Tubes (2 ml)	28706
Related products		
MinElute Reaction Cleanup Kit (50)	50 MinElute Spin Columns, Buffers, Collection Tubes (2 ml)	28204
MinElute Reaction Cleanup Kit (250)	250 MinElute Spin Columns, Buffers, Collection Tubes (2 ml)	28206
MinElute Gel Extraction Kit (50)	50 MinElute Spin Columns, Buffers, Collection Tubes (2 ml)	28604
MinElute Gel Extraction Kit (250)	250 MinElute Spin Columns, Buffers, Collection Tubes (2 ml)	28606
MinElute PCR Purification Kit (50)	50 MinElute Spin Columns, Buffers, Collection Tubes (2 ml)	28004
MinElute PCR Purification Kit (250)	250 MinElute Spin Columns, Buffers, Collection Tubes (2 ml)	28006
Individual buffers		
Buffer PB (500 ml)	500 ml Binding Buffer	19066
Buffer PN	500 ml Binding Buffer	19071
Buffer PE (concentrate)	100 ml Buffer PE (5x concentrate; final volume 500 ml)	19065
Buffer QG* (250 ml)	250 ml Solubilization and Binding Buffer (with pH indicator)	19063

* Additional Buffer QG may be required for routine purifications from gel slices >300 mg from gels containing >2% agarose.

Ordering Information

Product	Contents	Cat. no.
QIAcube and accessories		
QIAcube*	Robotic workstation for automated purification of DNA, RNA, or proteins using QIAGEN spin-column kits, 3-year warranty on parts and labor	9001292† 9001293‡
Starter Pack, QIAcube§	Pack includes: reagent bottle racks (3); rack labeling strips (8); 200 µl filter-tips (1024); 1000 µl filter-tips (1024); 1000 µl filter-tips, wide-bore (1024); 30 ml reagent bottles (18); rotor adapters (120); rotor adapter holder	990395
QIAvac manifolds and accessories		
QIAvac 24 Plus	Vacuum manifold for processing 1–24 spin columns: includes QIAvac 24 Plus Vacuum Manifold, Luer Plugs, Quick Couplings	19413
QIAvac 6S	Vacuum manifold for processing 1–6 QIAGEN 8-well strips: includes QIAvac 6S Top Plate with flip-up lid, Base, Waste Tray, Blanks, Strip Holder	19503
QIAvac 96	Vacuum manifold for processing QIAGEN 96 well-plates: includes QIAvac 96 Top plate, Base, Waste Tray, Plate Holder	19504
QIAvac Luer Adapter Set¶	For processing 1–24 QIAGEN spin columns on QIAvac 6S: 6 adapters with 4 luer connectors each, 24 plugs	19541
Vacuum Regulator	For use with QIAvac manifolds	19530
Vacuum Pump	Universal vacuum pump (capacity 34 L/min, 8 mbar vacuum abs.)	84000** 84010†† 84020‡‡

* Agreements for conprehensive service coverage are available; please inquire. † US, Canada, and Japan. ‡ Rest of world. § All starter pack items are available separately. ¶ Compatible only with QIAvac Top Plates containing flip-up lid. ** Japan. †† US and Canada. ‡‡ Rest of world.

The QIAcube is intended to be used only in combination with QIAGEN Kits for applications described in the respective Kit handbooks. All other Kits are intended for research use. No claim or representation is intended to provide information for the diagnosis, prevention, or treatment of a disease.

Trademarks: QIAGEN®, QIAEX®, QIAquick®, QIAprep®, MinElute®, QIAcube®, RNeasy® (QIAGEN Group); Tween® (ICI Americas Inc.)

Limited License Agreement

Use of this product signifies the agreement of any purchaser or user of the QIAquick PCR Purification Kit, the QIAquick Nucleotide Removal Kit and the QIAquick Gel extraction Kit to the following terms:

1. The QIAquick PCR Purification Kit, the QIAquick Nucleotide Removal Kit and the QIAquick Gel extraction Kit may be used solely in accordance with the QIAquick Spin Handbook and for use with components contained in the Kit only. QIAGEN grants no license under any of its intellectual property to use or incorporate the enclosed components of this Kit with any components not included within this Kit except as described in the QIAquick Spin Handbook and additional protocols available at www.qiagen.com .
2. Other than expressly stated licenses, QIAGEN makes no warranty that this Kit and/or its use(s) do not infringe the rights of third-parties.
3. This Kit and its components are licensed for one-time use and may not be reused, refurbished, or resold.
4. QIAGEN specifically disclaims any other licenses, expressed or implied other than those expressly stated.
5. The purchaser and user of the Kit agree not to take or permit anyone else to take any steps that could lead to or facilitate any acts prohibited above. QIAGEN may enforce the prohibitions of this Limited License Agreement in any Court, and shall recover all its investigative and Court costs, including attorney fees, in any action to enforce this Limited License Agreement or any of its intellectual property rights relating to the Kit and/or its components.

For updated license terms, see www.qiagen.com .

www.qiagen.com

Australia ■ Orders 03-9840-9800 ■ Fax 03-9840-9888 ■ Technical 1-800-243-066

Austria ■ Orders 0800/28-10-10 ■ Fax 0800/28-10-19 ■ Technical 0800/28-10-11

Belgium ■ Orders 0800-79612 ■ Fax 0800-79611 ■ Technical 0800-79556

Canada ■ Orders 800-572-9613 ■ Fax 800-713-5951 ■ Technical 800-DNA-PREP (800-362-7737)

China ■ Orders 021-51345678 ■ Fax 021-51342500 ■ Technical 021-51345678

Denmark ■ Orders 80-885945 ■ Fax 80-885944 ■ Technical 80-885942

Finland ■ Orders 0800-914416 ■ Fax 0800-914415 ■ Technical 0800-914413

France ■ Orders 01-60-920-926 ■ Fax 01-60-920-925 ■ Technical 01-60-920-930 ■ Offers 01-60-920-928

Germany ■ Orders 02103-29-12000 ■ Fax 02103-29-22000 ■ Technical 02103-29-12400

Hong Kong ■ Orders 800 933 965 ■ Fax 800 930 439 ■ Technical 800 930 425

Ireland ■ Orders 1800-555-049 ■ Fax 1800-555-048 ■ Technical 1800-555-061

Italy ■ Orders 02-33430411 ■ Fax 02-33430426 ■ Technical 800-787980

Japan ■ Telephone 03-5547-0811 ■ Fax 03-5547-0818 ■ Technical 03-5547-0811

Korea (South) ■ Orders 1544 7145 ■ Fax 1544 7146 ■ Technical 1544 7145

Luxembourg ■ Orders 8002-2076 ■ Fax 8002-2073 ■ Technical 8002-2067

The Netherlands ■ Orders 0800-0229592 ■ Fax 0800-0229593 ■ Technical 0800-0229602

Norway ■ Orders 800-18859 ■ Fax 800-18817 ■ Technical 800-18712

Singapore ■ Orders 65-67775366 ■ Fax 65-67785177 ■ Technical 65-67775366

Sweden ■ Orders 020-790282 ■ Fax 020-790582 ■ Technical 020-798328

Switzerland ■ Orders 055-254-22-11 ■ Fax 055-254-22-13 ■ Technical 055-254-22-12

UK ■ Orders 01293-422-911 ■ Fax 01293-422-922 ■ Technical 01293-422-999

USA ■ Orders 800-426-8157 ■ Fax 800-718-2056 ■ Technical 800-DNA-PREP (800-362-7737)

1051746 03/2008

Sample & Assay Technologies

Please tear here

Bench Protocol: QIAquick PCR Purification Microcentrifuge and Vacuum Protocol

New users are strongly advised to familiarize themselves with the detailed protocols and safety information provided in the *QIAquick Spin Handbook* before using this bench protocol.

Notes before starting

- Add ethanol (96–100%) to Buffer PE before use (see bottle label for volume).
- All centrifugation steps are carried out at 17,900 x *g* (13,000 rpm) in a conventional tabletop microcentrifuge at room temperature.
- Add 1:250 volume pH indicator I to Buffer PB. The yellow color of Buffer PB with pH indicator I indicates a pH of ≤7.5.

  Note: If the purified PCR product is to be used in sensitive microarray applications, it may be beneficial to use Buffer PB without addition of pH indicator I. Do not add pH indicator I to buffer aliquots.

Procedure

1. **Add 5 volumes of Buffer PB to 1 volume of the PCR reaction and mix.**
   If the color of the mixture is orange or violet, add 10 µl of 3 M sodium acetate, pH 5.0, and mix. The color of the mixture will turn yellow.
2. **Place a QIAquick column in ▲ a provided 2 ml collection tube or into ● a vacuum manifold.**
   See the *QIAquick Spin Handbook* for details on how to set up a vacuum manifold.
3. **To bind DNA, apply the sample to the QIAquick column and ▲ centrifuge for 30–60 s or ● apply vacuum to the manifold until all samples have passed through the column. ▲ Discard flow-through and place the QIAquick column back into the same tube.**
4. **To wash, add 0.75 ml Buffer PE to the QIAquick column and ▲ centrifuge for 30–60 s or ● apply vacuum. ▲ Discard flow-through and place the QIAquick column back in the same tube.**
5. **Centrifuge the column in a 2 ml collection tube (provided) for 1 min.**
6. **Place each QIAquick column in a clean 1.5 ml microcentrifuge tube.**
7. **To elute DNA, add 50 µl Buffer EB (10 mM Tris·Cl, pH 8.5) or water to the center of the QIAquick membrane and centrifuge the column for 1 min. For increased DNA concentration, add 30 µl elution buffer to the center of the QIAquick membrane, let the column stand for 1 min, and then centrifuge.**
8. **If the purified DNA is to be analyzed on a gel, add 1 volume of Loading Dye to 5 volumes of purified DNA. Mix the solution by pipetting up and down before loading the gel.**

Bench Protocol: QIAquick Nucleotide Removal Protocol

New users are strongly advised to familiarize themselves with the detailed protocols and safety information provided in the *QIAquick Spin Handbook* before using this bench protocol.

Notes before starting

- Add ethanol (96–100%) to Buffer PE before use (see bottle label for volume).
- All centrifugation steps are in a conventional in a conventional tabletop microcentrifuge.

Procedure

1. **Add 10 volumes of Buffer PN to 1 volume of the reaction sample and mix.**
2. **Place a QIAquick spin column in a provided 2 ml collection tube.**
3. **To bind DNA, apply the sample to the QIAquick column and centrifuge for 1 min at 6000 rpm.**
4. **For radioactive samples:**
   Place the QIAquick column into a clean 2 ml collection tube and discard the tube containing the radioactive flow-through appropriately.
   For non-radioactive samples:
   Discard the flow-through and place QIAquick column back into the same tube.
5. **For radioactive samples:**
   To wash QIAquick column, add 500 µl of Buffer PE and centrifuge for 1 min at 6000 rpm. Discard the flow-through appropriately and repeat wash with another 500 µl of Buffer PE.
   For non-radioactive samples:
   To wash QIAquick column, add 750 µl of Buffer PE and centrifuge for 1 min at 6000 rpm.
6. **Discard the flow-through and place the QIAquick column back in the same tube, which should be empty. Centrifuge for an additional 1 min at 13,000 rpm (17,900 x *g*).**
7. **Place the QIAquick column in a clean 1.5 ml microcentrifuge tube.**
8. **To elute DNA, add 100–200 µl of Buffer EB (10 mM Tris·Cl, pH 8.5) or water to the center of the QIAquick membrane and centrifuge the column for 1 min at 13,000 rpm (17,900 x *g*). Alternatively, for increased DNA concentration, add 30–50 µl elution buffer to the center of the QIAquick membrane, let the column stand for 1 min, and then centrifuge.**
9. **If the purified DNA is to be analyzed on a gel, add 1 volume of Loading Dye to 5 volumes of purified DNA. Mix the solution by pipetting up and down before loading the gel.**

Please tear here

Please tear here

Bench Protocol: QIAquick Gel Extraction Microcentrifuge and Vacuum Protocol

New users are strongly advised to familiarize themselves with the detailed protocols and safety information provided in the *QIAquick Spin Handbook* before using this bench protocol.

Notes before starting

- The yellow color of Buffer QG indicates a pH ≤7.5.
- Add ethanol (96–100%) to Buffer PE before use (see bottle label for volume).
- Isopropanol (100%) and a heating block or water bath at 50°C are required.
- All centrifugation steps are carried out at 17,900 x *g* (13,000 rpm) in a conventional table-top microcentrifuge.

Procedure

1. **Excise the DNA fragment from the agarose gel with a clean, sharp scalpel.**
2. **Weigh the gel slice in a colorless tube. Add 3 volumes of Buffer QG to 1 volume of gel (100 mg ~ 100 µl).**

   If the color of the mixture is orange or violet, add 10 µl of 3 M sodium acetate, pH 5.0, and mix. The color of the mixture will turn yellow.
3. **Incubate at 50°C for 10 min (or until the gel slice has completely dissolved). To help dissolve gel, mix by vortexing the tube every 2–3 min during the incubation.**

   For >2% gels, increase incubation time.
4. **After the gel slice has dissolved completely, check that the color of the mixture is yellow (similar to Buffer QG without dissolved agarose).**

   If the color of the mixture is orange or violet, add 10 µl of 3 M sodium acetate, pH 5.0, and mix. The color of the mixture will turn to yellow.
5. **Add 1 gel volume of isopropanol to the sample and mix.**
6. **Place a QIAquick spin column in ▲ a provided 2 ml collection tube or into ● a vacuum manifold.**

   See *QIAquick Spin Handbook* for details on how to set up a vacuum manifold.

QIAGEN

7. **To bind DNA, apply the sample to the QIAquick column and ▲ centrifuge for 1 min or ● apply vacuum to the manifold until all samples have passed through the column. ▲ Discard flow-through and place the QIAquick column back into the same tube.**

   The maximum volume of the column reservoir is 800 µl. For sample volumes of more than 800 µl, simply load and spin/apply vacuum again.

8. **Recommended: Add 0.5 ml of Buffer QG to QIAquick column and ▲ centrifuge for 1 min or ● apply vacuum. ▲ Discard flow-through and place the QIAquick column back into the same tube.**

   This step is only required when the DNA will subsequently be used for direct sequencing, in vitro transcription, or microinjection.

9. **To wash, add 0.75 ml of Buffer PE to QIAquick column and ▲ centrifuge for 1 min or ● apply vacuum. ▲ Discard flow-through and place the QIAquick column back into the same tube.**

   Note: If the DNA will be used for salt-sensitive applications, such as blunt-end ligation and direct sequencing, let the column stand 2–5 min after addition of Buffer PE, before centrifuging.

10. **Centrifuge the column in a 2 ml collection tube (provided) for 1 min at 17,900 x *g* (13,000 rpm).**

11. **Place QIAquick column into a clean 1.5 ml microcentrifuge tube.**

12. **To elute DNA, add 50 µl of Buffer EB (10 mM Tris·Cl, pH 8.5) or water to the center of the QIAquick membrane and centrifuge the column for 1 min. Alternatively, for increased DNA concentration, add 30 µl elution buffer to the center of the QIAquick membrane, let the column stand for 1 min, and then centrifuge for 1 min.**

13. **If the purified DNA is to be analyzed on a gel, add 1 volume of Loading Dye to 5 volumes of purified DNA. Mix the solution by pipetting up and down before loading the gel.**

APPENDIX D

Bayes-block used in TE_B molecular phylogenetic analysis for the TE_B alignment.

```
begin mrbayes;
log start filename=TotBbaylog.txt;

        [The following lines define four character sets, each corresponding to a gene]
        charset coi = 1-620;
        charset 16s = 621-1023;
        charset its = 1024-1512;
        charset 28s = 1512-2110;

        [The following line defines a partition called "by_gentyp" that divides the sites
into genes]
        partition by_gentyp = 4:16s,coi,28s,its;

        [The following line sets the current partition to the one we just defined above.
If we do not explicitly set the partition to the one we defined, MrBayes will use the
default partition.  The default partition divides the characters into sets based on their
data type (DNA, amino acid, etc)]
        set partition=by_gentyp;

        [The following line allows the genes to have different mutation rates. Without
the following line, all codon positions will be assumed to evolve at the same rate]
        prset ratepr=variable;

end;

begin mrbayes;
            unlink statefreq=(all) revmat=(all) shape=(all)
pinvar=(all);
            prset applyto=(all);
            lset applyto=(1) nst=6 rates=invgamma;
            [Modelselection coi by hLrt: GTR+I+G]

            lset applyto=(2) nst=2 rates=invgamma;
            [Modelselection 16s by hLrt: HKY+I+G]

                lset applyto=(3) nst=1 rates=equal;
            [Modelselection ITS by hLrt: JC]

                lset applyto=(4) nst=2 rates=inv;
            [Modelselection 28S by hLrt: HKY+I]
end;

begin mrbayes;
            mcmcp savebrlens=yes ngen=2000000;

end;
```

Zootaxa 2302: 31–47 (2009)
www.mapress.com/zootaxa/

Article

ISSN 1175-5326 (print edition)
ZOOTAXA
ISSN 1175-5334 (online edition)

Four new species of the family Lithodidae (Decapoda: Anomura) from the collections of the National Museum of Natural History, Smithsonian Institution

SALLY HALL[1] & SVEN THATJE

National Oceanography Centre, Southampton, School of Ocean and Earth Sciences, University of Southampton, SO14 3ZH, United Kingdom.

[1]E-mail: smh57@noc.soton.ac.uk

Abstract

Four new species of lithodid crab were identified in the collections of the National Museum of Natural History, Smithsonian Institution. These include three species of the genus *Paralomis*: *P. nivosa* from the Philippines, *P. makarovi* from the Bering Sea, and *P. alcockiana* from South Carolina; and one new species of the genus *Lithodes*, *L. galapagensis*, from the Galapagos archipelago. Two of these species, *P. nivosa* and *P. makarovi* were part of a collection of previously unidentified lithodid samples from the Albatross expeditions of 1906–1908. *Paralomis makarovi* may have been misidentified as *P. multispina* Benedict, 1894, or *P. histrix* (De Haan, 1844) in other collections owing to superficial similarities in carapace ornamentation and overlapping distributions.

Key words: king crab, *Lithodes*, *Paralomis*, Albatross expedition, new species, Anomura, Lithodidae

Introduction

The family Lithodidae Samouelle, 1819, is a commercially important group of crustaceans inhabiting subtidal waters at high latitudes, as well as the deep sea in most of the world's oceans (Hall & Thatje 2009). The family consists of 109 species described to date; most of these belonging to the deep-sea genera *Lithodes* Latreille, 1806 (20 species), and *Paralomis* White, 1856 (57 species) (Zaklan 2002; Macpherson & Chan 2008; Spiridonov *et al.* 2006).

The National Museum of Natural History, Smithsonian Institution, Washington D.C. (USNM) currently curates over 700 samples belonging to the family Lithodidae — 684 of which are identified to species level. Several of the unidentified samples were collected in the early part of the 20th century by the U.S. Bureau of Fisheries steamer, "Albatross".

The number of described species of the genus *Paralomis* has increased in recent decades (Takeda & Bussarawit 2007). We are beginning to understand the incredible diversity of deep-water forms at depths typically 500–1500 m.

No species of *Paralomis* have been previously reported from the Philippines, although the Albatross 1908–09 expedition to this region also yielded the holotype of *Paralomis ochthodes* Macpherson, 1988a, from the Gulf of Boni, about 1300 km to the south. In addition, *P. seagranti* Eldredge, 1976 and *P. haigae* Eldredge, 1976, were described from Guam, and *P. danida* Takeda & Bussarawit, 2007, was described from Thailand. Several species of *Paralomis*, including *P. dofleini* Balss, 1911, are known from Taiwan and Japan (Macpherson & Chan 2008; Takeda 1985; Takeda 1990; Takeda 1980; Sakai 1971; Sakai 1987).

The diversity of the family Lithodidae in the North Pacific is notably high, with most of the 14 lithodid genera being represented there. Only two species of *Paralomis* have been reported from the Bering Sea, namely *P. multispina* (Benedict, 1894) and *P. verrilli* (Benedict, 1894) (Sakai 1971). In this region, species of

Accepted by S. Ahyong: 30 Oct. 2009; published: 2 Dec. 2009

Paralomis have been encountered at depths of around 1500 m, whereas most other members of the Lithodidae in the North Pacific are found intertidally, based on data from the USNM holdings.

Several species of *Paralomis* are encountered in the Caribbean Sea: *P. cubensis* Chace, 1939, *P. pectinata* Macpherson, 1988b and *P. serrata* Macpherson, 1988b, and *P. arethusa* Macpherson, 1994. None are recorded in the waters off South Carolina, and the closest described species from the Atlantic coast of the USA is *P. bouvieri* Hansen, 1908 (see Macpherson 1988b) at 1460 m off the coast of Virginia.

To date, no specimen of Lithodidae has been recorded from the Galapagos Islands. The genus *Lithodes* is typically found between 200 and 1000 m, and it has been recorded from several locations in the Pacific Ocean — particularly around the islands chains of the western Pacific (Hall & Thatje 2009). The species of *Lithodes* occurring nearest to the Galapagos Islands are *L. wiracocha* Haig, 1974, and *L. panamensis* Faxon, 1893 from the coastal waters off Equador and Peru (Haig 1974).

Materials and methods

All specimens remain in the collections of the USNM. Measurements given are of carapace length (CL) excluding the rostrum. Terminology follows Macpherson (1988b).

Systematic account

Family Lithodidae Samouelle, 1819

***Paralomis alcockiana* n. sp.**
(Figs 1, 2)

Material examined. South Carolina: 31°20'N, 79°05'W, 1995, 570 m: male holotype, CL 44 mm (USNM 269032), S. Carolina Department of Natural Resources.

Etymology. This new species is named after Alfred W. Alcock, 19th century British carcinologist, and Fellow of the Royal Society who reported on the findings of the HMS Investigator in the Indian Ocean.

Description of holotype. Carapace about as long as broad; irregularly hexagonal and angular in outline (Fig. 1a). Surface covered in smoothly elliptical, raised tubercles becoming somewhat more acute towards anterolateral margins; some tubercles enlarged and more acute, with clustered rings of smaller tubercles at base (Fig. 1b). Gastric regions with five enlarged tubercles, largest in the centre of region. Cardiac region with four enlarged tubercles in a quadrilateral pattern. Branchial region with three enlarged tubercles. (Positions of enlarged tubercles corresponding to dorsal spines in other species of *Paralomis* such as *P. formosa* Henderson). Under magnification, all tubercles with irregular arrangements of very short setae, as seen in *Paralomis cubensis* (Fig. 1d).

No regions particularly inflated above dorsal surface, although gastric region slightly inflated in comparison to branchial and cardiac regions. Grooves delimit cardiac region, forming triangle in advance of posterior margin. Small anterior spine present on pterygostomian region, as typical of genus.

Median rostral spine nearly straight, surpassing length of ocular peduncle; ventral surface deeply keeled, bearing several small denticulate spinules (Fig 2a). Paired dorsal spines diverging at level of cornea; both spines much shorter than ventral spine (Figs 2a, b). Dorsally, base of rostrum covered with more or less acute tubercles. Base of the rostrum wide, partially obscuring bases of ocular peduncles in dorsal view.

External-orbital and anterolateral spine similar in size, shorter than ocular peduncle (Fig. 1a). Several irregularly spaced spines (10+) of varying size on lateral margins of anterior half of carapace. Posterior lateral margins with acute tubercles.

Ocular peduncles covered with short spines, and one larger spine disto-dorsal near cornea (Fig. 1c). Antennal acicle broad, with one large central spine, 4 or 5 long spines on outer border and 4 spines of similar length on inner border.

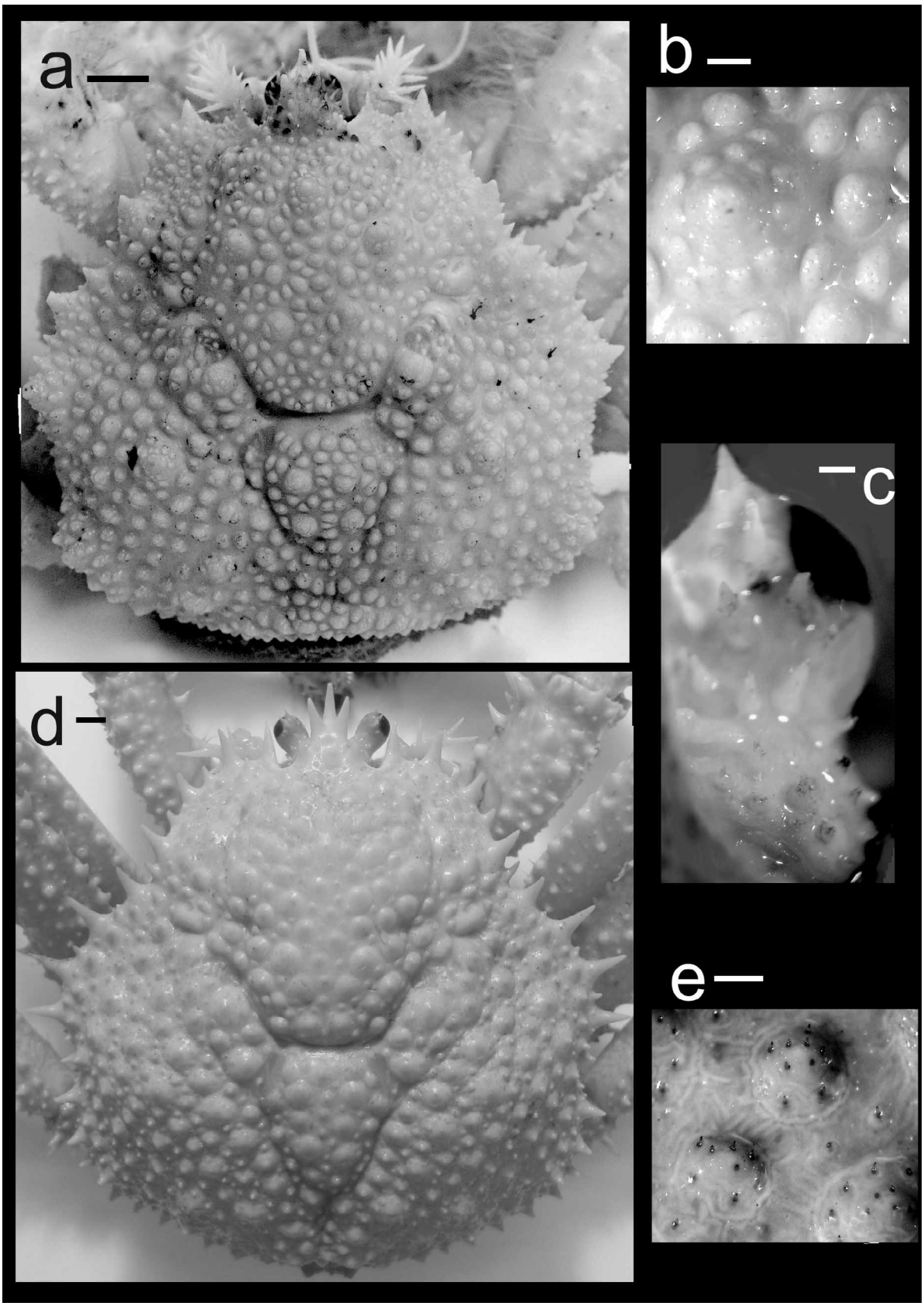

FIGURE 1. *Paralomis alcockiana* **n. sp.** a–c: male holotype, 44 mm CL (USNM 269032), South Carolina: 31°20'N, 79°05'W, 570 m. (a) carapace, dorsal. (b) carapace ornamentation, dorsal. (c) part of ocular peduncle visible below rostrum, dorsal. *Paralomis cubensis* Chace. d, e: Male, 46 mm CL (USNM 213542) (d) carapace, dorsal. (e) carapace ornamentation, dorsal. Scale bar = 5 mm for a, d; 1 mm for b, c, e.

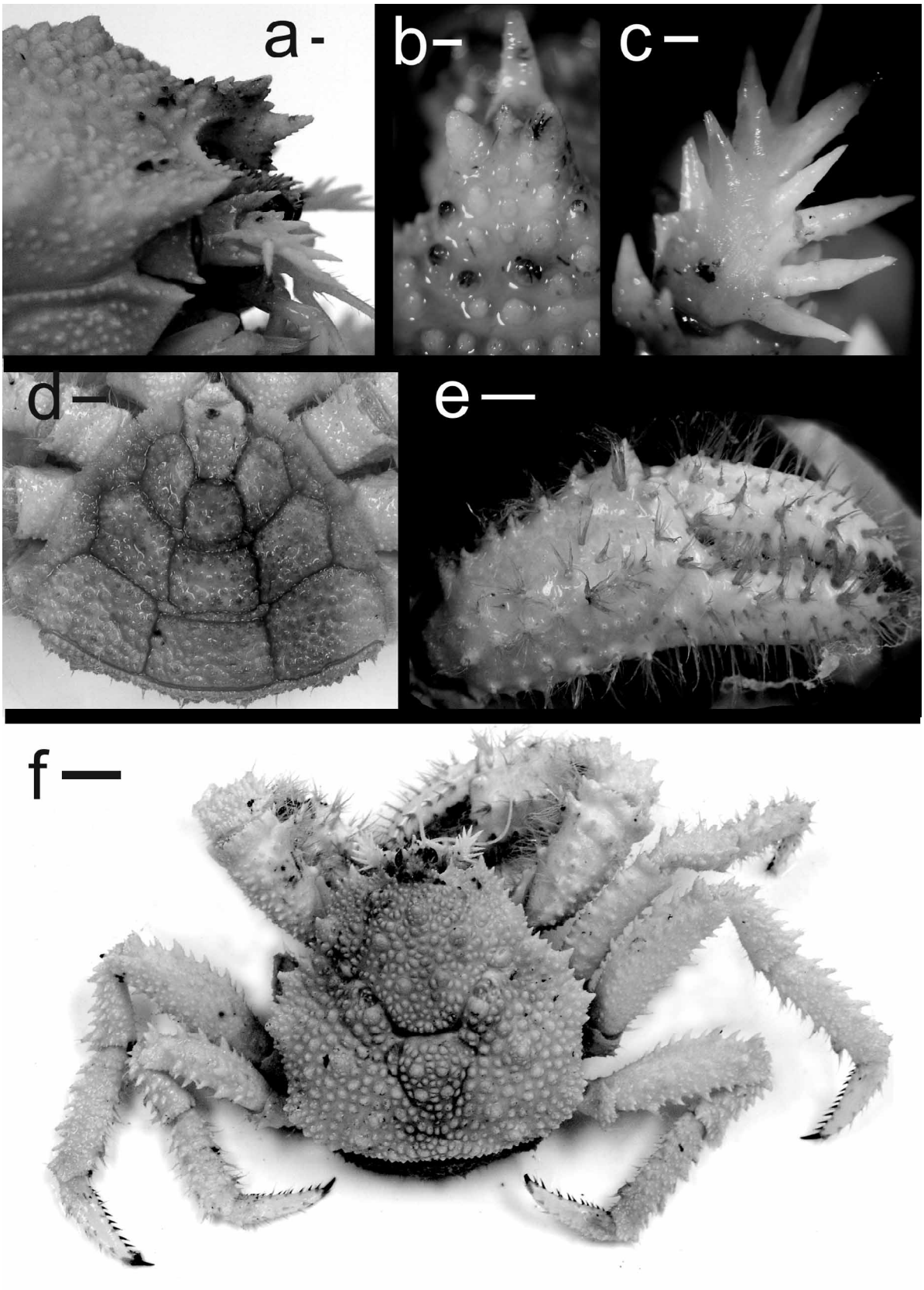

FIGURE 2. *Paralomis alcockiana* **n. sp.** a–f: male holotype, 44 mm CL (USNM 269032), South Carolina: 31°20’N, 79°05’W, 570 m. (a) anterior carapace, lateral. (b) rostral spines, dorsal. (c) right antennal acicle, dorsal. (d) abdomen. (e) right chela, lateral. (f) whole organism, dorsal. Scale bar = 1 mm for a–c; 5 mm for d–f.

Cheliped merus with numerous spiniform tubercles dorsally and on outer surface, larger distally, and one large spine distally on inner surface. Chela with numerous tufts of long yellow setae covering palm and fingers of both hands.

Merus of pereiopod 3 a little over half carapace length, and about four times as long as high, rectangular in cross-section. Several rows of spines on dorsal anterior margin and ventral posterior margin. Posterior, dorsal and ventral surfaces of merus covered with acute tubercles. Two rows of spines on dorsal surface of carpus, larger on anterior row. Propodus with one row of dorsal spines and one row of ventral spines; covered in acute tubercles. Dactylus ventral margin with row of long black needle-like spines, and one black spine at tip; dorsal margins with a few spines near the articulation with propodus; with tufts of long yellow setae.

Abdomen covered with tubercles smaller than on dorsal surface. Marginal plates expanded and fused on each of abdominal segments 3–5; marginal plates fused to lateral plates on segment 3 (Fig. 2d).

Remarks. *Paralomis alcockiana* n.sp. shares many characteristics with *P. cubensis*, which is found in the Gulf of Mexico and Caribbean Sea (Chace 1939) at similar depths to the new species. Some differences are listed in Table 1. The most notable distinguishing feature is the presence, in *P. alcockiana*, of some enlarged conical tubercles surrounded by a ring of smaller rounded tubercles (Fig. 1b).

TABLE 1. Key diagnostic differences between *Paralomis alcockiana* and two similar species.

	P. alcockiana **n. sp.** (Figs 1, 2).	*P. cubensis* Chace, 1939	*P. arethusa* Macpherson, 1994
Carapace outline	Irregularly hexagonal.	Circular in juveniles. Pyriform in adults.	Hexagonal.
Spinulation of lateral margins of carapace	Several irregularly spaced spines (10 +) of varying size on lateral margins of anterior carapace. Posterior lateral margins with acute tubercles.	More than 20 spines of different sizes spaced evenly around anterior and posterior margins	Three spines on each side of anterior margins, several small tubercles on posterior margins.
Spinulation of eyestalks	Several small spines or conical tubercles, largest terminal, extending well beyond cornea.	Several small spines or conical tubercles, largest terminal, extending well beyond cornea.	One distodorsal spine.
Antennal acicle	Broad; one large central spine, 4 or 5 long spines on outer border and 4 spines of a similar length on inner border.	4–6 spines, terminal pair longest, forming a fork. One spine proximal of inner spine of terminal pair and a fourth still more proximal on outer margin.	Large central spine not overreaching antennal peduncle; 2 spines on outer border. Inner border smooth.
Walking leg spinulation	Covered with irregular rows of spines and acute tubercles.	Covered with irregular rows of spines and acute tubercles.	Comb-like sets of spines on merus and carpus. Similar to *P. serrata* and *P. pectinata* from the Gulf of Mexico. Distinguishes all three in this group from *P. alcockiana*.

Paralomis alcockiana is similar in shape to *P. arethusa* from the Barbados accretionary prism, a species known only from a juvenile specimen of 18 mm CL. Although comparison is difficult between different growth stages (Ingle & Garrod 1987), some key diagnostic differences are listed in Table 1.

Paralomis alcockiana is somewhat similar to *P. inca* Haig, 1974, from Peru, and *P. grossmani* Macpherson, 1988b, from French Guiana, but under magnification, the setal coverage of the dorsal tubercles is very different. *Paralomis alcockiana* has rounded tubercles sparsely covered with a few short setae; *P. inca* has rounded or conical tubercles, densely covered with short setae on their apices; and *P. grossmani* has a distinct ring of longer setae around the apex of the tubercles on its dorsal surface. There are also differences in the shape of the carapace. *P. grossmani* is longer and thinner than *P. alcockiana*, especially in the anterior region, and has the gastric region inflated to a much greater level. *P. inca* has its posterior half very much expanded, in contrast to *P. alcockiana* which has a roughly hexagonal outline.

***Paralomis makarovi* n. sp.**
(Figs 3, 4)

Material examined. Bering Sea: Bowers Bank, 54°30'N, 179°17'E, Albatross station 4772, 4.06.1906, 629 m: male holotype, CL 23.8 mm; 3 male paratypes, CL 15–25 mm; 3 female paratypes. CL 12–23 mm (all USNM 1122582).

Etymology. This new species is named after V.V. Makarov, the author of an influential 1938 monograph on lithodid biogeography.

Description of the holotype. Carapace pear-shaped; rounded posteriorly, and longer than wide. Dorsal surface covered uniformly by conical spines, each with band of long setae half-way along length (Fig. 4c) No spines dorsally or laterally notably longer than any other — no prominent spine at apex of gastric or branchial regions. Gastric region rounded and more prominent than branchial and cardiac regions, which are relatively sunken. Grooves only partially delimiting regions.

Median spine of rostrum strongly curved upward, and without secondary spinules or tubercles on ventral surface; one pair of dorsal spines, and one pair of spinules at their base. Rostrum not pedunculated, such that dorsal spines do not surpass cornea in dorsal view (Figs 3f, 4f).

Spines on the lateral margins of carapace of similar size to those on dorsal surface; spines on frontal margin subequal, much shorter than eyestalk; 10–13 spines on each side of anterolateral margin; hepatic spines barely enlarged relative to others.

Ocular peduncles with long spine above cornea, and a few smaller spines along its length. Several setae above cornea (Fig. 3c).

Second peduncular segment of antenna with moderately-sized spine on outer angle, and small spine on inner angle. Antennal acicle longer than ocular peduncle, consisting of one central spine, with 2 or 3 long outer spines and 2 or 3 smaller inner spines; all spines with several setae (Fig. 3g).

Cheliped carpus with several spinules on medial face, without crest of large spines. Chelae with few spinules on dorsal border of palm, and several clusters of brush-like setae.

Merus of pereiopods 2–4 with 4 or 5 ill-defined rows of spines of various sizes; each row with 6 spines of a similar size to those on carapace. Dactylus of pereiopods 2–4 unarmed dorsally except for one at articulation and row of dark needle-like spines ventrally. Claw of dactylus recurved, with several clumps of setae.

Abdomen with marginal plates of segments 3–5 not separated from lateral plates, atypical of genus (Fig. 3d); surface of plates without spines, but with low tubercles and several clusters of setae.

Variations. With the exception of the abdominal asymmetry typical of this family, no notable differences are observed between the males and the females. All individuals agree closely with the holotype.

TABLE 2. Key diagnostic differences between *Paralomis makarovi*, *P. aspera* and *P. chilensis*.

	Paralomis makarovi **n. sp.** (Figs 2, 3)	*Paralomis aspera* Faxon	*Paralomis chilensis* Andrade
Carapace outline	Pear-shaped; rounded posteriorly. Longer than wide.	Pentagonal; as broad as long.	Pear shaped; broader than long.
Antennal acicle spinulation	One central spine, with 2 or 3 long outer spines and 2 or 3 smaller inner spines. All spines with several setae.	At least 7 fully developed spines, on inner and outer faces of the acicle.	Acicle with many spines above and below the plane.
Cheliped palms	Chelae with a few spinules on dorsal border of palm, and several clusters of brush-like setae	Thickly set with strong spines.	Thickly set with strong spines; fingers with no spines.
Abdomen	Surface of plates with low tubercles and several clusters of setae	Plates bear spines similar to those on the dorsal surface of carapace.	Plates bear spines similar to those on the dorsal surface of carapace.
Carapace regional differentiation	Poorly defined regions.	Well defined gastric, cardiac and branchial regions.	Strong definition of all regions.

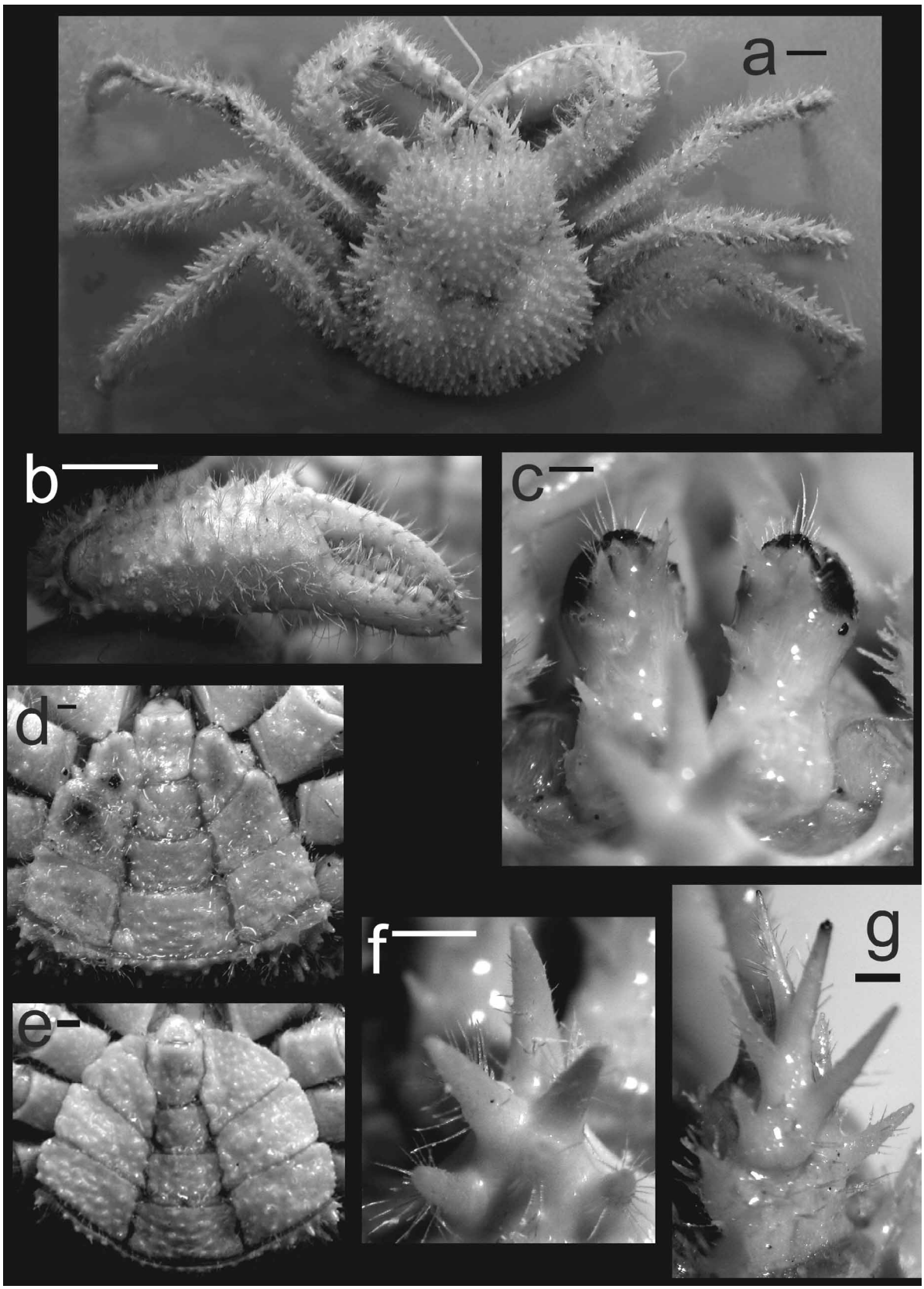

FIGURE 3. *Paralomis makarovi* **n. sp.** a–d, f–g: male holotype, 23.8 mm CL (USNM 1122582) , Bering Sea, Bowers Bank, 54°30'N, 179°17'E, 629 m. e: female paratype 24 mm CL (USNM 1122582). (a) whole organism, dorsal. (b) right chela, lateral. (c) ocular peduncles, dorsal. (d) male abdomen. (e) female abdomen. (f) rostral spines, dorsal. (g) antennal acicle, dorsal. Scale bar = 5 mm for a, b; 1 mm for c–g.

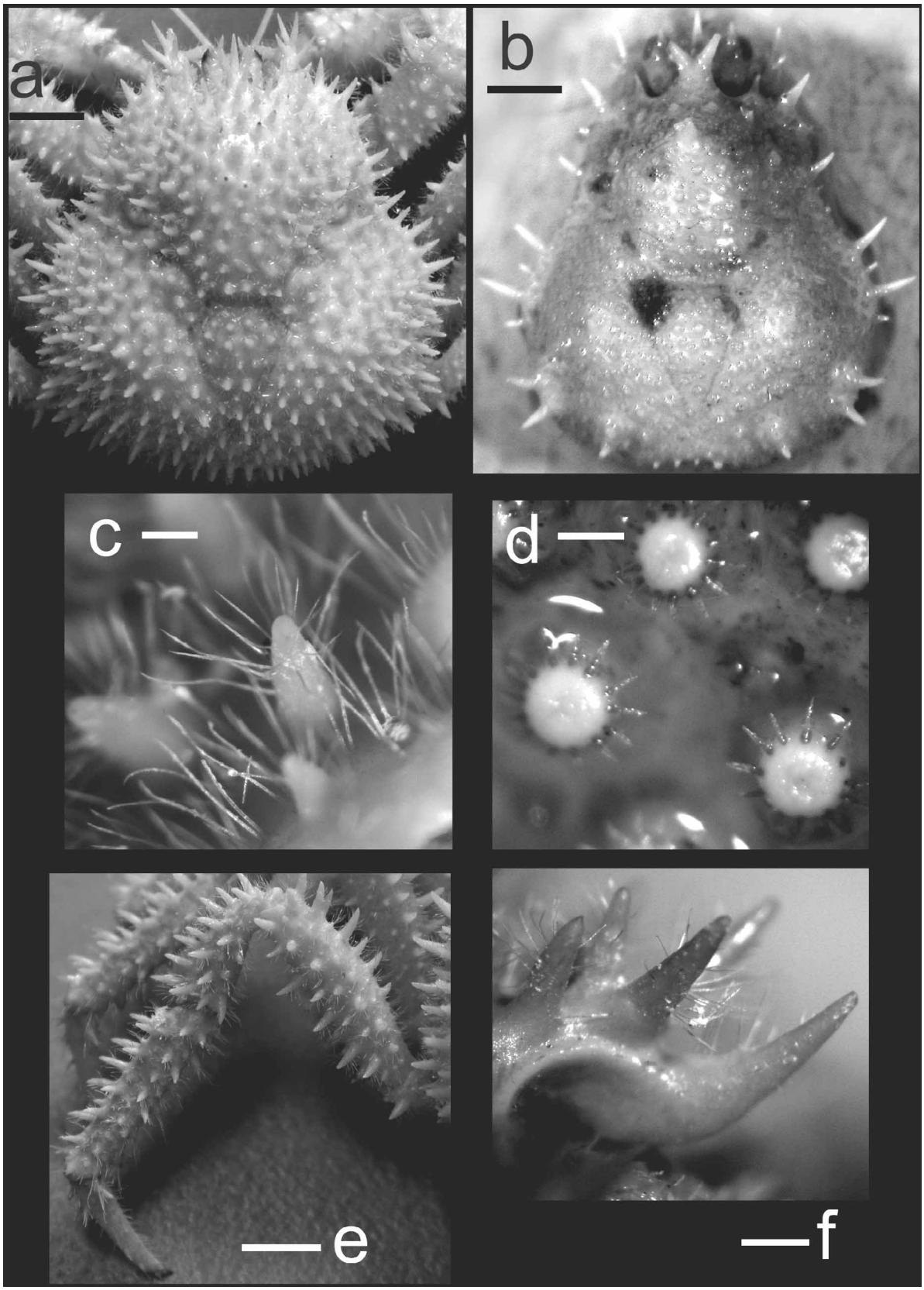

FIGURE 4. *Paralomis makarovi* **n. sp.** a, c, e, f: male holotype, 23.8 mm CL (USNM 1122582), Bering Sea, Bowers Bank, 54°30'N, 179°17'E, 629 m. (a) carapace, dorsal. (c) dorsal carapace spines, lateral. (e) left pereiopod 4, posterior. (f) rostrum, lateral. *Paralomis multispina* Benedict. b, d: USNM 18592, female, 20 mm CL. (b) carapace, dorsal. (d) mid-branchial carapace ornamentation, dorsal. Scale bar = 5 mm for a, b, e; 1mm for c, d, f.

Remarks. Several species of *Paralomis* have the dorsal part of their carapace covered in dense, uniform spines. Under magnification, however, the structure of the spines is similar only to *P. aspera* and *P. chilensis* from the coast of South America, both of which have conical spines with a band of long setae half way along the length. Diagnostic differences between these species are set out in Table 2.

Paralomis makarovi has a geographic proximity to *P. multispina* and *P. verrilli*. A uniform coverage of spines on the carapace and on the pereiopods, with no dorsal spine more prominent than any other easily distinguishes *P. makarovi* from *P. verrilli*. Specimens of *P. multispina* of a similar size to the types of *P. makarovi* (Fig. 4b) have been studied, and they are distinguished by the following features:

- No enlarged spine on the apex of the gastric region of *P. makarovi*, whereas a large spine is found in this position on all *P. multispina*, and is especially prominent in smaller specimens.
- Dorsal spines in *P. makarovi* conical, with a band of long setae half way down the spine. *P. multispina* has blunt spines with a single ring of short setae at the expanded apex (Figs 4c, d).
- *P. multispina* also has several long lateral spines on the carapace, whereas *P. makarovi* has none particularly more prominent than any other.
- A pedunculation of the base of the rostrum is found in *P. multispina*, and not in *P. makarovi*.

It is quite likely that specimens belonging to *P. makarovi* have been found previously, but misidentified as *P. multispina*. The equivalent growth stages of these two species are, however, substantially different (Figs 4a, b). Juvenile *P. histrix*, from Japan, also has a carapace covered with spines, but its spines are very long and are without setae. *Paralomis histrix* also has long spines on the abdomen, whereas the abdomen of *P. makarovi* lacks spines. *Paralomis bouvieri* Hansen, 1908, from the Northern Atlantic seems quite close to this species, except that spines have long setae eminating in a cluster from the apex in similar sized specimens.

***Paralomis nivosa* n. sp.**
(Figs 5, 6)

Material examined. Philippines: Palawan passage 10°57’45”N, 118°38’15”E, 27.12.1908, 685 m: female holotype CL 30 mm, collected on the 1907–1908 ‘Albatross’ expedition to the Philippines (USNM 1122581).

Etymology. This species is named *nivosa*, which is the Latin for snow-like or snowy. The name alludes to the fact that the carapace is angular and resembles a snowflake in dorsal view.

Description of holotype. Carapace angular in outline, with distinct angle at hepatic region (Fig. 6a). Gastric and branchial regions of similar size and moderately convex; cardiac region slightly sunken in comparison. Inflated whelt towards posterior of branchial regions and at medial entrance to cervical groove. Intestinal region flattened to posterior margin. Surface of carapace covered in low, rounded tubercles, each with a thick ring of short setae around sides and rounded non-setose apex (Fig. 5b). A few instances of clustered tubercles on gastric and cardiac regions. No spines or particularly prominent tubercles on dorsal surface. Lateral edges rounded and covered with similar ornamentation as dorsally. Five sharp spines on anterolateral portion of carapace: two on anterior margin; one on hepatic region, and two on anterior branchial margin. No spines on posterior or posterolateral branchial margin.

Rostrum pedunculate and wide, almost covering eyestalks in dorsal view. Base of rostrum dorsally covered in tubercles, similar to rest of dorsal carapace. Two short, sharp spines at end of this rostral prominence, at level of corneae. Median spine of rostrum extending beyond corneae; slightly keeled ventrally, and strongly curved upward (Figs 6b, d).

Eyestalks with several dorsal spines, one very long and extending past cornea (Fig 6e). Antennal acicle long, with one long medial spine, five long outer spines, and four short spines on internal surface. Several spinules on dorsal surface of acicle. All spines with uniform coverage of short setae along their length.

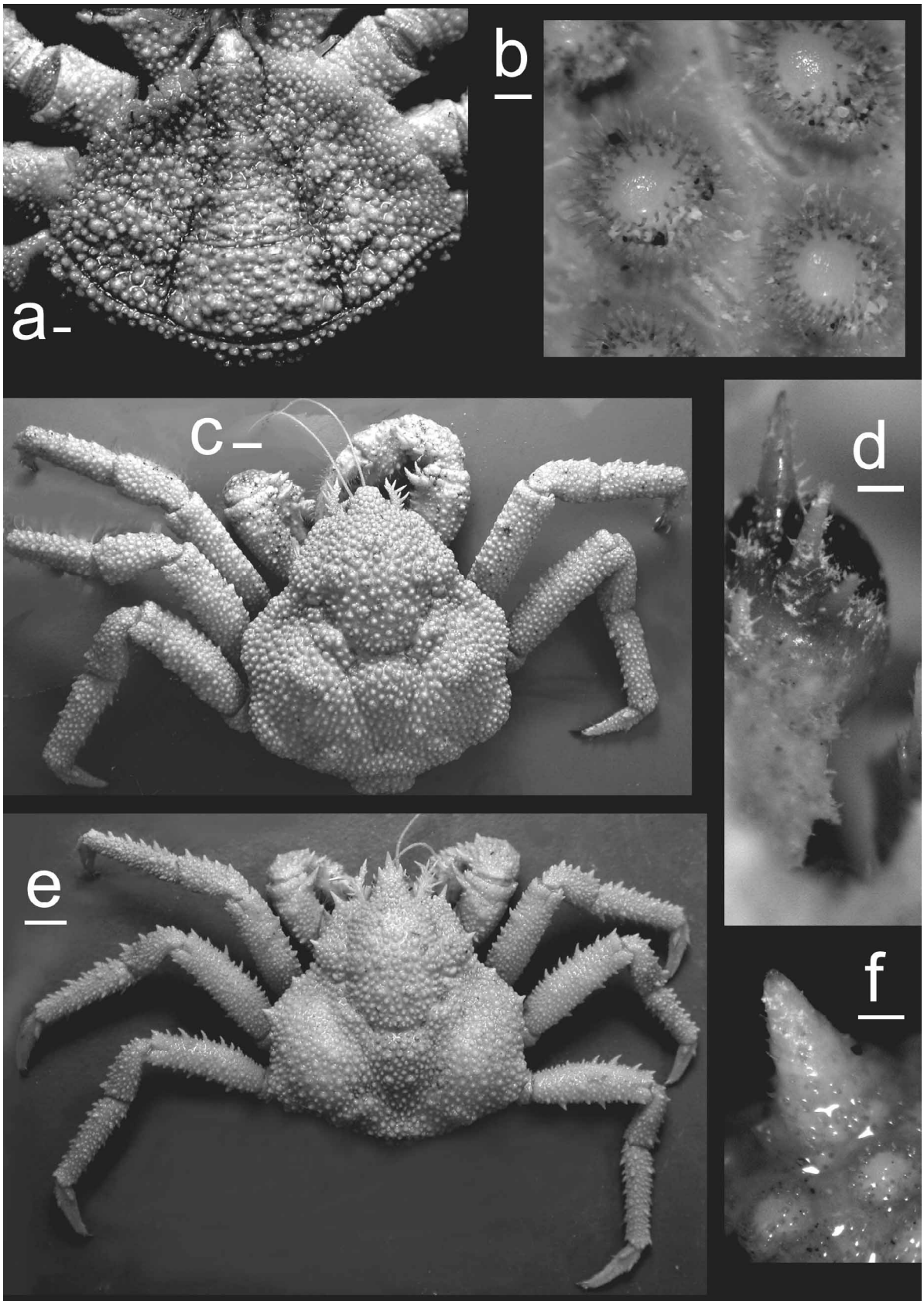

FIGURE 5. *Paralomis nivosa* **n. sp.** a, b, d–f: female holotype, 30 mm CL (USNM 1122581), Philippines, Palawan passage, 10°57'45"N, 118°38'15"E, 685 m. (a) abdomen. (b) mid-branchial carapace ornamentation, dorsal. (d) part of right ocular peduncle visible below rostrum, dorsal (e) whole organism, dorsal. (f) carapace lateral spine, dorsal. *Paralomis haigae* Eldredge. e: female 43.8 mm CL (MNHN-Pg4274), Samoa. (e) whole organism, dorsal. Scale bar = 1 mm for a–d; 5 mm for e, f.

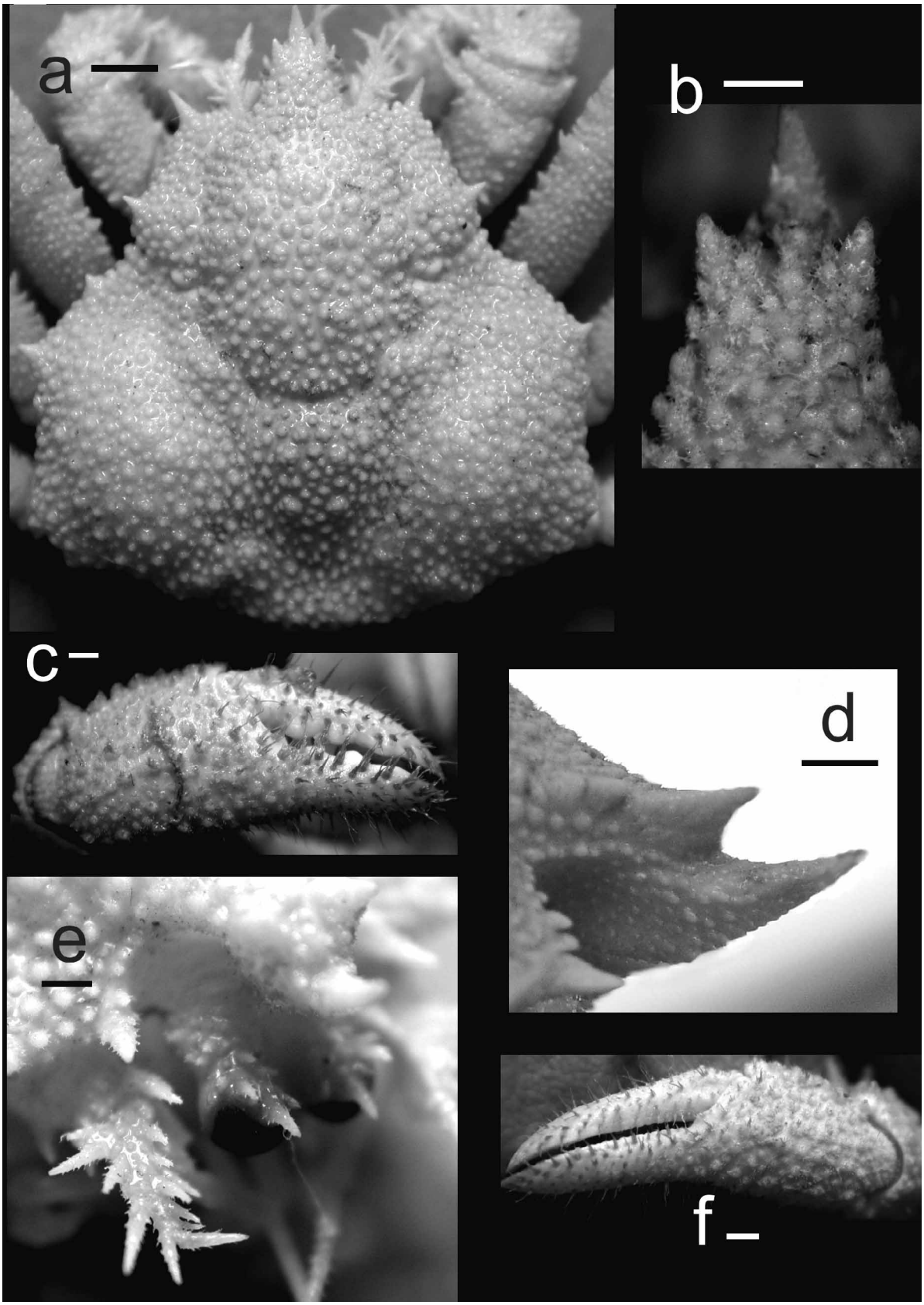

FIGURE 6. *Paralomis nivosa* **n. sp.** a–f: female holotype, 30 mm CL (USNM 1122581), Philippines, Palawan passage, 10°57'45"N, 118°38'15"E, 685 m. (a) carapace, dorsal. (b) rostral spines, dorsal. (c) right chela, lateral. (d) rostrum, lateral. (e) antennal acicle, frontal. (f) left chela, lateral. Scale bar = 5 mm for a; 1 mm for b–f

Cheliped carpus with a series of 4 enlarged spines on internal angle and a few tubercles on other surfaces. Very few spinules on surface of chelae palms, none on fingers. Fingers with row of clusters of setae external to cutting surfaces, and several setae on mobile finger.

Pereiopods uniformly covered with tubercles, with some prominent sharp spines as on lateral margins. Merus of pereiopod 4 about half carapace length and 1.5 times length of propodus, with rounded cross-section. Five prominent spines on dorsal anterior edge, and several sharp spinules on ventral posterior edge of walking leg meri. Sharp spinules covering carpus and propodus. Dactylus slightly shorter than propodus and compressed in cross-section. One or two spines in articulating region, but smooth surfaces elsewhere. With 5 short, black needle-like spines on ventral side of dactylus, as well as several tufts of setae.

Abdomen of holotype female asymmetrical, although with very little 'right-hand skew' — telson almost in line with body axis (Fig. 5a). Mid portion of second abdominal segment prominent in dorsal view. Medial and paired lateral plates on each abdominal segment 3–5. Marginal plates on left side separate from lateral plates. Surface of abdominal plates with low tubercles similar to those found dorsally.

Remarks. The dorsal ornamentation in *Paralomis nivosa* n.sp. is very similar to *P. haigae* Eldredge, 1976 (Fig 5c), and *P. dofleini* Balss, 1911 and this feature allies these three species within *Paralomis*. This specimen is a small adult; 30 mm in carapace length. Direct comparison with similar sized specimens of *P. haigae* and *P. dofleini* have been made at the USNM and Muséum National d'Histoire Naturelle, Paris (MNHN).

- *P. nivosa* has several sharp spines on the lateral borders, dorsally on the rostrum, and on the legs. There is no indication of any spines laterally in *P. haigae* or *P. dofleini*, with the exception of one on the anterior margin. No specimens of *P. haigae* studied have spines dorsally on the rostrum.
- The outline of the carapace *in P. nivosa* is quite angular, whereas in *P. haigae*, the carapace is more rounded.
- The rostrum in *P. haigae* and *P. dofleini* has a wide base, which ends in a blunt prominence above a short, straight ventral spine. In *P. nivosa*, the ventral spine is very prominent and curved upward.

***Lithodes galapagensis* n. sp.**
(Figs 7, 8)

Material examined. Galapagos Archipelago: Johnson Sea-Link II Cruise station 3101, Cabo Douglas, Fernandina Island, 00°17'30"S, 091°39'36"W, 17.07.1998, 648m: male holotype, CL 114 mm; female paratype, CL 84 mm, Seymour Island, 00°21'42"S, 090°15'00"W, 25.07.1998, 740 m (all USNM 1122586).

Etymology. This species is named after its type locality, the Galapagos Islands.

Description of the holotype. Carapace roughly pyriform in outline (Fig. 7d); as wide as long when measured at maximal width of carapace. Dorsal regions well defined; covered uniformly with small spinules more or less acute at apex, without setae (Fig. 7b). Gastric region convex and slightly more inflated than branchial and cardiac regions. One pair of slender spines 7 mm in length, emanating from the mid part of this region — level with hepatic spines on lateral margin. Spinules sparse on apex of gastric region and very few around base of prominent spines. Cardiac region depressed and separated from gastric region by smooth, wide, and saddle-shaped groove. Cardiac region depressed anteriorly, and more inflated posteriorly around single pair of long, slender spines in this region. A pair of acute spinules directly anterior to this pair. Triangular cardiac region separated from branchial regions by grooves which converge posteriorly, and then diverge close to the margin to describe posterior of branchial regions. Branchial regions each with single long, slender spine at apex; a few large, acute spinules posteriorly. A pair of conical spines in intestinal region almost on posterior margin.

Exterior orbital spine just surpassing length of eyestalks; anterolateral spine about equal in length or slightly smaller. Hepatic spines slightly inflated at base, with long slender spine reaching 20 mm. Two spines

on anterior portion of each branchial lateral margin, and several much smaller, conical spines interspersed between them and on posterolateral margins.

Rostrum with long, straight median projection rising dorsally from surface of carapace and terminating in pair of spines. Mid way along length of median projection emanate a pair of dorsal lateral spines of about the same length as terminal bifurcation. Base of rostrum narrow, without granulation. Ventrally, with long, smooth spine curving gently upward, terminating approximately at level of corneae.

Eyestalks prominent and without granulation, but with crenulation of dorsal edge of the corneal margin (Fig. 8b).

Second segment of antennal peduncle with long slender spine on exterior aspect. Antennal acicle reduced to very small conical process.

Cheliped merus and carpus with several strong spines on terminal border and poorly defined rows of short spines on dorsal, interior and exterior surfaces. Palm with several poorly defined rows of short spines on dorsal border and two rows on exterior surface leading to articulation with movable finger. Fingers 0.4 × total length of right hand, and 0.5 of left hand. Fingers bearing few tufts of short setae.

Walking legs long and slender. Merus of pereiopod 3 about 0.8 × length of carapace, and 0.2 × as high as long. Covered densely with spinules on dorsal/posterior surface, and smooth on ventral surface (Fig. 7c). Two or three rows of larger conical spines along length of merus and long spine on terminal border. Carpus of walking legs with spinulation on dorsal surfaces and smooth ventral surfaces, as well as two very long spines at proximal and distal ends of dorsal border. Propodus sparsely covered with irregular rows of spinules. Dactyli of walking legs over half length of merus and equal to length of carpus; very sharp, slender spines on dorsal border to tip; few or no spines on ventral border; no tufts of setae present.

Abdomen of a form typical of *Lithodes*, with nodules in the medial portion of segments 3–5; separate marginal and lateral plates well-calcified (Fig. 8f). Second abdominal segment with medial and lateral plates fused; marginal plates almost joined or with suture visible. Surface of abdominal plates with several warty tubercles on edges but no spines decorating surface.

Variations. The female paratype of this species is slightly smaller than the male. It differs from the holotype in having less acute spinules on the dorsal surface, and the less prominent spines on the proximal and distal angles of the walking-leg carpi.

Remarks. This species is distinguished from all other members of this genus, except *Lithodes wiracocha* Haig, from Peru, in that it has carapace and dorsal surface of the walking legs densely covered in spinules. This species differs from *L. wiracocha* in the following ways:

- The spines on the dorsal surface are less dense in *L. galapagensis* than in *L. wiracocha*.
- The walking legs of *L. galapagensis* have spinules only on the dorsal and not on the ventral surfaces of the walking-leg segments, whereas *L. wiracocha* has densely packed spinules covering the surface of all segments.
- In the holotype, and somewhat on the paratype of *L. galapagensis*, certain spines on the dorsal surface and on the walking legs are very long and slender, unlike the stout conical spines in *L. wiracocha*.
- The rostrum of *L. galapagensis* is very long and slender — similar in this respect to *Lithodes megacantha* Macpherson, 1991 from the central Pacific; however, the rostrum of *L. wiraconcha* is rather stout in comparison.
- There are no acute spinules on the dorsal base of the rostrum in *L. galapagensis*, whereas spines cover the proximal part of all of the lateral spines in *L. wiracocha*.
- No spines on the surface of the abdominal plates in *L. galapagensis*. Instead, plates are covered with low tubercles.

Other species close to this location include *Lithodes panamensis* Faxon from Panama and Peru, and *Lithodes santolla* Macpherson (1988b), from Patagonia, both of these are readily distinguishable from the present species because of the peculiar spination of *Lithodes galapagensis* in which a dense coverage of acute spinules are combined with the few very long spines and long rostrum.

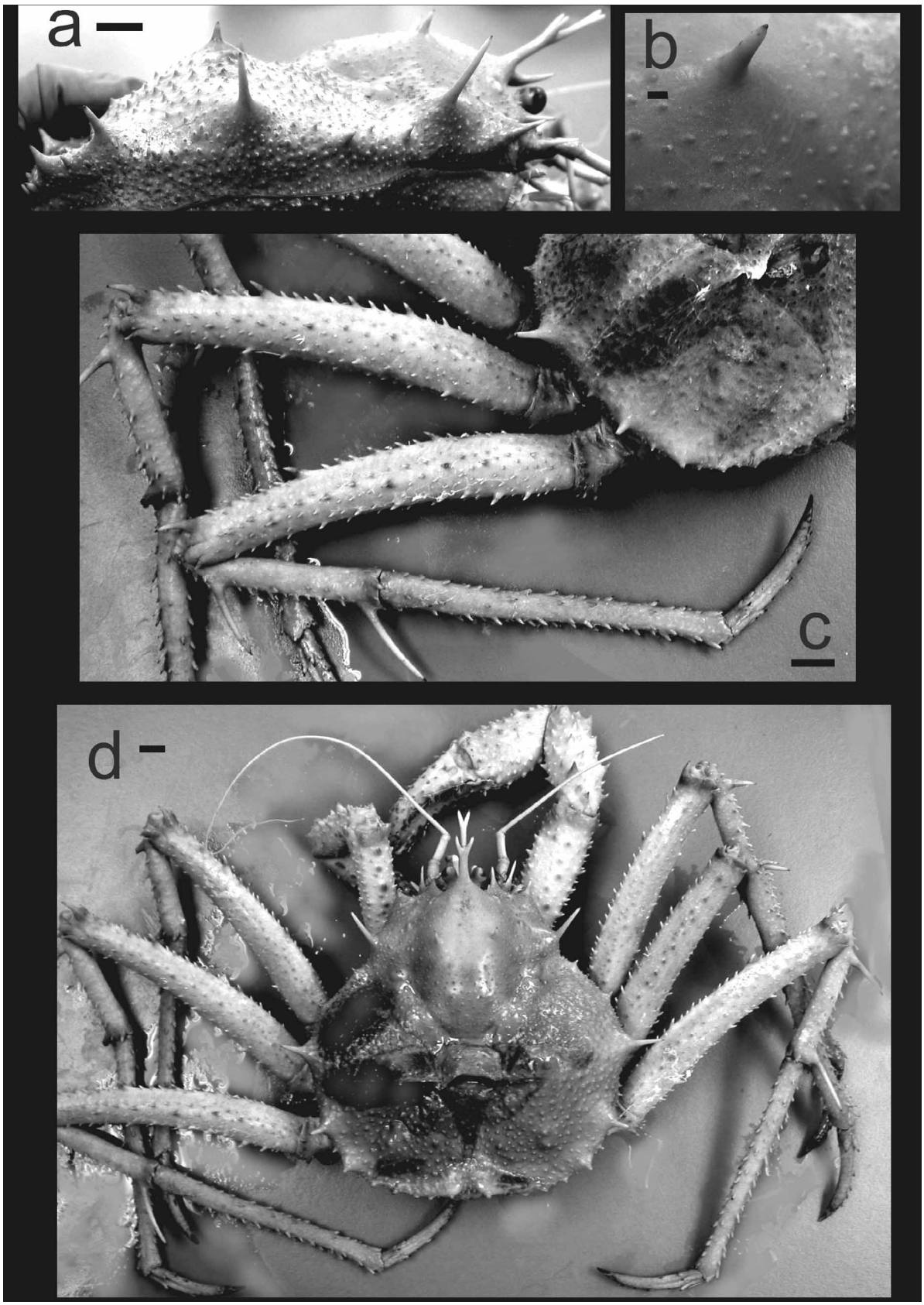

FIGURE 7. *Lithodes galapagensis* **n. sp.** a–d, male holotype, 114 mm CL (USNM 1122586), Galapagos Archipelago, Cabo Douglas, Fernandina Island, 00°17'30"S, 091°39'36"W, 648 m. (a) carapace, lateral. (b) dorsal carapace spine, lateral. (c) left walking leg 3, posterior. (d) whole organism, dorsal (note damage to carapace on the left branchial region). Scale bar = 10 mm for a, c, d; 1 mm for b.

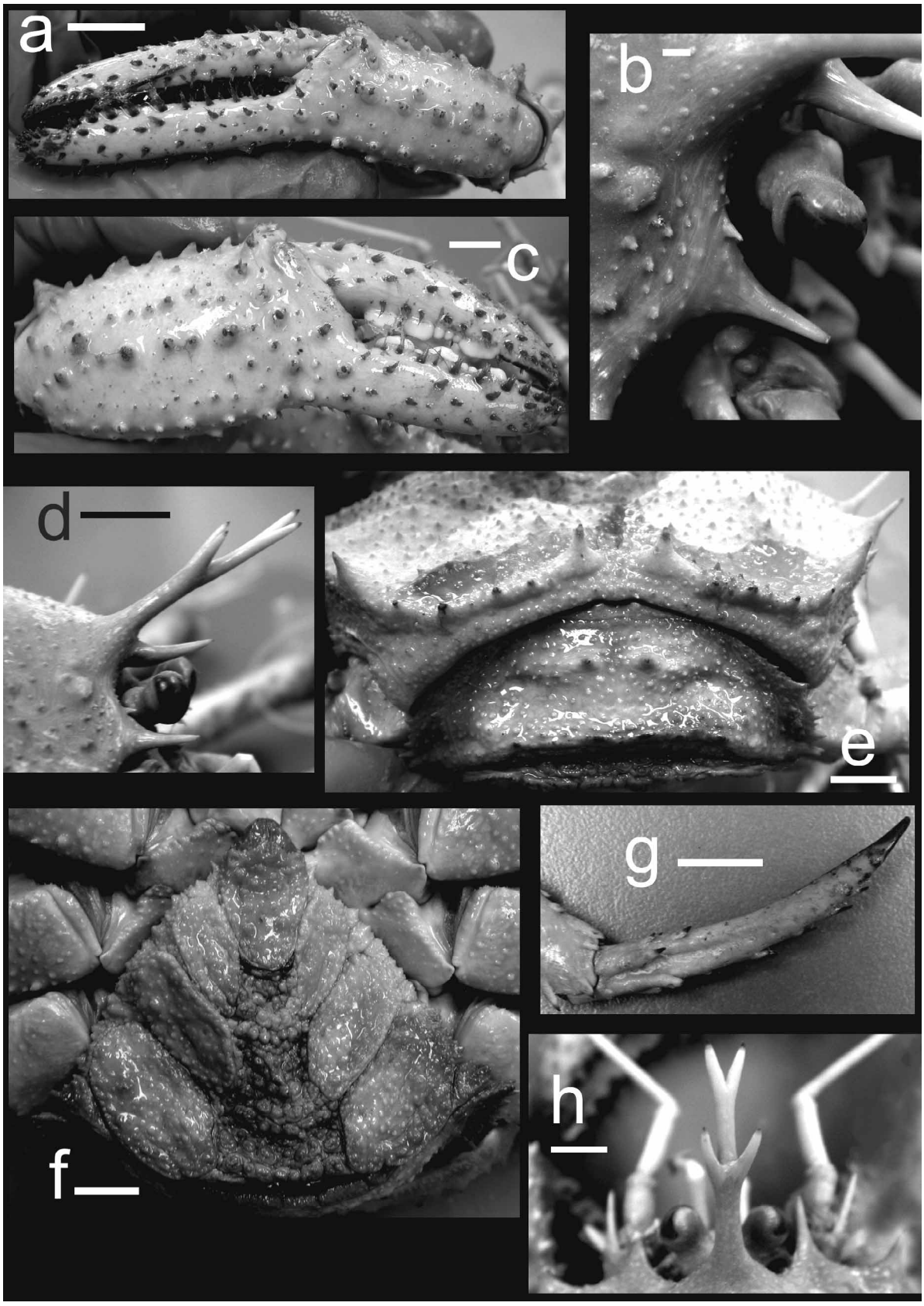

FIGURE 8. *Lithodes galapagensis* **n. sp.** a–h, male holotype, 114 mm CL (USNM 1122586), Galapagos Archipelago, Cabo Douglas, Fernandina Island, 00°17'30"S, 091°39'36"W, 648 m. (a) left chela, lateral. (b) ocular peduncle, frontal. (c) right chela, lateral. (d) anterior carapace, lateral. (e) second abdominal segment, posterior. (f) abdominal plates. (g) dactylus 3rd walking leg, posterior. (h) rostral spines, dorsal. Scale bar = 10 mm for a, c–h; 1 mm for b.

Discussion

The discovery of these species adds to the considerable number belonging to the genera *Lithodes* (now 21 species), and *Paralomis* (now 60 species). These genera have representatives in most areas of the world's oceans, and species numbers in different oceans probably reflects the more on the intensity of sampling in that locality than actual level of biodiversity. Especially in *Paralomis*, the highest species counts are found along the western coast of South America (9 species), and around Japan (10 species). A gap in knowledge is present around eastern Africa (and much of the Indian Ocean), and the Southern Ocean. The four species of *Paralomis* in the northern and central Indian Ocean are known only from their respective type localities. Only *P. birsteini* Macpherson 1988a and *P. stevensi* Ahyong & Dawson 2006, are known from the Southern Ocean above 60°S (Thatje *et al.* 2005, 2008). The full extent of diversity in *Paralomis* can only be found by an increase in sampling effort and reporting of novel morphotypes.

Acknowledgements

We sincerely thank Karen Reed and Rafael Lemaitre at the National Museum of Natural History, Smithsonian Institution, Washington D.C., who made this study possible. We would also like to thank Paul Clark at the Natural History Museum, London, Régis Cleva at the Muséum National d'Histoire Naturelle, Paris (MNHN), and Michael Türkay at the Senkenberg Museum, Frankfurt, who made other type specimens available for comparison. We thank Enrique Macpherson Shane Ahyong and an anonymous reviewer for their helpful comments on the manuscript. This work was supported by the Marine Biodiversity and Ecosystem Functioning Network of Excellence MarBEF (contract no. GOCE-CT-2003-505446) of the FP6.

References

Ahyong, S.T. & Dawson, E.W. (2006) Lithodidae from the Ross Sea, Antarctica, with descriptions of two new species (Crustacea: Decapoda: Anomura). *Zootaxa*, 1303, 45–68.

Balss, H. (1911) Neue Paguriden aus den Ausbeuten der Deutchen Tiefsee-Expedition 'Valdivia' und der Japanischen Expedition Prof. Dofleins. *Zoologischer Anzeiger*, 38, 1–9.

Chace, F.A.J. (1939) Reports on the scientific results of the first Atlantis expedition to the West Indies, under the joint auspices of the University of Havana and Harvard. Preliminary descriptions of one new genus and seventeen new species of decapod and stomatopod crustaceans. *Memorias de al sociedad cubana de historica Natural*, 13, 31–54.

Eldredge, L.G. (1976) Two new species of lithodid crabs from Guam. *Micronesica*, 12, 309–315.

Haig, J. (1974) Observations on the lithodid crabs of Peru, with a description of two new species. *Bulletin of the Southern California Academy of Science*, 73, 152–164.

Hall, S. & Thatje, S. (2009) Global bottlenecks in marine Crustacea: temperature constraints in the family Lithodidae (Crustacea: Decapoda: Anomura). *Journal of Biogeography*, 36, 2125-2135.

Hansen, H.J. (1908) Crustacea Malacostraca I. Bianco Luno, Copenhagen. Translated by H. M. Kyle. *The Danish Ingolf Expedition*, 3, 1–120.

Ingle, R.W. & Garrod, C. (1987) Ornamentation Changes Associated with Growth of Falkland Island Populations of *Paralomis granulosa* (Jacquinot, 1842–1847) (Decapoda, Lithodidae). *Crustaceana*, 52, 220–224.

Latreille, P.A. (1806) *Genera crustaceorum et insectorum secundum ordinem naturalem in familias disposita, iconibus exemplisque plurimus explicata*, Amand Koenig, Paris, 280 pp.

Macpherson, E. (1988a) Three new species of *Paralomis* (Crustacea, Decapoda, Anomura, Lithodidae) from the Pacific and Antarctic Oceans. *Zoologica Scripta*, 17, 69–75.

Macpherson, E. (1988b) Revision of the Family Lithodidae Samouelle, 1819 (Crustacea, Decapoda, Anomura) in the Atlantic Ocean. *Monografias de Zoologia Marina*, 2, 9–153.

Macpherson, E. (1994) Occurrence of two lithodid crabs (Crustacea: Decapoda: Lithodidae) in the cold seep zone of the South Barbados accretionary prism. *Proceedings of the Biological Society of Washington*, 107, 465–468.

Macpherson, E. & Chan. T.-Y. (2008) Some lithodid crabs (Crustacea: Decapoda: Lithodidae) from Taiwan and adjacent waters, with the description of one new species from Guam. *Zootaxa*, 1924, 43–52.

Sakai, K. (1987) Biogeographical records of five species of the family Lithodidae from the abyssal valley off Gamoda-Misaki, Tokushima, Japan. *Researches on Crustacea*, 16, 19–24.
Sakai, T. (1971) Illustrations of 15 species of crabs of the family Lithodidae, two of which are new to science. *Researches on Crustacea*, 4–5, 1–491.
Samouelle, G. (1819) *The Entomologist's useful Compendium*, Thomas Boys, London, 496, 12 pls pp.
Spiridonov, V., Türkay, M., Arntz, W.E. & Thatje, S. (2006) A new species of the genus *Paralomis* (Crustacea: Decapoda: Lithodidae) from the Spiess seamount near Bouvet Island (Southern Ocean), with notes on habitat and ecology. *Polar Biology*, 29, 137–146.
Takeda, M. (1980) A new species of *Paralomis* from the East China Sea. *Annotationes Zoologicae Japonsenses*, 53, 42–45.
Takeda, M. (1985) A new species of *Paralomis*, the crab shaped anomuran from the Kyushu-Palu submarine ridge. *Bulletin of the National Science Museum Series A (Zoology)*, 11, 137–140.
Takeda, M. (1990) A new species of the genus *Paralomis* from Minami-Ensei Knoll in the Mid Okinawa Trough. *Bulletin of the National Science Museum Series A (Zoology)*, 16, 79–88.
Takeda, M. & Bussarawit, S. (2007) A new species of the genus *Paralomis* White, 1856 (Crustacea, Decapoda, Anomura, Lithodidae) from the Andaman Sea. *Bulletin of the National Science Museum Series A (Zoology)*, 33, 51–59.
Thatje, S., Anger, K., Calcagno, J.A., Lovrich, G.A., Pörtner, H.O. & Arntz, W.E. (2005) Challenging the cold: Crabs reconquer the Antarctic. *Ecology*, 86, 619–625.
Thatje, S., Hall, S., Tyler, P.A., Hauton, C. & Held, C. (2008) Encounter of *Paralomis birsteini* on the continental slope of Antarctica, sampled by ROV. *Polar Biology*, 31, 1143–1148.
White, A. (1856) Some remarks on Crustacea of the genus *Lithodes*, with a brief description of a species apparently hitherto unrecorded. *Proceedings of the Zoological Society of London*, 24, 132–135.
Zaklan, S.D. (2002) Review of the family Lithodidae (Crustacea: Anomura: Paguroidea): distribution, biology, and fisheries. *In:* MacIntosh, R.A. (ed.), *Crabs in Cold Water Regions: Biology, Management, and Economics*. Alaska Sea Grant College Program AK-SG-02-01, Anchorage, 751–845.

Scientia Marina 74(3)
September 2010, 000-000, Barcelona (Spain)
ISSN: 0214-8358

DNA extraction from formalin-fixed tissue: new light from the deep sea

FERRAN PALERO [1], SALLY HALL [2], PAUL F. CLARK [3], DAVID JOHNSTON [3], JACKIE MACKENZIE-DODDS [3] and SVEN THATJE [2]

[1] Departament de Genètica, Facultat de Biologia, Universitat de Barcelona, Av. Diagonal 645, 08028 Barcelona, Spain. E-mail: fepapas@alumni.uv.es
[2] National Oceanography Centre, Southampton, University of Southampton, European Way, Southampton, SO14 3ZH, UK.
[3] Department of Zoology, Natural History Museum, Cromwell Road, London SW7 5BD, UK.

SUMMARY: DNA samples were extracted from ethanol and formalin-fixed decapod crustacean tissue using a new method based on Tetramethylsilane (TMS)-Chelex. It is shown that neither an indigestible matrix of cross-linked protein nor soluble PCR inhibitors impede PCR success when dealing with formalin-fixed material. Instead, amplification success from formalin-fixed tissue appears to depend on the presence of unmodified DNA in the extracted sample. A staining method that facilitates the targeting of samples with a high content of unmodified DNA is provided.

Keywords: tetramethylsilane, ethidium bromide, formalin, *Carcinus*, Lithodidae.

RESUMEN: Extracción de ADN a partir de tejido fijado en formol: nueva luz desde el mar abisal. – Muestras de ADN de distintos crustáceos decápodos fueron obtenidas independientemente a partir de tejidos fijados en etanol y tejidos fijados en formol mediante un nuevo protocolo basado en el Tetrametilsilano (TMS)-Chelex. Los resultados obtenidos muestran que el ADN no se encuentra atrapado de forma irreversible en una matriz proteica y que el éxito de amplificación no depende de la extracción de inhibidores de PCR solubles. Sin embargo, nuestros resultados indican que el éxito de amplificación depende de la presencia de ADN no modificado en la muestra. Se incluye un sencillo método de tinción que facilita la identificación de muestras con un alto contenido en ADN no modificado.

Palabras clave: tetrametilsilano, bromuro de etidio, formol, *Carcinus*, Lithodidae.

INTRODUCTION

Lithodids, commonly known as king crabs (Decapoda: Anomura: Lithodidae) are decapod crustaceans found in global cold and deep waters (Macpherson, 2003). Deep-sea marine specimens are expensive to collect and are rarely encountered, so that many lithodid species have been collected only once and are held as a precious resource by museums (Macpherson, 1988; Chase *et al.*, 1998). While there is much discussion in the literature, there is no agreement on a theory of Lithodidae evolution (Cunningham *et al.*, 1992; Thatje *et al.*, 2005), and lack of suitable material available for molecular analysis means that theories of phylogeny and early radiations cannot yet be fully tested (McLaughlin, 1983; Zaklan, 2002; Hall and Thatje, 2009). In order to launch a molecular phylogeny of Lithodidae, it is first necessary to obtain suitable DNA from museum specimens. However, museum material produced negative results when DNA extraction was attempted using silica-based columns (Díaz-Viloria *et al.*, 2005).

Historically, fluid-preserved museum specimens have been initially fixed in formalin and then later transferred into alcohol or industrial methylated spirit (IMS) for archival storage (Simmons, 1995). Generally, a sodium tetraborate (borax) or sodium phosphate buffer has been used to maintain the pH of the formalin

near neutrality, since buffering the formalin is essential to ensure satisfactory long-term storage of samples (Quay, 1974). In fact, many specimens prized for their morphological novelty have been kept in formalin for years (Thatje *et al.*, 2008). Therefore, it becomes desirable to overcome barriers to molecular analysis caused by the traditional processes of preservation and considerable resources are being invested in obtaining DNA from formalin-fixed museum specimens (Scatena and Morielle-Versute, 2008; Santos *et al*., 2009).

Extraction and amplification of DNA from such traditionally fixed material has proven to be difficult and the reason for this is not resolved yet (France and Kocher, 1996; Gilbert *et al*., 2007). Several hypotheses have been proposed for explaining the difficulties found with the polymerase chain reaction (PCR), including DNA being trapped in a matrix of cross-linked proteins, severe DNA damage caused by low pH or the presence of PCR inhibitors in solution (Shibata, 1994; Fang *et al*., 2002). Many reports have been published and numerous protocols have been proposed on extraction and amplification of DNA from formalin-fixed material, but the fact remains that no reproducible and generic method has been reported to date (Diaz-Cano *et al*., 1997; García-Vázquez *et al*., 2006). Furthermore, it should be pointed out that many of these protocols are problematic, since they require multiple wash steps or long incubation periods that increase the risk of contamination (Cawkwell and Quirke, 2000; Schander and Halanych, 2003).

As a suitable starting point, the present study follows up on the latest protocols introduced in the literature to resolve the problem of DNA extraction from formalin-fixed material, which are based on critical point drying (Fang *et al.*, 2002) and Chelex (García-Vázquez *et al*., 2006). In order to reduce costs and provide a similar effect to that proposed in Fang *et al*. (2002), tetramethylsilane (TMS) will be used as a strong dehydrating agent that maintains tissue structure (Ubero-Pascal *et al.*, 2005). Moreover, a series of investigations is set up to determine the specific way in which formalin acts to prevent amplification. Finally, tissue from both ethanol and formalin-fixed samples will be analysed in order to define a quick and inexpensive test for the validity of DNA extracts for molecular analysis.

MATERIALS AND METHODS

Thirty formalin-fixed and ten ethanol-preserved lithodid samples were extracted and amplified using a protocol based on Tetramethylsilane (TMS) (Fluka-Riedel de Haën, Seelze, Germany, cat. no. 87920) and Chelex 100 resin (sodium form) (Bio-Rad, Hemel Hemstead, Herts, UK) (Fang *et al*., 2002). Samples were obtained from the dactylus or propodal muscle tissue of lithodid specimens in the Natural History Museum (NHM), London; the Muséum National d'Histoire Naturelle, Paris; and the Centre Mediterrani d'Investigacions Marines i Ambientals, Barcelona. After cutting off a piece of the specimen (2 mm^3), the tissue sample was squeezed in a piece of absorbant paper, transferred to TMS (50-100 µl) and incubated with gentle agitation for 1h. This incubation may be carried out overnight, even though a shorter time is recommended to reduce contamination. Tissue was transferred to a new 1.5ml Eppendorf tube with 200 µl of 10% Chelex solution in TE pH 8.0 and 20 µl of proteinase K (20 mg/ml stock solution) and incubated for 2-3 h at 55ºC in a thermomixer. Finally, sample was centrifuged for 5-10 minutes at 10000 rpm and 100 µl of supernatant was transferred into a fresh tube and kept at 4ºC until used. About 1-2 µl of the supernatant was taken for each 25 µl total volume PCR reaction.

Initially, a total of 3 lithodid-specific primers were designed for amplifying hemi-nested fragments of the mitochondrial 16S gene region (440 bp) using multiplex PCR (LITF1: 5'-GCCGCAGTATTTTGACTGTGCGAA-3'; LITF2: 5'-GGCTTGAATGAAAGGTTGGACAA-3' and LITR1: 5'-TCTCTTATAGCGGCTGCACCA-3'). In order to check the specificity of the primers and optimise amplification conditions, multiplex PCR was first carried out on DNA extracted from ethanol-fixed lithodid samples, and spiny lobster tissue (obtained from *Palinurus elephas*) was used as a negative control. Multiplex amplification reactions were carried out in a 10 µl reaction containing 30 ng of genomic DNA, 0.5x QIAGEN Multiplex PCR Kit 2x and 0.2x of equimolar (1 mM) primer mix. The PCR thermal profile used was 94°C for 4 min for initial denaturation, followed by 30 cycles of denaturation at 94°C for 30 s, annealing temperature at 54°C for 30 s, extension at 72°C for 30 s, and a final extension at 72°C for 4 min. The PCR reaction was loaded to a 1% agarose gel in TBE with EtBr together with HyperLadder I and HyperLadder IV (Bioline). Sequences were obtained using the Big-Dye Ready-Reaction kit v3.1 (Applied Biosystems, Foster City, USA) on an ABI Prism 3770 automated sequencer from the Molecular Biology Unit, NHM.

To examine the effect of formalin on the process of DNA liberation from tissue, a 30 h time-series proteinase K digestion (proteinase K from *Tritirachium album*, Roche Diagnostics GmbH, Mannheim, Germany) of both formalin-fixed (n = 8) and control ethanol-fixed (n = 4) samples was carried out. The amount of DNA in solution (ng/µl) was measured using a NanoDrop™ 1000 Spectrophotometer (Thermo Fisher Scientific) at several time intervals. Secondly, in order to attempt to eliminate the effect of soluble PCR inhibitors, both physical (filtering) and chemical DNA cleaning techniques were applied to the Chelex-extracted DNA. Therefore, two different filtering systems provided by Millipore, namely the 96-well MultiScreen plates (Cat. MAPBMN310) together with a MultiScreen™ Vacuum Manifold, and the Microcon columns (YM-100) used with a Microcentrifuge (Eppendorf Model 5415D, VWR Int Ltd, Poole Dorset, UK) were applied to the crude DNA extract following the manufacturer's

guidelines (http://www.millipore.com/userguides/). The chemical-based DNA cleaning techniques were used in separate treatments of genomic extracts prior to PCR amplification. Both Phenol: Chloroform: Isoamyl alcohol purification (Sigma-Aldrich cat. P2069, Dorset, UK) and Isopropanol precipitation methods were carried out following the standard protocols included in Sambrook *et al.* (1989).

In addition, and in order to confirm the validity of a simple test for predicting PCR success, a total of 88 *Carcinus* samples collected from different localities were analysed. From these, 66 samples were obtained from NHM collections (Sandy Bay and Europa Point, Gibraltar and Ebro Delta, Spain; Clark *et al*., 2001) and 12 samples were obtained from recent ethanol-fixed material (Cullera, Spain; present study). Multiplex amplification reactions were carried out as previously stated but using Folmer *et al*. (1994) (LCO1490: 5'-GGTCAACAAATCATAAAGATATTGG-3'; HCO2198: 5'-TAAACTTCAGGGTGACCAAAAAATCA-3') and Darling *et al*. (2008) (COIF-PR115: 5'-TCWACNAAYCAYAARGAYATTGG-3'; COIR-PR114: 5'-ACYTCNGGRTGNCCRAARARYCA-3') mitochondrial cytochrome oxidase I (COI) primers at 45°C annealing temperature for 30 s. A one-side Fisher's exact probability test was carried out on the PCR success/failure table for the green/orange DNA as implemented in the function fisher.test of the stats package in R v2.9.1 (R Development Core Team, 2009). Fisher's exact probability test is recommended in order to test for differences in success rates from two-by-two contingency tables with moderate sample sizes (Martín Andrés *et al*., 2004).

RESULTS

Of the thirty formalin-fixed lithodid tissue samples analysed, 18 failed to produce 16S PCR products, 5 produced amplicons but were not successfully sequenced, and 7 samples with band sizes of 250-300 bp produced fully-sequenced PCR products (GenBank accession numbers: EU493266, EU493268-72 and EU493275). Moreover, all 10 ethanol-preserved lithodid samples produced fully-sequenced PCR products (GenBank accession numbers: EU493267, EU493273-74, EU493276-EU493278, FJ462644-45 and FJ462648). A database search in GenBank using Megablast (BLASTN v2.2.18) showed that sequences from formalin-fixed specimens were homologous to available lithodid sequences. Sequences from formalin-fixed samples were either closer to those obtained from species with similar geography and morphology, or they matched exactly with sequences that had been independently obtained from fresh specimens of the same species in other laboratories. For example, two specimens of *Paralomis cristata* (Takeda and Ohta, 1979) included in the present study correspond to one specimen preserved in formalin in 1987 and analysed in NHM (EU493266), and another sequence independently obtained in Germany by S. Hall from an ethanol-fixed sample (EU493267). Moreover, one of the successful samples from this study, *Lithodes turkayi* Macpherson, 1988 (NHM registration no. 2004.2994; GenBank code: EU493268) had been kept in formalin continuously since its fixation in 1932.

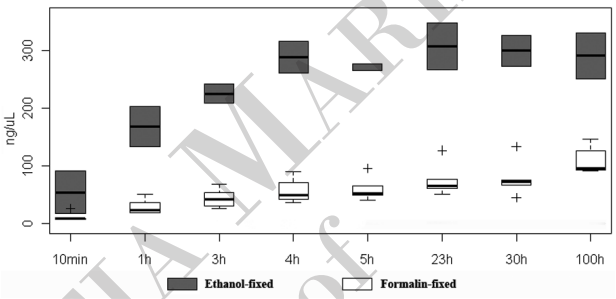

FIG. 1. – Time course of proteinase K-induced release of DNA obtained from formalin-fixed samples and from ethanol-fixed controls as measured by NanoDrop spectrophotometry.

The results obtained from the proteinase K time-series digestion experiment indicate that DNA can be released from formalin-fixed tissue (Fig. 1). Furthermore, gel electrophoresis of extracted DNA showed that despite increased DNA degradation in formalin-fixed samples, fragments larger than 1 Kb can still be found in formalin-fixed specimens (Fig. 2A). Nevertheless, the presence of large fragments of DNA could not be taken as an effective predictor of PCR success, since none of the four cleaning protocols tested (Millipore MultiScreen plates, Microcon columns (YM-100), Phenol: Chloroform: Isoamyl alcohol purification, and Isopropanol precipitation) gave positive 16S PCR results for those samples that had failed when processed directly from the Chelex extraction supernatant. In fact, our results from lithodid samples pointed out that rather than overall DNA fragment size, it was DNA staining behaviour that could be used as an effective predictor of PCR success.

In order to confirm the validity of our staining protocol for predicting PCR success from genomic DNA, two sets of ethanol-fixed (12) and formalin-fixed (66) *Carcinus* samples were analysed. After running 5 µl of DNA-Chelex supernatant on a 1% agarose gel and staining with ethidium bromide, the gel was photographed under UV light (250-360 nm) (Fig. 2A). This simple test identified two different types of extracted DNA; while PCR-negative samples only contained green autofluorescent material, both green autofluorescent and ethidium bromide-stained orange DNA could be observed on PCR-positive samples. When ethanol-preserved tissue from fresh specimens is analysed using this method, only ethidium bromide-stained orange DNA is observed (Fig. 2A). In fact, NHM *Carcinus* samples containing orange DNA yielded a considerably larger proportion of successes (9.2 times more success) than samples containing just green DNA. From 66 formalin-fixed NHM *Carcinus* samples, those with orange DNA provided a larger number of PCR

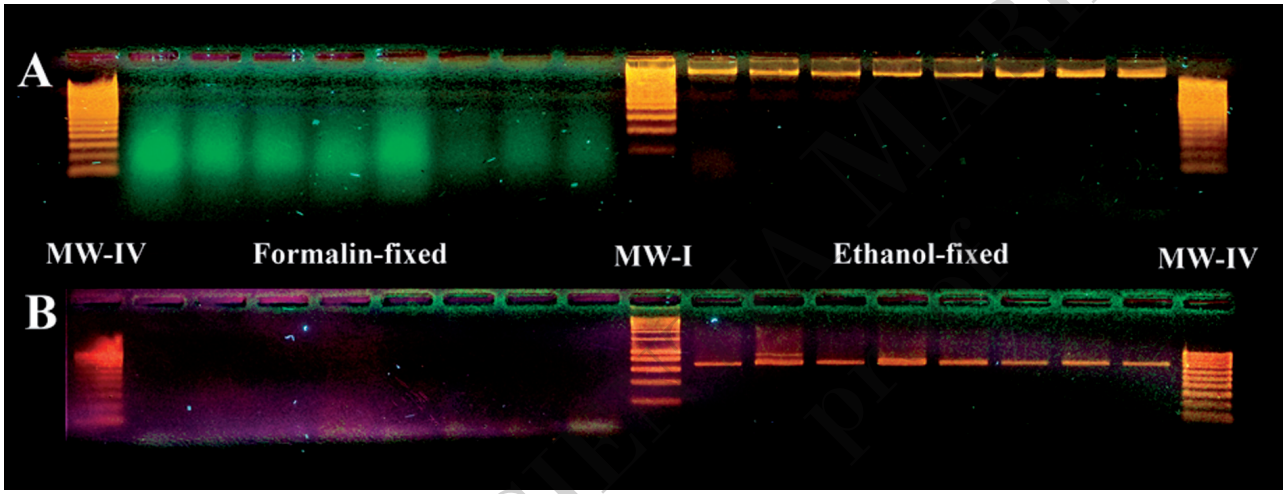

FIG. 2. – Different staining behaviour and PCR success of the COI gene from DNA obtained from formalin and ethanol-fixed material. Agarose gel analysis of (A) 5 µl of Chelex supernatant and (B) 3 µl of PCR amplicon (~640 bp) is presented. MW-I = DNA HyperLadder I; MW-IV = DNA HyperLadder IV. HyperLadder IV produces a pattern of 9 regularly spaced bands, ranging from 100 to 1000 bp.

bands (18) than negative results (10), while most samples with green DNA failed to amplify (32) and just 6 produced PCR bands (Fig. 2B). This difference in COI PCR success between formalin-fixed samples containing green DNA only and those containing green and orange DNA was found to be significant according to Fisher's exact probability test ($p<0.01$). All 12 ethanol-fixed *Carcinus* samples from Cullera provided positive results.

DISCUSSION

While previous studies using oligonucleotides or isolated DNA have described the presence of lesions in DNA exposed to formaldehyde (Huang and Hopkins, 1993), the present study indicates that, even though only 24% of lithodid samples gave positive results, fully reliable sequence data can still be retrieved from formalin-fixed museum specimens. The comparison of sequence data from formalin-fixed samples and fresh and ethanol preserved specimens collected at independent laboratories for the same species (i.e. *Paralomis granulosa* from Zaklan, 2002) confirms the validity of sequences obtained from formalin-fixed material. In other cases we have been able to compare sequence data from closely related species belonging to the same genus (i.e. *Paralomis africana* and *Paralomis granulosa*). Moreover, although the TMS-Chelex protocol is reported for the first time in this validation study, it has been used previously with success on formalin-fixed spiny lobster specimens from the National Museum of Natural History, Washington (Palero *et al*., 2009).

Among the most interesting results from this validation study, it is worth pointing out that none of the four cleaning protocols tested had a measurable effect on amplification success, which suggests that either no direct PCR inhibitor is present in the solution, or it could not be removed by these techniques. PCR inhibition did not seem to be caused by DNA shearing either, since positive results were obtained from museum samples with sheared-DNA. Therefore, by using a quick and inexpensive test on both successful and failed DNA extracts from formalin-fixed samples, it was inferred that green-stained material on the agarose gel corresponds to DNA molecules that have been modified by formalin (and are therefore unsuitable as PCR templates), while orange-stained material corresponds to unmodified DNA molecules (which can be used as functional PCR templates).

The results obtained in the present study indicate that formalin does directly modify DNA molecules themselves and impedes PCR without the need for other PCR inhibitors or protein complexes. These observations agree with predictions made by Chaw *et al*. (1980) concerning cross-link interactions among amino groups of nucleosides from DNA. Indeed, amplification success did not depend on digestion time, since DNA extracts from successful samples showed PCR band amplification after 1-3 h digestion while non-successful samples did not amplify irrespectively of the incubation time (results not shown). It is well known that PCR is sensitive enough to provide a million copies of a target DNA sequence from only a few molecules (Saiki *et al.*, 1988), so that it seems reasonable to expect positive results from formalin-fixed samples for which some unmodified DNA is still available. Therefore, the presence of unmodified DNA molecules in the samples analysed could explain the positive results for many (if not all) of the protocols previously proposed (Fang *et al.*, 2002; García-Vázquez *et al*., 2006).

Obtaining DNA sequences from specimens that have been initially fixed in formalin is not a straightforward task and more work is required to optimise methodologies, and reduce costs and handling times (Schander and Halanych, 2003). Indeed, the present study does not claim that a final solution has been found for any formalin-fixed tissue. Nevertheless, this study shows that it is possible to obtain reliable and in-

formative sequence data from formalin-fixed samples and presents an easy-to-use diagnostic test to assess the suitability of DNA extracts for molecular analysis. Factors such as pH and temperature can modify the effects of formalin fixation on DNA (Chang and Loew, 1994; Shi *et al.*, 2004) and it is possible that some unmodified DNA is still available in formalin-fixed samples preserved many years ago. The fact that this inexpensive method can be used as a simple and direct test for DNA modification in multiple samples, provides the opportunity for future studies to screen several tissues and select those most suitable for use in molecular analyses while optimising resources for PCR amplification and sequencing.

AKNOWLEDGEMENTS

The authors would like to thank two anonymous reviewers for their remarks, which helped to improve the manuscript. This project was supported by the Marine Biodiversity and Ecosystem Functioning Network of Excellence MarBEF (Contract no. GOCE-CT-2003-505446) of the 6th European Framework Programme (FP6), the Zoology Research Fund, Department of Zoology, NHM, London, a Research Grant from the Royal Society to S.T., and a pre-doctoral fellowship awarded by the Autonomous Government of Catalonia to F.P. (2006FIC-00082). This research received support from the SYNTHESYS Project http://www.synthesys.info/ which is financed by European Community Research Infrastructure Action under the FP6 "Structuring the European Research Area" Programme. Many thanks are due to J. Fortuño for suggesting TMS as an alternative to critical point drying, P. Crabb for helping with the UV-light photography setting and our colleagues/friends in the Molecular Biology Unit, Department of Zoology NHM

REFERENCES

Cawkwell, L. and P. Quirke. – 2000. Direct multiplex amplification of DNA from a formalin fixed, paraffin wax embedded tissue section. *J. Clinic. Pathol. Mol. Pathol.*, 53: 51-52.

Chang, Y. and G. Loew. – 1994. Reaction mechanisms of formaldehyde with endocyclic imino groups of nucleic acid bases. *J. Am. Chem. Soc.*, 116: 3548-3555.

Chase, M., R. Etter, M. Rex and J. Quattro. – 1998. Extraction and amplification of mitochondrial DNA from formalin-fixed deep-sea mollusks. *Biotechniques*, 24: 243-247.

Chaw, Y., L. Crane, P. Lange and R. Shapiro. – 1980. Isolation and identification of cross-links from formaldehyde-treated nucleic acids. *Biochemistry*, 19: 5525-5531.

Clark, P.F., M. Neale and P.S. Rainbow. – 2001. A morphometric analysis of regional variation in *Carcinus* Leach, 1814 (Brachyura: Portunidae: Carcininae) with particular reference to the status of the two species *C. maenas* (Linnaeus, 1758) and *C. aestuarii* (Nardo, 1847). *J. Crustac. Biol.*, 21: 288-303.

Cunningham, C., N. Blackstone and L. Buss. – 1992. Evolution of king crabs from hermit crab ancestors. *Nature*, 355: 539-542.

Diaz-Cano, S. and S. Brady. – 1997. DNA extraction from formalin-fixed, paraffin-embedded tissues: Protein digestion as a limiting step for retrieval of high-quality DNA. *Diagn. Mol. Pathol.*, 6: 342-346.

Díaz-Viloria, N., L. Sánchez-Velasco and R. Pérez-Enríquez. – 2005. Inhibition of DNA amplification in marine fish larvae preserved in formalin. *J. Plankton Res.*, 27: 787-792.

Fang, S., Q. Wan and N. Fujihara. – 2002. Formalin removal from archival tissue by critical point drying. *Biotechniques*, 33: 604-611.

France, S. and T. Kocher. – 1996. DNA sequencing of formalin-fixed crustaceans from archival research collections. *Mol. Mar. Biol. Biotech.*, 5: 304-313.

García-Vázquez E., P. Alvarez, P. Lopes, N. Karaiskou, J. Perez, A. Teia, J.L. Martinez, L. Gomes and C. Triantaphyllidis. – 2006. PCR-SSCP of the 16S rRNA gene, a simple methodology for species identification of fish eggs and larvae. *Sci. Mar.*, 70S2: 13-21.

Gilbert, M.T.P., T. Haselkorn, M. Bunce, J.J. Sanchez, S.B. Lucas, L.D. Jewell, E. van Marck and M. Worobey. – 2007. The isolation of nucleic acids from fixed, paraffin-embedded tissues - which methods are useful when? *PLoS ONE,* 2(6): e537. doi:10.1371/journal.pone.0000537.

Hall, S. and S. Thatje. – 2009. Global bottlenecks in the distribution of marine Crustacea: temperature constraints in the biogeography of the family Lithodidae. *J. Biogeogr.*, 36: 2125-2135.

Huang, H. and P. Hopkins. – 1993. DNA interstrand cross-linking by formaldehyde: Nucleotide sequence preference and covalent structure of the predominant cross-link formed in synthetic oligonucleotides. *J. Am. Chem. Soc.*, 115: 9402-9408.

Macpherson, E. – 1988. Revision of the family Lithodidae Samouelle, 1819 (Crustacea: Decapoda: Anomura) in the Atlantic Ocean. *Mon. Zool. Mar.*, 2: 9-153.

Macpherson, E. – 2003. Some lithodid crabs (Crustacea: Decapoda: Lithodidae) from the Solomon islands (SW Pacific Ocean) with the description of a new species. *Sci. Mar.*, 67: 413-418.

Martín Andrés, A., A. Silva Mato, J.M. Tapia García and M.J. Sánchez Quevedo. – 2004. Comparing the asymptotic power of exact tests in 2x2 tables. *Comp. Stat. & Data Anal.*, 47(4): 745-756.

McLaughlin, P. – 1983. Hermit crabs - are they really polyphyletic? *J. Crustac. Biol.*, 3: 608-621.

Palero, F., K.A. Crandall, P. Abelló, E. Macpherson and M. Pascual. – 2009. Phylogenetic relationships between spiny, slipper and coral lobsters (Crustacea: Decapoda: Achelata). *Mol. Phylogenet. Evol.*, 50: 152-162.

Quay, W. – 1974. Bird and mammal specimens in fluid-objectives and methods. *Curator*, 17: 91-104.

R Development Core Team. – 2009. R: A language and environment for statistical computing. R Foundation for Statistical Computing, Vienna, Austria. ISBN 3-900051-07-0, URL http://www.R-project.org.

Saiki, R., D. Gelfand, S. Stoffel, S. Scharf, R. Higuchi, G. Horn, K. Mullis and H. Erlich. – 1988. Primer-directed enzymatic amplification of DNA with a thermostable DNA polymerase. *Science*, 239: 487-491.

Sambrook, J., E. Fritsch and T. Maniatis - 1989. *Molecular cloning: A laboratory manual*. Cold Spring Harbor Laboratory, New York.

Santos, S., D. Sá, E. Bastos, H. Guedes-Pinto, I. Gut, F. Gärtner and R. Chaves. – 2009. An efficient protocol for genomic DNA extraction from formalin-fixed paraffin-embedded tissues. *Res. Vet. Sci.*, 86: 421-6.

Scatena, M. and E. Morielle-Versute. – 2008. Suitability of DNA extracted from archival specimens of fruit-eating bats of the genus *Artibeus* (Chiroptera, Phyllostomidae) for polymerase chain reaction and sequencing analysis. *Gen. Mol. Biol.*, 31: 160-165.

Schander, C. and K. Halanych. – 2003. DNA, PCR and formalinized animal tissue - a short review and protocols. *Org. Diver. Evol.*, 3: 195-205.

Shi, S., R. Datar, C. Liu, L. Wu, Z. Zhang, R. Cote and C. Taylor. – 2004. DNA extraction from archival formalin-fixed, paraffin-embedded tissues: Heat-induced retrieval in alkaline solution. *Histochem. Cell Biol.*, 122: 211-218.

Shibata, D. – 1994. Extraction of DNA from paraffin-embedded tissue for analysis by polymerase chain-reaction - new tricks from an old friend. *Human Pathol.*, 25: 561-563.

Simmons, J. – 1995. Storage in fluid preservatives. In: C. Rose, C. Hawks, H. Genoways (eds.), *Storage of natural history collections: A preventive conservation approach*, pp. 161-186. Society for the Preservation of Natural History Collections, Iowa.

Takeda, M. and Y. Ohta. – 1979. A new species of lithodidae from Suruga Bay, central Japan. *Bull. Natl. Sci. Mus. A*, 5: 195-200.

Thatje, S., K. Anger, J. Calcagno, H. Lovrich, H. Pörtner and W. Arntz. – 2005. Challenging the cold: Crabs reconquer the antarctic. *Ecology*, 86: 619-625.

Thatje, S., S. Hall, C. Hauton, C. Held, P.A. Tyler. – 2008. Encounter of lithodid crab *Paralomis birsteini* on the continental slope off Antarctica, sampled by ROV. *Polar Biol.,* 31: 1143-1148.

Ubero-Pascal, N., J. Fortuño and M. Puing. – 2005. New application of air-drying techniques for studying Ephermeroptera and Plecoptera eggs by scanning electron microscopy. *Micr. Res. Tech.*, 68: 264-271.

Zaklan, S. – 2002. Review of the family Lithodidae (Crustacea: Anomura: Paguroidea): Distribution, biology and fisheries. In: A. Paul, E. Dawe, R. Elner, G. Jamieson, G. Kruse, R. Otto, B. Sainte-Marie and T. Shirley (eds.), *Crabs in cold water regions: Biology, management and economics*, pp. 58-84. Alaska Sea Grant College Program, Fairbanks.

Scient. ed.: J. Viñas.
Received December 12, 2008. Accepted November 3, 2009

Polar Biol (2008) 31:1143–1148
DOI 10.1007/s00300-008-0457-5

SHORT NOTE

Encounter of lithodid crab *Paralomis birsteini* on the continental slope off Antarctica, sampled by ROV

Sven Thatje · Sally Hall · Chris Hauton · Christoph Held · Paul Tyler

Received: 29 February 2008 / Revised: 28 April 2008 / Accepted: 2 May 2008 / Published online: 27 May 2008

Abstract A population of stone crab (Lithodidae) was encountered on the continental slope off Antarctica in the Bellingshausen Sea between 1,123 and 1,304 m water depths using the ROV-*Isis* during leg 166 of the RV James Clark Ross, in January 2007. Specimens were video recorded and one specimen was retrieved by ROV for morphological and molecular identification. Based on morphology and molecular data from the mitochondrial COI gene, this specimen identified as *P. birsteini*, Macpherson, 1988a. The significance of the molecular data and their implications for biogeography and evolution of lithodids in the Southern Ocean are briefly discussed.

Keywords Southern Ocean · Stone crab · Molecular phylogeny · Biogeography

Introduction

The shallow waters of the Antarctic continental shelf are virtually free of benthic top predators, such as shark, rays, teleost fish, and crabs (Aronson et al. 2007). The absence of such predators results from harsh physiological constraints, mainly low temperature that has prevailed in this environment for tens of millions of years. The process of Antarctic cooling was initiated by the breakup of Gondwana in the early Eocene, with a last cooling step until about 14 million years ago that resulted in conditions similar to those as seen today (see Aronson et al. 2007, and references therein). Since then, and in the absence of top predators structuring the faunal community, the Antarctic benthos of the shallow continental shelf evolved and maintained a rather ancient structure that today is not found anywhere else on Earth (Aronson et al. 2007).

The increased records of lithodid crabs in deeper waters and on seamounts surrounding the Antarctic continent in recent years raised the question of established lithodid crab populations in the Southern Ocean (López Abellan and Balguerías 1993; Klages et al. 1995; Arana and Retamal 1999; Thatje and Arntz 2004; Thatje and Lörz 2005). Although the origin and especially the timescale of lithodid radiation in the Southern Ocean remains obscure (Thatje et al. 2005), there is consensus that these largest arthropods currently inhabiting the oceans are the most likely candidates to invade the shallow waters of the Antarctic continental shelf under conditions of climate change (Meredith and King 2005; Thatje et al. 2005). Warming is likely to remove physiological barriers on lithodid crabs that currently place a limit on the invasion of shallow waters of the high Antarctic; a scenario that is especially likely for waters off the Antarctic Peninsula (Aronson et al. 2007, and references therein).

First records of lithodid crabs of the species *Neolithodes capensis* and *Paralomis birsteini* from 1,408 to 1,947 m, respectively, were made on the continental rise of Antarctica in the Bellingshausen Sea (García Raso et al. 2005). *P. birsteini* now appears to be widespread in the Bellingshausen Sea and so far remains the most commonly recorded Antarctic lithodid species south of 60°S (Arana and Retamal 1999; Thatje and Arntz 2004; Ahyong and Dawson 2006).

In the present work, we present new records of *P. birsteini* Macpherson, 1988a (=*P. spectabilis* Birstein and

S. Thatje (✉) · S. Hall · C. Hauton · P. Tyler
National Oceanography Centre, Southampton,
School of Ocean and Earth Science,
University of Southampton, European Way,
Southampton SO14 3ZH, UK
e-mail: svth@noc.soton.ac.uk

C. Held
Alfred Wegener Institute for Polar and Marine Research,
Marine Animal Ecology, Am Alten Hafen 26,
27568 Bremerhaven, Germany

Vinogradov 1967, not Hansen 1908) from 1,100 to 1,400 m water depths in the Bellingshausen Sea, which constitute the shallowest records of lithodids on the continental slope/rise of Antarctica. Comparative analysis of a fragment of the mitochondrial cytochrome oxidase I gene from the sampled specimen of *P. birsteini* and sequences obtained from related species are discussed from a biogeographical and evolutionary point of view.

Materials and methods

Sampling—thirteen specimens of the lithodid genus *Paralomis* were video-recorded on the continental slope/rise off Antarctica in the Bellingshausen Sea between 1,123 and 1,394 m water depth using the ROV-*Isis* during leg 166 of the RV James Clark Ross in January 2007 (Fig. 1, dive stations 5 and 6, Tyler et al. 2007). One male specimen (Fig. 2a–d) was sampled using the ROV's manipulator arm (66°24′81 S; 71°30′79 W; 1,394 m). The specimen was surfaced and died shortly thereafter.

Species identification—Morphological identification followed descriptions by Macpherson (1988a) in the form of the carapace and the antennal acicle, and additional comparison was made with other specimens of *P. birsteini* from the Musée National d'Histoire Naturelle (MNHN) in Paris. The specimen examined was 65 mm of Carapace Length (CL), measured from the orbit to the posterior carapace

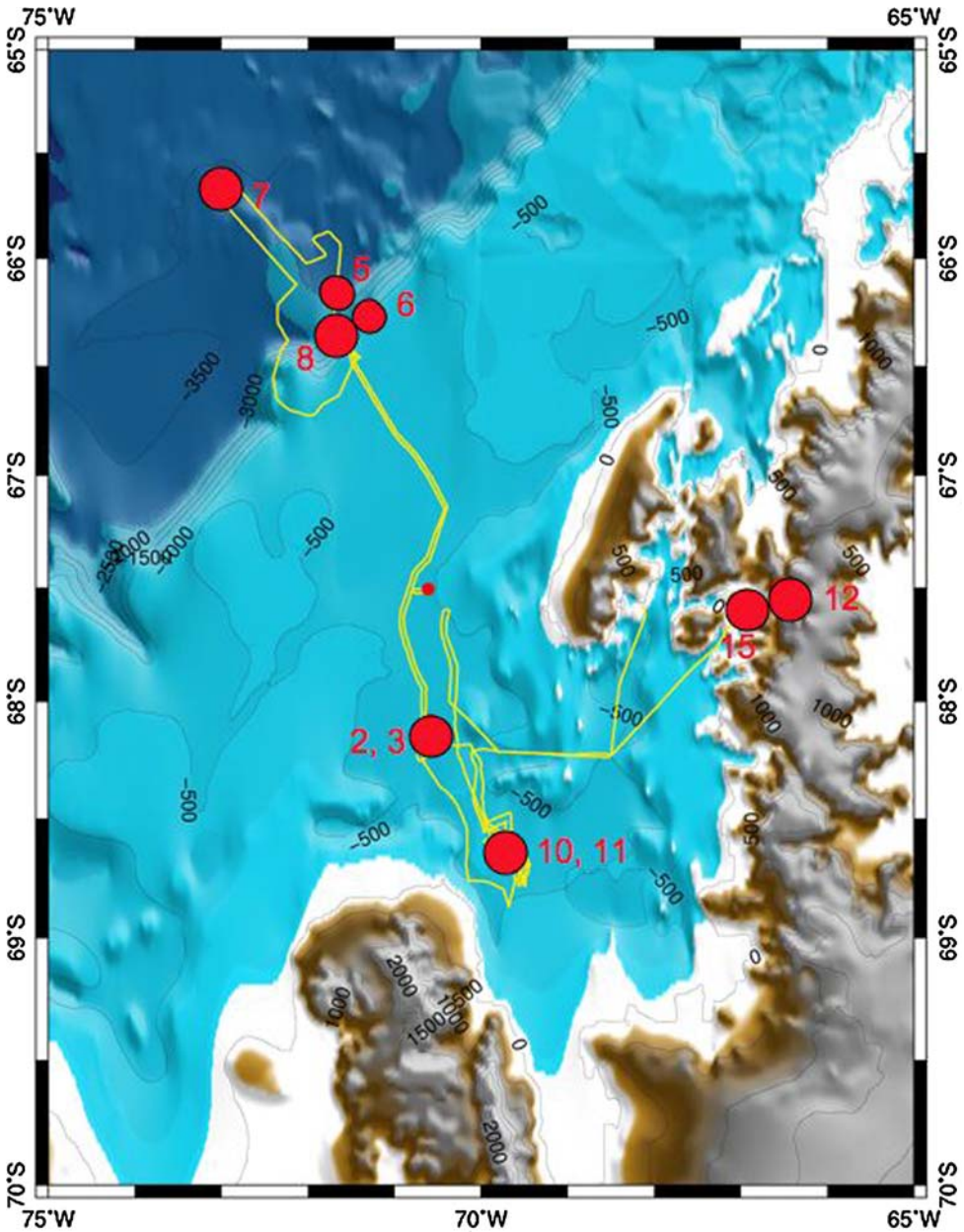

Fig. 1 Biological dive stations with the ROV-*Isis* during leg 166 of RV James Clark Ross to the Antarctic Bellingshausen Sea in January/February 2007. Specimens of the lithodid crab *Paralomis birsteini* were encountered during dive Nos. 5 & 6 (starting points: 68°23′48 S; 71°32′95 W and 66°24′24 S; 71°81′82 W, respectively) on the continental slope/rise off the Western Antarctic Peninsula

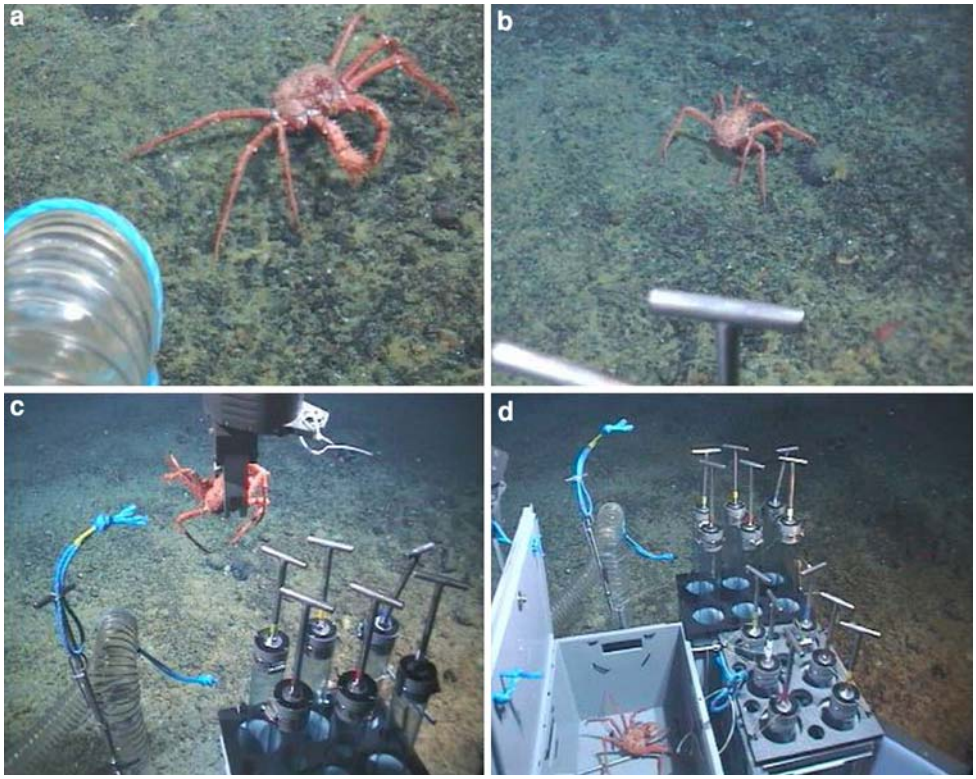

Fig. 2 Male specimen of *Paralomis birsteini* on the continental slope off Antarctica, Bellingshausen Sea, sampled by ROV-*Isis* during leg JCR166 on 25 January 2007. *P. birsteini* in its natural habitat (**a**, **b**), sampled by ROV-*Isis* (**c**, **d**), specimen CL = 64.9 mm

edge, and making it similar in size to the nominal *P. birsteini* (two paratypes studied: maximum CL = 67.78 mm; maximum CW = 67.74 mm).

DNA extraction, PCR, and sequencing—Tissue was sampled from the dactylus muscle of the retrieved sample and preserved in pre-cooled, 70% ethanol. Muscle samples from related species were also frozen very soon after death. DNA was extracted using Qiagen (Hilden, Germany) DNeasy Blood & Tissue kits following manufacturers' protocol. Using universal primers HCO2198 and LCO1490 (Folmer 1994) and Qiagen Taq polymerase approximately 850 bp of the mitochondrial COI gene were amplified (Saiki et al. 1988). The amplicons were cleaned using Qiagen QIAquick purification columns and sent to Macrogen Inc (Korea) for sequencing. Sequences can be retrieved from GenBank (Table 1).

Alignment and phylogenetic analyses—DNA sequences were aligned with no gaps or ambiguity using the Clustal W program (Thompson et al. 1994). Identical sequences were omitted from the analysis. Alignments were run through Modeltest 3.7 to obtain estimates of parameters for Maximum likelihood analysis. Phylogenetic trees were inferred

Table 1 Collection data for the lithodid specimens studied

Morphological ID	Lat	Long	Genbank accession	Identified by	Caught by
Paralomis spinosissima	53°36 S	36°38′ W	EU493258	S. Hall	Long line off South Georgia
Paralomis spinosissima	53°36′ S	36°38′ W	EU493259	S. Hall	Long line off South Georgia
Paralomis birsteini	66°24′81 S	71°30′79 W	EU493260	S. Hall	JCR166 ROV-*Isis*
Paralomis birsteini	48°2′ S	71°18′ E	EU493261	S. Hall	Palangrier Aldbaran, Kerguelen St Pal. 60 6/12/1999
Paralomis formosa	53°36′ S	36°38′ W	EU493262	S. Hall	Long line off South Georgia
Paralomis formosa	53°36′4.42″ S	36°38′43.86″ W	EU493265	M. Belchier	Long line off South Georgia
Paralomis granulosa	54°47′59.14″ S	65°15′0.15″ W	EU493264	G.A. Lovrich	Artisanal trap fisheries, Beagle Channel
Lithodes confundens	54°47′ S	65°15′ W	EU493257	S. Hall	ICEFISH 04, st 10T1
Neolithodes brodiei	14°44′48 S	167°8′40 E	EU493263	Original, E. Macpherson; Reviewed S. Hall	BOAO Alis CP 2312 Vanuatu, 15/11/2004
Pagurus bernhardus	Unknown	Unknown	AF483157	Young et al. Genbank	Unknown

from DNA sequences using PAUP 4 beta version 10. Outgroups were taken from both within the family Lithodidae (*Neolithodes brodiei* and *Lithodes confundens),* and from a closely related group (*Pagurus bernhardus).* Inclusion of either lithodid outgroup did not change the outcome. In addition, an iterative Bayesian analysis was run with Mrbayes 3.1 (Huelsenbeck and Ronquist 2001; Ronquist and Huelsenbeck 2003). The trees are presented for comparison (Fig. 3a, b).

Results

Thirteen specimens of *P. birsteini* were video recorded between about 1,123 and 1,394 m water depths on the Antarctic continental slope/rise in the Bellingshausen Sea (Figs. 1, 2). The present video footage included the record of one juvenile specimen of less than 2 cm CL in a gravel substratum that tried to escape the ROV's slurp gun and unfortunately was destroyed during hovering.

The genus *Paralomis* is well supported in the present molecular work, with species from the South Atlantic and Indian oceans clustering very closely together. While the phylogeny doesn't resolve fully with molecular methods, the recognized morphospecies of *Paralomis spinosissima* and *P. formosa* are upheld (Fig. 3a, b). It may be of significance that the specimens of *P. birsteini* from the Crozet Islands appear in this analysis distinct from the specimen in question despite close morphological similarity. Comparative analysis of a fragment of the mitochondrial cytochrome oxidase I gene from the sampled specimen of *P. birsteini* and sequences obtained from related species indicates a close affinity of species of *Paralomis* from either side of the Scotia arc and the Bellingshausen Sea (Fig. 3a, b). Relationships within this group cannot be further resolved based on the present data.

Discussion

Paralomis birsteini is morphologically closely related to *P. spectabilis*, which so far has only been found off Iceland and eastern Greenland at depths ranging from 1,470 to 2,075 m (Macpherson 1988b) and *P. formosa* Henderson,

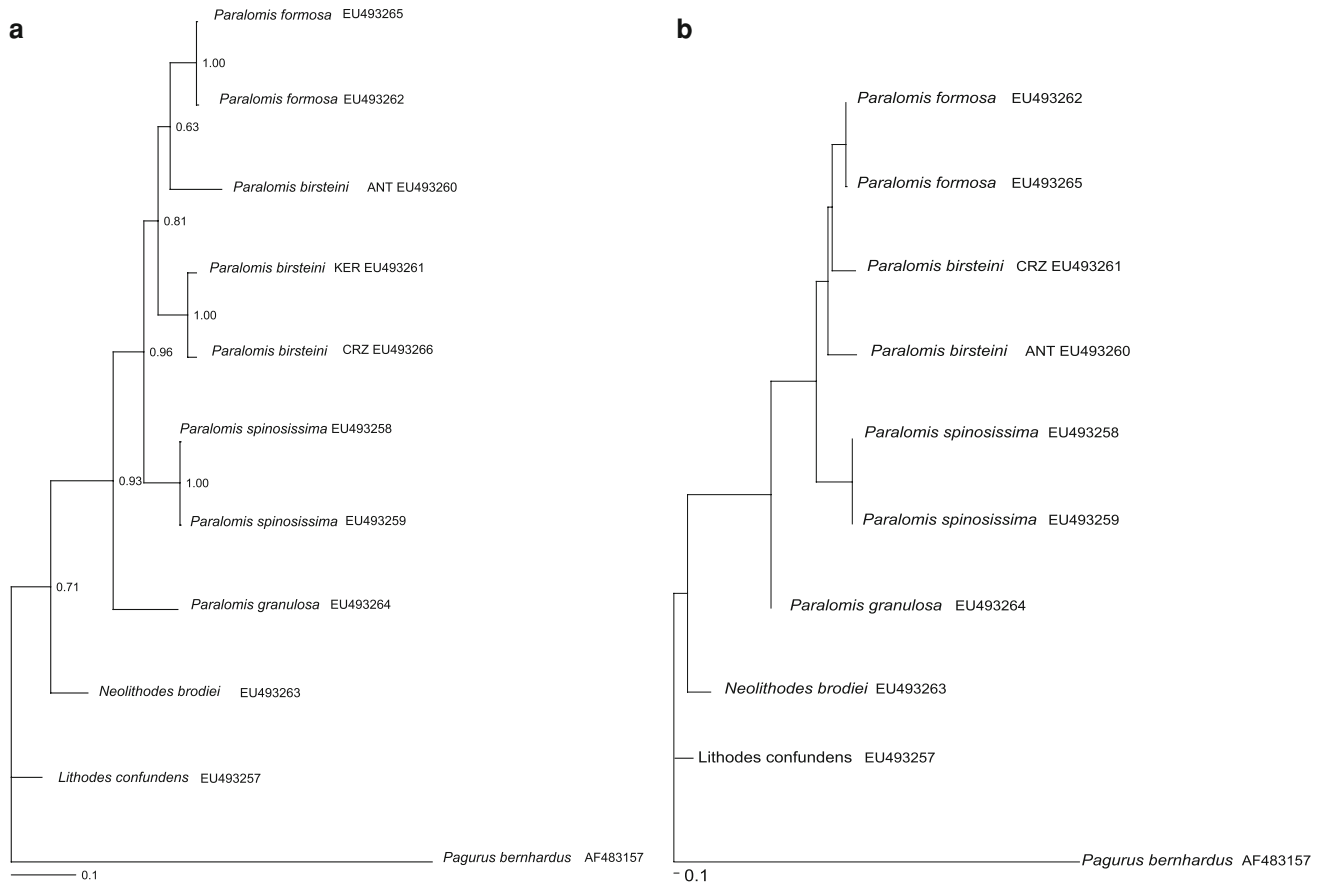

Fig. 3 **a** Phylogram produced using the Mrbayes program, displaying Bayesian posterior probabilities at the internal nodes. Genbank accession numbers provided. *ANT* Bellingshausen Sea, *CRZ* Crozet, *KER* Kerguelen Plateau. **b** Phylogram produced using PAUP 4 beta 10 using a Maximum Likelihood Method and a GTR_G_I model of substitution. *ANT* Bellingshausen Sea, *CRZ* Crozet, *KER* Kerguelen Plateau

which is common in waters off the island of South Georgia in the South Atlantic, at depths ranging from around 300 to 1,700 m (Thatje et al. 2005). *P. birsteini is* distinguished from *P. spectabilis* by shorter, stouter legs and the dactylus shorter than the propodus in *P. spectabilis*; the rostrum not pedunculate in *P. birsteini*, which is pedunculate in *P. spectabilis*; and the antennal acicle having short spines on its inner surface in *P. birsteini* (for details see Birstein and Vinogradov 1967; Macpherson 1988a). Personal observations of southern ocean *P. birsteini* specimens (Table 1) reveal a high degree of variability in these character states, and we recognize little substantial difference between the two species.

P. birsteini distinguishes from *P. formosa* in having longer legs and less prominent spines than in *P. formosa*; *P. formosa* has a large spine in the centre of its gastric region drawn out anteriorly which makes this region very convex. This spine is present but less pronounced in *P. birsteini. P. formosa* is also distinguishable by having long slender spines variable in number on both sides of its antennal acicle, and in having its carapace and walking legs covered completely in granules (although this disappears in larger individuals; for details see Macpherson 1988b).

Because only one specimen was retrieved by ROV for morphological and molecular studies it remains unclear whether other species of *Paralomis* co-occur with *P. birsteini* in the same habitat, which is not uncommon in this genus (Thatje and Arntz 2004). So far, species from other lithodid genera, *Neolithodes* and *Lithodes*, and *Paralomis* have been recorded for the Bellingshausen Sea and the Scotia arc region (Thatje and Arntz 2004; García Raso et al. 2005).

This record of a juvenile specimen of *P. birsteini* may indicate a reproductively active population in the area under investigation, given that lithodid species in the Southern Ocean are assumed to possess a low potential for larval dispersal. This was frequently discussed to be due to demersally drifting, lecithotrophic larvae with limited swimming ability, as found in several species from southern high latitudes based on field and laboratory observations (Lovrich 1999; Thatje et al. 2003; Watts et al. 2006; Reid et al. 2007). Radiation in Southern Ocean lithodids is thus likely dependent on adult migration, although one may indeed discuss the potential of demersally drifting larvae in bottom currents to distribute over long distance, given that larval development in Southern Ocean lithodids is likely exceeding 4–5 months in duration (Thatje et al. 2005). The topic needs much closer future investigation.

The phylogenetic analysis of the COI gene of *Paralomis* species from either side of the Scotia arc indicates a close affinity of species from South Georgia (*P. formosa* and *P. spinosissima*) with morphologically similar groups from as far away as Crozet in the Indian Ocean, and the Bellingshausen Sea (Table 1, Fig. 3a, b). Although defined species do show constant morphological characters that aid identification of morphospecies (Macpherson 1988a, b) the molecular analysis provides an initial suggestion of an ongoing or very recent speciation process within this group in the Southern Atlantic/Indian Ocean.

Analysis of the COI gene in the Bellingshausen Sea specimen of *Paralomis birsteini* allows us to suggest that gene flow within this morphotype is limited over distance, possibly to the extent of a cryptic speciation. Cryptic speciation has been previously discovered in other Antarctic taxa with limited dispersal potential (Held and Wägele 2005; Raupach and Wägele 2006). Genetic differences between *P. birsteini* from three different localities presented in this work (Fig. 3a, b) could point at a species complex that consists of at least two cryptic species. This supports the necessity of comparative analyses among type locality specimens from around Antarctica and adjacent seas in order to unravel biogeography and radiation patterns of Antarctic invertebrates in general.

Relatively close phylogenetic relationships between south Atlantic and Bellingshausen species supports hypothesis of a biogeographic relationship between these two areas (Gorny 1999), and gives further insight into the potential colonization of Antarctica from lower latitudes. Given that dispersal of larvae and thus potential gene flow between populations of Southern Ocean is discussed to be very low (Thatje et al. 2003; Watts et al. 2006), the close-relatedness of species across the Scotia Arc could point at a relatively recent separation of species and possible radiation in the Southern Ocean. Evolutionary timescales and exact radiation patterns of lithodid species remain obscure (Zaklan 2002; Thatje et al. 2005) and such work is so far particularly biased by the lack of sufficient numbers of lithodid specimens from Antarctic waters available for phylogenetic and molecular studies.

Acknowledgments We are grateful to the crew of R.V. James Clark Ross and the ROV-*Isis* team (NOCS) for help and assistance at sea, and to Julian Dowdeswell (SPRI, Cambridge) for the organization of leg JCR166. Molecular work was made possible by a travel grant from the German Academic Exchange Service (DAAD) to S.H. and a Research Grant from The Royal Society (2006-R2) to S.T. The ROV-cruise on board RV James Clark Ross was funded by NERC (project no. NE/D008352/1, P.I. Tyler). The authors are grateful for the valuable comments made by three anonymous reviewers. This work is a contribution to the Network of Excellence MarBEF under the sixth European Framework Programme (contract no. GOCE-CT-2003-505446).

References

Ahyong ST, Dawson EW (2006) Lithodidae from the Ross Sea, Antarctica, with descriptions of two new species (Crustacea: Decapoda: Anomura). Zootaxa 1303:45–68

Arana PM, Retamal MA (1999) Nueva distribución de *Paralomis birsteini* Macpherson 1988 en aguas antárticas (Anomura, Lithodidae, Lithodinae). Invest Mar (Valparaíso) 27:101–110

Aronson RB, Thatje S, Clarke A, Peck LS, Blake DB, Wilga CD, Seibel BA (2007) Climate change and invasibility of the Antarctic benthos. Annu Rev Ecol Evol Syst 38:129–154

Birstein YA, Vinogradov LG (1967) Occurrence of *Paralomis spectabilis* Hansen (Crustacea, Decapoda, Anomura) in the Antarctic. Explorations of the fauna of the sea. IV (XII). Biol Res Soviet Ant Exp 3:390–398 (Israel Program for Scientific Translations)

Folmer O, Black M, Hoeh W, Lutz R, Vrijenhoek R (1994) DNA primers for amplification of mitochondrial cytochrome C oxidase subunit I from metazoan invertebrates. Molec Mar Biol Biotech 3:294–299

García Raso JE, Manjón-Cabeza ME, Ramos A, Olasi I (2005) New record of Lithodidae (Crustacea, Decapoda, Anomura) from the Antarctic (Bellingshausen Sea). Polar Biol 28:642–646

Gorny M (1999) On the biogeography and ecology of the Southern Ocean decapod fauna. Scient Mar 63:367–382

Hansen HJ (1908) Crustacea Malacostraca. I. Dan Ingolf Exp 3:1–120

Held C, Wägele JW (2005) Cryptic speciation in the giant Antarctic isopod *Glyptonotus antarcticus* (Isopoda: Valvifera: Chaetiliidae). Scient Mar 69:175–181

Huelsenbeck JP, Ronquist F (2001) MRBAYES: Bayesian inference of phylogeny. Bioinformatics 17:754–755

Klages M, Gutt J, Starmans A, Bruns T (1995) Stone crabs close to the Antarctic continent: *Lithodes murrayi* Henderson, 1888 (Crustacea; Decapoda; Anomura) off Peter I Island (68°51′ S, 91°51′ W). Polar Biol 15:73–75

López Abellan LJ, Balguerías E (1993) On the presence of *Paralomis spinosissima* and *Paralomis formosa* in catches taken during the Spanish Survey ANTARTIDA 8611. CCAMLR Sci 1:165–173

Lovrich GA (1999) Seasonality of larvae of Brachyura and Anomura (Crustacea, Decapoda) in the Beagle Channel, Argentina. Scient Mar 63(Suppl 1):347–354

Macpherson E (1988a) Three new species of *Paralomis* (Crustacea, Decapoda, Anomura, Lithodidae) from the Pacific and Antarctic oceans. Zool Scripta 17:69–75

Macpherson E (1988b) Revision of the family Lithodidae Samouelle, 1819 (Crustacea, Decapoda, Anomura) in the Atlantic Ocean. Monogr Zool Mar 2:9–153

Meredith MP, King JC (2005) Rapid climate change in the ocean west of the Antarctic Peninsula during the second half of the 20th century. Geophys Res Lett 32:L19604

Raupach MJ, Wägele JW (2006) Distinguishing cryptic species in Antarctic Asellota (Crustacea: Isopoda) - a preliminary study of mitochondrial DNA in *Acanthaspidia drygalskii*. Antarct Sci 18:191–198

Reid W, Watts J, Clarke S, Belchier M, Thatje S (2007) Egg development, hatching rhythm and moult patterns in reared *Paralomis spinosissima* (Decapoda: Anomura: Paguroidea: Lithodidae) from South Georgia waters (Southern Ocean). Polar Biol 30:1213–1218

Ronquist F, Huelsenbeck JP (2003) MRBAYES 3: Bayesian phylogenetic inference under mixed models. Bioinformatics 19:1572–1574

Saiki R, Gelfand DH, Stoffel S, Scharf SJ, Higuchi R, Horn GT, Mullis KB, Erlich HA (1988) Primer directed enzymatic amplification of DNA with a thermostable DNA polymerase. Science 239:487–491

Thatje S, Calcagno JA, Lovrich GA, Sartoris FJ, Anger K (2003) Extended hatching periods in the Subantarctic lithodid crabs *Lithodes santolla* and *Paralomis granulosa* (Crustacea: Decapoda). Helgol Mar Res 57:110–113

Thatje S, Arntz WE (2004) Antarctic reptant decapods: more than a myth? Polar Biol 27:195–201

Thatje S, Lörz AN (2005) First record of lithodid crabs from Antarctic waters off the Balleny Islands. Polar Biol 28:334–337

Thatje S, Anger K, Calcagno JA, Lovrich GA, Pörtner HO, Arntz WE (2005) Challenging the cold: crabs reconquer the Antarctic. Ecology 86:619–625

Thompson JD, Higgins DG, Gibson TJ (1994) Clustal W. Nucleic Acids Res 22:4673–4680

Tyler PA and participants (2007) NERC Cruise report. James Clark Ross Cruise No. 166 (in association with JCR cruise no. 157). pp 18 (unpublished report)

Watts J, Thatje S, Clarke S, Belchier M (2006) A description of larval and early juvenile development in *Paralomis spinosissima* (Decapoda: Anomura: Paguroidea: Lithodidae) from South Georgia waters (Southern Ocean). Polar Biol 29:1028–1038

Zaklan SD (2002) Review of the family Lithodidae (Crustacea: Anomura: Paguroidea): Distribution, biology, and fisheries. In: Paul AJ, Dawe EG, Elner R, Jamieson GS, Kruse GH, Otto RS, Sainte-Marie B, Shirley TC, Woodby D (eds) Crabs in cold water regions: biology, management, and economics. University of Alaska Sea Grant College Program AK-SG-02–01, Fairbanks, pp 751–845

APPENDIX J

Table.a: Statistics relating to non-species-subdivided datasets for the *Lithodes* morphometric analysis (section B2).

Y_k	1^{st}; 2^{nd} order polynomial regression of undivided datasets x = CL; y = Y_k. **p** = probability that the coefficient of the highest term in the regression is zero.	ANOVA of $f_{CL}(Y_k)$ subdivided into 17 species. F statistic is explained. H_0: no difference in Y_k between species.	Shapiro-Wilk test for normality. **p**(N) = probability that all within-species samples are normally distributed.	F-test for equal variance. **p**(EV) = probability that all species have equal variance in the measurement Y_k.
AL	**1°: r^2** = 0.911 (**p** <0.001) ; **2°: r^2** = 0.000009 (**p** = 0.897)	**F =** 69.701 **p**(H_0) < 0.001	**p**(N) = 0.193	**p**(EV) =0.686
DL	**1°: r^2** = 0.911 (**p** 0 001); **2°: r^2** = 0.000723 (**p** = 0.264)	**F=** 34.685 **p**(H_0) < 0.001	**p**(N) = 0.606	**p**(EV) = 0.068
ML	**1°: r^2** = 0.805 (**p** < 0.001); **2°: r^2** = 0.00238 (**p** = 0.168)	**F=** 211.091 **p**(H_0) < 0.001	**p**(N) = 0.04	**p**(EV) = 0.032
PL	**1°: r^2** = 0.824 (**p** < 0.001); **2°: r^2** = 0.00131 (**p** = 0.285)	**F =** 17.865 **p**(H_0) < 0.001	**p**(N) = 0.02	**p**(EV) = 0.0299
GW	**1°: r^2** = 0.88 (**p** < 0.001); **2°: r^2** = 0.007 (**p** = 0.002)	**F =** 79.823 **p**(H_0) < 0.001	**p**(N) = 0.598	**p**(EV) = 0.095
LBH	**1°: r^2** = 0.797 (**p** < 0.001); **2°: r^2** = 0.0001 (**p** = 0.781)	**F =** 125.766 **p**(H_0) < 0.001	**p**(N) = 0.133	**p**(EV) = 0.188
GCL	**1°: r^2** = 0.619 (**p** < 0.001); **2°: r^2** = 0.0261 (**p** = 0.001)	**F=** 120.907 **p**(H_0) < 0.001	**p**(N) = 0.038	**p**(EV) = 0.154
DH	**1°: r^2** = 0.719 (**p** < 0.001); **2°: r^2** = 0.0181 (**p** = 0.001)	**F =** 53.325 **p**(H_0) < 0.001	**p**(N) = 0.067	**p**(EV) = 0.03
CAL	**1°: r^2** = 0.906 (**p** < 0.001); **2°: r^2** = 0.00023 (**p** = 0.532)	**F=** 27.456 **p**(H_0) < 0.001	**p**(N) = 0.0124	**p**(EV) = 0.034
LSH	**1°: r^2** = 0.797 (**p** < 0.001); **2°: r^2** = 0.000101 (**p** = 0.781)	**F=** 135.892 **p**(H_0) < 0.001	**p**(N) = 0.247	**p**(EV) = 0.105
GL	**1°: r^2** = 0.976 (**p** <	**F=** 19.819	**p**(N) = 0.671	**p**(EV) = 0.28

	0.001); **2°: r^2** = 0.00313 (**p** = 0.001)	**p**(H_0) < 0.001		
MW	**1°: r^2** = 0.753 (**p** < 0.001); **2°: r^2** = 0.0247 (**p** = 0.001)	**F** = 49.904 **p**(H_0) < 0.001	**p**(N) = 0.396	**p**(EV) = 0.269
ABL	**1°: r^2** = 0.866 (**p**<0.001); **2°: r^2** = 0.0093 (**p** = 0.112)	**F** = 65.067 **p**(H_0) < 0.001	**p**(N) = 0.057	**p**(EV) = 0.236
LHH	**1°: r^2** = 0.813 (**p** < 0.001); **2°: r^2** = 0.00038 (**p** = 0.572)	**F** =1.142 **p**(H_0) = 0.338	**p**(N) =	**p**(EV) = 0.124
HW	**1°: r^2** = 0.975 (**p** < 0.001); **2°: r^2** = 0.00268 (**p** = 0.001)	**F** = 2.714 **p**(H_0) = 0.006 H_0 is rejected based on these data with a confidence of 99%; however, in pair-wise comparisons, differences are found only between a single pair of species, and thus are not phylogenetically informative	**p**(N) =0.05	**p**(EV) = 0.433.
CDL	**1°: r^2** = 0.782 (**p** < 0.001); **2°: r^2** = 0.00047 (**p** = 0.56)	**F** = 1.875 **p**(H_0) = 0.07	**p**(N) =	**p**(EV) = 0.648
VRL	**1°: r^2** = 0.388* (**p** <0.001); **2°: r^2** = 0.0423 (**p** = 0.001) *indicating VRL is not well explained by correlation with CL	**F**=2.021 **p**(H_0) = 0.055	**p**(N) =	**p**(EV) = 0.058
OCW	**1°: r^2** = 0.648 (**p** <0.001); **2°: r^2** = 0.0058 (**p** = 0.112)	**F**=1.391 **p**(H_0) = 0.207	**p**(N) =	**p**(EV) = 0.217

b. Statistics relating to species-subdivided datasets for the *Lithodes* morphometric analysis.

K, n	r^2 test of linear regression within species, in which x = CL and y = $Y_{k,}$	Shapiro-Wilk test of normality	Sample number	Standardised within-species sample mean: $\bar{U}_{k,n}$	Standardised within-species sample standard

	$_n$/CL. p = probability that B=0 in the equation y = **A** + **B**x .	**p**(N) = probability that the sample is taken from a normally distributed population			deviation $S_{k,n}$
$AL_{L.aequispina}$	$\mathbf{r^2}$ = 0.0453 (**p** = 0.391)	**p**(N) = 0.507	18	8.993716	0.340765
$AL_{L.\ confundens}$	$\mathbf{r^2}$ = 0.120 (**p** = 0.361)	**p**(N) = 0.263	9	10.11531	0.269107
$AL_{L.\ couesi}$	$\mathbf{r^2}$ = 0.343 (**p** = 0.011)	**p**(N) = 0.713	18	8.399211	0.578858
$AL_{L.\ ferox}$	$\mathbf{r^2}$ = 0.522 (**p** = 0.005) **A** = 0.452 **B** = 0.0005	**p**(N) = 0.370	13	10.35392	0.456793
$AL_{L.\ galapagensis}$	N/A		2	10.45871	0.667137
$AL_{L.\ longispina}$	N/A		3	11.045	0.737178
$AL_{L.\ maja}$	$\mathbf{r^2}$ = 0.206 (**p** = 0.026)	**p**(N) = 0.126	24	10.69483	0.784147
$AL_{L.\ mammilifer}$	$\mathbf{r^2}$ = 0.151 (**p** = 0.518)	**p**(N) = 0.713	5	11.1458	0.39641
	N/A		3	11.22334	0.377259
$AL_{L.\ megacantha}$	$\mathbf{r^2}$ = 0.339 (**p** = 0.17)	**p**(N) = 0.034	7	10.89782	0.415116
$AL_{L.\ murrayi}$	$\mathbf{r^2}$ = 0.0397 (**p** = 0.4)	**p**(N) = 0.335	20	10.61635	0.368364
$AL_{L.\ richeri}$	$\mathbf{r^2}$ = 0.112 (**p** = 0.463)	**p**(N) = 0.581	7	11.133	0.324539
$AL_{L.\ santolla}$	$\mathbf{r^2}$ = 0.0446 (**p** = 0.488)	**p**(N) = 0.081	13	9.645107	0.237464
$AL_{P.\ californiensis}$				8.597065	0.037732
$AL_{P.\ camtschaticus}$	$\mathbf{r^2}$ = 0.796 (**p** = 0.017) **A** = 0.469 **B** = 0.0014	**p**(N) = 0.492		9.823005	0.614291

AL*P. platypus*	$\mathbf{r^2}$ = 0.451 (**p** = 0.215)	**p**(N) = 0.852		9.942947	0.137258
AL*P. rathbuni*	$\mathbf{r^2}$ = 0.242 (**p** = 0.508)	**p**(N) = 0.498		8.831877	0.155646
DL/CL					
DL*L.aequispina*	$\mathbf{r^2}$ = 0.0941 (**p** = 0.216)	**p**(N) = 0.02	18	9.669195	0.297442
DL*L. confundens*	$\mathbf{r^2}$ = 0.0140 (**p** = 0.762)	**p**(N) = 0.309	9	10.81185	0.653937
DL*L. couesi*	$\mathbf{r^2}$ = 0.371 (**p** = 0.762)	**p**(N) = 0.151	18	9.100429	0.379543
DL*L. ferox*	$\mathbf{r^2}$ = 0.00045 (**p** = 0.945)	**p**(N) = 0.148	13	10.77344	0.577214
DL*L. galapagensis*	N/A		2	9.603473	0.512549
DL*L. longispina*	N/A		3	10.38071	1.095118
DL*L. maja*	$\mathbf{r^2}$ = 0.0725 (**p** = 0.203)	**p**(N) = 0.035	24	9.484499	0.379517
DL*L. mammilifer*	$\mathbf{r^2}$ = 0.122 (**p** = 0.565)	**p**(N) = 0.061	5	10.40278	0.11246
DL*L. manningi*	N/A		3	10.59639	0.410021
DL*L. megacantha*	$\mathbf{r^2}$ = 0.123 (**p** = 0.0441)	**p**(N) = 0.222	7	10.41484	0.486243
DL*L. murrayi*	$\mathbf{r^2}$ = 0.333 (**p** = 0.008)	**p**(N) = 0.443	20	11.28695	0.470424
DL*L. richeri*	$\mathbf{r^2}$ = 0.00511 (**p** = 0.879)	**p**(N) = 0.371	7	11.12418	0.82368
DL*L. santolla*	$\mathbf{r^2}$ = 0.000879 (**p** = 0.923)	**p**(N) = 0.537	13	8.43482	0.530773
DL*P. californiensis*				9.334537	0.207762
DL*P. camtschaticus*	$\mathbf{r^2}$ = 0.132 (**p** = 0.478)	**p**(N) = 0.1		10.12561	0.388684
DL*P. platypus*	$\mathbf{r^2}$ = 0.00000001 (**p** = 0.999)	**p**(N) = 0.937		9.356586	0.345495
DL*P. rathbuni*	$\mathbf{r^2}$ = 0.437	**p**(N) =		10.67086	0.306723

	(**p** = 0.339)	0.159			
ML/CL					
$ML_{L.aequispina}$	$\mathbf{r^2}$ = 0.245 (**p** = 0.037)	**p**(N) = 0.795	18	8.758359	0.211606
$ML_{L.\ confundens}$	$\mathbf{r^2}$=0.032 (**p** = 0.644)	**p**(N) = 0.105	9	10.50912	0.190359
$ML_{L.\ couesi}$	$\mathbf{r^2}$=0.626 (**p** = 0.001) **A** = 0.648 **B** = 0.00124	**p**(N) = 0.996	18	9.43242	0.30952
$ML_{L.\ ferox}$	$\mathbf{r^2}$ = 0.231 (**p** = 0.097)	**p**(N) = 0.836	13	10.7681	0.313517
$ML_{L.\ galapagensis}$	N/A		2	9.920552	0.089123
$ML_{L.\ longispina}$	N/A		3	10.99919	0.576157
$ML_{L.\ maja}$	$\mathbf{r^2}$ = 0.000001 (**p** = 0.966)	**p**(N) = 0.723	24	9.311014	0.153171
$ML_{L.\ mammilifer}$	$\mathbf{r^2}$ = 0.00233 (**p** = 0.939)	**p**(N) = 0.988	5	10.83066	0.141209
$ML_{L.\ manningi}$	N/A		3	11.76072	1.084515
$ML_{L.\ megacantha}$	$\mathbf{r^2}$ = 0.0605 (**p** = 0.595)	**p**(N) = 0.485	7	11.88014	0.297333
$ML_{L.\ murrayi}$	$\mathbf{r^2}$ = 0.00365 (**p** = 0.8)	**p**(N) = 0.278	20	10.55907	0.156692
$ML_{L.\ richeri}$	$\mathbf{r^2}$ = 0.0368 (**p** = 0.68)	**p**(N) = 0.491	7	12.22601	0.482621
$ML_{L.\ santolla}$	$\mathbf{r^2}$ = 0.151 (**p** = 0.189)	**p**(N) = 0.379	13	9.447799	0.351335
$ML_{P.\ californiensis}$				9.183966	0.220888
$ML_{P.\ camtschaticus}$	$\mathbf{r^2}$ = 0.00561 (**p** = 0.888)	**p**(N) = 0.009	6	9.65186	0.398086
$ML_{P.\ platypus}$	$\mathbf{r^2}$ = 0.811 (**p** = 0.014) **A** = 0.59 **B** = 0.00151	**p**(N) = 0.937		9.162561	0.123303
$ML_{P.\ rathbuni}$	$\mathbf{r^2}$ = 0.822 (**p** = 0.093) **A** = 1.015	**p**(N) = 0.449		9.768982	0.232148

	B = 0.00314				
PL/CL					
$PL_{L.aequispina}$	$\mathbf{r^2}$ = 0.0446 (**p** = 0.4)	**p**(N) = 0.075	18	9.094656	0.151181
$PL_{L.\ confundens}$	$\mathbf{r^2}$ = 0.0186 (**p** = 0.726)	**p**(N) = 0.462	9	11.07691	0.275324
$PL_{L.\ couesi}$	$\mathbf{r^2}$ = 0.118 (**p** = 0.163)	**p**(N) = 0.021	18	9.32746	0.401518
$PL_{L.\ ferox}$	$\mathbf{r^2}$ = 0.111 (**p** = 0.266)	**p**(N) = 0.003	13	10.73205	0.415753
$PL_{L.\ galapagensis}$	N/A		2	10.15934	0.427966
$PL_{L.\ longispina}$	N/A		3	11.37872	0.554417
$PL_{L.\ maja}$	$\mathbf{r^2}$ = 0.0017 (**p** = 0.0848)	**p**(N) = 0.442	24	9.154187	0.27448
$PL_{L.\ mammilifer}$	$\mathbf{r^2}$ = 0.123 (**p** = 0.563)	**p**(N) = 0.054	5	10.34732	0.64231
$PL_{L.\ manningi}$	N/A		3	12.04794	1.079276
$PL_{L.\ megacantha}$	$\mathbf{r^2}$ = 0.155 (**p** = 0.383)	**p**(N) = 0.443	7	11.69353	0.322291
$PL_{L.\ murrayi}$	$\mathbf{r^2}$ = 0.188 (**p** = 0.056)	**p**(N) = 0.434	20	10.35934	0.204318
$PL_{L.\ richeri}$	$\mathbf{r^2}$ = 0.0519 (**p** = 0.623)	**p**(N) = 0.185	7	12.00916	0.487641
$PL_{L.\ santolla}$	$\mathbf{r^2}$ = 0.0107 (**p** = 0.736)	**p**(N) = 0.6	13	9.352897	0.390363
$PL_{P.\ californiensis}$				10.09239	0.170483
$PL_{P.\ camtschaticus}$	$\mathbf{r^2}$ = 0.0901 (**p** = 0.563)	**p**(N) = 0.023		9.493362	0.418149
$PL_{P.\ platypus}$	$\mathbf{r^2}$ = 0.775 (**p** = 0.021)	**p**(N) = 0.016		9.056738	0.189207
$PL_{P.\ rathbuni}$	$\mathbf{r^2}$ = 0.491 (**p** = 0.299) **A** = 0.968 **B** = 0.242	**p**(N) = 0.481		10.5876	0.29515
GW/CL					
$GW_{L.aequispina}$	$\mathbf{r^2}$ = 0.0251	**p**(N) =	18	9.304505	0.350607

	(**p** = 0.53)	0.206			
$GW_{L.\ confundens}$	$\mathbf{r^2}$ = 0.113 (**p** = 0.376)	**(P =** 0.532	9	9.619086	0.25986
$GW_{L.\ couesi}$	$\mathbf{r^2}$ = 0.556 (**p** = 0.001) **A** = 0.326 **B** = 0.000384	**p**(N) = 0.389	18	9.323632	0.42631
$GW_{L.\ ferox}$	$\mathbf{r^2}$ = 0.336 (**p** = 0.038)	**p**(N) = 0.328	13	10.06356	0.369597
$GW_{L.\ galapagensis}$	N/A		2	10.72544	0.37597
$GW_{L.\ longispina}$	N/A		3	11.37686	0.383897
$GW_{L.\ maja}$	$\mathbf{r^2}$ = 0.275 (**p** = 0.009)	**p**(N) = 0.346	24	9.725036	0.413565
$GW_{L.\ mammilifer}$	$\mathbf{r^2}$ = 0.234 (**p** = 0.409)	**p**(N) = 0.121	5	11.40718	0.164424
$GW_{L.\ manningi}$	N/A		3	10.83604	0.069428
$GW_{L.\ megacantha}$	$\mathbf{r^2}$ = 0.0284 (**p** = 0.718)	**p**(N) = 0.438	7	12.13541	0.415434
$GW_{L.\ murrayi}$	$\mathbf{r^2}$ = 0.000001 (**p** = 0.998)	**p**(N) = 0.850	20	10.67942	0.315608
$GW_{L.\ richeri}$	$\mathbf{r^2}$ = 0.0908 (**p** = 0.511)	**p**(N) = 0.193	7	11.87623	0.200978
$GW_{L.\ santolla}$	$\mathbf{r^2}$ 0.0591 (**p** = 0.424)	**p**(N) = 0.529	13	9.553519	0.558522
$GW_{P.\ californiensis}$	N/A		3	8.702118	0.1294
$GW_{P.\ camtschaticus}$	$\mathbf{r^2}$ = 0.0684 (**p** = 0.617)	**p**(N) = 0.767	6	9.725388	0.494413
$GW_{P.\ brevipes}$	$\mathbf{r^2}$ = 0.00642 (**p** = 0.88)	**p**(N) = 0.471	6	9.02056	1.226498
$GW_{P.\ rathbuni}$	$\mathbf{r^2}$ = 0.242 (**p** = 0.508)	**p**(N) = 0.854	4	8.065695	0.736115
$LBH_{L.aequispina}$	$\mathbf{r^2}$ = 0.0767 (**p** = 0.266)	**p**(N) = 0.775	18	10.83303	0.237455

LBH*L. confundens*	r^2 = 0.0163 (**p** = 0.743)	**p**(N) = 0.087	9	10.08844	0.310204
LBH*L. couesi*	r^2 = 0.0166 (**p** = 0.622)	**p**(N) = 0.257	18	11.77738	0.30553
LBH*L. ferox*	r^2 = 0.271 (**p** = 0.068)	**p**(N) = 0.725	13	9.962117	0.386866
LBH*L. galapagensis*			2	10.67933	0.240712
LBH*L. longispina*			3	9.507839	0.12971
LBH*L. maja*	r^2 = 0.0545 (**p** = 0.272)	**p**(N) = 0.549	24	9.190542	0.336479
LBH*L. mammilifer*			5	9.53221	0.359721
LBH*L. manningi*			3	9.903769	0.101375
LBH*L. megacantha*	r^2 = 0.0926 (**p** = 0.558)	**p**(N) = 0.993	7	8.970096	0.332112
LBH*L. murrayi*	r^2 = 0.0434 (**p** = 0.378)	**p**(N) = 0.564	20	8.887776	0.348895
LBH*L. richeri*	r^2 = 0.00110 (**p** = 0.944)	**p**(N) = 0.298	7	9.153715	0.248085
LBH*L. santolla*	r^2 = 0.00238 (**p** = 0.863)	**p**(N) = 0.556	13	9.93038	0.353551
LBH*P. californiensis*			3	11.36212	0.043419
LBH*P. camtschaticus*	r^2 = 0.321 (**p** = 0.241)	**p**(N) = 0.035	6	9.722175	0.252858
LBH*P. brevipes*	r^2 = 0.363 (**p** = 0.206)	**p**(N) = 0.903	6	10.31357	0.483531
LBH*P. rathbuni*	r^2 = 0.0535 (**p** = 0.769)	**p**(N) = 0.408	4	11.93921	0.18088
DH*L.aequispina*	r^2 = 0.00262 (**p** = 0.84)	**p**(N) = 0.015	18	9.435652	0.4824
DH*L. confundens*	r^2 = 0.244 (**p** = 0.176)	**p**(N) = 0.346	9	11.42958	0.190931
DH*L. couesi*	r^2 = 0.0937 (**p** = 0.232)	**p**(N) = 0.403	18	9.230104	0.396863
DH*L. ferox*	r^2 = 0.00178 (**p** = 0.891)	**p**(N) = 0.936	13	9.864549	0.57115
DH*L. galapagensis*			2	9.111268	0.490928

DH*L. longispina*			3	9.507137	1.296007
DH*L. maja*	$\mathbf{r^2}$ = 0.0434 (**p** = 0.329)	**p**(N) = 0.481	24	10.51581	0.159952
DH*L. mammilifer*	$\mathbf{r^2}$ = 0.300 (**p** = 0.453)	**p**(N) = 0.267	5	9.350418	0.454773
DH*L. manningi*			3	9.09492	0.549844
DH*L. megacantha*	$\mathbf{r^2}$ = 0.0183 (**p** = 0.772)	**p**(N) = 0.639	7	8.513598	0.182042
DH*L. murrayi*	$\mathbf{r^2}$ = 0.00548 (**p** = 0.756)	**p**(N) = 0.084	20	9.769846	0.410312
DH*L. richeri*	$\mathbf{r^2}$ = 0.126 (**p** = 0.434)	**p**(N) = 0.384	7	8.817117	0.773726
DH*L. santolla*	$\mathbf{r^2}$ = 0.0487 (**p** = 0.429)	**p**(N) = 0.364	13	10.46434	0.285082
DH*P. californiensis*			3	9.558699	0.153496
DH*P. camtschaticus*	$\mathbf{r^2}$ = 0.0633 (**p** = 0.631)	**p**(N) = 0.600	6	11.94297	0.388397
DH*P. brevipes*	$\mathbf{r^2}$ = 0.305 (**p** = 0.256)	**p**(N) = 0.184	6	12.25189	0.346648
DH*P. rathbuni*	$\mathbf{r^2}$ = 0.342 (**p** = 0.415)	**p**(N) = 0.895	4	10.0088	0.211561
CAL*L.aequispina*	$\mathbf{r^2}$ = 0.0587 (**p** = 0.333)	**p**(N) = 0.08	18	8.797777	0.403699
CAL*L. confundens*	$\mathbf{r^2}$ = 0.0873 (**p** = 0.44)	**p**(N) = 0.74	9	11.37621	0.16749
CAL*L. couesi*	$\mathbf{r^2}$ = 0.397 (**p** = 0.007) **A** = 0.337 **B** = 0.00068	**p**(N) = 0.155	18	8.63398	0.700755
CAL*L. ferox*	$\mathbf{r^2}$ = 0.0377 (**p** = 0.525)	**p**(N) = 0.356	13	10.37704	0.624178
CAL*L. galapagensis*			2	9.773678	0.376642
CAL*L. longispina*			3	10.94264	0.43293
CAL*L. maja*	$\mathbf{r^2}$ = 0.0859 (**p** = 0.164)	**p**(N) = 0.315	24	9.771101	0.293167
CAL*L. mammilifer*	$\mathbf{r^2}$ = 0.575 (**p** = 0.242) **A** = 0.577	**p**(N) = 0.251	5	9.861083	0.899345

	B = 0.00203				
CAL*L. manningi*			3	11.856	1.340678
CAL*L. megacantha*	$\mathbf{r^2}$ = 0.0616 (**p** = 0.592)	**p**(N) = 0.987	7	11.30805	0.251335
CAL*L. murrayi*	$\mathbf{r^2}$ = 0.0313 (**p** = 0.455)	**p**(N) = 0.06	20	10.42753	0.403432
CAL*L. richeri*	$\mathbf{r^2}$ = 0.0680 (**p** = 0.572)	**p**(N) = 0.831	7	11.48428	0.763249
CAL*L. santolla*	$\mathbf{r^2}$ = 0.00000359 (**p** = 0.984)	**p**(N) = 0.502	13	9.594548	0.364928
CAL*P. californiensis*			3	9.995611	0.176694
CAL*P. camtschaticus*	$\mathbf{r^2}$ = 0.553 (**p** = 0.09)	**p**(N) = 0.693	6	10.33845	0.118902
CAL*P. brevipes*	$\mathbf{r^2}$ = 0.72 (**p** = 0.033) **A** = 0.368 **B** = 0.00152	**p**(N) = 0.975	6	10.09338	0.355566
CAL*P. rathbuni*	$\mathbf{r^2}$ = 0.828 (**p** = 0.09) **A** = 0.640 **B** = 0.00216	**p**(N) = 0.42	4	10.38995	0.459331
GCL*L.aequispina*	$\mathbf{r^2}$ = 0.0690 (**p** = 0.292)	**p**(N) = 0.203	18	9.500899	0.140219
GCL*L. confundens*	$\mathbf{r^2}$ = 0.00537 (**p** = 0.851)	**p**(N) = 0.809	9	10.30991	0.113942
GCL*L. couesi*	$\mathbf{r^2}$ = 0.000874 (**p** = 0.910)	**p**(N) = 0.759	18	7.871441	0.203042
GCL*L. ferox*	$\mathbf{r^2}$ = 0.447 (**p** = 0.012) **A** = 0.306 **B** = 0.000820	**p**(N) = 0.036	13	10.25457	0.58069
GCL*L. galapagensis*			2	8.801645	0.272262
GCL*L. longispina*			3	9.475551	0.040274
GCL*L. maja*	$\mathbf{r^2}$ = 0.0374 (**p** = 0.365)	**p**(N) = <0.001	24	11.03019	0.315248
GCL*L. mammilifer*			5	10.13903	0.236683
GCL*L. manningi*			3	10.04336	0.12267

GCL*L. megacantha*	$\mathbf{r^2}$ = 0.0964 (**p** = 0.498)	**p**(N) = 0.001	7	10.07404	0.312334
GCL*L. murrayi*	$\mathbf{r^2}$ = 0.00293 (**p** = 0.821)	**p**(N) = 0.821	20	10.78131	0.391019
GCL*L. richeri*	$\mathbf{r^2}$ = 0.239 (**p** = 0.266)	**p**(N) = 0.671	7	10.45288	0.50648
GCL*L. santolla*	$\mathbf{r^2}$ = 0.0686 (**p** = 0.346)	**p**(N) = 0.493	13	10.2408	0.310962
GCL*P. californiensis*			3	8.645871	0.154222
GCL*P. camtschaticus*	$\mathbf{r^2}$ = 0.0000205 (**p** = 0.992)	**p**(N) = 0.781	6	10.57272	0.469242
GCL*P. brevipes*	$\mathbf{r^2}$ = 0.0337 (**p** = 0.728)	**p**(N) = 0.387	6	10.43554	0.305387
GCL*P. rathbuni*	$\mathbf{r^2}$ = 0.717 (**p** = 0.153)	**p**(N) = 0.473	4	8.472898	0.218867
GL*L.aequispina*	$\mathbf{r^2}$ = 0.00965 (**p** = 0.698)	**p**(N) = 0.137	18	10.98283	0.575082
GL*L. confundens*	$\mathbf{r^2}$ = 0.00537 (**p** = 0.851)	**p**(N) = 0.059	9	9.588729	0.501407
GL*L. couesi*	$\mathbf{r^2}$ = 0.268 (**p** = 0.033)	**p**(N) = 0.309	18	9.35232	0.705955
GL*L. ferox*	$\mathbf{r^2}$ = 0.651 (**p** = <0.001) **A** = 0.502 **B** = 0.000528	**p**(N) = 0.512	13	9.014984	0.683552
GL*L. galapagensis*			2	9.718241	0.370931
GL*L. longispina*			3	9.96155	0.638549
GL*L. maja*	$\mathbf{r^2}$ = 0.211 (**p** = 0.024)	**p**(N) = 0.43	24	9.86631	0.679434
GL*L. mammilifer*			5	10.13821	0.557084
GL*L. manningi*			3	10.08408	0.927541
GL*L. megacantha*	$\mathbf{r^2}$ = 0.00256 (**p** = 0.914)	**p**(N) = 0.067	7	11.75804	0.322581
GL*L. murrayi*	$\mathbf{r^2}$ = 0.000846 (**p** = 0.903)	**p**(N) = 0.289	20	10.28741	0.615497
GL*L. richeri*	$\mathbf{r^2}$ = 0.403 (**p** = 0.126)	**p**(N) = 0.063	7	10.58442	0.411954
GL*L. santolla*	$\mathbf{r^2}$ = 0.263	**p**(N) =	13	9.440825	0.938374

	(**p** = 0.051)	0.969			
GL*P. californiensis*			3	8.387551	0.389072
GL*P. camtschaticus*	**r²** = 0.0805 (**p** = 0.537)	**p**(N) = 0.033	6	10.43103	0.162219
GL*P. brevipes*	**r²** = 0.922 (**p** = 0. 002) **A** =0.567 **B** = 0.000924	**p**(N) = 0.681	6	10.89173	0.435418
GL*P. rathbuni*	**r²** = 0.699 (**p** = 0.164) **A** = 0.539 **B** = 0.00139	**p**(N) = 0.841	4	8.34934	0.730536
MW*L.aequispina*	**r²** 0.219 (**p** = 0.05)	**p**(N) = 0.412	18	10.17546	0.310988
MW*L. confundens*	**r²** 0.178 (**p** = 0.258)	**p**(N) = 0.707	9	11.34535	0.543003
MW*L. couesi*	**r²** 0.519 (**p** = 0.001)	**p**(N) = 0.034	18	8.850754	0.50265
MW*L. ferox*	**r²** 0.00251 (**p** = 0.871)	**p**(N) = 0.399	13	9.39566	0.49285
MW*L. galapagensis*			2	9.335397	0.987352
MW*L. longispina*			3	8.814645	0.330112
MW*L. maja*	**r²** 0.0327 (**p** = 0.409)	**p**(N) = 0.79	24	10.86658	0.466091
MW*L. mammilifer*			5	9.546072	0.268358
MW*L. manningi*			3	9.184509	0.322008
MW*L. megacantha*	**r²** 0.0608 (**p** = 0.594)	**p**(N) = 0.269	7	8.667802	0.311328
MW*L. murrayi*	**r²** 0.00931 (**p** = 0.686)	**p**(N) = 0.355	20	9.659591	0.419634
MW*L. richeri*	**r²** 0.304 (**p** = 0.2)	**p**(N) = 0.322	7	8.975221	0.302871
MW*L. santolla*	**r²** 0.131 (**p** = 0.184)	**p**(N) = 0.726	13	10.56871	0.665396
MW*P. californiensis*			3	9.63455	0.171989
MW*P. camtschaticus*	**r²** 0.418 (**p** = 0.165)	**p**(N) = 0.226	6	11.27363	0.294646
MW*P. brevipes*	**r²** 0.126 (**p** = 0.490)	**p**(N) = 0.361	6	11.81863	0.351257

MW*P. rathbuni*	r^2 0.00249 (**p** = 0.950)	**p**(N) = 0.285	4	9.616808	0.11746
ABL*L.aequispina*	r^2 0.282 (**p** = 0.023)	**p**(N) = 0.955	18	10.40658	0.284475
ABL*L. confundens*	r^2 0.0873 (**p** = 0.44)	**p**(N) = 0.74	9	9.374634	0.281969
ABL*L. couesi*	r^2 0.0298 (**p** = 0.508)	**p**(N) = 0.692	18	8.022824	0.378305
ABL*L. ferox*	r^2 0.0107 (**p** = 0.737)	**p**(N) = 0.651	13	10.2377	0.59691
ABL*L. galapagensis*			2	9.216119	0.997909
ABL*L. longispina*			3	10.25447	0.549117
ABL*L. maja*	r^2 0.00811 (**p** = 0.676)	**p**(N) = 0.485	24	10.26596	0.330769
ABL*L. mammilifer*			5	9.920055	0.301264
ABL*L. manningi*			3	10.17545	0.265388
ABL*L. megacantha*	r^2 0.0552 (**p** = 0.612)	**p**(N) = 0.355	7	10.10293	0.326542
ABL*L. murrayi*	r^2 0.0102 (**p** = 0.671)	**p**(N) = 0.478	20	10.31612	0.476831
ABL*L. richeri*	r^2 0.173 (**p** = 0.353)	**p**(N) = 0.12	7	9.249437	0.228422
ABL*L. santolla*	r^2 0.00388 (**p** = 0.825)	**p**(N) = 0.12	13	10.15058	0.380681
ABL*P. californiensis*			3	9.40676	0.339896
ABL*P. camtschaticus*	r^2 0.146 (**p** = 0.455)	**p**(N) = 0.526	6	11.99883	0.471287
ABL*P. brevipes*	r^2 0.000887 (**p** = 0.955)	**p**(N) = 0.626	6	12.00857	0.316465
ABL*P. rathbuni*	r^2 0.486 (**p** = 0.303)	**p**(N) = 0.476	4	9.0907	0.25753
LSH*L.aequispina*	r^2 0.252 (**p** = 0.034)	**p**(N) = 0.491	18	9.187146	0.372226
LSH*L. confundens*	r^2 0.00934 (**p** = 0.805)	**p**(N) = 0.828	9	9.646891	0.324516
LSH*L. couesi*	r^2 0.290	**p**(N) =	18	8.712032	0.26366

	(**p** = 0.026)	0.253			
LSH$_{L.\ ferox}$	**r**^{2} 0.0432 (**p** = 0.496)	**p**(N) = 0.982	13	10.8234	0.345012
LSH$_{L.\ galapagensis}$			2	10.82066	0.329379
LSH$_{L.\ longispina}$			3	10.56317	0.83799
LSH$_{L.\ maja}$	**r**^{2} 0.0000605 (**p** = 0.971)	**p**(N) = 0.118	24	9.52798	0.188441
LSH$_{L.\ mammilifer}$			5	10.9512	0.575335
LSH$_{L.\ manningi}$			3	11.83831	0.196639
LSH$_{L.\ megacantha}$	**r**^{2} 0.0585 (**p** = 0.644)	**p**(N) = 0.983	7	11.39405	0.353105
LSH$_{L.\ murrayi}$	**r**^{2} 0.0497 (**p** = 0.345)	**p**(N) = 0.288	20	11.19202	0.318441
LSH$_{L.\ richeri}$	**r**^{2} 0.0417 (**p** = 0.661)	**p**(N) = 0.128	7	11.53462	0.598638
LSH$_{L.\ santolla}$	**r**^{2} 0.585 (**p** = 0.385)	**p**(N) = 0.377	13	9.524453	0.286484
LSH$_{P.\ californiensis}$			3	8.945357	0.237272
LSH$_{P.\ camtschaticus}$			6	9.84386	0.354302
LSH$_{P.\ brevipes}$	**r**^{2} 0.168 (**p** = 0.420)	**p**(N) = 0.315	6	9.783048	0.279948
LSH$_{P.\ rathbuni}$			4	8.890207	0.101394

APPENDIX K

Table.a: Statistics relating to non-species-subdivided datasets for the *Paralomis* morphometric analysis (section B2).

Y_k	1^{st}; 2^{nd} order polynomial regression of undivided datasets x = CL; $y = Y_k$. **p** = probability that the coefficient of the highest order term is zero (α = 0.01).	ANOVA of $f_{CL}(Y_k)$ subdivided into 17 species. H_0: no difference in Y_k between species. (α = 0.01)	Shapiro-Wilk test for normality. **p**(N) = probability that all within-species samples are normally distributed (α = 0.01).	F-test for equal variance. **p**(EV) = probability that all species have equal variance in the measurement Y_k (α = 0.01).
LBH	**1°: r²** = 0.884 (**p <** 0.001); **2°: r²** = 0.00441 (**p** = 0.247)	**F =** 38.681 **p**(H_0) < 0.001	**p**(N) = 0.133	**p**(EV) = 0.188
HW	**1°: r²** = 0.928 (**p <** 0.001); **2°: r²** = 0.00360 (**p** = 0.01)	**F =** 72.55 **p**(H_0) < 0.001	**p**(N) = 0.04	**p**(EV) = 0.821
ML	**1°: r²** = 0.657 (**p <** 0.001); **2°: r²** = 0.00003 (**p** = 0.889)	**F =** 44.587 **p**(H_0) < 0.001	**p**(N) = 0.104	**p**(EV) = 0.078
GCL	**1°: r²** = 0.156 (**p <** 0.001); **2°: r²** = 0.024 (**p** = 0.016)	**F =** 68.794 **p**(H_0) < 0.001	X	**p**(EV) = 0.154
GL	**1°: r²** = 0.942 (**p <** 0.001); **2°: r²** = 0.0034 (**p(B=0)** = 0.001)	**F =** 50.576 **p**(H_0) < 0.001	**p**(N) = 0.233	**p**(EV) = 0.633
AL	**1°: r²** = 0.845 (**p <** 0 001); **2°: r²** = 0.00723 (**p(B=0)** = 0.01)	**F =** 150.6 **p**(H_0) < 0.001	X	**p**(EV) = 0.309
DL	**1°: r²** = 0.629 (**p <** 0.001); **2°: r²** = 0.00029 (**p(B=0)** = 0.664)	**F =** 74.8 **p**(H_0) < 0.001	**p**(N) = 0.05	**p**(EV) = 0.05
OCL	**1°: r²** = 0.961 (**p <** 0.001); **2°: r²** = 0.00026 (**p(B=0)** = 0.2)	**F =** 0.933 **p**(H_0) = 0.767		**p**(EV) = 0.23
OCW	**1°: r²** = 0.96 (**p**	**F =** 0.796 **p**(H_0)	X	**p**(EV) = 0.815

	< 0.001); **2°: r²** = 0.00015 (**p(B=0)** = 0.339)	= 0.711		
ABL	**1°: r²** = 0.850 (**p <** 0.001); **2°: r²** = 0.00192 (**p(B=0)** = 0.082)	**F =** 1.012 **p**(H_0) = 0.448	X	**p**(EV) **=** 0.431
LSH	**1°: r²** = 0.737 (**p <** 0.001); **2°: r²** = 0.000526 (**p(B=0)** = 0.484)	**F =** 1.271 **p**(H_0) = 0.2	**p**(N) = 0.05	**p**(EV) **=** 0.197
HL	**1°: r²** = 0.959 (**p <** 0.001); **2°: r²** = 0.000444 (**p(B=0)** = 0.103)	**F =** 1.059 **p**(H_0) = 0.395	**p**(N) = 0.06	**p**(EV) **=** 0.212
CDL	**1°: r²** = 0.719 (**p <** 0.001); **2°: r²** = 0.0011 (**p(B=0)** = 0.327)	**F =** 1.244 **p**(H_0) = 0.224	**p**(N) = 0.1	**p**(EV) = 0.296
GCW	**1°: r²** = 0.286 (**p <** 0.001); **2°: r²** = 0.00108 (**p(B=0)** = 0.544)	**F =** 1.174 **p**(H_0) = 0.282	**p**(N) = 0.050	**p**(EV) **=** 0.281
VRL	**1°: r²** = 0.541 (**p(A=0) <** 0.001); **2°: r²** = 0.000789 (**p(B=0)** = 0.517)	**F =** 0.614 **p**(H_0) = 0.894	**p**(N) = 0.050	**p**(EV) **=** 0.621
DH	**1°: r²** = 0.653 (**p <** 0.001); **2°: r²** = 0.000007 (**p(B=0)** = 0.943)	**F =** 1.53 **p**(H_0) = 0.402	**p**(N) = 0.01	**p**(EV) **=** 0.970
PL	**1°: r²** = 0.84 (**p <** 0.001); **2°: r²** = 0.000067 (**p(B=0)** = 0.748)	**F =** 0.634 **p**(H_0) = 0.878	X	**p**(EV) **=** 0.976
CAL	**1°: r²** = 0.946 (**p <** 0.001); **2°: r²** = 0.000479 (**p(B=0)** = 0.138)	**F =** 1.337 **p**(H_0) = 0.162	X	**p**(EV) **=** 0.312
MW	**1°: r²** = 0.649 (**p <** 0.001); **2°: r²** = 0.0011 (**p(B=0)** =	**F =** 1.124 **p**(H_0) = 0.328	X	**p**(EV) **=** 0.736

	0.378)			
MH	**1°: r²** = 0.621 (**p** < 0.001); **2°: r²** = 0.00358 (**p(B=0)** = 0.128)	**F** = 3.624 **p**(H_0) = 0.728		**p**(EV) = 0.86
LHH	**1°: r²** = 0.781 (**p** < 0.001); **2°: r²** = 0.00438 (**p(B=0)** =0.026)	**F** = 0.124 **p**(H_0) = 0.828		**p**(EV) = 0.86

b. Statistics relating to species-subdivided datasets for the *Paralomis* morphometric analysis.

K, n	r^2 test of linear regression within species, in which x = CL and y = $Y_{k,n}$/CL. **p** is the probability that B=0 in the equation y = **A** + **B**x (α = 0.01)	Shapiro-Wilk test of normality **p**(N) = probability that the sample is taken from a normally distributed population (α = 0.01)	Sample number	Standardised within-species sample mean: $\bar{U}_{k,n}$	Standardised within-species sample standard deviation: $S_{k,n}$
LBH*Pacu*	**r²** = 0.00618 (**p** = 0.674)	**p**(N) = 0.165	31	10.07737	0.399655
LBH*Pafr*	**r²** = 0.00000006 (**p** = 0.998)	**p**(N) = 0.931	15	10.63838	0.436698
LBH*Pana*	**r²** = 0.55 (**p** = 0.034) **A** = 0.287 **B** = 0.000988	**p**(N) = 0.964	8	9.855126	0.532302
LBH*Pbir*	**r²** = 0.116 (**p** = 0.336)	**p**(N) = 0.208	10	9.32681	0.477682
LBH*Pcri*	**r²** = 0.0864 (**p** = 0.354)	**p**(N) = 0.279	12	10.5219	0.363468
LBH*Pcub*	**r²** = 0.214 (**p** = 0.053)	**p**(N) = 0.137	18	9.084735	0.587059
LBH*Peri*	**r²** = 0.00915 (**p** = 0.715)	**p**(N) = 0.304	17	9.544979	0.349015
LBH*Pfor*			5	10.70678	0.274101
LBH*Pgra*	**r²** = 0.0854 (**p** = 0.211)	**p**(N) = 0.431	21	8.647572	0.443872
LBH*Phai*	**r²** = 0.0734 (**p** = 0.449)	**p**(N) = 0.995	10	9.920925	0.444535
LBH*Pinc*			5	12.46169	0.635755
LBH*Pmen*	**r²** = 0.00158	**p**(N) = 0.388	10	9.186788	0.470946

	(**p** = 0.919)				
LBH$_{Pmul}$	$\mathbf{r}^2$ = 0.0102 (**p** = 0.665)	**p**(N) = 0.232	17	11.36904	0.703783
LBH$_{Pots}$	$\mathbf{r}^2$ = 0.0006 (**p** = 0.953)	**p**(N) = 0.723	8	10.68333	0.411925
LBH$_{Pphr}$			5	10.47425	0.45228
LBH$_{Pspi}$	$\mathbf{r}^2$ = 0.0536 (**p** = 0.407)	**p**(N) = 0.533	15	10.44068	0.57987
LBH$_{Pste}$	$\mathbf{r}^2$ = 0.0231 (**p** = 0.656)	**p**(N) = 0.540	11	9.357028	0.491302
LBH$_{Pver}$	$\mathbf{r}^2$ = 0.0434 (**p** = 0.654)	**p**(N) = 0.178	7	10.19007	0.633344
LBH$_{loop}$	$\mathbf{r}^2$ = 0.6 (**p** = 0.04) **A** = 0.6 **B**=0.00047	**p**(N) = 0.674	8	8.63464	0.575908
LBH$_{gly}$	$\mathbf{r}^2$ = 0.0675 (**p** = 0.534)	**p**(N) = 0.361	8	11.34427	0.633841
HW$_{Pacu}$	$\mathbf{r}^2$ = 0.00827 (**p** = 0.627)	**p**(N) = 0.056	31	10.94449	0.438185
HW$_{Pafr}$	$\mathbf{r}^2$ = 0.0685 (**p** = 0.346)	**p**(N) = 0.011	15	10.26265	0.404355
HW$_{Pana}$	$\mathbf{r}^2$ = 0.614 (**p** = 0.021) **A** = 0.562 **B** = 0.00195	**p**(N) = 0.481	8	11.05168	0.491337
HW$_{Pbir}$	$\mathbf{r}^2$ = 0.0664 (**p** = 0.472)	**p**(N) = 0.873	10	10.1888	0.200508
HW$_{Pcri}$	$\mathbf{r}^2$ = 0.013 (**p** = 0.742)	**p**(N) = 0.815	12	9.580048	0.264079
HW$_{Pcub}$	$\mathbf{r}^2$ = 0.172 (**p** = 0.087)	**p**(N) = 0.032	18	11.70031	0.403616
HW$_{Peri}$	$\mathbf{r}^2$ = 0.0224 (**p** = 0.566)	**p**(N) = 0.833	17	9.869671	0.326062
HW$_{Pfor}$			5	9.705189	0.217291
HW$_{Pgra}$	$\mathbf{r}^2$ = 0.0576 (**p** = 0.295)	**p**(N) = 0.054	21	9.649103	0.426745
HW$_{Phai}$	$\mathbf{r}^2$ = 0.282 (**p** = 0.175)	**p**(N) = 0.508	10	10.17662	0.50601
HW$_{Pinc}$			5	7.959664	0.430677
HW$_{Pmen}$	$\mathbf{r}^2$ = 0.00911 (**p** = 0.822)	**p**(N) = 0.130	10	11.4048	0.230786
HW$_{Pmul}$	$\mathbf{r}^2$ = 0.147 (**p** = 0.116)	**p**(N) = 0.230	17	9.186394	0.36912
HW$_{Pots}$	$\mathbf{r}^2$ = 0.665 (**p** = 0.014) **B** = 0.00084	**p**(N) = 0.336	8	9.356245	0.40981
HW$_{Pphr}$			5	9.616889	0.3114
HW$_{Pspi}$	$\mathbf{r}^2$ = 0.369 (**p** = 0.016)	**p**(N) = 0.246	15	8.814251	0.408458
HW$_{Pste}$	$\mathbf{r}^2$ = 0.0622 (**p** = 0.46)	**p**(N) = 0.558	11	10.52866	0.306926
HW$_{Pver}$	$\mathbf{r}^2$ = 0.315 (**p** = 0.19)	**p**(N) = 0.260	7	8.819982	0.485916

HW$_{lop}$	$\mathbf{r}^2$ = 0.36 (**p** = 0.116)	**p**(N) = 0.229	8	8.586976	0.426809
HW$_{gly}$	$\mathbf{r}^2$ = 0.0171 (**p** = 0.758)	**p**(N) = 0.537	8	9.096016	0.26123
ML$_{cu}$	$\mathbf{r}^2$ = 0.0818 (**p** = 0.119)	**p**(N) = 0.562	31	10.628	0.455472
ML$_{Pafr}$	$\mathbf{r}^2$ = 0.156 (**p** = 0.145)	**p**(N) = 0.388	15	9.846502	0.583136
ML$_{Pana}$	$\mathbf{r}^2$ = 0.295 (**p** = 0.164)	**p**(N) = 0.216	8	10.39801	0.719802
ML$_{Pbir}$	$\mathbf{r}^2$ = 0.528 (**p** = 0.017) **B** =0.00319	**p**(N) = 1.0	10	10.97287	0.707838
ML$_{Pcri}$	$\mathbf{r}^2$ = 0.0429 (**p** = 0.518)	**p**(N) = 0.105	12	8.986513	0.337699
ML$_{Pcub}$	$\mathbf{r}^2$ = 0.00122 (**p** = 0.890)	**p**(N) = 0.492	18	9.847328	0.200707
ML$_{Peri}$	$\mathbf{r}^2$ = 0.104 (**p** = 0.223)	**p**(N) = 0.576	17	9.788864	0.364249
ML$_{Pfor}$			5	11.09682	0.389265
ML$_{Pgra}$	$\mathbf{r}^2$ = 0.470 (**p** = 0.001) **B** = 0.00218	**p**(N) = 0.682	21	8.810587	0.427371
ML$_{Phai}$	$\mathbf{r}^2$ = 0.00994 (**p** = 0.784)	**p**(N) = 0.629	10	9.497893	0.441702
ML$_{Pinc}$			5	9.417671	0.469464
ML$_{Pmen}$	$\mathbf{r}^2$ = 0.0369 (**p** = 0.62)	**p**(N) = 0.765	10	10.89536	0.528681
ML$_{Pmul}$	$\mathbf{r}^2$ = 0.1122 (**p** = 0.174)	**p**(N) = 0.619	17	11.46685	0.569493
ML$_{Pots}$	$\mathbf{r}^2$ = 0.273 (**p** = 0.184)	**p**(N) =0.422	8	10.53054	0.639866
ML$_{Pphr}$	$\mathbf{r}^2$ = 0.635 (**p** = 0.111) **B**= 0.0172	**p**(N) =0.963	5	10.75157	0.413327
ML$_{Pspi}$	$\mathbf{r}^2$ = 0.00005 (**p** = 0.979)	**p**(N) =0.953	15	10.16861	0.351904
ML$_{Pste}$	$\mathbf{r}^2$ = 0.0796 (**p** = 0.401)	**p**(N) = 0.464	11	9.652465	0.42286
ML$_{Pver}$	$\mathbf{r}^2$ = 0.125 (**p** = 0.437)	**p**(N) = 0.859	7	10.50686	0.58741
ML$_{lop}$	$\mathbf{r}^2$ = 0.0246 (**p** = 0.711)	**p**(N) = 0.462	8	7.591637	0.21614
ML$_{gly}$	$\mathbf{r}^2$ = 0.1122 (**p** = 0.987)	**p**(N) = 0.637	8	8.773115	0.548672
GCL$_{Pacu}$	$\mathbf{r}^2$ = 0.0119 (**p** = 0.56)	**p**(N) = 0.073	31	11.18331	0.36325
GCL$_{Pafr}$	$\mathbf{r}^2$ = 0.0766 (**p** = 0.410)	**p**(N) = 0.222	15	9.311326	0.226067
GCL$_{Pana}$	$\mathbf{r}^2$ = 0.00501 (**p** = 0.868)	**p**(N) = 0.11	8	10.68265	0.371433
GCL$_{Pbir}$	$\mathbf{r}^2$ = 0.00454 (**p** = 0.853)	**p**(N) = 0.025	10	10.33285	0.670977
GCL$_{Pcri}$	$\mathbf{r}^2$ = 0.00526	**p**(N) = 0.6	12	10.49385	0.284153

	(**p** = 0.823)				
GCL$_{Pcub}$	$\mathbf{r^2}$ = 0.0268 (**p** = 0.516)	**p**(N) = 0.091	18	9.881939	0.400301
GCL$_{Peri}$	$\mathbf{r^2}$ = 0.0194 (**p** = 0.594)	**p**(N) = 0.789	17	9.852932	0.244647
GCL$_{Pfor}$	$\mathbf{r^2}$ = 0.571 (**p** = 0. 626) **B** = 0.00277	**p**(N) = 0.626	5	9.680204	0.535297
GCL$_{Pgra}$	$\mathbf{r^2}$ = 0.0169 (**p** = 0.574)	**p**(N) = 0.201	21	10.04633	0.482462
GCL$_{Phai}$	$\mathbf{r^2}$ = 0.635 (**p** = 0.018) **A** = 0.308 **B** = 0.00124	**p**(N) = 0.124	10	10.48195	0.627109
GCL$_{Pinc}$	$\mathbf{r^2}$ = 0.32 (**p** = 0.321)	**p**(N) = 0.951	5	7.256676	0.28594
GCL$_{Pmen}$	$\mathbf{r^2}$ = 0.000755 (**p** = 0.948)	**p**(N) = 0.462	10	10.93959	0.283567
GCL$_{Pmul}$	$\mathbf{r^2}$ = 0.0651 (**p** = 0.307)	**p**(N) = 0.012	17	8.760209	0.441205
GCL$_{Pots}$	$\mathbf{r^2}$ = 0.0000472 (**p** = 0.987)	**p**(N) = 0.630	8	9.622753	0.213761
GCL$_{Pphr}$	$\mathbf{r^2}$ = 0.554 (**p** = 0.149) **A** = 0.366 **B** = 0.0027	**p**(N) = 0.862	5	9.598923	0.205949
GCL$_{Pspi}$	$\mathbf{r^2}$ = 0.00501 (**p** = 0.802)	**p**(N) = 0.155	15	10.51614	0.30719
GCL$_{Pste}$	$\mathbf{r^2}$ = 0.239 (**p** = 0.127)	**p**(N) = 0.572	11	10.64006	0.341553
GCL$_{Pver}$	$\mathbf{r^2}$ = 0.128 (**p** = 0.43)	**p**(N) = 0.497	7	9.312396	0.435655
GCL$_{lop}$	$\mathbf{r^2}$ = 0.0022 (**p** = 0.912)	**p**(N) = 0.175	8	10.24576	0.386466
GCL$_{gly}$	$\mathbf{r^2}$ = 0.138 (**p** = 0.364)	**p**(N) = 0.47	8	7.397069	0.339845
GL$_{Pacu}$	$\mathbf{r^2}$ = 0.00573 (**p** = 0.686)	**p**(N) = 0.381	31	11.40946	0.418209
GL$_{Pafr}$	$\mathbf{r^2}$ = 0.281 (**p** = 0.042)	**p**(N) = 0.05	15	8.839237	0.511072
GL$_{Pana}$	$\mathbf{r^2}$ = 0.00434 (**p** = 0.877)	**p**(N) = 0.547	8	11.00938	0.350855
GL$_{Pbir}$	$\mathbf{r^2}$ = 0.111 (**p** = 0.347)	**p**(N) = 0.588	10	11.12611	0.295765
GL$_{Pcri}$	$\mathbf{r^2}$ = 0.0144 (**p** = 0.711)	**p**(N) = 0.951	12	9.597378	0.330529
GL$_{Pcub}$	$\mathbf{r^2}$ = 0.0709 (**p** = 0.285)	**p**(N) = 0.914	18	10.23285	0.31773
GL$_{Peri}$	$\mathbf{r^2}$ = 0.00372 (**p** = 0.816)	**p**(N) = 0.044	17	10.28247	0.407034
GL$_{Pfor}$	$\mathbf{r^2}$ = 0.547 (**p** = 0.153) **A** = 0.626	**p**(N) = 0.422	5	10.24037	0.361653

	B = 0.00137				
GL$_{Pgra}$	$\mathbf{r}^2$ = 0.284 (**p** = 0.013)	**p**(N) = 0.799	21	10.26582	0.590133
GL$_{Phai}$	$\mathbf{r}^2$ = 0.271 (**p** = 0.123)	**p**(N) = 0.621	10	10.43765	0.529269
GL$_{Pinc}$	$\mathbf{r}^2$ = 0.109 (**p** = 0.587)	**p**(N) = 0.269	5	7.236884	0.198834
GL$_{Pmen}$	$\mathbf{r}^2$ = 0.0922 (**p** = 0.427)	**p**(N) = 0.499	10	10.21418	0.530511
GL$_{Pmul}$	$\mathbf{r}^2$ = 0.203 (**p** = 0.06)	**p**(N) = 0.916	17	9.524148	0.410944
GL$_{Pots}$	$\mathbf{r}^2$ = 0.0246 (**p** = 0.711)	**p**(N) = 0.514	8	9.648917	0.46497
GL$_{Pphr}$	$\mathbf{r}^2$ = 0.00652 (**p** = 0.897)	**p**(N) = 0.866	5	9.774755	0.584813
GL$_{Pspi}$	$\mathbf{r}^2$ = 0.033 (**p** = 0.517)	**p**(N) = 0.755	15	9.428599	0.452277
GL$_{Pste}$	$\mathbf{r}^2$ = 0.352 (**p** = 0.054)	**p**(N) = 0.34	11	9.52823	0.490308
GL$_{Pver}$	$\mathbf{r}^2$ = 0.00004 (**p** = 0.989)	**p**(N) = 0.04	7	9.570841	0.361237
GL$_{lop}$	$\mathbf{r}^2$ = 0.107 (**p** = 0.429)	**p**(N) = 0.787	8	9.44901	0.513755
GL$_{gly}$	$\mathbf{r}^2$ = 0.0122 (**p** = 0.795)	**p**(N) = 0.086	8	8.077554	0.619229
AL$_{Pacu}$	$\mathbf{r}^2$ = 0.0351 (**p** = 0.313)	**p**(N) = 0.184	31	11.34301	0.28009
AL$_{Pafr}$	$\mathbf{r}^2$ = 0.0141 (**p** = 0.674)	**p**(N) = 0.219	15	9.831723	0.167242
AL$_{Pana}$	$\mathbf{r}^2$ = 0.233 (**p** =0.226)	**p**(N) = 0.225	8	10.63229	0.464388
AL$_{Pbir}$	$\mathbf{r}^2$ = 0.119 (**p** = 0.328)	**p**(N) = 0.443	10	11.2289	0.193833
AL$_{Pcri}$	$\mathbf{r}^2$ = 0.137 (**p** = 0.236)	**p**(N) = 0.958	12	8.733416	0.167462
AL$_{Pcub}$	$\mathbf{r}^2$ = 0.187 (**p** = 0.073)	**p**(N) = 0.07	18	10.11957	0.30662
AL$_{Peri}$	$\mathbf{r}^2$ = 0.0618 (**p** = 0.336)	**p**(N) = 0.47	17	10.28855	0.280451
AL$_{Pfor}$	$\mathbf{r}^2$ = 0.00775 (**p** = 0.888)	**p**(N) = 0.856	5	9.811348	0.291521
AL$_{Pgra}$	$\mathbf{r}^2$ = 0.251 (**p** = 0.021)	**p**(N) = 0.925	21	8.363322	0.256719
AL$_{Phai}$	$\mathbf{r}^2$ = 0.104 (**p** = 0.364)	**p**(N) = 0.699	10	10.51178	0.415736
AL$_{Pinc}$	$\mathbf{r}^2$ = 0.459 (**p** = 0.209) **A** = 0.245 **B** = 0.000745	**p**(N) = 0.814	5	8.528309	0.162441
AL$_{Pmen}$	$\mathbf{r}^2$ = 0.00614 (**p** = 0.854)	**p**(N) = 0.037	10	10.59302	0.233494
AL$_{Pmul}$	$\mathbf{r}^2$ = 0.256 (**p** = 0.032)	**p**(N) = 0.08	17	10.00439	0.352856
AL$_{Pots}$	$\mathbf{r}^2$ = 0.74	**p**(N) = 0.494	8	9.808249	0.320035

	(**p** =0.006) **B** = 0.0007				
AL$_{Pphr}$	$\mathbf{r}^2$ = 0.0189 (**p** = 0.825)	**p**(N) = 0.452	5	11.073	0.161251
AL$_{Pspi}$	$\mathbf{r}^2$ = 0.0407 (**p** = 0.471)	**p**(N) = 0.03	15	10.6354	0.272651
AL$_{Pste}$	$\mathbf{r}^2$ = 0.0546 (**p** = 0.489)	**p**(N) = 0.113	11	9.867093	0.303527
AL$_{Pver}$	$\mathbf{r}^2$ = 0.0257 (**p** = 0.731)	**p**(N) = 0.071	7	9.654274	0.117158
AL$_{lop}$	$\mathbf{r}^2$ = 0.137 (**p** = 0.367)	**p**(N) = 0.790	8	8.711148	0.287283
AL$_{gly}$	$\mathbf{r}^2$ = 0.028 (**p** = 0.692	**p**(N) = 0.717	8	8.15583	0.113898
DL$_{Pacu}$	$\mathbf{r}^2$ = 0.0683 (**p** = 0.155)	**p**(N) = 0.01	31	10.95378	0.417343
DL$_{Pafr}$	$\mathbf{r}^2$ = 0.54 (**p** = 0.002) **A** = 0.263 **B** = 0.00313	**p**(N) = 0.394	15	9.964007	0.431166
DL$_{Pana}$	$\mathbf{r}^2$ = 0.319 (**p** = 0.145)	**p**(N) = 0.939	8	10.74625	0.664669
DL$_{Pbir}$	$\mathbf{r}^2$ = 0.217 (**p** = 0.175)	**p**(N) = 0.746	10	11.36447	0.299519
DL$_{Pcri}$	$\mathbf{r}^2$ = 0.00112 (**p** = 0.918)	**p**(N) = 0.65	12	9.518856	0.081091
DL$_{Pcub}$	$\mathbf{r}^2$ = 0.0865 (**p** = 0.236)	**p**(N) = 0.096	18	9.53168	0.165124
DL$_{Peri}$	$\mathbf{r}^2$ = 0.0048 (**p** = 0.799)	**p**(N) = 0.01	17	9.61102	0.21275
DL$_{Pfor}$	$\mathbf{r}^2$ = 0.374 (**p** = 0.273)	**p**(N) = 0.626	5	11.07164	0.427858
DL$_{Pgra}$	$\mathbf{r}^2$ = 0.602 (**p** = 0.01) **A** = 0.195 **B** = 0.00215	**p**(N) = 0.358	21	8.606782	0.41313
DL$_{Phai}$	$\mathbf{r}^2$ = 0.013 (**p** = 0.754)	**p**(N) = 0.157	10	9.066233	0.319837
DL$_{Pinc}$	$\mathbf{r}^2$ = 0.0405 (**p** = 0.746)	**p**(N) = 0.125	5	9.66038	0.360125
DL$_{Pmen}$	$\mathbf{r}^2$ = 0.0983 (**p** = 0.411)	**p**(N) = 0.537	10	10.41884	0.411826
DL$_{Pmul}$	$\mathbf{r}^2$ = 0.219 (**p** = 0.05)	**p**(N) = 0.192	17	11.15104	0.630466
DL$_{Pots}$	$\mathbf{r}^2$ = 0.607 (**p** = 0.023) **B** = 0.0026	**p**(N) = 0.061	8	10.52136	0.543332
DL$_{Pphr}$	$\mathbf{r}^2$ = 0.111 (**p** = 0.583)	**p**(N) = 0.88	5	10.37525	0.064954
DL$_{Pspi}$	$\mathbf{r}^2$ = 0.205 (**p** = 0.09)	**p**(N) = 0.968	15	10.38141	0.190245
DL$_{Pste}$	$\mathbf{r}^2$ = 0.00366 (**p** = 0.86)	**p**(N) = 0.249	11	9.211343	0.204303
DL$_{Pver}$	$\mathbf{r}^2$ = 0.23	**p**(N) = 0.720	7	10.60038	0.512587

	(**p** = 0.276)				
DL$_{lop}$	$\mathbf{r^2}$ = 0.185 (**p** = 0.288)	**p**(N) = 0.532	8	7.542282	0.149323
DL$_{gly}$	$\mathbf{r^2}$ = 0.00819 (**p** = 0.831)	**p**(N) = 0.309	8	9.373372	0.351435